



Programme Area: Carbon Capture and Storage

Project: DECC Storage Appraisal

Title: WP5E –Viking A Storage Development Plan

Abstract:

Storage of CO₂ in the Permian Leman Sandstone in the faulted horst block known as Viking A (UKCS block 49/12) in the Southern North Sea. Three well development of Viking A from a new unmanned platform supplied with CO₂ from Barmston via a 20" 185 km pipeline. Final investment decision in 2027 and first injection in 2031. The site stores 130Mt of CO₂, 5Mt/y for 26 years. Capital investment of £150 million (PV10, 2015), equating to £1.2 for each tonne stored. Capacity uncertainty is low, but can be reduced further through access to operator data (well rates and pressures) Heating is required to achieve the target injection rate in the initial very low reservoir pressure conditions.

Context:

This project, funded with up to £2.5m from the UK Department of Energy and Climate Change (DECC - now the Department of Business, Energy and Industrial Strategy), was led by Aberdeen-based consultancy Pale Blue Dot Energy supported by Axis Well Technology and Costain. The project appraised five selected CO₂ storage sites towards readiness for Final Investment Decisions. The sites were selected from a short-list of 20 (drawn from a long-list of 579 potential sites), representing the tip of a very large strategic national CO₂ storage resource potential (estimated as 78,000 million tonnes). The sites were selected based on their potential to mobilise commercial-scale carbon, capture and storage projects for the UK. Outline development plans and budgets were prepared, confirming no major technical hurdles to storing industrial scale CO₂ offshore in the UK with sites able to service both mainland Europe and the UK. The project built on data from CO₂ Stored - the UK's CO₂ storage atlas - a database which was created from the ETI's UK Storage Appraisal Project. This is now publically available and being further developed by The Crown Estate and the British Geological Survey. Information on CO₂Stored is available at www.co2stored.com.

Disclaimer:

The Energy Technologies Institute is making this document available to use under the Energy Technologies Institute Open Licence for Materials. Please refer to the Energy Technologies Institute website for the terms and conditions of this licence. The Information is licensed 'as is' and the Energy Technologies Institute excludes all representations, warranties, obligations and liabilities in relation to the Information to the maximum extent permitted by law. The Energy Technologies Institute is not liable for any errors or omissions in the Information and shall not be liable for any loss, injury or damage of any kind caused by its use. This exclusion of liability includes, but is not limited to, any direct, indirect, special, incidental, consequential, punitive, or exemplary damages in each case such as loss of revenue, data, anticipated profits, and lost business. The Energy Technologies Institute does not guarantee the continued supply of the Information. Notwithstanding any statement to the contrary contained on the face of this document, the Energy Technologies Institute confirms that the authors of the document have consented to its publication by the Energy Technologies Institute.

2016

Pale Blue Dot.



D14: WP5E –Viking A Storage Development Plan
10113ETIS-Rep-21-03

March 2016

www.pale-blu.com

www.axis-wt.com

© Energy Technologies Institute 2016

Contents

Document Summary						
Client	The Energy Technologies Institute					
Project Title	DECC Strategic UK CCS Storage Appraisal Project					
Title:	D14: Wp5e –Viking A Storage Development Plan					
Distribution:	A Green, D Gammer			Classification:	Client Confidential	
Date of Issue:	30/03/16					
	Name		Role		Signature	
Prepared by:	A James, S Baines & S McCollough		Chief Technologist, Scientific Advisor & Subsurface Lead			
Approved by:	S J Murphy		Project Manager			
Amendment Record						
Rev	Date	Description	Issued By	Checked By	Approved By	Client Approval
V01	14/03/16	Draft	D Pilbeam	A James	S Murphy	
V02	30/03/16	Final	D Pilbeam	A James	S Murphy	A Green
V03	20/04/16	Final (added PV10 Real values)	D Pilbeam	A James	S Murphy	A Green

Disclaimer:

While the authors consider that the data and opinions contained in this report are sound, all parties must rely upon their own skill and judgement when using it. The authors do not make any representation or warranty, expressed or implied, as to the accuracy or completeness of the report. There is considerable uncertainty around the development of CO₂ stores and the available data are extremely limited. The authors assume no liability for any loss or damage arising from decisions made on the basis of this report. The views and judgements expressed here are the opinions of the authors and do not reflect those of the ETI or any of the stakeholders consulted during the course of this project. The figures, charts and tables contained in this report comply with the intellectual property and copyright constraints of this project and in some cases this has meant that they have been simplified or their number limited.

© Energy Technologies Institute 2016

Table of Contents

CONTENTS I

1.0 EXECUTIVE SUMMARY 14

2.0 OBJECTIVES 19

3.0 SITE CHARACTERISATION 21

4.0 APPRAISAL PLANNING 155

5.0 DEVELOPMENT PLANNING 157

6.0 BUDGET & SCHEDULE 179

7.0 CONCLUSIONS & RECOMMENDATIONS 190

8.0 REFERENCES 194

9.0 CONTRIBUTING AUTHORS 196

10.0 GLOSSARY 197

11.0 APPENDICES 201

Detailed Table of Contents

CONTENTS	I
TABLE OF CONTENTS	II
FIGURES	VI
TABLES	XI
1.0 EXECUTIVE SUMMARY	14
2.0 OBJECTIVES	19
3.0 SITE CHARACTERISATION	21
3.1 GEOLOGICAL SETTING	21
3.2 SITE HISTORY AND DATABASE	22
3.3 STORAGE STRATIGRAPHY	26
3.4 SEISMIC CHARACTERISATION	28
3.5 GEOLOGICAL CHARACTERISATION	56
3.6 INJECTION PERFORMANCE CHARACTERISATION	86
3.7 CONTAINMENT CHARACTERISATION	130
4.0 APPRAISAL PLANNING	155
4.1 DISCUSSION OF KEY UNCERTAINTIES	155
4.2 PROPOSED APPRAISAL PLAN	156
5.0 DEVELOPMENT PLANNING	157
5.1 DESCRIPTION OF DEVELOPMENT	157
5.2 CO ₂ SUPPLY PROFILE	158
5.3 WELL DEVELOPMENT PLAN	158
5.4 INJECTION FORECAST	162

5.5	OFFSHORE INFRASTRUCTURE DEVELOPMENT PLAN	163
5.6	OTHER ACTIVITIES IN THIS AREA	174
5.7	OPTIONS FOR EXPANSION.....	174
5.8	OPERATIONS.....	175
5.9	DECOMMISSIONING.....	176
5.10	POST CLOSURE PLAN.....	176
5.11	HANDOVER TO AUTHORITY.....	176
5.12	DEVELOPMENT RISK ASSESSMENT.....	177
6.0	BUDGET & SCHEDULE	179
6.1	SCHEDULE OF DEVELOPMENT	179
6.2	BUDGET.....	181
6.3	ECONOMICS	187
7.0	CONCLUSIONS & RECOMMENDATIONS.....	190
7.1	CONCLUSIONS.....	190
7.2	RECOMMENDATIONS.....	193
8.0	REFERENCES	194
9.0	CONTRIBUTING AUTHORS	196
10.0	GLOSSARY	197
11.0	APPENDICES.....	201
11.1	APPENDIX 1 – RISK MATRIX	201
11.2	APPENDIX 2 – LEAKAGE WORKSHOP REPORT	201
11.3	APPENDIX 3 – DATABASE.....	201
11.4	APPENDIX 4 – GEOLOGICAL INFORMATION	201
11.5	APPENDIX 5 – MMV TECHNOLOGIES	201

11.6	APPENDIX 6 – WELL BASIS OF DESIGN	201
11.7	APPENDIX 7 – COST ESTIMATE.....	201
11.8	APPENDIX 8 – METHODOLOGIES.....	201
11.9	APPENDIX 9 – FRACTURE PRESSURE GRADIENT	201
11.10	APPENDIX 10 – SUBSURFACE UNCERTAINTY ANALYSIS.....	201
11.11	APPENDIX 11 – 3D GEOMECHANICAL MODELLING	201

Figures

FIGURE 1-1 VIKING A AND VIKING GAS FIELDS LOCATION MAP.....	16
FIGURE 1-2 VIKING A - CROSS SECTION ILLUSTRATING STORAGE RESERVOIRS AND SEALS	16
FIGURE 1-3 SUMMARY DEVELOPMENT SCHEDULE	17
FIGURE 2-1: THE FIVE PROJECT OBJECTIVES.....	19
FIGURE 2-2: SEVEN COMPONENTS OF WORKPACK 5	20
FIGURE 3-1 LOCATION MAP AND LEMAN SANDSTONE EXTENT	21
FIGURE 3-2 SEISMIC DATABASE SHOWING THE AGE OF THE SURVEYS	23
FIGURE 3-3 GEOPHYSICAL WELLS AND LOG DATABASE.....	25
FIGURE 3-4 STRATIGRAPHIC COLUMN AT THE NORTH VIKING SITE, SHOWING THE OVERLYING AND UNDERLYING GEOLOGICAL FORMATIONS.....	26
FIGURE 3-5 SYNTHETIC SEISMOGRAM	29
FIGURE 3-6 VIKING A NW-SE SEISMIC PROFILE ALONG THE CREST	30
FIGURE 3-7 VIKING A, F AND Fs SW-NE SEISMIC PROFILE	31
FIGURE 3-8 TOP CHALK TWO-WAY TIME MAP	33
FIGURE 3-9 BASE CHALK/BASE CRETACEOUS UNCONFORMITY TWO-WAY TIME MAP	34
FIGURE 3-10 TOP TRIASSIC TWO-WAY TIME MAP.....	34
FIGURE 3-11 TOP BUNTER SANDSTONE TWO-WAY TIME MAP.....	35
FIGURE 3-12 TOP ZECHSTEIN TWO-WAY TIME MAP	36
FIGURE 3-13 TOP LEMAN SANDSTONE TWO-WAY TIME MAP.....	37
FIGURE 3-14 3D VIEW OF THE TOP LEMAN SANDSTONE TIME INTERPRETATION	38
FIGURE 3-15 TOP LEMAN SANDSTONE SEMBLANCE SLICE	39
FIGURE 3-16 3D VIEW OF LEMAN SANDSTONE FAIRWAY MODELLED FAULTS.....	40
FIGURE 3-17 LOCATION OF PSUEDO WELLS IN SITE MODEL	41
FIGURE 3-18 LAYER CAKE DEPTH CONVERSION SUMMARY.....	42
FIGURE 3-19 TOP CHALK DEPTH MAP.....	43
FIGURE 3-20 BASE CHALK/BASE CRETACEOUS UNCONFORMITY DEPTH MAP	44
FIGURE 3-21 TOP TRIASSIC DEPTH MAP	45

FIGURE 3-22 TOP ZECHSTEIN RAW DEPTH MAP	45
FIGURE 3-23 TOP ZECHSTEIN DEPTH MAP EDITING WORKFLOW	46
FIGURE 3-24 TOP ZECHSTEIN DEPTH MAP	46
FIGURE 3-25 ZECHSTEIN ISOCHORE	47
FIGURE 3-26 TOP LEMAN SANDSTONE DEPTH MAP	48
FIGURE 3-27 TOP LEMAN SANDSTONE DEPTH MAP	48
FIGURE 3-28 3D VIEW OF THE TOP LEMAN SANDSTONE DEPTH INTERPRETATION	49
FIGURE 3-29 TOP BUNTER SANDSTONE RAW DEPTH MAP.....	50
FIGURE 3-30 TOP BUNTER SANDSTONE DEPTH MAP EDITING WORKFLOW	51
FIGURE 3-31 TOP BUNTER SANDSTONE DEPTH MAP	51
FIGURE 3-32 DEPTH CONVERSION SENSITIVITY.....	53
FIGURE 3-33 TOP LEMAN SANDSTONE DEPTH STRUCTURE MAP FOR VIKING A	56
FIGURE 3-34 WELL CORRELATION ACROSS THE VIKING A SITE	58
FIGURE 3-35 SUMMARY OF PETROPHYSICAL WORKFLOW	60
FIGURE 3-36 CROSS SECTION THROUGH THE 3D GRID AT WELL 49/12-2 SHOWING THE LAYERING WITHIN THE STATIC MODEL	66
FIGURE 3-37 EXAMPLE OF FACIES INTERPRETATION IN WELL 49/12-3	68
FIGURE 3-38 VERTICAL PROPORTION CURVES GENERATED FROM WELLS WITHIN THE SITE MODEL	70
FIGURE 3-39 CROSS SECTIONS AND LAYER SLICES THROUGH THE REFERENCE CASE FACIES MODEL	72
FIGURE 3-40 HISTOGRAM OF POROSITY WITHIN SAND FACIES, VIKING A, ALL ZONES	73
FIGURE 3-41 CROSS PLOT OF POROSITY VERSUS PERMEABILITY, COLOURED BY ZONE	74
FIGURE 3-42 HISTOGRAM OF HORIZONTAL PERMEABILITY WITHIN SAND FACIES, VIKING A ALL ZONES	75
FIGURE 3-43 CROSS PLOT OF HORIZONTAL VERSUS VERTICAL CORE PERMEABILITY (LOG SCALE), COLOURED BY WELL	75
FIGURE 3-44 W-E CROSS SECTION THROUGH WELL 49/12-3A COMPARING STATIC MODEL (LEFT) TO DYNAMIC MODEL (RIGHT) LAYERING	77
FIGURE 3-45 CROSS PLOT OF POROSITY VERSUS PERMEABILITY FOR ALL VIKING FIELDS	80
FIGURE 3-46 LAYER SLICES THROUGH FAIRWAY PROPERTY MODELS NTG, POROSITY.....	80
FIGURE 3-47 PROBABILISTIC VOLUMETRIC RESULTS	84
FIGURE 3-48 ADOPTED CO ₂ RESOURCE CLASSIFICATION	85

FIGURE 3-49 EFFECT OF IMPURITIES ON THE PHASE ENVELOPE	87
FIGURE 3-50 PRESSURE – TEMPERATURE PROFILES FOR LIQUID AND DENSE PHASE OPERATION.....	93
FIGURE 3-51 PRESSURE AND TEMPERATURE VS DEPTH FOR CASE 20	94
FIGURE 3-52 PERFORMANCE ENVELOPE FOR 7" TUBING - SUPERCRITICAL INJECTION	98
FIGURE 3-53 PERFORMANCE ENVELOPE FOR 7" TUBING - LIQUID PHASE INJECTION	99
FIGURE 3-54 LEMAN SANDSTONE UCS CUMULATIVE DISTRIBUTIONS	102
FIGURE 3-55 CRITICAL DRAWDOWN PRESSURE FOR VIKING A	102
FIGURE 3-56 MAXIMUM APPLIED PRESSURE	105
FIGURE 3-57 GAS PHASE INJECTION OPTION	109
FIGURE 3-58 LIQUID PHASE INJECTION OPTION	110
FIGURE 3-59 EXTENT OF VIKING GAS FIELD, SHOWING SEPARATE GAS ACCUMULATIONS AND MAIN PLATFORM LOCATIONS.....	111
FIGURE 3-60 VIKING GAS COMPOSITION PRESSURE-TEMPERATURE PLOT.....	114
FIGURE 3-61 VIKING A PRESSURE GRADIENT INCREASE DURING CO ₂ INJECTION.....	115
FIGURE 3-62 LOCATION WHERE PRESSURE LIMIT IS FIRST VIOLATED IN REFERENCE CASE MODEL.....	116
FIGURE 3-63 FAULT COMPARTMENTS WITHIN THE STORAGE SITE MODEL.....	116
FIGURE 3-64 GAS MATERIAL BALANCE ANALYSIS	118
FIGURE 3-65 CO ₂ PHASE DIAGRAM WITH VIKING A PRE-INJECTION, RESERVOIR AND WELLBORE CONDITIONS	119
FIGURE 3-66 CROSS SECTION THROUGH INJECTOR 2 WELL PATH SHOWING CO ₂ CONCENTRATION PER ZONE AFTER ONE YEAR OF INJECTION	120
FIGURE 3-67 VIKING A INJECTION WELL LOCATIONS AT TOP RESERVOIR DEPTH.....	120
FIGURE 3-68 TOTAL CO ₂ CONCENTRATION AT THE END OF INJECTION FOR THE 2 WELL AND 5 WELL CASES	121
FIGURE 3-69 SENSITIVITY ANALYSIS: COMPARISON OF CAPACITY PER CASE	123
FIGURE 3-70 SENSITIVITY ANALYSIS: COMPARISON OF DURATION OF INJECTION PER CASE.....	124
FIGURE 3-71 SUMMED CO ₂ CONCENTRATION AT YEAR 2058 AND 1000 YEARS AFTER INJECTION IS STOPPED.....	125
FIGURE 3-72 CO ₂ CONCENTRATION AT YEAR 2058, AT THE END OF INJECTION	126
FIGURE 3-73 CO ₂ CONCENTRATION 1000 YEARS AFTER THE END OF INJECTION.....	126
FIGURE 3-74 CO ₂ INJECTION WELL LOCATIONS.....	127
FIGURE 3-75 FIELD CO ₂ INJECTION FORECAST	128

FIGURE 3-76 REFERENCE CASE THP FORECASTS	128
FIGURE 3-77 ALLOCATION OF STORED CO ₂ TO THE VARIOUS TRAPPING MECHANISMS FOR THE PROPOSED VIKING A DEVELOPMENT	129
FIGURE 3-78 PROPOSED STORAGE COMPLEX BOUNDARY ON TOP LEMAN SST. DEPTH MAP	130
FIGURE 3-79 VIKING A - CROSS SECTION THROUGH THE OVERBURDEN MODEL.....	132
FIGURE 3-80 3D GEOMECHANICAL MODEL - VIKING A AND F AT TOP LEMAN SANDSTONE.....	134
FIGURE 3-81 CROSS SECTION THROUGH VIKING A GEOMECHANICAL MODEL	134
FIGURE 3-82 VIKING A BLOCK A WELLS	138
FIGURE 3-83 SCHEMATIC OF WELL 49/12-2 WITH POTENTIAL LEAK PATHS INDICATED	140
FIGURE 3-84 SCHEMATIC OF WELL 49/12-3 WITH POTENTIAL LEAK PATHS INDICATED	141
FIGURE 3-85 VIKING A RISK MATRIX OF LEAKAGE SCENARIOS	145
FIGURE 3-86 VIKING A COMPARISON OF 1D FORWARD MODELLING RESULTS FOR A) CASE 1 AND B) CASE 2	148
FIGURE 3-87 VIKING A COMPARISON OF 1D FORWARD MODELLING RESULTS FOR A) CASE 4 AND B) CASE 5	149
FIGURE 3-88 OUTLINE MONITORING PLAN FOR THE VIKING A STORAGE SITE	151
FIGURE 3-89 VIKING A STORAGE SITE - LEAKAGE SCENARIO MAPPING TO MMV TECHNOLOGY	152
FIGURE 3-90 OUTLINE CORRECTIVE MEASURES PLAN.....	154
FIGURE 5-1 CO ₂ SUPPLY PROFILE.....	158
FIGURE 5-2 PLATFORM DIRECTIONAL SPIDER PLOT	160
FIGURE 5-3 SLANT INJECTOR 1 DIRECTIONAL PROFILE	160
FIGURE 5-4 PIPELINE ROUTE	164
FIGURE 5-5 PIPELINE ROUTE AVOIDING DOGGER BANK WINDFARM.....	164
FIGURE 5-6 PIPELINE PRESSURE DROPS	166
FIGURE 5-7 VIKING A DEVELOPMENT PROCESS FLOW DIAGRAM.....	169
FIGURE 5-8 OPTIONS FOR EXPANDING THE DEVELOPMENT	174
FIGURE 6-1 SUMMARY LEVEL PROJECT SCHEDULE.....	180
FIGURE 6-2 PHASING OF CAPITAL SPEND.....	182
FIGURE 6-3 ELEMENTS OF COST OVER PROJECT LIFETIME.....	183
FIGURE 6-4 BREAKDOWN OF LEVELISED COSTS	188

FIGURE 6-5 BREAKDOWN OF LIFE-CYCLE COST 188

Tables

TABLE 1-1 - PROJECT COST ESTIMATE (PV10, 2015)	17
TABLE 3-1 WELLS SCREENED FOR PETROPHYSICAL EVALUATION	24
TABLE 3-2 INTERPRETED HORIZONS	32
TABLE 3-3 PETROPHYSICAL SUMMARY FOR INJECTION ZONES A, C & E	61
TABLE 3-4 STRATIGRAPHY, ZONATION AND LAYERING FOR THE PRIMARY STATIC MODEL	65
TABLE 3-5 VCLAY CUT-OFFS USED TO HELP DEFINE FACIES LOG	67
TABLE 3-6 WELLS IN VIKING A, F AND FS USED FOR FACIES AND POROSITY MODELLING	68
TABLE 3-7 INPUT PROPERTIES AND FINAL MODELLED PROPORTIONS FOR FACIES MODELLING	71
TABLE 3-8 INPUT SETTING FOR POROSITY AND PERMEABILITY SGS MODELLING	73
TABLE 3-9 AVERAGE SAND POROSITY PER ZONE WITHIN VIKING A	74
TABLE 3-10 AVERAGE HORIZONTAL SAND PERMEABILITY WITHIN VIKING A	75
TABLE 3-11 AVERAGE MODELLED VERTICAL PERMEABILITY VALUES AND Kv/Kh FOR EACH FACIES WITHIN VIKING A	76
TABLE 3-12 GROSS ROCK, PORE VOLUMES AND GIIP FOR NORTH VIKING SITE MODEL	76
TABLE 3-13 SUMMARY OF STATIC AND DYNAMIC MODEL LAYER NUMBERS	77
TABLE 3-14 STRATIGRAPHY, ZONATION AND LAYERING FOR THE FAIRWAY MODEL	78
TABLE 3-15 WELLS USED IN FAIRWAY MODEL	79
TABLE 3-16 INPUT SETTING FOR NTG AND POROSITY SGS MODELLING	79
TABLE 3-17 PVT DEFINITIONS	86
TABLE 3-18 VIKING A FIELD AND WELL DATA	90
TABLE 3-19 VIKING A RESERVOIR DATA	90
TABLE 3-20 VIKING IPR DEFINITIONS	90
TABLE 3-21 INJECTION PRESSURE AND TEMPERATURE LIMITS - SUPERCRITICAL INJECTION	91
TABLE 3-22 RATES ACHIEVABLE BY CASE - SUPERCRITICAL INJECTION	92
TABLE 3-23 INJECTION PRESSURE AND TEMPERATURE LIMITS - LIQUID PHASE INJECTION	95
TABLE 3-24 RATES ACHIEVABLE BY CASE - LIQUID PHASE INJECTION	96
TABLE 3-25 TUBING HEAD INJECTION TEMPERATURE SENSITIVITIES AND RESULTS	97

TABLE 3-26 DIMENSIONS AND PROPERTIES FOR THE DYNAMIC MODEL	112
TABLE 3-27 VIKING GAS COMPOSITION	113
TABLE 3-28 KEY INPUT PARAMETERS TO THE REFERENCE CASE DYNAMIC MODEL	122
TABLE 3-29 SUBSURFACE UNCERTAINTY PARAMETERS AND ASSOCIATED RANGE OF VALUES	123
TABLE 3-30 SUMMARY OF HORIZONS IN THE OVERBURDEN MODEL	132
TABLE 3-31 GUIDELINES FOR THE SUSPENSION AND ABANDONMENT OF WELLS	136
TABLE 3-32 VIKING RISK REVIEW	137
TABLE 3-33 VIKING LEGACY WELLS	139
TABLE 3-34 VIKING LEAKAGE SCENARIOS	144
TABLE 3-35 FLUID SUBSTITUTION CASES	146
TABLE 3-36 EXAMPLES OF IRREGULARITIES AND POSSIBLE IMPLICATIONS	153
TABLE 5-1 VIKING A WELL LOCATIONS.....	159
TABLE 5-2 SUMMARY WELL ACTIVITY SCHEDULE	161
TABLE 5-3 OUTLINE WELL CONSTRUCTION PROGRAMME -SLANT INJECTOR 1	162
TABLE 5-4 INJECTION PROFILE.....	162
TABLE 5-5 PLATFORM LOCATION	163
TABLE 5-6 PIPELINE CROSSINGS (BARMSTON TO VIKING).....	164
TABLE 5-7 MASTER EQUIPMENT LIST	168
TABLE 5-8 CO ₂ HEATERS	171
TABLE 5-9 OPTIONS FOR EXPANSION	174
TABLE 6-1 VIKING A DEVELOPMENT COST ESTIMATE SUMMARY.....	181
TABLE 6-2 PROJECT COST ESTIMATE BY COMPONENT	182
TABLE 6-3 VIKING A DEVELOPMENT TRANSPORT CAPEX (BASE CASE)	183
TABLE 6-4 VIKING A DEVELOPMENT FACILITIES CAPEX	184
TABLE 6-5 VIKING A DEVELOPMENT WELLS CAPEX.....	184
TABLE 6-6 VIKING A DEVELOPMENT OTHER CAPEX	185
TABLE 6-7 VIKING A DEVELOPMENT WELLS OPEX.....	185

TABLE 6-8 VIKING A DEVELOPMENT OTHER OPEX	185
TABLE 6-9 COST OF POWER SENSITIVITY ANALYSIS	186
TABLE 6-10 VIKING A DEVELOPMENT FACILITIES ABEX.....	186
TABLE 6-11 VIKING A DEVELOPMENT OTHER ABEX.....	186
TABLE 6-12 VIKING A DEVELOPMENT COST IN REAL AND NOMINAL TERMS	187
TABLE 6-13 VIKING A TOTAL TRANSPORT AND STORAGE COSTS	187
TABLE 6-14 VIKING A TRANSPORT AND STORAGE COSTS PER TONNE OF CO ₂	187
TABLE 6-15 UNIT COSTS IN DETAIL.....	189

1.0 Executive Summary

Storage of CO₂ in the Permian Leman Sandstone in the faulted horst block known as Viking A (UKCS block 49/12) in the Southern North Sea.

Three well development of Viking A from a new unmanned platform supplied with CO₂ from Barmston via a 20" 185 km pipeline.

Final investment decision in 2027 and first injection in 2031. The site stores 130Mt of CO₂, 5Mt/y for 26 years. Capital investment of £150 million (PV₁₀, 2015), equating to £1.2 for each tonne stored.

Capacity uncertainty is low, but can be reduced further through access to operator data (well rates and pressures)

Heating is required to achieve the target injection rate in the initial very low reservoir pressure conditions.

This Energy Technologies Institute (ETI) Strategic UK CCS Storage Appraisal project has been commissioned on behalf of the Department of Energy and Climate Change. The project brings together existing storage appraisal initiatives, accelerates the development of strategically important storage capacity and leverages further investment in building this capacity to meet UK needs.

The primary objective of the overall project is to down-select and materially progress the appraisal of five potential CO₂ storage sites on their path towards final investment decision (FID) readiness from an initial site inventory of over 500. The desired outcome is the delivery of a mature set of high quality CO₂ storage options for the developers of major power and industrial CCS project developers to access in the future. The work will add significantly to the de-risking of these stores and be transferable to storage developers to complete the more capital intensive parts of storage development.

The Viking Fields were selected as one of five target storage sites during a portfolio selection process. The full rationale behind the screening and selection is fully documented in the following reports:

- D04: Initial Screening & Down-Select (Pale Blue Dot Energy; Axis Well Technology, 2015)
- D05: Due Diligence and Portfolio Selection (Pale Blue Dot Energy; Axis Well Technology, 2015)

The Viking gas field area is a series of horst block structures located in the Southern North Sea, block 49/12, approximately 90 km off the Norfolk coast and 185 km from Barmston on Humberside. Viking A has been selected as the starting point for a CO₂ storage development in the area because it is the largest of these structures as illustrated in Figure 1-1. The gas reservoir and primary storage unit is within the Lemn Sandstone Formation of the Permian Rotliegend Group. These sandstones extend over most of the Southern North Sea (SNS).

The Lemn Sandstone Formation is comprised of moderate quality aeolian and fluvial sandstones with average porosity from logs between 13 – 16% and average permeability from core of 83mD. The depth to the crest of the structure is 2500m (8200 ft) tvdss. Total thickness of the Lemn Sandstone at the Viking A Site is approximately 137m (450 ft) but the original gas column height is a minimum of 426m (1400ft).

The caprock is provided by laterally extensive halites of the overlying Zechstein Group which are a proven seal for multiple hydrocarbon fields in the SNS and provides an excellent caprock for the storage complex.

The geophysical interpretation was based on the PGS Southern North Sea MegaSurvey. Synthetic seismograms were generated from well logs to link the formations identified in the wells to the main reflection events in the seismic volume. Faults and seismic horizons were picked using Schlumberger's proprietary PETREL software and the results gridded and converted to depth to build a Static Model of the fairway, the storage site and the overburden. Depth conversion and migration are considered to be the most significant geophysical uncertainties. This is due to the high variation in seismic velocity and steep dips in the overburden.

A seismic interpretation was carried out on the 1991 - 1996 3D seismic survey for which only the basic post-stack processing was available. The seismic survey is adequate structural interpretation at this stage of the development. A detailed geological model based on this and the petrophysical evaluation of 21 regional wells was built. The static model was upscaled and used in the dynamic compositional simulation model to generate the development plan.

The ultimate impact of these uncertainties on capacity is limited because this is a depleted gas field with a pore volume and connectivity well understood from the gas production history. Production from the A fault block ceased in 1991.

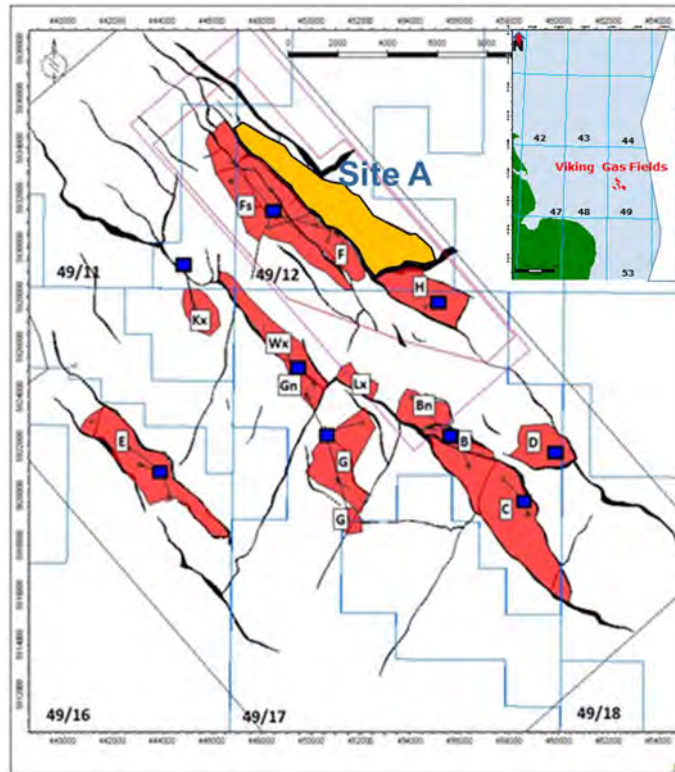


Figure 1-1 Viking A and Viking Gas Fields Location Map

The basis for the development plan is an assumed CO₂ supply of 5Mt/y to be provided from the shore terminal at the Barmston commencing in 2031. To maximise the economic benefit CO₂ will be transported offshore in liquid-phase via a new 185km 20” pipeline from Barmston to a newly installed Normally Unmanned Installation (NUI), minimum facilities platform on a 4-legged steel jacket standing in 28m (92 ft) of water. During the operational period two active wells are required to inject the supply profile.

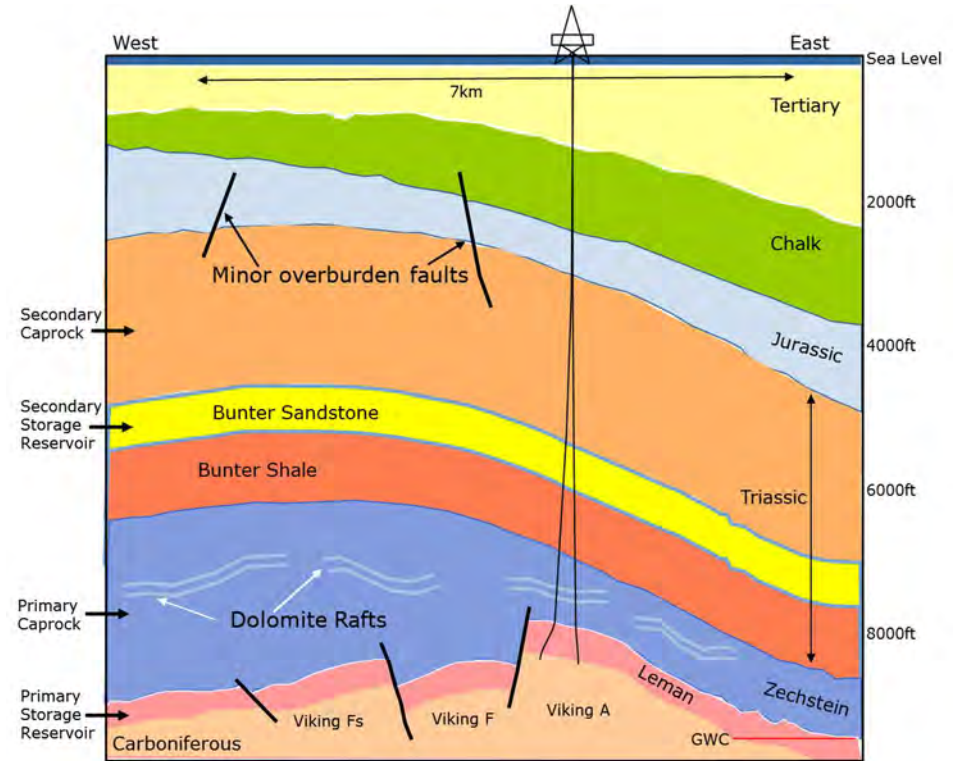


Figure 1-2 Viking A - Cross section Illustrating storage reservoirs and seals

The Viking A storage reservoir is a depleted gas field and has a very low reservoir pressure but relatively high temperature. Consequently, CO₂ will initially have to be injected in supercritical-phase until the reservoir pressure has increased sufficiently to support liquid-phase injection. Heating of the CO₂ will be required during the initial period to manage low temperature risks and ensure single phase conditions in the wells.

Geological and reservoir engineering work has concluded that the Viking A reservoir is very well connected hydraulically and storage capacity is relatively insensitive to well placement. Injection wells will be placed in the vicinity of the existing gas production wells, to minimise the geological risk. Injectivity is expected to be good and it is planned to inject CO₂ across the entire Leman Sandstone interval at the target injection rate of 5Mt/y.

During the operational periods, two of the wells are expected to be injecting at any point in time with the third as backup in the event of an unforeseen well problem. In this manner, the facilities will maintain a robust injection capacity and inject 5Mt/y of CO₂ for the 26-year project life whilst staying well within the safe operating envelope. Over the period a total of 130Mt CO₂ will have been stored.

No further appraisal drilling is considered necessary, although further desk based appraisal work can reduce uncertainty still further by gaining access to operator data such as well by well production and pressure data, abandonment records and the re-processed pre-stack depth migrated seismic data. This will help to further extend the confidence in the dynamic model.

The development schedule has five main phases of activity and is anticipated to require 6 years to complete, as illustrated in Figure 1-3. The schedule indicates that FEED, appraisal and contracting activities will commence 2-3 years prior to the final investment decision (FID) in 2027. The capital intensive activities of procurement and construction follow FID and take place over a 3-4 year period. First injection is forecast to be in mid-2031.

The development of the offshore transportation and injection infrastructure is estimated to require a capital investment of £150 million (in present value terms discounted at 10% to 2015), equating to £1.2/T. The life-cycle costs are

estimated to be £233M (PV₁₀), equating to a levelised cost of £23.4/T, as summarised in Table 1 1.

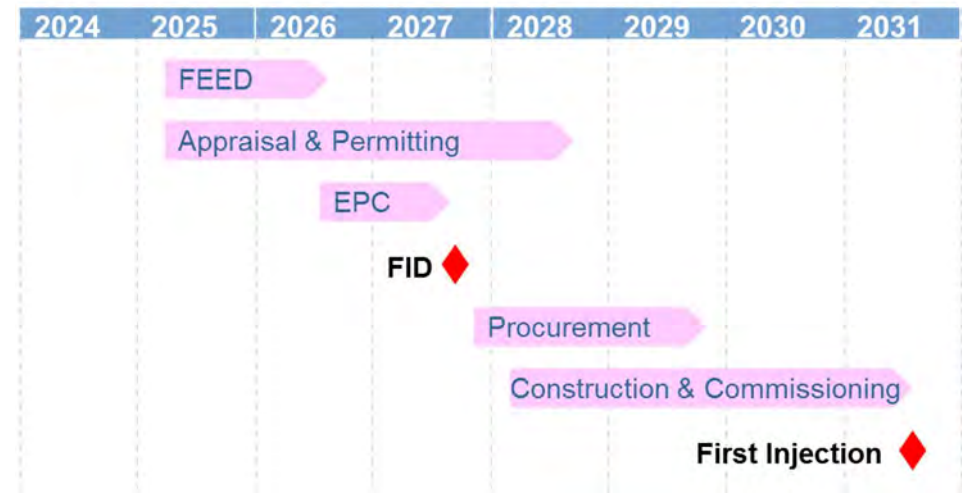


Figure 1-3 Summary Development Schedule

£million (PV ₁₀ , 2015)	Total
Transportation	74
Facilities	47
Wells	29
Opex	79
Decommissioning & MMV	4
Total	233

Table 1-1 - Project Cost Estimate (PV10, 2015)

Of the £23.4/T levelised cost, it is estimated that the heating required to manage the phase transition have contributed £3.3/T (14%). Whilst it is clearly more attractive to avoid such operations, they can be safely included within a storage development plan. It should also be noted that whilst the heavily depleted nature of the Viking reservoir creates some operational challenges, the project storage efficiency at 78% is almost four times greater than the best saline aquifer systems.

A series of recommendations for further work are provided towards the end of this report. The principal ones being:

- Further improve the confidence in the dynamic modelling by improving the pressure calibration of the model to well by well production and pressure data sourced from the gas field operator.
- Gain access to interpret the re-processed pre-stack depth migrated seismic data from the operator and build into the subsurface modelling ahead of any FID.
- Gain access to the Improve the characterisation of how the fracture pressure will evolve during the re-pressurisation of the reservoir.
- Commission further work to better understand the options for managing the CO₂ phase transition period of injection operations.
- Further work should consider how best to deliver the heating requirements and identify alternatives to the 10MW electrical heating options evaluated for this study.

2.0 Objectives

The Strategic UK CCS Storage Appraisal Project has five objectives, as illustrated in Figure 2-1.



Figure 2-1: The Five Project Objectives

Viking A is one of the five CO₂ storage targets evaluated as part of Work Pack 5 (WP5). The primary objective of this element of the project is to advance understanding of the nature, potential, costs and risks associated with developing the site, with the data currently available to the project and within

normal budget and schedule constraints. The output fits within the broader purpose of the project to “facilitate the future commercial development of UK CO₂ storage capacity”.

This report documents the current appraisal status of the site and recommends further appraisal and development options within the framework of a CO₂ storage development plan. An additional objective of this phase of the project is to provide a repository for the seismic and geological interpretations, subsurface and reservoir simulation models.

WP5 has seven principal components:

1. Data collection & maintenance.
2. Seismic interpretation and structural modelling.
3. Containment.
4. Well design and modelling.
5. Site performance modelling.
6. Development planning.
7. Documentation and library.

These components and their contribution to the storage development plan are illustrated in Figure 2-2.

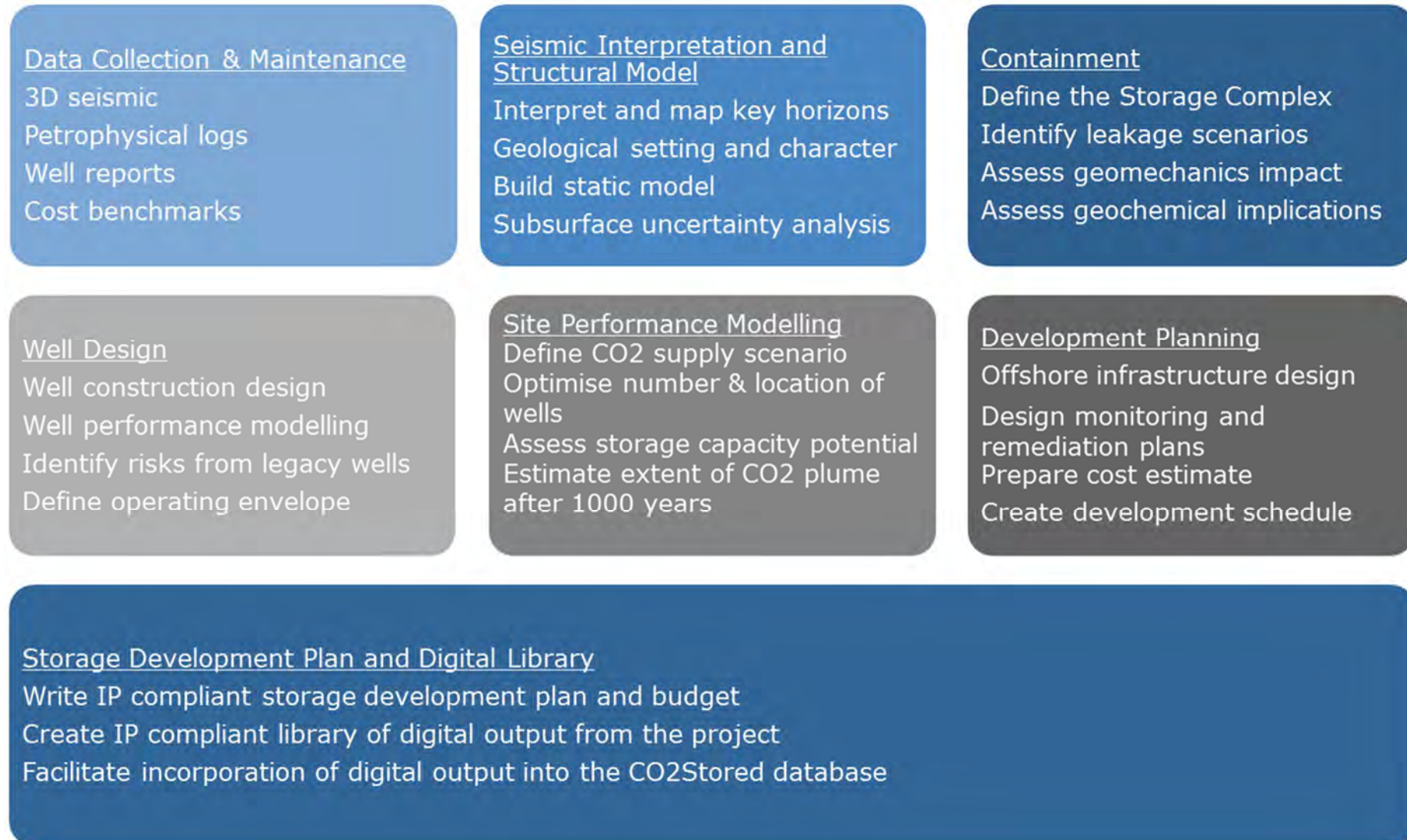


Figure 2-2: Seven Components of Workpack 5

3.0 Site Characterisation

3.1 Geological Setting

The Viking field area is located within Blocks 49/11a, 49/12a, 49/16 and 49/17 in the Southern North Sea, approximately 90km off the Norfolk coast and 140km off the Lincolnshire coast. Collectively, the Viking Fields are separate gas accumulations within a series of parallel elongated anticlinal fault blocks which trend NW-SE. The fields were discovered by well 49/12-2 in March 1969 and came on-stream in October 1972, (Riches, 2003).

The gas reservoir is the Lemna Sandstone Formation within the Early Permian Upper Rotliegendes Group. The location of the Viking Fields and the distribution of the Lemna Sandstone within the Southern North Sea are shown in Figure 3-1.

One of the fault components, Viking A was selected as the primary storage site. Production from the A fault block ceased in 1991.

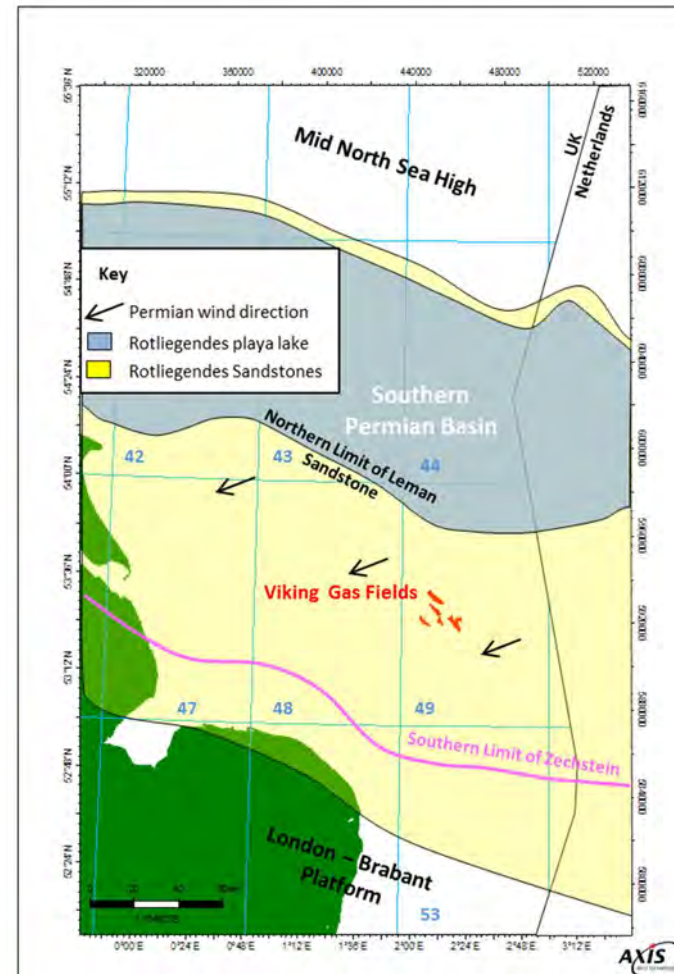


Figure 3-1 Location map and Lemna sandstone extent

3.2 Site History and Database

3.2.1 History

The Viking fields area lies on the north east edge of the Sole Pit Basin in the Southern North Sea. This was a locally active depositional centre within the southern Permian Basin. The Leman Sandstone in the Viking area lies unconformably above the partially eroded Carboniferous, and was deposited as a part of a major shifting sand dune system which passes northwards into playa lake silts and shales of the Silverpit Formation.

The Viking fields area is split into three, north, central and south. North Viking comprises Viking A, H, F and Fs reservoirs. Central Viking comprises Viking Bn, Lx, Wx and Yx reservoirs. The south Viking area is structurally more complex and includes the Viking B, C, D, E, G, Gn and KX accumulations.

The reservoirs of the north Viking fields lie close to the edge of a major dune belt, and are comprised of aeolian dune, fluvial and sabkha facies. The North Viking fields are within an elongated asymmetric anticline which has a NW-SE trending axis. Two trends of faulting can be seen within the Leman Sandstone. The major trend is NW-SE along which the A, F and Fs accumulations are aligned. These faults can be several kilometres long and form the boundaries and depositional trends for most of the Viking area fields. These originally normal faults are also prone to reactivation during periods of tectonic uplift and inversion. A second fault trend running NNE-SSW can also be identified on seismic. Although these typically show little throw (Section 3.4), these “De Keyser structures” are a recognised feature of the Southern North Sea geology and are often sealing to fluid flow. Many of the present day structural features are the result of inversion during the Late Cretaceous and mid Tertiary.

3.2.2 Hydrocarbon Exploration

The Rotliegend Sandstone, referred to as the Leman Sandstone Formation in the UK sector, is one of the most important gas reservoirs in NW Europe. Gas was sourced from the widespread underlying Carboniferous Westphalian coals and carbonaceous shales, and migration into the Rotliegend Group probably occurred during the Late Cretaceous to Early Tertiary. The top seal is formed by the overlying anhydrites and salts of the Permian Zechstein Group (Riches, 2003).

3.2.3 Seismic

The seismic data set used for the Viking A site and fairway interpretation was the PGS Southern North Sea MegaSurvey (PGS, 2015). These data were loaded to Schlumberger’s proprietary PETREL software where the seismic interpretation was undertaken. Figure 3-2 shows the extent of seismic available together with the area of the fairway interpretation and the Viking A CO₂ storage complex model. Seismic coverage over the fairway is complete although there is a data gap to the north east of the Viking A field which limits the extent of the interpretation in this direction. A 1999 3D seismic volume, a Schlumberger speculative survey, that covers this data gap was not available to this project.

The seismic volume is made up of several surveys that have been merged post stack (Figure 3-2). They were acquired between 1991 and 1996. Re-processed data sets are available in the area (Riches, 2003), however they were not available to this project. In the north west corner of the fairway there is a vertical step between two surveys resulting in a 40 to 50 ms offset of the reflectors (Figure 3-2). However, this area is away from the potential Viking storage sites.

Seismic data SEG-Y summary is provided in Appendix 3.

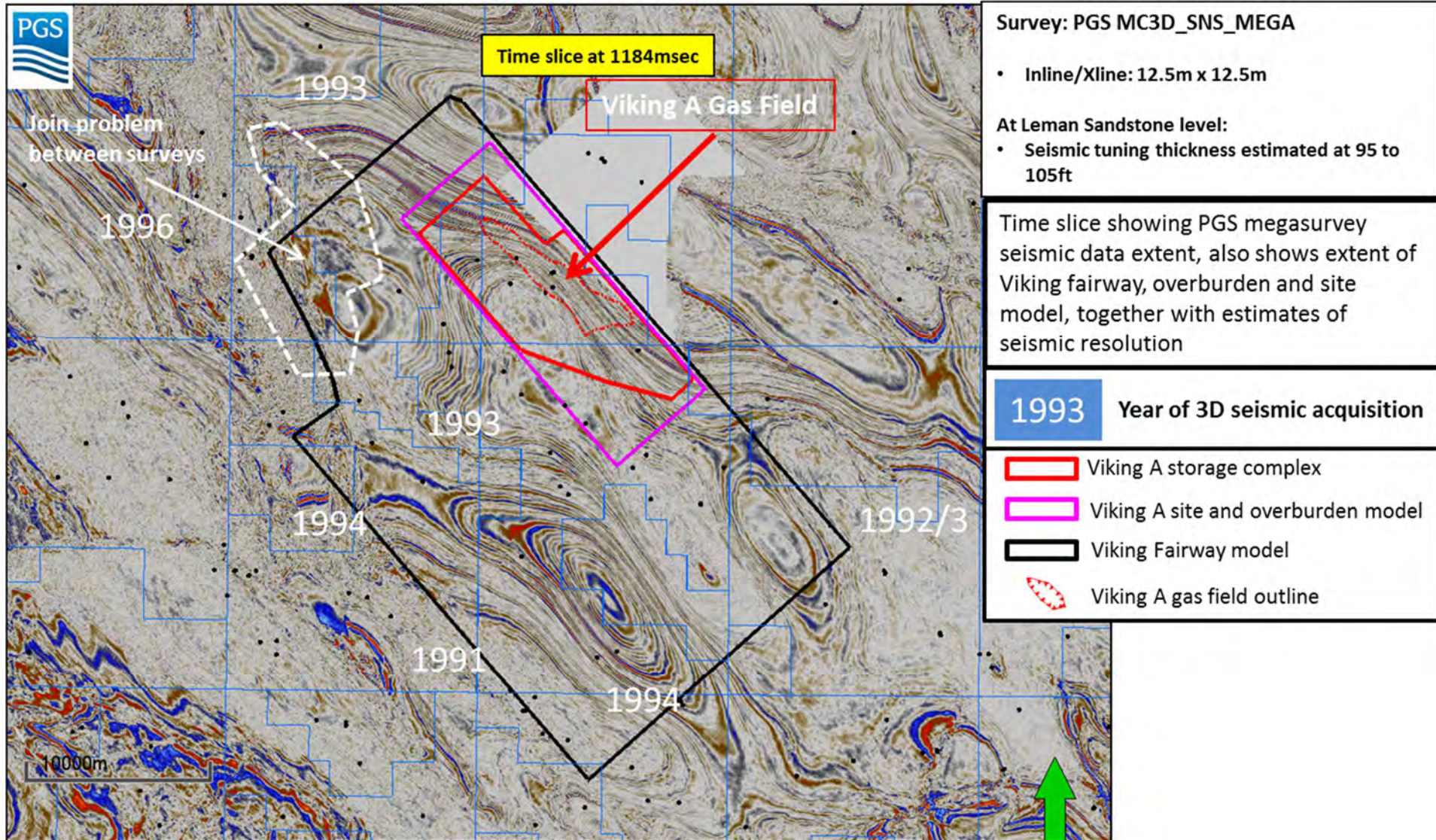


Figure 3-2 Seismic database showing the age of the surveys

3.2.4 Wells

All well log data were sourced from the publically available CDA database. These data are variable in range and quality, but generally included LIS or DLIS formatted digital data files, field reports, end of well reports, composite logs and core reports.

A total of 21 wells were screened for petrophysical evaluation (Table 3-1). 13 wells were selected that have suitable data for analysis over the area of interest, of these a sub-set of 4 have conventional core data with only one well having SCAL data (special core analysis).

The quality of data is generally very good, no major issues were identified and little manipulation was required to prepare the data for interpretation. Data were checked against the operator's composite logs to ensure consistency between the digital data and the operator's reports.

Figure 3-3 shows the wells used for the seismic interpretation. 17 wells have time depth information with 3 of those wells having sonic logs but no density logs.

Well	Wireline	MWD	Core	Mud Type
49/11a-6	✓		✓	OBM
49/12-1	No Data available		✓	
49/12-2	✓		✓	XC Poly
49/12-3	✓		✓	
49/12a-4	✓			XC Poly
49/12a-8	✓			
49/12a-9	✓		✓ + SCAL	OBM
49/12-A6	✓			
49/12-A10	✓			
49/12a-F1	✓			
49/12a-K2	✓			XC Poly
49/12a-K3	✓			XC Poly
49/12a-K4		✓		XC Poly
49/12a-K4Z		✓		XC Poly
49/16-3			✓	
49/17-1			✓	
49/17-2			✓	
49/17-4			✓	
49/17-5	No Data available			
49/17-6			✓	
49/17-7			✓	

Table 3-1 Wells screened for petrophysical evaluation

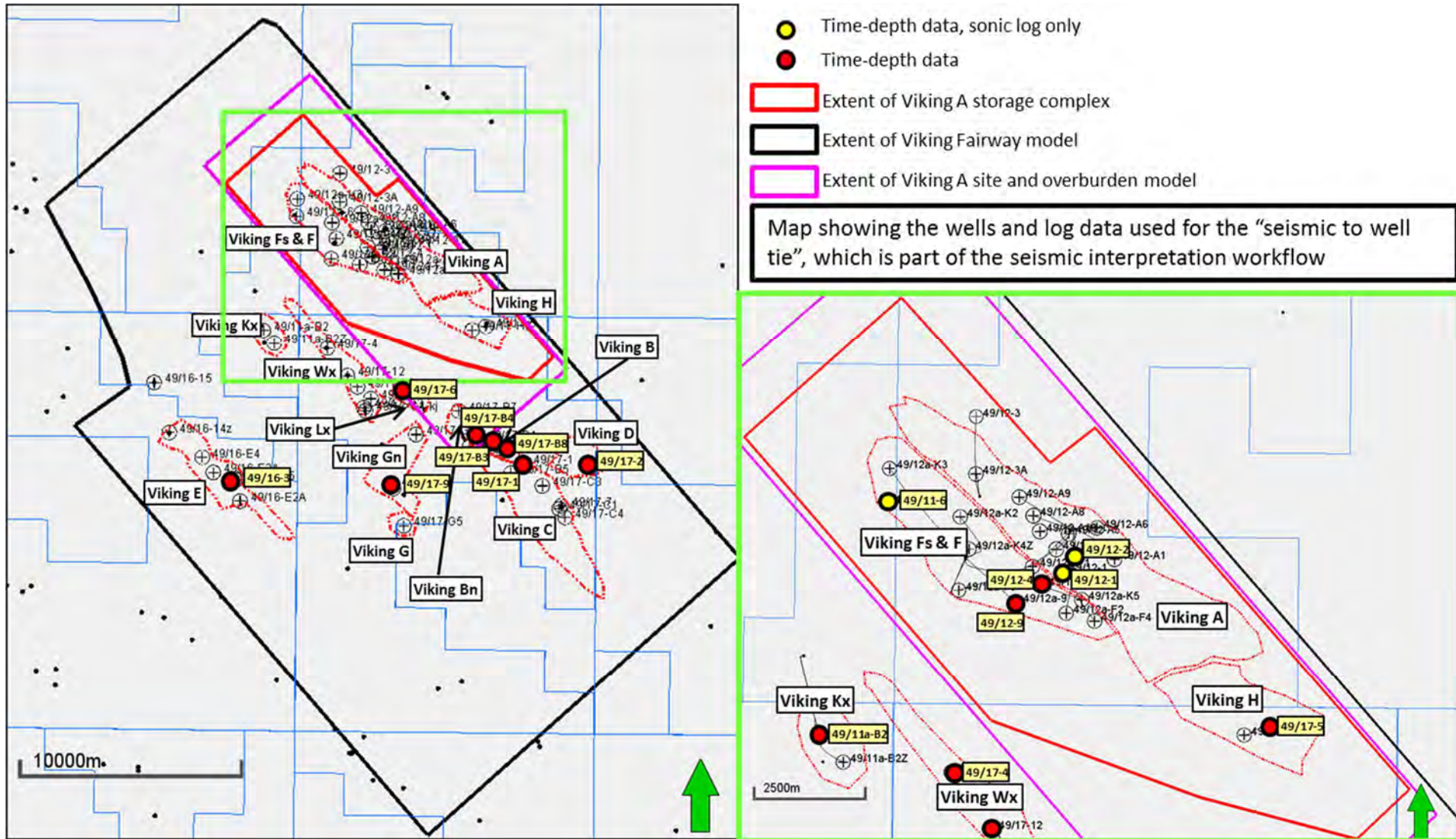


Figure 3-3 Geophysical wells and log database

3.3 Storage Stratigraphy

A stratigraphic column of the site area is shown in Figure 3-4.

Carboniferous

The majority of wells drilled in the north Viking area were drilled through to the Top Carboniferous. At the site location this is predominantly comprised of shales, clays and siltstone. Where sandstone inter-beds have been observed, these are described as being cemented and having poor visible porosity.

The Rotliegend Group lies unconformably on a large regional Carboniferous anticlinal structure. This extends NW-SE through blocks 49/16 and 49/1, exposing Westphalian A subcrop along its crest and successively younger Westphalian units on its flanks (Morgan, 1991).

Permian

The Viking field reservoirs are made up of continental deposits of the Rotliegend Group. These consist of aeolian and fluvial sandstones which are interbedded in the north of the area with silty shales deposited in a sabkha environment. These sandstones belong to the Lemna Sandstone Formation and pass laterally into the Silverpit Formation of playa lake silts and shales to the north. The thickness of Rotliegend Group varies regionally from 137 m (450 ft) at the site location to 213 m (700 ft) in the south Viking area. Thickening of the Rotliegend across the major faults suggests that faulting did exert some control on sedimentation during the Early Permian.

The Rotliegend Group is overlain by a thick sequence (365 m or 1,200 ft) of Permian Zechstein Group evaporites deposited in the hypersaline Zechstein Sea during the Late Permian. Werra, Stassfurt, Leine and Aller Formations

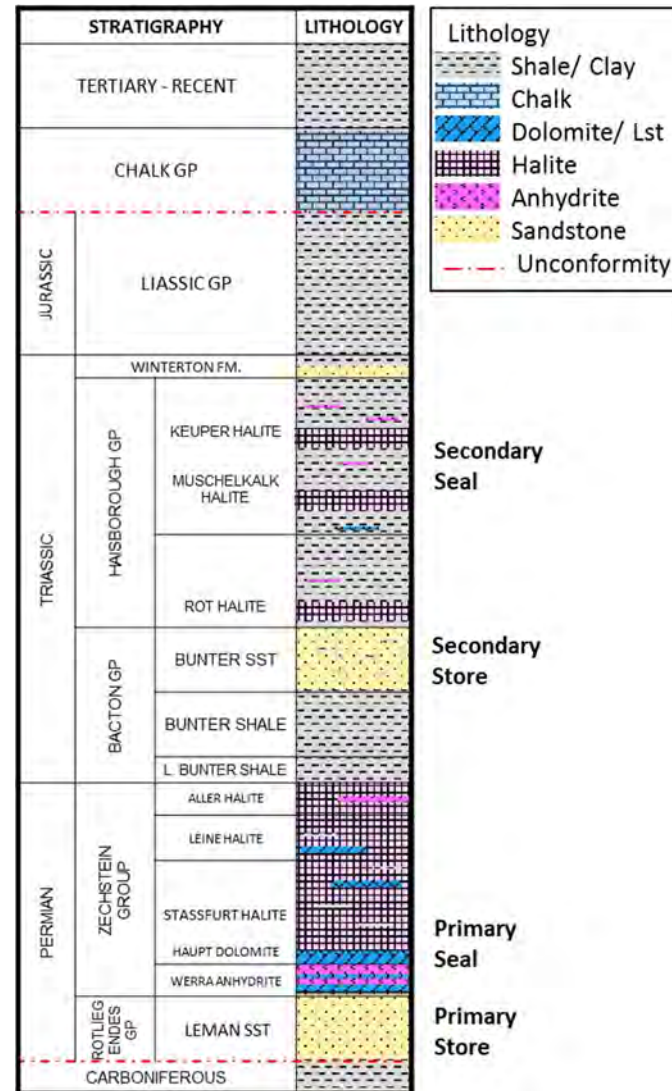


Figure 3-4 Stratigraphic column at the north Viking site, showing the overlying and underlying geological formations

which correspond to cycles Z1-Z4 are all represented. Most of the Zechstein sequence is dominated by halites with interbedded anhydrites and carbonates (Riches, 2003). Whilst dolomite sequences occur widely they are discontinuous and often rafted out. These evaporite sequences are the proven regional seal.

Triassic

The Zechstein Group sequence is overlain conformably by the Triassic. The continued contraction of the Zechstein Sea during the Early Triassic resulted in the SNS basin becoming the site of continental clastic sedimentation and the deposition of the Bacton Group. The Permian-Triassic boundary is associated with a distinct facies break where the Bunter shale overlies the Zechstein evaporites.

The thick clay and muds of the Bunter shale represent the maximum extent of an early Triassic playa lake. These were gradually replaced by deposition of the sands and silts of the Bunter Sandstone, prograding into the centre of the basin. The Bunter Sandstone thickness ranges from 0 – 350m (0 – 1150 ft) in the Southern North Sea being approximately 275m (900 ft) at the Viking A site.

The overlying Haisborough Group forms a thick and laterally extensive seal for the Bunter Sandstone.

It marks the re-establishment of marginal marine conditions and is comprised of a thick sequence of mudstones, claystones and evaporates commonly more than 500m (1640 ft) in thickness (Heinemann, Wilkinson, Pickup, Haszeldine, & Cutler, 2011), deposited as distal flood plain and shallow marine, alternating with coastal sabkha (Glennie, 1998).

Jurassic

Overlying the Triassic is approximately 305m (1000 ft) of massive calcareous mudstones of the Lower Jurassic Liassic Group, deposited in an open shallow marine environment as global sea levels rose.

The Upper Jurassic is absent in the area due to erosion.

Cretaceous

The Cromer Knoll is largely absent, although some isolated occurrences are observed in the NE of the area, with the Upper Cretaceous Chalk Group typically sitting directly on top of the Base Cretaceous Unconformity (BCU). The Chalk Group is widespread but variable in thickness, 250 – 600m (820-1970 ft) thick in the northern Viking area averaging approximately 300m (980 ft) over the site location.

Tertiary

Tertiary and Quaternary claystones and thin sandstones are present across the whole area and range in thickness from 400ft to over 2000ft in the north.

3.4 Seismic Characterisation

3.4.1 Database

Many 2D and 3D seismic surveys are available across the Viking fields area. Of these, the PGS Southern North Sea MegaSurvey (PGS, 2015) is the most comprehensive in terms of its areal coverage. The 3D seismic volume is made up of several different surveys that have been merged post stack (Figure 3-2) and were acquired between 1991 and 1996. Seismic coverage over the fairway is complete although there is a data gap to the north east of the Viking A field which limits the extent of the interpretation in this direction.

Data quality is good to excellent. However due to significant vertical and lateral velocity variations in the overburden there are lateral positioning errors inherent in the time migrated data. Seismic ray-path bending effects mean that raw seismic images do not correctly position dipping events. Normally these events are repositioned using ‘migration’ algorithms of various levels of sophistication and expense. The PGS MegaSurvey data was processed with a basic post-stack time migration whereas the published Viking field paper (Riches, 2003) reports that a more sophisticated post-stack depth migration produced lateral changes of up to 360m (1180 ft). The newer processing was not available for this project. It is likely that further reprocessing with modern pre-stack depth migration methods would produce further improvements in quality and more accurate positioning of steeply dipping events.

Wavelet extraction confirms the seismic volume to be SEG reverse polarity (North Sea normal) with a trough representing an increase in acoustic impedance and a peak representing a decrease in acoustic impedance. It also

shows the seismic volume is close to zero phase with a change in acoustic impedance (AI) being represented by either a peak or a trough.

To aid fault identification, a semblance volume was generated using the OpendTect open source software then exported and loaded into the Petrel project. A non-dip adapted semblance volume over the entire fairway was generated.

3.4.2 Horizon Identification

Whilst the seismic volume is recorded in terms of two-way travel time for a seismic wave to travel from the surface to the subsurface reflector and back again, well data are recorded in depth (ft or m). The well data are used to identify the seismic events within the 3D volume. Using checkshots, recorded in the well, a time vs depth relationship for the well is established. This time-depth relationship together with sonic and density logs are used to generate synthetic seismograms. The purpose of a synthetic seismogram is to forward model the seismic response of rock properties in the well bore to a seismic pulse at the well location, convolving the reflection coefficient log with the seismic pulse wavelet. This enables the interpreter to accurately match the position of certain seismic reflectors with respect to the known subsurface geology of an area.

Three synthetic well ties (49/11-6, 49/12-1, and 49/12-2, Figure 3-5) were produced using available sonic logs in each well.

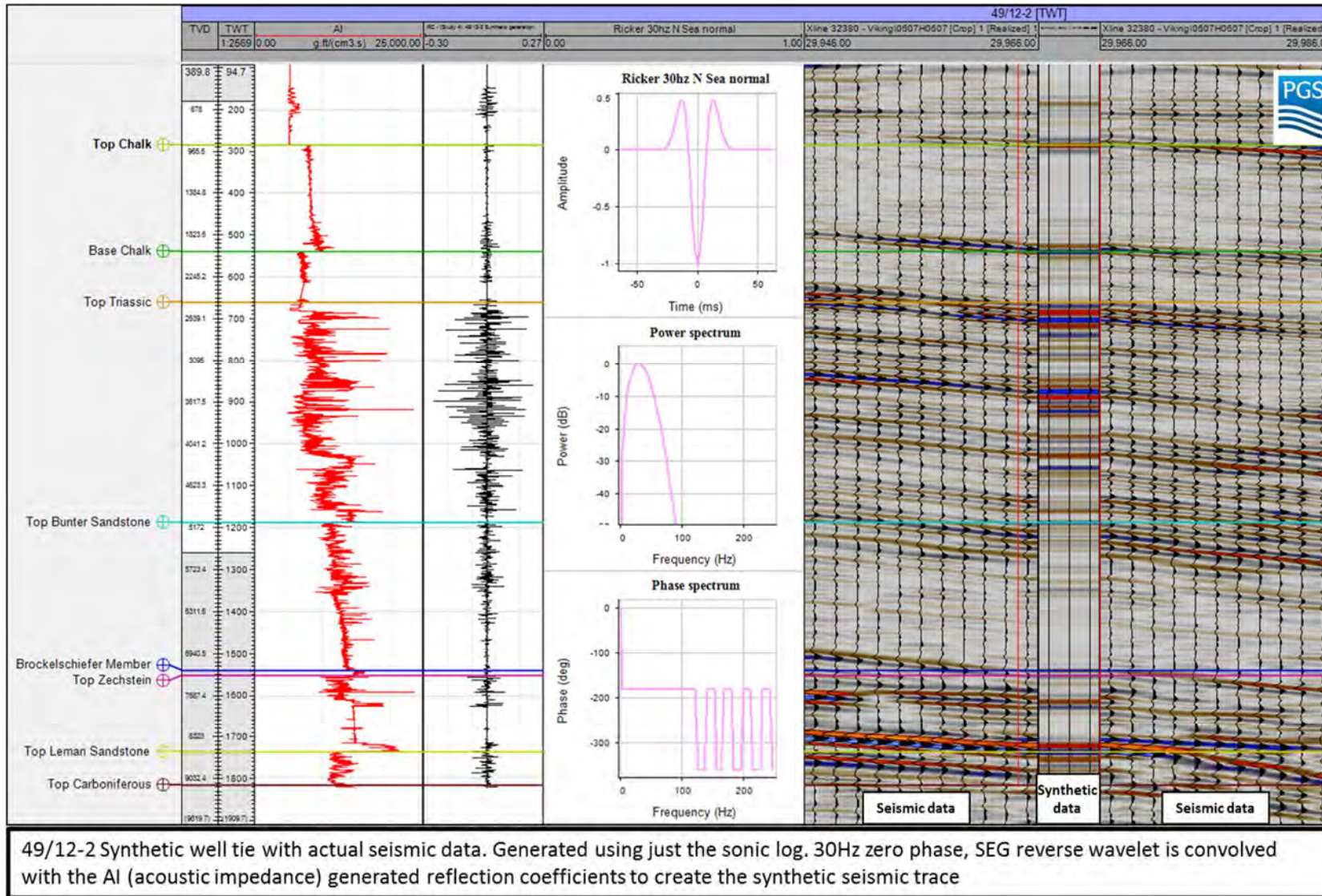


Figure 3-5 Synthetic seismogram

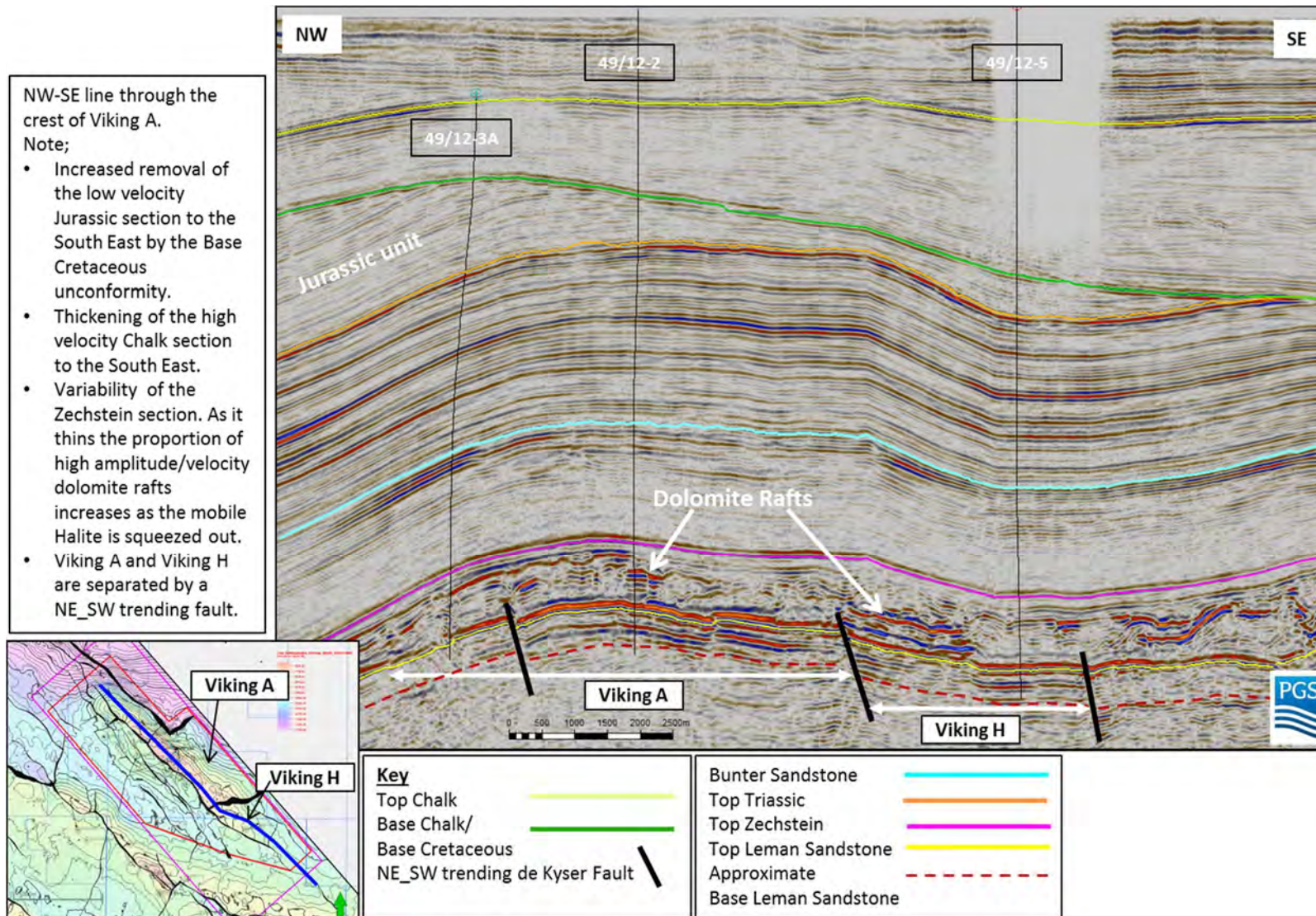


Figure 3-6 Viking A NW-SE seismic profile along the crest

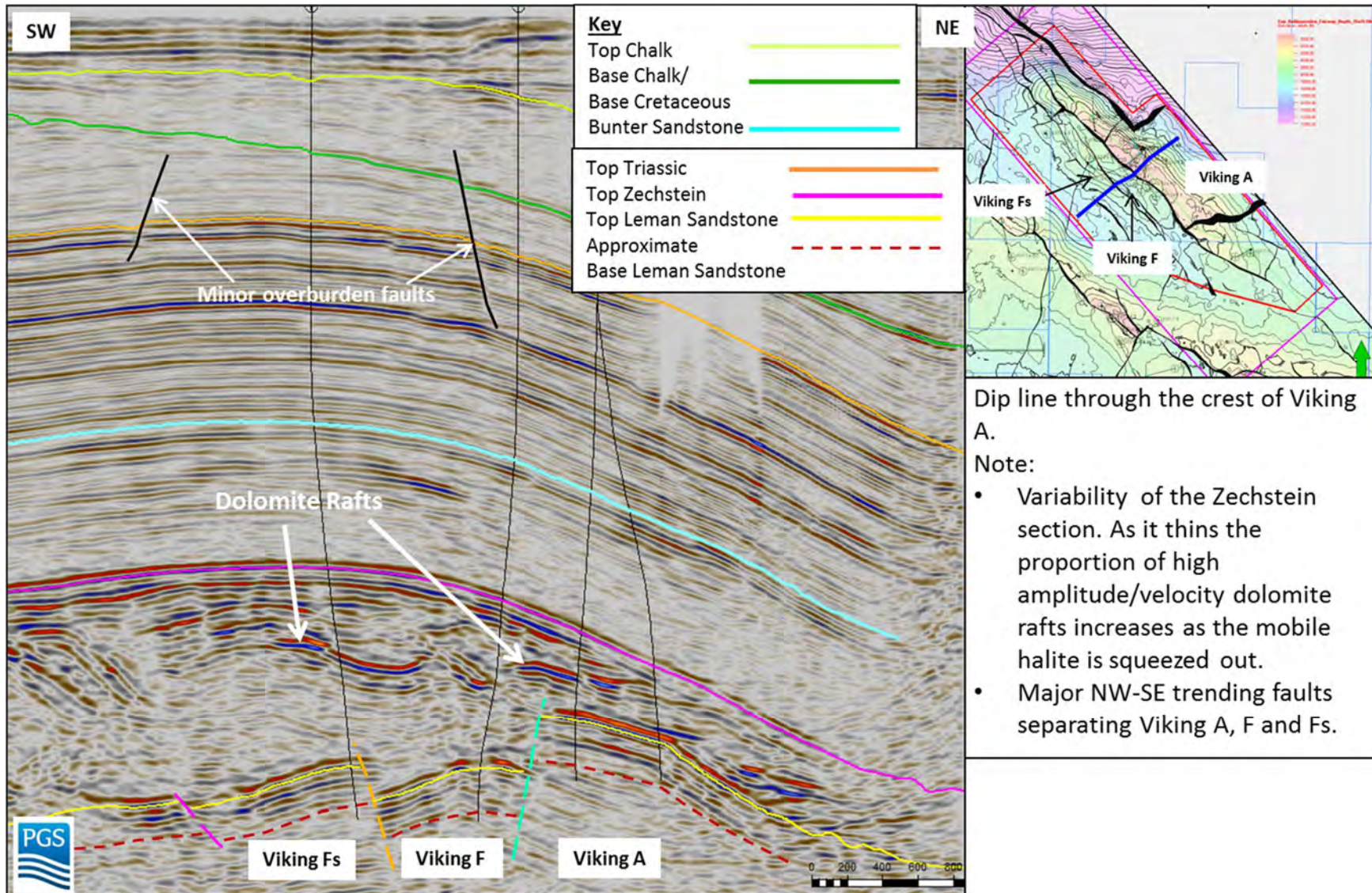


Figure 3-7 Viking A, F and Fs SW-NE Seismic profile

To generate the synthetic seismograms a theoretical Ricker wavelet was used with an appropriate frequency applied to each well (range 25-30Hz). The three wells containing sonic logs had no density logs and for these wells a constant density value was used in the synthetic generation. An example of a synthetic for well 49/12-2 is shown in Figure 3-5. The synthetic seismogram and actual seismic data display a very good match giving high confidence regarding correct horizon identification on the seismic data.

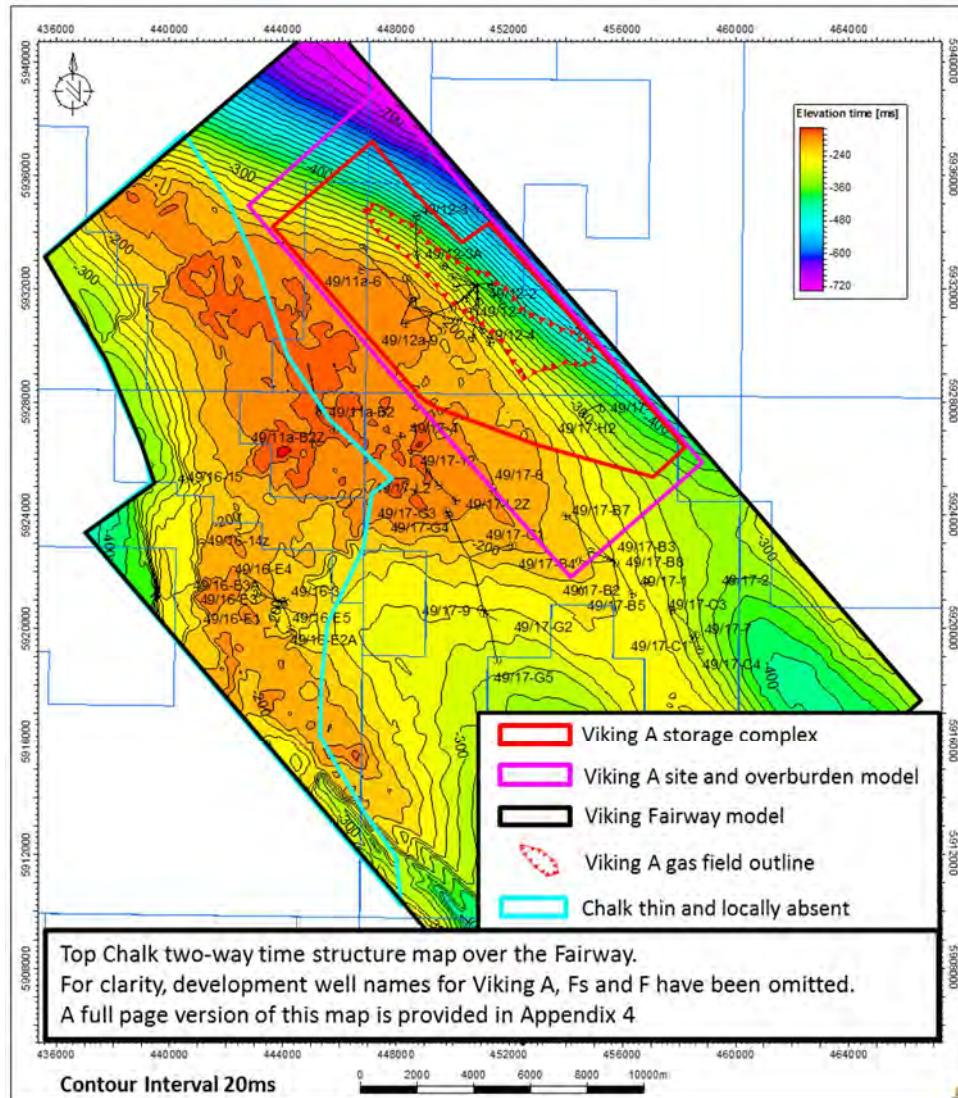
The identified horizons, their pick criteria and general pick quality are listed in Table 3-2 and illustrated on seismic lines in Figure 3-6 and Figure 3-7.

Horizon	Event Type	Display Response	Pick Quality
Top Chalk	Hard	Trough	Moderate to Very Good
Base Chalk/Base	Soft	Peak	Moderate to Very Good
Top Triassic	Soft	Peak	Very Good
Top Bunter	Soft	Peak	Moderate to Very Good
Top Zechstein	Soft	Peak	Very Good
Top Lemman Sandstone	Soft	Peak	Moderate to Very Good
Base Lemman Sandstone	-	Poor & variable	Very poor – not picked

Table 3-2 Interpreted horizons

3.4.3 Horizon Interpretation

A detailed seismic interpretation was carried out using a combination of seismic reflectivity and semblance volumes to provide input surfaces and faults to the Viking A site, fairway and overburden static models. In total six horizons from the seabed down to the Top Lemman Sandstone were interpreted across the 3D seismic data set (see Table 3-2, Figure 3-6 and Figure 3-7). The seismic quality is such that all events were picked on a seed grid and then autotracked. A polygon has been used to define the area of each surface (Figure 3-2 black polygon). The interpreted horizon values were then gridded at 25x25m grid increment and the resultant time maps are shown in Figure 3-8 to Figure 3-13. The interpreted seismic horizons are described below;



Top Chalk – The Top Chalk reflector is a high-amplitude trough, representing an increase in acoustic impedance at the top of the high velocity Chalk unit. It is a clear pick over the Viking A storage complex but becomes less distinct in the central and western parts of the fairway where the chalk unit rises towards the seabed and thins (several wells show it to be locally absent). This area of increased pick uncertainty is highlighted by the light blue polygon in Figure 3-8 and here the pick becomes more difficult to distinguish from the high amplitude seabed reverberations and the Base Chalk reflection. The Top Chalk horizon has been manually picked at a seed increment inline/crossline spacing of 64 enabling the event to be accurately autotracked with a high level of confidence (Figure 3-8). Minor editing and smoothing was required to correct cycle skips within the blue polygon area.

Base Chalk / Base Cretaceous Unconformity – In this part of the Southern North Sea the prominent regional Base Cretaceous unconformity coincides with the Base Chalk. The seismic response is a high-amplitude peak representing a decrease in acoustic impedance at the base of the high velocity Chalk interval. The event is continuous regionally across the entire fairway. However, like the Top Chalk, it becomes less distinct as the Chalk unit rises towards the seabed and thins. The Base Chalk horizon has been manually picked at a seed increment inline/crossline spacing of 64 enabling the event to be accurately autotracked with a high level of confidence (Figure 3-9). Across most of the fairway it is underlain by Jurassic sediments. However, to the south east the unconformity has eroded down into the upper part of the Triassic (Figure 3-6 and Figure 3-9).

Figure 3-8 Top Chalk two-way time map

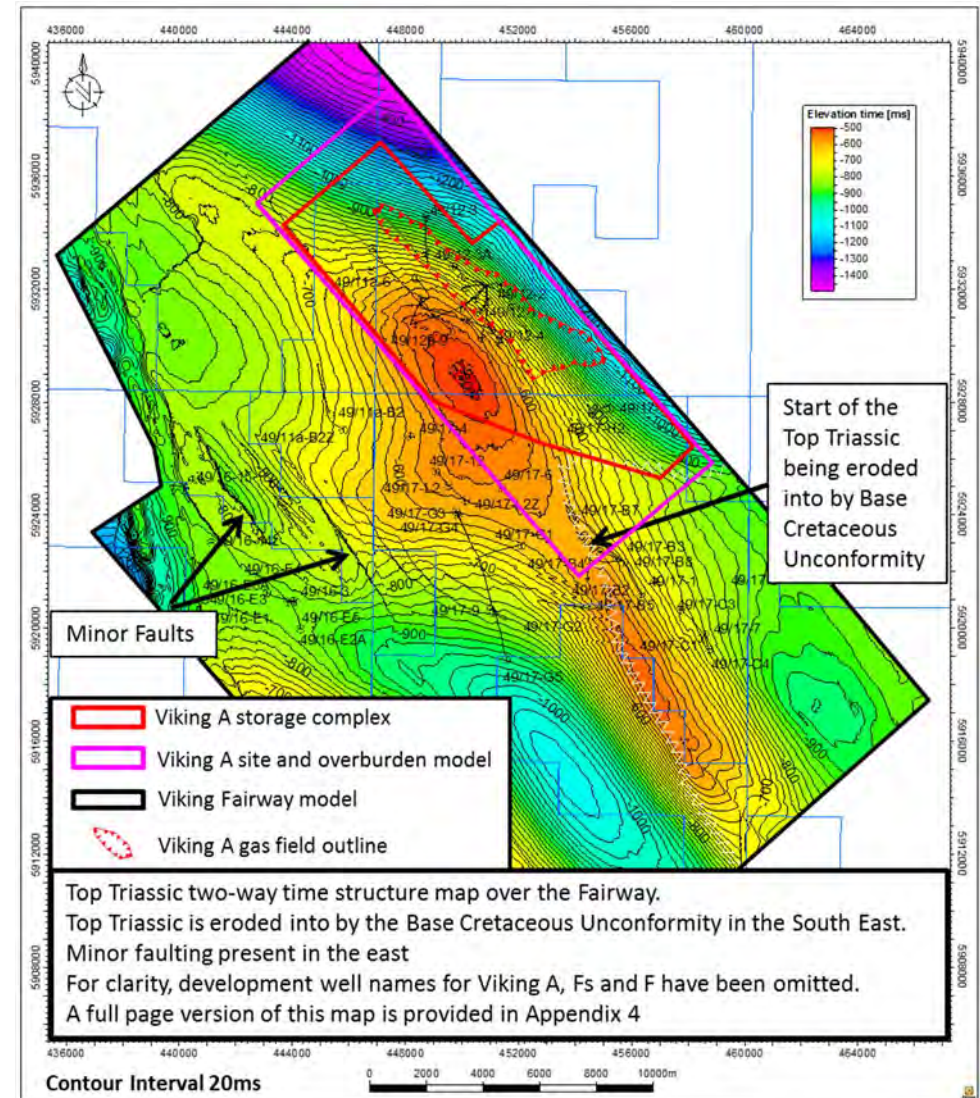
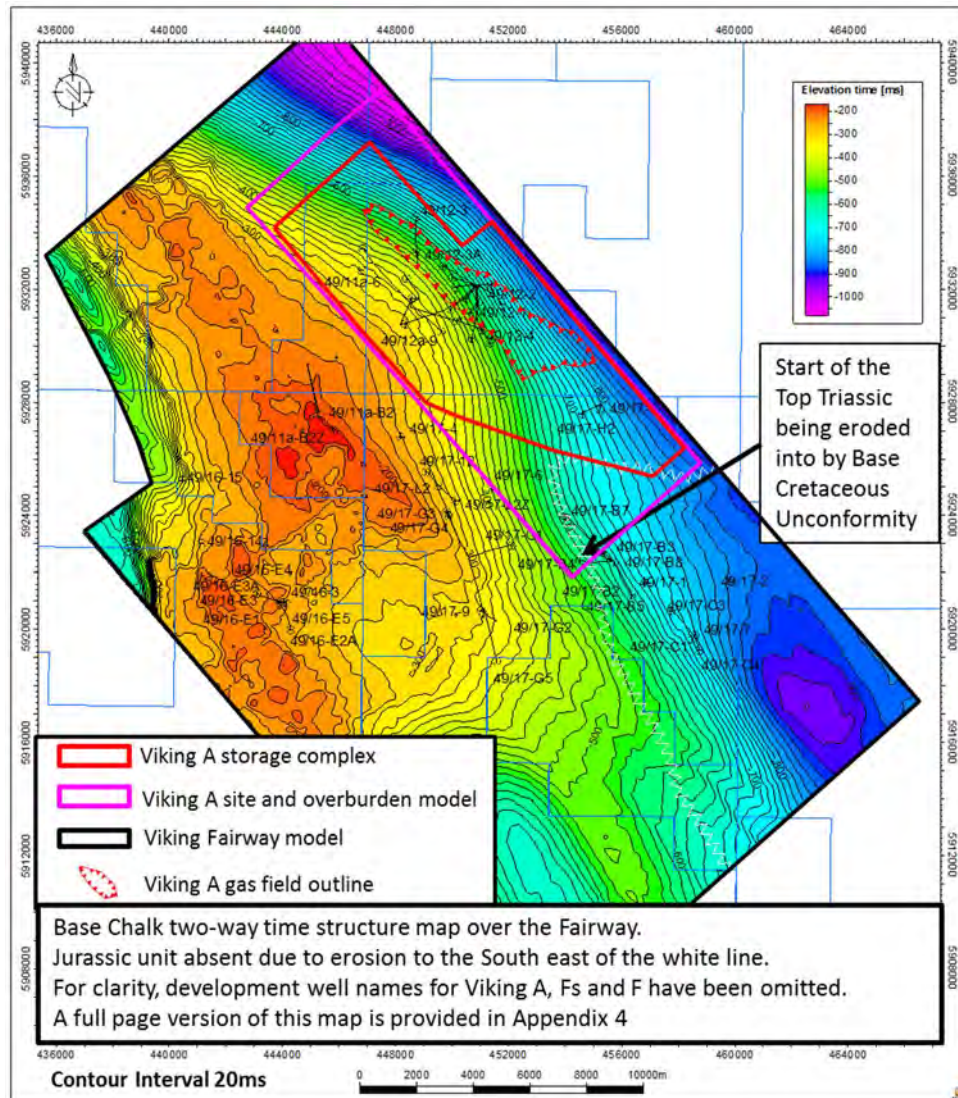


Figure 3-9 Base Chalk/Base Cretaceous unconformity two-way time map

Figure 3-10 Top Triassic two-way time map

Top Triassic – The Top Triassic is a distinct, medium amplitude peak representing a decrease in acoustic impedance caused by a 60ft thick low velocity shale at the top of the Winterton Formation. The event is absent in the south east corner of the fairway due to truncation by the overlying Base Cretaceous unconformity. For depth conversion purposes, at the truncation point, the Top Triassic and Base Chalk surfaces have been merged to form one continuous surface.

The Top Triassic horizon has been manually picked at a seed increment inline/crossline spacing of 64 enabling the event to be accurately autotracked with a high level of confidence (Figure 3-10). Minor faulting can be seen to the south west of the Viking A storage complex (Figure 3-10).

Top Bunter Sandstone – The seismic response of the event is predominately a moderate amplitude peak representing a decrease in acoustic impedance at the base of the Rot Halite. The event is continuous across the fairway and varies laterally in amplitude. The presence of halite cements is well documented within the Bunter Sandstone. Where it is present at the top of the unit the seismic response changes to a moderate trough due to the increase in acoustic impedance caused by the high velocity halite presence. In order to reduce uncertainty of exactly where this reflector changes character, the Top Bunter Sandstone seismic pick has been consistently interpreted as a black peak in this study over the whole fairway.

The Top Bunter Sandstone horizon has been manually picked at a seed increment inline/crossline spacing of 64 enabling the event to be autotracked with a medium level of confidence (Figure 3-11). Confidence in the horizon is high over Viking A storage complex and the middle part of the fairway. However, in the western part of the fairway confidence in the horizon is lower due to the

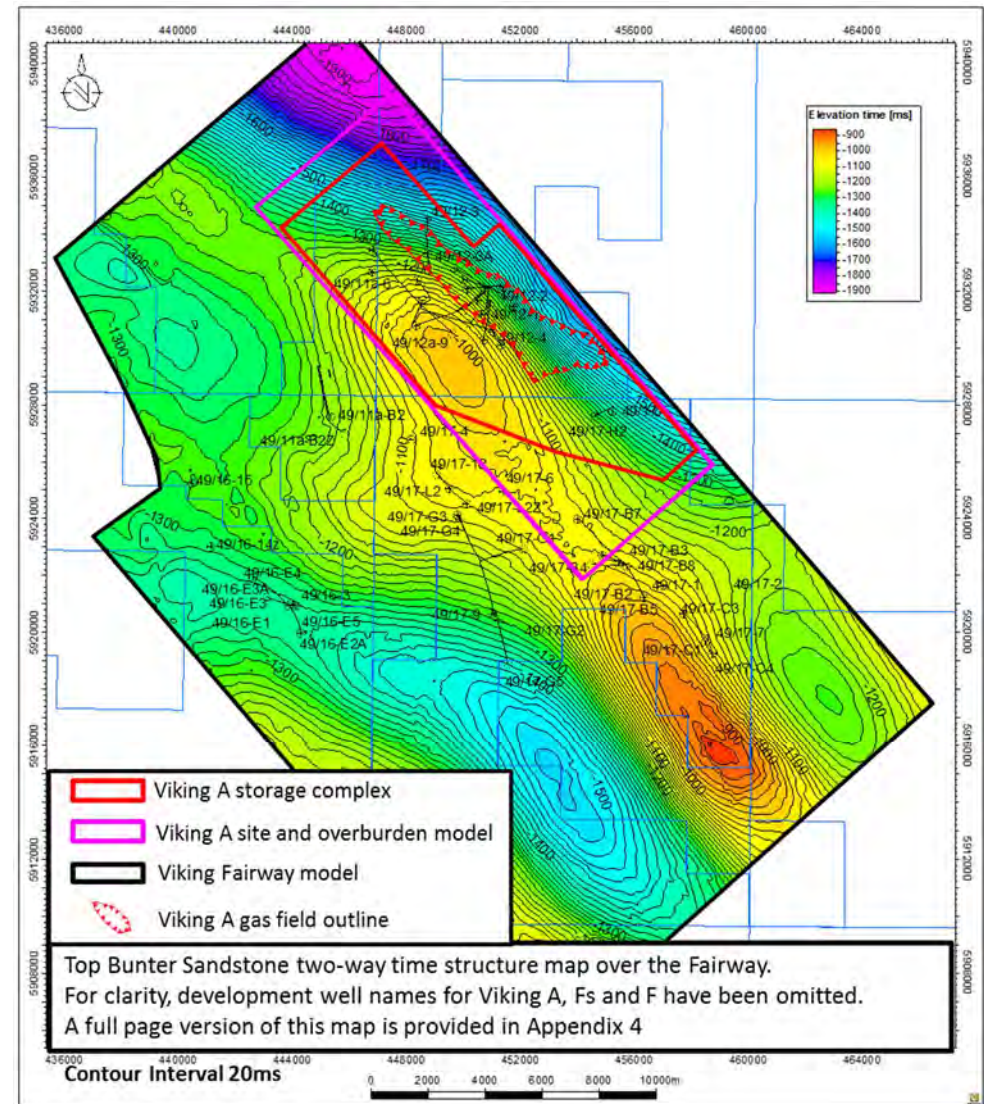


Figure 3-11 Top Bunter Sandstone two-way time map

events lower frequency and lower amplitude. Very few if any faults affect the Bunter Sandstone within the Viking A storage complex. There are a few very minor breaks at Top Bunter Sandstone to the south west of the Viking A storage complex.

Top Zechstein – The Zechstein evaporate system terminated with the deposition of the Brockelscheifer shales (McCann, 2008). These shales produce a hard seismic response immediately above the Top Zechstein. The well to seismic ties (Figure 3-5) show that the Brockelscheifer shale is a strong trough and that the Top Zechstein is a medium amplitude peak representing a decrease in acoustic impedance at the base of the shale.

The horizon forms a broad north west to south east trending ridge across the fairway (Figure 3-12) caused by movement of the underlying salt. Thinning of the salt to the east produces a steeply dipping flank to the ridge overlying the Viking A and H reservoirs which contributes to depth conversion complexity in this area. The movement of halite under overburden pressure within the Zechstein unit also breaks-up inter-bedded high velocity anhydrite and dolomite layers. These high velocity layers move apart and form ‘rafts’ within the salt which in turn increases depth conversion uncertainty further (Figure 3-6 and Figure 3-7).

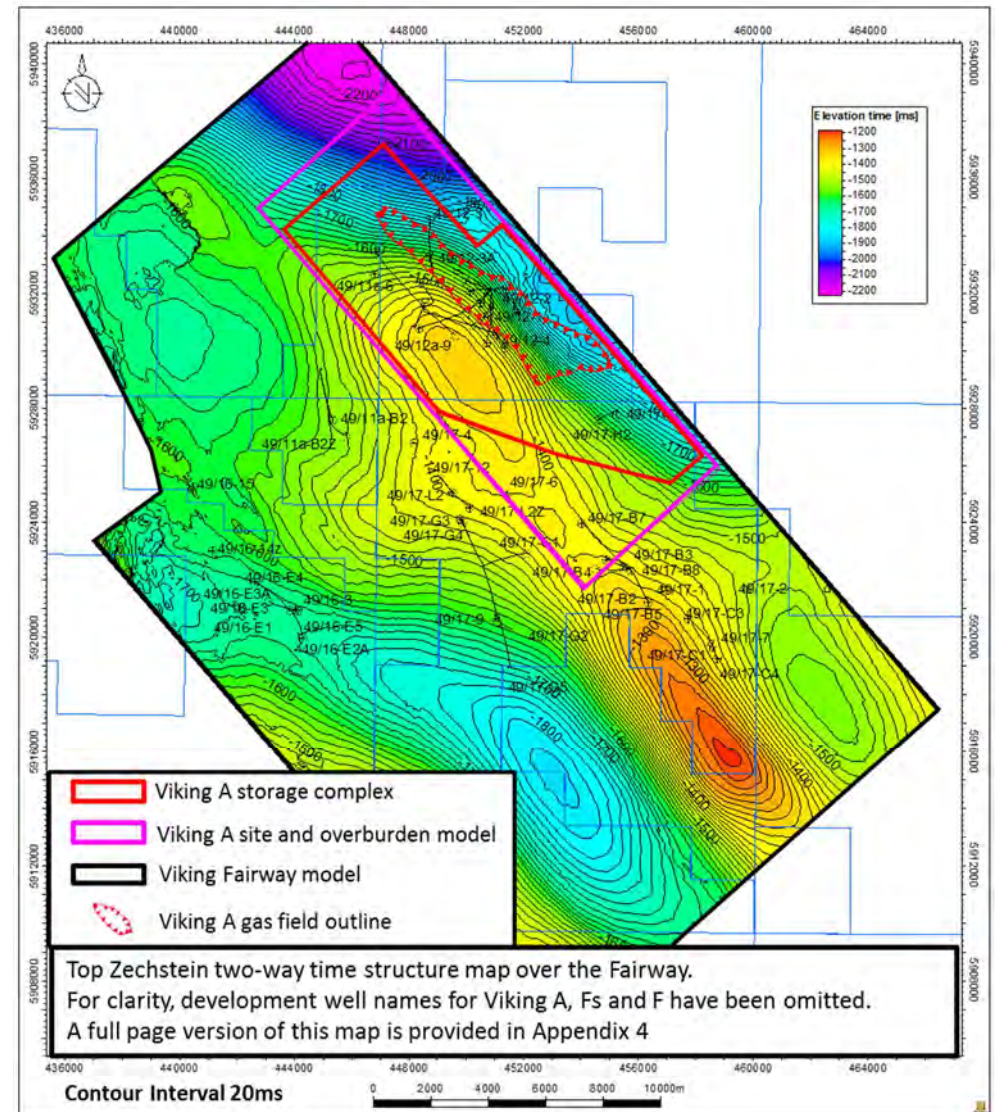


Figure 3-12 Top Zechstein two-way time map

Top Lemman Sandstone – The Top Lemman Sandstone is a high amplitude peak representing a decrease in acoustic impedance at the boundary of the Zechstein evaporites and the softer underlying Lemman Sandstone. Although the boundary generates a strong seismic peak (Figure 3-5), the horizon is highly faulted, sometimes steeply dipping and in places, overlain by high amplitude evaporate reflections that mask the Top Lemman Sandstone response. This complexity meant that the initial 128x128 seed grid was refined to 64x64 across the main structural highs with additional picks down to 4 line spacing near the more complex faults. The horizon picks were extended using Petrel’s 3D autotracking function with a stringent quality test applied so as to reduce the risk of incorrect picking of the horizon across faults. Fault polygons were generated from the 3D tracked horizon and applied as boundaries in the surface gridding process to produce the final gridded surface (Figure 3-13). Figure 3-14 shows a 3D view of the Top Lemman Sandstone two-way time surface; the faults have been omitted to allow a clear view of the surface.

Base Lemman Sandstone – The Lemman Sandstone lies unconformably on gently folded Carboniferous strata. The acoustic contrast between the Lemman and the Carboniferous is very low and within the fairway area it is not possible to accurately pick a Top Carboniferous horizon on the seismic. The approximate position of the Top Carboniferous is shown on the seismic lines (Figure 3-6 and Figure 3-7).

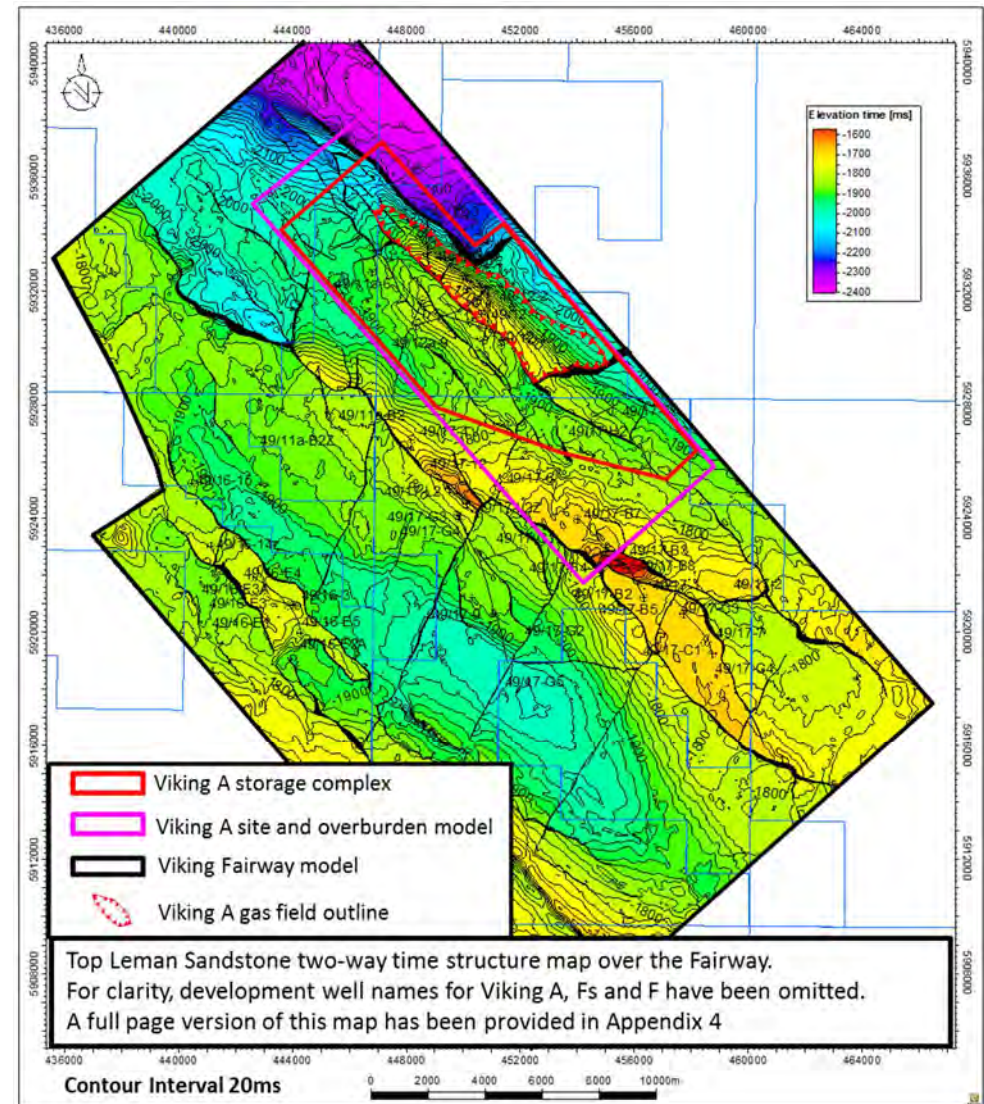


Figure 3-13 Top Lemman Sandstone two-way time map

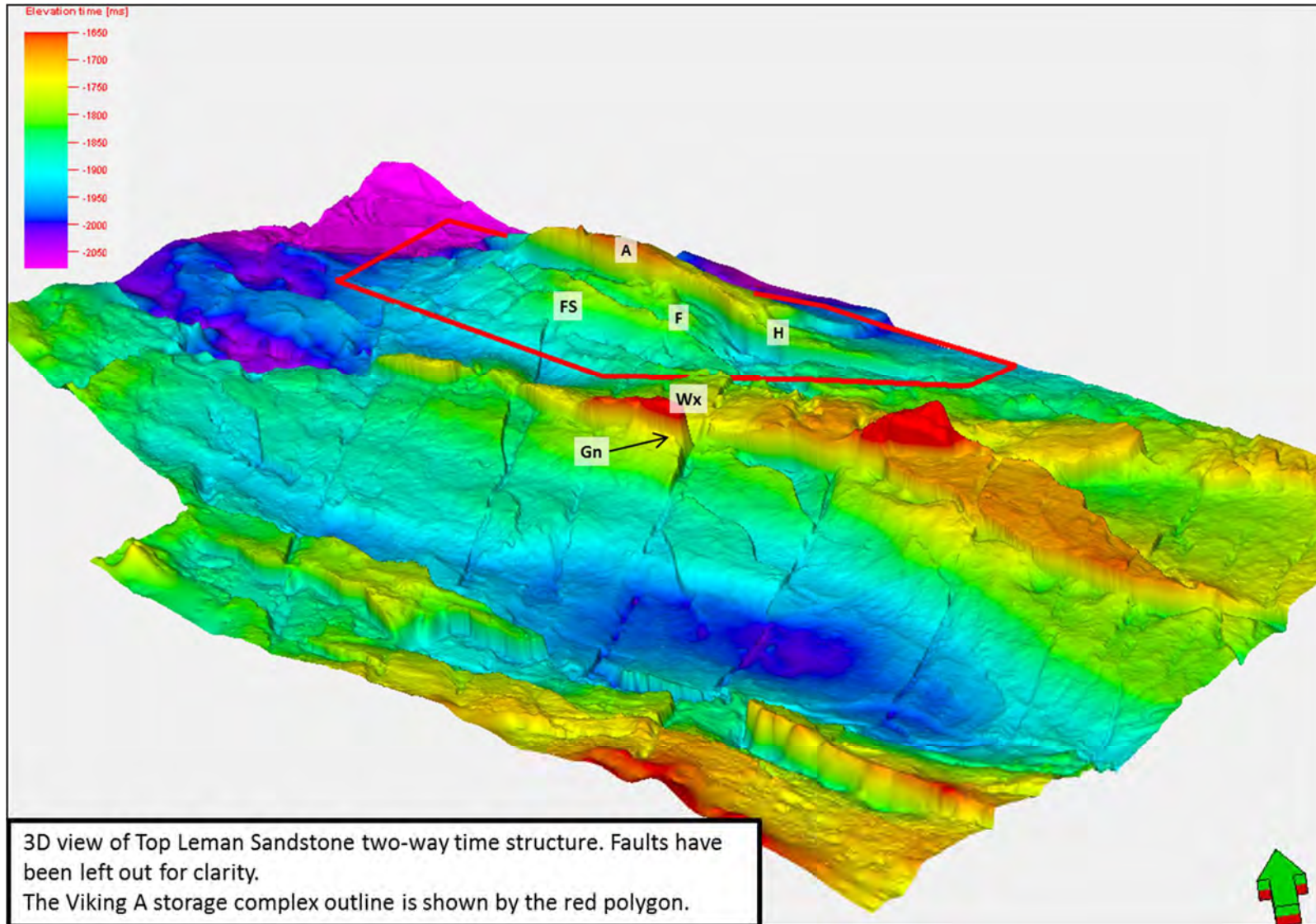


Figure 3-14 3D view of the Top Leman Sandstone time interpretation

3.4.4 Faulting

Two major fault trends exist at the Lemman Sandstone level. The dominant trend is NW-SE and these faults form the boundaries of most Southern North Sea gas fields. These faults have throws up to 400m (1300ft) and can completely offset the whole Lemman Sandstone unit. A second NNE-SSW trend is also present with several long lineaments clearly seen on the Semblance slice (Figure 3-15). These lineaments, known as 'De Keyser' lineaments, are a recognised feature of the Southern North Sea geology. The vertical offset across these lineaments is often very small and sometimes below seismic resolution with only a slight bend in the horizon present. They have been shown to seal in some Southern North Sea gas fields and are therefore important components in the final static model. A third, ENE-WSW structural trend can also be identified. They are generally short length faults and are most apparent in the F and Fs structures (Riches, 2003). The fault between Viking A and Viking H is ENE-WSW trending and production data shows these two fields to be separate despite having Lemman Sandstone juxtaposed against each other on either side of the fault.

Viking F and Fs have a 7m (22ft) difference in GWC. The NW-SE trending fault that separate the two gas accumulations must be sealing as there is Lemman Sandstone juxtaposed against Lemman Sandstone across the fault. Viking A maximum gas column height is 450m (1480ft). Viking H maximum gas column height is 270m (880ft). Viking F maximum gas column height is 215m (700ft). Viking Fs maximum gas column height is 235m (775ft).

The Southern North Sea area has been subjected to two phases of inversion in the late Cretaceous and mid Tertiary. A number of existing faulted structures have been deformed by this inversion resulting in both compressional and extensional geometries which results in both normal and reverse faults together

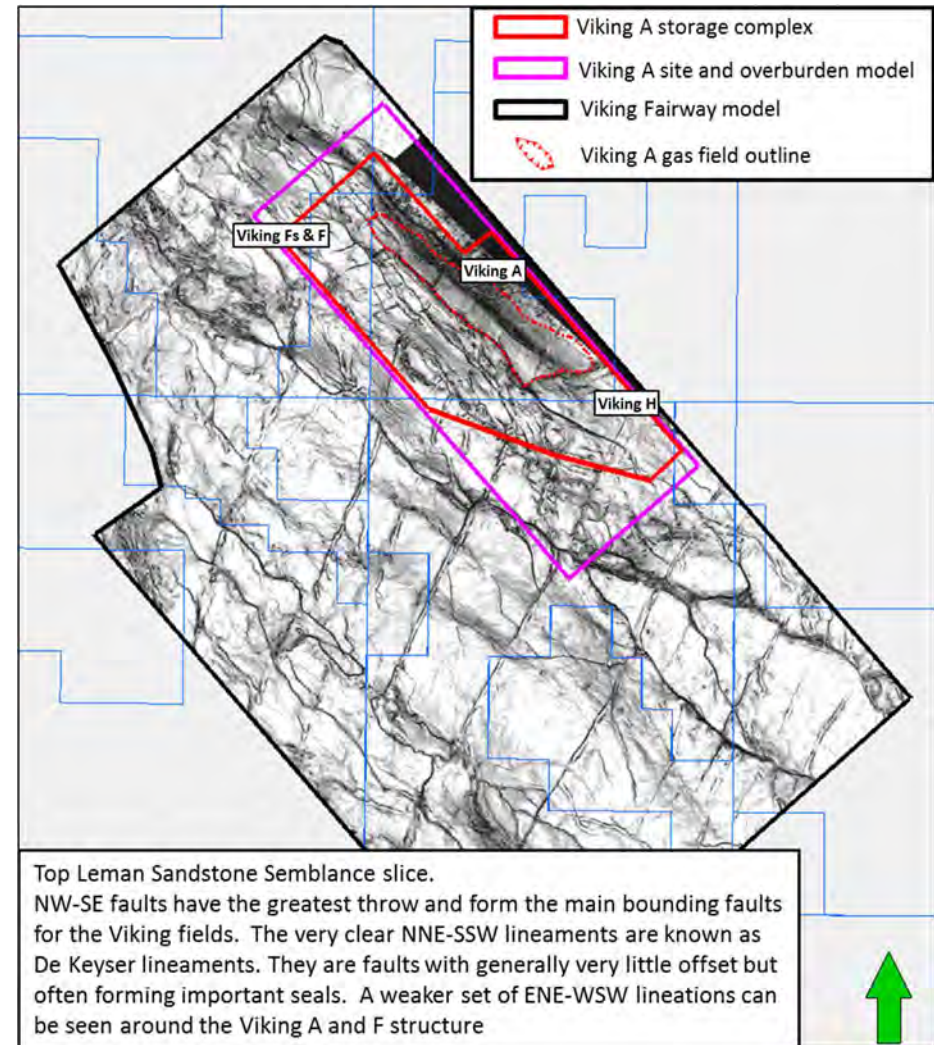


Figure 3-15 Top Lemman Sandstone semblance slice

with some faults having opposite throws along their length. The Viking Wx structure (Figure 3-14) is a north-east to south-west trending compressional structure formed by reactivation of a pre-existing normal fault. The reactivated fault is now a reverse fault which separates the Wx and Gn gas accumulations. Across the fault there is sand-to-sand contact of the Leman Sandstone but the gas fields have different GWCs which shows that the fault is sealing.

The Leman Sandstone faulting is controlled by the underlying structure of the Carboniferous with faults generally continuing well into the underlying Carboniferous. Above the Leman Sandstone the faults die out very quickly in the lower parts of the Zechstein.

Typically faults have been interpreted on inline and crossline orientations every 64 lines but this was refined to as close as every 2 lines at the more complex fault intersections. Figure 3-16 shows a 3D view of the faults that have been taken forward for building the Static Models.

The faulting in the overburden is limited to a few minor faults which can extend down from the Chalk unit into the Upper Triassic. Most of the faults sole out on the Upper Triassic halites with only a few very minor breaks at Top Bunter Sandstone to the south-west of the Viking A storage complex. These minor faults do not appear to offset the secondary seal (10m (33ft) of Solling Claystones and 60m (200ft) of Rot Halite) and have not been included in the overburden static modelling.

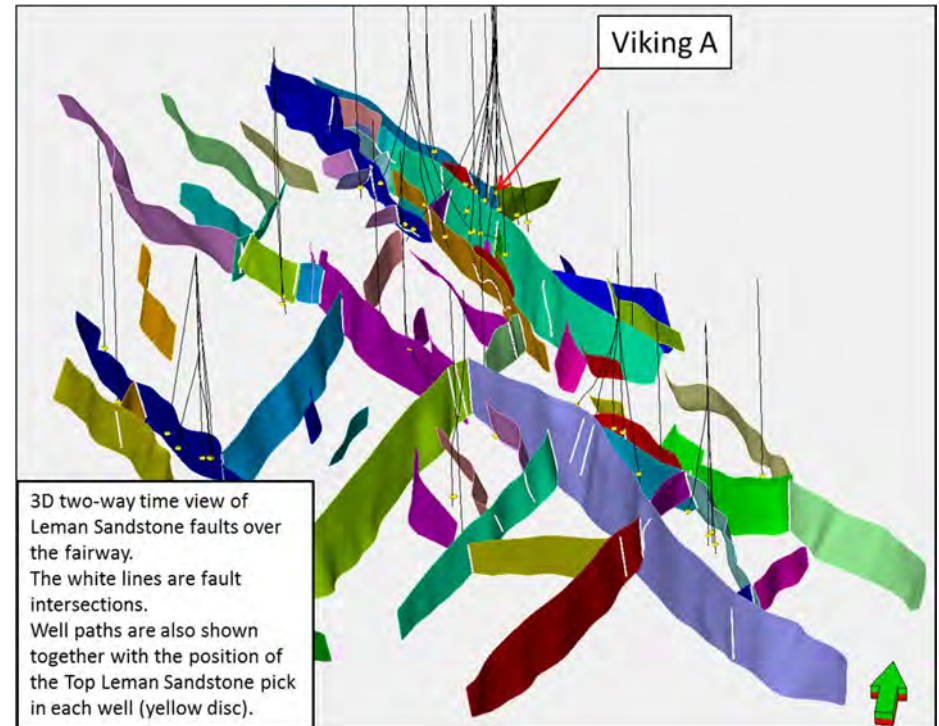


Figure 3-16 3D view of Leman Sandstone fairway modelled faults

3.4.5 Depth Conversion

Depth conversion in the Southern North Sea is complicated by the rapidly changing distribution and thickness of high and low velocity units in the post Zechstein section and the chaotic mixture of lithologies within the Zechstein. This indicates that a layer-cake depth conversion is the appropriate method to use.

The wells database presented a number of challenges for depth conversion. Many of the wells available on CDA, date from the 1960s and 1970s and have no digital checkshot data. Checkshot times for these wells were copied from often poor quality scans of original paper composite logs. Many wells are deviated production wells and pass through steeply dipping formations making the interval velocity values unreliable. In addition, many were not logged in the very shallow section so that the upper formation tops, namely top and base Chalk, are often based on relatively inaccurate analysis of cuttings.

Whilst exploring for and developing hydrocarbons in the Southern North Sea considerable time and effort is employed by operators to develop sophisticated depth conversion models that account for the highly variable velocity field. Depth conversion can often lead to significantly different depth structures to that produced from the original time data. However, given the constraints on the time and data available for this project it was decided to use a simpler approach and in areas of poor well control pseudo well tops have been used to modify the Top Lemman Sandstone depth surface to match the approximate position of the GWCs reported in the operators published Viking field paper (Riches, 2003).

With the focus of the dynamic modelling restricted to Viking A, the depth conversion design has also been focused on Viking A and its peripheral

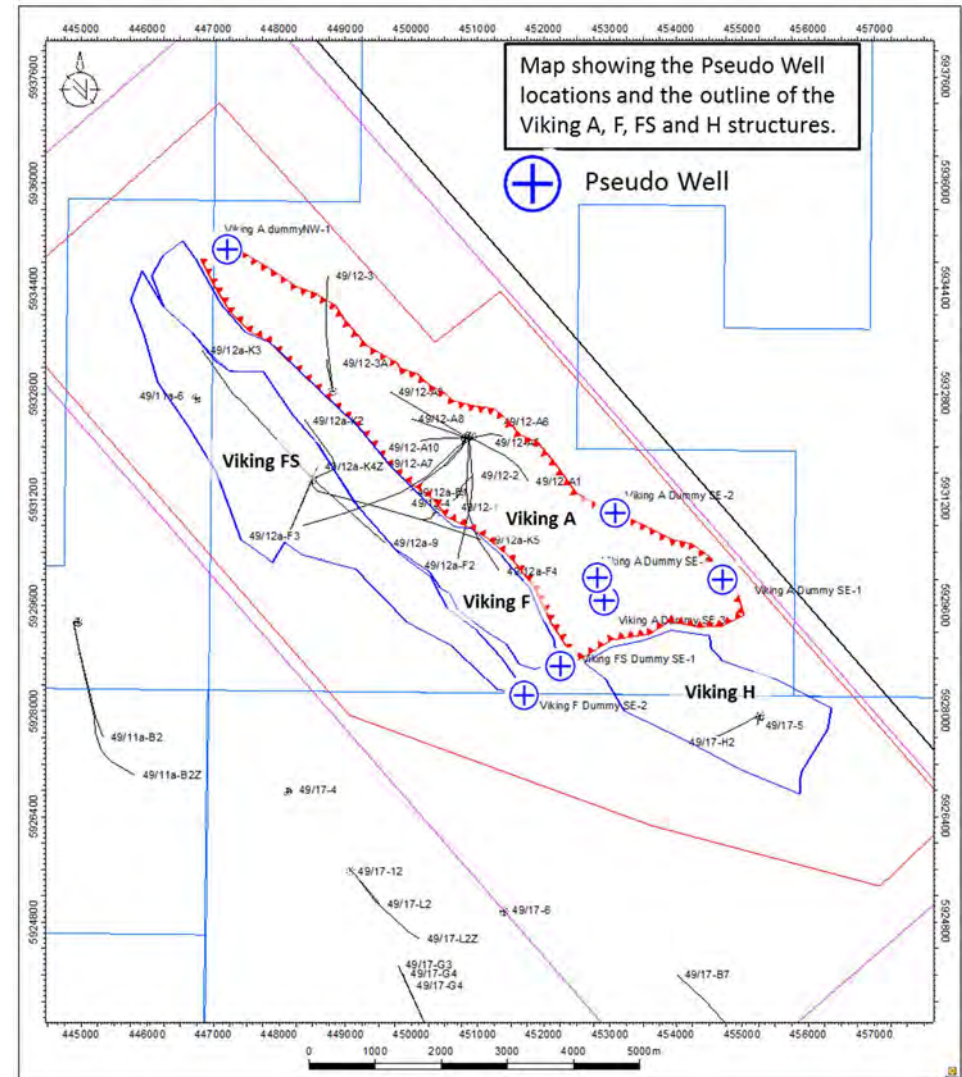


Figure 3-17 Location of psuedo wells in site model

structures Viking F, FS and H. Pseudo well tops (Top Leman Sandstone) have been positioned to the north and east of Viking A and to the south east of Viking F and FS (Figure 3-17) based on the operators published map (Riches, 2003).

The depth conversion was undertaken in the industry standard interpretation software PETREL. The depth conversion method for each interval or surface is outlined below and summarised in Figure 3-18.

The overburden down to Top Zechstein has been divided into four layers; Tertiary, Cretaceous, Jurassic and Triassic velocity units. Due to time constraints the Zechstein is depth converted as a single unit. Each interval was depth converted using oil industry standard depth conversion techniques and these are summarised in Figure 3-18 and outlined below in more detail. The depth conversion was undertaken in the PETREL software using the velocity modelling plug-in. Top Chalk, Base Chalk/Base Cretaceous Unconformity, Top Triassic, Top Bunter Sandstone and Top Zechstein were depth converted directly using the Petrel generated velocity model. Prior to depth converting the Zechstein interval the Top Zechstein required editing to remove depth imprints of overburden features caused by the layer cake method.

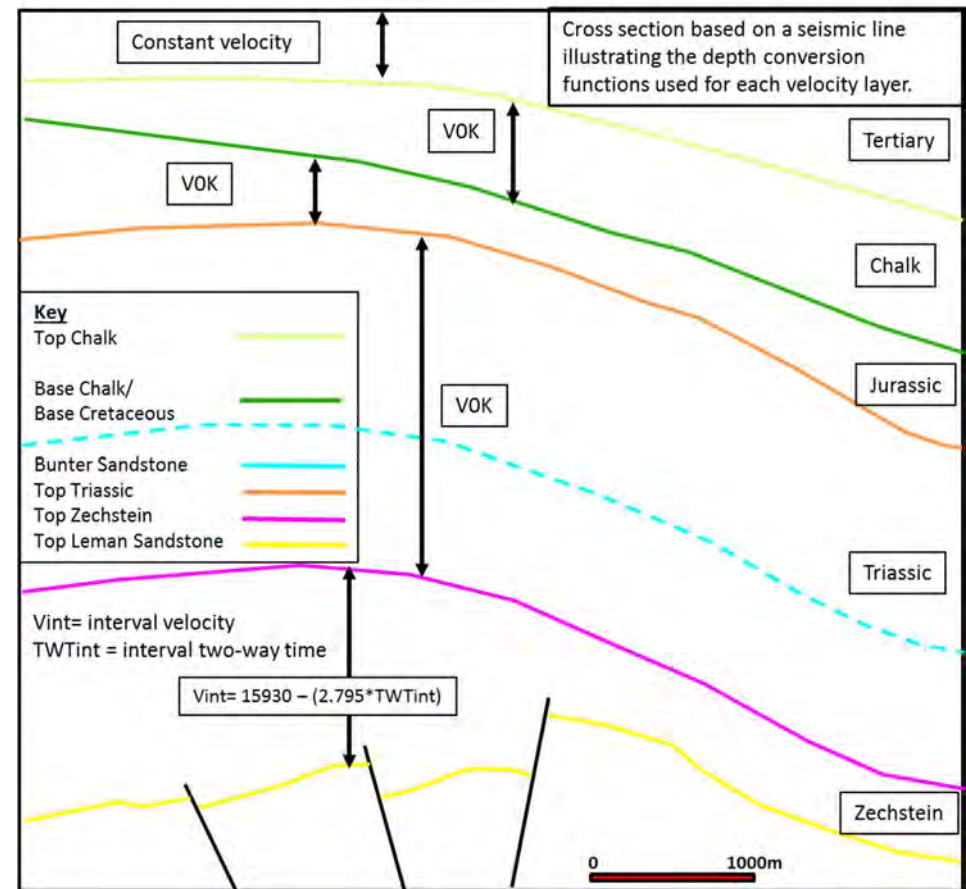
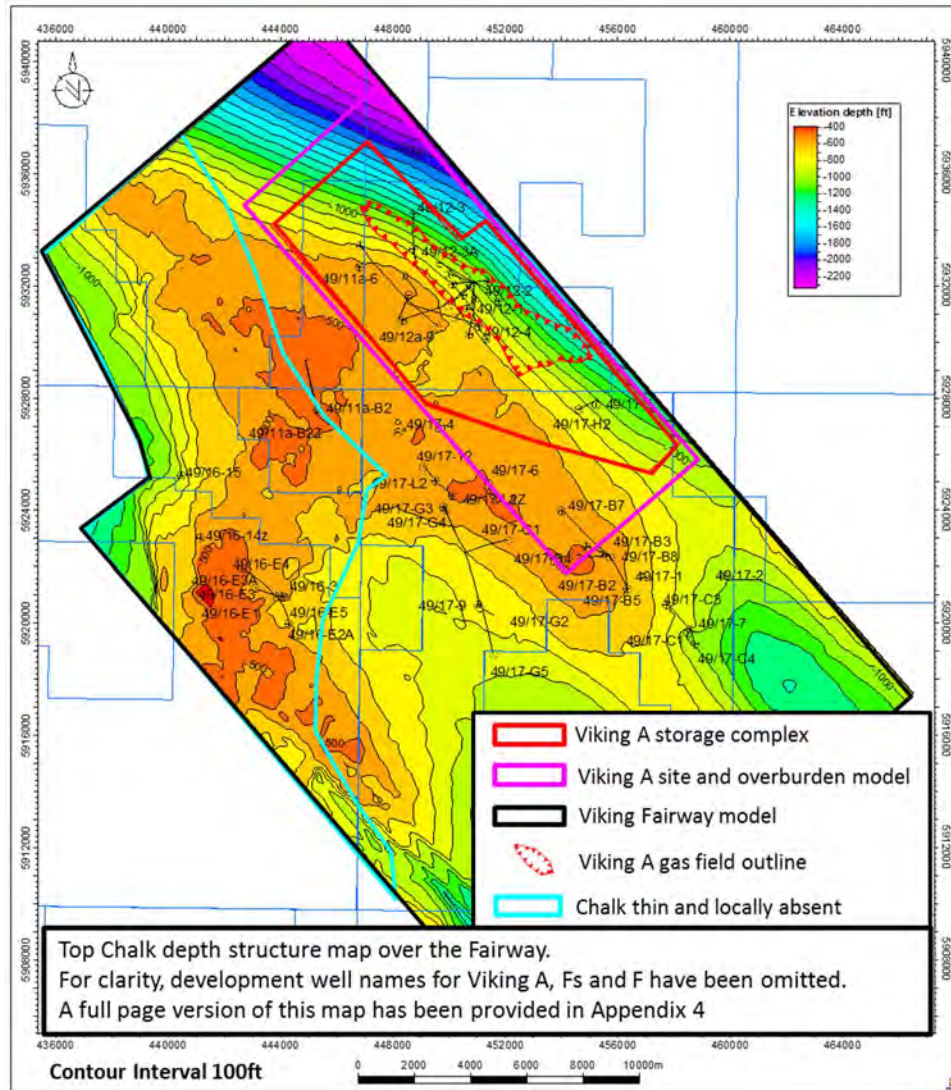


Figure 3-18 Layer cake depth conversion summary



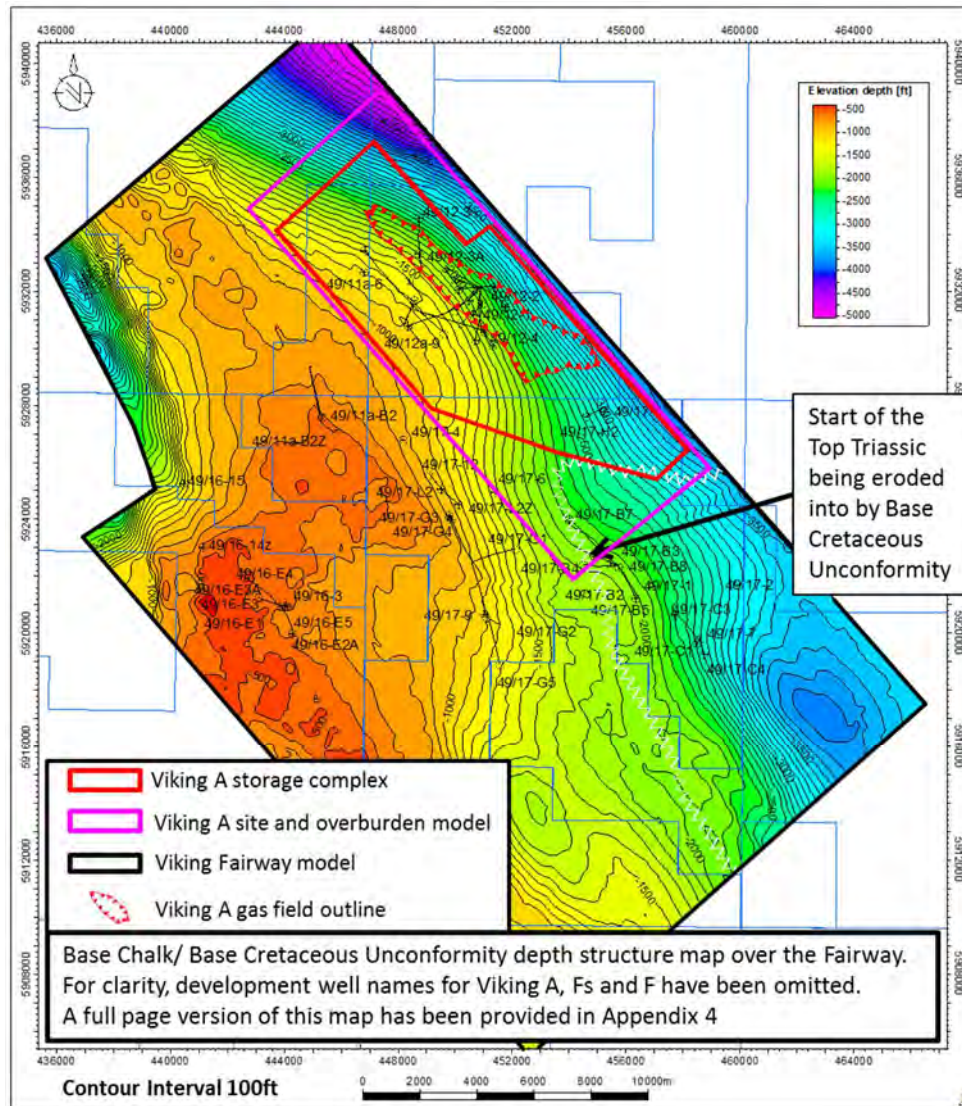
Mean Sea Level to Top Chalk

The checkshot, logs and tops data for the shallowest section is of variable quality. Any gradient of velocity increase with depth is very unreliable as the sign of the gradient changes depending on which outliers are included in the regression. Consequently, a single constant interval velocity of 6529ft/s was calculated for this layer. This is the average interval velocity calculated from the horizon times and logged formation depths in wells 49/11a-6, 49/12/A5, 49/12/2, 49/17/1, 49/17/5, 49/17/6, 49/17/9 and 49/17/12. The resulting depth surface is shown in Figure 3-19 and tied to the well depth using a depth residual correction grid.

Top Chalk to Base Chalk / Base Cretaceous Unconformity

The Chalk layer was depth converted using a V0+K function (constant K and a mapped V0 surface). The seismic times and well bore depths to the middle of the Chalk interval were used to generate a plot of interval velocity variation with depth. After removing bad data points, a regression line was fitted with a gradient of 2.61. The V0 surface was generated by gridding V0 values derived at the wells. The derived V0 grid ensures that the depth surface ties at the wells. The resulting depth surface is shown in Figure 3-20.

Figure 3-19 Top Chalk Depth Map



Base Chalk / Base Cretaceous Unconformity to Top Triassic (Jurassic Interval)

The Jurassic interval was also depth converted by applying a V0+K function using the same method as the overlying Chalk interval. The seismic time and well bore depth to the middle of the Jurassic interval were used to generate a plot of interval velocity variation with depth. After removing bad data points, a regression line was fitted with a gradient of 2.45. The V0 surface was generated by gridding V0 values derived at the wells. The derived V0 grid ensures that the depth surface ties at the wells. The resulting depth surface is shown in Figure 3-21.

Top Triassic to Top Zechstein (Triassic Interval)

The Triassic interval was also depth converted by applying a V0+K function using the same method as the overlying Chalk interval. The seismic time and well bore depth to the middle of the Triassic interval were used to generate a plot of interval velocity variation with depth. After removing bad data points, a regression line was fitted with a gradient of 0.70. The V0 surface was generated by gridding V0 values derived at the wells. The derived V0 grid ensures that the depth surface ties at the wells. The resulting depth surface is shown in Figure 3-22.

Figure 3-22 shows that there is a depth imprint of the overlying Chalk and Top Triassic rugosity on the Top Zechstein depth surface as a consequence of the multi-layer depth conversion. Although not present over Viking A storage complex it is present within the fairway and hence needs to be removed before progressing the depth conversion down to Top Lemna Sandstone. To remove the depth imprint edits are made in the velocity domain and Figure 3-23 illustrates this workflow. The final depth map is shown in Figure 3-24.

Figure 3-20 Base Chalk/Base Cretaceous Unconformity depth map

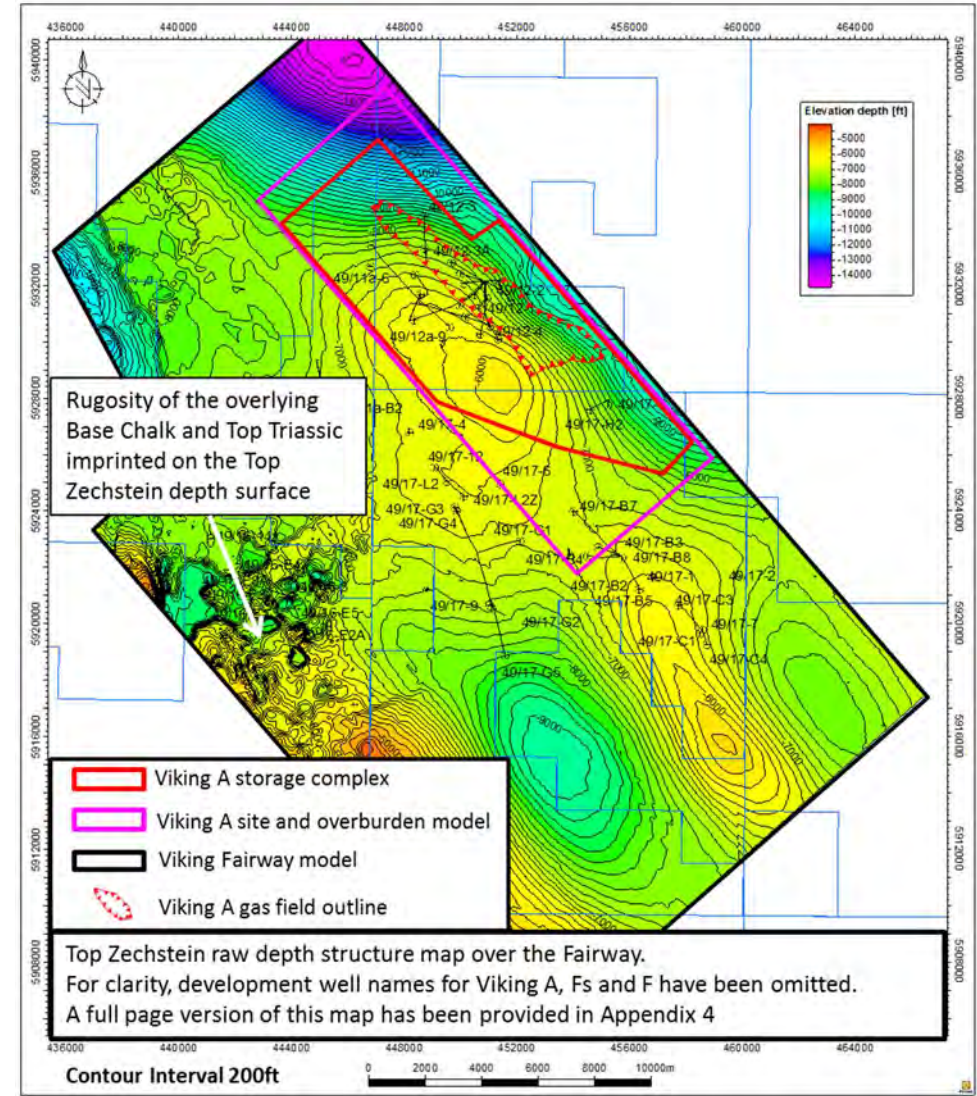
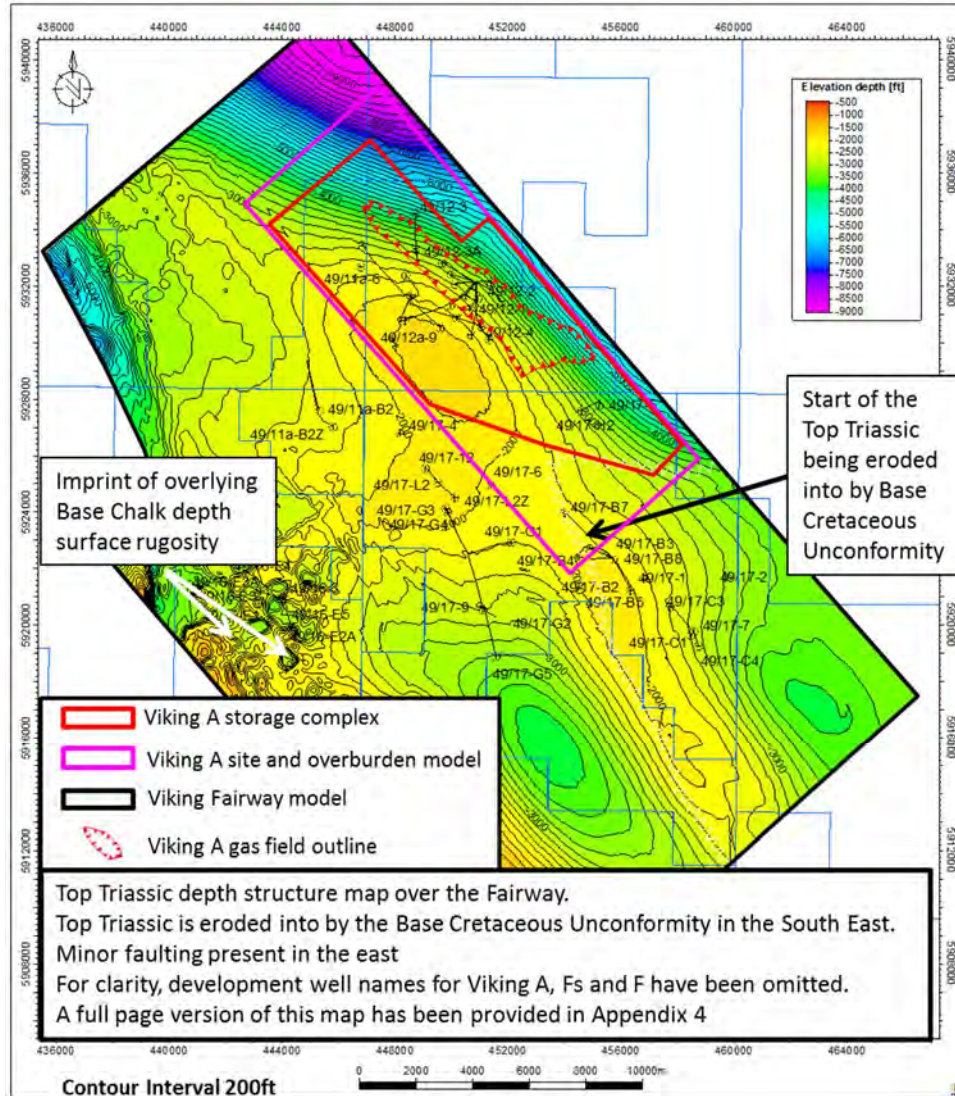


Figure 3-21 Top Triassic depth map

Figure 3-22 Top Zechstein raw depth map

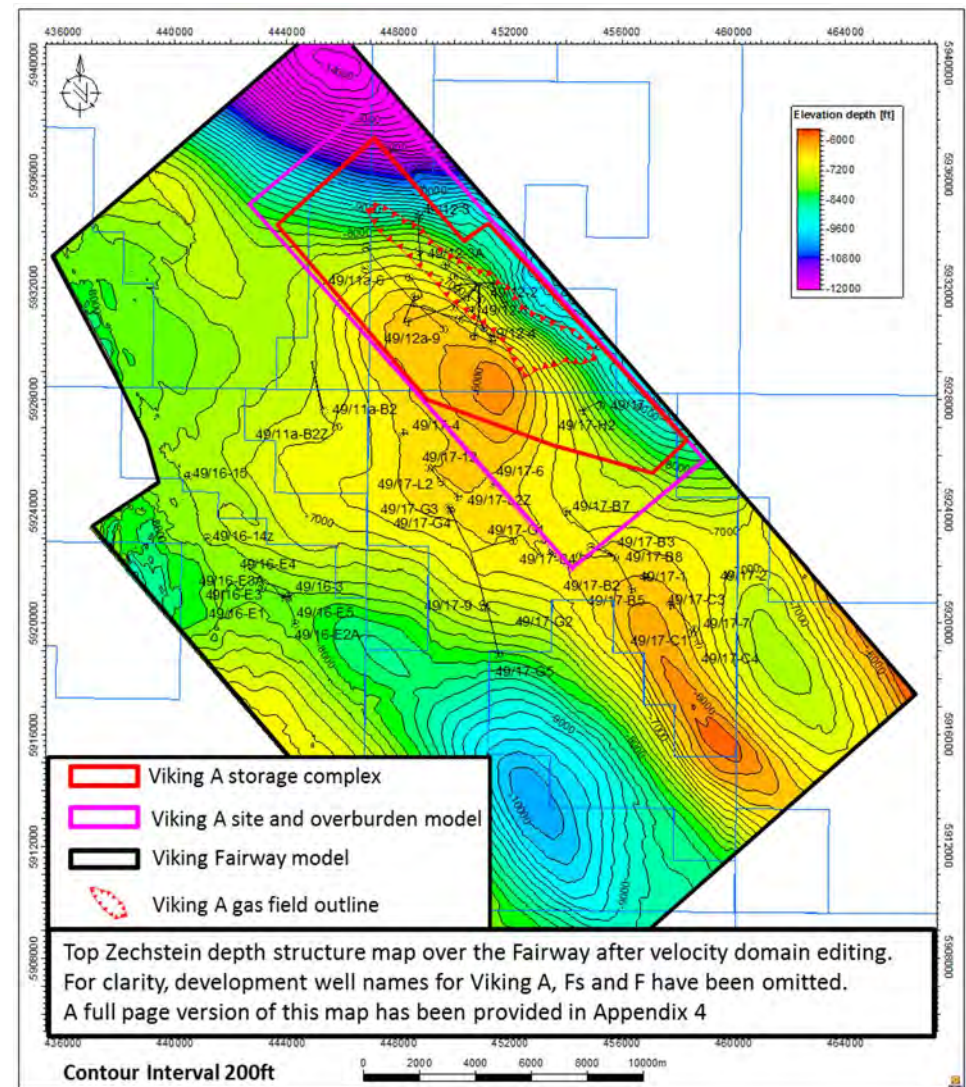
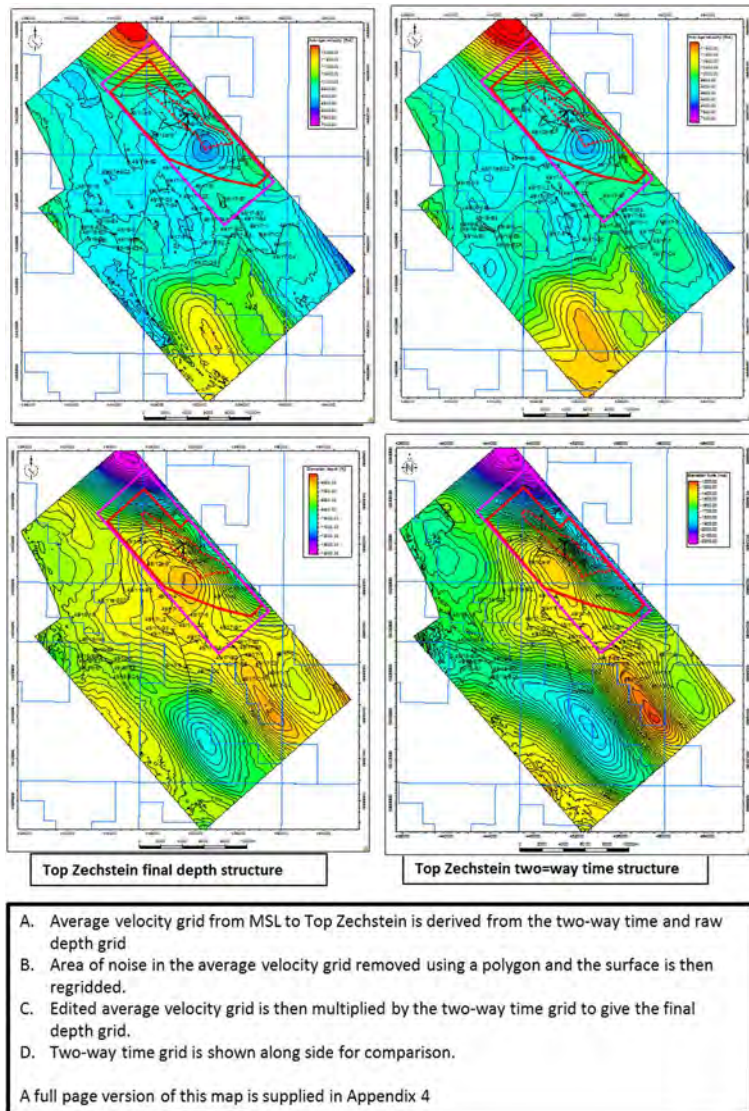


Figure 3-23 Top Zechstein depth map editing workflow

Figure 3-24 Top Zechstein depth map

Top Zechstein to Top Lemna Sandstone (Zechstein Interval)

This is a highly complex interval that is usually depth converted with a detailed interpretation of three, often discontinuous different velocity units within the evaporite sequence. This three layer depth conversion can be approximated by a relationship between interval thickness and interval velocity as the proportion of high velocity dolomite increases as the overall thickness decreases. The seismic interval time (TWTint) and well bore derived isochore for the Zechstein interval were used to calculate interval velocities and hence derive a plot of interval velocity variation with interval time. After removing bad data points, a linear regression line was fitted with the relationship $V_{int} = 15930 - (2.795 * TWT_{int})$. The function was used to generate an interval velocity surface within Petrel and this was used as the final layer of the velocity model.

The Top Lemna Sandstone time surface was depth converted using the Zechstein interval velocity surface which was multiplied by the Zechstein isochron to generate an isochore (Figure 3-25). The isochore was added to the Top Zechstein depth surface to generate a Top Lemna Sandstone raw depth surface. This surface was then flexed to tie the well tops. As discussed above, several pseudo Top Lemna Sandstone well tops (Figure 3-17) were used to ensure that the areal extent and spill points of Viking A, F and FS structures were approximately the same as what has been published by the operator (Riches, 2003). The resulting depth surface is shown in Figure 3-26. A larger scale map of the Viking A storage complex is shown in Figure 3-27 and a 3D view of the same surface is shown in Figure 3-28.

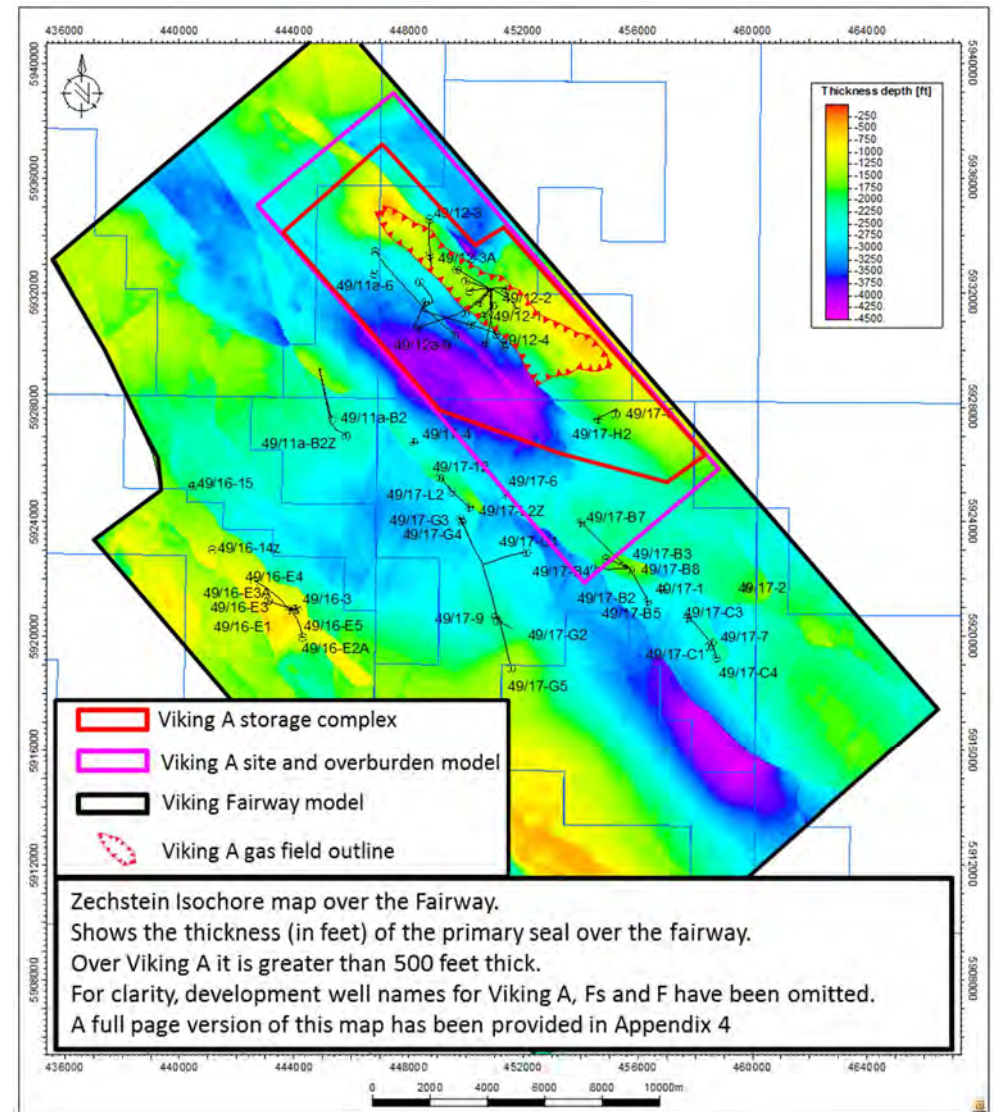


Figure 3-25 Zechstein Isochore

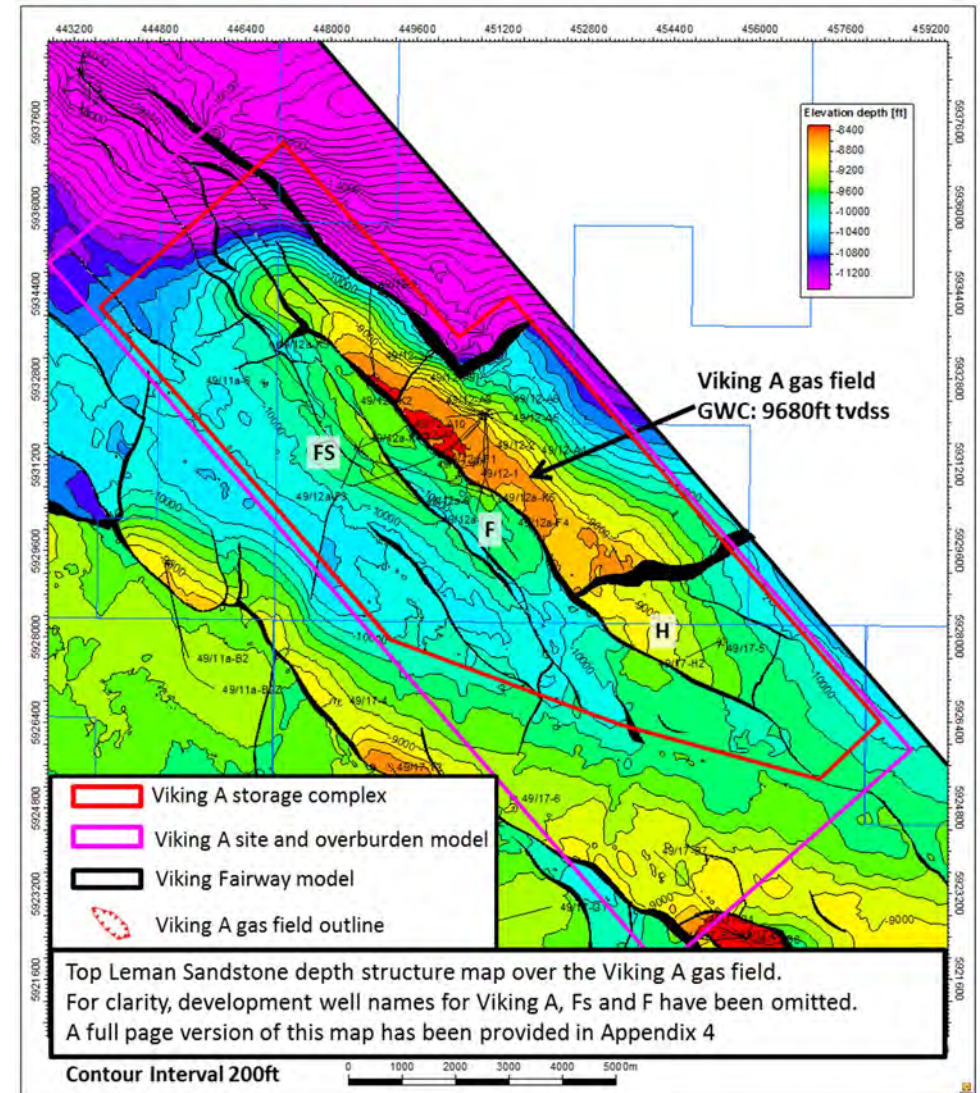
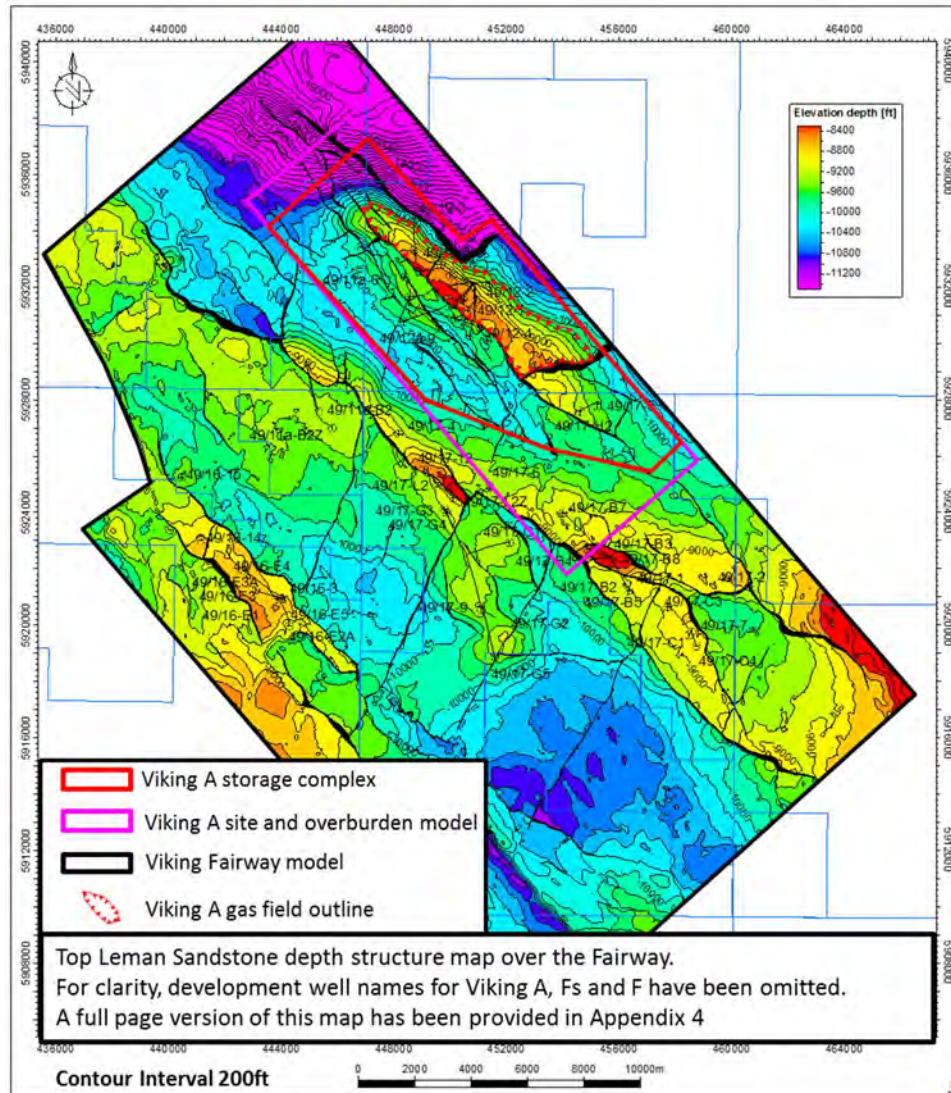


Figure 3-26 Top Leman Sandstone depth map

Figure 3-27 Top Leman Sandstone depth map

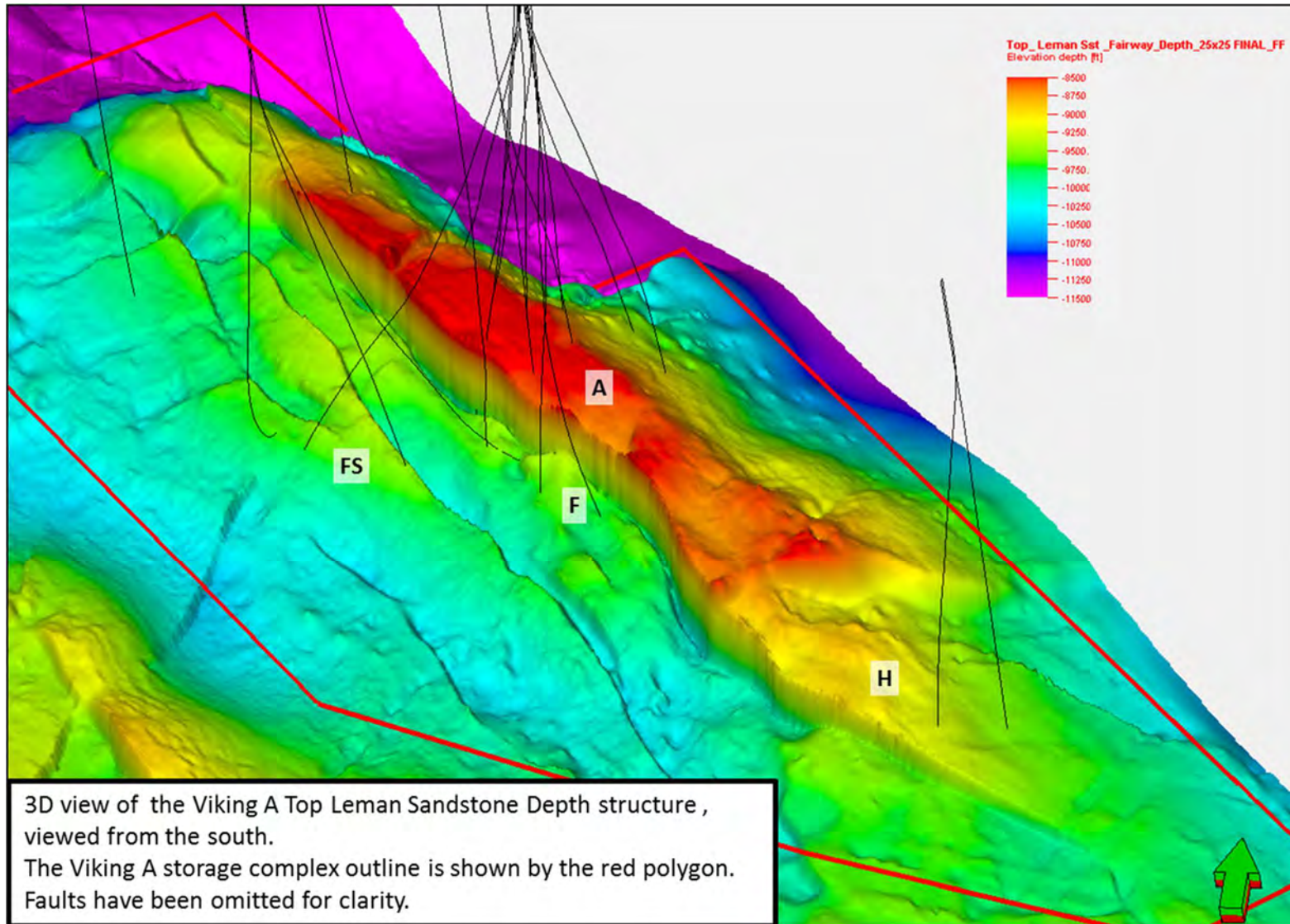


Figure 3-28 3D view of the Top Leman Sandstone depth interpretation

Top Bunter Sandstone

Although not a specific event used in the velocity model, the Top Bunter Sandstone time surface was depth converted directly using the Petrel velocity model described above. The resulting Top Bunter Sandstone depth surface is shown in Figure 3-29. As with the raw Top Zechstein depth surface the Top Bunter Sandstone raw depth surface has a depth imprint of the overlying Chalk and Top Triassic rugosity. Although not present over the Viking A storage complex it is present within the fairway and hence needs to be removed. This has been accomplished by making edits in the velocity domain and Figure 3-30 illustrates this workflow which is the same as that applied to the Top Zechstein raw depth surface. The final depth map is shown in Figure 3-31. There is a large 4-way dip closure at Top Bunter Sandstone known as Bunter Closure 3 (227.007 in CO₂Stored) that has an estimated capacity of 409MT (Pale Blue Dot Energy; Axis Well Technology, 2015). It is offset to the south west of Viking A but it is partially within the Viking A storage complex.

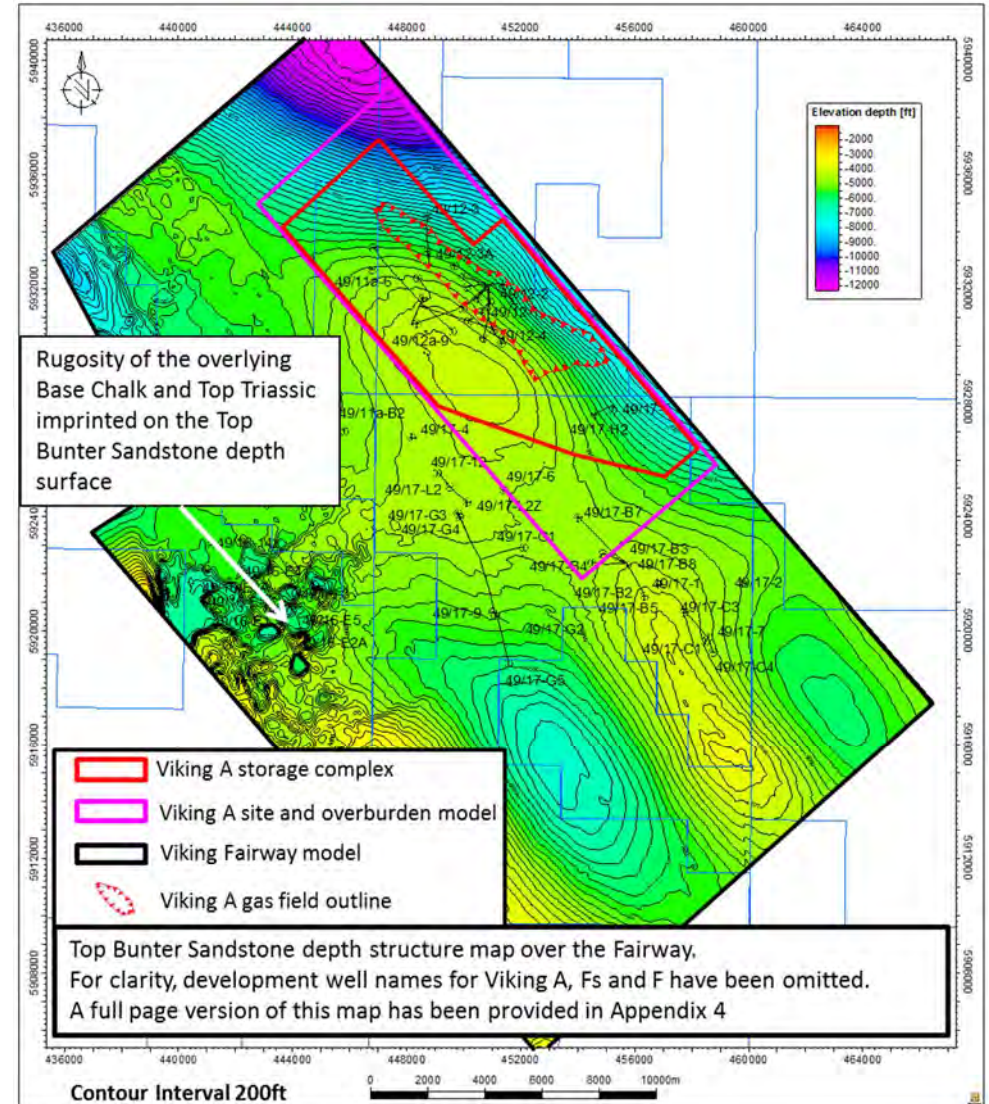


Figure 3-29 Top Bunter Sandstone raw depth map

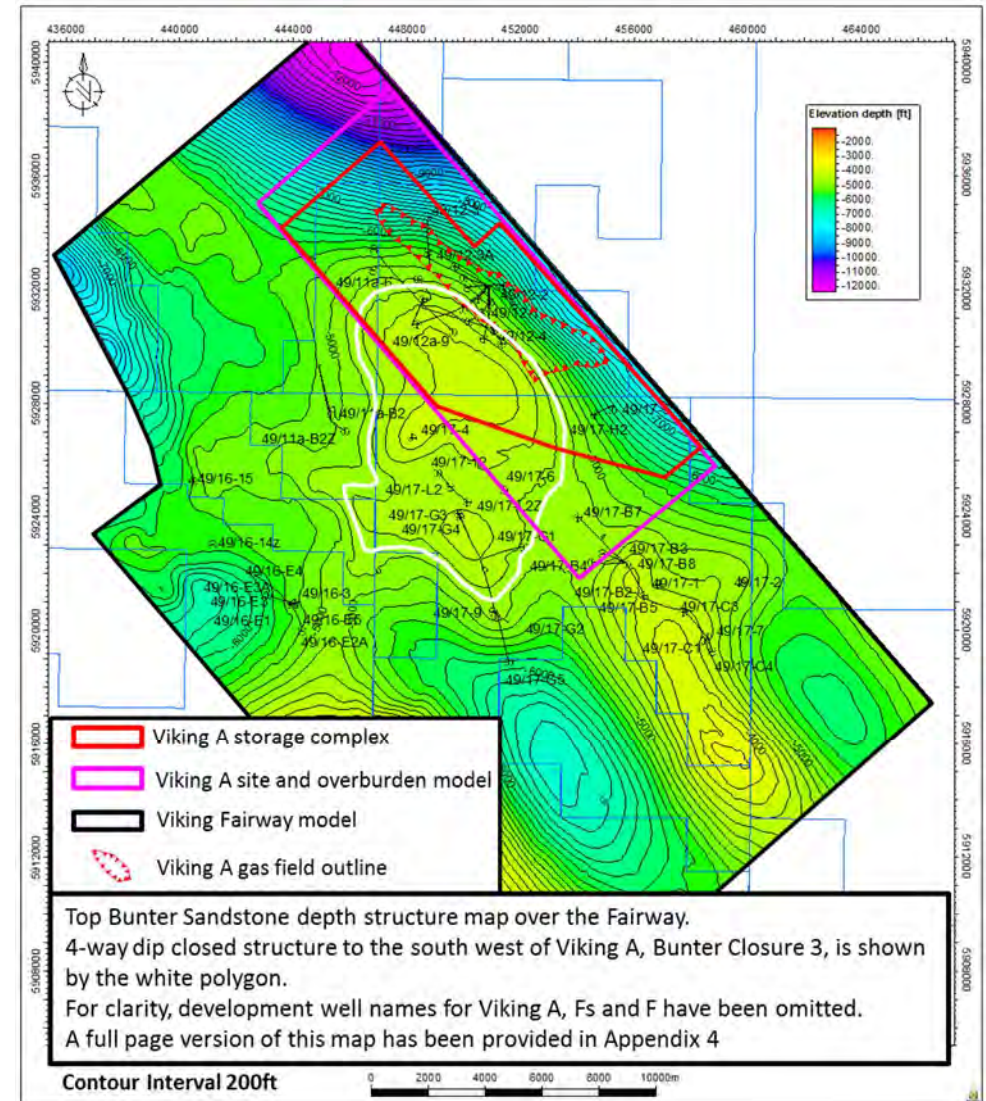
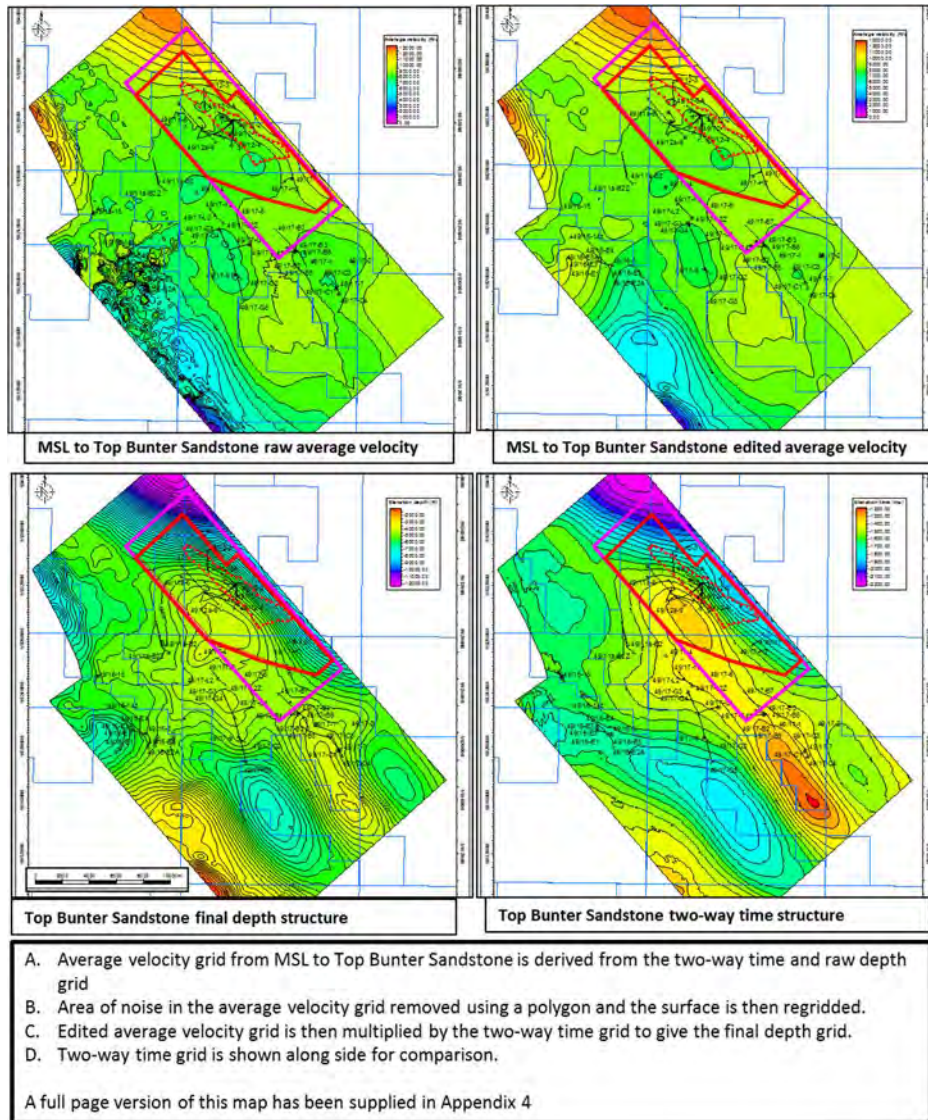


Figure 3-30 Top Bunter Sandstone depth map editing workflow

Figure 3-31 Top Bunter Sandstone depth map

3.4.6 Depth Conversion Uncertainty

The structural and lithological variations across the Viking area of the Southern North Sea allow considerable variation in velocity models and in the resulting depth surfaces. Fortunately, the appraisal maturity of the Viking gas fields has resulted in good well coverage across the crestal areas of the main structures at the Leman Sandstone level. Remaining depth uncertainty is restricted to the flanks of the structures particularly the eastern and northern flanks of Viking A which are steep and have no well control.

Figure 3-32 shows Top Leman Sandstone depth surface variation from different velocity models on two arbitrary cross-sections through Viking A. A simple model with constant velocities in each layer and no well ties (lilac) differs by over 300m (985ft) vertically from more sophisticated models which take into account lateral velocity changes within the layers. Using time varying functions for each layer of the velocity model produces a better fit to wells (green) and this fit is improved by laterally varying the V0 component of each layer to ensure well ties at the formation tops (red).

The well distribution means there is little depth uncertainty across the crest of the Viking A storage site but this increases at the north and east edges. The final model (black line in Figure 3-32) incorporates the areal extent of the field from the operators published map (Riches, 2003) to position pseudo well tops in areas of insufficient data. It is assumed that the edge of the field on the map is at the Viking A GWC depth of 2950m (9680 ft) tvdss. The different velocity models produce vertical depth variation of up to 300m (985ft) relative to the final model.

The operators published paper (Riches, 2003) shows that further uncertainty exists in the lateral movement of faults by up to 360m (1180ft) between the

original data and the newer depth migrated data. However, the details of this variation cannot be investigated without access to the newer processing of the seismic data.

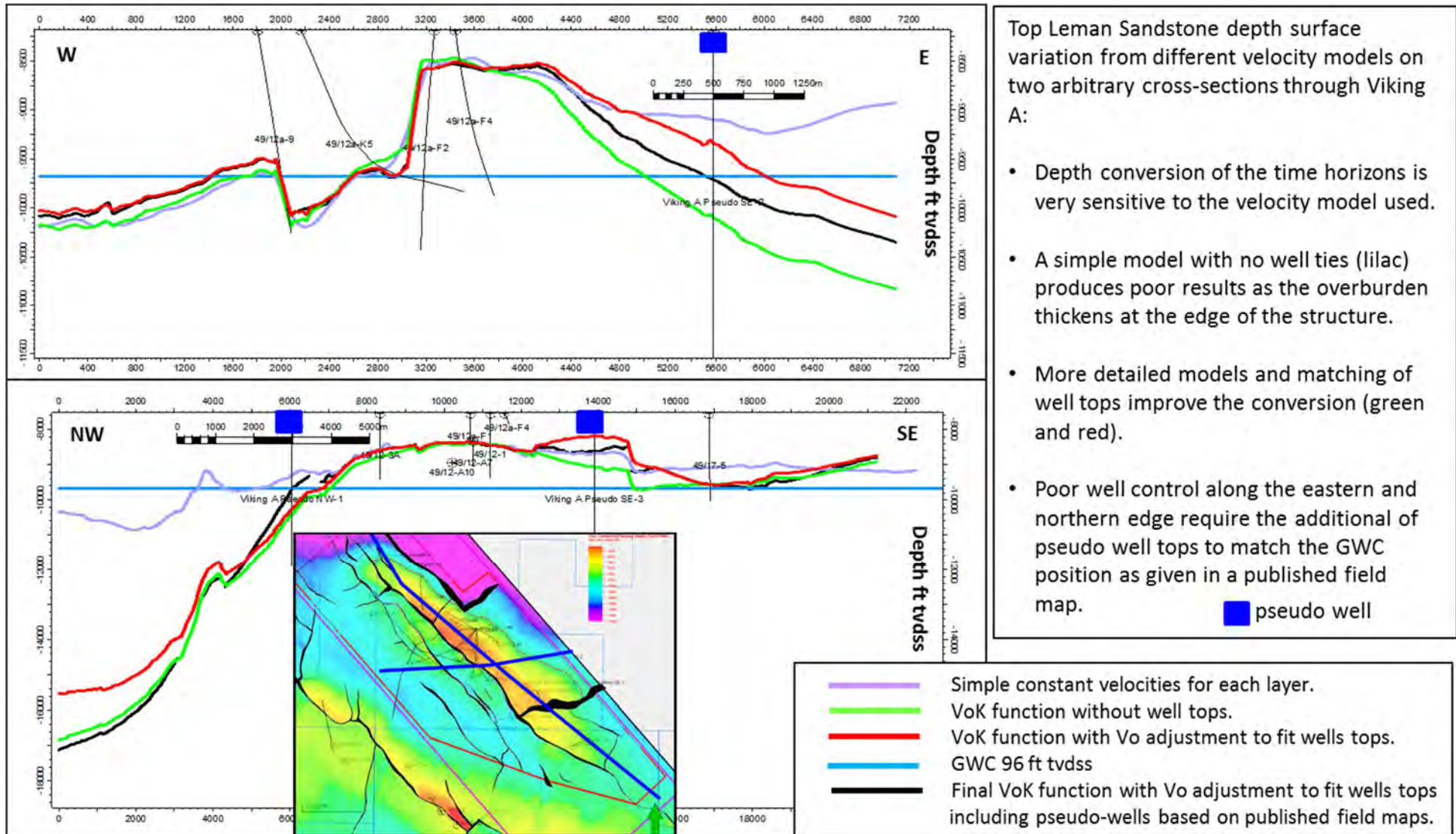


Figure 3-32 Depth conversion sensitivity

3.4.7 Seismic Attributes

Seismic attribute displays have been generated and used for a range of applications in this characterisation of the Viking fairway. The attributes fall into two primary application groups:

Supporting structural definition - these include semblance attributes which describe the degree to which a trace in the 3D volume resembles its adjacent neighbouring traces. Where there is a strong and laterally continuous seismic reflection across an area then the semblance measure will be high. Where such a seismic reflection is broken or discontinuous then the semblance will be low. Semblance can be calculated relative to a constant time value or it can be dip adapted so that continuous, but sloping reflectors will also display high semblance. Semblance can be used to quickly identify faults and structural features in the subsurface detected by the seismic data as an important aid to interpretation. Under certain circumstances the semblance can also identify stratigraphic features such as channel margins etc. Semblance has a similar function to other attributes like similarity, continuity, coherency. At the Viking A Site this attribute has been used to characterise structural detail at each interpreted horizon, including the key search for small faults at the top of the primary reservoir (Leman Sandstone).

Supporting interval characterisation - these include seismic amplitude which describe the magnitude of the signal peak or trough of the reflected seismic wave. This is related to the acoustic impedance contrast between the layers in the earth and can be used to infer some information about the properties of one layer relative to an adjacent layer. In ideal conditions this can be used to quantify lateral variation in overall reservoir quality. Various windowed seismic attribute extractions within the Leman Sandstone interval produced no useful results.

3.4.8 Conclusions

The PGS Southern North Sea MegaSurvey seismic volume (PGS, 2015) which extends over the Viking Fields complex has been interpreted. The key horizons have been identified, interpreted and mapped. Seismic data quality is considered adequate for structural interpretation but is not sufficient to confidently map the depth to the base of the Leman Sandstone. Leman Sandstone faults are clearly interpretable on the seismic volume and are seen to die out rapidly within the lower part of the Zechstein (primary seal). The Zechstein evaporite unit is continuous and over 150m (500ft) thick at the Viking A storage complex.

There is a seismic data gap to the north east of Viking A, while the available data has been sufficient to assess the Viking A site, there is other commercial 3D available to fill this data gap. This should be accessed prior to storage permitting.

The mapped time surfaces have been depth converted using a combination of a V0+k and interval velocity layer cake depth conversion method. A layer cake depth conversion was identified as the most technically robust approach, due to thickness and velocity variations in the overburden units.

The steep dips, rapid lateral changes in velocity and chaotic structures within the Zechstein produce complex ray paths that distort the geometry in the raw seismic section. These distortions have not been fully corrected by the post stack time migration processing applied to the available seismic volume. This distortion together with the complex depth conversion leads to considerable uncertainty in the final depth surfaces on the north and east flanks of the Viking A structural high due to the lack of well control. However, a known volume of gas has been extracted from Viking A by the operator and by incorporating

pseudo well points based on their published map (Riches, 2003) the final depth surface is considered a reasonable representation of the structure (and hence gross rock volume) and adequate for static and dynamic modelling purposes. Future appraisal programmes should address the need for more sophisticated seismic processing and depth conversion techniques to reduce the depth uncertainty of the flanks.

A large 4-way dip closure at Top Bunter Sandstone level (secondary storage unit) has been identified. However, it is offset to the south west of Viking A but is partially within the Viking A storage complex. Only a few very minor faults at Top Bunter Sandstone have been identified but they don't appear to offset the secondary seal (Solling Claystone and Rot Halite) and have not been included in the Static Modelling.

Depth converted structure grids and Leman depth converted faults have been taken forward and used as input data for fairway, site and overburden 3D static models.

3.5 Geological Characterisation

3.5.1 Primary Store

3.5.1.1 *Depositional Model*

The primary storage reservoir for Viking A is the Lemna Sandstone Formation of the Permian Rotliegend Group. This sandstone is pressure depleted after a long period of natural gas production. Post production repressuring and formation pressure estimation are discussed in Section 3.6.7.

The depth to the crest of the structure is approximately 2500 m (8200 ft) tvdss. The Top Lemna Sandstone depth structure map for the site is shown in Figure 3-33.

The Lemna Sandstone was deposited in an arid continental environment as part of a major shifting sand dune system that transitions northwards to the Silverpit playa (sabkha) lake. Depositional facies are primarily aeolian in nature with locally developed fluvial (wadi) deposits and playa lake margin sabkha facies.

The formation rock quality is very variable across the Viking field area. Reservoir quality is best in the northern Viking area (Viking A, H, F and Fs reservoirs) where porosities of up to 25% and permeabilities of 1000mD have been measured in core samples. In the adjacent Central Viking fault blocks (Wx, Yx, Lx and Bn) reservoir quality has been severely degraded due to deeper burial depths. This has often reduced permeabilities to less than 1mD.

The zonation within the Lemna Sandstone is clear in the north Viking area with sandy sequences of dune or fluvial facies interlayered with poorer, impermeable sabkha facies and can be correlated across the area. This becomes less clear in the south where the sabkha facies is replaced by dry aeolian facies. The

reservoir is divided into 5 zones based on log correlation and core descriptions. These are described below in depth order, from the deepest to the shallowest.

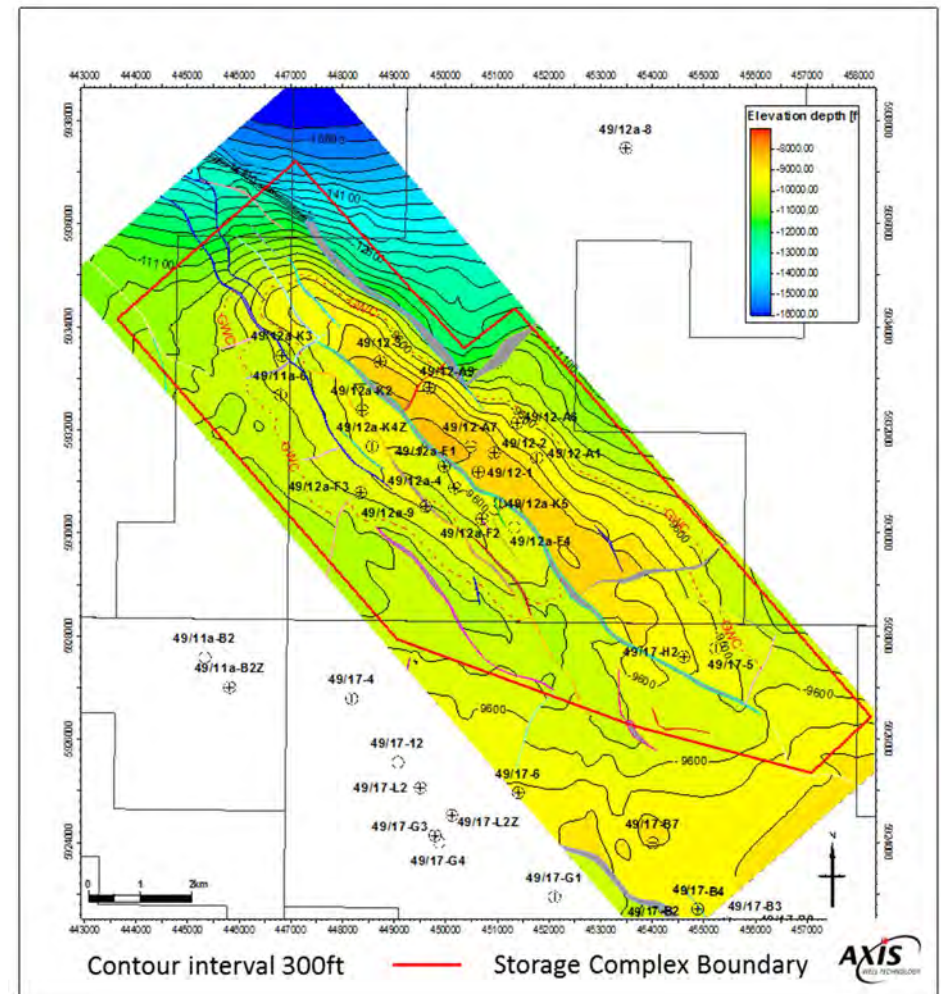


Figure 3-33 Top Lemna Sandstone depth structure map for Viking A

Zone E is a high net to gross (NTG) interval (85%) dominated by clean, well sorted, aeolian dune sandstones interbedded in the north and west with thin sabkha silts. Historically this has been the most productive zone with average well porosities of 13 – 20% and permeabilities in excess of 500 mD (average 75 mD). The average thickness across the northern Viking area is 60 m (200 ft).

Zone D can be correlated across the site and represents a regional climatic change corresponding to a rise in the groundwater table and a southward expansion of the Silverpit desert lake to the north. The northern Viking area is comprised of 22 m (77ft) of sabkha silts and fluvial sands. The reservoir quality is poor in this zone with a low NTG of 33%, average well porosities of 10 – 16% and maximum permeabilities of less than 50mD (average 5mD), it therefore acts as a horizontal permeability barrier to vertical flow between zones.

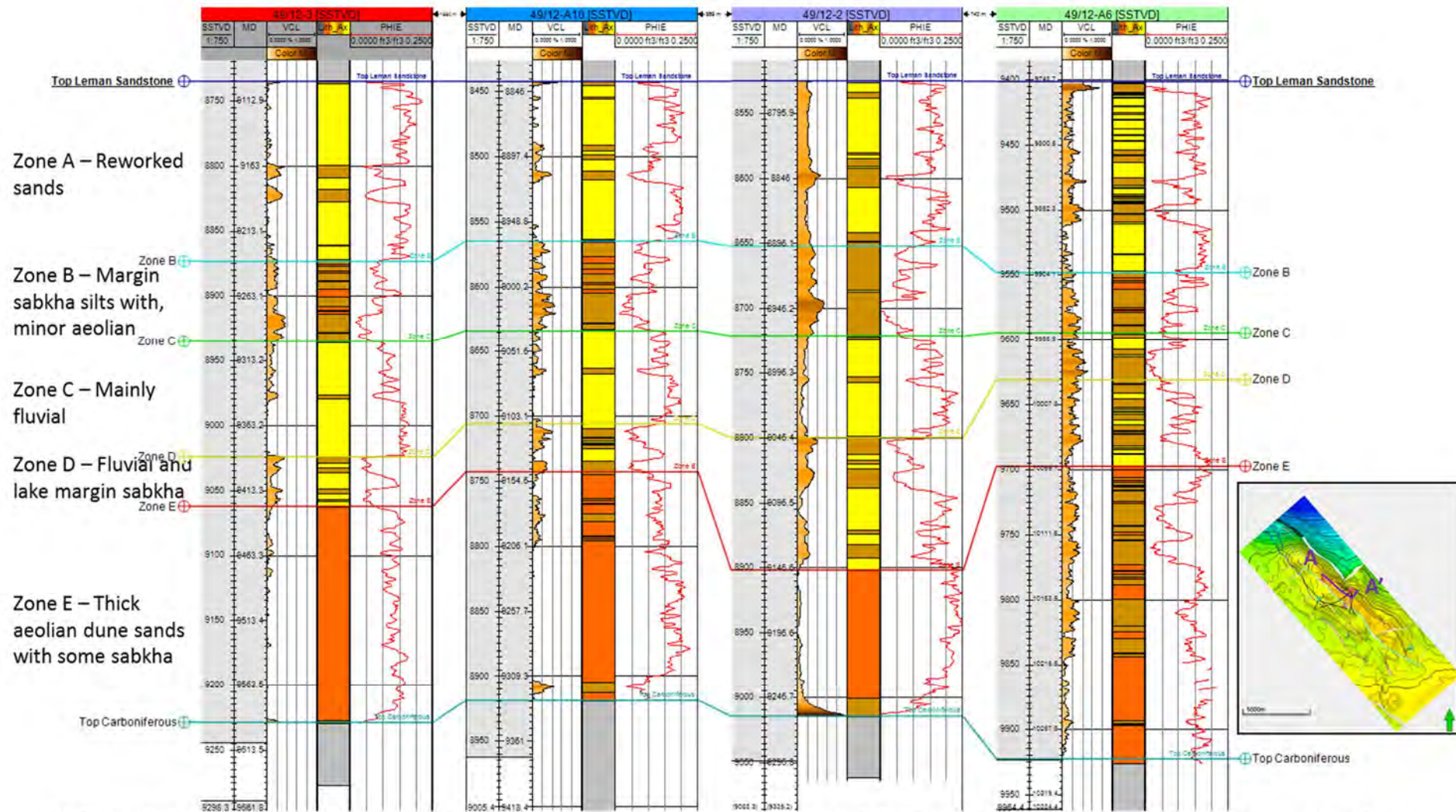
Zone C is dominated by fluvial sands, with minor dune sand intervals, in the north Viking area. Reservoir quality is moderate with a NTG of 66%, average well porosities of 12 – 16% and permeabilities over 100 mD measured in core (averaging 60 mD). Within the south Viking area (Viking B, C, D, E, G, Gn and KX), the zone is predominantly aeolian dune facies.

Zone B marks the encroachment of the Silverpit lake and a return to lake margin sabkha deposits which are correlatable across the North Viking area. Average thickness over the north Viking area is 26 m (85 ft). The reservoir quality is poor with a low NTG of 25%, an average net porosity of 13% and an average permeability of approximately 10 mD. This unit acts as a barrier to vertical flow between zones.

Zone A is a relatively continuous interval of fluvial and reworked sands interbedded with sabkha and silt facies. Reservoir quality is good with a high NTG of 85%. The average thickness is 41 m (136 ft) over the north Viking area

and average well porosities of approximately 15% and measured permeabilities up to over 800 mD (average core permeability is 110 mD).

Figure 3-36 shows the well correlation section NW – SE through the Viking A site.



Well correlation across the Viking A site showing the Leman Sandstone zonation and dominant lithofacies. Flattened on Top Leman Sandstone.

Figure 3-34 Well correlation across the Viking A site

3.5.1.2 *Rock and Fluid Properties*

The petrophysical database is outlined in Section 3.2.4 and was sourced from the publically available CDA database. The data quality was generally very good, no major issues were identified and little manipulation was required to prepare the data for interpretation. The hole condition, interpreted from the calliper and DRHO curves over the zones of interest, was generally good with only the following few exceptions.

- 49/12-2 data are limited to GR-DT-Rt; a basic interpretation was possible with this data.
- 49/12-A10 had marked depth offsets between the data files available from CDA; it was decided to use the higher resolution neutron-density curve as the depth reference and match the offset logs to this reference.
- 49/12a-K2 is reported to be pipe conveyed logging, the hole quality is notably poor in parts and the well logs characterised by 90ft interval ‘spikes’ where connections of the drill pipe were made.

The CDA data were checked against the operator’s composite logs to ensure consistency between the digital data and the operator’s reports. No environmental corrections were made to these data, and the OBM flag was set for interpretations where this was the drilling fluid used to drill the zone of interest.

Only four wells were identified with both core and wireline data within the study area of interest (49/12-1, 49/12-2, 49/12-3, 49/12a-9), these data include Grain Density, Helium Porosity, Horizontal and Vertical Permeability.

Limited special core analysis (SCAL) data were available for this study (well 14/12a-9 only). Archie saturation exponents calculated using this data were

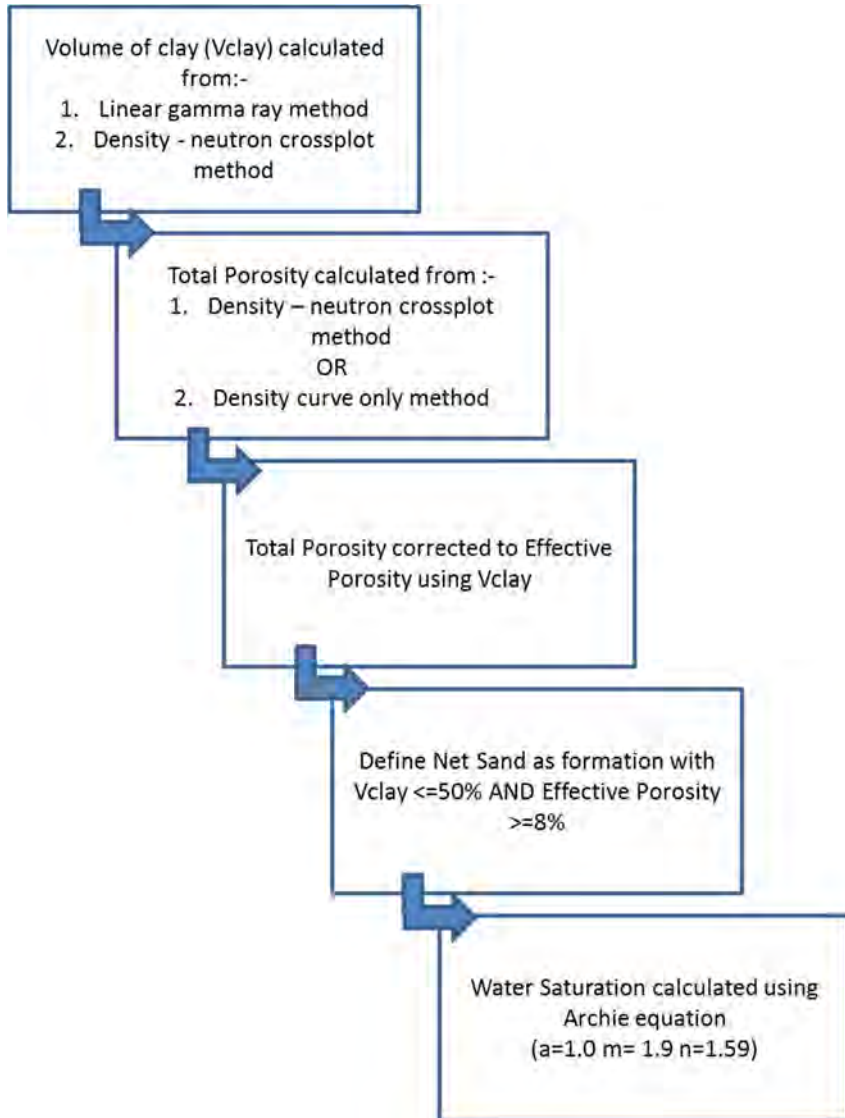
slightly different to those quoted by the operator. For this study it has been assumed that the operator had a more comprehensive database when defining their petrophysical model, on this basis the operators model parameters have been selected for these interpretations ($a = 1.0$, $m = 1.9$, $n = 1.59$).

R_{wa} is calibrated in all the water zones and gives a fairly consistent estimate of formation water resistivity. Formation water resistivity (R_w) is assumed to be 0.0545 at 60 °F for the main area of this study.

For the purposes of quantitative evaluation of reservoir rock properties from wireline logs, a standard oilfield approach to formation evaluation has been adopted. This is outlined in Appendix 8 and illustrated in Figure 3-35.

The results of the petrophysical analysis are summarised below across the wells reviewed. Computer Processed Interpretation (CPI) plots for each analysed well showing derived calculated information are also provided in Appendix 4. Note that the input curves have been provided under CDA license and are not reproduced in this report. Table 3-3 is a summary of the net reservoir properties for the Viking area Lemna Sandstone fairway.

Permeability has not been estimated based on wireline data, but was computed within the primary static model using core based porosity versus permeability relationships (Section 3.5.4).



Well	Zone	Block	Top (ft)	Bottom (ft)	Gross (ft)	Net (ft)	N/G	AvPhi	AvVcl
49/11a-6	A	Fs	10,025	10,151	126	53	0.42	0.089	0.113
49/12-2	A	A	8,771	8,898	127	118	0.92	0.157	0.228
49/12-3	A	A	9,098	9,236	138	125	0.90	0.154	0.038
49/12a-4	A	Fs	9,740	9,875	134	118	0.87	0.110	0.027
49/12a-8	A		11,082	11,518	436	166	0.38	0.129	0.096
49/12a-9	A	Fs	11,029	11,185	156	144	0.92	0.155	0.057
49/12a-A10	A	A	8,838	9,329	491	418	0.85	0.149	0.055
49/12a-A6	A	A	9,750	9,902	152	127	0.83	0.150	0.137
49/12a-F1	A	F	10,688	10,814	126	103	0.82	0.113	0.097
49/12a-K2	A	F	10,245	10,864	619	436	0.70	0.128	0.050
49/12a-K3	A	Fs	11,451	11,624	173	125	0.72	0.101	0.089
49/12a-K4	A	Fs	10,876	11,304	427	189	0.44	0.094	0.132
49/12-K4Z	A	F	10,876	11,304	428	172	0.40	0.095	0.077
49/11a-6	C	Fs	10,222	10,250	28	28	1.00	0.116	0.115
49/12-2	C	A	8,967	9,046	78	75	0.96	0.165	0.140
49/12-3	C	A	9,298	9,387	89	85	0.96	0.136	0.053
49/12a-4	C	Fs	9,965	10,037	72	72	1.00	0.145	0.037
49/12a-9	C	Fs	11,285	11,377	92	92	1.00	0.176	0.018
49/12a-A6	C	A	9,950	9,988	38	8	0.22	0.112	0.131
49/12a-F1	C	F	10,879	10,956	77	65	0.84	0.115	0.095
49/12a-K2	C	F	11,405	11,567	162	150	0.92	0.111	0.042
49/12a-K3	C	Fs	11,804	11,959	155	132	0.85	0.114	0.092
49/12-K4Z	C	F	11,756	12,031	275	1.0	0.004	0.091	0.059
49/11a-6	E	Fs	10,292	10,587	295	265	0.90	0.134	0.096

Figure 3-35 Summary of petrophysical workflow

Well	Zone	Block	Top (ft)	Bottom (ft)	Gross (ft)	Net (ft)	N/G	AvPhi	AVVci
49/12-2	E	A	9,148	9,261	113	107	0.95	0.201	0.069
49/12-3	E	A	9,425	9,592	167	161	0.96	0.133	0.018
49/12a-4	E	Fs	10,087	10,363	276	273	0.99	0.138	0.022
49/12a-9	E	Fs	11,419	11,638	219	214	0.98	0.152	0.044
49/12a-A6	E	A	10,057	10,294	237	185	0.78	0.150	0.142
49/12a-F1	E	F	11,030	11,233	203	195	0.96	0.141	0.033
49/12a-K2	E	F	11,709	12,182	473	362	0.76	0.104	0.044
49/12a-K3	E	Fs	12,069	14,103	2,034	1,680	0.82	0.116	0.126

Table 3-3 Petrophysical summary for injection zones A, C & E

Table 3-3 is a petrophysical summary for the injection zones A,C & E only. A full summary of all zones is provided in Appendix 4.

3.5.1.3 Relative Permeability and Capillary Pressure

There is no specific relative permeability or capillary pressure SCAL data available from the Viking A storage site data set within CDA. This is discussed further in section 3.6.

3.5.1.4 Geomechanics

3D Geomechanical modelling has been completed across the crestal part of the Viking A structure and up into the overburden section. This is outlined in Section 3.7.1.4 and also Appendix 11. This concluded that the risk of geomechanical failure of either the primary storage reservoir or reactivation of faults under the proposed development plan is minimal.

3.5.1.5 Geochemistry

It is anticipated that all geochemical reactions between the existing Leman Sandstone mineralogy and injected CO₂ will be slow (low rate constants for dissolution). The average, quartz-rich, mineralogy of the Leman Sandstone is not considered especially reactive to the CO₂ and, as such, it is not expected that the reservoir sandstones will undergo major mineral volume (porosity) changes due to CO₂ injection.

However, within the reservoir sandstones some minor geochemical reactions will occur with injected CO₂. The authigenic mineral assemblage for the Leman Sandstone commonly includes illite and kaolinite clay minerals, plus early carbonate cements (siderite and dolomite; often partially dissolved during late burial) and anhydrite. Illite and kaolinite are likely to react with the CO₂ and Na-rich formation water and lead to the precipitation of dawsonite (Na-Al carbonate), whilst dolomite may undergo minor dissolution. Any anhydrite will remain stable. The reaction rates will still be slow given the CO₂ injection and storage timescale – relatively little dawsonite is likely to be precipitated even on the 1000's year timeframe.

The vast dominance of unreactive quartz means that there can be relatively little effect on porosity; there should be negligible effects on an injection timescale and only very minor effects even after 10,000 years.

The effect on the permeability of the sandstone is unknown since it is not possible to predict the fabric of the artificially altered rock (by CO₂ injection). It seems likely that any newly formed minerals will sit in pores and block pore throats suggesting that there could be a minor loss of permeability (on a 10,000 year time-scale). It is considered unlikely that reactions in the near-well bore area will impact (reduce) the injectivity.

3.5.2 Primary Caprock

3.5.2.1 Depositional Model

The Lemn Sandstone is directly overlain by a thin interval (~1m) of Kupferschiefer shale, a dark grey anoxic shale which represents the initial flooding of the basin. This in turn is overlain by a thick sequence of Zechstein evaporites, which were extensively deposited across the Southern North Sea.

These evaporites (halites interbedded with anhydrites and carbonates) provide the primary top seal for the Lemn Sandstone and are a proven seal in Southern North Sea gas fields, including the all of the Viking area fields themselves.

The evaporites were deposited following the transgression of the Zechstein Sea due in part to global sea level rise. In the Southern North Sea up to four main evaporite cycles can be recognised (Z1 – Z4). These cycles of limestone -> dolomite-> anhydrite-> halite reflect the influence of increasing salinity due to restricted in flow of sea water.

The extent of the Zechstein and its thickness are shown in Figure 3-24 and Figure 3-25.

3.5.2.2 Rock and Fluid Properties

There are no measured core data available for the overlying Zechstein Group at the site location. Halite and anhydrite are impermeable, and the Zechstein Group provides the top seal for all Lemn Sandstone gas fields in the UK sector of the Southern North Sea. It can therefore be reasonably assumed that the effective porosity and permeability is zero.

3.5.2.3 Relative Permeability and Capillary Pressure

There are no direct capillary pressure measurements available for the cap rock formation of Viking A.

3.5.2.4 Geomechanics

3D Geomechanical modelling has been completed across the crestal part of the Viking A structure and up into the overburden section. This is outlined in Section 3.7.1.4 and also Appendix 11. This work concluded that the risk of geomechanical failure of either the primary caprock or reactivation of faults under the proposed development plan is minimal.

3.5.2.5 Geochemistry

Geochemical modelling of the primary caprocks for the Viking field was carried out to evaluate the likely impact of CO₂ injection on the rock fabric and mineralogy following the injection period and the long term post-closure period. The main objective was to gain a better understanding of the key geochemical risks to injection site operation and security of storage. Specifically, the main objective in this study was to assess if, increasing the volume (partial pressure) of CO₂ in the Lemn Sandstone leads to mineral reactions which result in either an increase or decrease of the porosity and permeability of the overlying Kupferschiefer or Zechstein caprocks.

The approach, methodology used and the results are described in more detail in Appendix 8 but were focussed on one key question:

- Will increasing the amount (partial pressure) of CO₂ in the Lower Permian Lemn sandstone lead to mineral reactions which result in either increase or decrease of porosity and permeability of the Kupferschiefer and Zechstein Group sealing lithologies which overlie the field reservoir sandstones?

A dataset of water and gas compositional data for the Viking Field and the Kupferschiefer and Zechstein Formations and their mineralogy was compiled from both published data and technical reports available in the CDA and the

public domain. These data were then used to establish the pre-CO₂ geochemical conditions in the primary reservoir and the assumption was then made that similar conditions existed in the caprock.

A kinetic study of geochemical reactions in the caprock was then undertaken with appropriate estimates of rock fabric and the selection of appropriate kinetic constants for the identified reactants to evaluate the realistic impact of CO₂ injection with regard to time, using 10,000 years as the target timeframe.

Summary of Geochemical Impact of CO₂ Injection

Kupferschiefer Formation

The main changes modelled in the clay-rich Kupferschiefer caprock are the major dissolution of kaolinite due to CO₂ influx, the relatively minor loss of muscovite (illite) over 10,000 years of addition of CO₂ and the replacement of Mg, Si and Al-bearing chlorite. The products of this clay mineral breakdown are shown by the increase in volume of the quartz, dolomite and dawsonite.

Overall, there is a solid volume increase due to CO₂ flooding of the Kupferschiefer Formation meaning that there is no increase in porosity and thus no increase in permeability. The solid volume increase is considerable, probably leading to significant decrease of porosity and permeability of the top seal. Migration of CO₂ into the Kupferschiefer caprock should not initiate leakage from the top seal.

In the clay-rich Kupferschiefer:

1. The kaolinite and, to a lesser extent illite, react with sodium in the formation water and the incoming CO₂ to create dawsonite and quartz
2. Chlorite reacts to form dolomite (and dawsonite and quartz)

These reactions lead to a solid volume increase thus diminishing porosity and permeability.

Zechstein Group

Three caprock lithologies were modelled for the Zechstein: dolomitic (98% dolomite, 2% anhydrite), anhydritic dolomite (55% anhydrite, 45% dolomite) and anhydrite (98% anhydrite, 2% dolomite). All showed similar results from the kinetic modelling with the main variation relating to the volume of dolomite initially present. Key results are:

1. Dolomite undergoes a small amount of dissolution as CO₂ injection proceeds and pH drops.
2. Sr-sulphate initially forms due to the elevated Sr in the formation water – it then partially dissolves.
3. No change to the volume of anhydrite was observed. No change in halite is anticipated.

Overall, a very small solid volume decrease can be expected with any CO₂ ingress into the Zechstein Group where dolomite is present, meaning that there is a very small increase in porosity. Where dolomite is absent, such as where faults juxtapose Lemna Sandstone against Zechstein Halite or Anhydrite then there is no reaction and no volume change due to the chemical stability of both the anhydrite and halite in the presence of CO₂.

In summary, by flooding the Viking A Lemna Sandstone reservoirs with CO₂, the overlying caprock lithologies are unlikely to be geochemically-affected in a manner which significantly alters the existing permeability character.

The Zechstein may undergo minor dissolution due to the presence of CO₂ where dolomite is present but anhydrite and halite is fully stable.

The combination of Kupferschiefer-loss of porosity and the stability of the anhydrite-dominated Zechstein probably means there is negligible risk of top seal dissolution due to elevated CO₂ concentration in the reservoir.

3.5.3 Secondary Store

The high quality sands of the Triassic Bunter Sandstone Formation of the Bacton Group provide the most likely secondary store above the injection site. It is an extensive sandstone unit that stretches from the Poland, Germany and Denmark in the East, to the UK sector of the Southern North Sea, outcropping UK onshore as the Sherwood Sandstone, and stretching to the East Irish Sea where it is known as the Ormskirk Sandstone.

The thick mudstones and evaporites of the overlying Haisborough Group provide the top seal for the Bunter Sandstone. This includes approximately 10m of Solling Claystone and 60m of Rot Halite immediately above the Bunter Sandstone. The Haisborough Group is laterally extensive and the total thickness is commonly over 500m, only being absent in the very south and north of the basin.

3.5.3.1 Depositional Model

The contraction of the Zechstein Sea during the Early Triassic resulted in the Southern North Sea basin becoming the site of continental clastic sedimentation and the deposition of the Bacton Group. The Permian-Triassic boundary is associated with a distinct facies break where the Bunter shale overlies the Zechstein evaporites.

The thick clay and muds of the Bunter shale represent the maximum extent of an early Triassic playa lake. These were gradually replaced by deposition of the

sands and silts of the Bunter Sandstone, prograding into the centre of the basin as a series of progressive encroachments.

The Bunter Sandstone was deposited in a fluviially dominated environment, mainly as sheet floods on a broad low relief alluvial plain in an arid to semi-arid climate (Ritchie & Pratsides, 1993). Sediments are interpreted as being deposited from the west and southwest, draining into a playa lake towards the north-northeast.

The overlying rocks of the Haisborough Group, which form the top seal, mark the re-establishment of marine conditions and were deposited as distal flood plain and shallow marine, alternating with coastal sabkha.

A full characterisation of the secondary store potential has not been performed and would require further work. It does however provide a combination of further trapping security and also possible upside capacity potential at this location.

3.5.4 Static Modelling

Three static geological models have been developed as part of the characterisation effort of the Viking A site:

- **Primary Static Model** – The primary static model has been built over an area which includes the north Viking gas fields (A, F, Fs and H fields) only. The purpose of this model is to serve as the basis for building an effective reservoir simulation model over the site.
- **Fairway Model** – The fairway model is semi regional in nature and covers the full Viking fields area. The purpose of this model is to characterise the full area.
- **Overburden model** – The overburden model builds upon the footprint of the primary static model, but extends to describe the

overburden geology. The model is primarily used for consideration of containment issues which are detailed in Section 3.7.

3.5.4.1 Primary Static Model (Site)

Grid Definition

The static model described in this section focuses on the site geological model for the north Viking area which comprises of A, H, F and Fs accumulations. A map of Top Lemman Sandstone for the modelled site area is shown in Figure 3-27.

The area selected for the site model covers an approximate area of 17km x 6.5km, the coordinates of the site model boundary are:

X Min 442817.49 X Max 458767.49

Y Min 5922031.13 Y Max 5938981.13

Reservoir modelling has been carried out using Petrel v2014.

The reference system used ED50 (UTM31).

The stratigraphic interval for the site model is from 60 m (200 ft) above the Top Lemman Sandstone to the Top Carboniferous, the Lemman Sandstone interval has an average thickness of approximately 235 m (770 ft) thick. The primary seal for the Lemman Sandstone interval is the overlying Zechstein. The stratigraphic definition of the primary static model is outlined in Table 3-4, and is based upon the zonation scheme defined during the well correlation.

Horizon	Zone	Source	Number of Layers
Top Model	Zechstein	Calculated as 60 m (200 ft) above Top Lemman	1
Top Lemman Sst	Zone A	Direct seismic interpretation and depth conversion	28
Top Zone B	Zone B	Built down from Top Lemman using well derived thickness (Isochore)	12
Top Zone C	Zone C	Built down from Top Zone B using well derived thickness (Isochore)	28
Top Zone D	Zone D	Built down from Top Zone C using well derived thickness (Isochore)	12
Top Zone E	Zone E	Built down from Top Zone D using well derived thickness (Isochore)	40
Top Carboniferous	-	Built down from Top Zone E using well derived thickness (Isochore)	-

Table 3-4 Stratigraphy, zonation and layering for the primary static model

The Top Lemman Sandstone depth horizon within the static model was created from the depth surface interpreted from the seismic and time to depth converted (Section 3.4). The depth horizon has been tied to the well tops using a radius of 800 m.

The top of the model is taken as an arbitrary 60 m (200 ft) above the Top Lemman Sandstone and was generated by subtracting 60 m (200 ft) from the Top Lemman Sandstone depth surface. This is included in the model as a single layer.

The horizons below Top Lemman (Top Zone B – Top Zone E, Top Carboniferous) have been calculated from well thickness information, derived from the well correlation.

There are 39 faults which have been interpreted and incorporated into the site model, these fall within two major fault trends. The dominant trend is NW-SE, with a second minor NNE-SSW trend.

A cross section through the structure showing the different zones and layering within the model through 49/12-2 is shown in Figure 3-36.

The primary static model 3D grid was built with a rotation of 41° and grid cells of 100m x 100m in the X, Y direction. The resulting grid has approximately 1.8 million grid cells.

Proportional layering has been used for all zones. The number of layers has been selected in order to effectively model the geological heterogeneity, specifically capturing the thin sabkha / silts observed in the well data. The layering per zone is shown in Table 3-4.

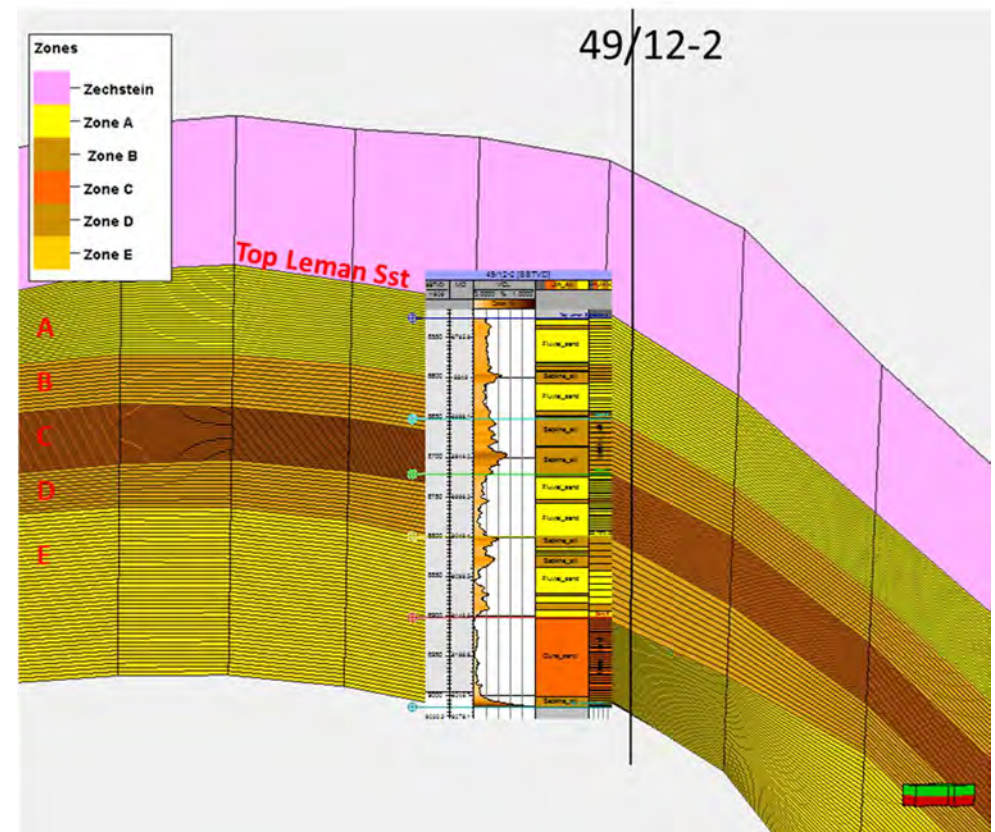


Figure 3-36 Cross section through the 3D grid at well 49/12-2 showing the layering within the static model

3.5.4.2 *Property Modelling*

As described in Section 3.5, the Leman Sandstone was deposited in an arid environment and consists of aeolian and fluvial sandstones interbedded with sabkha facies.

The Leman Sandstone zones A, C and E are high NTG sand dominated intervals. These are separated by two poor quality, low NTG, sabkha dominated intervals representing wet cycles which can be correlated across the North Viking area (Zones B and D). These form horizontal barriers to vertical flow between the zones.

Within the high NTG zones interbedded sabkha facies represent local baffles to flow through the otherwise clean, good quality sands. To allow for the impact of these baffles to be captured within the static model a facies model has been built.

Reservoir quality varies across the different fault blocks within the Viking fields area, with porosity and permeability reduced within the F and Fs blocks.

The porosity and permeability for blocks A/ H and F/ Fs have been modelled separately due to their different reservoir quality characteristics. The results are then combined to give the final property result.

Porosity calculations have been constrained to the facies model using the available interpreted PHIE log.

Permeability has been modelled within the 3D grid using the available measured core data and correlated to the modelled porosity.

NTG is not explicitly modelled and is a function of the distribution of net (sand) and non-net (sabkha/ silt) facies.

3.5.4.3 *Facies Log Interpretation*

There is a limited amount of core data available across the Viking A site area. A lithology log has been created using a combination of interpreted Vclay log cutoffs, with QC and manual interpretation using additional wireline data (neutron, density) where available. The Vclay cut-off varies by zone and well, it has been calibrated against the log response observed in the full wireline suite and core reports where available.

Sand facies are identified as those with a clean (low) Vclay signature, separation of the neutron density logs and good porosity. The sand facies classification (dune or fluvial) is based upon the dominant facies within the zone as described in core. A summary of the Vclay cut-offs used for the Viking A wells is shown in Table 3-5.

	Zone A	Zone B	Zone C	Zone D	Zone E
49/12-2	0.25	0.25	0.25	0.20	0.15
49/12-A6	0.20	0.15	0.25	0.20	0.15
49/12-A10	0.15	0.15	0.25	0.20	0.15
49/12-3A	0.15	0.20	0.25	0.20	0.15

Table 3-5 VClay cut-offs used to help define facies log

The raw lithology curve is generated at the sample rate of 0.15 m (0.5 ft), this has been upscaled into the modelling grid using the ‘most of’ upscaling method. The upscaling has been weighted to ensure that a representative proportion of the thin sabkha silts have been captured within the gridded model.

Facies logs have been calculated for the wells shown in Table 3-6, and these have been used to control the facies modelling:

Viking A	Viking F	Viking Fs
49/12-2	49/11a-6	49/12a-K2
49/12-A6	49/12a-K3	49/12a-K5
49/12-A10	49/12a-K4Z	49/12a-4
49/12-3	49/12a-9	49/12a-F2
		49/12a-F4
		49/12a-F1

Table 3-6 Wells in Viking A, F and Fs used for facies and porosity modelling

An example of the lithology log and upscaled lithology log from well 49/12-3A is shown in Figure 3-37.



Figure 3-37 Example of facies interpretation in well 49/12-3

3.5.4.4 *Facies Modelling*

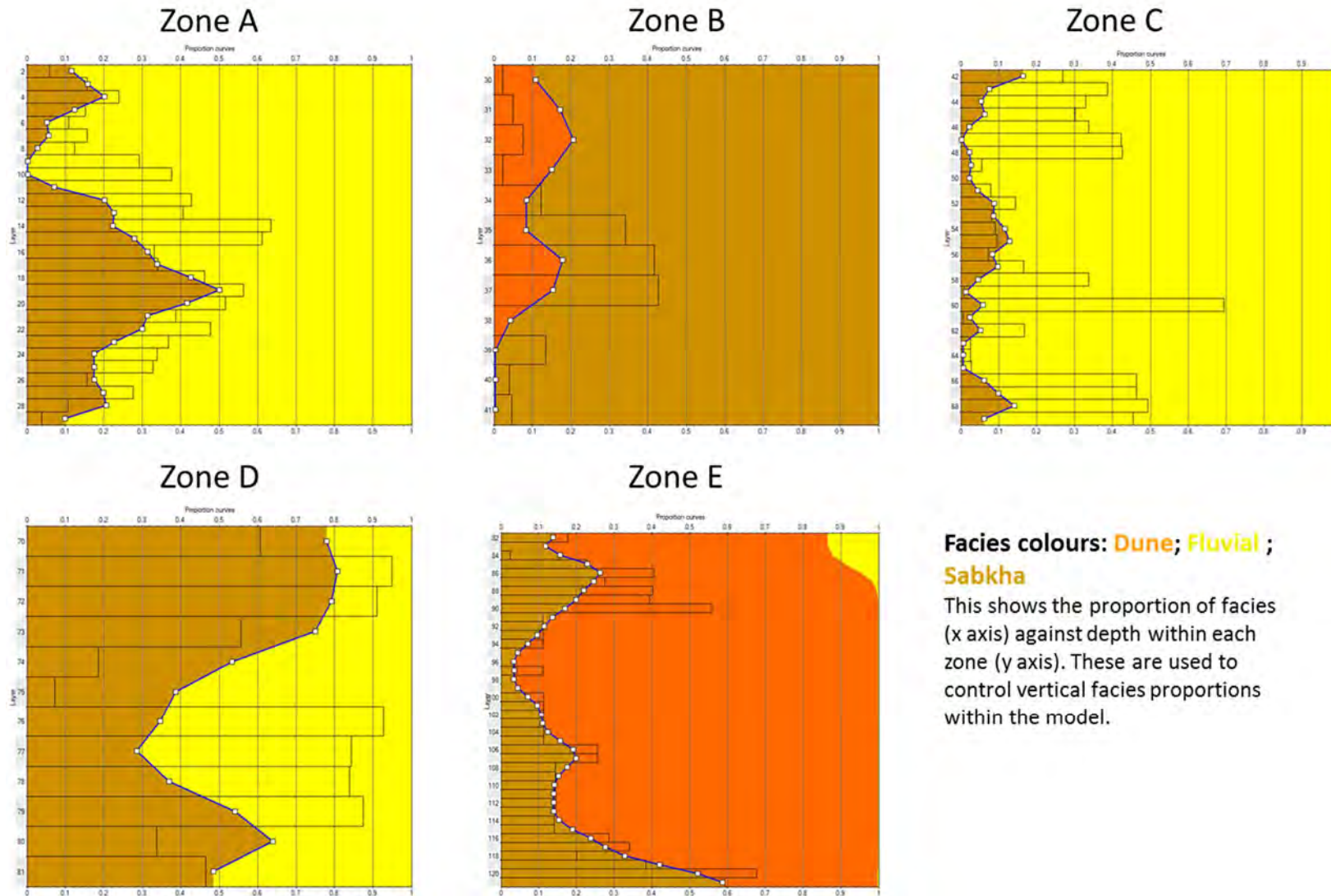
The dune, fluvial and sabkha facies have been modelled in each zone using the Sequential Indicator Simulation (SIS). The chosen length and orientation of the variograms for each facies type have been selected based on the depositional environment.

With transverse dunes and palaeowinds mainly from the east or south east, dunes would have their long axis orientated NE-SW. It is expected that any fluvial/ wadi deposition would be towards the silverpit basin in the North (i.e. long axis NE-SW).

The proportion of each facies modelled has been calculated based on well data within the site area, for each zone in the model. The vertical distribution of facies within each zone is controlled by vertical proportion curves, calculated from the well data (Figure 3-38). Within the site model area lateral facies trends have not been interpreted or used within the modelling.

The orientation of the long axis of the sabkha silts, dune and fluvial sands has been aligned with the depositional direction, approximately NE-SW. Variogram ranges, orientations and modelled proportions are summarised in Table 3-7.

Cross sections and layer slices through the facies model are shown in Figure 3-39.



Facies colours: Dune; Fluvial ; Sabkha

This shows the proportion of facies (x axis) against depth within each zone (y axis). These are used to control vertical facies proportions within the model.

Figure 3-38 Vertical proportion curves generated from wells within the site model

Zone	Facies	Method	Variogram type	Orientation[Degrees]	Major width[m]	Minor width[m]	Modelled Volume %
Zone A	Sabkha	SIS	Spherical	10	6000	3000	20
	Sand	SIS	Spherical	10	6000	3000	80
Zone B	Sabkha	SIS	Spherical	10	6000	3000	88
	Dune Sand	SIS	Spherical	10	2000	3000	12
Zone C	Sabkha	SIS	Spherical	10	6000	3000	8
	Dune Sand	SIS	Spherical	10	2000	1000	2
	Fluvial Sand	SIS	Spherical	10	6000	3000	90
Zone D	Sabkha	SIS	Spherical	10	6000	3000	57
	Fluvial Sand	SIS	Spherical	10	6000	3000	42
Zone E	Sabkha	SIS	Spherical	10	6000	3000	19
	Dune Sand	SIS	Spherical	10	2000	1000	79
	Fluvial Sand	SIS	Spherical	10	6000	3000	2

Table 3-7 Input properties and final modelled proportions for facies modelling

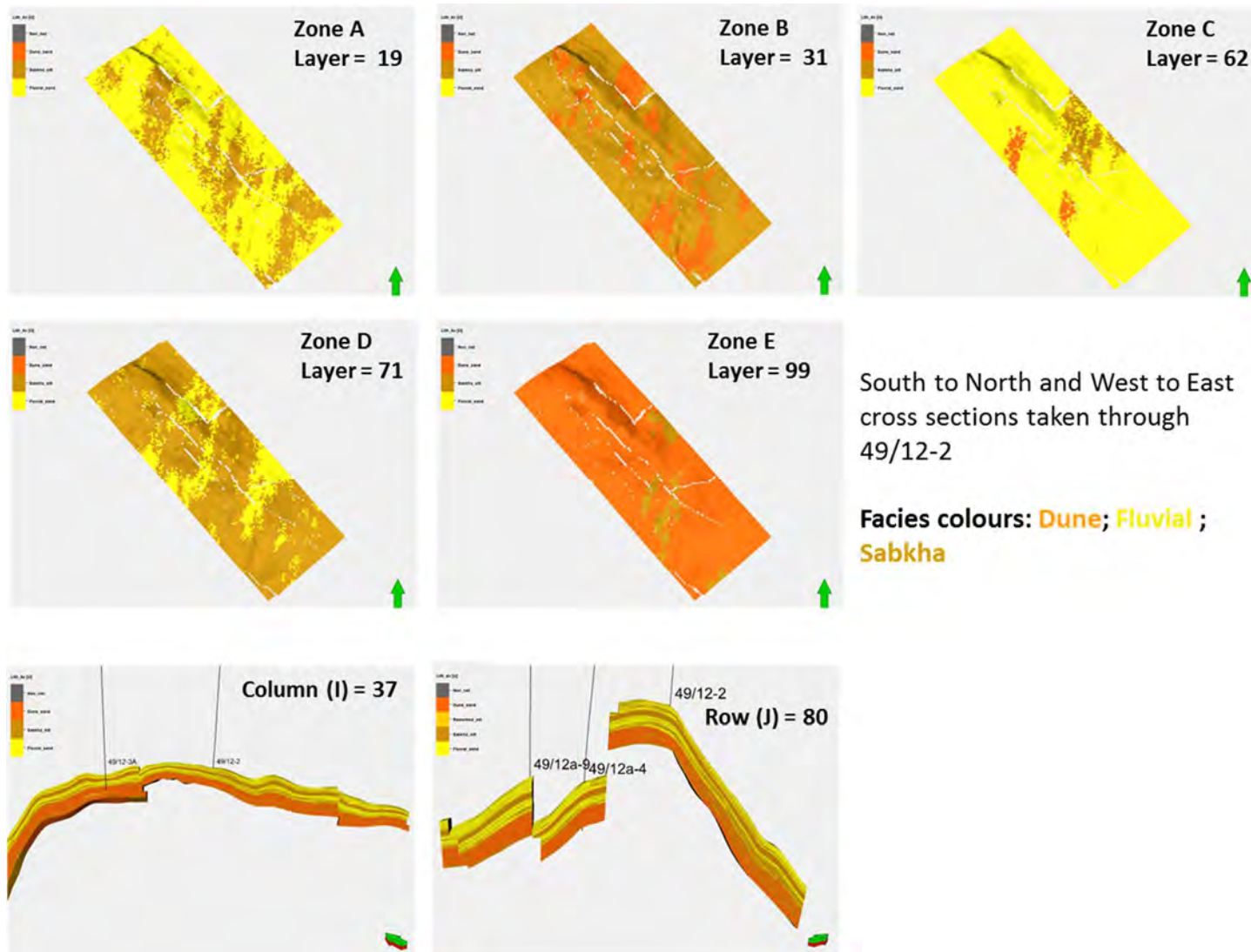


Figure 3-39 Cross sections and layer slices through the reference case facies model

3.5.4.5 Porosity Modelling

The interpreted PHIE log was upscaled to the grid scale using arithmetic averages, biased to the interpreted facies logs. This ensures that the porosity distribution (mean and standard deviation) for each facies is correct. Blocks A/ H and F/ Fs have been modelled separately due to their different burial histories and reservoir quality characteristics. The final results were combined into a single porosity model.

Table 3-6 shows the wells used for input to the porosity modelling.

Porosity modelling was performed for each zone. Properties within the sand facies were distributed in the model, between wells, using a Sequential Gaussian Simulation method (SGS) and constrained to the facies model. This ensures that the property distributions (mean and standard deviation) in the original log porosity data are maintained in the final model. Due to the low porosity and permeability of the sabkha facies, these were assumed to be non-net and assigned porosity values of 0%.

Settings for the SGS modelling of the sand facies porosity are shown in Table 3-8.

In addition to the well data and facies model, the distribution of porosity within each zone is also controlled by depth trends where observed in the original well log data. Where present these are not significant.

A histogram showing a comparison of the porosity well log input versus the modelled porosity for the sand facies is shown in Figure 3-40.

A comparison of average modelled porosity versus average well porosity, by zone for Viking A, is shown in Table 3-9.

Facies	Type	Major Axis [m]	Minor Axis [m]	Vertical [m]	Azimuth [deg]
Dune sand	Spherical	2000	1000	10	10
Fluvial sand	Spherical	6000	3000	20	10
Sabkha silt	Spherical	6000	3000	20	10

Table 3-8 Input setting for porosity and permeability SGS modelling

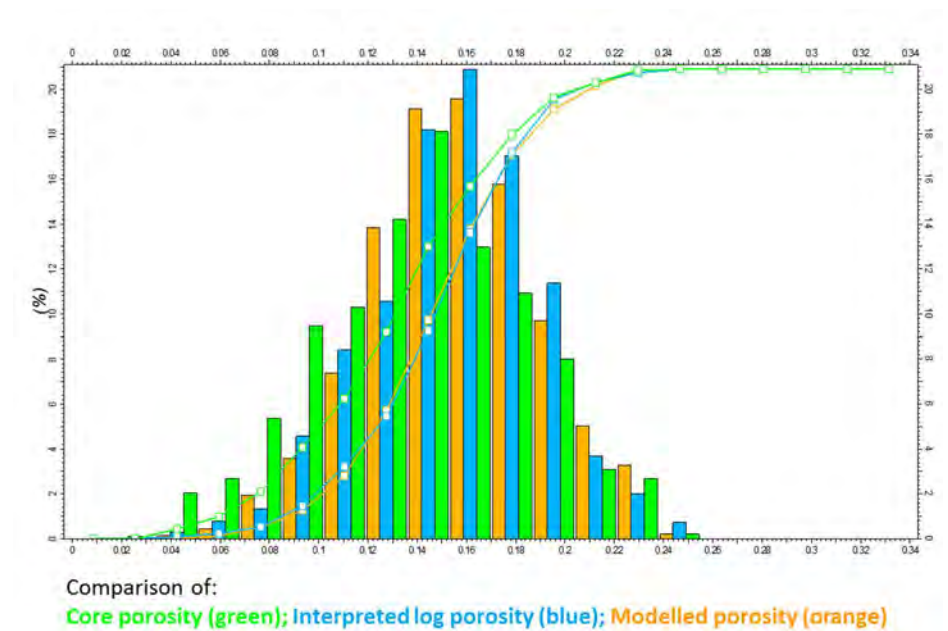


Figure 3-40 Histogram of porosity within sand facies, Viking A, All zones

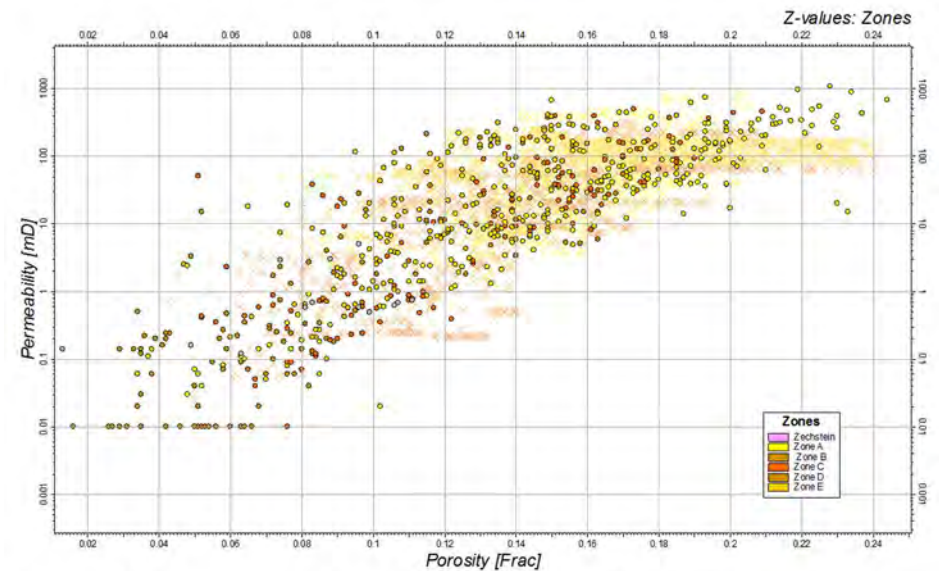
Zone	Wells	Model
Zone A	0.16	0.16
Zone B	0.13	0.14
Zone C	0.15	0.15
Zone D	0.14	0.13
Zone E	0.16	0.16
All zones	0.16	0.16

Table 3-9 Average sand porosity per zone within Viking A

3.5.4.6 Permeability Modelling

A strong positive correlation between the measured core porosity and core permeability is observed. Horizontal permeability within the sand facies is modelled using a bivariate distribution method, allowing for this correlation and distribution to be used directly and ensure that the final permeability distribution matches that of the measure core data. The modelled porosity is used as a secondary property input, ensuring that the resulting permeability model also remains correlated with the modelled porosity, i.e. a cell with a high porosity will have a high permeability. The variogram settings used are the same as those used for the porosity modelling. The sabkha facies were given a permeability of 0 mD.

A cross plot of porosity versus permeability for both the measure core data and final modelled data are shown in Figure 3-41.



Comparison of core measurements (circle) versus modelled results (cross)

Figure 3-41 Cross plot of porosity versus permeability, coloured by zone

The average horizontal permeability from core within Viking A is 87 mD which compares to the average modelled horizontal permeability of 83 mD. A histogram showing the modelled horizontal permeability for Viking A is shown in Figure 3-42.

The average horizontal permeability values within the sand facies for Viking A are shown in Table 3-10.

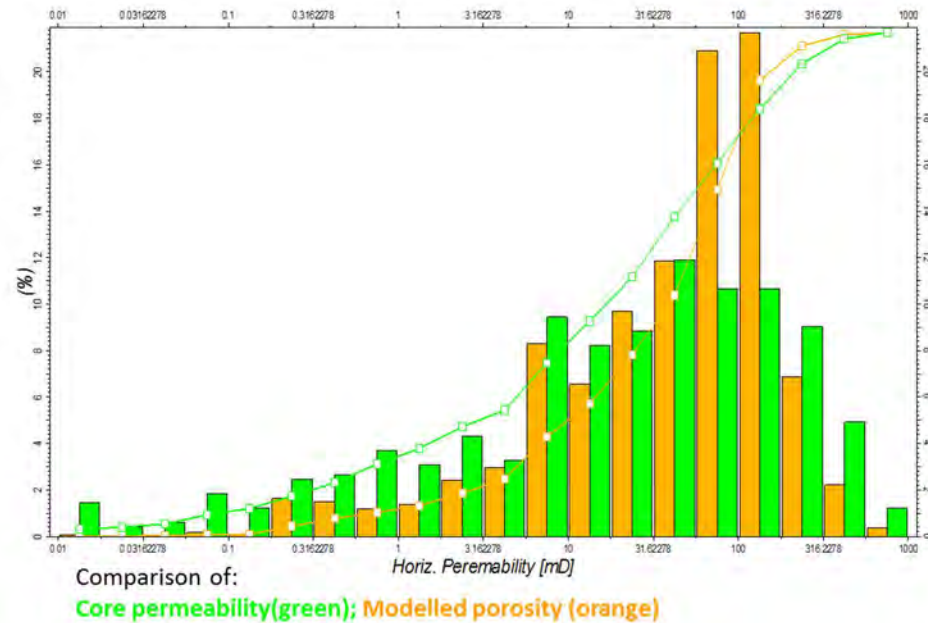


Figure 3-42 Histogram of horizontal permeability within sand facies, Viking A all zones

Zone	Hor. Perm.
Zone A	96 mD
Zone B	39 mD
Zone C	60 mD
Zone D	12 mD
Zone E	102 mD
All Zones	83 mD

Table 3-10 Average horizontal sand permeability within Viking A

A strong relationship exists between horizontal and vertical permeability at the core scale. This has been incorporated into the model through the use of a function, derived from core data, which has been applied directly to the modelled horizontal permeability (Figure 3-43). The function used is shown below.

$$\text{Vertical Permeability} = 10^{(0.831262 \cdot \text{Log}(\text{Horiz Permeability}) - 0.203608)}$$

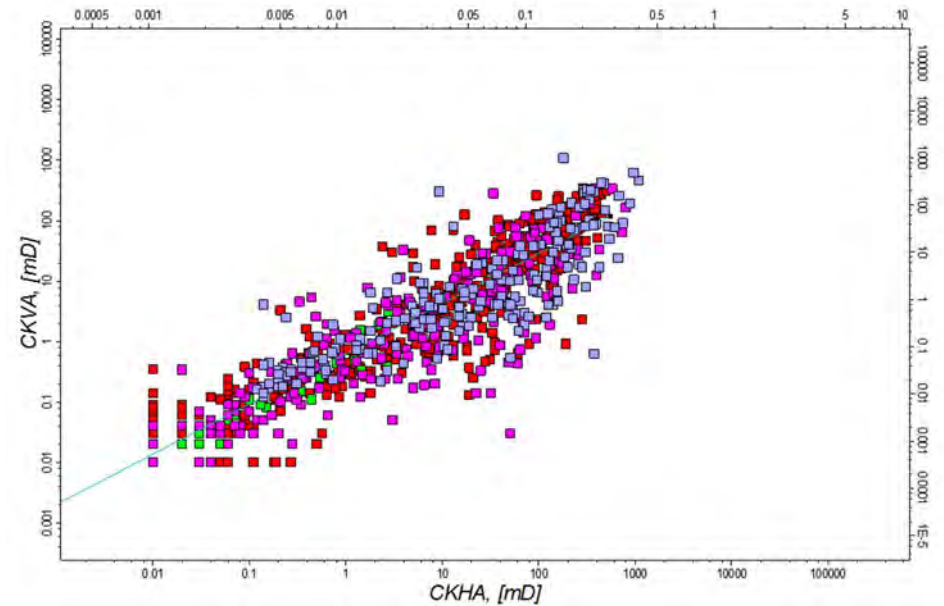


Figure 3-43 Cross plot of horizontal versus vertical core permeability (log scale), coloured by well

Average vertical permeability and Kv/ Kh per facies, at the static model scale, within Viking A are shown in Table 3-11.

	Kv [mD]	Kv/ Kh
Fluvial	73	0.81
Dune	98.8	0.83

Table 3-11 Average modelled vertical permeability values and Kv/Kh for each facies within Viking A

3.5.4.7 Water Saturation (Sw) Modelling

Modelling of initial reservoir Sw was carried out directly in the model using capillary pressure based method (Leverett J Function) generated during the petrophysical analysis from the available SCAL data. This is a standard oilfield approach and is documented in more detail in Appendix 8.

The Sw function used is:

$$SW_j = \left(6.1204 \times \text{Height} \times 0.0314 \times \sqrt{\frac{K}{\phi}} \right)^{-0.2828}$$

Height = Height above the GWC in feet.

3.5.4.8 Static Volumes

Initial gas in place volumes have been calculated for each of the fault blocks within the static model, using the operators quoted GWC.

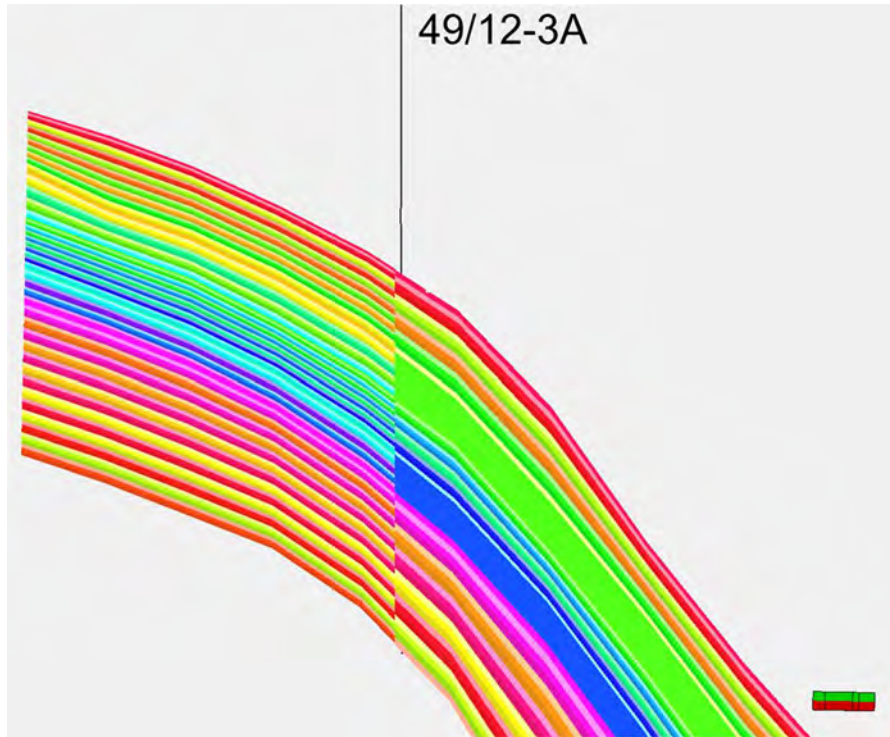
Blocks	Gas Water Contact	Bulk volume	Pore volume	GIIP
	(ft TVDSS)	[*10^6 rm^3]	[*10^6 rm^3]	[Bscf]
Viking A	9680	1654	211	1542
Viking H	9680	362	48	338
Viking F	10103	356	34	222
Viking Fs	10125	508	46	254
Total		2880	339	2356

Table 3-12 Gross rock, pore volumes and GIIP for North Viking site model

3.5.4.9 Simulation Model Gridding and Upscaling

To enable dynamic simulation models to run within a reasonable time frame, a coarser simulation grid and model was generated. Vertical coarsening from 121 layers in the static model to 51 layers in the dynamic model has been used to reduce the number of cells from approximately 1.8 million to 938,556. The area of interest (6.5km x 17km), zonation (5 zones within Leman Sandstone), lateral cell size (100m x 100m), and grid orientation (41°) remain the same as the finer scale static model.

A comparison of the layering between static and dynamic models is shown in Figure 3-44. The layering scheme is summarised in Table 3-13.



A check of static model versus dynamic model pore volumes was carried out and the difference was less than 1%.

Zone	Number of Layers Static Model	Dynamic Model Layers
Above reservoir	1	1
Zone A	28	14
Zone B	12	1
Zone C	28	14
Zone D	12	1
Zone E	40	20

Table 3-13 Summary of static and dynamic model layer numbers

Figure 3-44 W-E cross section through well 49/12-3A comparing static model (left) to dynamic model (right) layering

Porosity, horizontal permeability and vertical permeability have been upscaled (averaged) from the fine scale grid into the coarser scale simulation grid using standard hydrocarbon industry upscaling methods.

- Porosity: Volume weighted arithmetic average
- Horizontal Permeability: Volume weighted arithmetic average
- Vertical Permeability: Volume weighted harmonic average

3.5.5 Fairway Static Model

A fairway static model has been built which covers the full Viking fields area (Figure 3-27). This covers an area of approximately 29 km x 16 km. The purpose of this model is to characterise the Viking fields area. The stratigraphic interval for the site model is from 60 m (200 ft) above the Top Leman Sandstone to the Top Carboniferous.

The model stratigraphy is shown in Table 3-14; this is the same zonation used for the primary static model and is based upon the zonation scheme defined during the well correlation.

The fairway model 3D grid was built with a rotation of 41° and grid cells of 200m x 200m in the X, Y direction. The number of cells has been kept to a minimum due to the regional scale of the model. Proportional layering has been used for all zones, the layering per zone is shown in Table 3-14. The resulting grid has approximately 1.08 million grid cells. A total of 72 faults have been incorporated into the model.

At this time the fairway model has not been used to assess plume mobility into other areas outside Viking A as the proposed development plan has been designed to retain all the injected CO₂ within original gas field closure. No migration of CO₂ into other structures is envisaged.

Horizon	Zone	Source	Number of Layers
Top Model	Zechstein	Calculated as 60 m (200 ft) above Top Leman	1
Top Leman Sst	Zone A	Direct seismic interpretation and depth conversion	14
Top Zone B	Zone B	Built down from Top Leman using well derived thickness (Isochore)	1
Top Zone C	Zone C	Built down from Top Zone B using well derived thickness (Isochore)	14
Top Zone D	Zone D	Built down from Top Zone C using well derived thickness (Isochore)	12
Top Zone E	Zone E	Built down from Top Zone D using well derived thickness (Isochore)	20
Top Carboniferous	-	Built down from Top Zone E using well derived thickness (Isochore)	-

Table 3-14 Stratigraphy, zonation and layering for the Fairway model

3.5.5.1 Property Modelling

Due to the regional focus of the fairway model, no facies modelling was carried out. Net to Gross (NTG) and net porosity have been modelled using available interpreted well log data.

Permeability has been modelled using available measured core data, correlated to porosity.

3.5.5.2 NTG and Porosity Modelling

Full petrophysical analysis was only carried out for a limited number of wells, and was focused on the storage site model area (Section 3.5.4). To enable the fairway model to be built, density porosity was calculated for additional wells across the Viking fields complex area (those wells which contained a density log were used).

For the purposes of the fairway modelling, a NTG log was calculated based on an 8% porosity cut-off (i.e. NTG= 1 where Porosity >= 8%). This has then been used to generate a net porosity log, which is used for the modelling of porosity.

In total 17 wells have been used for the modelling of NTG and porosity in the fairway model (Table 3-15), with zones A, H, F and Fs also being in the site model.

Block	Wells Used in Modelling
Viking A	49/12-3A, 49/12-2, 49/12-A10, 49/12-A6
Viking F	49/12a-K2, 49/12a-F1, 49/12a-F2, 49/12a-F4
Viking Fs	49/12a-F3, 49/11a-6, 49/12a-K3, 49/12a-K4z, 49/12a-9
Viking B	49/17-B3, 49/17-B4, 49/17-1
Viking D	49/17-2
Viking E	49/16-3, 49/16-E2A, 49/16-E1
Viking G	49/17-G4, 49/17-G5, 49/17-G2

Table 3-15 Wells used in fairway model

NTG and porosity modelling is performed separately for each zone. The central Viking fault blocks were also modelled separately due to their different poro-perm characteristics. The results have then been combined to give a final property result.

Within the Lemna Sandstone the NTG and net porosity log data have been upscaled to the grid scale using arithmetic averages and distributed between wells using Sequential Gaussian Simulation method (SGS), a standard hydrocarbon field modelling method. This ensures that the property distributions (mean and standard deviation) in the original logs are maintained in the final model.

NTG and Porosity in the overlying Zechstein (seal) interval have been modelled as 0.

Settings for the SGS were the same for both NTG and porosity, and are shown in Table 3-16.

Type	Major Axis [m]	Minor Axis [m]	Vertical [m]	Azimuth [deg]
Spherical	3000	1500	25	10

Table 3-16 Input setting for NTG and porosity SGS modelling

The fairway model has also been calibrated and checked against the site model to ensure consistency.

3.5.5.3 Permeability Modelling

Permeability has been modelled within the 3D grid using the available measured core data, correlated to the modelled porosity.

Within the central Viking area, there is a significant reduction in permeability, this is believed to be due to the Rotliegend formations in this area originally being buried to much greater depths than the neighbouring areas, prior to subsequent inversion (Riches, 2003). Figure 3-45 shows a cross plot of core porosity versus core permeability for the north Viking area and the central Viking wells. These correlations have been used to model the permeability data for the central Viking area and the rest of the Viking complex.

Core permeability data at the wells has been upscaled using an arithmetic average. Horizontal permeability is distributed between wells using Sequential Gaussian Simulation method (SGS), a co-simulation option is used to ensure the strong correlation between porosity and permeability is maintained. As with NTG and porosity, the Central Viking fault block was modelled separately due to the different poro-perm relationship, the results have then been combined to give a final horizontal permeability model.

Average permeability within central Viking is 2.5 mD compared to 195 mD for the rest of the Viking fields area.

Final properties for the fairway model are shown in Figure 3-46.

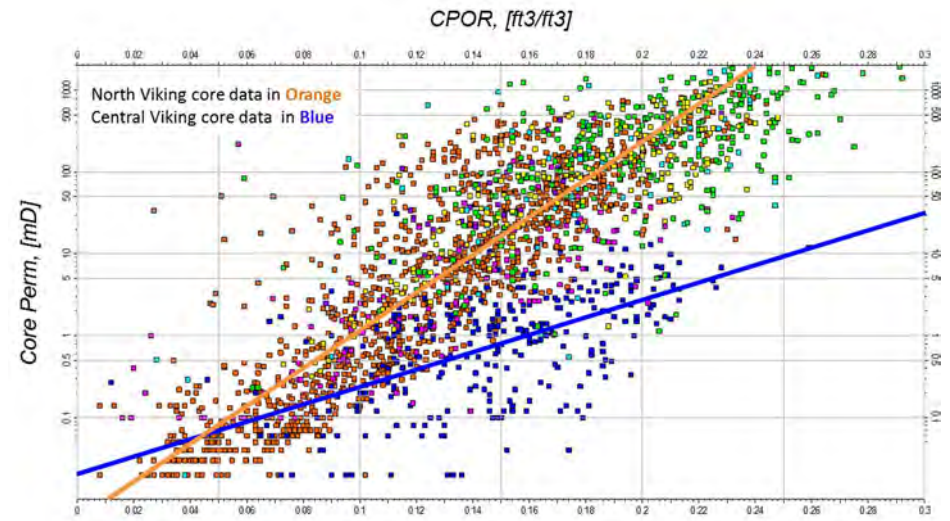


Figure 3-45 Cross plot of porosity versus permeability for all Viking fields

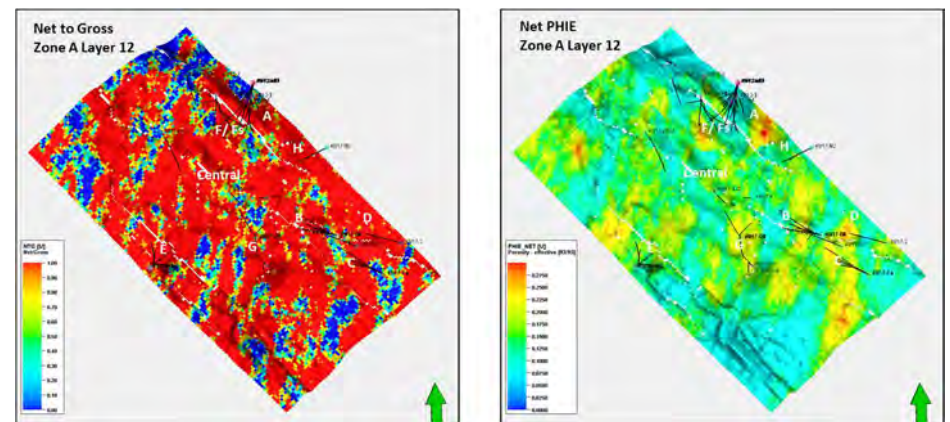


Figure 3-46 Layer Slices through fairway property models NTG, porosity

3.5.6 Probabilistic Volumetrics

The sensitivity analyses in the static and dynamic modelling work have provided a range of estimates for rock volume, pore volume and dynamic CO₂ storage capacity. The complexity of the models and the number of variables conspire to make a full exploration of this uncertainty space impractical. A simple probabilistic approach to estimation has been adopted to provide a context within which the specific runs from the static and dynamic modelling can be considered.

The approach used has been adopted from oil and gas industry practice for the estimation of oil and gas volume estimates where:

$$\text{STOIP} = \text{GRV} \times \text{NGR} \times \text{PHI} \times (1-\text{SW}) \times \text{Bo}$$

Where:

STOIP - Stock tank oil initially in place.

GRV - Gross rock volume - the geometric volume of the gross reservoir interval from its top surface to the deepest level that contains hydrocarbons.

NGR - Net to gross ratio - The average vertical proportion of the gross reservoir interval that can be considered to be effective (net) reservoir.

PHI - The average effective porosity of the net reservoir volume.

SW - The average proportion of the net reservoir volume pore space that is saturated with water.

Bo - The shrinkage (oil) or expansion (gas) factor to convert the hydrocarbon volumes from reservoir conditions to surface conditions.

This equation has been modified here to be:

$$\text{Dynamic Capacity} = \text{GRV} \times \text{NGR} \times \text{PHI} \times \text{CO}_2 \text{ Density} \times E$$

Where:

CO₂ Density - the average density of CO₂ in the store at the end of the injection period.

E - the Dynamic storage efficiency which is the volume proportion of pore space within the target storage reservoir volume that can be filled with CO₂ given the development options considered.

To consider probabilistic estimations of capacity, a Monte Carlo model has been developed around this equation. Each input parameter is described by a simple probability distribution function and then each of these is sampled many times to calculate a large range of possible dynamic capacity estimates.

The input to the calculation and the results are outlined below.

3.5.6.1 Gross Rock Volume

For the purposes of this calculation, the gross rock volume is the potential gross storage reservoir with an uncertainty of +/- 20% due to the depth conversion and connected volume and in particular the uncertainties regarding fault positioning with the current seismic data. A simple triangular distribution is assumed weighted heavily to a reference case volume of 1654*10⁶ m³.

3.5.6.2 Net to Gross Ratio

An average net to gross ratio of 80% for the closure has been extracted from the static model. This is derived from an interpolation of the petrophysics from well control throughout the model appropriately weighted to the gas bearing zone. An upper and lower value of 90% and 70% have been assigned from consideration of the well data in the area.

At this stage, the project has assumed a 10% porosity cut-off value to differentiate net from non net and therefore NTG but does recognise that this will ultimately depend on the commercial arrangements of the development. NTG cut-off is actually a commercial consideration. In oil and gas developments it is also a function of oil price. In a high oil price regime NTG cut off might be lower than 10% whilst in a low oil price regime it can be much greater than 10%.

3.5.6.3 Porosity

An average porosity of 16% has been extracted from the static model. This is derived from an interpolation of the petrophysics from well control. A triangular distribution has been assumed with a small variance from 13% to 19%.

3.5.6.4 CO₂ Density

A range of 0.77 to 0.79 and 0.81 tonnes/m³ was established after consideration of low and high ranges of final temperature and pressure at the end of the injection cycle for the midpoint of the storage reservoir using an equation of state to compute the CO₂ density. A simple triangular distribution has been used.

3.5.6.5 Dynamic Storage Efficiency

Since each dynamic model run is based upon the same model volume, the results can be used to extract estimates of E, the dynamic storage efficiency factor. This accounts for the average CO₂ saturation achieved in each dynamic simulation together with the vertical and areal sweep efficiency. It also fully accounts for limiting factors such as the fracture pressure limit. In the Viking A storage project, the dynamic storage efficiency is tightly constrained at around 0.78 to 0.8 as a result of the ready diffusion of the injected CO₂ into the space occupied by low pressure natural gas. These efficiencies are very high as a result of the very high recovery factor experienced with gas production and the fact that the development plan has not had to displace water to inject CO₂. High

mobility associated with the initial injection in super-critical phase also support these high efficiencies. There was one dynamic model run with a much lower injected inventory, this describes a situation where the fracture pressure does not recover from its reduced value at the point of maximum pressure depletion. Whilst considered to be very unlikely, if there was an issue such as this which made the transition from super-critical phase to liquid phase injection complex or costly, then a much smaller dynamic storage efficiency factor can be anticipated of perhaps 0.49. This is captured in the Monte Carlo outcomes.

Well by well production and pressure data are not available to this project, but some pressure data have been published and were used to match performance over production time (Section 3.6.7).

3.5.6.6 Probabilistic Volumetric Results

Figure 3-47 captures the inputs and outputs of the Monte Carlo assessment of dynamic CO₂ storage capacity for the Viking A storage site. The P90 value (i.e 90% chance of exceeding) is 107MT, with P50 (50% chance of exceeding) of 128MT and a P10 (10% chance of exceeding) of 150MT. These numbers provide the context for the “deterministic” estimates from the dynamic modelling work for the “development reference case” of 130MT.

This shows that whilst there is downside capacity uncertainty with the proposed development plan which is largely associated with the risk of complexities arising from the transition between gas and liquid phase injection, there is at the same time, very little upside anticipated within Viking A itself. This is because of the confidence in the accessible pore space volume which has been provided by the matching of the volume to the historical production data.

Since there is no formalised resource classification system currently in use by the CCS industry for CO₂ storage resources, a scheme has been adopted from

the SPE petroleum resource world (Society of Petroleum Engineers, 2000) and is outlined in Figure 3-48.

There are no CO₂ storage reserves currently assessed for the Viking A storage site. The resource base cannot be considered to be commercial at this time as FID has not been concluded and there is no commercial contract in place for its development with an emitter. As a result, the assessed volumes all fall within the sub-commercial contingent resources category. The storage site is of course proven and there is excellent evidence from wells, seismic and very importantly historical production data that the site could be developed. Without a matched emissions point the resource has been characterised on the basis of this probabilistic assessment as:

“Contingent Resources – Development unclarified”

1C – 107MT – P90

2C – 128MT – P50

3C – 150MT – P10

The full scope of the probabilistic dynamic CO₂ storage capacity ranges from a P100 of 64MT to a P0 of 190MT.

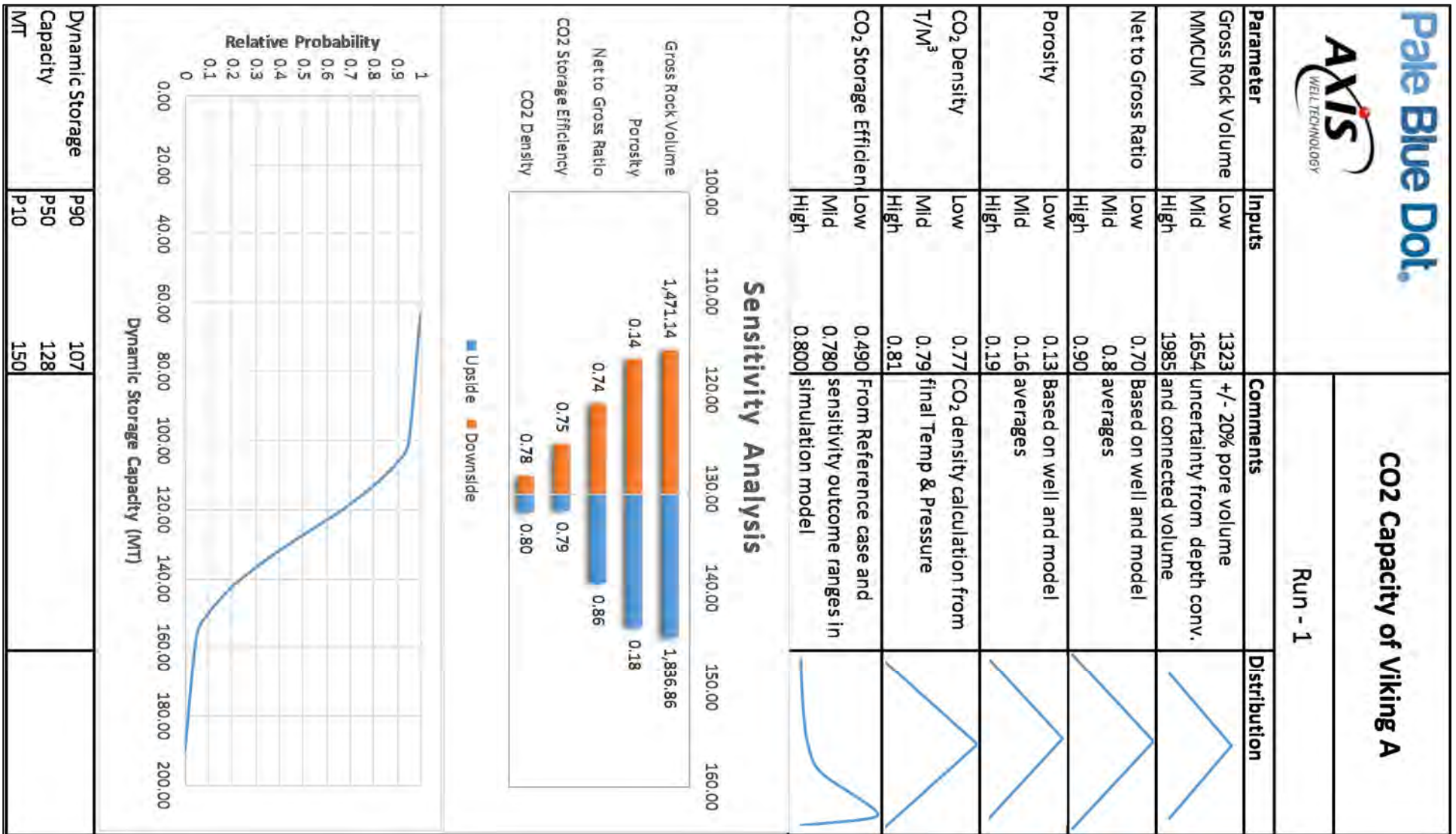


Figure 3-47 Probabilistic volumetric results

CO2 Storage Resource Classification					<- Increasing Confidence in Capacity Estimation									
					Proved	P90	Probable	P50	Possible	P10			Narrative - Key Events	
Increasing maturity and chance of commerciality ->	Total Theoretical Capacity	Discovered Pore Space	Commercial	Injected Inventory	Actual Metered						Practical Storage Capacity	Narrative - Key Events		
				Reserves	On Injection							At the end of Injection Operations		
				Approved for Development	Matched Storage Capacity							Based upon injected inventory		
			Justified for Development	1P	2P				3P					
			Sub-Commercial	Contingent Resources	Development Pending							<- Positive FID and Contract with Emitter in place		
					Development unclarified or on hold	1C	2C					3C		
		Development Not Viable									Cut off criteria on volumes / conflict of interest etc			
		Undiscovered Pore Space	Prospective Resources	Unusable - IEAGHG Cautionary									Effective Capacity	<- Discovery of accessible pore space
				Prospect							Theoretical Storage Capacity	Volumes calculated on area, average thickness and porosity basis		
				Lead	low	best				high				
Play														
Unusable - IEAGHG Cautionary														

Figure 3-48 Adopted CO₂ resource classification

3.6 Injection Performance Characterisation

3.6.1 PVT Characteristics

The PVT properties were modelled using the Peng Robinson equation of state and the CO₂ density correction implemented by Petroleum Experts for modelling CO₂ injection. The injection fluid was modelled as 100% CO₂ in compliance with project CO₂ composition limits (Scottish Power CCS Consortium, 2011). The PVT description used is shown in Table 3-17.

Property	Units	Value
Critical Temperature	°C	30.98
Critical Pressure	bara	73.77
Critical Volume	m ³ /kg.mole	0.0939
Acentric Factor	None	0.239
Molecular Weight	None	44.01
Specific Gravity	None	1.53
Boiling Point	°C	-78.45

Table 3-17 PVT definitions

CO₂ physical properties that strongly affect tubing flow and hence transport are density (ρ) and viscosity (μ). To test the validity of the Prosper PVT model, predicted in-situ CO₂ densities and viscosities were compared with pure component CO₂ properties calculated using the thermophysical properties of fluid systems (National Institute of Standards and Technology, 2016).

Comparisons were carried out for a range of temperatures and pressures (temperatures of 4 °C to 100 °C and pressures of 5 bara to 450 bara), with the following results:

- Density differs from the NIST calculated value by a maximum of 1.1% with an average of 0.3%.
- Viscosity differs from the NIST calculated value by a maximum of 14.3% with an average of 7.3%.

These results were considered adequate for the purposes of this study.

3.6.1.1 CO₂ Impurity Sensitivity

The well and tubing design work has been carried out assuming that the CO₂ is contaminant free. In practice, however, a small amount of other gases may be present in the injection gas. The main effect of this is that the phase envelope, which simplifies to a line in the case of pure CO₂, has a two phase region and the minimum injection pressures required to ensure single phase liquid injection have to be raised (Figure 3-49). For small amounts of impurities this shift is minor, but in order to simulate the effect of possible contamination a 10% safety region has been defined around the pure CO₂ phase envelope and this region has been avoided during the well design work.

A further effect of the presence of contaminants is that the fluid viscosity and density will change, which has an effect on the flow behaviour, which should be minor if contaminant content is insignificant.

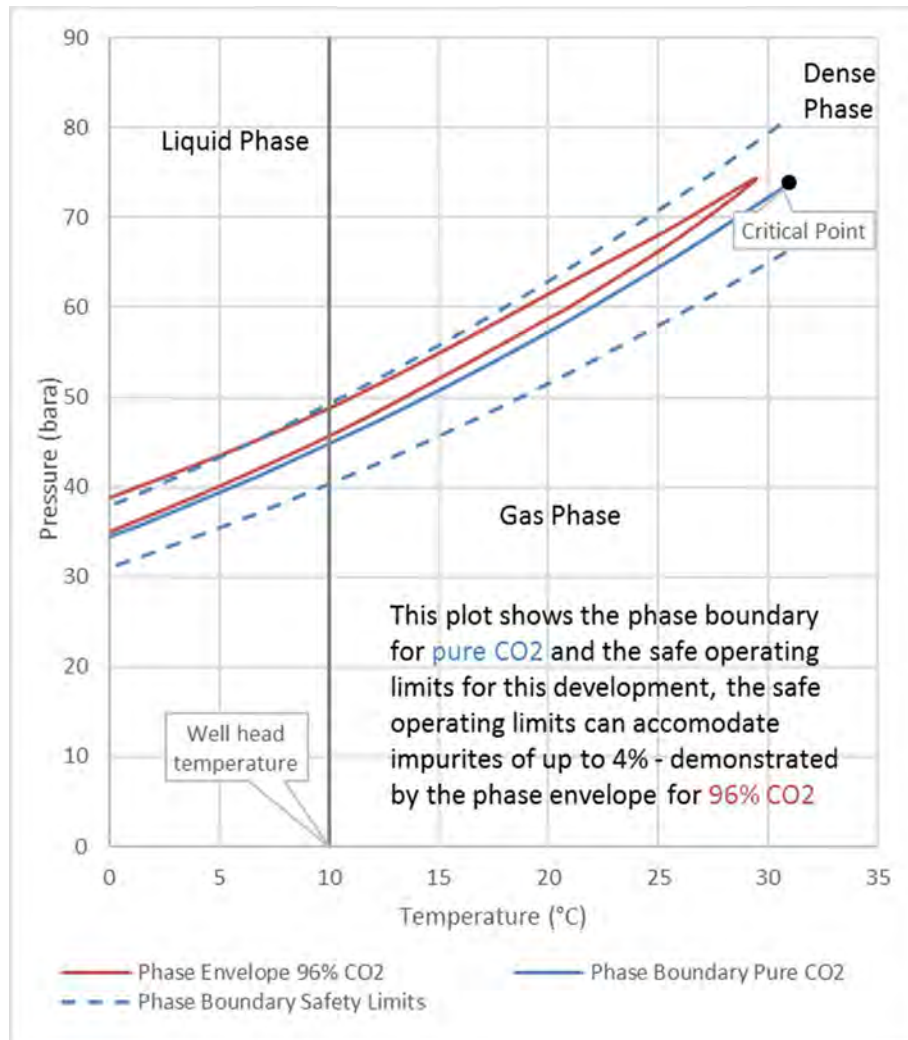


Figure 3-49 Effect of impurities on the phase envelope

3.6.2 Well Placement Strategy

In order to model well injection performance, the well deviation profiles (route from surface to reservoir) need to be determined. This was done following a well placement strategy review.

The Viking A field produced hydrocarbon gas from 1972 to 1991 (19 years total production and 44 years since first production). It is assumed in this study that the existing infrastructure will not be suitable for re-use. Well and platform placement is therefore independent of existing facilities. 10 long term producing wells are located in the 'A' block and it is useful to take advantage of the reduction in geological risk offered by the data from these wells, by siting the new wells in this area.

Geological and reservoir engineering work has concluded that within the Viking A fault block, the reservoirs are laterally very well connected. There is also some potential for upside in fault blocks to the west and south east. As such, the development is relatively insensitive to well placement, providing the well penetrates through the entire vertical reservoir sequence. Some laterally extensive non-pay units (sabkha silts) do create vertical permeability barriers, requiring vertical or low angle wells to access the three primary sand units. Injectivity is moderately high and therefore acceptable injection rates can be achieved without the full reservoir interval being open. However, as with all injection wells operating below fracture pressure (matrix injection), the concern with respect to maintaining long term injectivity is formation plugging. This occurs when small particulates accumulate in the near wellbore, reducing the near wellbore reservoir permeability over time. The source of particulates can be entrained solids from corrosion products from pipeline, wells or process plant, scale or re-injected formation fines. Formation fines may be back produced

during shut-in, providing plugging material when injection restarts. While some particulates can be filtered out of the injection stream at surface, it is not possible to eliminate all solids in the system. Therefore, the larger the sand face area open to injection, the longer it will take to plug, based on volume of particulates per square foot of sand face. Best practice dictates, therefore, that as much sand face is exposed as practicable in order to maintain adequate injectivity for the planned well life. However, due to the depleted nature of the reservoir, very high angle drilling carries significant risk of differential sticking. The compromise angle of 60 degrees from the vertical was therefore selected, in order to access all sand units and maximise sandface without compromising well delivery. However, well deviation may be considered an optimisation at a later stage in the process.

Reservoir engineering work suggests that two large injection wells would provide sufficient injection capacity to meet target CO₂ volumes over field life. Given that this injection capacity needs to be maintained at all times to meet likely contractual obligations, this means that two injection wells are required for field life (heated and unheated liquid phase) plus a single back-up well.

As offshore heating and filtering will be required (as well as water wash – see Section 3.6.4), a wellhead platform is the appropriate facility for Viking A. This then dictates a single drill centre location for all development wells. The only other constraint considered (other than drilling constraints) was that each bottom hole target should be separated by a minimum 1,000m in order to eliminate the superposition of temperature effects.

3.6.2.1 Monitoring Well

Data acquisition is required in order to confirm reservoir response, monitor CO₂ saturation changes, observe reservoir temperature effects and to ensure

fracture pressure limits are not exceeded (both during injection and in the long term). This data acquisition could be done via regular wireline intervention or by permanent data acquisition systems installed in the wells. Likewise, the data can be acquired in injection wells (providing that some shut-in time is allowed for reservoir equilibrium) or in a dedicated monitoring well.

Due to the cost and risk associated with well intervention, permanent data acquisition systems are recommended.

A dedicated monitoring well is a costly addition to a two well development. However, additional injection capacity may be required during a well 'outage' (well shut-in for intervention, short or long term damage) in order to meet contractual obligations. It is therefore recommended that a further deviated well is drilled to serve as both a monitoring and back-up injection well.

3.6.3 Well Performance Modelling

The purpose of well performance modelling is to help select a suitable injection tubing size and to evaluate some of the factors that may limit injection performance. The results of this modelling are then made available in the form of lift curves, where they are used to predict well performance in the reservoir simulation models.

All modelling needs to respect the safe operating limits described in section 3.6.6.

3.6.3.1 Methodology

Well modelling was carried out using Petroleum Experts' Prosper software. Because the assumed initial reservoir pressure is relatively close to the maximum pressure for gas phase injection, the field development plan strategy is for initial super-critical injection at 35°C tubing head temperature and then

later switching to cold injection in liquid phase. The details of when the switch from hot to cold injection occurs is discussed in Section 3.6.6. The base case development plan requires two CO₂ injection wells for Viking A, reached from a single platform.

As the wells are expected to be similar it was decided to evaluate well performance using a single prototype well, Injector 1 (INJ1). The performance of this well was evaluated for both super-critical and cold liquid phase injection. The input of the well models is described in the following sections.

3.6.3.2 Downhole Equipment

Since part of the purpose of this study was to determine the optimal tubing size for the Viking A wells a set of sensitivity cases was defined on downhole equipment.

3.6.3.3 Wellbore Trajectory

The wellbore trajectory used for the Viking A well models were simplified from the deviation surveys provided by the well design study provided in Appendix 6.

3.6.3.4 Temperature Model

Prosper offers three heat transfer models; rough approximation, improved approximation and enthalpy balance.

The rough approximation model estimates heat transfer and hence fluid temperatures from background temperature information, an overall heat transfer coefficient and user-supplied values for the average heat capacity (C_p value) for oil, gas and water. In an application in which accurate temperature prediction is vital this model is considered too inaccurate, especially since it neglects Joule-Thomson effects, which can be vital in predicting the behaviour of a CO₂ injector. For this reason this model was not considered.

The full enthalpy balance model performs more rigorous heat transfer calculations (Petroleum Experts Ltd., 2015) (including capturing Joule-Thomson effects) and estimates the heat transfer coefficients as a function of depth from a full specification of drilling information, completion details and lithology. However, at the current stage in the design cycle many of the input parameters are still unknown (e.g. mud densities). For this reason the improved approximation model was chosen for this work. The sole difference between this model and the full enthalpy balance model is that the user supplies reasonable values for the heat transfer coefficient rather than having them estimated from the completion information and lithology. In line with Petroleum Experts recommendations, a uniform heat transfer coefficient of 3 BTU/h/ft²/F (17.04 W/m²/K) was chosen.

For the modelling a base case delivery and seabed temperature of 10°C was assumed and the required background temperature gradient was defined as 10°C at the seabed and reservoir temperature at top perforation depth. Sensitivities on a range of seabed temperatures between 6 and 16°C were performed where appropriate.

3.6.3.5 Reservoir Data and Inflow Performance Relationship (IPR)

A full review of likely reservoir and field parameters was carried out and estimates on which the IPR modelling was based are summarised in Table 3-18 and Table 3-19.

Parameter	Unit	Best Estimate
Water Depth	m (ft)	26 (86)
Total Field Drainage Area	km ² (acres)	10 (2471)
Temperature Gradient	°C/100 m (°F/100 ft)	2.596 (1.522)
Initial Pore Pressure Gradient	bar/100 m (psi/100 ft)	1.33 (5.86)

Table 3-18 Viking A field and well data

Parameter	Unit	Low	Best Estimate	High
Formation Top Depth (Datum)	m (ft) TVDSS		2664 (8740)	
Formation Gross Thickness	m (ft)	143 (470)	153 (503)	171 (561)
Formation NTG	-	0.34	0.72	1.00
Current (Depleted) Reservoir Pressure	bara (psia)		34.2 (496) ¹	
Reservoir Temperature (assumed depth datum as top of reservoir)	°C (°F)		83.9 (183)	
Permeability	mD	0.65	35.0	111.0
Permeability Anisotropy (K _v /K _h)	-	0.09	0.13	0.57
Formation Water Salinity	ppm		150,000	

Table 3-19 Viking A reservoir data

Notes:

Corrected from a pressure of 500 psia at a depth of 8958 ft TVDSS using a pressure gradient of 0.0091 psi/ft to top depth of 8527.02 ft TVDSS

Permeabilities within Viking are highly variable, with lower permeability in blocks that have been buried to a greater depth (due to burial diagenesis). With limited core data it was deemed appropriate to cover a wide range of permeabilities based on the entire Viking area.

Using these data three IPR models were defined in Prosper to represent high, medium and low reservoir performance. These are summarised in Table 3-20.

Parameter	Unit	Low	Mid	High
Top Depth	m (ft) TVDSS	2600 (8527)		
Depleted Reservoir Pressure @ top perforation depth	bara (psia)	34.2 (496)		
Initial Cold Phase Injection Reservoir Pressure @ top perforation depth	bara (psia)	252.9 (3668)		
Reservoir Temperature @ top perforation depth	°C (°F)	82.1 (179.8)		
IPR Model	n/a	Jones		
Permeability	mD	0.65	35.0	111.0
Reservoir Thickness	m (ft)	49 (160)	110 (362)	171 (561)
Well Drainage Area	km ² (acres)	5 (1236)		
Dietz Shape Factor	n/a	19.41		
Perforation Interval	m (ft)	49 (160)	110 (362)	171 (561)
Skin	(-)	+20	+10	0

Table 3-20 Viking IPR definitions

3.6.3.6 Tubing Selection

Tubing selection was carried out for both the super-critical and liquid injection phases.

Injection Limits – Supercritical Injection

Some pressure and temperature limits on super-critical injection operations have been defined and have been summarised in Table 3-21.

Parameter	Unit	Value
Fracture Limit at Top Perforation Depth (Depleted)	<i>bara (psia)</i>	227.5 (3300)
Minimum Fluid Temperature at Perforation Depth	°C	0
Maximum Pipeline Delivery Pressure at Wellhead	<i>bara (psia)</i>	160 (2321)

Table 3-21 Injection pressure and temperature limits - supercritical injection

Note:

- The fracture limit at top reservoir depth has been derived using a fracture gradient of 0.43 psi/ft, which is the assumed depleted fracture gradient, and a top reservoir depth of 2600m (8527ft) TVDSS. An uncertainty factor of 0.9 was applied to the calculated fracture pressure.
- The minimum fluid temperature at reservoir depth exists to prevent formation water from freezing during injection.

Sensitivity Cases – Supercritical Injection

The sensitivity cases considered for super-critical injection are summarised in Table 3-22. The high, medium and low reservoir cases are as described in Table 3-19. The tubing head pressures have been chosen in order to span a reasonable range of operating rates. Since the tubing head injection temperature is above the critical temperature a larger range of tubing head pressures can be considered than is possible with gas or liquid phase injection.

Results – Supercritical Injection

Table 3-22 summarises the rates achievable for the various sensitivity cases and the achievable rates for each tubing size. Prosper uses volumetric flow rates and the conversion to mass flowrate is based on a density of 1.8714 kg/m³ at standard conditions.

Case	Reservoir Case	Tubing Size	THP (bara)	THT (°C)	Gas Rate (MMscf/d)	Gas Rate (MMte/yr)
1	High	5-1/2" (17 ppf)	22	35	1.3	0.025
2	Medium		22		0.7	0.013
3	Low		22		0.1	0.002
4	High		50		32.9	0.637
5	Medium		50		25.6	0.495
6	Low		50		1.2	0.024
7	High		85		154.2	2.982
8	Medium		85		142.1	2.749
9	Low		85		1.7	0.033
10	High		160		246.4	4.767
11	Medium		160		214.4	4.147
12	Low		160		2.3	0.045
13	High	7" (29 ppf)	22		3.5	0.068
14	Medium		22		0.9	0.018
15	Low		22		0.1	0.002
16	High		50		59.1	1.144
17	Medium		50		38.8	0.75
18	Low		50		1.2	0.024
19	High		74		129.3	2.5
20	Medium		74		107.4	2.077
21	Low		74		1.5	0.03
22	High		95		335.5	6.489
23	Medium		95		257.1	4.974
24	Low		95		1.8	0.035
25	High	9-5/8" (47 ppf)	22		6.8	0.131
26	Medium		22		1.2	0.023
27	Low		22		0.1	0.002
28	High		50		133.3	2.579
29	Medium		50		55.7	1.078
30	Low		50		0.8	0.015
31	High		69		244.7	4.734
32	Medium		69		130.7	2.527
33	Low		69		0.9	0.017
34	High		75.5		332.9	6.44
35	Medium		75.5		257.4	4.978
36	Low		75.5		0.9	0.018

Note that the tubing head pressures (THP) quoted in the table above have been chosen as follows:

- The minimum pressures have been chosen to illustrate the minimum achievable injection rates.
- For the 5½” tubing, maximum injection pressures are limited by the maximum assumed pipeline delivery pressure at the wellhead. Otherwise, the maximum pressures are the pressures which ensure that the entire field target rate of 5 MMte/yr can be injected using a single well and is therefore the highest pressure that could be required.
- The medium pressures have been chosen to illustrate what tubing head pressures are required to approximately inject the target rate of 2.5 MMte/yr per well.

The results show that for the low reservoir quality cases (3,6,9,12,15,18,21,24,27,30,33 and 36) the achievable rates are substantially below the target rate and this issue cannot be addressed by tubing choice or injection pressure. In practice new well locations should be chosen close to existing production wells in order to avoid areas of low reservoir quality. The low reservoir quality cases have therefore been excluded from any further analysis.

Figure 3-50 shows the pressure and temperature behaviour along the tubing plotted as pressure versus temperature for the three tubing sizes. Also shown is the phase boundary with an upper and lower safety limit and the temperature and fracture limits. Figure 3-51 shows the pressure and temperature profile versus depth for an example case (Case 20).

Table 3-22 Rates achievable by case - supercritical injection

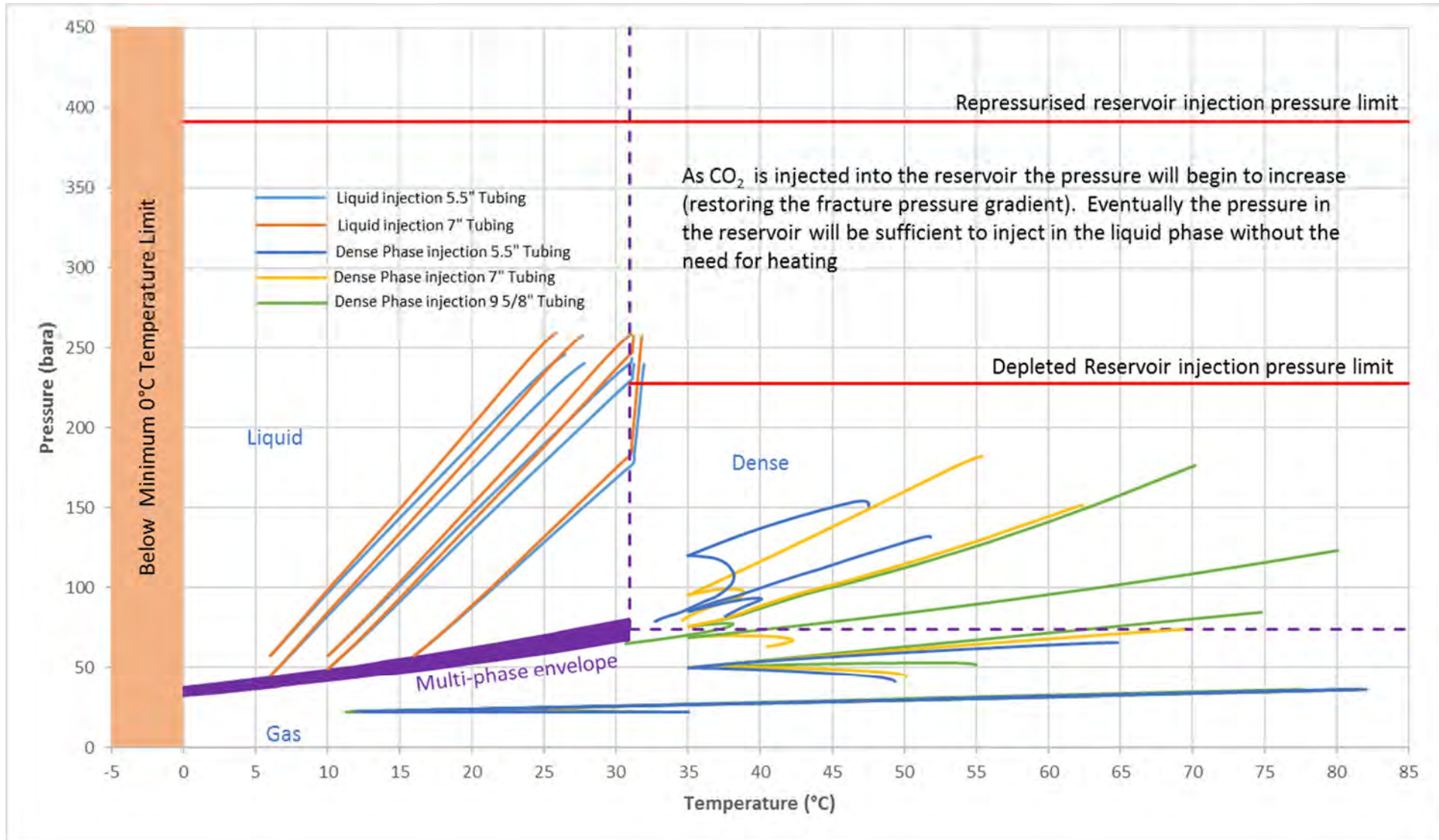


Figure 3-50 Pressure – Temperature profiles for liquid and dense phase operation

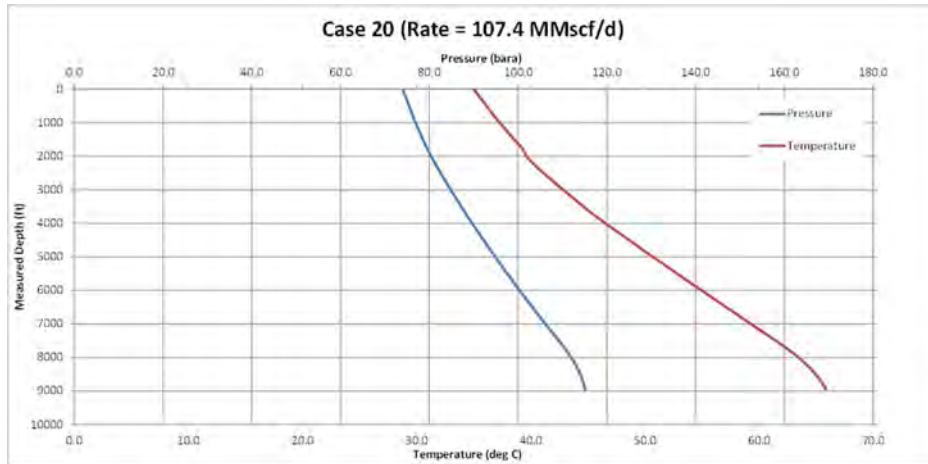


Figure 3-51 Pressure and temperature vs depth for case 20

The results can be summarised as follows:

- Both the 7" and the 9-5/8" tubing sizes allow the target injection rate and also a reasonable range of injection rates to be achieved with super-critical injection. For the 5 1/2" tubing the target injection rate can be achieved but the achievable range of rates is slightly more limited in that the field target injection rate of 5 MMte/yr cannot be injected into a single well given the THP bounds considered. In addition, at an injection pressure of 160 bara a phase change to liquid injection occurs for the best ("high") reservoir case at 75.8 bara. However, this phase change is continuous and since the target rate is 2.5 MMte/yr this scenario may also not be relevant for practical purposes.
- Apart from the 5 1/2" tubing, where injection rates are limited by the pipeline delivery pressure limit, the tubing head pressures are determined by the need to keep the rates within the limits imposed

by the available CO₂ injection gas. In other words, higher injection pressures will achieve higher rates than contract supplies (or will result in phase change in the wellbore).

- For the cases considered there should be no phase changes (between gas and liquid injection) in the wellbore, although the fluid may change from super-critical to gas phase or in one case liquid phase, which are both continuous transitions. The 0 °C FBHT and fracture pressure limits are not broken.
- Reservoir engineering consideration suggests that the 7" tubing is required to sustain target injection rates as reservoir pressure increases. 7" is therefore selected for the supercritical (heated) phase of this development.
- 9 5/8" tubing is not considered further as it is expected to represent a higher cost but deliver no additional benefit. Its performance is also limited at low rates.

Injection Limits – Liquid Phase Injection

After completing the initial supercritical injection stage there are several technically viable production strategies for later life injection. These include the following:

- Continuation of the supercritical injection at a well head temperature of 35 °C using the 7" tubing as described above
- A switch to unheated liquid injection at a well head temperature of 10 °C (base case) using 5 1/2" tubing
- A switch to unheated liquid injection at a well head temperature of 10 °C (base case) using 7" tubing

Continuing to heat the CO₂ for continuous supercritical injection is attractive, in that no changes are required throughout the injection period. However, heating the liquid CO₂ to 35 degrees (or thereabouts) incurs an additional cost and the shorter this period is, the better the overall economics of the project. The first option has not been considered for this study as a result.

Reservoir engineering work has shown that the supercritical (heated) phase of the development can be shortened by around 4 years if 5-1/2” tubing is used with unheated liquid injection. However, the smaller tubing imposes greater friction pressure losses and the maximum operating pressure is reached earlier, resulting in loss of total storage capacity. As a switch to 5-1/2” completions would also involve a workover in all 3 wells, the cost of heating needs to be significant in order to pursue this option.

The third option therefore appears the most suitable. The following sections illustrate the injection behaviour of the chosen option, predicted injection limits and the impact of changes in the well head injection temperature due to seasonal variations.

The pressure and temperature limits on liquid phase injection operations have been summarised in Table 3-23.

Parameter	Unit	Value
Fracture Limit at Top Perforation Depth (Depleted)	bara (psia)	391.6 (5679)
Minimum Fluid Temperature at Perforation Depth	°C	0
Maximum Pipeline Delivery Pressure at Wellhead	bara (psia)	160 (2321)

Table 3-23 Injection pressure and temperature limits - liquid phase injection

Note:

- The fracture limit at top reservoir depth has been derived using a fracture gradient of 0.74 psi/ft and a top reservoir depth of 2600m (8527 ft) TVDSS. An uncertainty factor of 0.9 was applied to the calculated fracture pressure. While this is the fully re-pressurised fracture limit (and there is a fracture pressure ramp to consider), it is not considered limiting until late in field life, where this is the best estimate available.
- The fluid temperature and pipeline delivery pressure limits are as for supercritical injection.

Sensitivity Cases – Liquid Phase Injection

The sensitivity cases considered for liquid phase injection are summarised in Table 3-24. Note that ambient temperature only is considered.

The high, medium and low reservoir cases are as described in Table 3-19. The minimum tubing head pressure is the minimum safe injection pressure to ensure

single liquid phase injection throughout the tubing; the maximum THP is the maximum pipeline delivery pressure considered.

Results – Liquid Phase Injection

Table 3-24 summarises the rates predicted for the various sensitivity cases provides a graphical representation. As mentioned above Prosper uses volumetric flow rates and the conversion to mass flowrate is based on a density of 1.8714 kg/m³ at standard conditions.

Case	Reservoir Case	Tubing Size	THP (bara)	THT (°C)	Rate (MMscf/d)	Rate (MMte/yr)
1	High	7" (29 ppf)	49.32	10	126.9	2.454
2	Medium		49.32		50.5	0.977
3	Low		49.32		0.1	0.002
4	High		160		353.6	6.839
5	Medium		160		227	4.39
6	Low		160		1	0.02

Table 3-24 Rates achievable by case - liquid phase injection

As for supercritical injection the results show that the for the low reservoir quality cases (3 and 6) the achievable rates are substantially below the target rate and this issue cannot be addressed raising the injection pressure within reasonable limits. In practice the well locations should be chosen in order to avoid these low quality areas. Again, these cases have been excluded from any further analysis.

Figure 3-50 shows the pressure and temperature behaviour along the tubing plotted as pressure versus temperature for the various tubing head pressures and viable reservoir cases. The graphs also show the phase boundary with an upper and lower safety limit and the temperature and fracture limits.

The results can be summarised as follows:

- Target injection rates are approximately 2.5 MMte/yr per well and the rates predicted for the 7" tubing at the minimum injection pressure are close to that rate for the "high" reservoir case. Note that the initial reservoir pressure for liquid injection has been chosen during reservoir simulations with this aim in mind.
- Maximum rates achievable are between 4.4 and 6.8 MMte/yr depending on reservoir case.
- In the scenarios considered no issues with discontinuous phase changes in the tubing should be encountered. The fracture limit should not be broken and the bottom hole temperature limit not be breached.

Injection Temperature Sensitivity

As discussed in Section 3.6.3 the seabed temperature at the Viking location varies seasonally between approximately 6 °C and 16 °C and this has an impact on the arrival temperature of the injection gas.

For super-critical injection any impact of arrival temperatures on injection performance is negated by the fact that the injection gas will be heated to 35 °C to optimise injection performance. The arrival temperature will of course impact the heating load.

For liquid phase, however, no heating will be in place and therefore arrival temperature will have an effect on injection temperature and performance. This effect is twofold:

- A higher injection temperature implies a higher minimum injection pressure to ensure single phase injection throughout the tubing.

- Higher temperatures imply lower fluid density and increased friction leading to lower injection rates at the same injection pressure.

To evaluate these effects for the Viking liquid phase injector the sensitivities summarised in Table 3-25 below were run. The tubing head pressures chosen for cases 1-3 are the minimum required to ensure safe single phase injection at the various injection temperatures. Cases 4 and 5 illustrate the impact of arrival temperature on injection rate for the fixed tubing head pressure (from Case 3).

The table below also summarises the results. The impact on temperature along the tubing is show in Figure 3-50 below.

Case	Reservoir Case	Tubing Size	THP (bara)	THT (°C)	Rate (MMscf/d)	Rate (MMte/yr)
Case 1	High	7" (29 ppf)	44.47	6	130.7	2.527
Case 2	High		49.32	10	126.9	2.454
Case 3	High		57.20	16	125.6	2.430
Case 4	High		57.20	6	171.3	3.314
Case 5	High		57.20	10	154.2	2.982

Table 3-25 Tubing head injection temperature sensitivities and results

The results can be summarised as follows:

- Differences in injection rates from the base case (case 2, injection at 10 °C) are up to 35.1%.
- The differences in minimum rates achievable, taking into account the different minimum injection pressures, are negligible. In particular,

this means that target injection rates can be achieved for the range of seasonal temperature variation considered.

- There are no discontinuous (gas / liquid) phase changes and the fracture and temperature limits are not broken.

As the dynamic reservoir modelling work is not rate constrained by well delivery, the effects of changes in delivery temperature are not considered critical. However, it is recommended that a full system delivery temperature sensitivity be performed during the FEED work.

Tubing Size Selection Summary

From the work done above, together with the reservoir engineering modelling, it has been concluded that for this study, the base case tubing size is 7" throughout the life of the field. This maximises injection rates, while minimising cost. However, there are several possible optimisations, which should be considered in any future work. The main optimisation is to reduce the period during which heating is required. Current estimates suggest this period may be as long as 20 years. The reason the change from heated to unheated injection takes so long is that, in the cold dense phase (with a high hydrostatic column pressure), Tubing Head Pressures (THP) remain stubbornly low, despite reservoir pressure increasing past critical point. Options to increase THP, and allow earlier transition include:

- Reduce tubing ID (this is what has been considered in the 7" + 5.5" scenario). However, due to higher frictional losses, this reaches THP limits earlier and capacity is lost. THP could be increased past 160 bar with higher pipeline specs or with platform based boost pumps to regain this lost (contractual – plateau) capacity.

- More wells could be drilled, but with smaller tubing ID (5.5” or 4.5”). This would help, as the target injection rate per well is reduced, but at the cost of additional wells.
- For the transition phase, the well PI could be artificially reduced. However, wells would shut-in earlier as fracture gradient would be reached earlier and only a small gain in transition timing would be achieved.
- Perform sensitivities with heating (different injection temperatures – higher / lower).
- Reduce target injection rate to be able to live with 5.5” wells for life of field (avoiding costly workovers). It would extend storage life, but not increase capacity. This would take longer to pressure up the reservoir, but transition would be at a slightly lower pressure.

- Gas Rates: 5 MMscf/d to 130 MMscf/d in 20 steps

The performance envelope of the well is shown in Figure 3-52. It was ensured that for all points shown on the curves no gas / liquid phase changes occurred throughout the tubing and that the temperature limit of 0 °C was not broken.

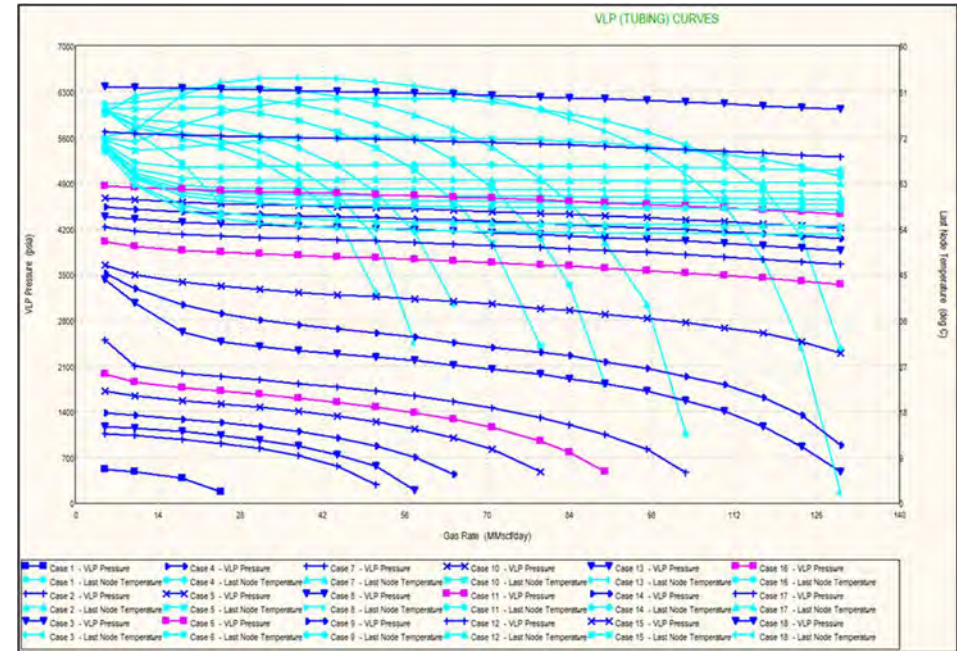


Figure 3-52 Performance envelope for 7" tubing - supercritical injection

It is recommended that these sensitivities / alternate scenarios are considered in detail during the FEED stage.

3.6.3.7 Vertical Lift Performance Curve Generation

Vertical lift performance (VLP) curves were generated for the Viking wells for both supercritical and liquid phase injection with the tubing chosen for each case. To allow sensitivities to injection pressure limits and other quantities to be run in Eclipse without extrapolation, the curves were generated for pressures and rates that were adjusted to Eclipse requirements rather than reflecting limits to these values discussed above.

Supercritical Injection

Input parameters were as follows:

- Tubing Head Pressures: 324 psia (22.3 bara) to 3000 psia (206.8 bara) in 18 steps

Liquid Phase Injection

Input parameters were as follows:

- Tubing Head Pressures: 715 psia (49.32 bara) to 2321 psia (160 bara) in 20 steps
- Gas Rates: 30 MMscf/d to 200 MMscf/d in 17 steps

The performance envelope of the well is shown in Figure 3-53. It was ensured that for all points shown on the curves no gas / liquid phase changes occurred throughout the tubing and that the temperature limit of 0 °C was not broken.

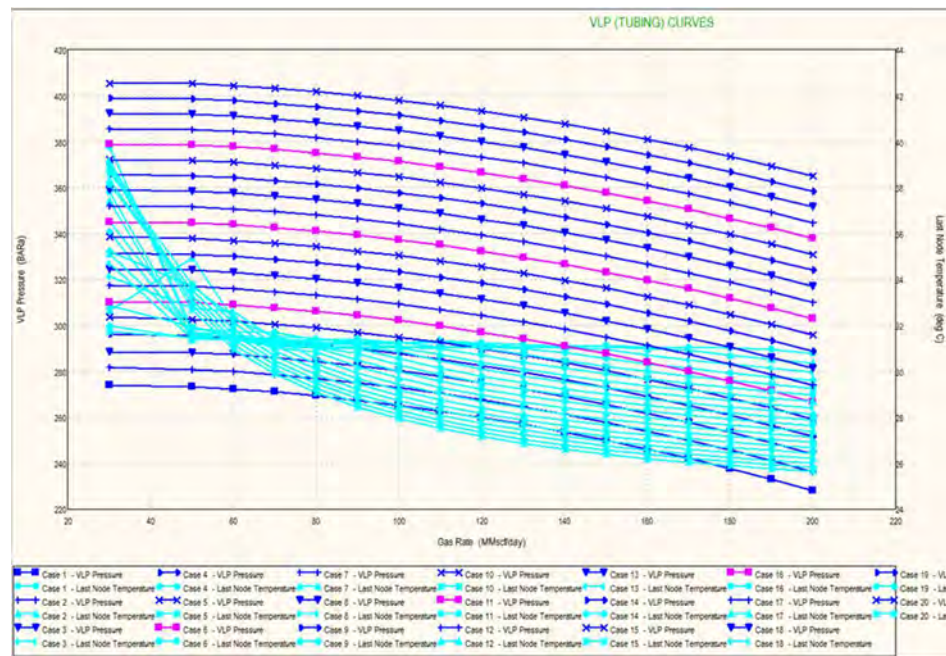


Figure 3-53 Performance envelope for 7" tubing - liquid phase injection

3.6.4 Injectivity and Near Wellbore Issues

The effects of long term CO₂ injection into a sandstone reservoir are not yet fully defined. Despite some experience of the process gained in the industry, each reservoir rock, each injection profile and each development scenario is different. The reservoir rock is subject to pressure and thermally induced stresses, applied in sometimes random patterns (cyclic stressing from variations in supply conditions). These stresses can lead to rock failure or damage to the rock fabric and therefore permeability changes. Interaction of CO₂ with in-place reservoir rock and fluids may also alter the ability of the rock to conduct fluids.

Some of the more recognised issues are discussed below, along with their effect on the Viking A storage potential.

3.6.4.1 Halite

The Lemna Sandstone formation water at Viking A is a moderate to high saline brine, typically with 220,000 ppm (Riches, 2003). There is uncertainty in the composition of this brine, but some nearby fields have reported very high salinity (salt content) values, close to salt saturation. As a gas reservoir, the Viking A brine will be primarily connate water (water adsorbed on the surface of the rock grains or on the walls of the pore channels). With water saturations around 10 - 14% in the Viking A reservoir, water volumes are relatively low with respect to pore volume, and therefore the salt content in a 150,000 to 220,000 ppm salt solution will be limited to no more than 3% of pore volume.

When supercritical CO₂ is injected into formations containing high salinity connate water, CO₂ will absorb the water phase, thus precipitating the salt out of solution. In other words, the near wellbore is dehydrated, leaving the salts behind. This dehydration process can increase the CO₂ saturation and therefore its relative permeability. The salt precipitation in pore throats can reduce

permeability if salt crystals are mobilised and form bridges / plugs in the matrix rock pore throats.

Given the relatively large injection area (sand face) planned in the Viking A wells, CO₂ velocity through the matrix will be moderate to low and salt crystal mobilisation may not occur. If it does occur (CO₂ in Viking A will be relatively viscous), it is likely to be in the very near wellbore region only, and once removed, should not re-occur. The only exception to this might be due to connate water re-saturation in the near wellbore due to capillary pressures. In this case, more halite is fed into the system leading to a reduction in pore volume and considerably higher risk of pore throat plugging. However, with high permeabilities and no apparent aquifer contact in Viking A, capillary pressure re-saturation is unlikely. Overall no significant impact on permeability or porosity is anticipated as a result of dehydration.

At the start of CO₂ injection (after 18 years of hydrocarbon gas production ended), considerable dehydration is likely to have occurred already in the reservoir. The halite crystals may have formed bonds with the matrix rock and may no longer be considered mobile. However, this has not yet been experienced in any CO₂ storage site and considerable uncertainty remains surrounding the actual halite risk to injectivity. Ultimately, concerns over absolute permeability degradation due to halite may be eclipsed by the anticipated increase in relative permeability as single phase flow dominates in the “dry out” zone (Mathias, Gluyas, Gonzalez, Bryant, & Wilson, 2013).

The effect of halite precipitation can be mitigated by ‘washing’ the near wellbore with fresh or low salinity water (seawater is relatively low salinity at 35,000 ppm). The wash water dissolves the salt and carries it away from the near wellbore region, where the effects of permeability reduction have most impact. As the impacts of halite precipitation are not yet fully understood for Viking A, it is

recommended that provision is made for early time wash water operations. Note that a full column of fresh water is slightly higher than the minimum initial fracture pressure assumptions (0.433 psi/ft vs 0.43 psi/ft), and therefore it is recommended that slugs of fresh water are introduced into the CO₂ stream until sufficient re-pressurisation has occurred to increase the fracture gradient past the water gradient. Wash water should be treated with corrosion inhibitor, antioxidants and biocide. Hydrate inhibitor (MEG) may also be required to prevent hydrate formation.

Water wash facilities have been incorporated in the platform facilities to account for these operations.

3.6.4.2 Thermal Fracturing

The CO₂ stream injected into the Lemna Sandstone is colder (varies from 25 to 80°C, depending on rate and phase of operations – heated or unheated etc) than the modelled ambient reservoir temperature (~84°C). This reduction in temperature may be quite extensive (thermal modelling done on similar, but cooler, reservoirs suggests that this may extend to a radius of 1,500ft) but depends on the specific heat capacity of the formation. A drop in temperature will have an effect on the near wellbore stresses, and will make rock more liable to fracture (tensile failure). This thermal effect on the fracture pressure has not been investigated in this report. The applied safety margin (10%) on reservoir rock fracture pressure, and the thickness and strength of the cap rock, provides some security with respect to cap rock fracturing and containment issues. It is recommended that these issues be reconciled in the FEED stage.

3.6.4.3 Sand Failure

As with water injection wells, there is a potential for sand failure in CO₂ injection wells. The principal causes of this are similar:

- Flow back (unlikely to occur in CO₂ injection wells without some form of pre-flow pad)
- Hammer effects during shut-in
- Downhole crossflow during shut-in (from and to formation zones with different charging profiles)
- Well to well crossflow during shut-in (if individual wells are charged to different pressures and surface valves are left open, allowing cross-flow via injection manifold)

The effects of sand failure are that near wellbore injectivity can be reduced (failed sand packs the perforation tunnels or plugs the formation) or the well can be filled with sand (reducing injectivity and potentially plugging the well completely).

The pre-requisite for sand failure is that the effective near wellbore stresses, as a result of depletion and drawdown, exceed the strength of the formation.

The in-situ stresses at the wellbore wall, while predominantly a function of the overburden and tectonic forces, will vary dependent on the trajectory (deviation and azimuth) of the proposed wellbore. So, while field wide values can be generalised, the specifics of the well can impact on the required conditions for failure of the formation.

These notes apply a generic critical drawdown process to selected well strength logs to provide a guide for the pressure drops required for failure in a CO₂ injector. More detailed work would be required once the well trajectory and injection scheme parameters are better defined.

Critical Drawdown for Sanding

The critical drawdown for sanding was estimated using the methodology presented in Bellarby (2009) and SPE 78235. This method relates mechanical rock properties and the stress condition.

$$p_{w(\text{crit})} = \frac{3\sigma_1 - \sigma_2 - \sigma_{\text{yield}} - p_r A}{2 - A}$$

Where:

$$A = \frac{(1 - 2\mu)}{(1 - \mu)} \alpha$$

The cumulative rock strength (UCS) in the Lemna Sandstone as calculated from logs for the wells with sonic log available (49/12-2, 49/11a-6, 49/12a-K4 and 49/12a-K5) are shown in Figure 3-54, where the average range is between 4000 psi to 5400 psi.

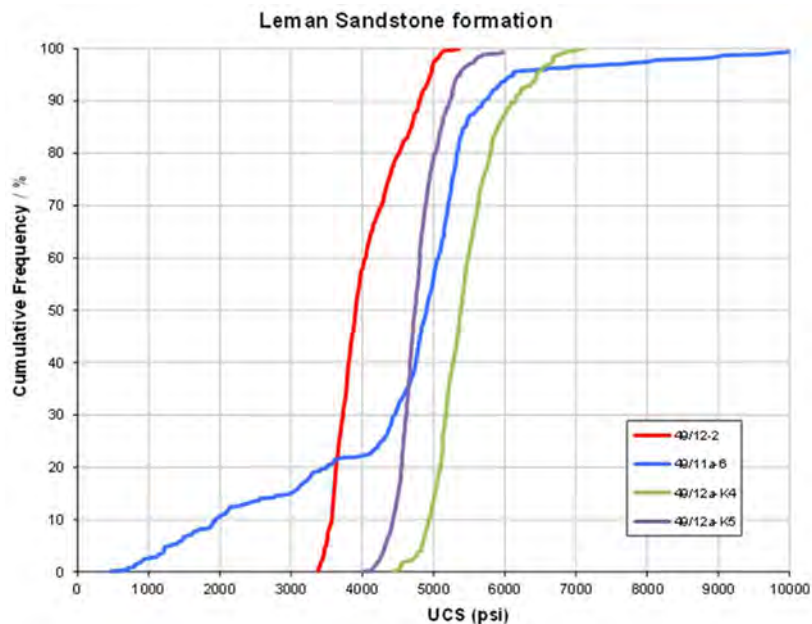


Figure 3-54 Lemn sandstone UCS cumulative distributions

Two cases were considered in this analysis of the critical total drawdown (CTD, sometimes referred to as CDP – Critical Drawdown Pressure) for sanding: a) at original reservoir pressure condition; and b) at depleted reservoir conditions. The following figures indicate the CTD for the four wells evaluated in the Lemn Sandstone in Viking A, including original and depleted reservoir pressure conditions.

As can be seen, the CTD at original reservoir condition for wells 49/12-2, 49/12a-K4 and 49/12a-K5 are above 1800 psi, indicating a low risk for sanding. For the well 49/11a-6 apparent weak zones are present that seem to bring a risk of sanding even at original reservoir conditions. However, these are regarded as log artefacts and are therefore unreliable.

For the depleted conditions, all four wells have a risk of sanding, where the worst cases are wells 49/12a-K4 and 49/12a-K5 where any drawdown will induce sand production (e.g. drawdown due to water hammer effect). However, it is worth mentioning that this is based on an uncalibrated rock strength so uncertainty remains.

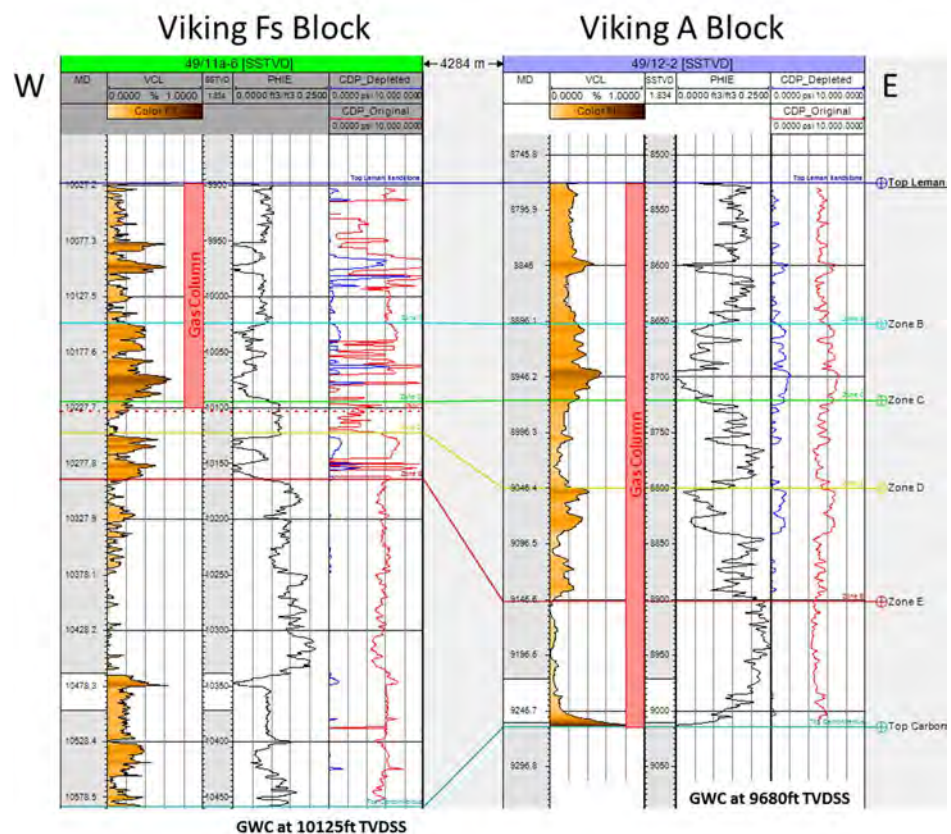


Figure 3-55 Critical drawdown pressure for Viking A

Impact on Well Completion

Following the guidelines from SPE 39436 (Morita, E, & Whitebay, 1998), the Leman Sandstone in Viking A could be considered as a Case A, suggesting that gravel-pack or open-hole with pre-packed screen could be suitable.

However the choice of a sand control completion is not an obvious one. Gravel pack operations at such low pressures are problematic as they require a full column of viscous fluid to surface, which may be beyond the initial fracture pressure limit. With three different sand bodies in the Viking A block, there is potential for cross-flow during shut-in. This makes standalone sand screens vulnerable to plugging from failed shales, especially if a natural sand pack is not formed in the screen annulus (unlikely in the CO₂ injection scenario) to prevent annular mobilisation.

This leaves two options: a standard cased and perforated completion, where intermittent sand production is tolerated through the drilling of a significant sump (allows produced sand to fall clear of the perforations, preventing any plugging), or a more complex ICD (Interval Control Valve) type sand control completion, where the valve prevents backflow. Both options have merits:

Cased and Perforated

A simple solution, providing the drilled sump has sufficient capacity for failed sand until such time as the reservoir pore pressure increases sufficiently to reduce failure stresses past the critical point for sanding. It also has the benefit of the perforations by-passing the inevitable near wellbore damage likely to occur in an underbalanced reservoir during drilling and completion operations. However, cementing a production liner in place on Viking under initial reservoir conditions may be challenging due to the uncertainty in fracture pressure (potentially less than the hydrostatic column during the cementing operation).

Fracture pressure lies in a range, somewhere between 0.54 psi/ft and 0.43 psi/ft. There are several options for low pressure cementing, including stage cementing and nitrified, or other light weight, cements. However, these add to the complexity and cost of the development.

ICD Completion

This is a shrouded sand screen, which allows the injected fluid to enter via a port before reaching the sand screen and annulus. They are separated by external isolation packers, preventing annular hydraulic communication between different sand zones. The injection port has a form of variable back-pressure valve that can be set (at surface before installation) to equalise the injection into each target sand zone. Some variants of these valves incorporate a one way valve option that will prevent back flow. This would make the sand screen option less susceptible to plugging by shales through backflow, thus negating the need for a natural sand pack to form for conformable sand control. Furthermore, injection into each zone can be appropriately distributed (potentially reducing the likelihood of backflow) and additional back pressure can be imposed on the injection pressure, allowing earlier transition to unheated CO₂ injection. The main issues with this option are the formation clean-up challenges (removing drilling mud damage prior to lower completion installation) and ensuring the completion is set on depth (off depth will set the wrong valves across the target formation).

While the ICD option meets all the well sand control objectives (and may provide other significant benefits), this form of lower completion has never been trialled in a CO₂ injection well. There may be issues surrounding temperature drop at the control valves. Furthermore, back pressure modelling has not been done to simulate the effects on storage rate and capacity. The more conservative cased and perforated option has therefore been adopted for the purposes of this study,

but the ICD option is recommended to be fully investigated in any FEED work. Note that no evidence of sand production in the Viking gas production wells has been found in literature reviews, but this does not exclude the possibility that sanding may have occurred.

3.6.5 Transient Well Behaviour

In both the heated and unheated injection stages, the maximum tubing head pressure (THP) limit is primarily determined by the pipeline delivery pressure and the supply rate of CO₂. Towards the end of field life, formation fracture pressure becomes more relevant and imposes a restriction that determines the end of sustainable injection.

Bottom hole temperature (BHT), which must remain above 0°C to avoid the formation of ice (note that this limit is lower than 0°C for saline brine, but the presence of fresh ‘wash water’ has been assumed) has not imposed any restrictions on injection in the case of Viking A due to the depth (and therefore temperature) of the Leman Sandstone. Hydrate risk during normal injection operations was therefore minimal. However, more work on this may be required at any FEED stage, with the construction of a full thermal model.

As noted earlier (Section 3.6.4), the injection of a full column of wash water in the well may result in the unintentional fracturing of the formation. It is therefore recommended that wash water, if required, is injected in batches smaller than the well tubing volume, chased by CO₂ or nitrogen. The water may require to be heated (or an inhibitor such as MEG added) in order to prevent the formation of ice or hydrates.

Transient effects in the period before the reservoir pressure can support a full column of CO₂ in the wellbore remain problematic. Should the hydrostatic pressure of a full column of liquid CO₂ be applied to the reservoir during the

transition from injection to shut-in, the depleted fracture pressure limit will be surpassed. Furthermore, maintaining single phase in the wellbore during start-up of injection (before an injection back-pressure can be established) may be problematic. These transient issues require further well modelling in order to assess the true limits, which should be assessed in the FEED stage. Other transient effects include significant temperature drops during shut-in and well restart. These effects, and proposed mitigations, are discussed below.

Two transitional effects in the liquid phase injection have been identified:

- Shut-in at surface with a full column of CO₂ in the well
- Restarting CO₂ injection during the transition period or after a water wash

3.6.5.1 Shut-in at Surface with a Full Column of CO₂ in the Well

If the injection pressure is high and this pressure is transferred to the formation at shut-in on top of a static column of CO₂, then the formation fracture pressure could be exceeded (depending on where on the fracture pressure hysteresis curve the well is operating at the time of shut in). This is considered as a ‘worst case’, similar to a water hammer effect (which induces high and low pressures into the system). This is unlikely to happen in practice because of the ‘fall-off’ pressure profile in the well: after shut-in the fluids continue to inject and the frictional pressure losses in the tubing act to reduce the bottom hole pressure at the same time as the surface injection pressure dissipates. Calculations using 160 bar (2320 psi) applied pressure and expected static gradients of CO₂ at 3 significant points in field life, suggest that this worst case remains below minimum expected fracture pressure at each stage.

It is more likely that with a surface shut-in, the pressure at the top of the well, below the shut-in point, falls to below the phase boundary, so gas will evolve,

leading to significant cooling (and gas slugging when injection starts up again). When injection starts again, the pressure will be low at the wellhead at the top of the CO₂ column and there will be a short transitional period of high pressure liquid entering a low pressure gas environment, leading to further cooling effects.

Stage	Average Reservoir Pressure	Average Static Gradient	Equivalent Pressure Gradient
	psi	psi/ft	psi/ft
Start of injection	538	0.027	0.299
End of heated CO ₂ injection	3585	0.287	0.559
End of injection	5636	0.348	0.620

Figure 3-56 Maximum applied pressure

The transient pressure effects of a surface shut-in could be modelled using a simulator such as OLGA, for example. This would give a better prediction of the maximum and minimum pressures in the wellbore and highlight if the pressure variations cause problems with exceeding fracture pressures or fall below sand face failure pressures.

3.6.5.2 Restarting CO₂ injection during the Transition Period or After a Water Wash

During the early time heated injection period, where the reservoir pressure is below critical, we are not concerned about the evolution of gas in the wellbore, as the injected CO₂ is heated above the critical point, ensuring a continuous evolution from supercritical fluid to gas and vice versa. The only transitional effect that is of concern is therefore the loss of pressure and / or cooling of the gas or supercritical CO₂ in such a way as to cross the gas / liquid phase

boundary. As cooling will only occur near the top of the well (towards seawater temperatures) where pressures are low, it is likely that the CO₂ will remain in gas phase. When heated injection (supercritical) re-starts, there is no phase transition. The main transition concern, therefore, is the failure of heating or the introduction of cold water for water wash purposes. Safeguards should therefore be put in place to prevent injection during heating 'outages' and the heating of wash water should also be considered.

During the un-heated injection phase, where liquid CO₂ is being injected, the reservoir may support a full column of CO₂ in the wellbore, but we are still relying on well and reservoir 'back pressure' to maintain single phase in the wellbore to surface. However, when shutting in the well at surface, the reservoir pressure may be insufficient to maintain wellbore pressure at surface above the gas phase boundary and gaseous CO₂ will evolve filling a part of the wellbore. When starting injection again, the back pressure is not yet generated and the high pressure liquid CO₂ will flash to gas in the wellbore. This will create a considerable temperature drop in the wellbore, with a final limit determined by the reservoir pressure (and thus THP) at the time.

If a large volume water wash is required in the unheated (liquid phase injection) period, the potential cooling effects on restarting CO₂ injection are more serious (see section 3.6.4 for near wellbore issues). At the end of a water wash, with a column of fresh water in the well, the surface pressure will be below the CO₂ gas – liquid phase boundary. When injection restarts and high pressure liquid is introduced there is rapid cooling. If water is present at the interface, an ice plug may form. This might be mitigated by heating the water or the introduction of sufficient MEG into the wash water, and this is a contingency that is allowed for in the platform design. As stated previously, if water washing is required, small

batches of fresh water injection may be preferred to large continuous water injections, although the effectiveness of this is, as yet, undetermined.

3.6.5.3 Solution to Transient Effects

As the Viking A platform facility will have CO₂ heating capacity, the simplest solution to transient effects during liquid phase re-start is to temporarily heat the CO₂ past critical temperature, allowing continuous property transition from supercritical to gas (i.e. no phase change). This does, however, require that the heating facilities are made available (kept maintained) for the entire storage injection period.

A possible alternative solution to these transitional effects, and one that allows for failure of the heating system, involves adding a deep-set shut-in valve to the completion. The deep-set valve would act as the primary shut-in. While not eliminating the problem entirely, it would move the issues away from the wellhead to a much deeper – and hotter – location in the wellbore. If the valve could be reliably operated as a flow control valve, all phase transition effects could be moved to the lower completion temporarily, before transitioning to the reservoir,

Shut-in closer to the formation reduces the hydrostatic head of CO₂ acting on the formation and removes the risk of exceeding formation fracture pressures. After shut-in the well could be left with the CO₂ supply pressure applied and therefore mitigate cooling effects at the wellhead on restart. The pressure differential across the downhole valve, however, will still be considerable and may cause problematic transitional effects, although the higher temperatures at depth may limit these issues. Some modelling with suitable transitional software (e.g. OLGA) would be required to determine the minimum depth of shut-in and a suitable valve specified.

A similar approach could be taken for a water wash: the system left pressured above the deep set valve at the end of the treatment (or re-pressured before restarting CO₂ injection). The higher pressure would mitigate the cooling at the CO₂ / water interface when injection restarts. However, higher pressure would need to be modelled in a hydrate prediction software in order to ensure that hydrates were avoided.

The oil and gas industry offers a range of subsurface isolation valves that could be evaluated. Preferred features would be:

- Surface controlled – hydraulic control lines
- Ball valve
- Flow control functionality
- Metal-to-metal sealing
- Bi-directional sealing
- Deep set functioning
- Wireline retrievable
- Reliable

Potential candidate valves are currently available on the market. These are surface-controlled, tubing-retrievable isolation barrier valves. Open/close is achieved by applying hydraulic pressure to the tool via dual control lines. They have metal-to-metal sealing body joints, full bore internal diameter, bi-directional sealing and a deep-set capability (the actuation mechanisms in these valves mean that the setting depth is unrestricted). Some have a contingency mechanical shifting capability.

The preferred features not available are the ability to retrieve/set the valves on wireline, which means a workover is required to retrieve it in case of failure, and track record as flow control valves. Including these valves in the completion adds

some complexity and slows the completion running/pulling time because of the need to run dual control lines. However, if they can be operated reliably, they considerably simplify the well shut-in and start-up procedure and would be beneficial over the project life.

These valves are tested to ISO 28781 Barrier Valve Certification. However, before incorporating them into a completion for CO₂ injection there should be a comprehensive evaluation of the historic reliability of these valves under similar operating conditions to give confidence that their inclusion does not compromise the efficient operation of the injection program.

For the purposes of this work, it is assumed that a suitable mechanism is available to perform the downhole shut-in function, and that this is installed as back up to the primary heating option. However, further work is required in the FEED stage to substantiate this approach, or to provide alternate solutions

3.6.6 Safe Operating Envelope Definition

With respect to CO₂ injection, safe operating limits are those that allow the continuous injection of CO₂ without compromising the integrity of the well or the geological store. Since wells are designed to cope with the expected injection pressures and temperatures, the primary risk to integrity is uncontrolled fracturing of the formation rock, leading to an escape of CO₂ through the caprock (adjacent to the wellbore or at a point anywhere in the storage complex). The pressure at which fractures can propagate through formation rock is called the fracture pressure and is usually defined as a gradient, as it varies with true vertical depth.

In order to prevent CO₂ leaking from a storage complex, fractures in the caprock need to be avoided. This can be done by limiting the pressure to which the caprock is exposed, in both the near wellbore and the storage site complex as a whole. The pressure limit at any one point depends on the caprock properties, including strength, elasticity and thickness. Given that there is always uncertainty in rock properties as you move away from 'control' wells, and that caprock properties are generally not measured and documented to the same degree as permeable formation rock, there is a high degree of uncertainty surrounding caprock fracture initiation pressures and the vertical extent of any resulting fracture (fully penetrating or partially penetrating). For this reason, this study has used the permeable formation fracture pressure as the pressure limit (which, in the overwhelming majority of cases considered for CO₂ storage, is lower than the caprock fracture pressure) rather than that of the caprock itself. This provides a conservative approach, and also allays concerns over the concentration of cold CO₂ at high pressure that might be delivered to the caprock boundary through fracture propagation in the target formation. A further safety

margin of 10% is taken from the estimated formation fracture pressure in order to allow for variations (and unknowns) within the formation rock properties.

A further risk to well integrity and the well injection performance is the poor understanding of operating a CO₂ injection well close to the gas / liquid phase boundary. Due to the characteristics of CO₂, changes in phase can be accompanied by significant changes in temperature as well as flow performance (pressure drops due to friction within the wellbore). Across the phase boundary, CO₂ is boiling and condensing, making it an extremely complex system to model, from both a temperature and flow perspective. This complexity introduces significant uncertainty.

3.6.6.1 *Fracture Pressures*

In order to determine the fracture pressure for Viking A, to be used as an upper injection pressure constraint, a geomechanical review was performed on the available well data. Several key data requirements for this study were not available, including confirmed current (depleted) reservoir pressure, rock strength data from core and actual in-situ stress orientation. With this data missing, several assumptions had to be made. For example, the current reservoir pressure – or pore pressure – was assumed to be 500 psi (Section 3.6.3). Regional stress maps were used in the assumption of a NW-SE maximum stress orientation. Correlations from well log data were used to determine rock strength. Different geomechanical correlations use different measured parameters from logs to estimate rock strength and these often result in a range of fracture pressure estimates, some more conservative than others. Field data is normally used to determine which of these correlations might be more representative of the in situ rock.

The geomechanics review was performed on well data acquired when the wells were drilled – in other words at original reservoir pressure. This resulted in the

initial – un-depleted - fracture gradient estimate of 0.74psi/ft from literature being confirmed. As the pressure in the reservoir depletes through production, relative stresses change and the horizontal stress reduces. This means that the rock can fracture at lower applied pressures. Again, various correlations exist to allow this process to be modelled analytically. Using the best fit correlation, a depleted fracture gradient of 0.54psi/ft was determined. This figure is thought to be a reasonable estimate for well design and drilling purposes. Should the fracture gradient be lower, it may be necessary to modify drilling techniques to suit. A further study, utilising a 3D geomechanical model, suggested a more conservative depleted fracture pressure gradient of 0.43 psi/ft if using the Mohr Coulomb relationship.

As the reservoir is re-pressured with CO₂ injection, the accepted convention is that fracture pressure will increase back towards the original value. Wells drilled at a later stage in the field life will therefore be less exposed to fracture pressure limitations. It should be noted, however, that there is considerable uncertainty over the stress path during re-pressurisation (whether it follows back up the depletion path or whether there is a hysteresis effect) and this is considered a high project risk. However, this can be considerably de-risked by determining the true depleted fracture pressure as a starting point. It is therefore recommended that the current operators of the Viking field are approached, prior to field abandonment, in order to acquire fracture pressures from the current well stock (extended leak off tests for example).

For reservoir engineering and well modelling purposes, where fracture pressure is an intrinsic limitation for CO₂ injection (nothing can be done about it), a conservative approach was taken to establish the safe operating limit by applying a 10% margin for safety to the lowest estimated depleted fracture pressure. Thus the depleted fracture pressure limit applied was 0.9×0.43 psi/ft =

0.387 psi/ft and the re-pressurised (original) fracture pressure limit was 0.9×0.74 psi/ft = 0.666 psi/ft.

3.6.6.2 Phase Envelope

In order to minimise the risk associated with the uncertainty introduced by operating wells across the liquid to gas phase boundary, all injection in the wells will be engineered to avoid the liquid to gas phase transition. With the reservoir pressure at the start of CO₂ injection (~35 bara) being below the critical point for CO₂ (74 bara), initial injection options are therefore limited either to gas or supercritical phase. As the reservoir temperature of 84 °C is well above the CO₂ critical temperature of around 31 °C, transition from supercritical to gas phase can occur in the reservoir without phase change.

Initial gas phase injection was explored and could be considered. However, to achieve target injection rates (>1mmte/yr), large injection tubulars were required (9-5/8"). Due to well construction limitations, it was only possible to deliver 9-5/8" tubulars to a few hundred feet above the top Zechstein, requiring a hybrid 9-5/8" x 7" completion. Furthermore, in order to avoid phase change, injected CO₂ required to be heated to at least 30 °C (Figure 3-57). Injection pressures were also required to be close to the phase boundary, meaning that either the pipeline should be operated in liquid phase with a liquid to HP gas heater / convertor or operated in gas phase with a compressor on the platform. Given that the gas phase injection period might be fairly limited in time (initial reservoir pressure being relatively high compared to other depleted gas fields) and that several injection wells might be required to achieve a target injection rate of 5mmte/yr, it was decided not to pursue the gas phase injection route.

Injecting in the liquid phase is problematic for low pressure reservoirs, as there is insufficient back pressure to prevent a phase change from liquid to gas within the wellbore. It is therefore necessary to either create the back pressure

artificially (through downhole back pressure valves, limited reservoir entry or deliberate reservoir damage) or to heat the liquid CO₂ past the critical temperature so that any change to gas phase does not cross the phase boundary (continuous evolution in density and enthalpy). The use of back pressure systems in the well bores themselves is the simplest solution, but keeps the phase change within the lower wellbore, with all the associated issues of extremely low temperatures and unpredictable well behaviour. Limited entry and deliberate reservoir damage (induced 'skin') can lead to the requirement for extra wells in order to achieve target injection rates as the reservoir pressure increases, and would not be a preference where new wells are being delivered.

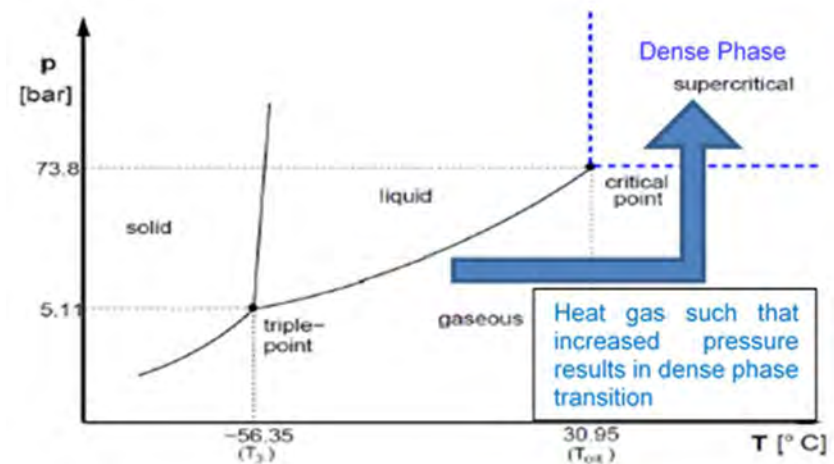


Figure 3-57 Gas phase injection option

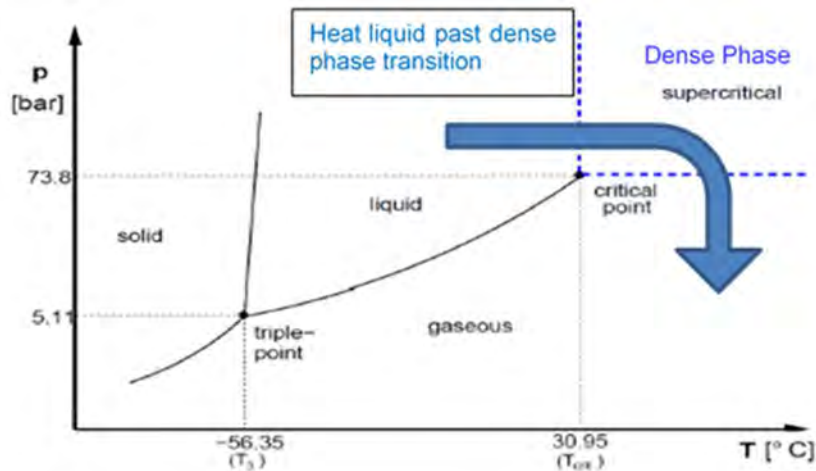


Figure 3-58 Liquid phase injection option

For Viking A, therefore, the preference is to heat the liquid phase CO₂ past critical temperature for an initial period (see Figure 3-58), until reservoir pressure is sufficiently high to support unheated CO₂ injection. This allows liquid phase pipeline delivery (most cost effective), with a liquid phase heater for the dense phase located on the platform, which can be by-passed after sufficient re-pressurisation of the reservoir is achieved. This helps 'front load' the project with respect to offshore maintenance, reducing requirements as the facilities age. No change in well architecture is required between the heated and un-heated phases of the store life.

It is recommended that the pros and cons of all options listed above should be further investigated in a FEED study with further optimisation being possible in order to reduce the heating requirements.

3.6.7 Dynamic Modelling

The Viking gas field is comprised of a number of gas accumulations within separate fault compartments. Each of these accumulations could provide CO₂ storage potential but as they are isolated fault compartments dedicated injectors will be required for each fault compartment. The field extends over a large area of approximately 108 km² and has been developed by two main platforms A and B, and a number of satellite platforms. It is clear from the literature that the area is very complex and although there is a high level understanding of the field performance, the detailed production performance per fault block or by well is not available to this study. For CO₂ storage in a depleted gas field the storage capacity is dependent on the volume of produced hydrocarbon gas from the reservoir that is connected to the injection wells. There is significant uncertainty in the connectivity, if any, between the separate gas accumulations within the Viking field as a whole which could be reduced considerably if historical production and pressure data can be made available.

For this study a primary storage complex was selected for evaluation with the understanding that additional potential exists elsewhere in the Viking field area for further phases of storage development. The north Viking area was selected. This comprises fault blocks A, H, F and Fs. Production performance including references to compartmentalisation within this area is well documented (Riches, 2003). Block A is the main injection target area as it is the largest fault block. Production from Block A ceased in 1991 after 1124 Bscf gas had been produced. This equates to approximately 40%, a significant proportion, of the estimated total gas production from the entire Viking field area.

The location of northern area within the Viking gas field is shown in Figure 3-59.

The dynamic modelling was carried out using the ECLIPSE compositional simulator to allow CO₂ injection into a depleted hydrocarbon gas reservoir to be modelled. A representative dynamic model, referred to as the reference case model, was constructed for the storage complex area. The inputs and results from the dynamic modelling are discussed in the following sections.

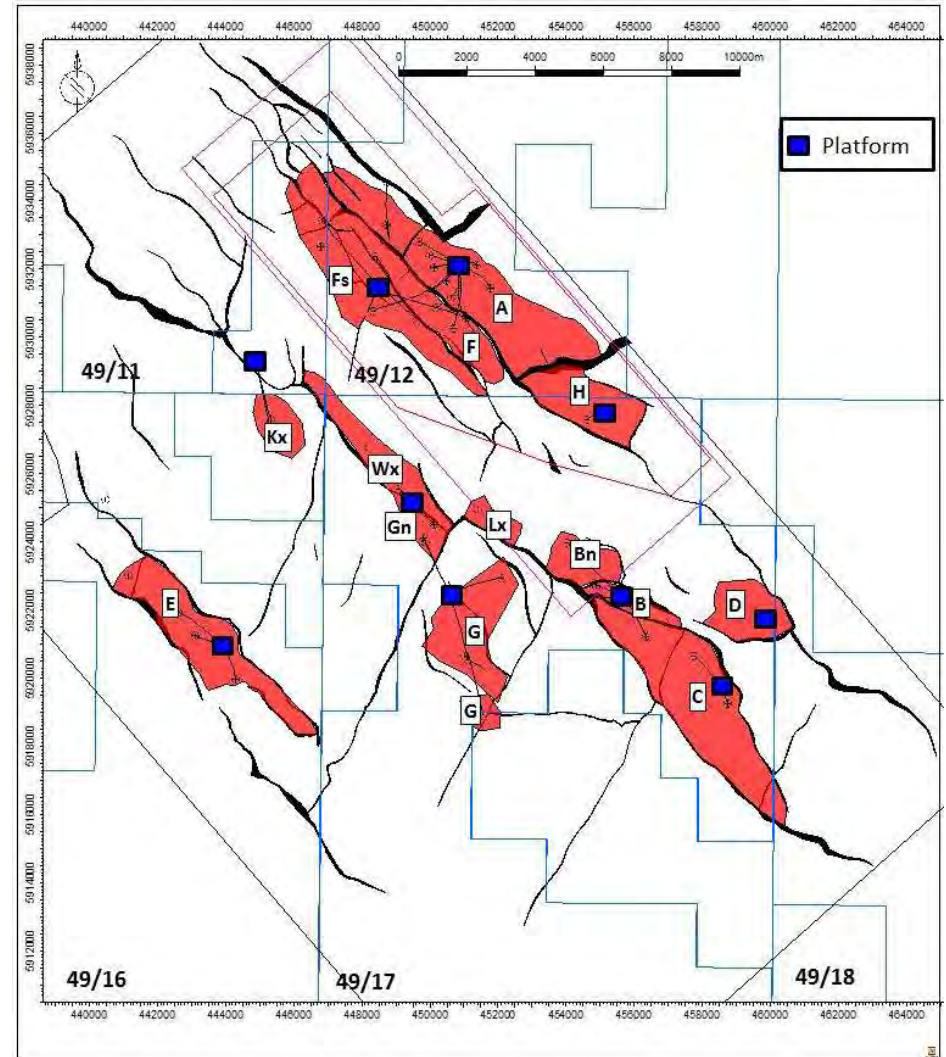


Figure 3-59 Extent of Viking Gas Field, showing separate gas accumulations and main platform locations.

3.6.7.1 *Model Inputs**Structural Grid and Reservoir Modelling*

The structural grid and reservoir properties modelling are discussed in detail in section 3.5. The grid and properties were upscaled to a suitable engineering scale to allow for reasonable run times. Grid cells are 100m by 100m in the x and y directions and the number of active cells is approximately 468,000.

The storage capacity is dependent on the connected reservoir pore volume. It is therefore important to understand the impact of subsurface uncertainties on the reservoir connectivity. Fault transmissibility, horizontal barriers to vertical flow and permeability have been identified as key subsurface uncertainties. The impact of these on the storage site performance has been evaluated and is discussed in the uncertainty analysis section. Internal faults exist within Block A. All faults in Block A are assumed to be sealing with the exception of the north western fault.

Dynamic model parameters	Model 1: Fine Scaled
Dimensions (NX x NY x NZ)	62 x 174 x 87
Cell Dimensions (m)	100 x 100
Cell thickness range / average (m)	0.08-86.5 /4.3
Number of cells	938,556
Number of active cells	468,174
GIIP (m ³ g / Bscf)	68 / 2385
GIIP (m ³ g / Bscf) – Block A	44 / 1553
WIIP (m ³ g)	806,137
WIIP (m ³ g) – Block A	807
Permeability (horizontal) average (mD)	49
Permeability (horizontal) average (mD) – Block A	78
Permeability (vertical) average (mD)	26
Permeability (vertical) average (mD) – Block A	45
GWC Blocks A and H (m tvdss)	2950
GWC Blocks F (m tvdss)	3079
GWC Blocks Fs (m tvdss)	3086
Pre-production pressure (@2544 mtvdss) (bara)	305
Pressure at start of CO ₂ injection (@2544 mtvdss) (bara)	34.1
Pressure at end of CO ₂ injection (@2544 mtvdss) (bara)	383.3
Reservoir Temperature (°C)	83.8

Table 3-26 Dimensions and properties for the dynamic model

Equilibration and Volumes in Place

The gas initially in place (GIIP) of Viking A in the dynamic model is 1553 Bscf, within 0.8% of the static model GIIP which is an acceptable accuracy. The volume for block A aquifer is 5081MMbbls. No additional aquifer volume has been added to the block A as there is no evidence from production history to support any additional aquifer support, aquifer influx is only documented in blocks F, G and Gn (Morgan, 1991).

PVT Management within Eclipse

Compositional modelling is required to model CO₂ storage in a depleted gas field. In a compositional simulator oil and gas phases are represented by a multi-component mixture rather than by single or binary component representation in a black oil simulator. The compositional simulator can account for effects of phase behaviour and compositionally dependent phase properties such as viscosity and density on miscible displacement. In the case of CO₂ injection into the depleted Viking A gas field, the reservoir pressure is initially below the critical pressure of CO₂ (74 bar/1071 psi). However, due to continuous CO₂ injection, the reservoir pressure will increase beyond the critical pressure resulting in CO₂ changing from gas phase to dense phase in the reservoir, because the reservoir temperature is above the critical temperature of CO₂ (31.5 °C). Supercritical CO₂ has a liquid like density and a gas like viscosity. The viscosity of CO₂ also changes with pressure. Using the Peng Robinson equation of state, in the ECLIPSE compositional simulator, the density and viscosity changes with increase in reservoir pressure can be modelled correctly.

In addition to modelling the phase change behaviour of CO₂ correctly, a compositional simulator is required to model the natural gas and CO₂ gas system as there is a significant difference between the properties and phase

behaviour of natural gas and CO₂. A Black Oil simulator is limited to modelling a single gas within the fluid system and is therefore not suitable for modelling CO₂ injection into a depleted gas field correctly.

The Viking gas properties and initial reservoir conditions were sourced from well data from CDA.

The Viking gas composition is shown in Table 3-27.

Component	CO ₂	N ₂	C ₁	C ₂	C ₃	C ₄	C ₅	C ₆	C ₇
Mole fraction	0.35	2.77	90.31	4.58	1.18	0.48	0.16	0.09	0.08

Table 3-27 Viking gas composition

The initial reservoir pressure is 307 bara (4452 psia) at a depth of 2647 m TVDSS (8685 ft TVDSS) and the temperature is 83.8 °C (183 °F). This was used as input to the PVT model.

The component library in Petrel was used for the component properties. Petrel uses the original PVTi library, but with molecular weight, density, boiling points, critical properties and acentric factors taken from additional sources (Katz & Firoozabadi, 1978) (Ksler & Lee, 1976). The pressure - temperature plot for the Viking field gas composition is shown in Figure 3-60.

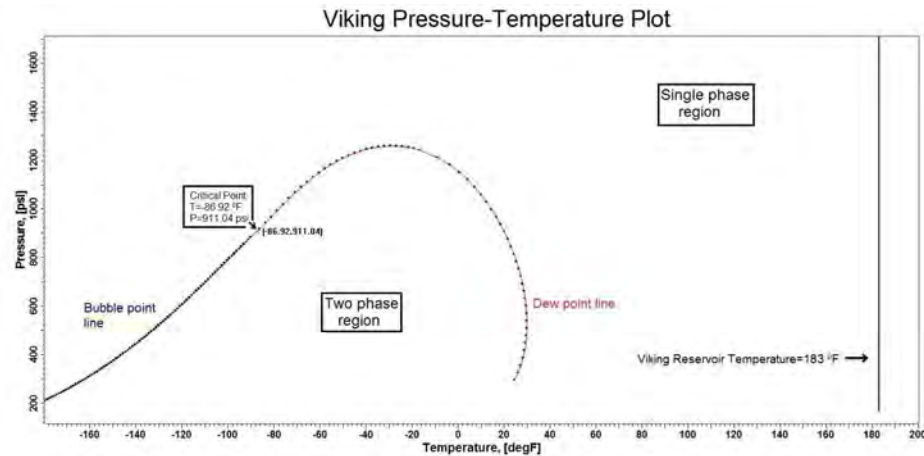


Figure 3-60 Viking Gas Composition pressure-temperature plot

The black vertical line in Figure 3-60 represents the Viking field reservoir temperature. This line is to the right of the dew point line indicating that the reservoir behaves as a dry gas.

A salinity value of 220,000 ppm was used. The salinity of water is used to tune the CO₂ solubility in water. The density of water was also modified to account for dissolved salts.

Relative Permeability

In compositional simulation three phase relative permeability curves are used. The phases are oil, gas and water. The ECLIPSE compositional simulator solves for molar concentration and then uses the calculated critical temperature to label the phase as oil or gas. Oil and gas phases then use the respective relative permeability curves. ECLIPSE calculates an average critical temperature of the fluid. When this critical temperature is above the cell temperature it labels a single phase hydrocarbon as oil otherwise it is labelled gas. The pressure is not

accounted for within the phase labelling of a single phase cell, only the temperature.

Software limitations dictate that CO₂ storage in a gas field can only be modelled in an isothermal mode, and as pressure is not accounted for in the phase labelling, CO₂ is labelled as either a gas or oil throughout the simulation run. The CO₂ phase change in the reservoir is modelled correctly but the dense phase CO₂ is labelled as gas. Therefore, in the Viking A CO₂ storage model, both methane and CO₂ (gas and dense phase) use the gas relative permeability curve i.e. methane, gas phase CO₂ and dense phase CO₂ have the same mobility. The relative movement of CO₂ and hydrocarbon gas is dominated by density and viscosity differences.

Indications from the limited available production data and literature review are that there is no significant pressure support from a connected aquifer into Block A and no water influx i.e. water is relatively immobile. It is therefore unlikely that there has been any significant movement in the GWC. The modelling results also indicate that very little CO₂ dissolves into the aquifer. As the interaction between CO₂ and water is expected to have very little impact on the CO₂ storage site performance, the relative permeability input curves are expected to have little impact on the results. A sensitivity, to relative permeability inputs, was carried out as part of this study and the results confirm that the relative permeability inputs are not key controlling parameters.

Pressure Constraints

The northern area of the Viking field has been selected as the primary CO₂ storage complex for this evaluation, with injection into the Viking A fault block. 1124 Bscf of gas was produced from Block A from 1972 to 1991 and with very limited pressure support into this area. As a result, very significant pressure

depletion of approximately 273 bara has been observed. A 1990 estimate of reservoir pressure for Block A is 34.3 bara at a depth of 2647m tvdss. This was supplied by the operator. It has been assumed that there will be no re-pressurisation between 1990 and when injection starts. This is an uncertain but reasonable assumption given the volumetric depletion observed at Site A during production.

For this study it has been assumed that CO₂ injection will commence in 2031. As CO₂ is injected into the reservoir the reservoir pressure will increase. As discussed in section 3.6.6, it is important that the reservoir pressure is maintained below the fracture pressure to minimise the risk of losing caprock integrity. There is significant uncertainty in estimating the fracture pressure in the Viking field. The initial fracture pressure gradient decreases under pressure depletion and then increases when the reservoir is repressurised under CO₂ injection. It is likely that the fracture pressure gradient will return to the original value at the same rate that it decreased during the depletion phase but it is possible that this might not be the case. Hysteresis might occur resulting in a lower fracture pressure gradient than that experienced during depletion. In the worst case scenario, the fracture pressure gradient could remain at the lowest value seen during the depletion phase. This is considered to be a very unlikely scenario but it has been evaluated as part of the sensitivity analysis.

A conservative approach has been adopted for the dynamic modelling inputs selection. To avoid any chance of fracturing the reservoir the maximum operating pressure is limited to 90% of the fracture pressure limit. The model is set up so that if the pressure in any cell in the model reaches its fracture pressure constraint then injection is stopped. At the start of CO₂ injection, into the depleted reservoir, the fracture pressure is estimated to be 0.097bar/m (0.43psi/ft). The most likely case is that the fracture pressure gradient will return to the initial

fracture pressure gradient (pre-production) of 0.167bar/m (0.74psi/ft). The increase in fracture pressure gradient with increasing pressure is compared to the model pore pressure gradient prediction, per well and per region, for the reference case in Figure 3-61.

The final reservoir pressure is 383.3bar at a depth of 2544m TVDSS. The fracture pressure at this depth is 426bar.

In all sensitivities it was found that the pressure limit was first met close to the north-west to south east trending boundary fault and injector I2. The location of the grid cells where the pressure limit is first met in the reference case model is shown in Figure 3-62

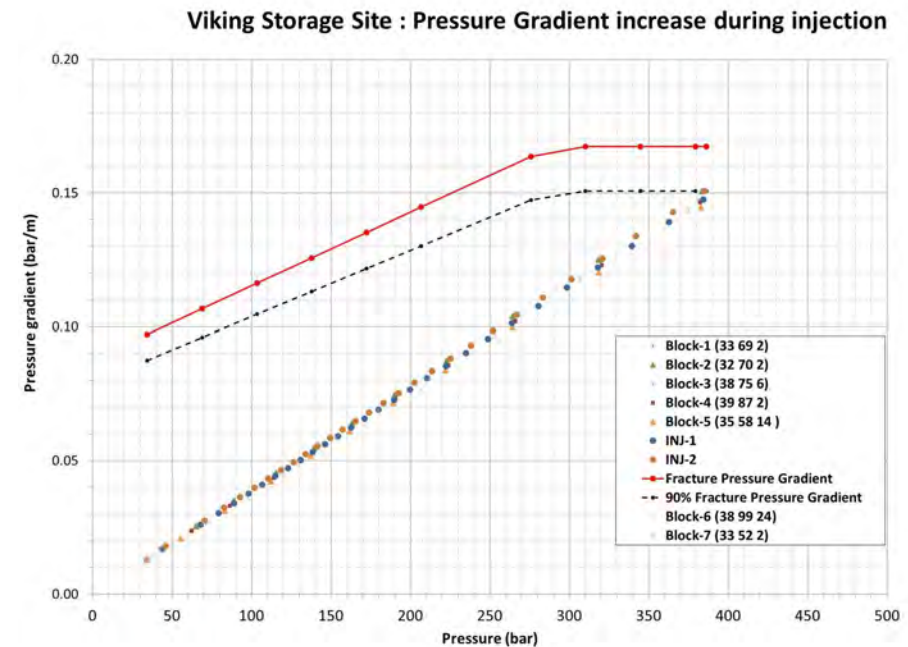


Figure 3-61 Viking A Pressure gradient increase during CO₂ injection

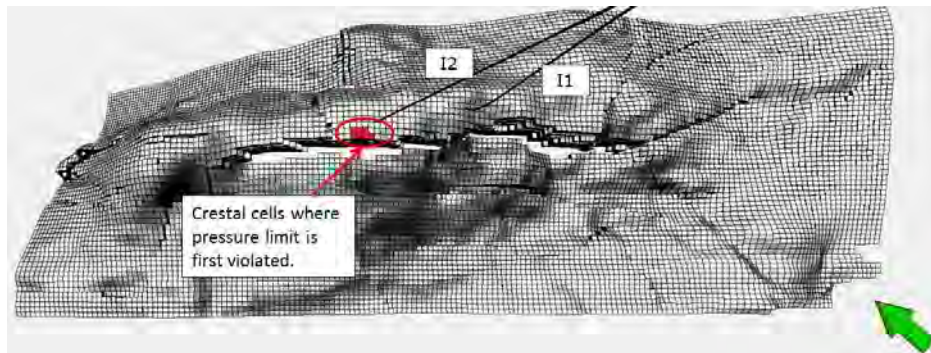


Figure 3-62 Location where pressure limit is first violated in reference case model

Well Modelling

3.6.7.2 Model Calibration

The storage complex comprises the north Viking gas accumulations, namely Block A, Block H, Block F and Block Fs (F south). The fault block regions within the site model are shown in Figure 3-63.

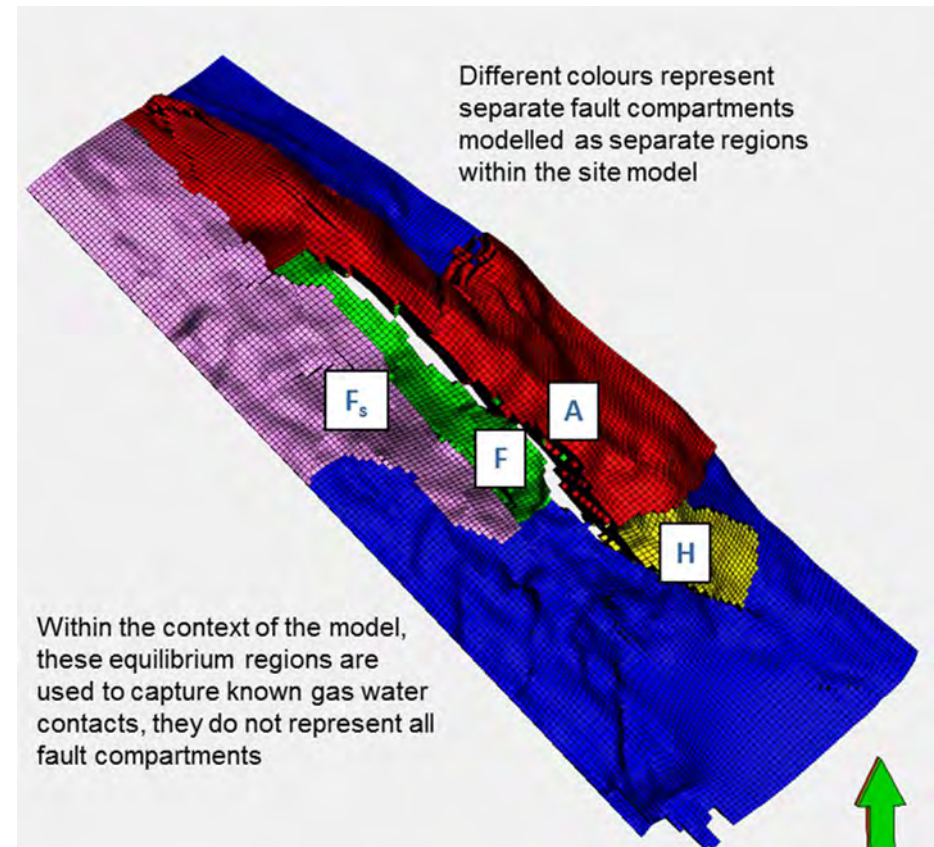


Figure 3-63 Fault compartments within the storage site model

Block A and Block H have the same initial GWC however, production and pressure responses during depletion indicate that the fault blocks are not hydraulically connected. These regions are modelled as separate regions in the site model. The downthrown fault blocks of Block A, Block F and Block Fs, have different GWCs and are also not hydraulically connected to Block A itself. This has been captured in the site model.

Injectivity into all the fault compartments has been tested and the primary injection site for this evaluation is Block A as there is more well control and therefore greater confidence in the subsurface properties as well as a significantly larger capacity. It is recommended that the development potential of Blocks H, F and Fs is evaluated in more detail when production, pressure and well data are made available.

Viking Block A was produced from October 1972 until April 1991, using ten gas producers. Production data are available through DECC but the database is incomplete for Viking as first production records are available from 1983, 11 years after Viking started producing. In addition, the production is not split by fault block. With no production history available for Block A, the model could not be finely calibrated to production performance. It is recommended that a full model calibration is carried out to improve confidence in the model's predictions when pressure and production data becomes available. The cumulative production from Block A was reported in the literature to be 1124 Bscf, (Riches, 2003), and, although there is uncertainty in this volume, it has been used as guidance during the model calibration.

Some pressure data were supplied by the Operator for Viking A in the form of a single reservoir pressure and this has been used in combination with pressure data sourced from CDA abandonment reports to estimate a reservoir pressure at the start of CO₂ injection to be 34.1bara at a depth of 2544m TVDSS. The model has been initialised with this pressure in all regions. As there is considerable uncertainty in the pressure depletion, sensitivities have been run using initial pressures of 21 bara and 48 bara to evaluate the impact of the pressure uncertainty in the site storage performance. This is discussed in more detail in the uncertainty analysis.

Initial Gas in Place

The modelled GIIP for Block A is 1553 Bscf with a total GIIP of 2385 Bscf in the site model. There is no data available to confirm if this is representative. As the CO₂ storage capacity is dependent on the GIIP connected to the injector well locations, a material balance, using P/Z analysis, was carried out to gain more confidence in the modelled volume.

There is believed to be good pressure communication within the reservoir zones A, C and E, the targeted sands for CO₂ injection and storage. However, these zones are separated by extensive muds and shales that act as horizontal barriers to vertical flow. Internal faulting within Block A enables the reconnection of these sands through juxtaposition thus allowing pressure communication between zones A, C and E. Although communication between the zones could be through a tortuous pathway the assumption is that the injection wells are connected to the total GIIP in Block A. Based on the limited pressure data available, 19 years of production with no water influx and the information from available literature, it is unlikely that there is much if any aquifer pressure support into Block A.

Inputs to the material balance analysis include an initial pressure of 305 bara and a depleted pressure of 34.1 bara after 1124Bscf gas had been produced from Block A. Based on these inputs the GIIP is estimated to be 1270Bscf, 18% less than the modelled volume. This corresponds to a recovery factor of 89 % compared to a recovery of 77% of the modelled volume.

The P/Z plot is shown in Figure 3-64.

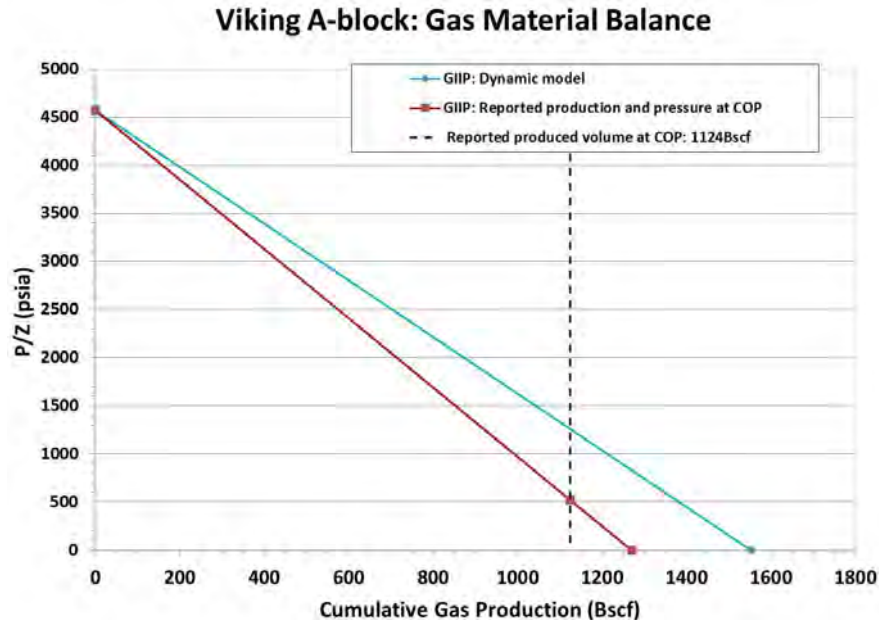


Figure 3-64 Gas material balance analysis

As mentioned previously there is considerable uncertainty in both the volume produced from Block A and the final depleted pressure in Block A. Without this data being available there was considered to be too much uncertainty to justify carrying out a modification to the structural model to match the lower GIIP estimated using material balance. However, the impact of a lower GIIP volume was evaluated during the sensitivity analysis.

3.6.7.3 Modelling Results

Development Strategy

Viking Block A is a depleted gas field that ceased production in 1991. The reservoir pressure at the start of the CO₂ injection is estimated to be 34.1 bara

at a depth of 2544m TVDSS and the reservoir temperature is estimated to be 83.8°C.

In order to minimise the risk associated with the uncertainty introduced by operating wells across a phase boundary, all injection in the wells will be limited to single phase operation. With the reservoir pressure of Viking A at the start of CO₂ injection being below the critical point for CO₂ (74 bara), initial injection options are limited to gas or supercritical phase. As the reservoir temperature is well above the CO₂ critical temperature (31°C), transition from supercritical to gas phase can occur in the reservoir without phase change. The pre injection CO₂ conditions in the reservoir and wellbore are illustrated on the phase diagram in Figure 3-65.

The development options are discussed in detail in Section 3.6.6. The currently preferred development for Viking A is to heat the supplied liquid phase CO₂ past critical temperature for an initial period, until the reservoir pressure is sufficiently high to support unheated CO₂ injection.

The injection rate target for Viking A is 5Mt/y. Numerous sensitivities were run to establish the duration of the injection plateau. For the reference case, which is described in the following sections, the plateau extends for 26 years. The proposed development case requires two 7" injection wells. The CO₂ is initially injected at a wellhead temperature of 35°C. After 20 years the reservoir has been re-pressurised to a pressure that can support unheated CO₂ injection and liquid CO₂ injection will continue, but at a wellhead temperature of 10°C.

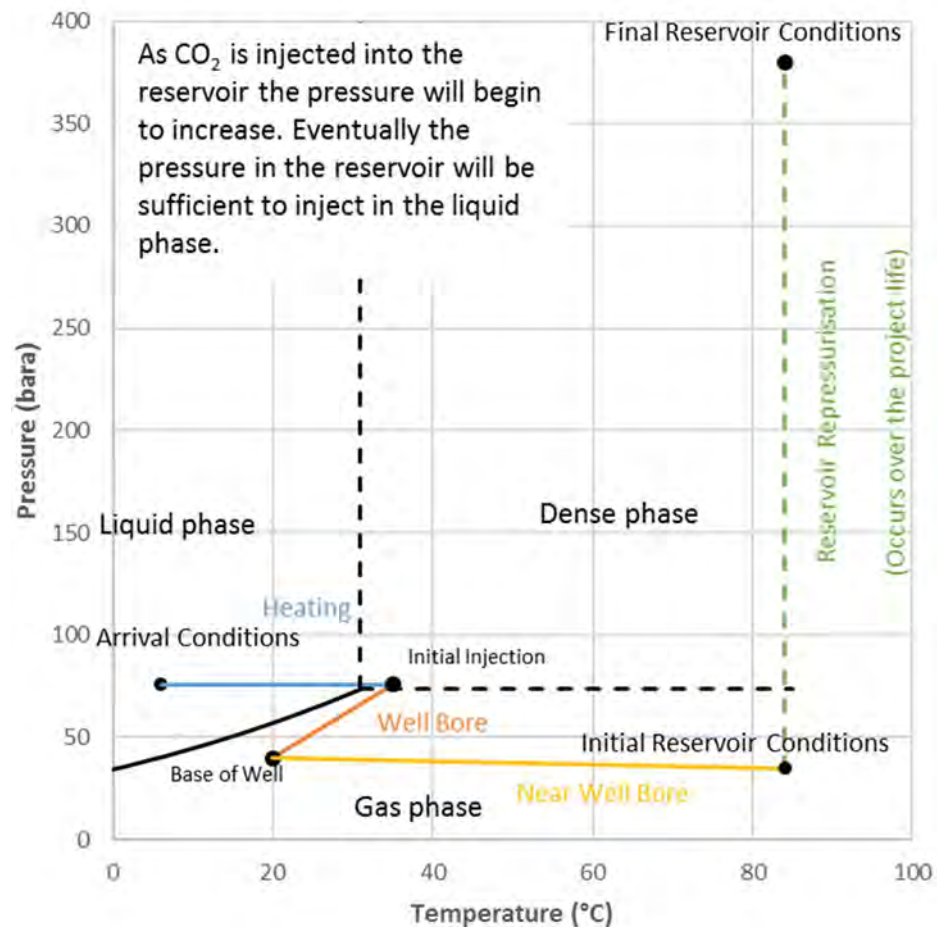


Figure 3-65 CO₂ Phase diagram with Viking A pre-injection, reservoir and wellbore conditions

Well Placement

Injectivity into all the fault compartments was tested in the model. Block A was selected as the primary injection site as it contains the largest storage capacity potential with 65% of the total site GIIP located in Block A. In addition, there are 10 development wells located in Block A providing more well control than in the other fault compartments and therefore considerably reducing the subsurface uncertainty associated with Block A.

There are three productive sand units, A, C and E that will be targeted for CO₂ storage. These units are separated by laterally extensive non-pay units (sabkha silts) that act as horizontal barriers to vertical flow. Communication between the sand units does occur where the sands are juxtaposed at the internal faults. The wells will penetrate all sand units, at an angle of 60 degrees from the vertical, to optimise injectivity and CO₂ placement in the reservoir. A cross section showing the well location through the reservoir and the sand juxtaposition at the fault is shown in Figure 3-66.

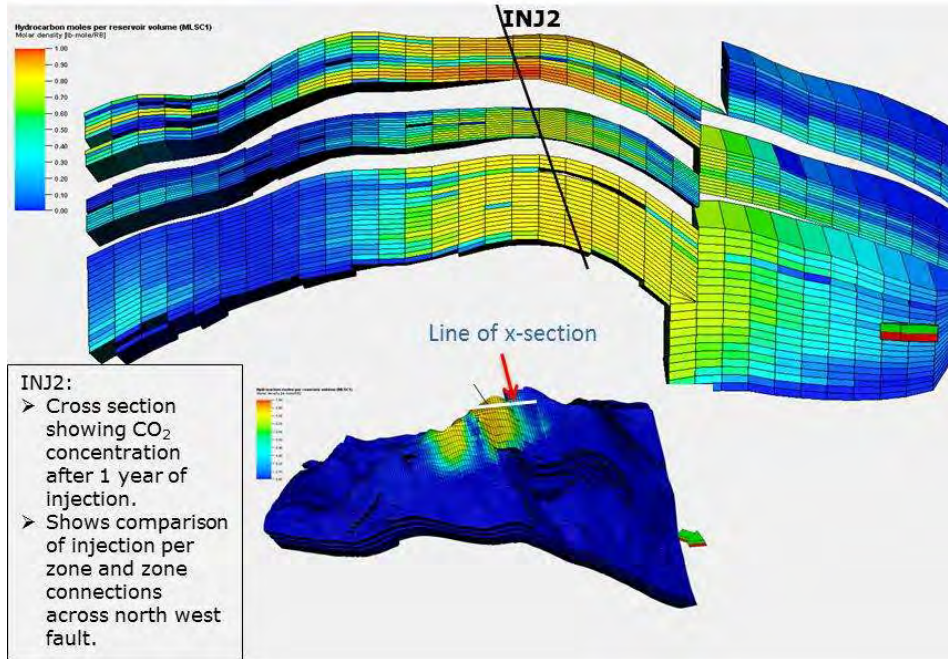


Figure 3-66 Cross section through injector 2 well path showing CO₂ concentration per zone after one year of injection

Within the model there is good lateral connectivity within the sand units (no significant barriers to flow). Simulation results indicate that injectivity and capacity are relatively insensitive to the well location within Block A, providing the well penetrates through the entire vertical sequence. The injection wells have therefore been located in the crest of Block A close to the development wells, therefore minimising the subsurface risk regarding reservoir quality. Three injection well locations are shown in Figure 3-67, injector 1 and 2 are the development wells and injector 3 is the required spare injector.

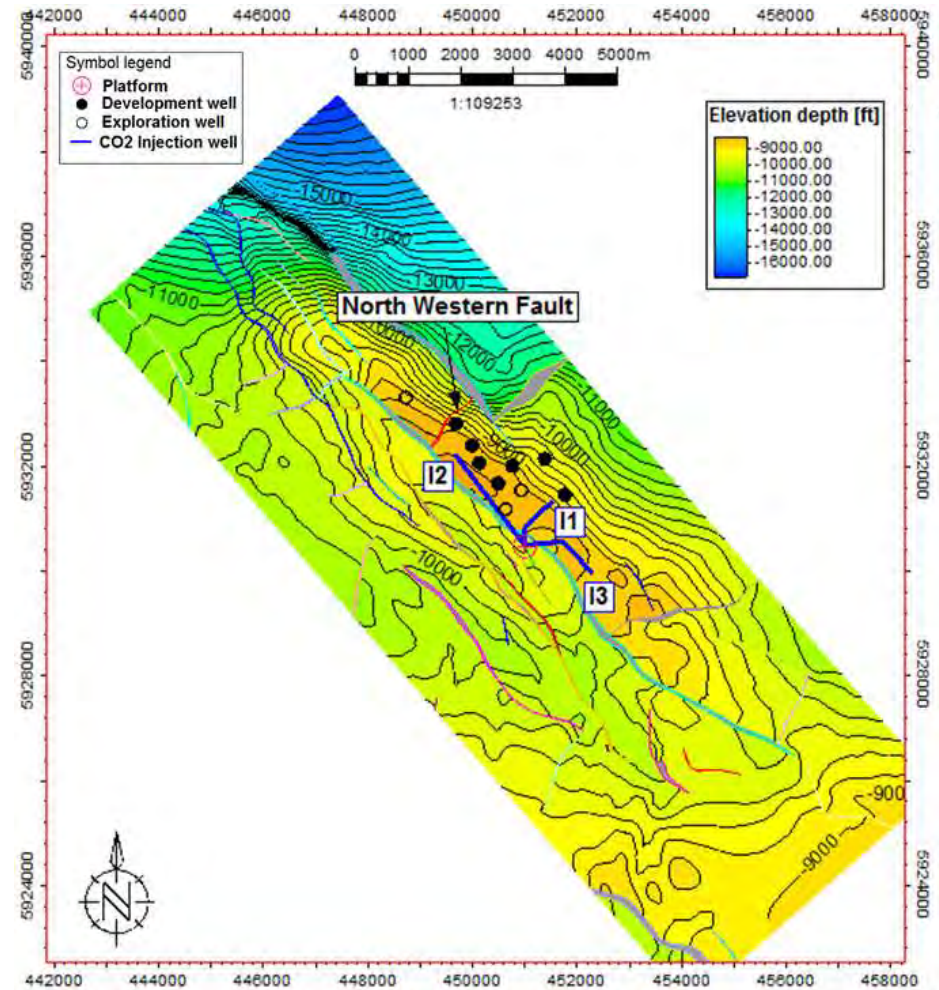


Figure 3-67 Viking A Injection Well locations at Top Reservoir Depth

Well Injectivity Potential

The Viking Block A reservoir is a moderate quality sand system with an average permeability of 78mD and a gas zone thickness of approximately 200m. Target injection rates per well are 2.5Mt/y. Initially this will be achieved by heating the liquid CO₂ at the wellhead to 35°C. 5 ½”, 7” and 9 ⅝”, tubing sizes were evaluated. 5 ½” wells have limited injectivity potential however the 7” tubing size meets the injectivity requirements for supercritical CO₂ injection. The minimum THP required to inject at the rate of 2.5Mt/y is estimated to be 73 bara. The well injectivity potential increases with increasing THP.

The well performance modelling is discussed in detail in section 3.6.3 and the THP limits are incorporated into the VLP curves used in the dynamic model.

Well Number

Sensitivities were run to determine the impact of the number of injectors on the storage site performance. Cases with 2, 3 and 5 wells were evaluated. In each case the total injection rate was fixed at 5Mt/y, the target supply rate for Viking. The inclusion of additional injectors had no significant impact on the storage capacity (<1% difference).

In addition to having minimal impact on capacity, additional wells had little impact on the storage efficiency of the site. For all injection locations the CO₂ plume migration is similar. CO₂ is injected into all reservoir layers and under injection the CO₂ migration is dominated by gravity. The lateral migration is dependent on the vertical transmissibility i.e. the CO₂ moves along the top of non-permeable layers. However, if the CO₂ can move downwards it will do so because it is denser than methane. At Viking A, the CO₂ continues to move down until it reaches the GWC. This is in contrast to CO₂ injected at an aquifer site which would rise to the top of the reservoir because of its buoyancy. With

continued injection the reservoir fills from the bottom and the depleted gas region (gas reservoir) is filled until the fracture pressure limit is reached. In the 5 well case, additional injectors are placed in the north west region, across the fault from the development well locations. In this case there is a small improvement in CO₂ stored in this region, with 26% of the CO₂ being injected into the north west area compared to 22% in the reference case. The well locations and CO₂ distribution are illustrated in Figure 3-68 below.

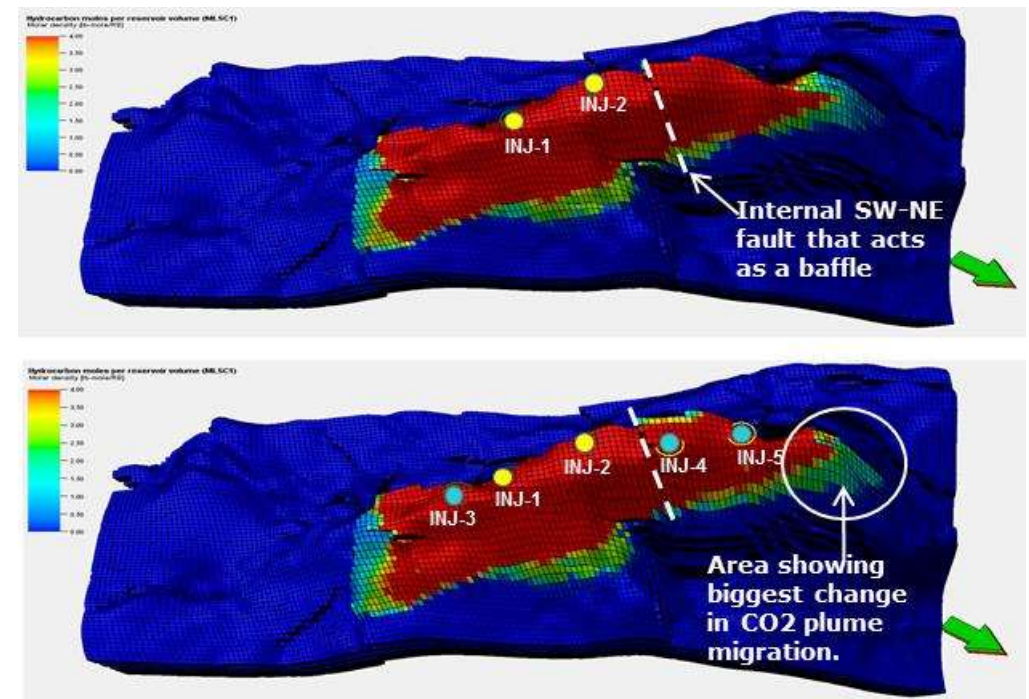


Figure 3-68 Total CO₂ concentration at the end of injection for the 2 well and 5 well cases

Sensitivity Analysis

A number of subsurface and development uncertainties were identified through the course of the project and assessed for their impact on CO₂ injectivity and site performance.

The reference case is described with respect to the sensitivity parameters in Table 3-28, for clarity the main input parameters presented throughout the body of this report are consolidated in in this table and provided as a summary.

Note that the density and viscosity ranges refer to conditions at the start and end of injection.

The uncertainty parameters and the associated range of values is summarised in the sensitivity matrix in Table 3-29 and the results are summarised in Figure 3-69, a bar chart showing the capacity and in Figure 3-70, a bar chart showing the duration of the injection period.

Input Parameter	Value / Description
Datum depth (mTVDSS)	2544
Initial Pressure (pre-injection) at datum (bar)	34.1
Temperature at datum (°C)	83.8
Rock compressibility	1.423x 10 ⁻⁵
CO ₂ density at datum (kg/m ³)	56 - 799
CO ₂ viscosity at datum (cp)	0.017 – 0.069
Brine Salinity (NaCl eq.) (ppm)	220000
Porosity (mean) (fraction)	0.13
Permeability (model mean / range) mD	49.2 (0 – 962)
Aquifer Volume (MMm ³)	806.5
Well Number	2
Injection Rate per well (Mt/y)	2.5
Tubing Size (“)	7”

Table 3-28 Key input parameters to the reference case dynamic model

Uncertainty Parameter	Unit	Input Values		
		Low	Reference	High
Pre-injection reservoir pressure	bara	20.4	34.1	47.1
Fault seal	m ³	sealed	open	-
Fracture pressure limit (bar/m)	bar/m	0.09	0.15	-
Connected Volume in Block A	MMm ³ (Bscf)	36 (1269)	44 (1553)	52 (1837)
Permeability (kx)	mD	26	78	230
kv/kh		0.20	0.58	-
Connection through zones B and D		-	None	Low transmissibility
Number of wells		-	2	5
Injection rate	MT/y	2	5	10

Table 3-29 Subsurface uncertainty parameters and associated range of values

Sensitivity analysis: Capacity

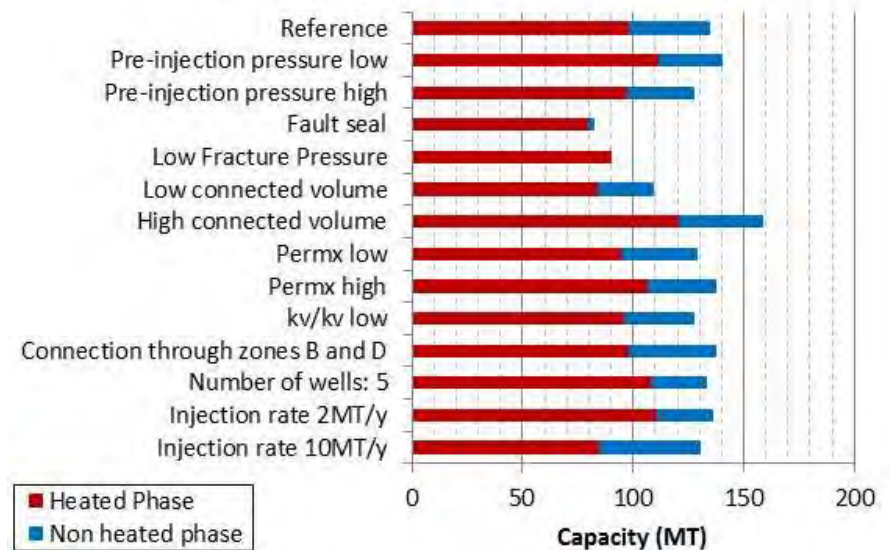


Figure 3-69 Sensitivity analysis: comparison of capacity per case

Injection into the Viking A site ceases when any cell in the model violates the imposed pressure constraint which is 90% of the fracture pressure. The injected mass at this time represents the storage capacity of the Viking A site. Based on the sensitivity analysis the range of capacity for Viking A ranges from 82.7Mt to 158.8MT, with a reference case capacity of 134.5MT. The parameters that have the biggest impact on capacity are the fracture pressure limit and the connected GIIP volume.

Sensitivity analysis: Injection duration

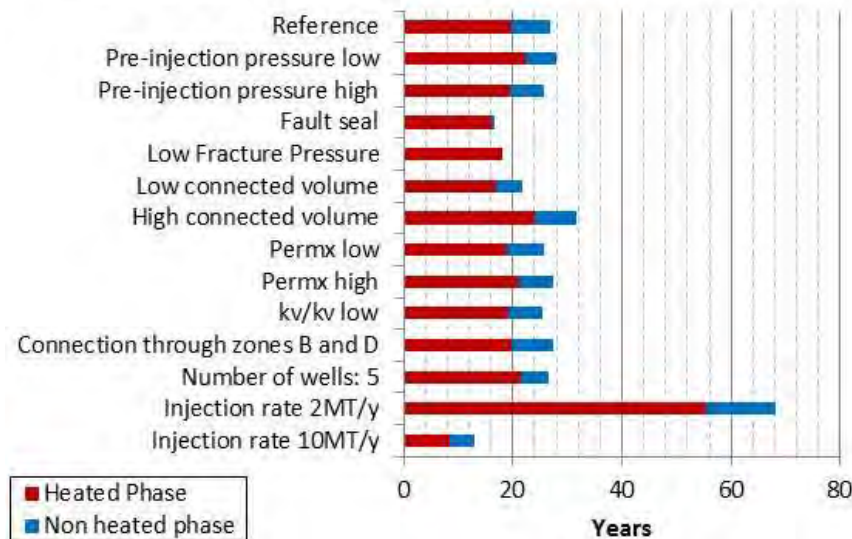


Figure 3-70 Sensitivity analysis: comparison of duration of injection per case

As stated previously, there is some uncertainty associated with the fracture pressure limit prediction, particularly for a depleted gas field, due to the uncertainty in the depleted reservoir pressure and also the uncertainty associated with the change in fracture pressure during re-pressurisation. The worst case scenario is that the fracture pressure remains at the low depleted fracture pressure during injection but this is considered to be very unlikely. In this case the capacity is reduced from 134.5MT to 90MT.

The uncertainty in the connected pore space has been discussed previously with regards to the uncertainty in the connected GIIP in Block A. To evaluate the impact of this uncertainty on the site performance a pore volume multiplier was applied in the model to represent a low case (-18% GIIP) which matches the

results of the material balance analysis and a high case (+18% GIIP) which captures the structural uncertainty related to the depth conversion and improved reservoir connectivity. The capacity for the low and high cases is 109MT and 159MT respectively.

Fault seal also influences the connected pore space available for CO₂ storage. The fault to the north west of the injection wells could potentially act as a barrier. If this is the case the capacity is reduced from 134.5MT to 82.7MT. In this case the connected GIIP is 1225Bscf, similar to the GIIP estimated from material balance (1270Bscf). This GIIP volume is comparable to the low pore volume case but it is concentrated in a small area with the result of a faster pressure build up rate and a shorter injection profile.

No attempt was made to model the impact of a brine producer since the field produced very little water during its long production lifetime.

The impact of the uncertainties on the Viking A storage site performance is discussed in more detail in Appendix 10.

Based on the data available for this study, the reference case is considered to be the most representative model and is the basis for the storage development evaluation.

3.6.7.4 CO₂ Plume Migration

There are three productive sand units, A, C and E that will be targeted for CO₂ storage. These units are separated by laterally extensive non-pay units (sabkha silts) that act as horizontal barriers to vertical flow. Communication between the sand units does occur where the sands are juxtaposed at the internal faults. The wells will penetrate all sand units, at an angle of 60 degrees from the vertical, to optimise injectivity and CO₂ placement in the reservoir. CO₂ is injected into the three reservoir zones. The lateral migration is dependent on the vertical transmissibility i.e. the CO₂ moves along the top of non-permeable layers. However, if the CO₂ can move downwards it will as it is denser than the hydrocarbon gas remaining in the reservoir. The CO₂ moves down until it reaches the GWC. This is in contrast to CO₂ injected at an aquifer site which would rise to the top of the reservoir because of its buoyancy. A very small proportion of the CO₂ dissolves into the aquifer (<1MT of the 130MT injected) but most of the CO₂ remains above the GWC and with continued injection the reservoir fills from the bottom up until the pressure constraint is met. In the proposed development case 130MT is injected into the store. When injection stops the CO₂ concentration equilibrates throughout the field area but does not migrate beyond the storage complex.

Although the A and H fields have the same initial GWC of 9680 ft (2950 m) sub-sea, pressure tests indicate separate drainage (Riches, 2003).

The change in CO₂ distribution from the end of injection to 1000 years after injection is stopped is shown in Figure 3-71. These images clearly show the migration of CO₂, during the shut-in period, to the deeper regions if no impermeable barriers restrict flow. The methane is concentrated in the structural high areas.

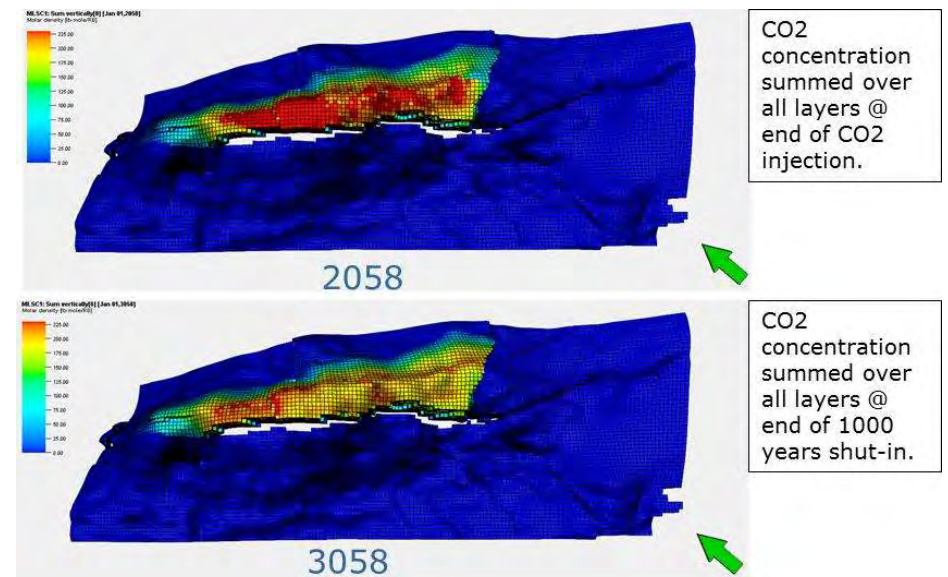


Figure 3-71 Summed CO₂ concentration at year 2058 and 1000 years after injection is stopped

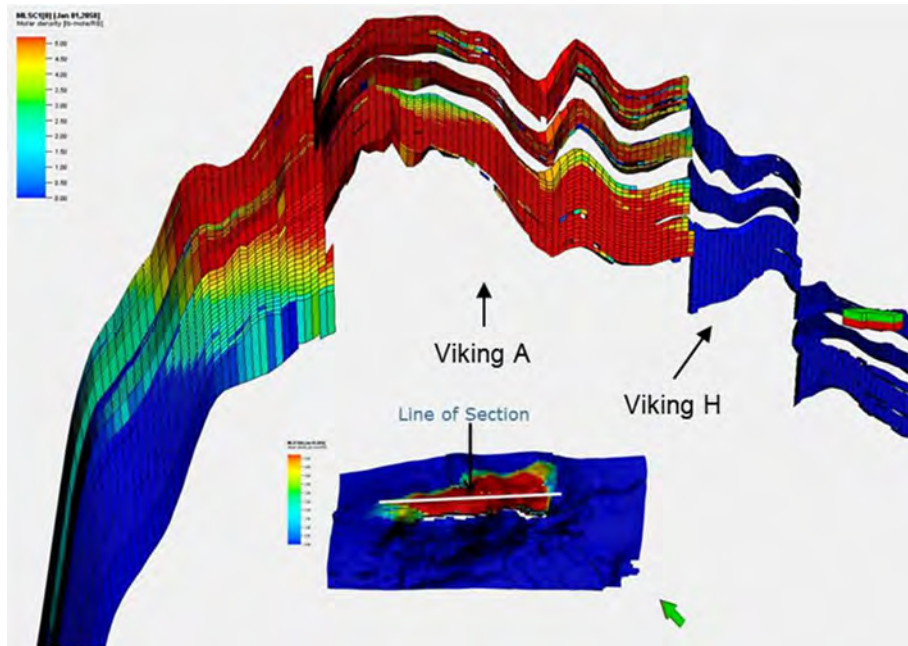


Figure 3-72 CO₂ concentration at year 2058, at the end of injection

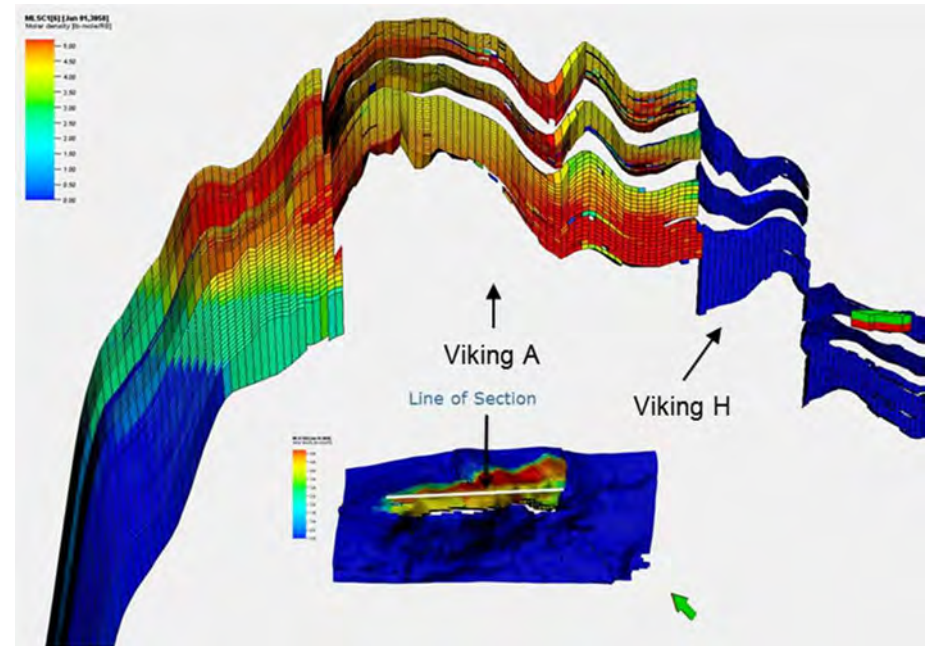


Figure 3-73 CO₂ concentration 1000 years after the end of injection

3.6.7.5 Storage Site Development Plan

Viking Block A is a depleted gas field that ceased production in 1991. The reservoir pressure at the start of the CO₂ injection is estimated to be 34.1 bara at a depth of 2544m TVDSS and the reservoir temperature is estimated to be 83.8°C.

In order to minimise the risk associated with the uncertainty introduced by operating wells across a phase boundary, all injection in the wells will be limited to single phase. With the reservoir pressure of Viking at the start of CO₂ injection being below the critical point for CO₂ (74 bara) the supplied liquid CO₂ requires to be heated past the critical temperature for an initial period, until the reservoir pressure is sufficiently high to support unheated CO₂ injection.

The CO₂ supply profile for Viking A is assumed to be 5Mt/y for 26 years, commencing in 2031. 130MT CO₂ will be injected and stored in the site. The proposed development case requires two 7" injection wells. The CO₂ is initially heated and injected at a wellhead temperature of 35°C. After 20 years the reservoir has been re-pressurised to a pressure that can support unheated CO₂ injection and liquid CO₂ injection will continue, but at a wellhead temperature of 10°C.

A third well will be drilled as a spare injector to ensure that in the event that an injector is shut-in the supply injection rate can still be accommodated.

The injection well locations are shown on a top depth map in Figure 3-74 below.

The total injection forecast and the cumulative injected mass forecast are shown in Figure 3-75.

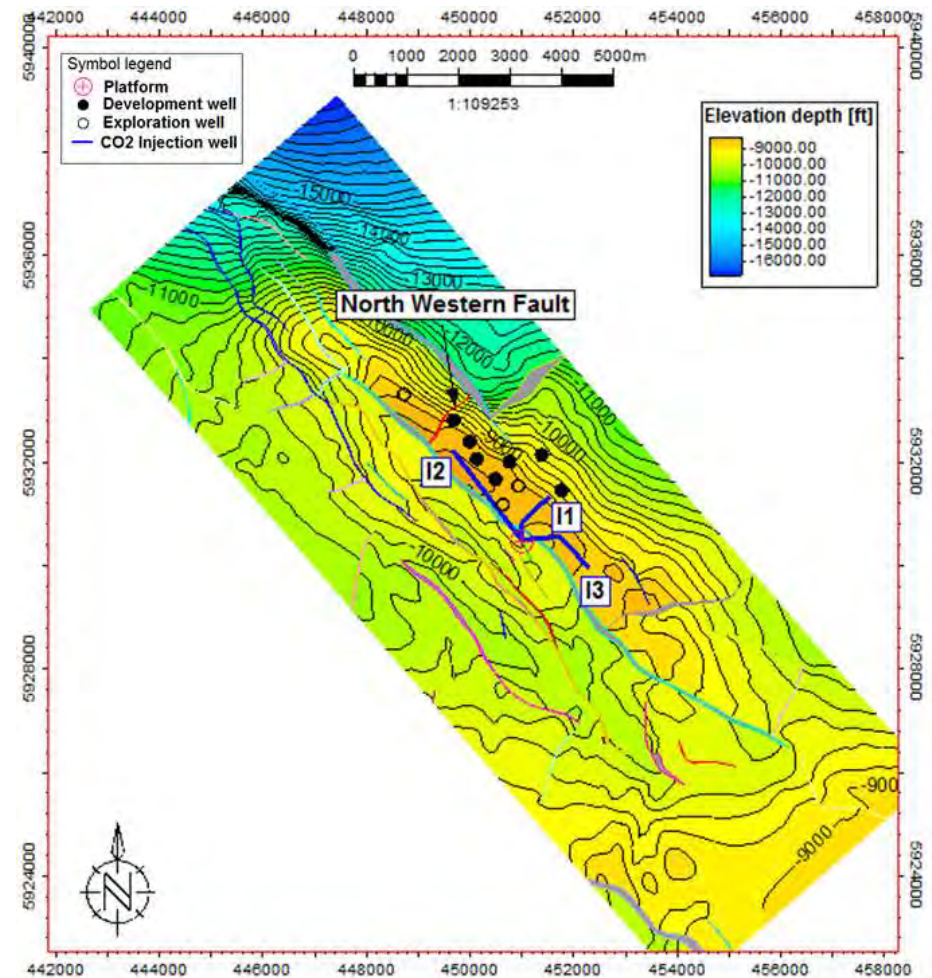


Figure 3-74 CO₂ injection well locations

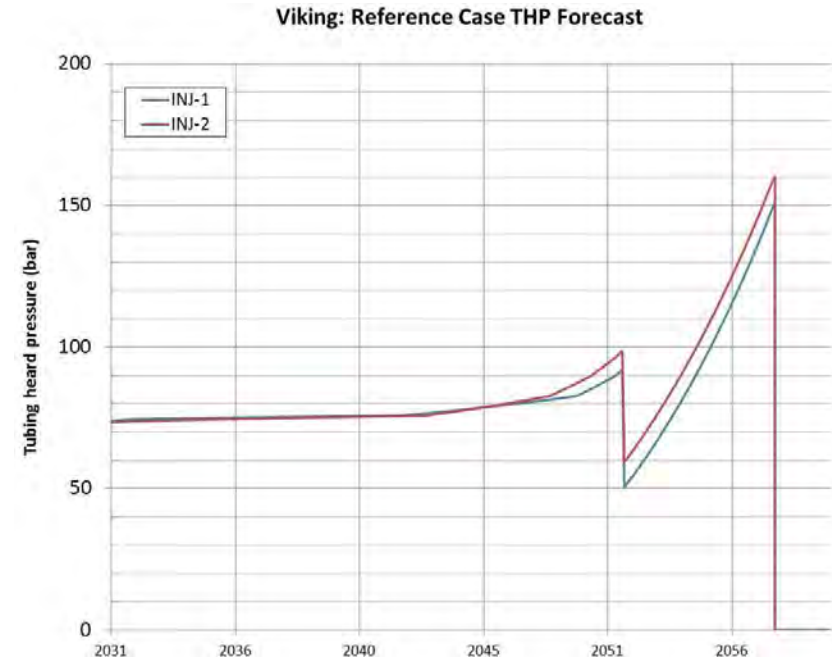
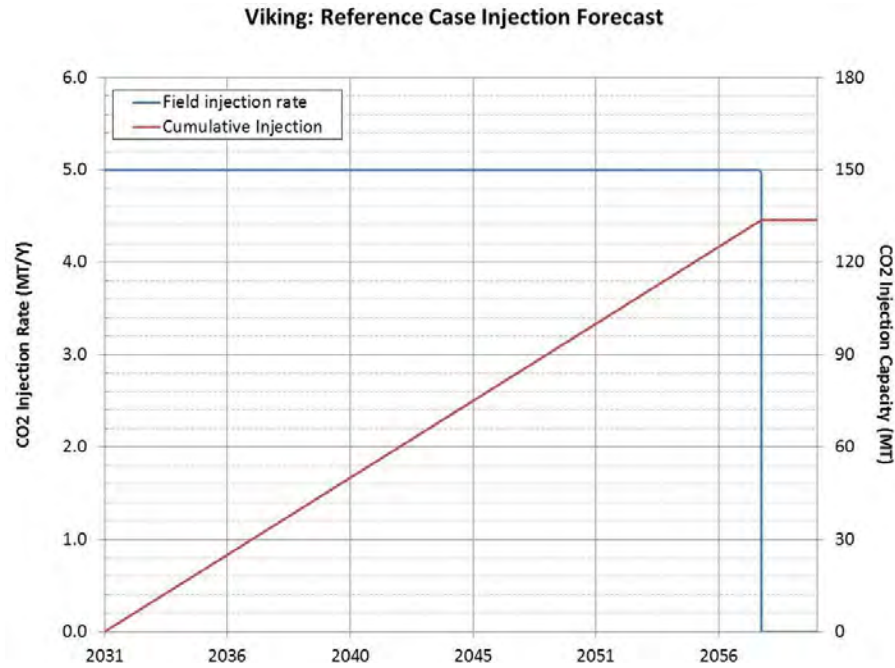


Figure 3-75 Field CO₂ injection forecast

Figure 3-76 Reference case THP forecasts

Both wells inject at 2.5Mt/y during the injection period. The predicted THP for each well is shown in Figure 3-76.

3.6.7.6 Trapping Mechanism

Greater than 99% the CO₂ injected into Viking A ends up structurally trapped. Less than 1Mt out of 130MT injected dissolves into the aquifer.

3.6.7.7 Dynamic Storage Capacity

Injection into the Viking A site ceases when any cell in the model violates the imposed pressure constraint which is 90% of the fracture pressure. The injected mass at this time represents the storage capacity of the Viking site. Pressure increases relatively uniformly throughout the field during injection and the rate of pressure increase is dependent on the injected mass. The pressure reaches the limit close to the North West-South East fault boundary and the I2 well, as shown in Figure 3-62. The capacity for the reference case is 130MT and is largely independent of the rate of injection.

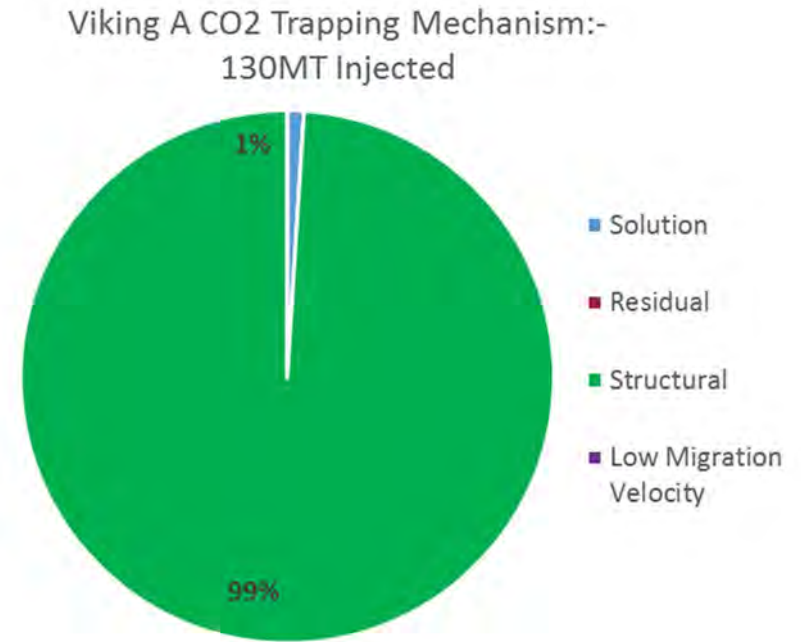


Figure 3-77 Allocation of stored CO₂ to the various trapping mechanisms for the proposed Viking A development

3.7 Containment Characterisation

3.7.1 Storage Complex Definition

The Viking A storage complex is a subsurface volume whose upper boundary is the top of the Keuper Halite, and base boundary is 61 m (200 ft) below the Top Carboniferous (or 61 m (200 ft) below the Viking A gas water contact (GWC), whichever is deeper).

The lateral limits of the storage complex are broadly defined by the location of the GWC within block A and the adjacent blocks F, Fs to the west and H to the south. Block A site containment is supported by dip closure to the north west and north east and by boundary faults. The southern bounding fault has a large offset which offsets the Lemna Sandstone reservoir in Viking A and Viking F. The fault at the eastern end, separating Viking A from Viking H, is shown to be sealing by post gas production data.

The complex boundary is defined as a slightly enlarged area which includes the full north Viking Fields area and accounts for the anticipated positioning error caused by seismic imaging challenges.

It should be noted that Viking A partly underlies Bunter Closure 3 which itself is a potentially outstanding quality CO₂ storage site. The integrity of this site is not considered here in detail. Bunter Closure 3 represents an obvious back up as build out opportunity for Viking A. It would operate at liquid phase injection throughout.

The proposed storage complex is illustrated in Figure 3-78.

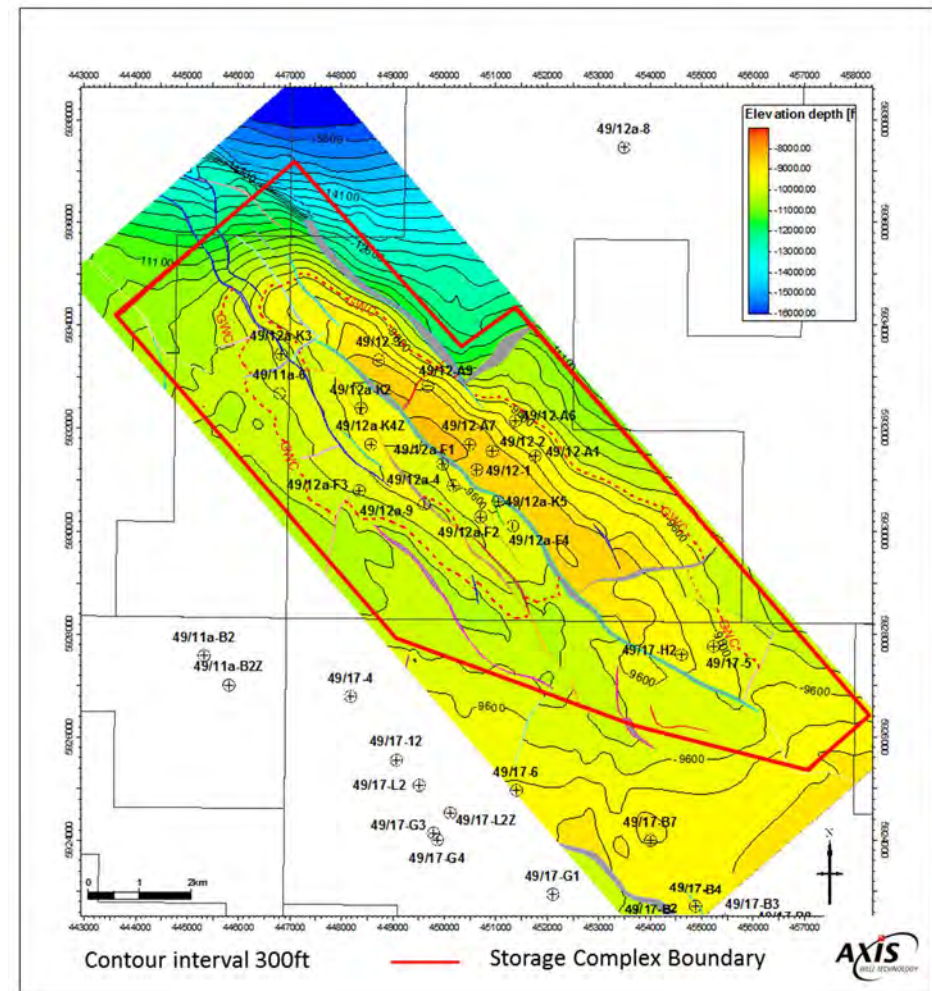


Figure 3-78 Proposed Storage Complex Boundary on Top Lemna Sst. Depth Map

3.7.1.1 Hydraulic Communication between Geological Units

One of the key attributes of the Lemna Sandstone as a CO₂ storage reservoir is that it is overlain by multiple sequences of Zechstein Group evaporites, which provide an excellent proven caprock. The Zechstein Group is laterally extensive across the Southern North Sea and at the site location they are in excess of 300 m (985 ft) thick.

The base of the Lemna Sandstone is underlain by Carboniferous sediments of Westphalian A age. Based upon a review of the available composite logs and well reports the Carboniferous interval below the Lemna Sandstone is predominantly shales, clays and siltstone. Where sandstone inter-beds have been observed these are described as being cemented and having low porosity. Measurements from core where taken also indicated low permeabilities. No hydrocarbon gas shows are reported from the Carboniferous intervals drilled. Field data also report no aquifer support or water ingress during production within the northern Viking fields.

Dynamic modelling work has shown that very little CO₂ is expected to dissolve into the aquifer at the GWC, when injected into the depleted gas leg. The GWC therefore forms an effective floor to free CO₂ migration downwards into the aquifer.

The Lemna Sandstone is a depositionally extensive interval that can be correlated across the region, however lateral hydraulic connectivity across the region is not anticipated as it is known to be structurally complex with observed isolated compartments. These are difficult to characterise at this time due to lack of publically available pressure data for the gas fields on a well by well basis, although published literature supports this assumption.

All Southern North Sea fields are expected to have ceased production by the time CO₂ injection is scheduled to start at the Viking A site in 2031. This includes the nearby V fields (Viking, Victoria, Vixen, Victor, Valiant, Viscount, Vanguard, Vampire).

3.7.1.2 Top and Base Seal

The primary seal is provided by the thick extensive sequence of Zechstein Group evaporites which is a proven seal in the Viking Fields area and most other hydrocarbon fields in the SNS.

The extensive faulting within the Lemna Sandstone is controlled by the underlying Carboniferous structure with faults generally continuing down well into the Carboniferous. Above the Lemna Sandstone the faults die out very quickly in the lower parts of the Zechstein and do not breach the top seal.

The risk of leak paths into the overburden above the Zechstein is minimal, with an additional thickness of Bunter shale above the Zechstein Group it is very unlikely that there will be any leak paths into the Bunter Sandstone secondary store. This is the reason why the gas accumulations in the Bunter Sandstone are rare and restricted to the edges of the Zechstein basin.

The faulting in the overburden above the secondary storage reservoir is limited to a few minor faults which extend down from the Chalk unit into the Upper Triassic. Most of the faults sole out on the Upper Triassic halites with only a few very minor breaks at Top Bunter Sandstone to the south east of the Viking A storage complex. These represent a very small risk to the containment of the Bunter Sandstone secondary store.

3.7.1.3 Overburden Model

A simple overburden model was built covering the same area of interest as the site static model. Interpretation of overburden horizons is described in Section 3.4.

As the purpose of the overburden model was to help and inform the discussion on geological containment, no petrophysical analysis or property modelling have been carried out within the overburden.

Formation	Source
Seabed	Constant depth of 25 m (80 ft) based on well water depth averages
Top Chalk	Direct seismic interpretation and depth conversion.
Base Chalk/ BCU	Direct seismic interpretation and depth conversion.
Top Triassic	Direct seismic interpretation and depth conversion.
Top Rot Halite	Built based on Top Bunter using a well derived isochore.
Top Bunter Sandstone	Direct seismic interpretation and depth conversion.
Lower Bunter	Built down from Top Bunter using a well derived isochore.
Top Zechstein	Direct seismic interpretation and depth conversion.
Top Leman Sandstone	Direct seismic interpretation and depth conversion.
Top Carboniferous	Built down from Top Leman Sandstone using a well derived isochore.

Table 3-30 Summary of Horizons in the Overburden Model

A cross section through the overburden model is shown in Figure 3-79.

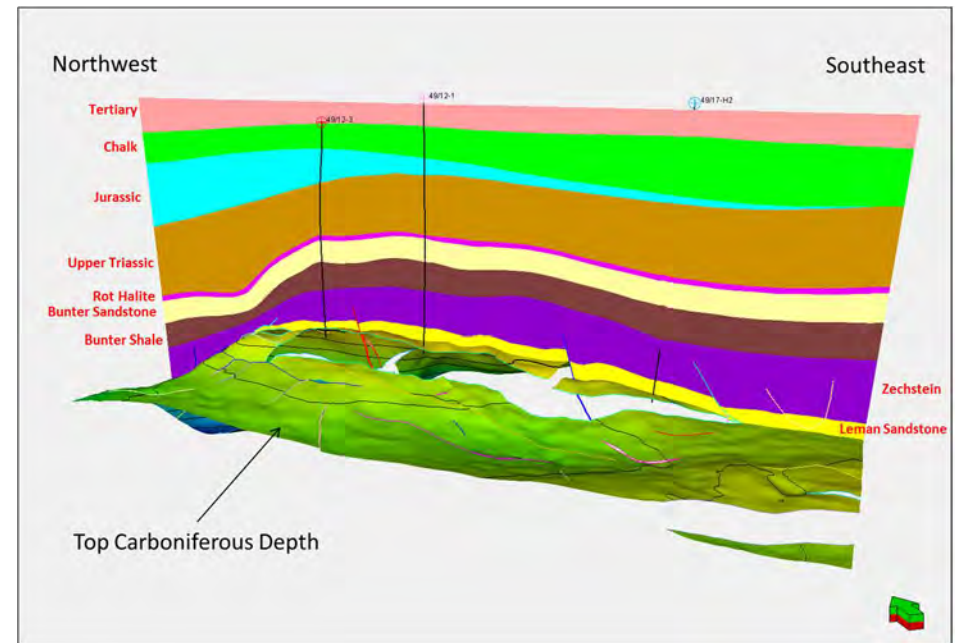


Figure 3-79 Viking A - Cross Section through the Overburden Model

3.7.1.4 3D Geomechanical Analysis and Results

A 3D geomechanical model was constructed to investigate the mechanical robustness of the seal and possibilities of fault reactivation in an area over the crest of the Viking A and F structures and the effects on the fracture gradient of depletion during gas production followed by injection. The process involves creating a small-strain finite element model (i.e. the grid is not deformed) that allows elastic stress/strain relations and plastic failure effects to be investigated as a response to the actual production and proposed injection scheme. The reported parameters include the following:

- Displacement vectors to assess degree of overburden uplift
- Failure criteria thresholds (shear or tensile) in the Lemna Sandstone or overburden
- Matrix strains
- Fault reactivation strains
- Total and effective stress evolution
- Stress path analysis (elastic response to pore pressure changes)

The Viking A static model was used as a basis for building a simplified 3D geomechanical model. This model has the same top and base as Primary static model within the Lemna Sandstone Figure 3-80 and Figure 3-81.

The various steps required to construct, initialise, run and analyse a 3D geomechanical model with specific reference to Viking A are included in Appendix 11.

The purpose of the geomechanical modelling was to run some scenarios to assess the potential for depletion / injection pressure related failure in the Lemna Sandstone, the cap-rock or the reservoir faults. One case was run with non-linear Mohr-Coulomb material properties and one with Drucker-Prager material properties within the Lemna Sandstone. Both were run in non-linear mode with faults. This was primarily to assess the impact of depletion followed by injection on the fracture gradient and the potential for fault reactivation.

Results indicate that varying levels of elastic and plastic strain can be modelled on Viking A, but virtually all of it is restricted to within the Lemna Sandstone interval. Some minor 'Pico' scale seismic events have been modelled that can be widespread on faults or more localised. Most of these would have occurred during production but a few may occur during injection. Note that the absolute

amounts of displacement associated with these events is unlikely to cause any significant failure and/or fault reactivation.

The 3D geomechanical modelling indicates that with variable material properties and stress paths and the inclusion of faults on the structure, the plastic strains and associated slip events are of a very small size. Note that all the properties in this model are log derived and uncalibrated to core or other data so other values are possible for key parameters such as rock strength and the elastic moduli. However, the Lemna Sandstone is usually a well cemented hard rock so extensive strain of the matrix is unlikely. It is also possible that hysteresis of the fracture gradient could occur after depletion (Santarelli, Havmoller, & Naumann, 2008) which is a remaining risk. Weaker faults could occur which may lead to larger plastic strains over larger areas. However, the change in fault properties would have to be significant to produce appreciable plastic strains. This is regarded as unlikely.

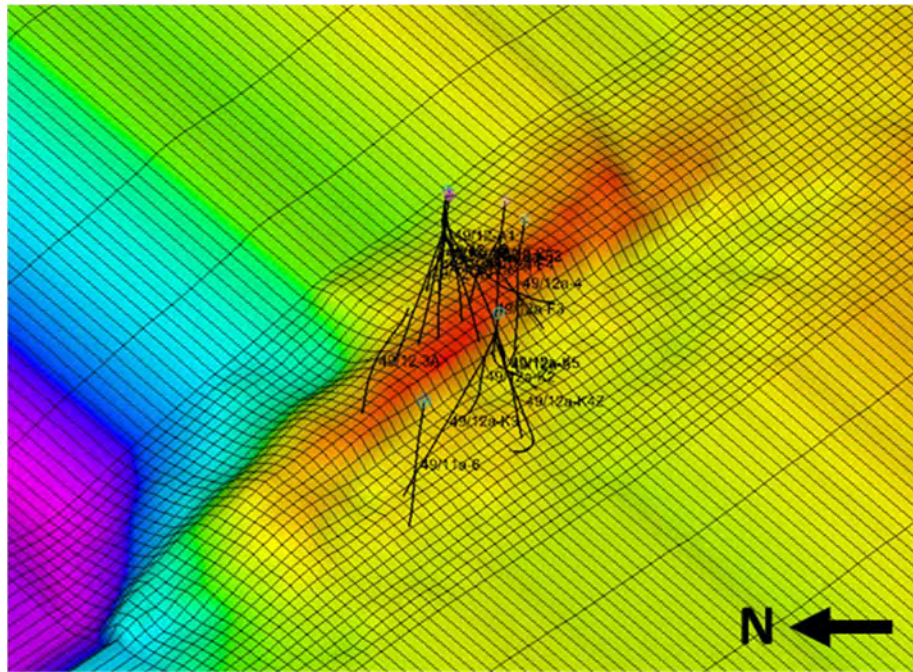


Figure 3-80 3D Geomechanical model - Viking A and F at Top Lemna Sandstone

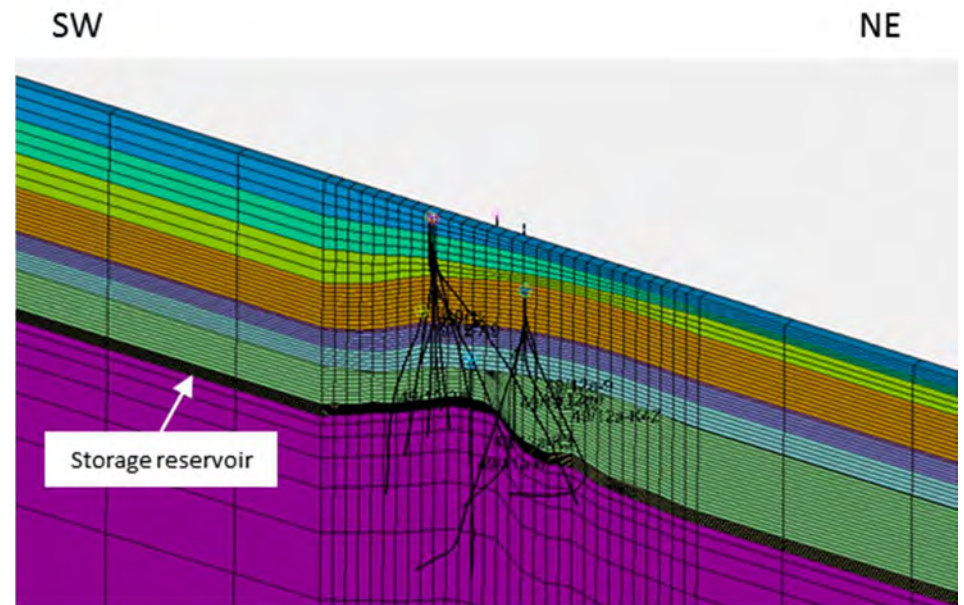


Figure 3-81 Cross section through Viking A Geomechanical model

3.7.1.5 Geochemical Degradation Analysis and Results

A geochemical stability review of the reservoir and caprock are outlined in sections 3.5.1.5 and 3.5.2.5. In summary, by flooding the Viking A field Leman Sandstone reservoirs with CO₂, the overlying caprock lithologies are unlikely to be geochemically-affected in a manner which significantly alters the existing permeability character.

In the clay-rich Kupferschiefer:

1. The kaolinite and, to a lesser extent illite, react with sodium in the formation water and the incoming CO₂ to create dawsonite and quartz
2. Chlorite reacts to form dolomite (and dawsonite and quartz)

These reactions lead to a solid volume increase thus diminishing porosity and permeability

The Zechstein may undergo minor dissolution due to the presence of CO₂ where dolomite is present but anhydrite and halite are fully stable.

The combination of Kupferschiefer loss of porosity and the stability of the anhydrite dominated Zechstein probably means there is negligible risk of top seal dissolution due to elevated CO₂ concentration in the reservoir.

3.7.2 Engineering Containment Integrity Characterisation

In order to contain the CO₂ injected into the Viking A Leman Sandstone reservoir, the integrity of the caprock must be maintained. The 'man made' (or engineered) risks to this containment represent the potential damage done through the application of excessive pressure (fracturing) or the failure to maintain an effective seal in the wells that penetrate the caprock. The following section explores the engineered containment risk for the Viking A storage site.

3.7.2.1 Leak Risk

Engineered containment risk that man-made reservoir penetrations may leak, resulting in a loss of CO₂ to the environment depends on several factors, most of which are well specific.

Risk, in this case, is considered to be the probability of a leak occurring. The quantification of the leakage volume is not considered at this stage, but has been fully described in AGR's report for DECC (AGR, 2012).

The main conclusion from this paper that has been used as an input to the current risk review, is that the range of leak risk from abandoned wells is between 0.12% and 0.5% per well per 100 years depending on age / type of abandonment. The risk of leakage is higher for abandoned wells where the storage target is above the original well target (hydrocarbon reservoir) due to less attention being paid to non-hydrocarbon bearing formations.

The characterisation of abandoned wells (time period of abandonment and the location of the well target depth) was determined by a review of the CDA database.

3.7.2.2 Abandonment Practices and Guidelines

Well abandonment practices have improved (become more rigorous) over time, resulting in the current practices for wells abandoned in the reservoir having the lowest risk. All earlier abandonment practices, and those where wells have been completed below the storage reservoir target, have less rigorous practices. As a result, a well abandoned prior to 1986 (when API guidelines were first published) where the well is targeted at a reservoir below the storage reservoir has the highest risk.

Guideline	API RP 57	UKOOA	UKOOA	UKOOA	UKOOA	UKOOA
Year	1986 - 1994	1994 - 2001	2001 - 2005	2005 - 2009	2009 - 2012	Post 2012
Issue/Rev	n/a	Issue 0	Issue 1	Issue 2	Issue 3	Issue 4

Table 3-31 Guidelines for the suspension and abandonment of wells

A brief summary of the main oil and gas abandonment guidelines relating to exploration/appraisal wells are detailed below with reference to major changes over the years:

1. Permanent barrier material – cement. Not specifically detailed until Issue 4 when a separate guideline was introduced for cement materials.
2. Bridge plug or viscous pill to support cement plug introduced in Issue 3 (2009) but mentioned in API RP 57.
3. Two permanent barriers for hydrocarbon zones. One permanent barrier for water bearing zones.
4. One permanent barrier to isolate distinct permeable zones.

5. Cement plug to be set across or above the highest point of potential inflow.
6. Position of cement plug to be placed adjacent to the cap rock introduced in Issue 4.
7. Length of cement plug typically 500 ft thick to assure a minimum of 100 ft of good cement.
8. Internal cement plugs are placed inside a previously cemented casing (lapped) with a 100ft minimum annulus cement for good annulus bond or 1000 ft annulus cement if the top of cement (TOC) is estimated rather than measured.
9. Plug verification – cement plug tagged/weight tested and/or pressure tested.
10. All casing strings retrieved to a minimum of 10 ft below the seabed.

For the Viking A site, a total of 9 wells were plugged and abandoned. A total of 3 legacy wells were reviewed from the details in the CDA database. Using these details, the actual well abandonment practises were compared to the assumed abandonment practises at that time. The risk scoring is verified if the abandonment has been performed as per the guidelines at that time and as per the assumptions. Any significant departure (better or worse) is documented and highlighted with the legacy wells. The risk assessment is categorised as low/medium/high and defined as follows:

- Low – does not meet the guidelines at that time
- Medium – meets the guidelines at that time
- High – exceeds the guidelines at that time

3.7.2.3 Benchmark Abandonment Practices

As a benchmark for CO₂ storage, the Goldeneye abandonment proposal (Scottish Power CCS Consortium, 2011) could be considered. This has a critical seal across the caprock and milled window providing a plug with a rock-to-rock seal. Shallow cement plugs provide a barrier for the water bearing zone. Cement retainer or inflatable plug provides support for the cement plug and prevents slumping. This exceeds current guidelines, UKOOA Issue 4, as no milled window is required if the casing cement is considered good but does provide a good benchmark example of an abandoned well.

3.7.2.4 Review of Legacy Wells

Initial Risk Assessment (Due Diligence)

The initial risk assessment of the Viking fields (Pale Blue Dot Energy; Axis Well Technology, 2015) considered only the hydrocarbon storage areas down to the gas – water contacts, incorporating Viking A, B, C, D, E, F, FS and H fields (Table 3-32). This was a limited area of 47 km², but contained over seventy wells. The assessed containment risk was moderately high, with a 12% probability of a leak within 100yrs across the whole greater Viking area if every legacy well was exposed to CO₂. However, it was recognised that the whole area would not be exposed to CO₂, and that the risk was dependant on the selected injection site.

	Initial Review	Risk	Final Review	Risk
Total Number of Wells	74		13	
Total Number of Abandoned Wells	27		2	
Total Number Abandoned before 1986	15		2	
Total Number of at Risk Wells	73		13	
Probability of a Well Leak in 100 yrs	0.12		0.018	
Storage Area (km²)	47		13	
Well Density (wells/km²)	1.54		1.0	
Leakage Risk Assessment (well density x leak probability)	0.18		0.018	

Table 3-32 Viking risk review

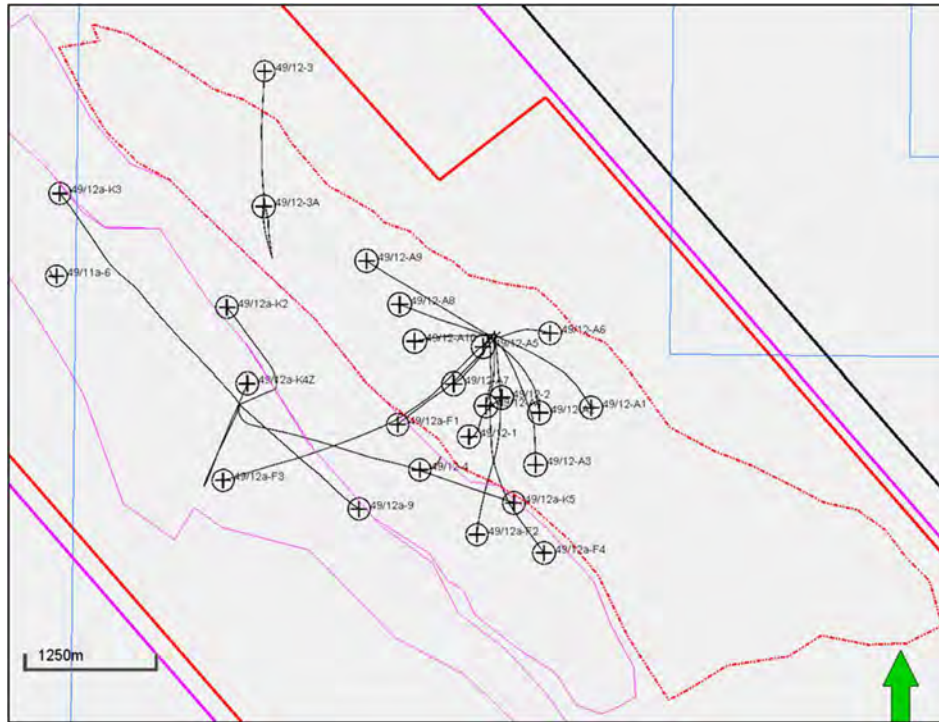


Figure 3-82 Viking A Block A wells

Detailed Risk Assessment

The detailed risk assessment was performed using the historical well data in the CDA data base. These data included the Final Well Reports or Abandonment Reports for the legacy wells. A total of 9 wells in the Viking site were plugged and abandoned.

It should be noted that there is some uncertainty in current well status. The status of the wells considered above are detailed in the CDA database. The database lists the majority of Viking A block wells as completed (not abandoned). However, in 1996, various structures on the field (platforms AC, AD, AP and FD) were removed. Furthermore, in the CDA database there are 'abandonment' logs or reports from several of the A block wells (A6 and A9 are the exceptions). This might suggest that the CDA database may not be current and that more wells have been abandoned than has been assumed in this assessment. Given that any abandoned wells were completed in the hydrocarbon store and therefore are likely to have been abandoned to a reasonable specification. The leakage risk would not, therefore, be considerably higher than that described in Table 3-32.

The review of the 3 legacy wells from the Viking is summarised below.

Well	UKOOA or API	Above/Below or In Store Depth	Meets/ Exceeds/ Fails Spec	Comments
49/12-2 1969	API RP 57	In store depth	Fails	Well side track from 49/12-1. Openhole well with 2 cement plugs and both supported with cement retainer. Not clear if cement plugs lapped with annulus cement. Limited info and no well schematic. Hydrocarbon sands. Store depth isolated with undersized cement plugs. Does not meet spec – shallow set cement plug not lapped with annulus cement.
49/12-3 1970	API RP 57	In store depth	Fails	Openhole well with 3 cement plugs. Lower cement plug in openhole. Casing cement plugs supported with bridge plug. Shallow set cement plug only 100 ft thick. Not clear if cement plugs lapped with annulus cement. Limited info and no well schematic. Hydrocarbon sands. Store depth isolated with undersized cement plugs. Does not meet spec – shallow set cement plug not lapped with annulus cement.
49/12a- K4Z 2000	Issue 0	In store depth	Meets	Openhole well with 2 cement plugs. Lower cement plug supported with bridge plug and across the top of the liner (TOL) and lapped with annulus cement. Upper plug lapped with cement and isolates bunter sands from surface. Well suspended with wellhead and can be abandoned by severing casing only if required.

Table 3-33 Viking legacy wells

The 3 legacy wells cover the specification API RP 57 and UKOOA Issue 0. There was limited well information in the CDA database and a number of the wells did not have abandonment well schematic.

Well 49/12a-K4Z (2000) meets the specification. The well is located in the Viking Fs block but is within the storage complex for the Viking A site. The target Leman Sandstone was in the open hole section at 11736 ft MDRKB and is the same as the store depth. Log interpretation indicated that the reservoir was lower than anticipated and the well path was too close to the top of the Leman Sandstone and had encountered mostly non-net sandstone. The wellbore was abandoned (49/12a-K4) with a cement plug from 10795 to 11236 ft (inside the casing shoe). A low sidetrack was then drilled to enter the reservoir approximately 40ft lower (49/12a-K4Z). Logs indicated that the reservoir drilled was gas bearing but was of poorer quality rock than expected. The well is suspended with two cement plugs. The first cement plug is across the liner and is supported with a bridge plug. The second cement plug is in the 9 5/8" casing across the Bunter Sandstone. Both cement plugs are lapped with annulus cement. The well can be permanently abandoned by severing the casing.

However, wells 49/12-2 and 49/12-3 fail to meet specification and are examined in more detail below. Both wells are reliant on undersized cement plugs with unknown top of cement (TOC) and shallow set cement plugs which are not lapped with annular cement to provide a secondary barrier for a leak up through the A annulus.

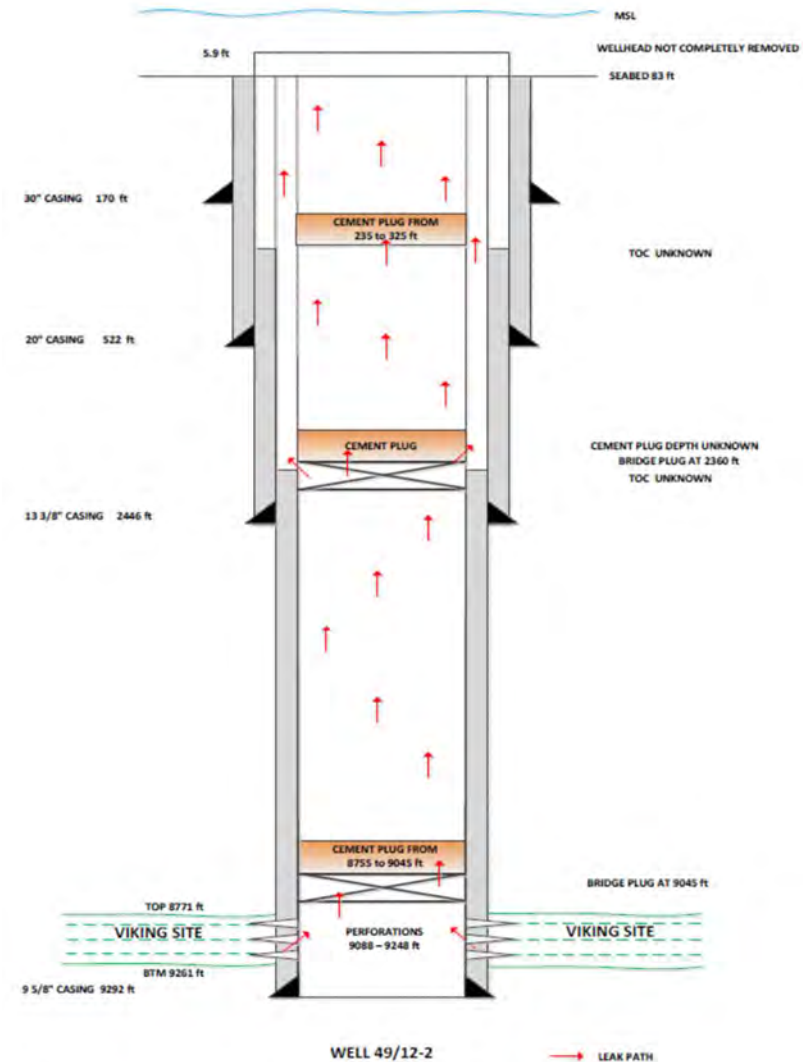


Figure 3-83 Schematic of well 49/12-2 with potential leak paths indicated

Well 49/12-2

The reservoir target is at the store depth and there is annular cement (perforated) in the 9 5/8" across the Leman Sandstone. A potential leak path through the bridge plugs and cement plugs would take the CO₂ directly up the wellbore or through the 9 5/8" casing above the TOC and directly up through the annulus. There is limited well information with no abandonment well schematic and a lack of clarity regarding cement plug placement. Furthermore, it is not clear whether the cement plugs are lapped with annulus cement as there is no detail on the TOC. The well is a sidetrack from 49/12-1. Integrity relies on the bridge plugs and undersized cement plugs or the unknown cement column inside the 13 3/8" casing. The shallow set cement plug is not lapped with annulus cement. The wellhead is not completely removed.

Well 49/12-3

The reservoir target is in the store depth. The cement plug is in the open hole, with the plug top 143 ft below the top of the store depth. The potential leak path from the top of the store depth, through the bridge plug and cement plug takes the CO₂ directly up the wellbore or through the 9 5/8" casing above the TOC and then directly up through the annulus. There is limited well information with no abandonment well schematic and a lack of clarity regarding cement plug placement. Furthermore, it is not clear whether the cement plugs are lapped with annulus cement as there is no detail on the TOC.

The original well was abandoned in the Zechstein Lower Magnesian Limestone zone after encountering uphole difficulties. An abortive attempt was made to sidetrack at 6660ft MD but further uphole difficulties caused this to be

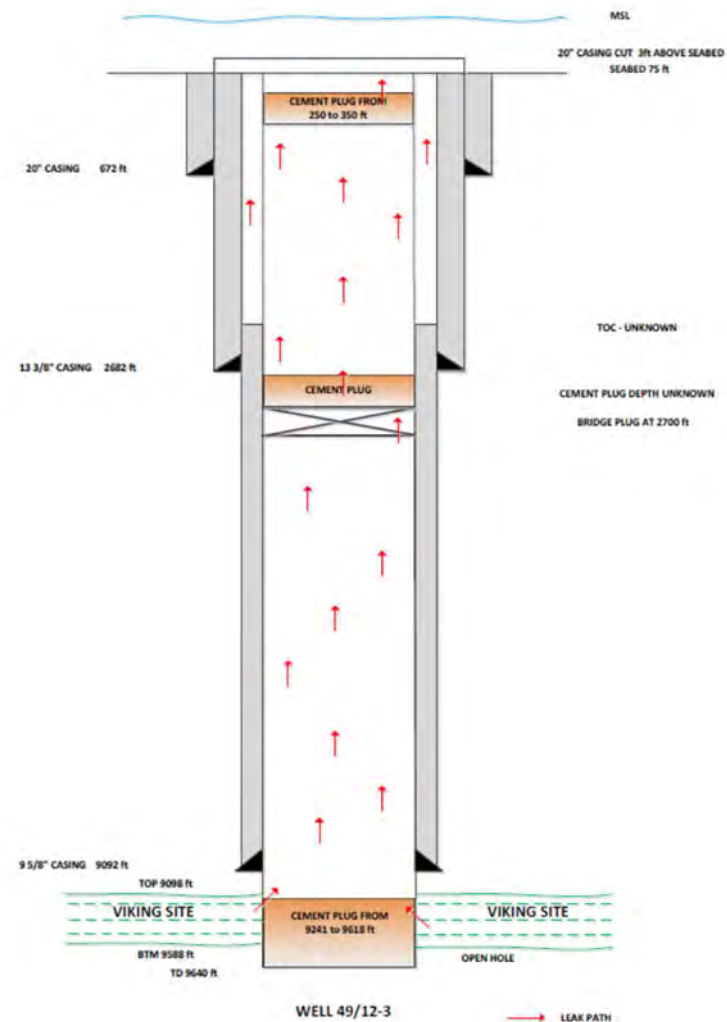


Figure 3-84 Schematic of well 49/12-3 with potential leak paths indicated

abandoned at 6715 ft MD. Side track No 2 commenced at 3167 ft MD and was successfully completed.

The well integrity relies on the bridge plug and undersized cement plugs. Also the shallow set cement plug is not lapped with annulus cement. In summary, the cement plug barriers are all undersized, the TOC is unknown, and the shallow cement plug is not lapped with cement to provide a secondary barrier for a leak up the A annulus. The wellhead is not completely removed.

3.7.2.5 Degradation

It has been shown that long term exposure of well construction materials to CO₂ and water leads to a process of chemical degradation. Cement used to seal the well casing annuli and for creating barrier plugs can degrade over time, with chemical reactions creating an increase in porosity and permeability of the cement and decreasing its compressive strength. However, cement has a 'self-healing' mechanism of carbonate precipitation that reduces the rate of this degradation in the short term. If a cement is fully integral at the outset of exposure to CO₂, degradation is likely to be an extremely slow process. However, if a weakness such as a fracture, micro-annulus or flow path exists in the cement, the subsequent degradation process may be accelerated. Further work is required to identify the rate of cement degradation under all conditions in order to establish a minimum height of integral cement to prevent leakage in the storage time frame and to produce a range of potential leak rates. This should then be applied to all legacy wells, bearing in mind that it is likely that hydrocarbon gas is most likely to form a 'buffer zone' at the top of the reservoir, preventing significant exposure of the well construction materials at the penetration point from being exposed to high concentrations of CO₂.

Carbon steel casing (as used in legacy wells) is also subject to degradation through exposure to CO₂. Corrosion rates are more predictable at up to 2.73 mm/yr in carbon steel for Viking conditions, when exposed to CO₂ and water. Under static conditions, the corrosion rate reduces significantly. A constant flux adjacent to the casing is therefore required to cause degradation concern. Note that, for the new injector wells, the corrosion rate for 13%Cr material is considerably lower. As the legacy wells are likely to be exposed to a flux of CO₂ during the injection period, it can be assumed that all casing strings in the reservoir section that are not protected by cement will be subject to significant corrosion. However, casing strings above the reservoir will only be affected if a leak path is initiated and there is no hydrocarbon gas 'buffer' as explained above.

3.7.2.6 Engineering Containment Risk Summary

As noted above, the final engineering containment risk is low, with 13 wells considered at risk of leakage in Viking A. Two of these wells – 49/12-1 and 49/12-3A – that were plugged and abandoned in 1969 and 1970 respectively represent the highest risk. The other wells remaining operational, according to the CDA database. While both abandoned wells are abandoned to a lower standard than suggested by the guidelines in place at the time, the leak risk from these wells is still only moderate and, should a leak occur, the leak rate is likely to be severely constrained.

Should Viking A be progressed as a CO₂ storage site, then wells that have not yet been plugged and abandoned should be abandoned to the benchmark standards noted above. As the abandoned wells were abandoned to seal a hydrocarbon gas reservoir, it is expected that the risk of CO₂ leakage will be low. Furthermore, with CO₂ gas being denser than hydrocarbon gas, as it is stored in the reservoir it will sink to the bottom, displacing hydrocarbon gas to the top

of the reservoir, adjacent to the well penetration points. It is therefore expected that well penetrations will suffer only modest long term exposure to CO₂ at the highest points of the reservoir.

A full review of the well's current status should be performed in the FEED stage.

3.7.2.7 Well Remediation Options

Appendix 5 includes a catalogue of the well containment failure modes and the associated effect, remediation and estimated cost. The remediation options available will be specific to the well and depend on:

- The type of failure.
- The location of the failure.
- The overall design of the well

It is recommended that a detailed well integrity management system is adopted to ensure well integrity is optimised throughout the life of the project (Smith, Billingham, Lee, & Milanovic, 2010).

3.7.3 Containment Risk Assessment

A subsurface and wells containment risk assessment was completed and the results are detailed in Appendix 2. The workflow considered ten specific failure modes or pathways for CO₂ to move out of the primary store and/or storage complex in a manner contrary to the development plan. Each failure mode might be caused by a range of failure mechanisms. Ultimately, pathways that could

potentially lead to CO₂ moving out with the storage complex were mapped out from combinations of failure modes. The pathways were then grouped into more general leakage scenarios. These are outlined in Table 3-34 Viking Leakage Scenarios and displayed in a risk matrix plot in Figure 3-85

The key containment risks perceived at the present time involve existing legacy wells:

- Escape of CO₂ from existing legacy wells leading to seabed release of CO₂.

This risk can be mitigated by careful monitoring of abandoned well heads, as laid out in the monitoring plan.

The bounding fault leakage likelihood is considered low due to the presence of gas in Viking Block A, which has been held for millions of years. Reactivation is also considered very low as a result of initial 3D geomechanical modelling. The injection pressure will be limited to 90% of the reservoir fracture pressure and the Zechstein caprock has a very high fracture pressure and is considered “self-healing”.

There are some uncertainties over well abandonment spec due to limited information, but not the same concerns with specific wells as for some of the other sites

Secondary containment within the overlying Bunter provides an additional barrier to the surface, should loss of containment occur.

Leakage scenario	Likelihood	Impact	Matrix Position
Vertical movement of CO ₂ from Primary store to overburden through caprock	1	3	
Vertical movement of CO ₂ from Primary store to overburden via existing wells	2	3	
Vertical movement of CO ₂ from Primary store to overburden via injection wells	2	3	
Vertical movement of CO ₂ from Primary store to overburden via caprock & wells	1	3	
Vertical movement of CO ₂ from Primary store to upper well/ seabed via P&A wells	2	4	
Vertical movement of CO ₂ from Primary store to upper well/ seabed via suspended wells	2	4	
Vertical movement of CO ₂ from Primary store to upper well/ seabed via injection wells	2	4	
Vertical movement of CO ₂ from Primary store to upper well/ seabed via caprock & wells	1	4	
Lateral movement of CO ₂ from Primary store out with storage complex	1	3	
Lateral movement of CO ₂ from Primary store via bounding faults	2	3	
Vertical movement of CO ₂ from Primary store to underburden via existing wells	1	2	
Vertical movement of CO ₂ from Primary store to underburden via store floor (out with storage complex)	1	3	

Table 3-34 Viking Leakage Scenarios

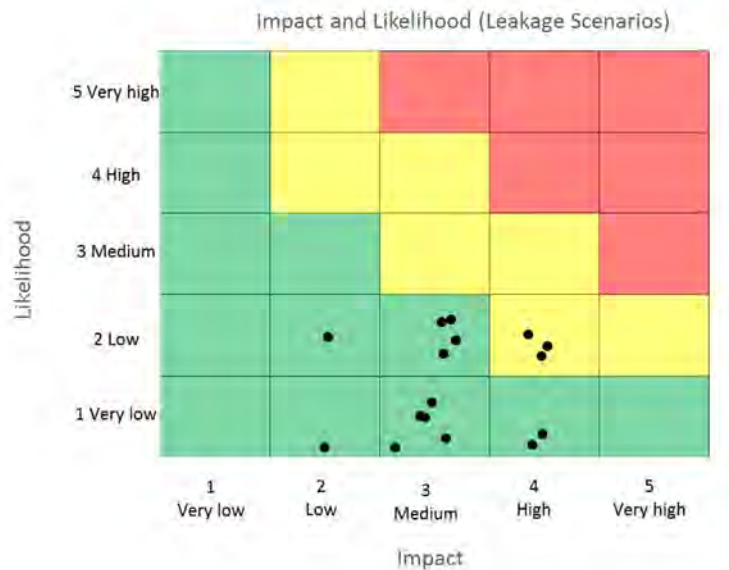


Figure 3-85 Viking A Risk matrix of leakage scenarios

3.7.4 MMV Plan

Monitoring, measurement and verification (MMV) of any CO₂ storage site in the United Kingdom Continental Shelf (UKCS) is required under the EU CCS Directive (The European Parliament And The Council Of The European Union, 2009) and its transposition into UK Law through the Energy Act 2008 (Energy Act, Chapter 32, 2008). A comprehensive monitoring plan is an essential part of the CO₂ Storage Permit.

For more information about the purposes of monitoring and the different monitoring phases and domains, please see Appendix 5 MMV Technologies.

3.7.4.1 Monitoring Technologies

Many technologies which can be used for offshore CO₂ storage monitoring are well established in the oil and gas industry.

Monitoring of offshore CO₂ storage reservoirs has been carried out for many years at Sleipner and Snohvit in Norway and at the K12-B pilot project in the Netherlands. Onshore, Ketzin in Germany has a significant focus on developing MMV research and best practice.

A comprehensive list of existing technologies has been pulled together from (National Energy Technology Laboratory, US Department of Energy, 2012) and (IEAGHG, 2015). This list of monitoring technologies and how they were screened is provided in Appendix 5.

3.7.4.2 Viking A Seismic Response of CO₂

With the significant cost of seismic surveys, it is essential to understand if they can detect and delineate CO₂ in the storage site. During injection, the CO₂ replaces and mixes with in-situ pore fluid, changing the density and

compressibility of the fluid in the pore space, which may change the seismic response enough to be detected.

This can be modelled prior to injection using a technique known as 1D forward modelling. A 1D model of the subsurface is built from well-log data and fluid substitution is carried out over the injection interval, substituting CO₂ for brine. The seismic response of this new fluid mixture is modelled via a synthetic seismogram and any visible changes give an indication that seismic will be able to detect the stored CO₂ at the site.

Modelling Inputs

The Lemn Sandstone in well 49/12-2 (Viking Block A) was modelled with a bulk mineral density of 2.69g/cc (from petrophysics), brine density of 1.1g/cc, gas density of 0.2g/cc, Vp from well logs, Vs derived from Vp and a constant density. The initial hydrocarbon gas saturation was set at 90%. Several fluid substitution cases were modelled, which are summarised below.

In all cases, CO₂ had a density of 0.8g/cc. A 30Hz North Sea (reverse SEG) polarity Ricker wavelet was used to generate the synthetic seismogram.

The software uses low-frequency Gassmann equations, which relate the saturated bulk modulus of the rock (Ksat) to its porosity, the bulk modulus of the porous rock frame, the bulk modulus of the mineral matrix and the bulk modulus of the pore-filling fluids. The saturated bulk modulus can also be related to P-wave velocity (Vp), S-wave velocity (Vs) and density (rho) and so these data can be taken from well logs.

Case	Description	Rationale
1	90% gas/ 10% brine (at depleted, pre-injection pressure)	Representative of reservoir conditions post hydrocarbon production and pre CO ₂ injection (with no water influx)
2	10% brine, 80% CO ₂ , 10% gas	Representative of reservoir conditions towards the end of the injection period (high CO ₂ saturation case)
3	10% brine, 45% CO ₂ , 45% gas	Representative of reservoir conditions towards the end of the injection period (low CO ₂ saturation case)
4	100% brine	Representative of a water-bearing location out with Block A
5	20% CO ₂ / 80% brine	Representative of dense phase CO ₂ migration into a water-bearing location out with Block A

Table 3-35 Fluid substitution cases

The software takes Vp and Vs from well logs (either directly or derived), and rho as the specified value, to determine the bulk modulus of the saturated rock over the modelled interval and then determines the mineral matrix and bulk modulus of the pore fluid from specified user inputs. It then essentially "removes" the in-situ fluid to calculate the bulk modulus of the rock matrix only and substitutes the pore fluid with the desired fluid to be modelled (in this case CO₂). Once the desired fluid is substituted it calculates the bulk modulus of the rock saturated with the new fluid and, as mentioned above, a new Vp, Vs and density can be determined from the saturated bulk modulus. This new Vp, Vs and density is then used with the synthetic wavelet to generate a synthetic seismogram.

Results

Figure 3-86 shows the results of the 1D modelling comparing Case 1 with Case 2 and Figure 3-87 Case 4 with Case 5.

As can be seen in Figure 3-86, the seismic response of CO₂ within the Leman Sandstone is very poor. It is likely to be extremely challenging to detect any CO₂ within the Viking Block A.

Figure 3-87 shows a similarly poor response and so it is likely to be challenging to detect any lateral migration of CO₂ out with Viking Block A.

The reason for the limited change in seismic response from the presence of CO₂ is due to the high impedance contrast between the overlying Zechstein salts and the Leman Sandstone.

Despite the suggested poor performance of 4D seismic for imaging the CO₂ plume development within the Leman Sandstone, it has been included in the monitoring plan at this time for detection of any CO₂ in the overburden (for example in the Bunter Sandstone, which was modelled for the Bunter Closure 36 site and showed that CO₂ should be detectable using 4D seismic).

Further modelling will be required during FEED to understand the phase transition of CO₂ in the reservoir more fully (from gaseous phase, to a dense phase fluid thereafter) and if there is any distinguishable amplitude versus offset (AVO) response, which may help with CO₂ detection.

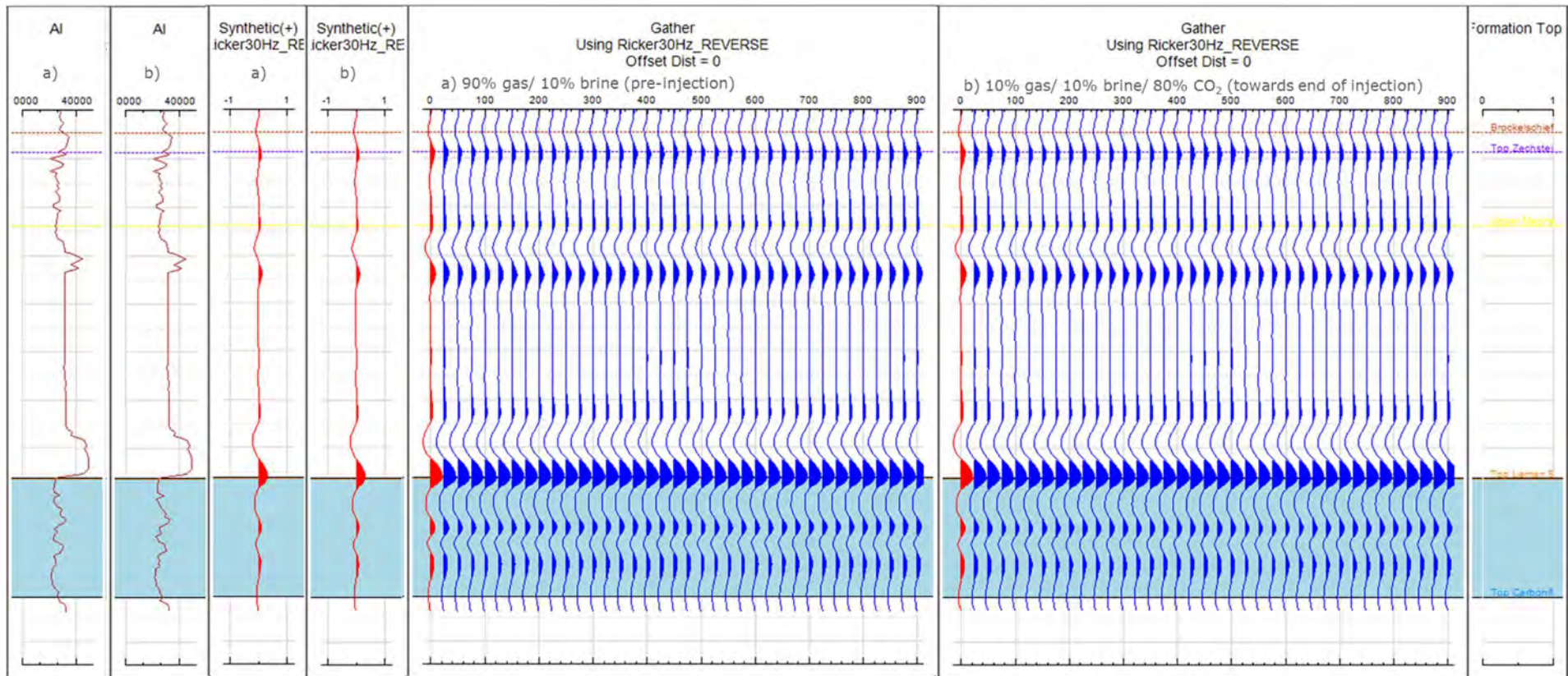


Figure 3-86 Viking A Comparison of 1D forward modelling results for a) Case 1 and b) Case 2

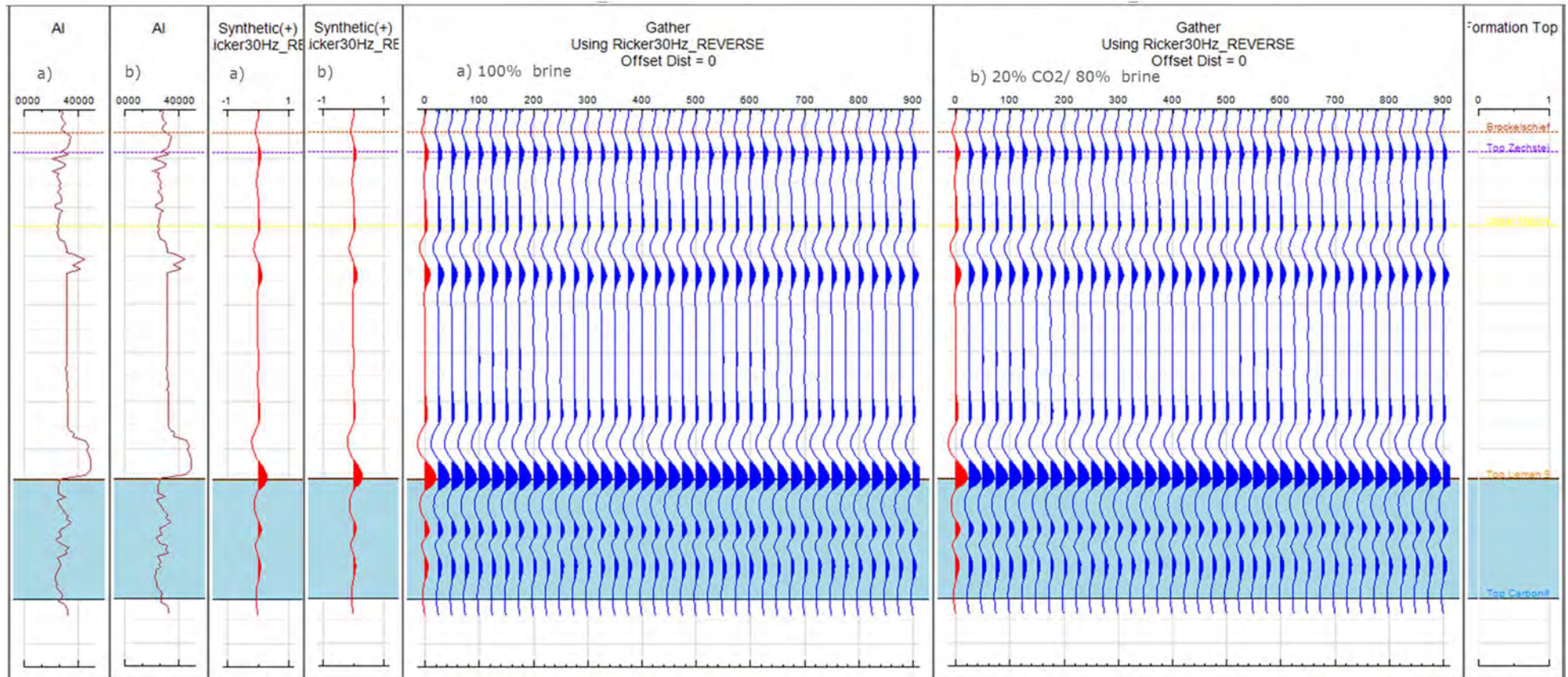


Figure 3-87 Viking A Comparison of 1D forward modelling results for a) Case 4 and b) Case 5

3.7.4.3 Outline Base Case Monitoring Plan

The outline monitoring plan has been developed to focus on the leakage scenarios as identified in Appendix 2, with the most applicable technologies at the time of writing.

49 technologies that are used in the hydrocarbon industry and existing CO₂ storage projects were reviewed and 35 were found to be suitable for CO₂ storage offshore. A list and description of the offshore technologies is in Appendix 5.

The monitoring plan for the Viking A storage site is shown in Figure 3-88, with the rationale and timing for each technology contained in tables in Appendix 5. The plans are based on using technologies from a general offshore UKCS Boston Square (see Appendix 5), which plots a technology's cost against its value of information, and are from either the "just do it" (low cost, high benefit) or "focussed application" (high cost, high benefit) categories.

Other technologies that are in the "consider" (low cost, low benefit) category require additional work during FEED to more fully assess the value for the Viking storage site. Note that some of the "consider" technologies are less commercially mature, but may move to the "just do it" category over time.

The 1D forward modelling results show that it is unlikely CO₂ will be detected within Viking Block or out with it in a brine-filled location (if lateral loss of containment occurred), however seismic surveys could still potentially pick up the presence of CO₂ in the overburden (e.g. the Bunter sandstone, secondary store) in the event of a leak.

Therefore the frequency of 4D seismic surveys should be reconsidered in the future, perhaps during FEED, once additional modelling has ruled out detectability of CO₂ using other seismic techniques such as AVO.

Figure 3-89 maps the selected technologies to the leakage scenarios discussed in Appendix 2.

Outline Monitoring Plan Viking - depleted gas site		Baseline		Operational					Post Closure					
		2020	2025	2030	2035	2040	2045	2050	2055	2060	2065	2070		2075
Monitoring Technology	Seabed sampling, ecosystem response monitoring, geochemical analyses of water column		◆	◆	◆	◆	◆	◆	◆	◆	◆	◆	◆	Handover to government
	Sidescan sonar survey; chirps, boomers & pingers		◆	◆	◆	◆	◆	◆	◆	◆	◆	◆	◆	
	4D seismic survey		◆	◆	◆	◆	◆	◆	◆	◆	◆	◆	◆	
	Wireline logging suite		◆		◆		◆							
	DTS, downhole and well head P/T gauge and flow meter													
	Data management													

Figure 3-88 Outline monitoring plan for the Viking A storage site

			Risk ranking			Monitoring Technology				
			Likelihood	Impact	Ranking	Seabed sampling, ecosystem response monitoring, geochemical analyses of water column	Sidescan sonar survey, chirps, boomers & pingers	4D Seismic	Wireline logging	Permanently installed wellbore tools (DTS), downhole and wellhead P/T gauge and flow meter
Leakage Scenario	Overburden	Vertical movement of CO ₂ from Primary store to overburden through caprock	1	3	●			X		X
		Vertical movement of CO ₂ from Primary store to overburden via pre-existing wells	2	3	●			X		
		Vertical movement of CO ₂ from Primary store to overburden via injection wells	2	3	●			X		X
		Vertical movement of CO ₂ from Primary store to overburden via both caprock & wells	1	3	●			X		X
	Seabed	Vertical movement of CO ₂ from Primary store to seabed via P&A wells	2	4	●	X	X			
		Vertical movement of CO ₂ from Primary store to seabed via suspended wells	2	4	●	X	X			
		Vertical movement of CO ₂ from Primary store to seabed via injection wells	2	4	●	X	X		X	X
		Vertical movement of CO ₂ from Primary store to seabed via both caprock & wells	1	4	●	X	X	X	X	X
	Lateral	Lateral movement of CO ₂ from Primary store out with storage complex	1	3	●			?*		
		Lateral movement of CO ₂ from Primary store via bounding faults	2	3	●			?*		
	Underburden	Primary store to underburden via existing wells	1	2	●			X		
		Primary store to underburden via store floor	2	2	●			X		

- Critical
- Serious
- Moderate
- Minor

*Seismic response of CO₂ within the Rotliegend is very poor so it may be extremely challenging to detect any lateral migration of CO₂

Figure 3-89 Viking A Storage site - Leakage scenario mapping to MMV technology

3.7.4.4 Outline Corrective Measures Plan

The corrective measures plan will be deployed if either leakage or significant irregularities are detected from the monitoring, measurement and verification plan above. Some examples of significant irregularities and their implications are shown in Table 3-36.

Once a significant irregularity has been detected, additional monitoring may be carried out to gather data which can be used to more fully understand the irregularity. A risk assessment should then be carried out to decide on the appropriate corrective measures to deploy, if any. It may be that only further

monitoring is required. Depending on the implication of the significant irregularity, some measures may be needed to control or prevent escalation and remediation options may be required.

The risk matrix provided as Appendix 1 contains examples of mitigation actions (controls) and potential remediation options. For the leakage scenarios discussed in Appendix 2 and mapped to MMV technologies in Figure 3-89. Some examples of control actions and remediation options are shown in Figure 3-90.

Monitoring technology	Example of significant irregularity	Implication
Wireline logging suite (incl well bore integrity)	Indication that wellbore integrity compromised	Injection process at risk
4D seismic survey	CO ₂ plume detected out with the storage site or complex (e.g. laterally or vertically)	Potential CO ₂ leakage or unexpected migration
Sidescan sonar survey Chirps, boomers & pingers	Bubble stream detected near P&A wellbore	Potential CO ₂ leakage to seabed via P&A wells
Seabed sampling, ecosystem response monitoring, geochemical analyses of water column	Elevated CO ₂ concentrations above background levels detected in seabed	Potential CO ₂ leakage to seabed
DTS, downhole and wellhead P/T gauge and flow meter readings	Sudden temperature drop along tubing Sudden pressure or temperature drop in reservoir	Potential CO ₂ leakage from injection wellbore Storage site integrity compromised (e.g. caprock fractured) - CO ₂ potentially

Table 3-36 Examples of irregularities and possible implications

		Outline Corrective Measures		
		Control/ mitigation actions	Potential Remediation Options	
Leakage Scenario	Overburden	Vertical movement of CO2 from Primary store to overburden through caprock	Investigate irregularity, assess risk, update models if required, increased monitoring to ensure under control	Increased monitoring to ensure under control (CO2 should be trapped by additional geological barriers in the overburden)
		Vertical movement of CO2 from Primary store to overburden via pre-existing wells	Investigate irregularity, assess risk, update models if required, increased monitoring to ensure under control	Increased monitoring to ensure under control. Consider adjusting injection pattern if can limit plume interaction with pre-existing wellbore. Worst case scenario would require a relief well (re-entry into an abandoned well is complex, difficult and has a very low chance of success)
		Vertical movement of CO2 from Primary store to overburden via injection wells	Stop injection, investigate irregularity, acquire additional shut-in reservoir data, update models	Replacement of damaged well parts (e.g. tubing or packer) by workover. Worst case scenario would be to abandon the injection well.
		Vertical movement of CO2 from Primary store to overburden via both caprock & wells	Investigate irregularity, assess risk, update models if required, increased monitoring to ensure under control	Increased monitoring to ensure under control (CO2 should be trapped by additional geological barriers in the overburden)
	Seabed	Vertical movement of CO2 from Primary store to seabed via P&A wells	Stop injection, investigate irregularity via additional monitoring at seabed and acquisition of shut-in reservoir data, assess risk, update models	Re-entry into an abandoned well is complex, difficult and has a very low chance of success. A relief well is required.
		Vertical movement of CO2 from Primary store to seabed via suspended wells	Stop injection, investigate irregularity via additional monitoring at seabed and acquisition of shut-in reservoir data, assess risk, update models	Re-entry into a suspended well may be easier than an abandoned well. Engage Operator.
		Vertical movement of CO2 from Primary store to seabed via injection wells	Stop injection, shut in the well and initiate well control procedures, investigate irregularity via additional monitoring at seabed and acquisition of shut-in reservoir data, assess risk, update models	Replacement of damaged well parts (e.g. tubing or packer) by workover. Worst case scenario would be to abandon the injection well.
		Vertical movement of CO2 from Primary store to seabed via both caprock & wells	Stop injection, investigate irregularity via additional monitoring at seabed, assess risk	If injection well - replacement of damaged well parts (e.g. tubing or packer) by workover. Worst case scenario would be to abandon the injection well. If P&A well - a relief well may be required.
	Lateral	Lateral movement of CO2 from Primary store out with storage complex	Investigate irregularity, assess risk, update models if required, increased monitoring to ensure under control	Continue to monitor, licence additional area as part of Storage Complex.
		Lateral movement of CO2 from Primary store via bounding faults	Investigate irregularity, assess risk, update models if required, increased monitoring to ensure under control	Continue to monitor, licence additional area as part of Storage Complex.
	Underburden	Primary store to underburden via existing wells	Investigate irregularity, assess risk, update models if required, increased monitoring to ensure under control	Continue to monitor, licence additional area as part of Storage Complex. Worst case scenario: a relief well may be required (re-entry into an abandoned well is complex, difficult and has a very low chance of success)
		Primary store to underburden via store floor (out with storage complex)	Investigate irregularity, assess risk, update models if required, increased monitoring to ensure under control	Continue to monitor, licence additional area as part of Storage Complex.

Figure 3-90 Outline Corrective Measures Plan

4.0 Appraisal Planning

4.1 Discussion of Key Uncertainties

The Leman Sandstone of the Southern North Sea province and the Viking field area has been explored and appraised since the 1960's. The area as a whole is extremely well characterised through the development and production of a series of major gas fields including Viking A itself which has been developed for gas extraction with 10 production wells. Together these have produced 1124 Bscf of gas from 1972 to 1991. The injection wells are located very close to the gas production wells in order to limit reservoir quality uncertainty.

As a result of its hydrocarbon history, the Viking A site is considered to be exceptionally well appraised. There are however some key remaining uncertainties which could be reduced significantly ahead of any final investment decision.

1. Whilst the seismic data are not critical to the definition of reservoir volume given the hydrocarbon production, it would be prudent for a storage operator to obtain re-processed pre stack depth migrated 3D seismic data before any FEED programme evaluation. Acquisition of seismic data covering the gap to the north east of Viking A would also be beneficial for storage permitting. This may be accessed through an existing commercial 3D volume.
2. It is essential to obtain the well by well production and pressure records for all of the production wells so that this can be used to refine the calibration of the dynamic model in FEED. Where possible this should include final reservoir pressures before well abandonment.

3. The recovery of mechanical strength of the reservoir and caprock as the reservoir is re-pressurised is not well understood and may have a significant negative impact upon capacity if it does not recover. Further general research and analysis of this factor is required ahead of any FID, perhaps using one of many Leman Sandstone gas storage reservoirs as a close analogue.
4. Further investigation of the fault seals and aquifer connectivity where sandstone is juxtaposed against sandstone should be carried out to further improve confidence around connected volume and the number of injection wells required. This should include some consideration of re-pressurisation scenarios between the end of production and initial injection.
5. Finally, there is a key uncertainty remaining regarding the operational management of the phase change to minimise or preferably eliminate the requirement for heating of the CO₂ at the wellhead early in the project. A specific project should be focussed upon drawing together the experience of phase management in CO₂ injection wells around the world from both a theoretical, modelling and practical experience.

4.2 Proposed Appraisal Plan

Appraisal Drilling: with ten wells on the Viking A block itself and many others in the nearby vicinity to help characterise the subsurface, all with reasonably modern log and core data focussed upon the evaluation Leman Sandstone reservoir for gas production, no further appraisal drilling is considered necessary at this time.

Seismic Acquisition: No further pre-FID seismic acquisition is considered necessary; however it would be beneficial to obtain the re-processed pre stack depth migrated 3D from the operator to assist in more accurate positioning of subsurface features such as boundary faults. It is however recommended that a new baseline survey is acquired before injection starts for the specific purpose of monitoring.

Other Appraisal Activity: Further subsurface evaluation and modelling work should be completed once well by well production and rate data are obtained from the operator. This will assist the refinement of the dynamic model calibration during the gas production history of the Viking A field.

5.0 Development Planning

5.1 Description of Development

The Viking field is a gas development located within blocks 49/12, 49/16 & 49/17 and comprises seven normally unmanned platforms in the Southern North Sea plus one manned main complex, Viking B, and the associated outlying Vixen subsea satellite, together with significant offshore and onshore facilities used for extracting, transporting and processing reserves.

The Viking area is located 140 km from the Lincolnshire coast of England and has been in production since 1972, with COP expected prior to commencement of this project. The Viking A area ceased production in 1991. The Viking reservoir will therefore be a depleted gas field that will have a very low reservoir pressure (but relatively high temperature). The CO₂ will be transported as a liquid, it is therefore anticipated that CO₂ heating will initially be required to manage low temperature risks and ensure single phase (supercritical) conditions going downhole (i.e. to avoid gas formation in the well bore). The CO₂ will therefore be injected in two stages, via 2 wells (plus a monitoring well and a spare):

Stage 1 – Heated CO₂ Injection (Continuous CO₂ heating);

Stage 2 – Un-heated CO₂ Injection (Intermittent or no CO₂ heating).

Note that the same two wells are used during Stage 1 and Stage 2, with workovers etc. as described in Appendix 6.

The current base case for the Viking A CO₂ storage development consists of a new 185km 20" pipeline from Barmston to a newly installed Normally Unmanned Installation (NUI) located at the Viking A site.

The NUI will take the form of a conventional 4-legged steel jacket standing in 27.5m water depth and supporting a multi-deck minimum facilities topsides. The steel jacket will be piled to the seabed and provide conductor guides which in conjunction with a 4 slot well bay will enable cantilevered jack-up drilling operations for the injection wells.

A 90km power cable will provide electrical power to the Viking A NUI from Bacton. The installation will be controlled from shore via dual redundant satellite links with system and operational procedures designed to minimise offshore visits.

The installation will be capable of operating in unattended mode for up to 90 days with routine maintenance visits scheduled approximately every six weeks to replenish consumables (chemicals, etc.), and carry out essential maintenance and inspection activities.

5.2 CO₂ Supply Profile

The assumed supply profile for the reference case is for 5 Mt/y to be provided for the shore terminal at Barmston for the duration of the 26 year injection period, this is illustrated in Figure 5-1.

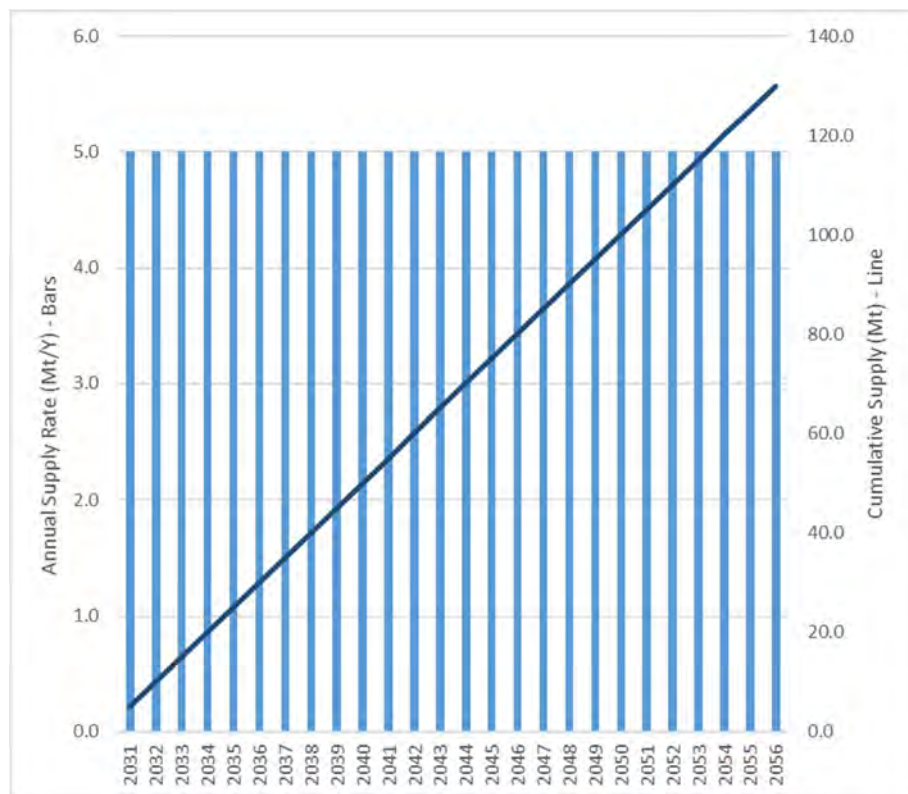


Figure 5-1 CO₂ supply profile

5.3 Well Development Plan

Geological and reservoir engineering work has concluded that the Viking A reservoir is very well connected laterally (no significant lateral barriers to the field limits, although there is some potential for upside in a potential fault block to the north west) and is thus relatively insensitive to well placement, providing the well penetrates through the entire vertical sequence.

Reservoir engineering analysis suggests that two large injection wells would provide sufficient injection capacity to meet target CO₂ volumes over field life. Given that this injection capacity needs to be maintained at all times to meet likely contractual obligations, this means that two injection wells are required for field life (heated and unheated liquid phase) plus a single back-up well.

As offshore heating and filtering will be required, a wellhead platform is the appropriate facility for Viking. This then dictates a single top hole well location for all development wells. The only other constraint considered (other than drilling constraints) was that each bottom hole target should be separated by a minimum 1,000m in order to eliminate the superposition of temperature effects.

5.3.1 Well Design

The Viking A injector well basis of design can be summarised as follows:

1. The injector wells will be drilled from a NUI platform by standard North Sea jack-up
2. The wells will be a deviated (up to 60°) in the target Leman Sandstone
3. The injector wells will consist of 26" conductor, 18-5/8" surface casing, 13-3/8" intermediate casing and 9-5/8" production casing,

with a 7” cemented liner (or open hole sand control completion). The wells will be completed with 7” production tubulars

4. All flow wetted surfaces will be 13%Cr material with higher grade CRA for the lower sections
5. Maximum injection rates will be 6.84 Mte/yr (354 mmscf/day) depending on reservoir quality
6. Maximum FTHP will be 160 bar
7. Maximum SITHP (<190bar)
8. Maximum WHT will be 35°C
9. Minimum Design Temperature (to be confirmed by transient modelling)

5.3.1.1 Well Construction

The following reservoir targets have been identified for the Lemman Sandstone reservoir:

Target Name	TVDSS (m)	UTM North (m)	UTM East (m)
INJ-01 Top Lemman	2,598.9	5,931,001.0	451,161.7
INJ-01 TD	2,844.7	5,931,272.0	451,473.2
INJ-02 Top Lemman	2,556.3	5,931,975.0	449,877.5
INJ-02 TD	2,703.3	5,932,169.0	449,708.5
INJ-03 Top Lemman	2,593.3	5,930,401.0	451,911.2
INJ-03 TD	2884.0	5,930,019.0	452,243.5

Table 5-1 Viking A well locations

Note:

Well INJ-03 is currently defined as the monitoring well and/or spare injector

The coordinate system in use is UTM, ED50 Common Offshore, Zone 31N (0° to 6° East)

The conceptual directional plans for the CO₂ injectors have been designed on the following basis:

1. All wells will be drilled as slant wells, including the monitoring well which will also act as a spare injector.
2. All wells will be drilled vertically to 640m TVDSS (i.e. to below the surface casing shoe).
3. All wells will be kicked off below 640m MD, with a planned dogleg severity of 3.0° per 30m. The wells will be built to the required tangent angle, while turning the wellpath onto the required azimuth.
4. A build section will be drilled from the surface shoe to the depth at which inclination is sufficient to reach the identified reservoir target.
5. A turn and build / drop section will be drilled in the 12 ¼” hole section to deliver an inclination of 60° at the top of the Lemman Sandstone while turning the well path onto the desired azimuth.
6. The reservoir section will be drilled as a tangent section, holding inclination at 60° to TD below the base of the Lemman Sandstone.

A directional well spider plot is provided in Figure 5-2. The directional profile for platform slant injector 1 is provided in Figure 5-3. Full details for all wells are provided in Appendix 6.

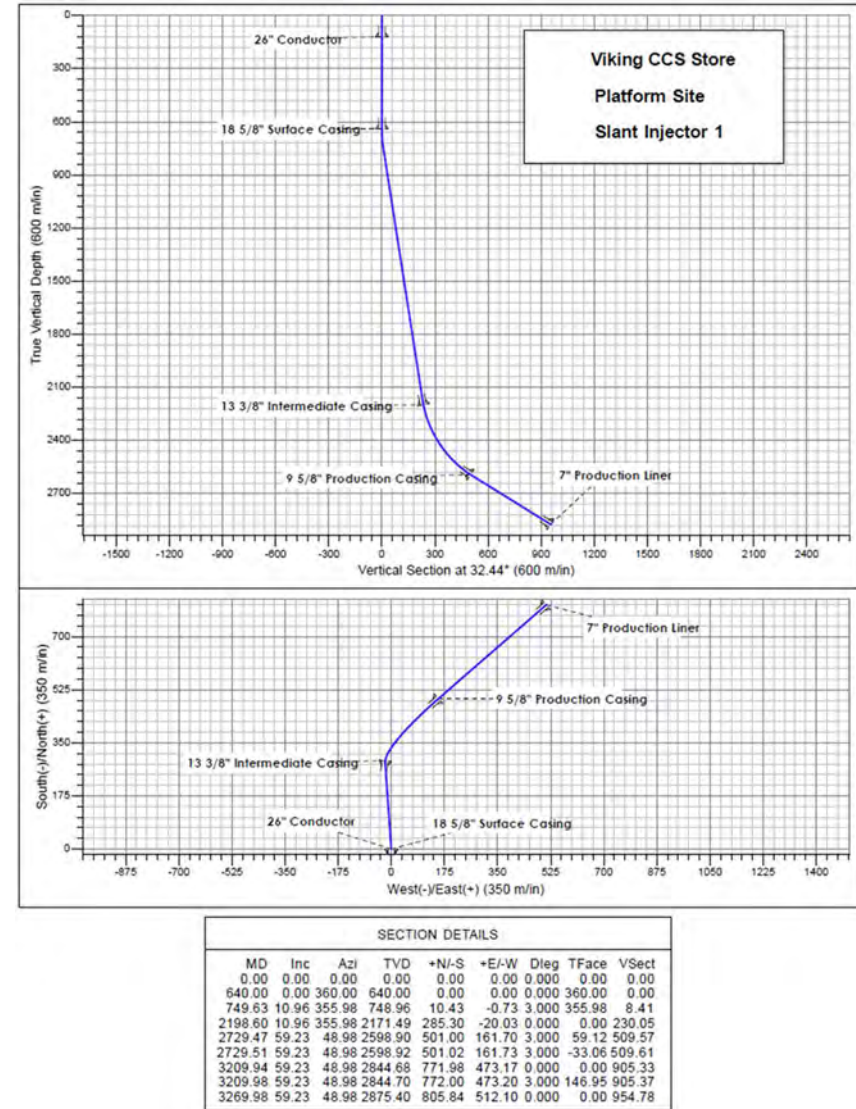
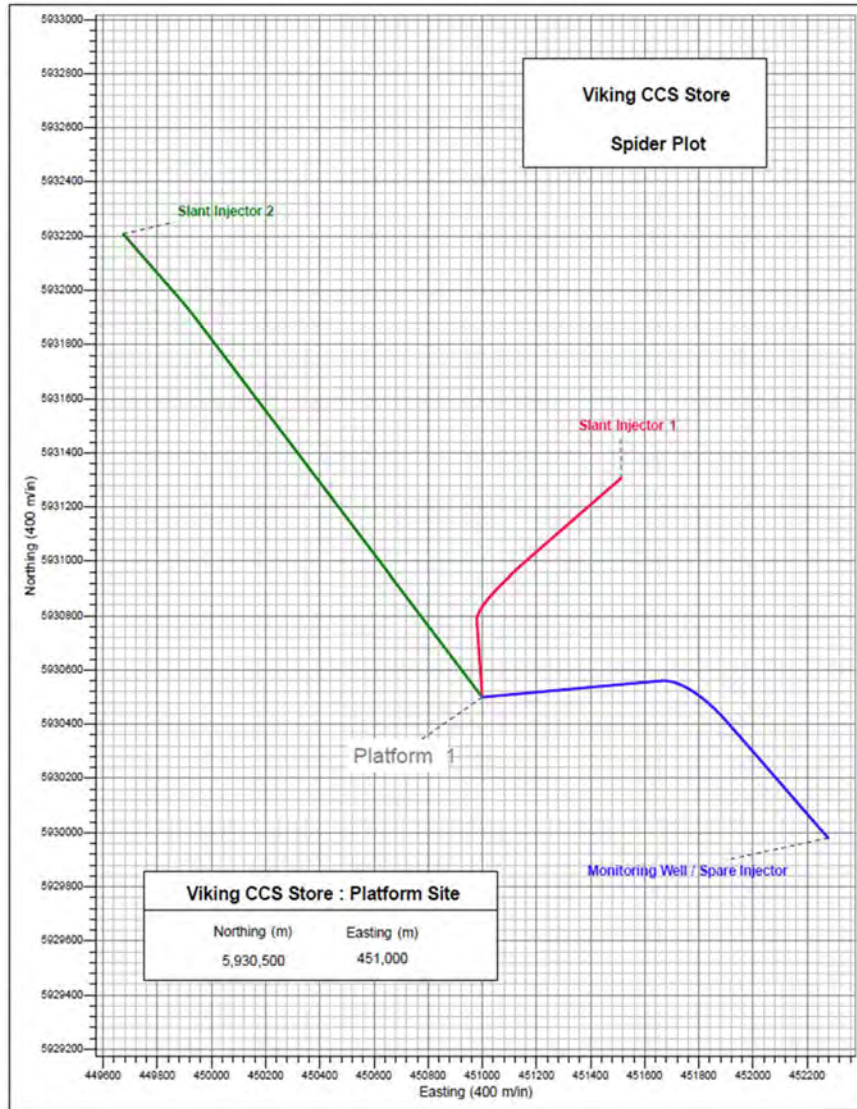


Figure 5-2 Platform directional spider plot

Figure 5-3 Slant injector 1 directional profile

5.3.1.2 Well Completion

The upper completion consists of a 7” tubing string, anchored at depth by a production packer in the 9-5/8” production casing, just above the 7” liner hanger. Components include:

1. 7” 13Cr tubing (weight to be confirmed with tubing stress analysis work) with higher grade CRA from Barrier Valve to tailpipe
2. Tubing Retrievable Sub Surface Safety Valve (TRSSSV)
3. Deep Set Surface-controlled Tubing-Retrievable Isolation Barrier Valve (wireline retrievable, if available)
4. Permanent Downhole Gauge (PDHG) for pressure and temperature above the production packer
5. Optional DTS (Distributed Temperature Sensing) installation
6. 9-5/8” V0 Production Packer

The DTS installation will give a detailed temperature profile along the injection tubulars and can enhance integrity monitoring (leak detection) and give some confidence in injected fluid phase behaviour. The value of this information should be further assessed, if confidence has been gained in other projects (tubing leaks can be monitored through annular pressure measurements at surface, leaks detected by wireline temperature logs and phase behaviour modelled with appropriate software). If possible, the DTS should be run across the full sandface (possibly behind casing) in order to provide an injection profile and monitor minimum temperatures in the wellbore.

5.3.2 Number of Wells

Geological and reservoir engineering work has concluded that the Viking A reservoir is very well connected laterally (no significant lateral barriers to the field

limits, although there is some potential for upside in a potential fault block to the south east) and is thus relatively insensitive to well placement, providing the well penetrates through the entire vertical sequence. First pass reservoir engineering also suggested that two large injection wells would provide sufficient injection capacity to meet target CO₂ volumes over field life. Given that this injection capacity needs to be maintained at all times to meet likely contractual obligations, this means that two injection wells are required for field life (heated and unheated liquid phase) plus a single back-up well.

5.3.3 Drilling Programme

The summary well drilling and completion schedule for the life of the project is illustrated in Table 5-2.

Well Activity	0	5	10	15	20	26
Drill and New injection Well	2					
Drill and Complete New Monitoring Well / Spare Injector	1					
Workover			1			
Local Sidetrack from Existing Platform Slot			2			
Abandonment						3

Table 5-2 Summary well activity schedule

5.3.3.1 Well Construction Programme

The outline drilling, casing and mud programmes for platform wells are provided in Table 5-3.

Section	Casing	Comments
Surface (Driven)	26", 95m below mudline Carbon Steel	
Surface Seawater (22")	18 5/8", 610m Carbon Steel Cemented to mudline	
Intermediate (17 1/2") Oil based mud	13 3/8", 2,200m Carbon Steel Cemented to 100m inside 18 5/8" shoe	Isolate the weaker Bunter Shale prior to drilling Zechstein salt mobile
Intermediate (12 1/4") Oil based mud	9 5/8", 2580m 13Cr below packer Cemented to 200m inside the 13 3/8" shoe	Isolate Zechstein salt Isolate dolomite rafts Provide a good cementing job over the mobile Zechstein Halites
Injection (8 1/2") Oil based mud	7", 2940m 13Cr Cemented over the entire length	

Table 5-3 Outline well construction programme -slant injector 1

5.4 Injection Forecast

Injection commences in 2031 and continues for approximately 26 years, the final year of injection is 2056. The injection forecast for the reference case is for 5 Mt/y for the 26 year store life. This forecast results in a cumulative injection of 130 Mt of CO₂.

Year	Rate (Mt/y)	Total (Mt)	Year	Rate (Mt/y)	Total (Mt)
2031	5	5	2044	5	70
2032	5	10	2045	5	75
2033	5	15	2046	5	80
2034	5	20	2047	5	85
2035	5	25	2048	5	90
2036	5	30	2049	5	95
2037	5	35	2050	5	100
2038	5	40	2051	5	105
2039	5	45	2052	5	110
2040	5	50	2053	5	115
2041	5	55	2054	5	120
2042	5	60	2055	5	125
2043	5	65	2056	5	130

Table 5-4 Injection profile

5.4.1 Movement of the CO₂ Plume

In the proposed development at Viking A, CO₂ is injected into the three permeable reservoir layers. Whilst there are strong baffles between these layers that hinder direct vertical communication, the layers are thought to be reasonably well connected as a result of internal faults which serve to connect the sands through juxtaposition. With little or no evidence for any aquifer influx during production, the injected CO₂ is expected to move downwards within the low pressure gas column left after the gas field development. Modelling suggests that it will move down until it reaches the GWC in block A. Below this depth the permeability is significantly reduced. Injection is halted when the weakest point in the storage reservoir approaches the fracture limit constraint.

CO₂ concentration equilibrates well over the 1000 years modelled period across the field, but does not move outside the storage complex.

5.5 Offshore Infrastructure Development Plan

The optimum platform location for the Viking A NUI has been determined through drilling studies, UTM coordinates are presented in the table below.

Platform	UTM Coordinates	
	Eastings (m)	Northings (m)
Viking A NUI	451000	5930500

Table 5-5 Platform Location

5.5.1 CO₂ Transportation Facilities

This section provides an overview of the Viking A CO₂ transportation (pipelines) development plan. CO₂ will be transported in the liquid phase.

5.5.1.1 Pipeline Routing

Figure 5-4 shows the pipeline route from Barmston to the Viking A NUI.

The pipeline route from Barmston to Viking has been selected to minimise the pipeline route length while avoiding existing facilities (hydrocarbon developments) and maintaining appropriate crossing angles. There are several other potential storage sites (including hydrocarbon fields) along the pipeline route and in the vicinity of Viking that could be utilised for step out CO₂ storage / EOR in the future, further discussion is included in Section 5.7.

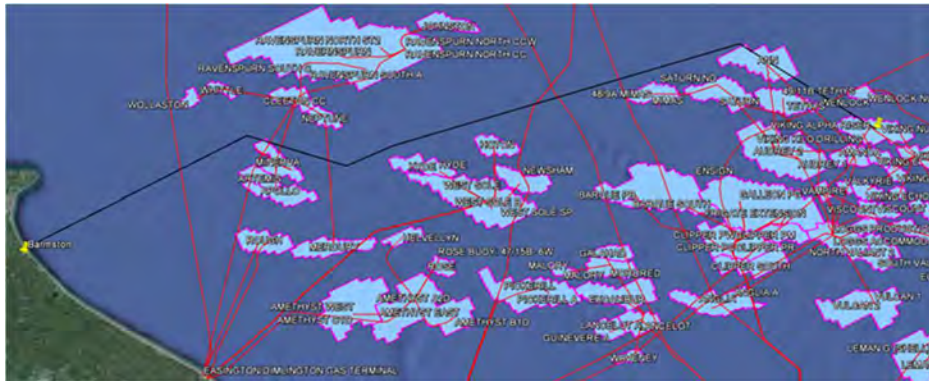


Figure 5-4 Pipeline route

The pipeline route shown crosses several pipelines and umbilicals as summarised in Table 5-6.

Pipeline	Surface Laid / Trenched	Operator
44” Langedled	Surface Laid	Gassco
36” Cleeton to Dimlington	Surface Laid	BP Exploration
Cleeton Umbilical	Trenched and Buried	BG
10” Neptune-Mercury	Trenched and Buried	BG
4” MEG to Murdoch	Trenched and Buried	ConocoPhillips
34” Shearwater	Surface Laid	Shell UK
24” Esmond to Bacton	Surface Laid	Perenco
20” Carrack Gas Export	Surface Laid	Shell UK

Table 5-6 Pipeline crossings (Barmston to Viking)

It is worth noting that the Dogger bank wind farm project is currently ongoing, with the UK government granting planning consent for the first and second phase of the project in 2015. Should this project be sanctioned it may necessitate a re-route to the south adding 5-10km to the overall route length, as well as a significant number of pipeline crossings, as shown below (an approximation of the round 3 wind farm zone is shown in yellow).

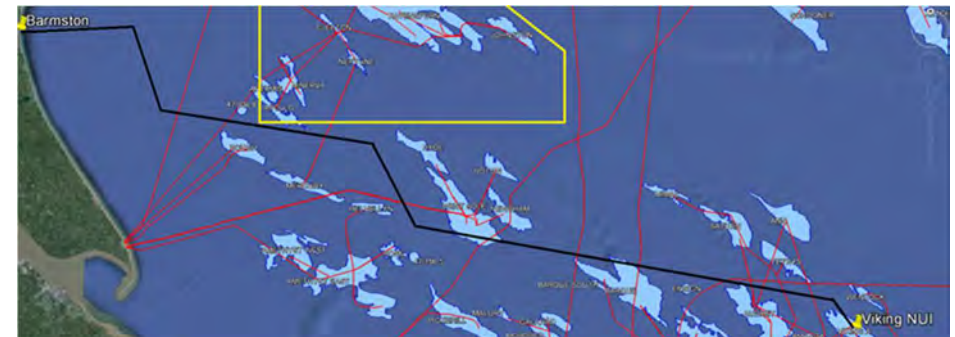


Figure 5-5 Pipeline route avoiding Dogger bank windfarm

A full desktop study will also be required to confirm the pipeline route and ensure that all seabed obstructions (wells, platforms, pipelines, umbilicals and cables etc) and seabed features (rocks, sandwaves, pockmarks, mud slides etc) are identified and accounted for appropriately. It is worth noting that the seabed in the Southern North Sea can be highly mobile and can include sandwaves and smaller ripple features. It is therefore recommended the desktop study is performed as early as possible to determine whether seabed rectification (presweeping, dredging etc) will be required due to the combination of shallow water, high tidal currents and mobile sand waves resulting in a problematic and dynamic seabed topography.

The pipeline will be taken offshore using either a cofferdam constructed on the beach/subtidal area, or using a caisson (which can be constructed entirely subtidally). The pipeline will be trenched in the nearshore out to 30m depth (approximately 15km offshore).

5.5.1.2 Preliminary Pipeline Design

Preliminary line sizing calculations have been performed to determine the Viking A pipeline outer diameter. The pipeline route length is 185 km.

The CO₂ will be transported in the liquid phase. The arrival pressures at the Viking A NUI are such that the CO₂ is in liquid phase under ambient sea temperatures throughout the year. An overview of the Viking A well development plan is presented in Section 5.3.

Due to the low pressure and relatively high temperature in the Viking depleted gas reservoir, the CO₂ will initially be heated prior to injection to ensure that the CO₂ is injected as a supercritical/dense phase fluid and to avoid multiphase conditions downhole (i.e. gas formation in the well bore). This first stage will last for approximately 20 years, until the reservoir pressure (and temperature) is sufficient to maintain a liquid column of CO₂ in the well bore (Stage 2). This second stage is estimated to last approximately 6 years, giving a total injection duration of approximately 26 years. Note that the same two wells are used during stage 1 and stage 2, with workovers as described in Section 5.3. Further discussion on the heating/operating philosophy is included in Section 3.6.

Operating the pipeline in liquid phase reduces the size of the pipeline but it will require significant amounts of offshore heating prior to injection in order to ensure supercritical/dense phase conditions going downhole and to manage low temperatures. Pressures in the liquid phase pipeline should also be kept to a strict limit both to avoid gas forming and to avoid large pressure drop across the

injection chokes which would in turn require further heating. Note that this operating philosophy will be highly dependent on the composition of the supplied CO₂, and will require confirmation during FEED (steady state and transient analysis).

The required mass flow rate of 5 MT/Year has been selected to ensure a sustainable plateau rate over the 26 year design life (130 MT total injected). It has been assumed that the Barmston pump station delivers up to approximately 200 bar in pressure therefore the maximum allowable pressure drop is in the region of 40 bar.

There are a number of other potential storage sites and oil/gas developments along the pipeline route and in the vicinity of the Viking A site which could be utilised for future build out of CO₂ storage. There is therefore merit in pre-investing in an increased ullage (larger) pipeline from Barmston with future tie-in structures (valved tees) at set locations along the route to facilitate future expansion (discussed further in Section 5.7). The cost estimates in Section 6 include provision for two in-line tee structures.

It can be seen from Figure 5-6. that a 20" pipeline Barmston is sufficient to meet the Viking CO₂ profile whilst still providing a level of spare capacity. At a flow rate of 5 MTPA results in a pressure drop of approximately 23 bar. At a flow rate of 7.5 MTPA this increases to approximately 45 bar. Therefore, there is sufficient ullage in the 20" pipeline for an additional Viking injection well, beyond which additional pumping will likely be required. Further results are provided in Appendix 8.

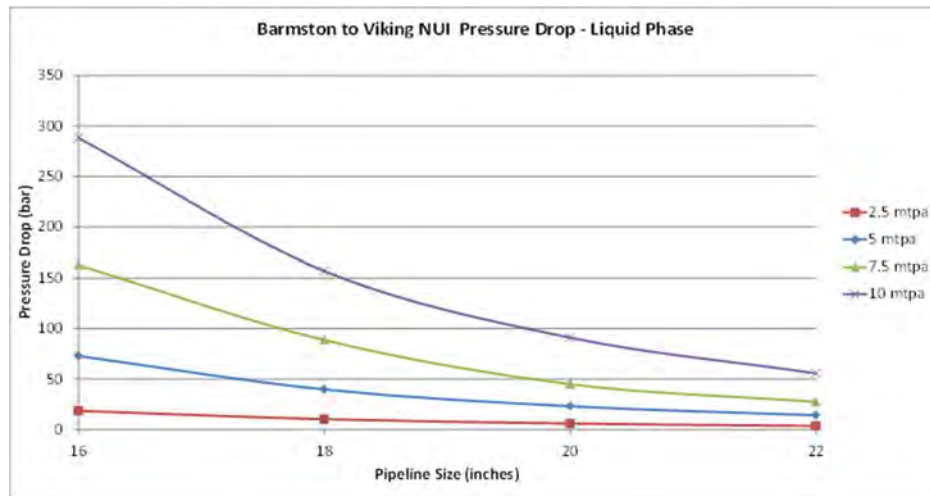


Figure 5-6 Pipeline pressure drops

The Viking A pipeline is sufficiently large (OD \geq 16") that it does not require burial or rockdumping for protection purposes. Instead it is proposed the pipelines be surface laid and protected/stabilised with concrete weight coating, which necessitates installation by S-lay. The near shore section will require burial for stability against wave and current forces.

5.5.1.3 Subsea Isolation Valve (SSIV)

For conservatism development costs include for an actuated piggable ball valve SSIV structure being installed on the 20" pipeline adjacent to the Viking A NUI Jacket. The requirement for SSIVs to be installed on CO₂ service pipelines feeding a normally unmanned installation (NUI) is not clear-cut. The Peterhead CCS Project Offshore Environmental statement (Shell, 2014) states that a new SSIV will be put in place to support the proposed project and provide a means of isolation in the event of loss of containment close to the platform. The Offshore Environmental Statement for the White Rose CCS project (National Grid Carbon

Ltd; Carbon Sentinel Ltd; Hartley Anderson Ltd, 2015) states that the White Rose 4/52 pipeline will not have a subsea isolation valve (SSIV). Comparatively the inventory of the proposed White Rose pipeline is greater than that of Goldeneye. The requirement for an SSIV for the Viking A pipeline should be fully appraised in FEED. The Viking A platform import riser will be fitted with an emergency shutdown valve (ESDV) and the riser located so as to mitigate risk of collision damage by support vessels. Full dispersion modelling will be required in order to position the ESDV and Riser and any temporary refuge facilities specified accordingly in compliance with PFEER regulations. If an SSIV is deemed necessary for the Viking pipeline then consideration must be given to the pressure rating of the piping, spools and riser to allow for thermal expansion of any potential trapped CO₂ inventory.

5.5.2 Offshore CO₂ Injection Facilities

It is proposed that CO₂ is injected into Viking from a single Normally Unmanned Installation (Platform) with a 4 slot wellbay that will enable Jack Up drilling and completion of dry injection trees. A NUI platform is considered as both the most economical and technically suited development concept for the Viking A site.

The key input parameters used to size and cost the NUI platform for Viking are listed below, and a master equipment list is provided in Table 5-7:

NUI Jacket:

- 27.5m water depth
- 26 year design life
- 10,000 year return wave air gap
- Jacket supported conductor guide frames
- J-tube and riser to facilitate future tie back

NUI Topsides:

- Minimum Facilities Topsides
- Pre-Injection CO₂ heaters (x6)
- Power supplied via power cable from shore (Bacton) with transformers
- Well and valve controls HPU and MCS package
- HVAC package
- Low temperature valving and manifolding pipework package
- Sampling and Metering package
- No compression / pumping
- Availability for a water wash skid
- Consumable tanks sized for 90 days self sustained operations

A process flow diagram of the Viking A development is presented in Figure 5-7.

Requirement	Quantity/Value	Comment
Design Life	26 Years	2 wells, plus a spare injector and a spare slot.
Platform Well Slots	4	Heated CO ₂ injection for approx. 20yrs, followed by 6 yrs Un-heated CO ₂ injection.
Platform Wells	3	
Trees (XT)	3	-
Diesel Generator	1	Emergency (back-up) power generation only
Satellite Communications	2 x 100%	Dual redundant VSAT systems
Risers	2	1 spare for future tie-back/expansion
J-Tube	3	For future tie-back/expansion
Subsea Isolation Valve (SSIV)	1	SSIV at Viking only
Temporary Refuge	1	4 Man
Lifeboat	1	TEMPSC and Life rafts
Helideck	1	-
Pig Launcher Receiver	Permanent	-
CO ₂ Filters	Yes	Bypassable
CO ₂ Heaters	6	3 x 2.5 MW heaters per injector well. To manage low temperature risks and ensure single phase conditions going downhole
Transformers and Distributors	2	Conversion from 33kV to 690V
Crane	1	Electric crane
Vent Stack	1	Low Volume
Leak detection and monitoring	1	
Chemical Injection	MEG	MEG for start-ups/restarts c/w storage, injection pumps and ports. Temporary Water Wash Facilities with Inert Gas for pressurisation
General Utilities	Yes	Open hazardous drains etc.

Table 5-7 Master equipment list

VIKING A

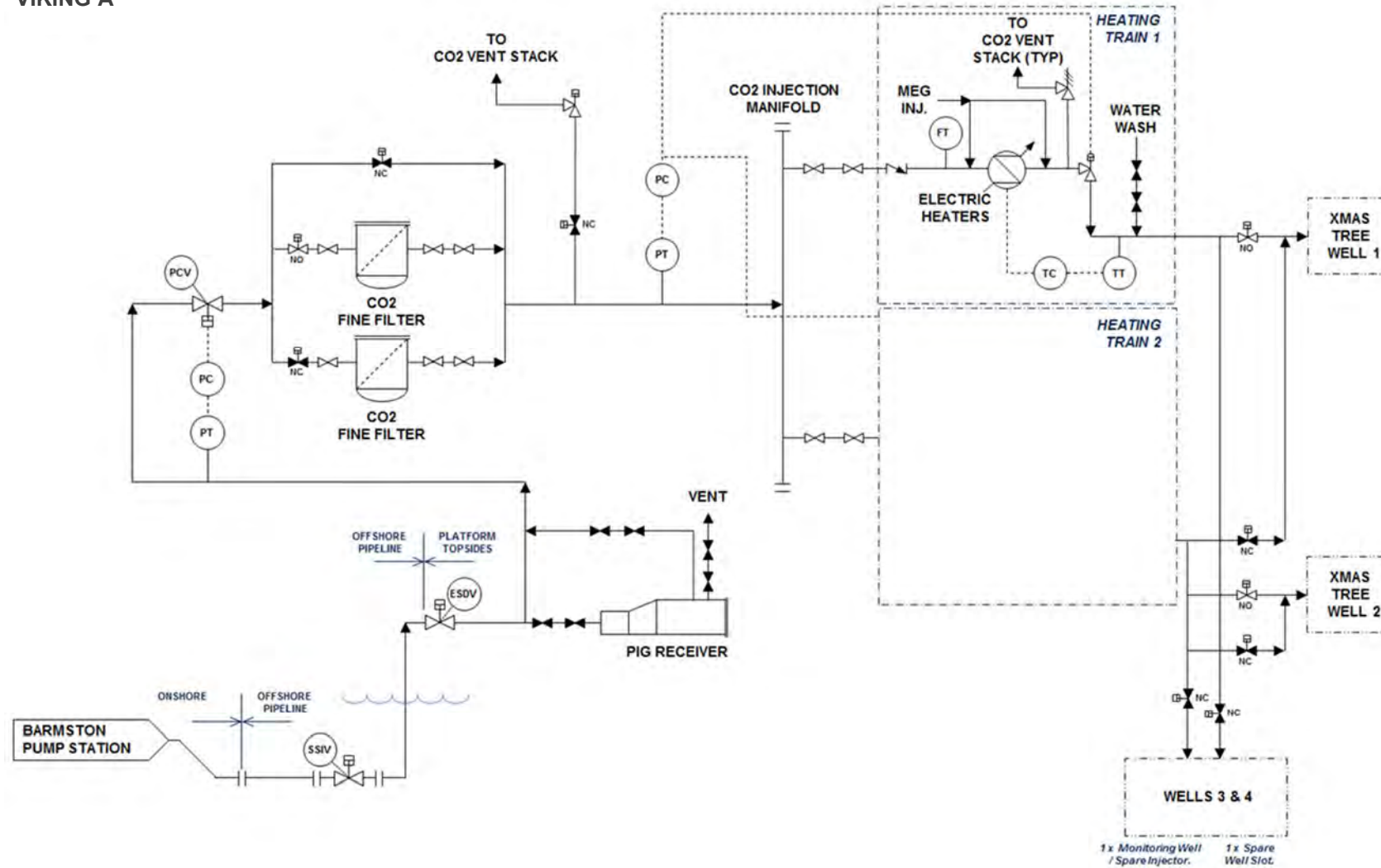


Figure 5-7 Viking A development process flow diagram

5.5.2.1 Platform Infrastructure

Jacket Design:

A conventional 4-legged steel jacket has been assumed. The jacket will be piled to the seabed and will be sufficiently tall to ensure an air gap is maintained between the topsides structure and the 10,000 year return period wave crest height. The jacket would be protected by sacrificial anodes and marine grade anti-corrosion coat paint. The water depth is such that a SeaKing design jacket may be employed which would reduce the associated CAPEX and fabrication time of the jacket. Suitability of such a jacket design would require to be fully appraised during FEED.

Jacket Installation:

The jacket will be fabricated onshore, skid loaded onto an installation barge, towed to site, and launched. Mudmats will provide temporary stability once the jacket has been upended and positioned; with driven piles installed and grouted to provide load transfer to the piled foundations.

Topsides Design:

The installation topsides are proposed to be constructed as a single lift topsides module. A multi-level topsides module consisting of a weather deck, a mid level, a lower cellar deck and a cantilevered helideck has been assumed.;

The weather deck will be of solid construction to act as a roof for the lower decks, it will provide a laydown area for the crane and house the HVAC package and VSAT domes. A helideck will be cantilevered out over the weather deck.

The mid level deck will only partially cover the topsides footprint and will serve to house the manifolding pipework, and pig receiver.

The cellar deck will house the wellhead Xmas trees and associated piping, a master control station (MCS), hydraulic power unit (HPU), process equipment including CO₂ heaters, emergency power generation package, chemical and diesel tanks, control and equipment room and short stay accommodation unit.

The jacket and topsides will be sized and arranged so as to enable jack-up set up on two faces, in order to access the 6 well slots.

Platform Power:

A power cable will provide electrical power to the Viking A NUI from Bacton. The power cable itself is discussed in Section 5.5.3.

The power cable will provide high voltage (HV) and low voltage (LV) power to the Viking A NUI. LV power supply shall be sufficient to power the MCS, HPU, plus the crane, HVAC system and all ancillary equipment.

A 690 voltage 3 phase power supply will be required for the CO₂ heaters. Table 5-8 provides the estimated continuous power loads for the system (during dense phase injection). It is envisaged that there will be three heaters per well, with one or two in operation as required (due to varying conditions), plus a spare/back-up.

The required capacity of the heaters depends on the injection rate, the down hole pressure and the required temperature rise. The power required to convert the liquid CO₂ into supercritical phase has been estimated to be 10 MW (at 5 MTPa flowrate) equivalent to 5MW per CO₂ injector well. This requires further assessment to account for the range in ambient temperature conditions (both subsea and air), flow rates, CO₂ compositions and injection pressure and temperature requirements.

Well	Number of CO ₂ Heaters	Assumed Power Capacity per Heater
Platform Injector 1	2 + 1 spare	2.5 MW
Platform Injector 2	2 + 1 spare	2.5 MW

Table 5-8 CO₂ heaters

Topsides Process:

The primary platform injection facilities will consist of a topsides emergency shutdown valve (ESDV), a pressure control valve (PSV) which will serve to safeguard the pipeline pressure and maintain the CO₂ in the pipeline in liquid phase, fines filters that will prevent solid contaminants entering the injection well bores, a vent stack to enable blowdown of the topsides pipework for maintenance, and an injection manifold which will facilitate injection of the CO₂ to the respective wells. As the CO₂ will be transported in the liquid phase the gas phase injector wells will also incorporate CO₂ heaters (x3) in the process pipework to manage low temperature risks and ensure single phase conditions going downhole.

Topsides pig receiving facilities will also be provided to enable periodic pipeline integrity monitoring, there is no foreseen requirement for operational pigging. All the topsides process pipework will use low temperature stainless steel materials in the event that a low pressure event occurs (i.e. venting).

Drains:

An open hazardous drains system will exist to drain the drip trays from equipment in environmental pollutant service i.e. the fuel and chemical tanks,

power generation package, and HPU. These drain sources shall be positioned below the weather deck to minimise rainwater runoff from the equipment into the hazardous open drain system. The hazardous open drains tank shall be emptied during routine maintenance. There is no foreseen requirement for a closed drains system.

Closed Loop Hydraulic system:

Topsides and tree valves will be hydraulically actuated and will utilise a water based hydraulic fluid. Dual redundant (2x100%) HPUs will be provided to allow offline maintenance.

Crane:

An electric crane will enable load transfer between vessel and NUI, and enable load transfer between the working decks of the installation.

5.5.2.2 Rationale for Development Concept

The following provides a brief overview of why a NUI Platform comprising a steel jacket and topsides has specifically been selected as the reference case for the Viking A development:

The Viking A development requires two injection wells (plus a spare injector and a spare slot) over the field life of 26 years. The proposed trajectories of the wells are such that they can be drilled from a single drill centre. The water depth at the proposed drilling location of Viking is 27.5m. This is sufficiently shallow to enable the wells to be drilled by a jack up drill rig cantilevered over a platform with 4 well slots (2 wells + spare injector + spare slot).

The Viking A development will involve the injection of CO₂ into a depleted gas reservoir. Liquid injection of CO₂ at ambient arrival temperatures from the outset is not feasible due to the reduced pressure and relatively high temperature of

the reservoir, therefore the injection strategy for Viking A is based on initial dense phase (supercritical) injection of CO₂ (heated CO₂ injection, stage 1) until the reservoir pressure is sufficient to maintain a liquid column of CO₂ in the well bore (un-heated CO₂ injection, stage 2). Note that the same two wells are used during stage 1 and stage 2, with workovers etc. as described in Section 5.3.

This requires either supercritical transport of the CO₂ to the Viking development, which would require a heated pipeline, or transporting the CO₂ offshore as a liquid, and incorporating a vaporisation unit (consisting of a heating train and a choke valve) to facilitate injection into the wells as a supercritical fluid. The latter philosophy has been adopted for the Viking A development.

The offshore heating would not be feasible on a subsea development, and is required to ensure single phase flow (i.e. to avoid gas formation in the well bore) and to protect the reservoir and wells from the very low temperatures generated by differential pressure across the choke valves (Joule Thompson effect). The well development plan is discussed in detail in Section 5.3. The first stage (heated injection) is estimated to last in the region of 20 years, and will require continuous pre-injection heating of the CO₂. Stage 2 is estimated to last an additional 6 years, and may require intermittent heating.

Electrical heaters have been identified as the most feasible option for adding heat to the CO₂ on the Viking A NUI. A fired heater train would likely require a manned platform, and excessive diesel storage or a fuel gas import pipeline. The power required to convert the liquid CO₂ into dense/supercritical phase has been estimated to be 10 MW (at 5 MTPa flowrate). Three (x3) 2.5 MW electrical heaters on each of the injector wells (upstream of the choke) will therefore have sufficient redundancy, and can be powered by a 3 phase power cable from the shore. The power cable is discussed in Section 5.5.3.

From a commercial viewpoint the design, build and installation of a NUI platform will exceed the CAPEX of an entirely subsea development however this will be eroded by the increased CAPEX of drilling subsea wells (approximately 25% more expensive to drill and complete than dry wells) and would not facilitate the CO₂ heating that is required, as described above.

Platform based wells will also improve the availability of the injection wells due to more readily achievable and inexpensive maintenance and well intervention. The OPEX for intervening on subsea wells will typically exceed that of dry wells by an order of magnitude. A platform also enables the provision of enhanced process capabilities, including (where required) the provision of the following which are not readily achievable with subsea wells:

- Pre-injection filtering (filters pipeline corrosion / scaling products), which becomes more critical for a long pipeline and is especially critical when planning matrix (as opposed to fracture) injection.
- Choke heating.
- Physical sampling facilities to ensure CO₂ injection quality.
- Pressure monitoring of all well casing annuli for integrity monitoring.
- Pig receiver.
- Venting
- Future connections are easier as the connections are above water thereby avoiding water ingress into existing systems and it's easier to dry any future pipelines

Providing the following process facilities to subsea wells is possible but will be more costly than for platform based wells:

- Process monitoring, and well allocation metering for reservoir management.

- Process chemical injection of MEG, and N₂ for transient well conditions and wash water for halite control.

Due to the requirement of a heavy lift vessel to remove the platform and topsides at the end of field life the ABEX costs associated with decommissioning a NUI platform is likely to exceed that of a subsea development, however the P&A (plug and abandonment) of subsea wells will be approximately 25% more costly than the P&A of platform wells.

5.5.3 Power Supply

A power cable will provide electrical power to the Viking A NUI from Bacton.

The power required to convert the CO₂ from liquid phase into dense phase is significant and has been estimated to be 10 MW for the 5Mtpa forecasted supply rates. This is above normal power generation on offshore facilities and requires special attention. There are three main options to consider for securing offshore power, namely:

- A self-contained generation and distribution network (typically gas turbine or diesel) – this requires extensive offshore power generation infrastructure as well as large fuel tanks and bunkering. This has been rejected due to the increase in offshore CAPEX costs, the additional manning requirements to service the generators and supply the fuel and the increase in the overall carbon footprint of the project.
- Utilising offshore renewable power from existing and or future offshore windfarms. There are wind farms operating within the region although none in the direct vicinity of the site due to the distance from shore. Also, as the heating is required continuously for an extended period of time, an alternative power source would be required during

periods of low wind supply to avoid downtime. A combination of local generation and renewable power could be feasible and would reduce the carbon deficit associated with local power generation but it would also result in high expenditure as it factors two independent power sources.

- Securing supplies from an onshore electricity distribution network connection using a 90 km subsea cable – this minimises offshore infrastructure and allows power to be procured from a wide range of sources including renewables.

A detailed description of each of these is presented in the appendices, and gives an overview of the key factors to be considered in securing a power supply from an onshore source. A breakdown of the Capex and Opex costs is also included.

A 90km 33 kV power cable from Bacton has been selected as the preferred solution. Utilising higher voltages (132kV) or DC systems are not necessary and cost considerably more. There may be a drive to increase the reliability of the system through the use of redundant systems however the cost of installing a completely separate power connection, transformer set and cable will increase the cost by almost an order of magnitude. A reliability and availability assessment is recommended to determine the optimum level of redundancy. More details are provided in Appendix 8.

5.6 Other Activities in this Area

There are several hydrocarbon fields in the vicinity of the Viking A site. The nearest of these are shown in the figures in Section 5.5.1. The pipeline is routed to avoid a number of existing hydrocarbon developments. The Viking field itself is a depleted gas reservoir, which was operated by ConocoPhillips.

Other activities in the area that are pertinent to the Viking A development are fishing and shipping.

A protection philosophy should be produced for the Viking A development, the results of which should be adopted to ensure all risks are identified and mitigated/minimized. To ensure the risks of any interaction with dropped anchors or fishing gear are minimized it is also recommended that any new infrastructure associated with the Viking A development is entered into fishing and marine charting systems to notify other marine users.

5.7 Options for Expansion

There are a number of potential future storage sites and oil/gas developments that have been identified along the pipeline route and in the vicinity of the Viking A NUI, therefore there is merit in pre-investing in an increased ullage (larger) pipeline from Barmston with future tie-in structures (valved tees) at set locations along the route to facilitate future expansion

These sites were checked against the WP3 rankings (top 20). It can be seen the Bunter Closure sites are favoured, being the only ones that ranked in the top 20 with the exception of the Hewett gas field.

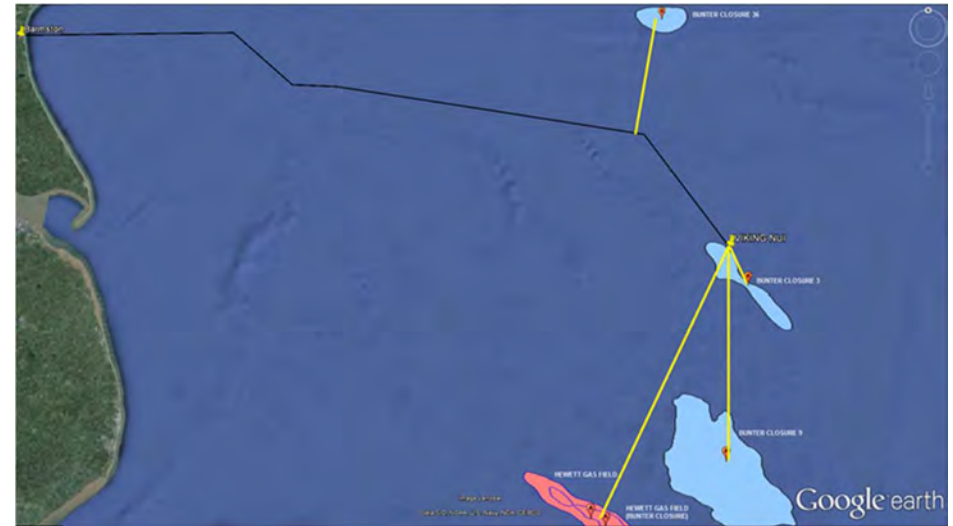


Figure 5-8 Options for expanding the development

Field	Type	Tie-in Distance	Tee / Tie-Back	WP3 Ranking
Bunter Closure 9	Aquifer	45km	Tie-Back	1
Bunter Closure 3	Aquifer	10km	Tie-Back	4
Bunter Closure 36	Aquifer	32km	Tee	6
Hewett Gas Field	Gas	65km	Tie-Back	5
Hewett Gas Field (Bunter)	Gas	65km	Tie-Back	7

Table 5-9 Options for expansion

The potential for EOR in the UK Sector of the Central North Sea is detailed in Energy Research Partnerships “Prospects for CO₂-EOR in the UKCS” report

published in October 2015. The nearby hydrocarbon developments are shown in Figure 5-4, however the Energy Research Partnership did not identify any potential fields in the Southern North Sea that would be suitable for CO₂-EOR.

5.8 Operations

The Viking A development will inject CO₂ at a constant injection rate of 5 MTPa, via two platform based injector wells over 26 years. The wells will be operated as ‘hot’ wells for the first 20 years and will require continuous CO₂ heating followed by a period of 6 years where heating will only be required during start-up conditions.

The Viking A platform will be a Normally Unmanned Installation (NUI), and will be capable of operating unattended for approximately 3 months (90 days). A power cable will provide electrical power to the Viking A NUI from Bacton. The NUI will be controlled from the beach, utilizing dual redundant satellite links.

The NUI will require regular IMR (Inspection, Maintenance and Repair), and it is envisaged that visits will typically be required every six weeks. Routine maintenance activities will include the following:

- Replenishing chemicals;
- Replenishing fuel (for emergency back-up generator, as required);
- IMR of lifeboats;
- IMR of telecommunications system (satellite comms);
- IMR of mechanical handling (crane);
- IMR of HVAC system;
- IMR of venting system;
- IMR and certification of metering system for CO₂ injection;
- IMR of chemical injection system including pumps, tanks and associated equipment;

- IMR of CO₂ heaters;
- IMR of CO₂ filters;
- IMR of hazardous open drains (drain tanks, heaters and pumps);
- IMR of non-hazardous open and closed drains (drain tanks, heaters and pumps);
- IMR of fire and gas detection systems, fire pumps and firewater systems;
- IMR of nitrogen system;
- IMR of emergency power generation system;
- Painting (fabric maintenance);
- Cleaning.

The pipeline and power cable will also require regular IMR. This will include regular (typically bi-annual) surveys (ROV) to confirm integrity. Although pigging facilities are available, the frequency will be minimal subject to an integrity management risk assessment of the control of the CO₂ quality.

5.9 Decommissioning

The decommissioning philosophy assumed for the Viking A facilities is as follows:

Note that this philosophy is subject to the outcome of the comparative assessment process and subsequent approval by DECC.

- Wells plugged and abandoned
- Topside facilities are cleaned, prepared and disconnected
- Removal of topsides (reverse installation)
- Steel jacket completely removed and taken ashore for dismantling and recycling.
- Pipeline is cleaned and left in place, part end recovery and ends protected by burial/rockdump
- Viking pipelines are assumed to be covered by the UK fisheries offshore oil and gas legacy trust fund
- Pipeline spools to be recovered
- Subsea structures to be recovered (SSIV)
- Subsea concrete mattresses and grout bags recovered

The crossed pipelines and umbilical(s) are discussed in Section 5.5.1. Note that if either of these are still in service the decommissioning of the pipeline crossing will likely have to occur as part of the associated crossed cable decommissioning.

5.10 Post Closure Plan

The aim of post-injection/closure monitoring is to show that all available evidence indicates that the stored CO₂ will be completely and permanently contained. Once this has been shown the site can be transferred to the UK Competent Authority.

In the Viking depleted gas field, this translates into the following performance criteria:

- The CO₂ has not migrated laterally or vertically from the storage site. (This is not necessarily the original site, if CO₂ has migrated then the site will have been extended and a new volume licensed.)
- The CO₂ within the structural containment storage site has reached a gravity stable equilibrium. Any CO₂ in an aquifer storage containment site is conforming to dynamic modelling assumptions – i.e. its size and rate of motion match the modelling results.
- The above are proven by two separate post closure surveys – with a minimum separation of five years.

The post closure period is assumed to last for a minimum of 20 years after the cessation of injection. During this time monitoring will be required, as detailed in Appendix 5.

5.11 Handover to Authority

Immediately following the completion of the post closure period the responsibility for the Viking A CO₂ storage site will be handed over to the UK Competent Authority. It is anticipated that a fee, estimated at ten times the annual cost of post closure monitoring will accompany the handover.

5.12 Development Risk Assessment

The following development risks have been identified:

Survey data: A full pipeline route survey is required. There is a risk that this may identify unknown seabed obstructions or features that will necessitate route deviations.

CO₂ composition/chemistry: This is unknown and therefore there is a risk of it being significantly different than that assumed throughout this study, with unforeseen consequences. There are going to be challenges operating the system in an operating pressure window that is affected by impurities, temperature fluctuations and well performance. Thorough steady state and transient modelling of these effects is required and may require strict control during operations.

Confirmation of heating requirements requires further work as this can significantly impact the size of the heating facilities, the amount of heating and therefore the overall CAPEX and OPEX figures.

The following opportunities have been identified and should be considered as part of further work:

Additional work to accurately determine the amount of heating required, heating technology and the process steps required to gasify the CO₂.

A value engineering exercise should be carried out to assess all equipment to ensure all specified equipment is technically justified in its application and not included on the basis of accepted oil and gas practice. Some examples are provided:

CO₂ Screens: A reduction in CAPEX and OPEX could be realized by removing the requirement for CO₂ screens.

Venting: Opportunity to remove the requirement for venting, with all venting performed from the beach.

Pig Receiver: Temporary v Permanent. Should permanent facilities not be required this will result in a reduction in topsides weight and the associated savings in CAPEX/OPEX.

SSIV: Requirement for an SSIV can be challenged during FEED and potentially omitted which would reduce the requirement for increased pressure rating of the riser and associated piping between SSIV and ESDV, to account for thermal expansion of riser inventory during shut in.

SSIV Location: If it is not possible to remove the requirement for an SSIV the location should be optimized with consideration to the impact of the riser volume on temporary refuge specification.

Helideck: A significant reduction in cost may be realised by removing the helideck and relying on walk to work vessels for platform visits. Helidecks have typically been specified for hydrocarbon producing NUI's due to the requirement for personnel to be on the facility to restart production following a shutdown, and the associated cost of deferred production until the restart can be enacted. Removing this requirement by enabling remote restart of CO₂ injection will improve uptime and negate the requirement for a helideck for platform visits.

Pipeline: The pipeline has been sized to allow for future expansion/step outs (additional ullage) which results in a 20" pipeline. If this requirement were removed, then it may be feasible to install an 18" diameter. This should be considered further during FEED.

Pipeline design: Pipeline design to be progressed to confirm wall thickness and remove uncertainties in mechanical design. Pipeline design to be performed to

either PD8010 Part 2 or DNV OS F101, and should follow the requirements of DNV RP J202.

Geotechnical data – site surveys result in complex foundations and increased costs. Ensure early development of desktop study and geotechnical testing programme performed/supervised by experienced geotechnical specialists.

Risk of pipeline leak/rupture – ensure pipeline is designed in accordance with DNV RP J202 Design and Operation of CO₂ pipelines, for the full range of design conditions, with an appropriate corrosion and fishing protection measures, integrity management plans and operating procedures.

Legislation – development of UK legislation could result in modifications to facilities requirements (e.g. emissions, safety case requirements, MMV).

Seabed conditions may require expensive seabed intervention to avoid pipeline instability and free-spanning. Metocean and geophysical surveys are required to confirm seabed conditions.

The water depth is such that a SeaKing design jacket may be employed which would reduce the associated CAPEX and fabrication time of the jacket. Suitability of such a jacket design would require to be fully appraised during FEED. The SeaKing design is an advancement of the SeaHorse platform design that allows for a larger well count (up to 6 wells) whilst maintaining the key characteristics of the highly successful SeaHorse family of platform designs that have been extensively utilised for minimum facility platforms in the UKCS.

Consideration should be given to utilising the power cable to supply all electrical power, signal, hydraulics and chemicals to the Viking development. This would increase the cost of the cable however it could reduce the running costs of the NUI.

Further process studies should also be performed to determine whether it would be prudent to include a heating train on the NUI vent line and the overall venting philosophy.

6.0 Budget & Schedule

6.1 Schedule of Development

A level 1 schedule (up to first CO₂ injection) has been produced and is included in Figure 6-1. The schedule is built up using the same breakdown structure as the cost estimate to allow for cost scheduling and is based on the following assumptions:

- Project kick off first quarter 2025.
- 12 months of EPC ITTs, contract and financing negotiation prior to FID.
- Project sanction / FID summer year 2027.
- Detailed design commences immediately following sanction.
- Viking A NUI jacket and topsides installed prior to drilling (facilities on critical path).
- The pipeline and facilities are pre-commissioned following completion of construction.
- Drilling and completing of the two platform injector wells commencing 2030.
- The pipeline, facilities and wells are commissioned in a continuous sequence of events.
- First CO₂ injection Q3 2031 which coincides with the projected supply profile

Total project duration from FEED to first injection is projected to be just over 6 years.

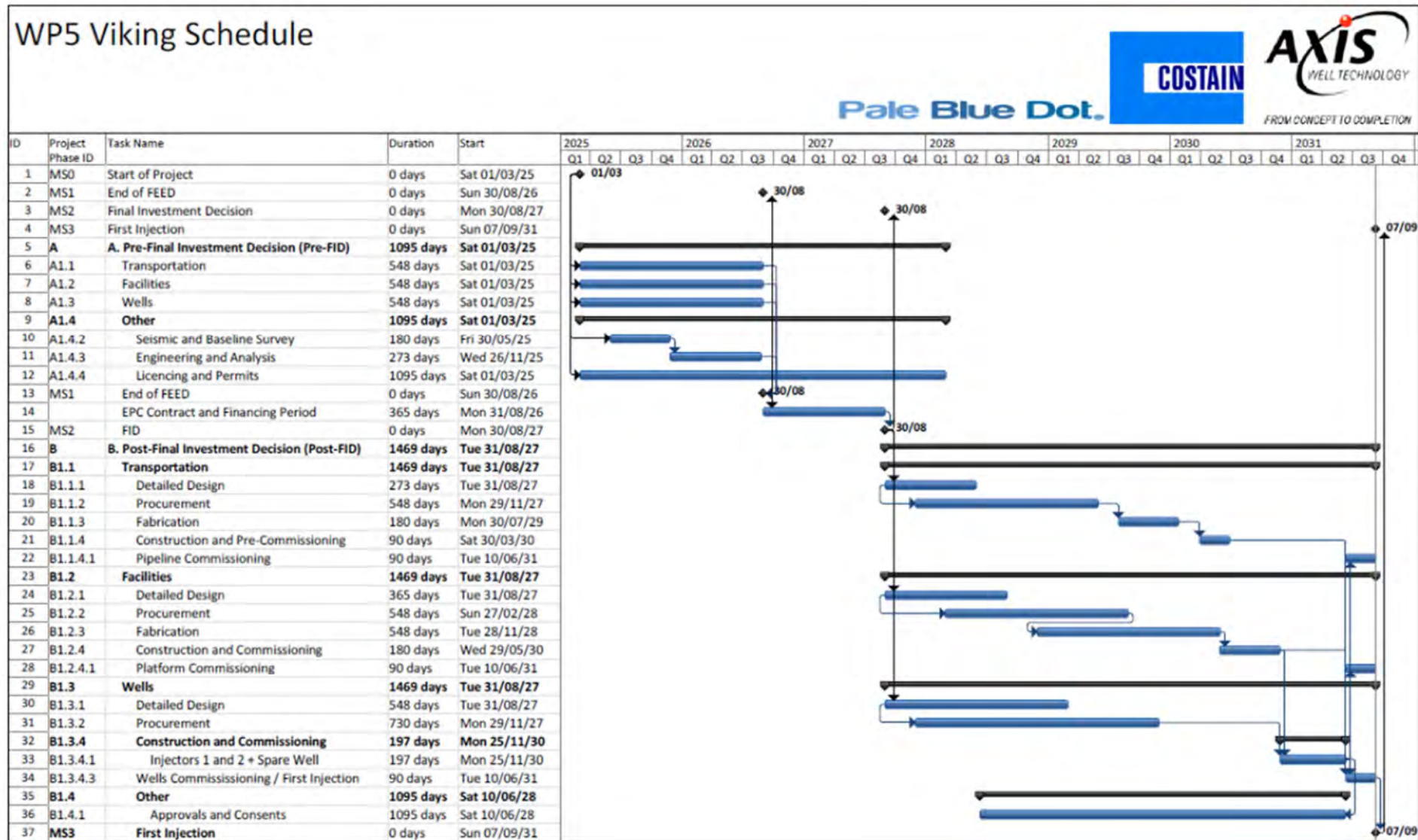


Figure 6-1 Summary level project schedule

6.2 Budget

The costs associated with the capital (CAPEX), operating (OPEX) and abandonment (ABEX) phase expenditures have been calculated for the engineering, procurement, construction, installation, commissioning, operation and decommissioning of the Viking A facilities. The OPEX has been calculated based on a 26 year design life. A 30% contingency has been included throughout.

An overview of the Viking A development (transportation, facilities, wells) is given in Section 5. The cost estimate is made up of the following components

- 20" Pipeline from Barmston to the Viking A NUI;
- Viking NUI (jacket and topsides);
- Two platform wells, plus a spare injector for field life of 26 years.

6.2.1 Cost Estimate Summary

The cost estimate summary for the Viking A development is outlined in Table 6-1. These numbers are current day estimates for the base case development. Details are provided in Appendix 7. Note that the total OPEX includes energy costs for the CO₂ heating calculated at £50/MW. A sensitivity was performed to investigate the effect on development costs if this were increased to £100/MW. The total 26 year OPEX increases to £756.4 MM, and the total development cost increases by approximately 10% to £1321 MM. It is expected that the additional financial returns to the power plant for such an increase in energy price would far exceed the additional cost of heating.

In the tables that follow estimates are provided in Real, 2015 terms and Nominal, 2015 PV10 terms.

- Real, 2015. These values represent current-day estimates and exclude the effects of cost escalation, inflation and discounting.
- Nominal, 2015 PV10. These values incorporate the time value of money into the estimates (i.e. including the effects of cost escalation and inflation (2%) that are then discounted back to a common base year of 2015 using an annual discount rate of 10%).

Unless specified otherwise, costs are presented in real, 2015 terms.

Category	Total Viking Development (Real, 2015, £ MM)
CAPEX	456.4
OPEX	639.1
ABEX	108.5
Total Cost	1204.0
Cost CO₂ Injected (£ per Tonne)	9.26

Table 6-1 Viking A development cost estimate summary

It should be noted that the cost estimates in Table 6-1 are 2015 estimates for 2015 activity and the present value estimates are provided in Table 6-2.

The cost over time is illustrated in Figure 6-2 (values are not inflated or discounted).

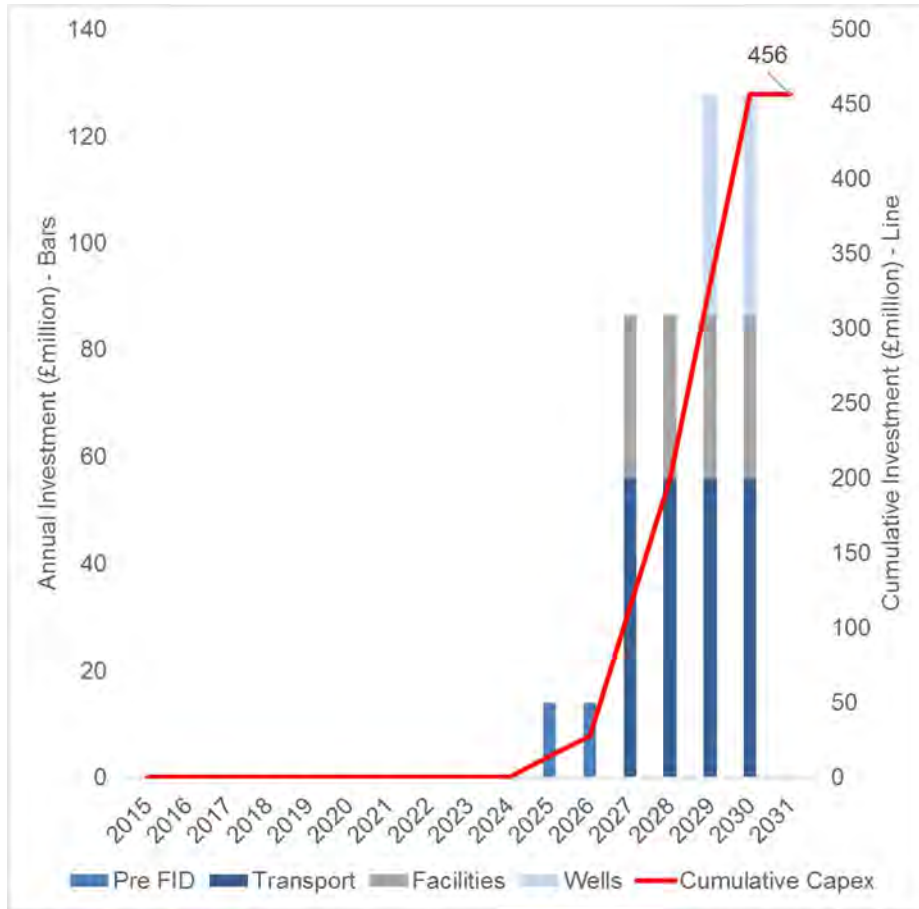


Figure 6-2 Phasing of capital spend

6.2.2 Life Cycle Costs

The total project costs, inflated at 2% p.a. with a discount factor of 10% p.a., are summarised in Table 6-2.

Category	£millions (PV ₁₀ , 2015 Nominal)
Transport	74
Facilities	47
Wells	29
Opex	79
Decommissioning & Post Closure Activity	4
Total	233

Table 6-2 Project cost estimate by component

Details of when these costs are incurred based on 2015 spending activity are shown in Figure 6-3.

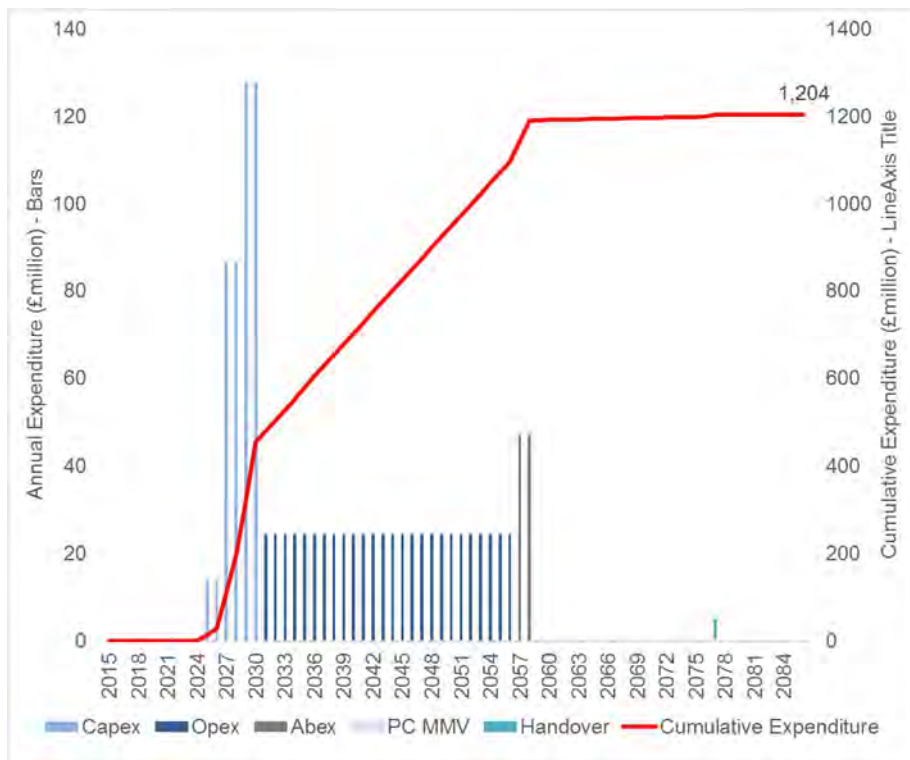


Figure 6-3 Elements of cost over project lifetime

6.2.2.1 Capital Expenditure

The CAPEX estimates for the Viking A development are summarised in the following tables. The costs are split up into transportation, facilities, wells and “other”. The cost estimates in these tables are in 2015 Real terms.

Phase	Category	Total (£ MM)	Viking	Development
Pre-FID	Pre-FEED	0.4		
	FEED	0.5		
Post-FID	Detailed Design	0.7		
	Procurement	99.6		
	Fabrication	30.1		
	Construction & Commissioning	93.1		
Total CAPEX – Transportation (£MM)		224.6		

Table 6-3 Viking A development transport CAPEX (Base case)

The CAPEX for the Viking A facilities is summarised in Table 6-4. The Viking A NUI (jacket and topsides) was generated using the Que\$stor cost estimating software, and benchmarked using Costain Norms. The power system costs were developed using Costain Norms.

Phase	Category	Total Viking Development (£ MM)
Pre-FID	Pre-FEED	6.1
	FEED	10.6
Post-FID	Detailed Design	16.9
	Procurement	40.1
	Fabrication	8.1
	Construction & Commissioning	57.4
Total CAPEX – Facilities (£MM)		139.2

Table 6-4 Viking A development facilities CAPEX

The well expenditure (CAPEX) for the Viking A development is summarised in Table 6-5.

Phase	Category	Total Viking Development (£ MM)
Pre-FID	Pre-FEED / FEED PM&E	2.9
	Detailed Design	2.9
Post-FID	Procurement	22.5
	Construction and Commissioning (Drilling)	54.5
Total CAPEX – Wells (£MM)		82.8

Table 6-5 Viking A development wells CAPEX

The “other” CAPEX associated with the Viking development is summarised below.

Phase	Category	Total (£ MM)	Viking	Development
Pre-FID	Seismic and Baseline Survey	1.8		
	Appraisal Well	-		
	Engineering and Analysis	2.9		
	Licencing and Permits	2.6		
Post-FID	Licencing and Permits	2.6		
Total CAPEX – Other Costs (£MM)		9.8		

Table 6-6 Viking A development other CAPEX

6.2.2.2 Operating Expenditure

The 26 year OPEX for the Viking A development has been estimated to be £639.1 million based on the following:

- Transportation at 1% of pipeline CAPEX per year
- Offshore facilities at 5.5% of facilities CAPEX per year plus cost to provide power (discussed in the appendices and is equivalent to approximately £4.4MM per year (£50/MWh) on average).
- Wells based on requiring workovers and local sidetracks as described in Section 3 of the report and summarised in Table 6-7.
- Other, as summarised in Table 6-8

OPEX Estimate	Total (£ MM)	Viking	Development
Major workover or local sidetrack	41.9		
Workovers	10.1		
Total	52.0		

Table 6-7 Viking A development wells OPEX

OPEX Estimate	Total (£ MM)	Viking	Development
Measurement, Monitoring and Verification	9.7		
Financial Securities	94.0		
Ongoing Tariffs and Agreements	0.0		
Total	103.7		

Table 6-8 Viking A development other OPEX

It is assumed that the supplier covers 3rd party tariffs.

A sensitivity to the power component of OPEX was conducted by increasing the cost of power to £100/MWh. This increased the life-cycle cost by approximately 7% in either Real or PV10, 2015 terms. Table 6-9 shows the results of the analysis.

	Life-cycle costs (£MM)	
	Real, 2015	PV ₁₀ , Nominal, 2015
Power @ £52/MWh	1208.7	233.7
Power @ £100/MWh	1321.3	247.6
Difference	112.6	13.9
Difference (%)	8.5	5.6

Table 6-9 Cost of Power Sensitivity Analysis

6.2.2.3 Abandonment Expenditure

Abandonment costs for the Viking A CO₂ transportation (pipeline) system has been estimated at 10% of transportation CAPEX.

The decommissioning costs for the offshore facilities are summarised Table 6-10, these costs were also generated using Que\$tor.

ABEX Decommissioning	Total Viking Development (£ MM)
Transportation	32.1
Facilities	38.2
Wells	24.1
Total	94.5

Table 6-10 Viking A development facilities ABEX

A breakdown of the ABEX associated with “other” costs is presented below.

Other	Total Viking Development (£ MM)
Post Closure Monitoring	9.7
Handover	4.4
Total	14.1

Table 6-11 Viking A development other ABEX

6.3 Economics

This section summarises the cost based economic metrics for the proposed development.

6.3.1 Project Component Costs

£million	Real (2015)	Nominal (MOTD)	PV ₁₀ (Nominal, 2015)
Transport	225	293	74
Facilities	139	181	47
Wells	93	122	29
Opex	639	1136	79
Decommissioning & Post Closure Activity	109	262	4
Total	1204	1994	233

Table 6-12 Viking A development cost in real and nominal terms

6.3.2 Transportation and Storage Costs

The contribution of each major element of the development to the overall cost is summarised in Table 6-13.

£million	Real (2015)	Nominal (MOTD)	PV ₁₀ (Nominal, 2015)
Transportation	333	503	85
Injection	871	1492	149
Total	1204	1994	233

Table 6-13 Viking A total transport and storage costs

6.3.3 Unit Costs

The life-cycle costs of the development are summarised in Table 6-14, Table 6-15, Figure 6-4 and Figure 6-5.

£/T	Real (2015)	Levelised (PV ₁₀ , Real 2015)	Nominal (MOTD)	Levelised (PV ₁₀ , Nominal, 2015)
Transportation	3	7	4	8
Injection	7	10	11	15
Total	9	17	15	23

Table 6-14 Viking A transport and storage costs per tonne of CO₂

Note: The levelised cost includes the discounted value of the CO₂ stored (10MT rather than the undiscounted value of 130MT).

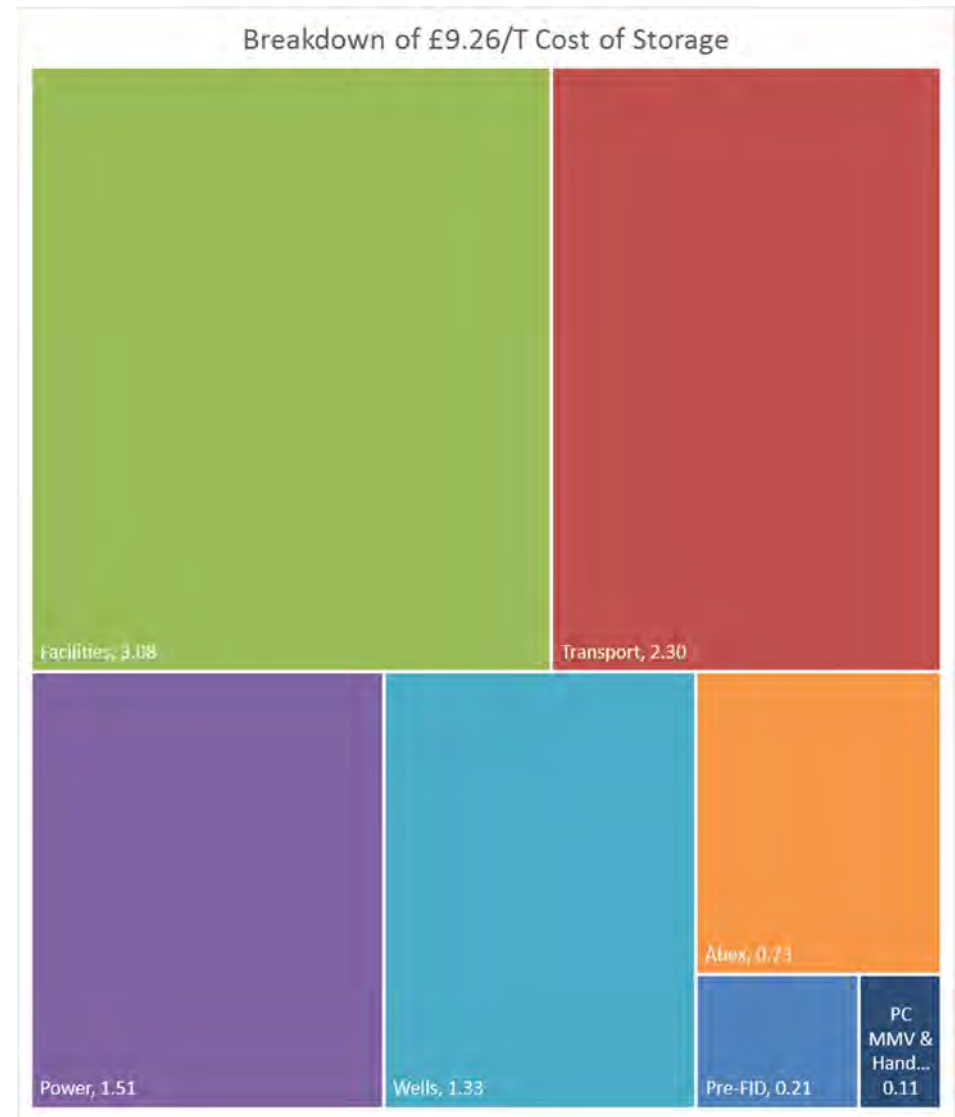
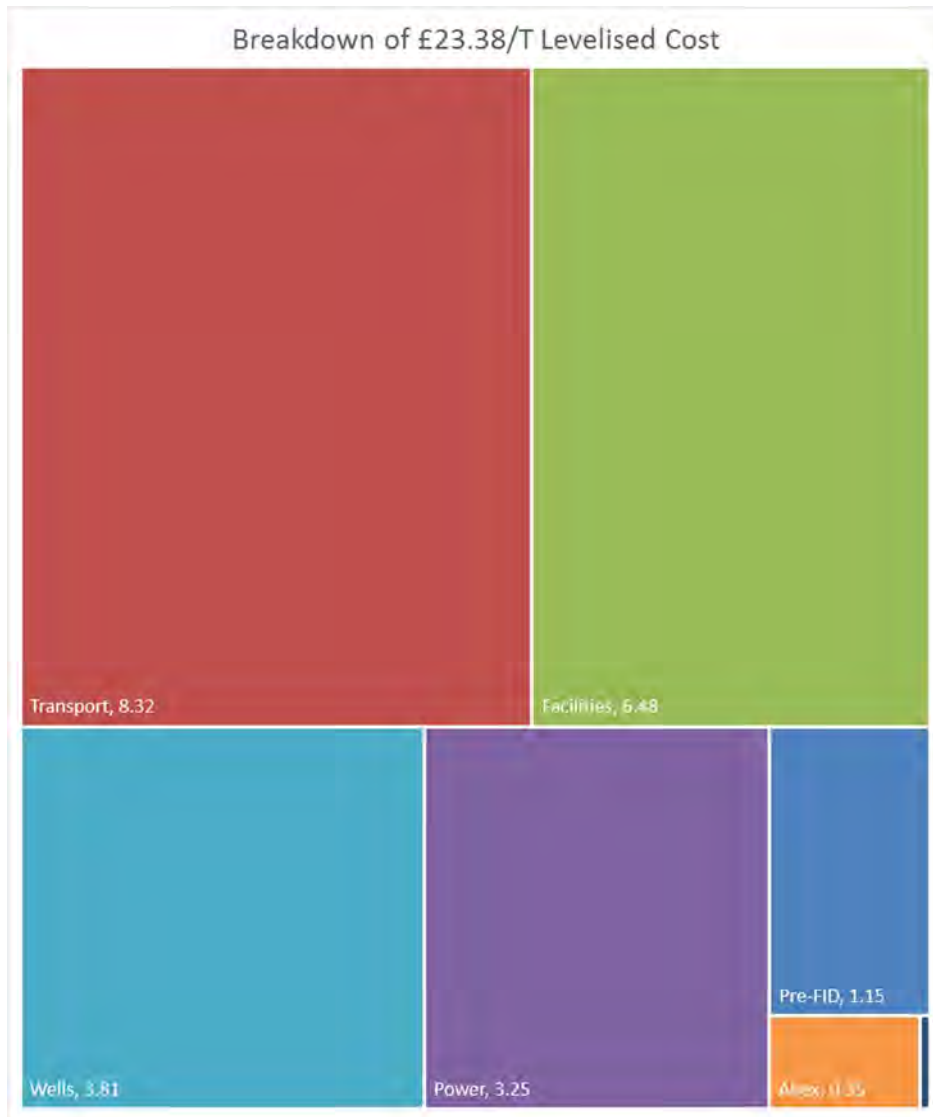


Figure 6-4 Breakdown of Levelised Costs

Figure 6-5 Breakdown of Life-cycle Cost

The charts shown in Figure 6-4 and Figure 6-5 show the components of unit cost on a levelised and real basis and illustrate the relative rank of each component for the two calculations. The levelised cost calculation (DECC, 2013) includes both inflation and discounting and therefore shows the impact of the timing of the timing of expenditure and injection. Thus expenditure far in the future such as MMV and handover (dark blue rectangles) appear smaller than on an undiscounted basis, as shown in Figure 6-5.

The variation between the Levelised and Real cost is due to both the timing of the expenditures as well as the rate at which the expenditure takes place.

£/T	Real (2015)	Levelised (PV ₁₀ , Real, 2015)	Nominal (MOTD)	Levelised (PV ₁₀ , Nominal, 2015)
Pre-FID	0.21	0.93	0.26	1.15
Transport	2.30	6.25	3.29	8.32
Facilities	3.08	4.40	5.24	6.48
Power	1.51	2.21	2.53	3.25
Wells	1.33	2.71	2.01	3.81
Abex	0.73	0.15	1.69	0.35
PC MMV & Handover	0.11	0.01	0.33	0.02
Total	9.26	16.66	15.34	23.38

Table 6-15 Unit Costs in Detail

7.0 Conclusions & Recommendations

7.1 Conclusions

Data

- There is 3D seismic coverage across the whole of the storage complex and the nearby relevant fairway. The seismic volume comprises data from several surveys carried out between 1991 – 1996. Data quality is good to excellent.
- There is a significant challenge in positioning subsurface features accurately with the 3D because of raypath bending through the complex velocity distribution in the overburden. Improved positioning would result from using re-processed post stack depth migration if available.
- There is good regional well coverage and good to very good well data available within the storage complex including modern logs, core and SCAL data.
- Comprehensive historical well by well production and pressure exists for Viking but was not available to this project. This represents a notable gap in the data set and accounts for much of the uncertainty in the simulation modelling.

Containment

- The primary storage reservoir for the Viking A site is the Leman Sandstone Formation of the Permian Rotliegend Group.
- Rock properties are generally moderate with porosity typically around 16% and the average permeability is 83mD.

- There is a high level of confidence that over 130Mt of CO₂ can be contained within the Leman Sandstone in the Viking A site.
- 1000 years after injection has ceased the CO₂ plume is still contained within the Viking A structure and the defined storage complex.
- The primary top seal is provided by a 365m sequence of halites with interbedded anhydrites and carbonates of the Permian Zechstein Group.
- Underlying the Leman Sandstone is approximately 400 m (1200 ft) of Carboniferous sediments of Westphalian age. These are predominantly shales, clays and siltstone with low permeability, and provide an effective containment feature at the floor of the store.
- Viking has minimal risk of caprock or fault failure for the modelled stress conditions, reservoir and overburden properties and fault properties. No adverse geochemical reactions are anticipated with the reservoir or caprock that might reduce the formations strength and integrity.
- The geomechanical models do not account for thermal effects in the near well bore area and these effects may reduce the fracture pressure near the wells.

Site Characterisation

- The PGS Southern North Sea MegaSurvey seismic volume which extends over the Viking A site and the regional fairway has been interpreted. The key horizons have been identified, interpreted and

mapped. Seismic data quality is considered adequate for structural interpretation at this stage of the development.

- The seismic data quality is not adequate to confidently map the base of the Lemna Sandstone.
- There is a high degree of confidence in the depth conversion in crestal areas due to the high density of wells in the field. Confidence is lower on the steep flanks of the structure where there is little well control.
- The steep dips, rapid lateral changes in velocity and chaotic structures within the Zechstein produce complex ray paths that distort the geometry in the raw seismic section. These distortions have not been fully corrected by the post-stack time migration processing applied to the available seismic volume.
- The limitations of the migrated volume together with the complex depth conversion leads to considerable uncertainty in the final depth surfaces especially on the flanks of the structural highs away from well control.
- The main reservoir event is a clear pick over the storage site.
- The Viking A structure is bounded by large faults and the horst block is split by numerous faults creating a complex geometry. Internal faults seem to be restricted to sand-to-sand contact.
- Faults are clearly interpretable in the seismic data within the Lemna Sandstone and are seen to die out rapidly within the lower part of the Zechstein.
- Seismic attributes extracted from the full stack 3D seismic volume, available to this project, produced no useful results.

Capacity

- There is a high degree of certainty on most of the subsurface variables: the pore volume is well known from the volume of hydrocarbons extracted over Viking's operational life; there is good well data coverage with little variation and relative permeability to water is not relevant in a depleted gas field with an immobile water leg.
- Estimates of capacity range between 107 - 150 Mt (P90 to P10) and are largely independent of injection rate, but they are strongly dependent on the amount of hydrocarbon production and complexities of CO₂ phase behaviour during the transition period.
- In the unlikely event that the fracture pressure limit does not recover during re-pressurisation it may limit capacity to around 90Mt.

Appraisal

- No further appraisal drilling is considered necessary at this time.
- No further 3D seismic data acquisition is required before the final investment decision, although it would be beneficial to gain access to the operators pre stack depth migrated 3D data.
- A key uncertainty is around how the fracture pressure of the reservoir formation will evolve as the store is re-pressured during CO₂ injection. Appraisal activity should address this issue.
- A further key uncertainty exists regarding the optimum way to manage the operations during the phase transition from gas to liquid CO₂ injection.

Development

- Final investment decision needs to be in 2027 in order to achieve the first injection date of 2031.
- The planning work indicates that approximately 6 years are required to finalise the evaluation and develop the store.
- A £150 million (in present value terms discounted at 10% to 2015) capital investment is required to design, build, install and commission the pipeline, platform and wells.
- The development is designed to accommodate the reference case supply profile of 5Mt CO₂/year from 2031 for approximately 26 years.
- Viking is estimated to have a current reservoir pressure of approximately 34 bara and a temperature of 83°C at a datum depth of 2544m. These conditions are close to the limit for gas-phase injection. Consequently, the development scheme is split into two periods. During the first 20 years continuous heating is required to ensure the injected CO₂ remains in supercritical-phase in the well-bore and the in the subsequent 6 years the CO₂ is anticipated to only require intermittent heating to remain in liquid-phase in the wellbore.
- The reference case development includes all new infrastructure: a minimum facilities platform; 185km of 20" pipeline from Barmston and two active injection wells.
- 7" completions are suitable for both the supercritical-phase injection and the liquid-phase injection periods.
- The main potential opportunities for cost reduction are: fewer well interventions, heating requirements and potential re-use of some of the existing SNS infrastructure.

Operations

- At the end of the injection period, reservoir pressure is calculated to be 383bar at the datum depth of 2522m. The fracture pressure at this depth will then be 426bar.
- The safe operating envelope for the wells is based on geomechanical analysis and the maximum allowable reservoir pressure has been constrained to 90% of the fracture pressure gradient (0.097bar/m and 0.167bar/m respectively) which increases as the reservoir is re-pressurised.
- The wells will require a total of approximately 10MW of heating during the initial period of operations to accommodate the 5Mt/y CO₂ supply profile. The power will be provided via a 90km subsea cable from Bacton. This accounts for approximately 14% of the life-cycle cost of the development.

7.2 Recommendations

Appraisal Programme

- Complete a more sophisticated reprocessing of the seismic data to reduce the distortion issues and improve accuracy of the imaging of the flanks and confidence in depth conversion in those areas.
- Gain more detailed access to the field data set so that well status and abandonment status can be fully understood. Work to ensure that the Operator is familiar with the potential for CO₂ storage in the area and seek collaboration to leverage cost reductions from potential synergies that this might present.
- Gain access to detailed well by well pressure and production rate records so that the dynamic model can be finely calibrated to the performance of the gas production development. This will significantly reduce uncertainty regarding CO₂ storage capacity.
- Improve the characterisation of how the fracture pressure will evolve during the re-pressurisation of the reservoir.
- Identify additional studies that could confirm the design and specification of 4D seismic to ensure maximum effectiveness as a monitoring tool.

Operational Planning

- Identify synergies with other offshore operations. Whilst re-use is unlikely due to the age of the infrastructure, this should include a careful review of the existing Viking area platforms and wells to check whether there might be a viable and cost effective re-use option.

- Commission further work to better understand the options for managing the operations during the CO₂ phase transition period and how best to select a preferred strategy.
- Further investigation into the range of operational issues identified in Section 5.
- Existing operational wells should be abandoned using best practice available to preserve the site for future CO₂ storage service.

Development Planning

- Consider the commercial aspects required for the development of Viking A in the light of past petroleum use to ensure that all existing rights are honoured whilst enabling the development to proceed.
- Incorporate the regulatory licensing and permitting requirements into the development plan.
- Work with the petroleum operator of Viking A and the regulator to ensure that the wells are abandoned using all best practice to secure the CO₂ integrity of the site.
- Review the current assumption that heating during the supercritical-phase operation is more beneficial than drilling additional wells.
- Further work should consider how best to deliver the heating requirements and identify alternatives to the 10MW electrical heating options evaluated for this study.
- Examine options for extending storage development to other nearby operations such as the other Viking area gas fields and the nearby Bunter Closure 3. Due diligence was completed on this 4-way dip closure in an earlier phase of this project (Pale Blue Dot Energy; Axis Well Technology, 2015).

8.0 References

- AGR. (2012). *CO2 Storage Liabilities in the North Sea: An Assessment of the Risks and Financial Consequences; Summary Report (including Annexes) for DECC*.
- DECC. (2013). *Electricity Generation Costs 2013*. HMG.
- (2008). *Energy Act, Chapter 32*. Retrieved from http://www.legislation.gov.uk/ukpga/2008/32/pdfs/ukpga_20080032_en.pdf
- Glennie, K. W. (1998). *Petroleum Geology of the North Sea. Basic Concepts and Recent Advances*.
- Heinemann, N., Wilkinson, M., Pickup, G. E., Haszeldine, R. S., & Cutler, N. A. (2011). CO2 Storage in the Offshore UK Bunter Sandstone Formation. *International Journal of Greenhouse Gas Control*, 6, 210-219.
- IEAGHG. (2015). *CCS Deployment in the Context of Regional Development in Meeting Long-Term Climate Change Objectives*.
- Katz, D. L., & Firoozabadi, A. (1978). *Predicting phase behaviour of condensate/crude-oil systems using methane interaction coefficients*. SPE 6721.
- Ksler, M. G., & Lee, B. I. (1976). Improved predictions of enthalpy of fractions. *Hydro. Proc.*, 153-158.
- Mathias, S. A., Gluyas, J. G., Gonzalez, G., Bryant, S., & Wilson, D. (2013). On Relative Permeability Data Uncertainty and CO2 injectivity estimation for brine aquifers. *International Journal of Greenhouse Gas Control*, 200-212.
- McCann, T. (2008). *The Geology of Central Europe: Precambrian and Palaeozoic*.
- Morgan, C. (1991). The Viking Complex, Blocks 49/12a, 49/16, 49/17, UK North Sea. *Abbots, I.L. (eds). United Kingdom Oil and Gas Fields, Commemorative Millenium Volume, Geological Society Memoir No 14*, pp. 509-515.
- Morita, N., E. D., & Whitebay, L. (1998). *Guidelines for Solving Sand Problems in Water Injection Wells*. SPE Paper 39436.
- National Energy Technology Laboratory, US Department of Energy. (2012). *Best Practices for Monitoring, Verification and Accounting of CO2 Stored in Deep Geologic Formations*.
- National Grid Carbon Ltd; Carbon Sentinel Ltd; Hartley Anderson Ltd. (2015). *Yorkshire and Humber CCS Offshore Pipeline and Storage Project: Offshore Environmental Statement*. Retrieved from http://nationalgrid.opendebate.co.uk/files/nationalgrid/ccshumber/Pages_from_D41752015_-_Yorkshire_and_Humber_CCS_Offshore_Pipeline_and_Storage_Project_ES-_main_report.pdf

- National Institute of Standards and Technology. (2016). *Thermophysical Properties of Fluid Systems*. Retrieved from <http://webbook.nist.gov/chemistry/fluid>
- Pale Blue Dot Energy; Axis Well Technology. (2015). *D04: Initial Screening and Downselect - Strategic UK CCS Storage Project*. The Energy Technologies Institute.
- Pale Blue Dot Energy; Axis Well Technology. (2015). *D05: Due Diligence and Portfolio Selection - Strategic UK CCS Storage Project*. The Energy Technologies Institute.
- Pale Blue Dot Energy; Axis Well Technology. (2015). *D05: Due Diligence and Portfolio Selection - Strategic UK CCS Storage Project*. The Energy Technologies Institute.
- Petroleum Experts Ltd. (2015). *User Manual IPM Prosper Version 13*.
- PGS. (2015). *The PGS Mega surveys*. Retrieved from [http://www.pgs.com/upload/31007/MegaSurvey%20\(1366Kb\).pdf](http://www.pgs.com/upload/31007/MegaSurvey%20(1366Kb).pdf)
- Riches, H. (2003). The Viking Field, Blocks 49/12a, 49/16, 49/17, UK North Sea. *Gluyas, J.G. & Hichens, H.M. (eds) United Kingdom Oil and Gas Fields, Commemorative Millenium Volume, Geological Society, London, Memoir, 20*, pp. 871-880.
- Ritchie, J. S., & Pratsides, P. (1993). The Caister Fields, Block 44/23-a, UK North Sea. *Petroleum Geology of Northwest Europe: Proceedings of the 4th Conference* (pp. 757-769). London: The Geological Society .
- Santarelli, F. J., Havmoller, O., & Naumann, M. (2008). Geomechanical aspects of 15 years water injection on a field complex: An analysis of the past to plan the future. *SPE North Africa Technical Conference & Exhibition* . Society of Petroleum Engineers.
- Scottish Power CCS Consortium. (2011). *UK Carbon Capture and Storage Demonstration Competition; Post Feed End-to-End Basis of Design*.
- Scottish Power CCS Consortium. (2011). *UK Carbon Capture and Storage Demonstration Competition; Well Abandonment Concept*.
- Shell. (2014). *Offshore Environmental Statement* .
- Smith, L., Billingham, M. A., Lee, C.-H., & Milanovic, D. (2010). *SPE-13660 CO2 Sequestration Wells - the Lifetime Integrity Challenge*. Society of Petroleum Engineers.
- Society of Petroleum Engineers. (2000). *Petroleum Resources Classification System and Definitions*. Retrieved from Petroleum Resources Classification System and Definitions
- The European Parliament And The Council Of The European Union. (2009). Directive 2009/31/Ec Of The European Parliament And Of The Council On The Geological Storage Of Carbon Dioxide. *Official Journal of the European Union*, 114-135.

9.0 Contributing Authors

First Name	Last Name	Company
Wahab	Ahmed	Axis Well Technology
Shelagh	Baines	Pale Blue Dot Energy
Hazel	Clyne	Pale Blue Dot Energy
Sybille	Handley-Schachler	Axis Well Technology
Dave	Hardy	Axis Well Technology
Charlie	Hartley-Sewel	Pale Blue Dot Energy
Ian	Humberstone	Axis Well Technology
Alan	James	Pale Blue Dot Energy
Ken	Johnson	Axis Well Technology
Doug	Maxwell	Axis Well Technology
Sharon	McCollough	Axis Well Technology
Steve	Murphy	Pale Blue Dot Energy
David	Pilbeam	Pale Blue Dot Energy
Angus	Reid	Costain
Ryan	Robbins	Costain

First Name	Last Name	Company
David	Sweeney	Axis Well Technology
Jamie	Telford	Costain
Lynsey	Wardlaw	Axis Well Technology
Tim	Wynn	Axis Well Technology

10.0 Glossary

Defined Term	Definition
Aeolian	Pertaining to material transported and deposited (aeolian deposit) by the wind. Includes clastic materials such as dune sands, sand sheets, loess deposits, and clay
Alluvial Plain	General term for the accumulation of fluvial sediments (including floodplains, fan and braided stream deposits) that form low gradient and low relief areas, often on the flanks of mountains.
Basin	A low lying area, of tectonic origin, in which sediments have accumulated.
Base Year	The common year (2015) to which discounted quantities are referenced for all stores
Bottom Hole Pressure (BHP)	This the pressure at the midpoint of the open perforations in a well connected to a reservoir system
Clastic	Pertaining to rock or sediment composed mainly of fragments derived from pre-existing rocks or minerals and moved from their place of origin. Often used to denote sandstones and siltstones.
Closure	A configuration of a storage formation and overlying cap rock formation which enables the buoyant trapping of CO ₂ in the storage formation.
CO₂ Plume	The dispersing volume of CO ₂ in a geological storage formation
Containment Mechanism	Failure The geological or engineering feature or event which could cause CO ₂ to leave the primary store and/or storage complex
Containment Modes	Failure Pathways for CO ₂ to move out of the primary store and/or storage complex which are contrary to the storage development plan
Containment Scenario	Risk A specific scenario comprising a Containment Failure Mechanism and Containment Failure Mode which might result in the movement of CO ₂ out of the primary store and/or storage complex
Darcy	Industry unit of permeability equal to 10 ⁻¹² m ²

Defined Term	Definition
Erg	An erg (also sand sea or dune sea, or sand sheet if it lacks dunes) is a broad, flat area of desert covered with wind-swept sand with little or no vegetative cover.
Evaporite	Sediments chemically precipitated due to evaporation of water. Common evaporates can be dominated by halite (salt), anhydrite and gypsum. Evaporites may be marine formed by the evaporation within an oceanic basin, or non-marine typically formed in arid environments.
Facies (Sedimentary)	A volume of rock that can be defined and recognised by a particular set of characteristics (physical, compositional, chemical) often reflecting its environment of deposition
Fault	Fracture discontinuity in a volume of rock, across which there has been significant displacement as a result of rock movement
Fluvial	Pertaining to or produced by streams or rivers
Formation	A formation is a geological rock unit that is distinctive enough in appearance and properties to distinguish it from surrounding rock units. It must also be thick enough and extensive enough to capture in a map or model. Formations are given names that include the geographic name of a permanent feature near the location where the rocks are well exposed. If the formation consists of a single or dominant rock type, such as shale or sandstone, then the rock type is included in the name.
Gardener's Equation	A relationship between seismic velocity V in ft/s (ie. The inverse of the sonic log measured in $\mu\text{s}/\text{ft}$) and density ρ in g/cm^3 for saturated sedimentary rocks. The equation was proposed by Gardener et al (1974) based on lab experiments and is of the form $\rho = aV^b$. Typically $a = 0.23$ and $b = 0.25$ but these values should be refined if measured V and ρ are available for calculation.
Geological Formation	Lithostratigraphical subdivision within which distinct rock layers can be found and mapped [CCS Directive]
Halokinesis	The study of salt tectonics, which includes the mobilization and flow of subsurface salt, and the subsequent emplacement and resulting structure of salt bodies
Hydraulic Unit	A Hydraulic Unit is a hydraulically connected pore space where pressure communication can be measured by technical means and which is bordered by flow barriers, such as faults, salt domes, lithological boundaries, or by the wedging out or outcropping of the formation (EU CCS Directive);
Leak	The movement of CO_2 from the Storage Complex

Defined Term	Definition
Levelised Cost	The levelised cost of transportation and storage for a development is the ratio of the discounted life cycle cost to the discounted injection profile. Both items discounted at the same discount rate and to the same base year.
Maximum Flooding Surface (MFS)	This is a geological surface which represents the deepest water facies within any particular sequence. It makes the change from a period of relative sea level rise to a period of relative sea level fall. An MFS commonly displays evidence of condensed or slow deposition. Such surfaces are key aids to understanding the stratigraphic evolution of a geological sequence.
Outline Storage Development (OSDP) Plan	The Outline Storage Development Plan defines the scope of the application process for a storage permit, including identification of required documents. These documents, include a Characterization Report (CR), an Injection and Operating Plan (IOP) (including a tentative site closure plan), a Storage Performance Forecast (SPF), an Impact Hypothesis (IH), a Contingency Plan (CP), and a Monitoring, Measurement and Verification, (MMV) plan.
Playa Lake	A shallow, intermittent lake in a arid or semiarid region, covering or occupying a playa in the wet season but drying up in summer; an ephemeral lake that upon evaporation leaves or forms a playa.
Primary Migration	The movement of CO ₂ within the injection system and primary reservoir according to and in line with the Storage Development Plan
Risk	Concept that denotes the product of the probability (likelihood) of a hazard and the subsequent consequence (impact) of the associated event [CO ₂ QUALSTORE]
Sabkha	A flat area of sedimentation and erosion formed under semiarid or arid conditions commonly along coastal areas but can also be deposited in interior areas (basin floors slightly above playa lake beds).
Secondary Migration	The movement of CO ₂ within subsurface or wells environment beyond the scope of the Storage Development Plan
Silver Pit Basin	Located in the northern part of the Southern North Sea. Over much of the basin up to 400 m of Silverpit Formation interbedded shales and evaporites are present. The absence of the Leman Sandstone reservoir over much of the basin has meant that gas fields predominate in the Carboniferous rather than in the Permian, as is the case in the Sole Pit Basin to the South.
Site Closure	The definitive cessation of CO ₂ injection into a Storage Site
Storage Complex	The Storage Complex is a storage site and surrounding geological domain which can have an effect on overall storage integrity and security; that is, secondary containment formations (EU CCS Directive).

Defined Term	Definition
Storage Site	Storage Site is a defined volume within a geological formation that is or could be used for the geological storage of CO ₂ . The Storage Site includes its associated surface and injection facilities (EU CCS Directive);
Storage Unit	A Storage Unit is a mappable subsurface body of reservoir rock that is at depths greater than 800 m below sea level, has similar geological characteristics and which has the potential to retain CO ₂ (UKSAP)
Stratigraphic Column	A diagram that shows the vertical sequence of rock units present beneath a given location with the oldest at the bottom and youngest at the top.
Stratigraphy	The study of sedimentary rock units, including their geographic extent, age, classification, characteristics and formation.
Tectonic	Relating to the structure of the Earth's crust, the forces or conditions causing movements of the crust and the resulting features.
Tubing Head Pressure (THP)	The pressure at the top of the injection tubing in a well downstream of any choke valve

11.0 Appendices

The following appendices are provided separately:

11.1 Appendix 1 – Risk Matrix

11.2 Appendix 2 – Leakage Workshop Report

11.3 Appendix 3 – Database

11.4 Appendix 4 – Geological Information

11.5 Appendix 5 – MMV Technologies

11.6 Appendix 6 – Well Basis of Design

11.7 Appendix 7 – Cost Estimate

11.8 Appendix 8 – Methodologies

11.9 Appendix 9 – Fracture Pressure Gradient

11.10 Appendix 10 – Subsurface Uncertainty Analysis

11.11 Appendix 11 – 3D Geomechanical Modelling

2016

Pale Blue Dot.



D14: WP5E –Viking A Storage Development Plan
10113ETIS-Rep-21-02 Appendices

March 2016

www.pale-blu.com

www.axis-wt.com

© Energy Technologies Institute 2016

Contents

Document Summary						
Client	The Energy Technologies Institute					
Project Title	DECC Strategic UK CCS Storage Appraisal Project					
Title:	D14: Wp5e –Viking A Storage Development Plan					
Distribution:	A Green, D Gammer			Classification:	Client Confidential	
Date of Issue:	30/03/16					
	Name		Role		Signature	
Prepared by:	A James, S Baines & S McCollough		Chief Technologist, Scientific Advisor & Subsurface Lead			
Approved by:	S J Murphy		Project Manager			
Amendment Record						
Rev	Date	Description	Issued By	Checked By	Approved By	Client Approval
V01	14/03/16	Draft	D Pilbeam	A James	S Murphy	
V02	30/03/16	Final	D Pilbeam	A James	S Murphy	

Disclaimer:

While the authors consider that the data and opinions contained in this report are sound, all parties must rely upon their own skill and judgement when using it. The authors do not make any representation or warranty, expressed or implied, as to the accuracy or completeness of the report. There is considerable uncertainty around the development of CO₂ stores and the available data are extremely limited. The authors assume no liability for any loss or damage arising from decisions made on the basis of this report. The views and judgements expressed here are the opinions of the authors and do not reflect those of the ETI or any of the stakeholders consulted during the course of this project. The figures, charts and tables contained in this report comply with the intellectual property and copyright constraints of this project and in some cases this has meant that they have been simplified or their number limited.

© Energy Technologies Institute 2016

Table of Contents

CONTENTS I

 FIGURES III

 TABLES VIII

11.0 APPENDICES **10**

 11.1 APPENDIX 1 – RISK REGISTER 10

 11.2 APPENDIX 2 – LEAKAGE WORKSHOP 11

 11.3 APPENDIX 3 – DATABASE 15

 11.4 APPENDIX 4 – GEOLOGICAL INFORMATION 25

 11.5 APPENDIX 5 – MMV TECHNOLOGIES 57

 11.6 APPENDIX 6 – WELL BASIS OF DESIGN 83

 11.7 APPENDIX 7 – COST ESTIMATE 118

 11.8 APPENDIX 8 – METHODOLOGIES 119

 11.9 APPENDIX 9 – FRACTURE PRESSURE GRADIENT CALCULATION 151

 11.10 APPENDIX 10 – SUBSURFACE UNCERTAINTY ANALYSIS 164

 11.11 APPENDIX 11 – 3D GEOMECHANICAL MODELLING 173

Figures

FIGURE 11-1 CONTAINMENT FAILURE MODES	11
FIGURE 11-2 RISK MATRIX OF LEAKAGE SCENARIOS.....	13
FIGURE 11-3 PGS SNS MEGA SURVEY TIME SLICE SHOWING THE SEG-Y DATA EXTENT AND TILES	16
FIGURE 11-4 SEISMIC DATABASE ILLUSTRATING DATA GAP TO THE NORTH EAST OF VIKING A.....	17
FIGURE 11-5 TOP CHALK TWO-WAY TIME MAP	25
FIGURE 11-6 BASE CHALK/ BASE CRETACEOUS UNCONFORMITY TWO-WAY TIME MAP.....	26
FIGURE 11-7 TOP TRIASSIC TWO-WAY TIME MAP	27
FIGURE 11-8 TOP BUNTER SANDSTONE TWO-WAY TIME MAP	28
FIGURE 11-9 TOP ZECHSTEIN TWO-WAY TIME MAP	29
FIGURE 11-10 TOP LEMAN SANDSTONE TWO-WAY TIME MAP	30
FIGURE 11-11 TOP CHALK DEPTH MAP	31
FIGURE 11-12 BASE CHALK/BASE CRETACEOUS UNCONFORMITY DEPTH MAP	32
FIGURE 11-13 TOP TRIASSIC DEPTH MAP.....	33
FIGURE 11-14 TOP ZECHSTEIN RAW DEPTH MAP	34
FIGURE 11-15 TOP ZECHSTEIN DEPTH MAP EDITING.....	35
FIGURE 11-16 TOP ZECHSTEIN DEPTH MAP.....	36
FIGURE 11-17 ZECHSTEIN ISOCHORE	37
FIGURE 11-18 TOP LEMAN SANDSTONE DEPTH MAP.....	38
FIGURE 11-19 VIKING A TOP LEMAN SANDSTONE DEPTH MAP.....	39
FIGURE 11-20 TOP BUNTER SANDSTONE RAW DEPTH MAP	40
FIGURE 11-21 TOP BUNTER SANDSTONE DEPTH MAP EDITING.....	41
FIGURE 11-22 TOP BUNTER SANDSTONE DEPTH MAP.....	42
FIGURE 11-23 WELL 49/11A-6 CPI	43
FIGURE 11-24 WELL 49/12-2 CPI	44
FIGURE 11-25 WELL 49/12-3 CPI	45
FIGURE 11-26 WELL 49/12-4 CPI	46

FIGURE 11-27 WELL 49/12A-8 CPI	47
FIGURE 11-28 WELL 49/12A-9 CPI	48
FIGURE 11-29 WELL 49/12A-A6 CPI	49
FIGURE 11-30 WELL 14/12A-A10 CPI	50
FIGURE 11-31 WELL 49/12A-F1 CPI	51
FIGURE 11-32 WELL 49/12A-K2 CPI	52
FIGURE 11-33 WELL 49/12A-K3 CPI	53
FIGURE 11-34 WELL 49/12A-K4 CPI	54
FIGURE 11-35 WELL 49/12A-K4Z CPI	55
FIGURE 11-36 PETROPHYSICAL SUMMARY FOR ALL ZONES.....	56
FIGURE 11-37 BOSTON SQUARE PLOT OF MONITORING TECHNOLOGIES APPLICABLE OFFSHORE	60
FIGURE 11-38 VIKING A WELL 49/12-2 (ORIGINAL CONDITION) SAFE MUDWEIGHT ANALYSIS.....	84
FIGURE 11-39 VIKING A WELL 49/11A-6 (ORIGINAL CONDITION) SAFE MUD WEIGHT ANALYSIS	85
FIGURE 11-40 VIKING A WELL 49/12A-K4 (ORIGINAL CONDITION) SAFE MUD WEIGHT ANALYSIS.....	85
FIGURE 11-41 VIKING A WELL 49/12A-K5 SAFE MUD WEIGHT ANALYSIS.....	86
FIGURE 11-42 VIKING A WELL 49/12-A6 (ORIGINAL CONDITIONS) SAFE MUD WEIGHT ANALYSIS.....	86
FIGURE 11-43 VIKING A WELL 49/12-A10 (ORIGINAL CONDITIONS) SAFE MUD WEIGHT ANALYSIS.....	87
FIGURE 11-44 VIKING A WELL 49/12-2 (ORIGINAL CONDITION) WELL TRAJECTORY ANALYSIS	88
FIGURE 11-45 VIKING A WELL 49/11A-6 (ORIGINAL CONDITION) WELL TRAJECTORY ANALYSIS	88
FIGURE 11-46 VIKING A WELL 49/12A-K4 (ORIGINAL CONDITION) WELL TRAJECTORY ANALYSIS.....	88
FIGURE 11-47 VIKING A WELL 49/12A-K5 (ORIGINAL CONDITION)	88
FIGURE 11-48 VIKING A WELL 49/12-A6 (ORIGINAL CONDITION) WELL TRAJECTORY ANALYSIS.....	89
FIGURE 11-49 VIKING A WELL 49/12-A10 (ORIGINAL CONDITION) WELL TRAJECTORY ANALYSIS.....	89
FIGURE 11-50 VIKING A WELL 49/12-2 (ORIGINAL/DEPLETED) SAFE MUD WEIGHT ANALYSIS.....	90
FIGURE 11-51 VIKING A WELL 49/11A-6 (ORIGINAL/DEPLETED) SAFE MUD WEIGH ANALYSIS.....	90
FIGURE 11-52 VIKING A WELL 49/12A-K4 (ORIGINAL/DEPLETED) SAFE MUD WEIGHT ANALYSIS	91
FIGURE 11-53 VIKING A WELL 49/12A-K5 (ORIGINAL/DEPLETED) SAFE MUD WEIGHT ANALYSIS	91

FIGURE 11-54 VIKING A WELL 49/12-A6 (ORIGINAL/DEPLETED) SAFE MUD WEIGHT ANALYSIS	92
FIGURE 11-55 VIKING A WELL 49/12-A10 (ORIGINAL/DEPLETED) SAFE MUD WEIGHT ANALYSIS	92
FIGURE 11-56 VIKING A WELL 49/12-2 (DEPLETED CONDITION) WELL TRAJECTORY ANALYSIS.....	93
FIGURE 11-57 VIKING A WELL 49/11A-6 (DEPLETED CONDITION) WELL TRAJECTORY ANALYSIS.....	93
FIGURE 11-58 VIKING A WELL 49/12A-K4 (DEPLETED CONDITION) WELL TRAJECTORY ANALYSIS	94
FIGURE 11-59 VIKING A WELL 49/12A-K5 (DEPLETED CONDITION) WELL TRAJECTORY ANALYSIS	94
FIGURE 11-60 VIKING A WELL 49/12-A6 (DEPLETED CONDITION) WELL TRAJECTORY ANALYSIS	94
FIGURE 11-61 VIKING A WELL 49/12-A10 (DEPLETED CONDITION) WELL TRAJECTORY ANALYSIS	94
FIGURE 11-62 PLATFORM DIRECTIONAL SPIDER PLOT	101
FIGURE 11-63 SLANT INJECTOR 1 DIRECTIONAL PROFILE	102
FIGURE 11-64 SLANT INJECTOR 2 DIRECTIONAL PROFILE	103
FIGURE 11-65 MONITORING WELL / SLANT INJECTOR 3 DIRECTIONAL PROFILE.....	103
FIGURE 11-66 EXAMPLES OF UNDERGROUND CABLES.....	123
FIGURE 11-67 EXAMPLE OF A CONSTRUCTION SWATHE FOR A LAND CABLE	124
FIGURE 11-68 POSSIBLE ELECTRICAL TOPOLOGIES FOR THE VIKING A DEVELOPMENT.....	128
FIGURE 11-69 SUMMARY OF PETROPHYSICAL WORKFLOW	135
FIGURE 11-70 RECORDED BOTTOM HOLE PRESSURE FROM WIRELINE DATA	135
FIGURE 11-71 MEASURED FORMATION RESISTIVITY FACTOR 'M'.....	136
FIGURE 11-72 MEASURED FORMATION SATURATION COMPONENT 'N'	136
FIGURE 11-73 CAPILLARY PRESSURE SAMPLES	137
FIGURE 11-74 MULTI-WELL GAMMA RAY DISTRIBUTION.....	138
FIGURE 11-75 MULTI-WELL NEUTRON DENSITY CROSSPLOT	139
FIGURE 11-76 MEASURED CORE GRAIN DENSITY	140
FIGURE 11-77 MEASURED CORE POROSITY.....	140
FIGURE 11-78 CORE POROSITY-PERMEABILITY CROSS PLOT	142
FIGURE 11-79 J-CURVE TREND NORMALISATION	143
FIGURE 11-80 CAPILLARY BASED SW HEIGHT CURVES.....	143

FIGURE 11-81 GEOCHEMICAL MODELLING WORKFLOW..... 145

FIGURE 11-82 MINERAL DISSOLUTION AND GROWTH WITH TIME AND CO₂ CONCENTRATION 148

FIGURE 11-83 MINERAL DISSOLUTION AND GROWTH WITH TIME AND CO₂ CONCENTRATION (ZECHSTEIN DOLOMITIC CAPROCK)..... 149

FIGURE 11-84 MINERAL DISSOLUTION AND GROWTH WITH TIME AND CO₂ CONCENTRATION (ZECHSTEIN ANHYDRITIC DOLOMITIC CAPROCK)..... 149

FIGURE 11-85 MINERAL DISSOLUTION AND GROWTH WITH TIME AND CO₂ CONCENTRATION (ZECHSTEIN ANHYDRITIC CAPROCK) 150

FIGURE 11-86 VIKING STRESS ORIENTATION 152

FIGURE 11-87 VIKING A FIELD 152

FIGURE 11-88 VIKING A WELL 49/12-2 CALCULATED STRESS CURVES 154

FIGURE 11-89 VIKING A WELL 49/12-2 ROCK MECHANICAL PROPERTIES..... 155

FIGURE 11-90 VIKING A WELL 49/11A-6..... 155

FIGURE 11-91 VIKING A WELL 49/11A-6..... 156

FIGURE 11-92 VIKING A WELL 49/12A-K4 156

FIGURE 11-93 VIKING A WELL 49/12A-K4 ROCK MECHANICAL PROPERTIES 157

FIGURE 11-94 VIKING A WELL 49/12A-K5 CALCULATED STRESS CURVES..... 157

FIGURE 11-95 VIKING A WELL 49/12A-K5 ROCK MECHANICAL PROPERTIES 158

FIGURE 11-96 VIKING A WELL 49/12-A6 CALUCLATED STRESS CURVES..... 158

FIGURE 11-97 VIKING A WELL 49/12-A6 ROCK MECHANICAL PROPERTIES 159

FIGURE 11-98 VIKING A WELL 49/12-A10 CALCULATED STRESS CURVES..... 159

FIGURE 11-99 VIKING A WELL 49/12-A10 160

FIGURE 11-100 VIKING A WELL 49/12-2 DEPLETED FRACTURE GRADIENT ANALYSIS..... 161

FIGURE 11-101 STRESS PATHS FOR VIKING AT THE 49/12-2 WELL LOCATION..... 162

FIGURE 11-102 COMPARISON OF CAPACITY PER CASE..... 166

FIGURE 11-103 COMPARISON OF INJECTION DURATION PER CASE 166

FIGURE 11-104 INJECTION FORECASTS FOR RESERVOIR PRESSURE SENSITIVITIES 167

FIGURE 11-105 NORTH WEST FAULT LOCATION SHOWN ON CO₂ DISTRIBUTION MAP AT THE END OF INJECTION 168

FIGURE 11-106 INJECTION FORECASTS FOR FAULT SEALING SENSITIVITIES 168

FIGURE 11-107 FRACTURE PRESSURE GRADIENT VS INJECTION CAPACITY 169

FIGURE 11-108 INJECTION FORECASTS FOR PORE VOLUME SENSITIVITES 170

FIGURE 11-109 INJECTION FORECASTS FOR THE HORIZONTAL PERMEABILITY SENSITIVITES 170

FIGURE 11-110 VIKING A RELATIVE PERMEABILITY FUNCTIONS..... 171

FIGURE 11-111 INJECTION FORECASTS FOR THE HORIZONTAL PERMEABILITY SENSITIVITES 172

FIGURE 11-112 VIEW TO SE OF VIKING A AND VIKING F TOP LEMAN SANDSTONE SURFACE IN THE GEOMECHANICAL MODEL 175

FIGURE 11-113 GEOMECHANICAL MODEL ZONATION IN SW-NE SECTION THROUGH CREST 175

FIGURE 11-114 POISSON'S RATIO IN THE GEOMECHANICAL MODEL, HIGH VALUES ARE FOR THE SALT LAYERS 175

FIGURE 11-115 FAULT CELLS (PLASTIC SHEAR STRAIN PROPERTY) AT K LAYER 58 IN THE LEMAN SANDSTONE..... 175

FIGURE 11-116 VIKING PRESSURE EVOLUTION FROM VIRGIN CONDITIONS (1972), DEPLETED STATE (2031), EARLY INJECTION IN VIKING F (2034) AND LATE INJECTION IN VIKING A (2058) MAP FROM K LAYER 58 WITHIN THE LEMAN SANDSTONE..... 176

FIGURE 11-117 MOHR-COULOMB RUN LH COLUMN ROCKDISZ ON VIKING CREST AT KEY TIMESTEPS DESCRIBED IN TEXT RH COLUMN STRAINZZ PROPERTY..... 177

FIGURE 11-118 MOHR-COLUMB RUN, FAULT RELATED PLASTIC SHEAR STRAIN AT END DEPLETION 177

FIGURE 11-119 MOHR-COLOUMB RUN, MICROSEISMIC EVENTS ASSOCIATED WITH FAULT RELATED PLASTIC STRAINS. EVENTS SCALE IN SIZE AND COLOUR FROM MAGNITUDE -4.56 TO -2.74 AND YELLOW TO RED RESPECTIVELY 178

FIGURE 11-120 MODIFIED DRUCKER-PRAGER RUN, LH COLUMN ROCKDISZ ON VIKING CREST AT KEY TIMESTEPS RH COLUMN, STRAINZZ PROPERTY 179

FIGURE 11-121 MODIFIED DRUCKER-PRAGER RUN, MICROSEISMIC EVENTS ASSOCIATED WITH PLASTIC SHEAR STRAIN AT END PRODUCTION IN 1990. EVENTS SCALE IN SIZE AND COLOUR FROM MAGNITUDE -3.88 TO -2.16 AND YELLOW TO RED RESPECTIVELY..... 180

FIGURE 11-122 STRESS PATHS FOR VIKING AT THE 49/12-2 WELL LOCATION..... 180

Tables

TABLE 11-1- LEAKAGE SCENARIOS 12

TABLE 11-2 - IMPACT CATEGORIES 14

TABLE 11-3 - LIKELIHOOD CATEGORIES 14

TABLE 11-4 SEG-Y SURVEY DATUM AND MAP PROJECTIONS 15

TABLE 11-5 SEG-Y TILES FOR THE VIKING STORAGE SITE EVALUATION 15

TABLE 11-6 WELL LOG DATA SUMMARY 23

TABLE 11-7 CORE DATA SUMMARY 24

TABLE 11-8 MONITORING DOMAINS 58

TABLE 11-9 OFFSHORE TECHNOLOGIES FOR MONITORING 72

TABLE 11-10 BASELINE MONITORING PLAN 73

TABLE 11-11 OPERATIONAL MONITORING PLAN 74

TABLE 11-12 POST CLOSURE MONITORING PLAN 75

TABLE 11-13 ACTIVE WELL CONTAINMENT FAILURE MODES AND ASSOCIATED EFFECTS AND REMEDIATION OPTIONS 81

TABLE 11-14 ABANDONED WELL CONTAINMENT FAILURE MODES AND ASSOCIATED EFFECTS AND REMEDIATION OPTIONS 82

TABLE 11-15 VIKING A RESERVOIR TARGETS 101

TABLE 11-16 CEMENT DEGRADATION RATES IN CO₂ LABORATORY TEST RESULTS 110

TABLE 11-17 MATERIAL SELECTION VS CONTAMINANTS 111

TABLE 11-18 FIELD LIFE WELL ACTIVITY 113

TABLE 11-19 TIME AND COST ESTIMATE SUMMARY 114

TABLE 11-20 PLATFORM INJECTOR TIME AND COST ESTIMATE 115

TABLE 11-21 MONITORING WELL TIME AND COST ESTIMATE 115

TABLE 11-22 WORKOVER TIME AND COST ESTIMATES 116

TABLE 11-23 LOCAL SIDETRACK TIME AND COST ESTIMATE 116

TABLE 11-24 WELL ABANDONMENT TIME AND COST ESTIMATE 117

TABLE 11-25 BARMSTON TO VIKING A NUI PIPELINE PRESSURE DROP 120

TABLE 11-26 VIKING A DEVELOPMENT PIPELINE SPECIFICATIONS 120

TABLE 11-27 CAPEX ASSOCIATED WITH A LARGER DIAMETER PIPELINE FROM BARMSTON TO VIKING A NUI	121
TABLE 11-28 COST ESTIMATE WBS.....	122
TABLE 11-29 TYPICAL ELECTRICAL CONNECTIONS FOR A 10 MW ELECTRICAL LOAD	126
TABLE 11-30 APPRAISAL OF ELECTRICAL CONNECTION TYPES.....	129
TABLE 11-31 CAPITAL COST ESTIMATES FOR A RANGE OF SUBSEA ELECTRICAL CABLE OPTIONS.....	130
TABLE 11-32 MAINTENANCE AND REPAIR COST ESTIMATES FOR SUBSEA CABLING OPTIONS	132
TABLE 11-33 TYPICAL AC LOAD LOSSES	133
TABLE 11-34 OPEX COST ESTIMATES FOR SUBSEA CABLING OPTIONS.....	134
TABLE 11-35 UNCERTAINTY IN ARCHIE PARAMETERS.....	136
TABLE 11-36 IMPACT OF UNCERTAINTY ON SW	137
TABLE 11-37 CORE GRAIN DENSITY SUMMARY.....	140
TABLE 11-38 CORE POROSITY SUMMARY	141
TABLE 11-39 CLAY PARAMETER SELECTION	141
TABLE 11-40 POROSITY AND WATER SATURATION PARAMETER SELECTION	142
TABLE 11-41 WATER GEOCHEMICAL COMPOSITION DATA USED IN MODELLING.....	146
TABLE 11-42 GAS GEOCHEMICAL COMPOSITION DATA USED IN MODELLING	147
TABLE 11-43 KINETIC MODELLING MINERAL VOLUME RESULTS FOR THE KUPFERSCHIEFER FORMATION.....	148
TABLE 11-44 RESULTS FOR THE SIMULATED ZECHSTEIN FORMATION CAPROCK LITHOLOGIES (DOLOMITIC, ANHYDRITIC DOLOMITE AND ANHYDRITIC).....	150
TABLE 11-45 KEY INPUT PARAMETERS TO THE REFERENCE CASE DYNAMIC MODEL.....	164
TABLE 11-46 SUBSURFACE UNCERTAINTY PARAMETERS AND ASSOCIATED RANGE OF VALUES	165
TABLE 11-47 COMPARISON OF INJECTION PROFILE FOR THE UNCERTAINTY CASES	165
TABLE 11-48 SEISMIC EVENT MAGNITUDES VS LENGTH SCALES	178

11.0 Appendices

11.1 Appendix 1 – Risk Register

Provided separately in Excel and PDF format.

11.2 Appendix 2 – Leakage Workshop

11.2.1 Objectives

The objectives for this workshop were to discuss and capture the leakage scenarios for the Viking A storage site & their risk (likelihood & impact).

11.2.2 Methodology

The Leakage Scenario Definition Workshop (WP5D.T23) covered all aspects of natural and engineering integrity. The project team of subsurface experts came together to brainstorm an inventory of potential leak paths (both geological and engineered) for the Viking A storage site. These potential leak paths were then assessed for their likelihood and impact, based on all the available evidence.

The scope of the workshop was for the Viking A site only, from the subsurface to the wellhead and did not include offshore facilities or pipeline transportation.

The roles in the room included:

- Facilitator, timekeeper, note-taker
- Geophysics expert
- Geology expert
- Reservoir Engineering expert
- Wells expert
- CO₂ Storage expert

The workshop focussed one at a time on each of the following 10 containment failure modes (pathways for CO₂ to move out of the primary store and/or storage complex which are contrary to the storage development plan):

1. Flow through Primary Caprock

2. Lateral Exit from Primary Store
3. Lateral Exit from Secondary Store
4. Flow through Secondary Caprock
5. CO₂ entry into a post operational or legacy well
6. CO₂ flow upwards in wellbore zone within Storage Complex
7. CO₂ exit from wellbore zone outside Primary Store
8. CO₂ flow upwards in wellbore zone beyond Storage Complex boundary
9. CO₂ flow through Store floor and beyond storage complex boundary
10. CO₂ flow downwards in wellbore zone beyond Storage Complex boundary

These are summarised in the following diagram:

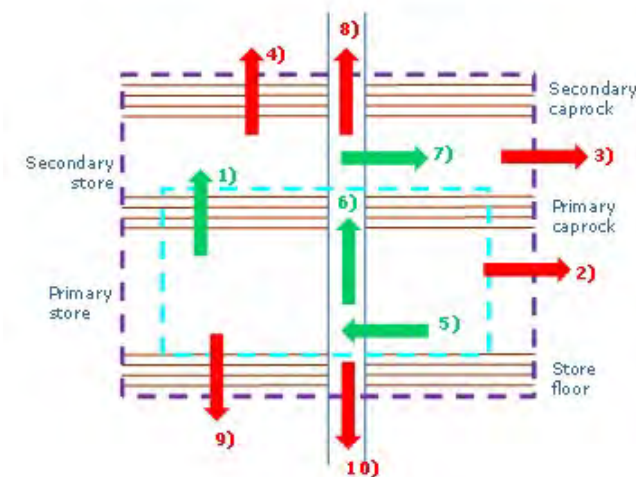


Figure 11-1 Containment failure modes

For each failure mode, a number of containment failure mechanisms were discussed. A containment failure mechanism is a geological or engineering

feature, event or process which could cause CO₂ to move out of the primary store and/or storage complex (contrary to the storage development plan). An example is: fault reactivation in primary caprock.

The likelihood and impact of each containment failure mechanism was discussed, based on the CO₂QUALSTORE (DNV, 2009) (DNV, 2010) framework shown in Table 11-2 and Table 11-3.

The failure mechanisms were then cross-checked with the Quintessa CO₂ FEP (feature, event, process) database (Quintessa, 2014) to ensure all possibilities were considered.

Pathways that could potentially lead to CO₂ moving out with the storage complex were mapped out from combinations of failure modes. For each pathway, the likelihood was taken as the lowest from likelihood of any of the failure modes that made it up and the impact was take as the highest. The pathways were then grouped into more general leakage scenarios.

11.2.3 Results

Leakage scenario	Likelihood	Impact	
Vertical movement of CO ₂ from Primary store to overburden through caprock	1	3	Green
Vertical movement of CO ₂ from Primary store to overburden via existing wells	2	3	Green
Vertical movement of CO ₂ from Primary store to overburden via injection wells	2	3	Green
Vertical movement of CO ₂ from Primary store to overburden via caprock & wells	1	3	Green
Vertical movement of CO ₂ from Primary store to upper well/ seabed via P&A wells	2	4	Yellow
Vertical movement of CO ₂ from Primary store to upper well/ seabed via suspended wells	2	4	Yellow
Vertical movement of CO ₂ from Primary store to upper well/ seabed via injection wells	2	4	Yellow
Vertical movement of CO ₂ from Primary store to upper well/ seabed via caprock & wells	1	4	Green
Lateral movement of CO ₂ from Primary store out with storage complex	1	3	Green
Lateral movement of CO ₂ from Primary store via bounding faults	2	3	Green
Vertical movement of CO ₂ from Primary store to underburden via existing wells	1	2	Green
Vertical movement of CO ₂ from Primary store to underburden via store floor (out with storage complex)	1	3	Green

Table 11-1- Leakage Scenarios

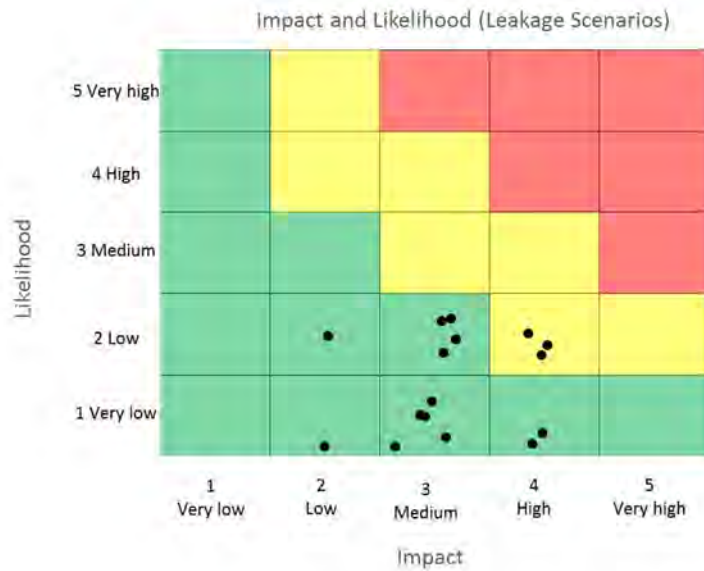


Figure 11-2 Risk matrix of leakage scenarios

The scenarios with the highest risk relate to existing (P&A and development) and injection wells as they provide a potential leakage pathway directly from the storage site to seabed.

The bounding fault leakage likelihood is considered low due to the presence of gas in Viking Block A, which has been held for millions of years. Reactivation is also considered very low. The injection pressure will be limited to 90% of the reservoir fracture pressure and the Zechstein caprock has a very high fracture pressure and is considered “self-healing”.

There are some uncertainties over well abandonment spec due to limited information, but not the same concerns with specific wells as for some of the other sites.

Secondary containment within the overlying Bunter provides an additional barrier to the surface, should loss of containment occur.

Score	1	2	3	4	5
Name	Very Low	Low	Medium	High	Very High
Impact on storage integrity	None	Unexpected migration of CO ₂ inside the defined storage complex	Unexpected migration of CO ₂ outside the defined storage complex	Leakage to seabed or water column over small area (<100m ²)	Leakage seabed water column over large area (>100m ²)
Impact on local environment	Minor environmental damage	Local environmental damage of short duration	Time for restitution of ecological resource <2 years	Time for restitution of ecological resource 2-5 years	Time for restitution of ecological resource such as marine Biosystems, ground water >5 years
Impact on reputation	Slight or no impact	Limited impact	Considerable impact	National impact	International impact
Consequence for Permit to operate	None	Small fine	Large fine	Temporary withdrawal of permit	Permanent loss of permit

Table 11-2 - Impact Categories

Score	1	2	3	4	5
Name	Very Low	Low	Medium	High	Very High
Description	Improbable, negligible	Remotely probably, hardly likely	Occasional, likely	Probable, very likely	Frequent, to be expected
Event (E)	Very unlikely to occur during the next 5000 years	Very unlikely to occur during injection operations	Likely to occur during injection operations	May occur several times during injection operations	Will occur several times during injection operations
Frequency	About 1 per 5000 years	About 1 per 500 years	About 1 per 50 years	About 1 per 5 years	About 1 per year or more
Feature (F)/ Process (P)	Disregarded	Not expected	50/50 chance	Expected	Sure

Table 11-3 - Likelihood Categories

11.3 Appendix 3 – Database

11.3.1 Viking: SEG-Y data summary

The seismic 3D survey used for the evaluation of Viking A storage site came from PGS UK CNS Mega Survey:

- Survey: MC3D_SNS_MEGA (UK Sector)
- Final Merged Migration (22 Tiles)

The SEG-Y data were supplied on a USB hard drive and have the following survey datum and map projections:

Survey Datum	Name:	ED50
Ellipsoid:	INTERNATIONAL 1924	
Semi Major Axis	6378388	
1/Flattening	297	
Map Projection	Projection	UTM 31N
Central Meridian	3 EAST	
Scale Factor on Central Meridian	0.9996	
Latitude of Origin	0.00N	
False Northing	0	
False Easting	500000	

Table 11-4 SEG-Y survey datum and map projections

The following tiles of SEG-Y data were used for the Viking site selection and evaluation:

File Name	Format	Tile	IL Range	XL Range
MC3D_SNS_MEGA_I06P	SEG-Y	I06	25001 - 30000	32001 - 36000
MC3D_SNS_MEGA_I07P	SEG-Y	I07	30001 - 35000	32001 - 36000
MC3D_SNS_MEGA_H06	SEG-Y	H06	25001 - 30000	28001 - 32000
MC3D_SNS_MEGA_H07P	SEG-Y	H07	30001 - 34259	28001 - 32000

Table 11-5 SEG-Y tiles for the Viking storage site evaluation

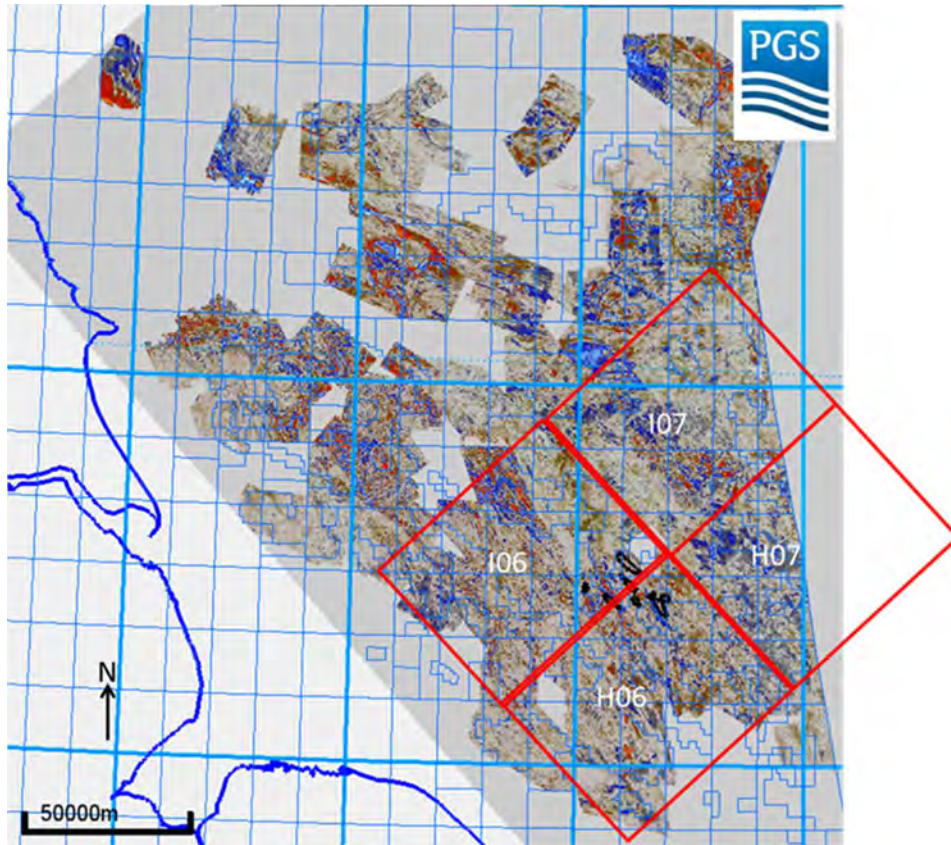


Figure 11-3 PGS SNS Mega survey time slice showing the SEG-Y data extent and tiles

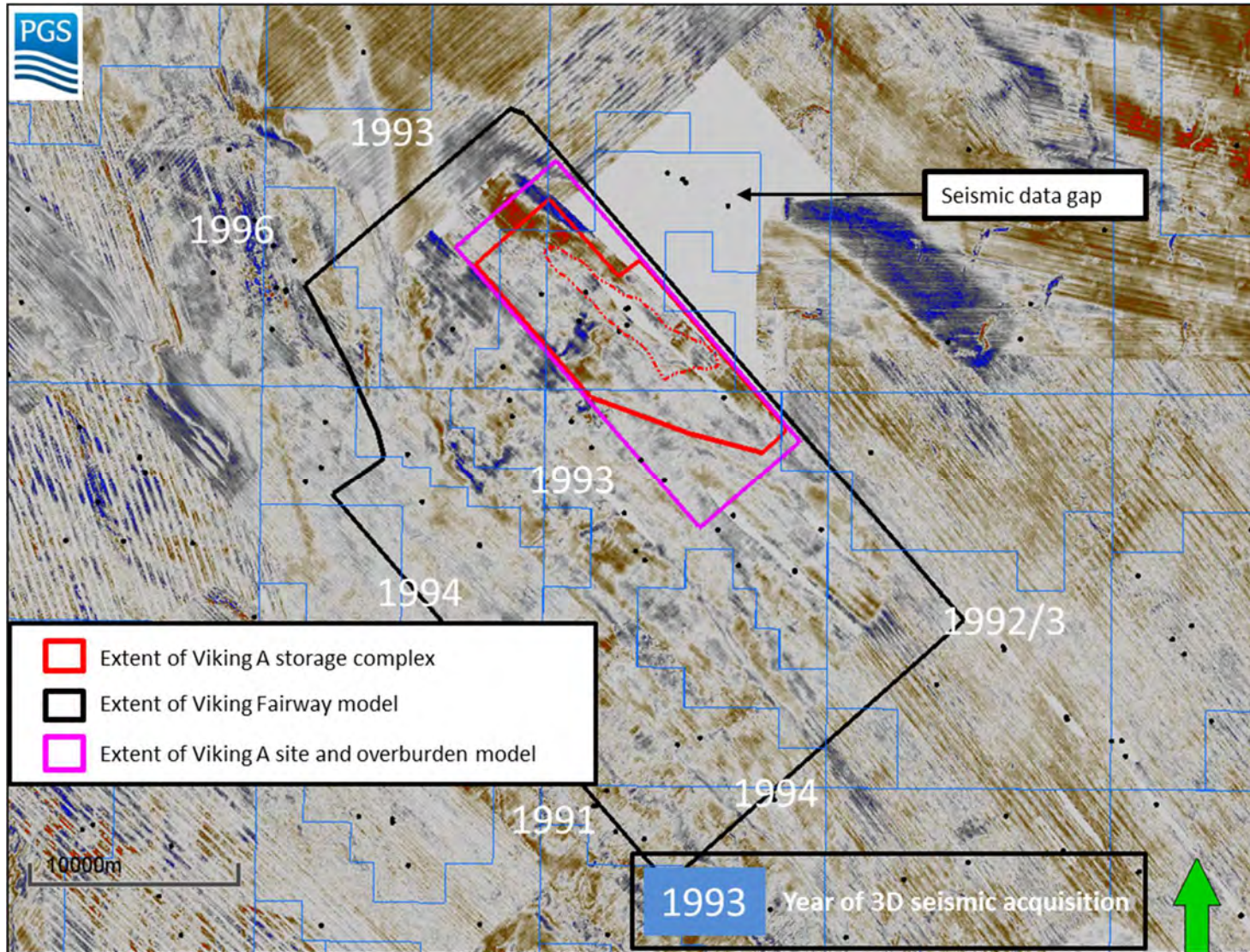


Figure 11-4 Seismic database illustrating data gap to the north east of Viking A

11.3.2 Viking storage site: Well log data summary

The table below shows a summary of the well log data for the Viking A storage site, downloaded from CDA.

Field	Well	Completion Date	E/A/D	DLIS or LAS?	GR	Neutron	Density	DT/Sonic	SP	Comp Log	Geol Report/Final Well Report	Digital Checkshots	Deviation Data	Well Tops	Core Data over Viking
Viking A	49/12-2	24/03/1969	E	DLIS	Y	N	N	Y	N	Y	Y	N	Y	Y	Y
	49/12-A1	30/07/1971	D	No Digital Logs	N	N	N	N	N	Y	N	N	Y	Y	N
	49/12-A5	01/03/1971	D	No Digital Logs	N	N	N	N	N	Y	Y	N	Y	Y	N
	49/12-A6	05/09/1971	D	DLIS	Y	Y	Y	N	N	Y	N	N	Y	Y	N
	49/12-A7	30/09/1971	D	No Digital Logs	N	N	N	N	N	Y	N	N	Y	Y	N
	49/12-A8	25/12/1971	D	No Digital Logs	N	N	N	N	N	Y	N	N	Y	Y	N
	49/12-A9	18/11/1970	D	No Digital Logs	N	N	N	N	N	Y	N	N	Y	Y	N
	49/12-A10	09/01/1972	D	DLIS	Y	Y	Y	N	N	Y	N	N	Y	Y	N
	49/12-3	09/03/1970	E	LAS	Y	Y	Y	N	N	Y	N	N	Y	Y	Y
	49/12-1	06/02/1969	E	DLIS	Y	Y	Y	Y	N	N	Y	Y	Y	Y	Y
Viking F	49/12a-K2	18/10/1998	D	DLIS	Y	N	Y	Y	N	Y	Y	N	Y	Y	N
	49/12a-K5	11/08/2000	D	DLIS	Y	N	N	Y	N	Y	Y	N	Y	Y	N
	49/12a-4	08/08/1973	E	DLIS	Y	Y	Y	Y	N	Y	N	Y	Y	Y	N
	49/12a-F2	22/02/1976	D	DLIS	Y	Y	Y	N	N	Y	N	N	Y	Y	N

Field	Well	Completion Date	E/A/D	DLIS or LAS?	GR	Neutron	Density	DT/Sonic	SP	Comp Log	Geol Report/Final Well Report	Digital Checkshots	Deviation Data	Well Tops	Core Data over Viking
	49/12a-F4	19/03/1976	D	DLIS	Y	Y	Y	Y	Y	Y	N	N	Y	Y	N
	49/12a-F1	19/02/1976	D	DLIS & LAS	Y	N	N	N	N	Y	N	N	Y	Y	N
Viking Fs	49/11a-6	24/12/1987	E	DLIS	Y	N	N	Y	Y	Y	Y	Y	Y	Y	Y
	49/12a-K3	14/10/1998	D	DLIS	Y	N	Y	Y	N	Y	Y	N	Y	Y	N
	49/12a-K4Z	19/10/2000	D	DLIS	Y	N	N	Y	N	Y	Y	N	Y	Y	N
	49/12a-F3	19/03/1976	D	DLIS	Y	Y	Y	N	N	N	Y	N	Y	Y	N
	49/12a-9	30/04/1994	A	DLIS	Y	N	Y	Y	N	Y	Y	Y	Y	Y	Y
Viking H	49/17-5	07/09/1969	E	No Digital Logs	N	N	N	N	N	Y	Y	Y	Y	Y	Y
	49/17-H2	03/01/2015	D	No Digital Logs	N	N	N	N	N	Y	N	N	Y	Y	N
	49/17-1	04/12/1965	E	DLIS	Y	Y	Y	Y	N	Y	Y	Y	Y	Y	Y
	49/17-B2	25/11/1972	D	No Digital Logs	N	N	N	N	N	Y		N	Y	N	N
	49/17-B3	05/12/1972	D	DLIS	Y	Y	Y	N	N	Y	Y	Y	Y	Y	N
	49/17-B4	18/04/1973	D	DLIS	Y	Y	Y	Y	N	Y	Y	Y	Y	Y	N
	49/17-B5	23/04/1973	D	No Digital Logs	N	N	N	N	N	N	N	N	Y	Y	N

Field	Well	Completion Date	E/A/D	DLIS or LAS?	GR	Neutron	Density	DT/Sonic	SP	Comp Log	Geol Report/Final Well Report	Digital Checkshots	Deviation Data	Well Tops	Core Data over Viking
Viking B	49/17-B7	05/03/1973	D	No Digital Logs	N	N	N	N	N	Y	N	N	Y	Y	N
	49/17-B8	29/12/1978	D	No Digital Logs	N	N	N	N	N	Y	N	Y	Y	N	N
Viking C	49/17-C1	23/05/2015	D	DLIS	Y	N	N	N	N	N	N	N	Y	Y	N
	49/17-C3	27/05/2015	D	DLIS	Y	N	N	Y	Y	Y	N	N	Y	Y	N
	49/17-C4	30/05/2015	D	DLIS	Y	N	N	Y	Y	Y	Y	N	Y	Y	N
	49/17-7	14/12/1969	E	No Digital Logs	Y	N	N	N	N	N	Y	N	N	Y	Y
Viking D	49/17-2	26/05/1968	E	DLIS	Y	Y	Y	Y	N	Y	Y	Y	Y	Y	Y
Viking E	49/16-E3	16/07/1975	D	DLIS	Y	Y	Y	N	N	Y	N	N	Y	Y	N
	49/16-E3A	31/12/1979	D	No Digital Logs	N	N	N	N	N	Y	Y	N	Y	Y	N
	49/16-E4	03/08/2015	D	DLIS	Y	N	N	Y	Y	Y	Y	N	Y	Y	N
	49/16-E5	10/08/2015	D	LIS	N	N	N	N	N	Y	N	N	Y	Y	N
	49/16-E1	24/07/1975	D	DLIS	Y	Y	Y	N	N	N	N	N	Y	Y	N

Field	Well	Completion Date	E/A/D	DLIS or LAS?	GR	Neutron	Density	DT/Sonic	SP	Comp Log	Geol Report/Final Well Report	Digital Checkshots	Deviation Data	Well Tops	Core Data over Viking
	49/16-3	17/01/1975	E	DLIS	Y	N	N	Y	N	Y	Y	Y	Y	Y	Y
	49/16-E2A	07/08/1975	D	DLIS	Y	N	Y	N	N	N	N	N	Y	Y	N
Viking G	49/17-G1	25/08/2014	D	No Digital Logs	N	N	N	N	N	Y	Y	N	Y	Y	N
	49/17-G2	09/07/1976	D	DLIS	Y	Y	Y	N	N	Y	N	N	N	Y	N
	49/17-G3	11/07/1976	D	DLIS	Y	Y	Y	N	N	Y	N	N	Y	Y	N
	49/17-G4	15/08/2014	D	DLIS	Y	Y	Y	N	N	Y	N	N	Y	Y	N
	49/17-G5	12/08/2014	D	DLIS	N	Y	Y	N	N	Y	Y	N	Y	Y	N
	49/17-9	02/02/1973	A	DLIS	Y	N	N	Y	N	Y	Y	Y	Y	Y	Y
Central Viking	49/17-4	18/06/1969	E	No Digital Logs	N	N	N	N	N	Y	Y	Y	Y	Y	Y
	49/17-12	24/92015	A	DLIS	Y	N	Y	N	N	Y	Y	Y	Y	Y	Y
	49/17-6	13/10/1969	E	No Digital Logs	N	N	N	N	N	Y	Y	Y	Y	Y	Y
	49/11a-B2	11/04/1995	D	DLIS	Y	N	N	Y	N	Y	Y	Y	Y	N	N
	49/11a-B2Z	25/05/1995	D	DLIS	Y	N	N	Y	N	Y	Y	N	Y	N	N
	49/17-L2	16/01/1999	D	DLIS	Y	N	N	N	N	N	Y	N	N	Y	Y

Field	Well	Completion Date	E/A/D	DLIS or LAS?	GR	Neutron	Density	DT/Sonic	SP	Comp Log	Geol Report/Final Well Report	Digital Checkshots	Deviation Data	Well Tops	Core Data over Viking
	49/17-L2Z	25/09/2015	D	DLIS	Y	N	N	N	N	Y	Y	N	Y	Y	N
	49/12a-8	15/02/1989	A	DLIS	Y	N	N	Y	Y	Y	N	N	Y	N	N

Table 11-6 Well log data summary

11.3.3 Viking Storage site: Core data summary

The table below show a summary of the core data available over the Viking A storage site.

Well	Cored interval (MD ft)	CKHA	CHKL	CKVA	CKVL	CPOR
49/12-2	8780 - 9013.5	Y	Y	Y	Y	Y
49/12-3	9118 - 9523	Y	Y	Y	Y	Y
49/12-1	9421 - 9505	Y	Y	Y	Y	Y
49/11a-6	10039.1 - 10203.8	Y	N	Y	N	Y
49/12a-9	11074 - 11713	Y	N	Y	N	Y
49/17-5	9677 - 9727	Y	Y	Y	Y	Y
49/17-1	8989 - 9330	Y	N	Y	N	Y
49/17-7	8976 - 9032	Y	Y	Y	Y	Y
49/17-2	8773 - 9006	Y	N	Y	N	Y
49/16-3	8885 - 9429	Y	Y	N	N	Y
49/17-9	9908 - 10143	Y	Y	N	N	Y
49/17-4	9204 - 9495	Y	Y	Y	Y	Y
49/17-12	8645 - 8858	Y	N	Y	N	Y
49/17-6	9345 - 9649	Y	Y	Y	Y	Y

Table 11-7 Core data summary

11.3.4 Data from Operators

Limited data from Operators in the area were provided as input to the Viking A storage site work.

11.4 Appendix 4 – Geological Information

11.4.1 Maps

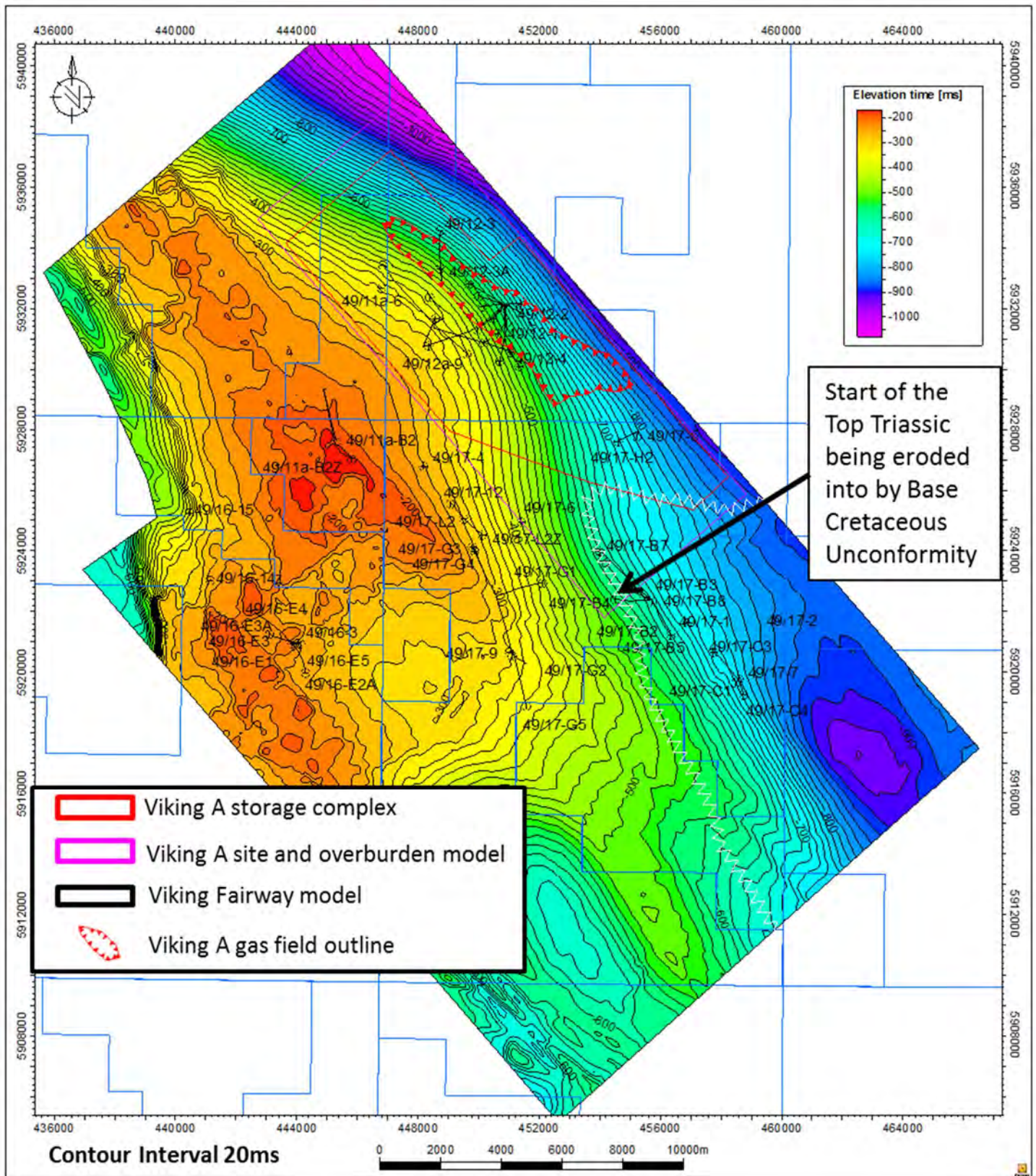


Figure 11-5 Top Chalk Two-Way Time Map

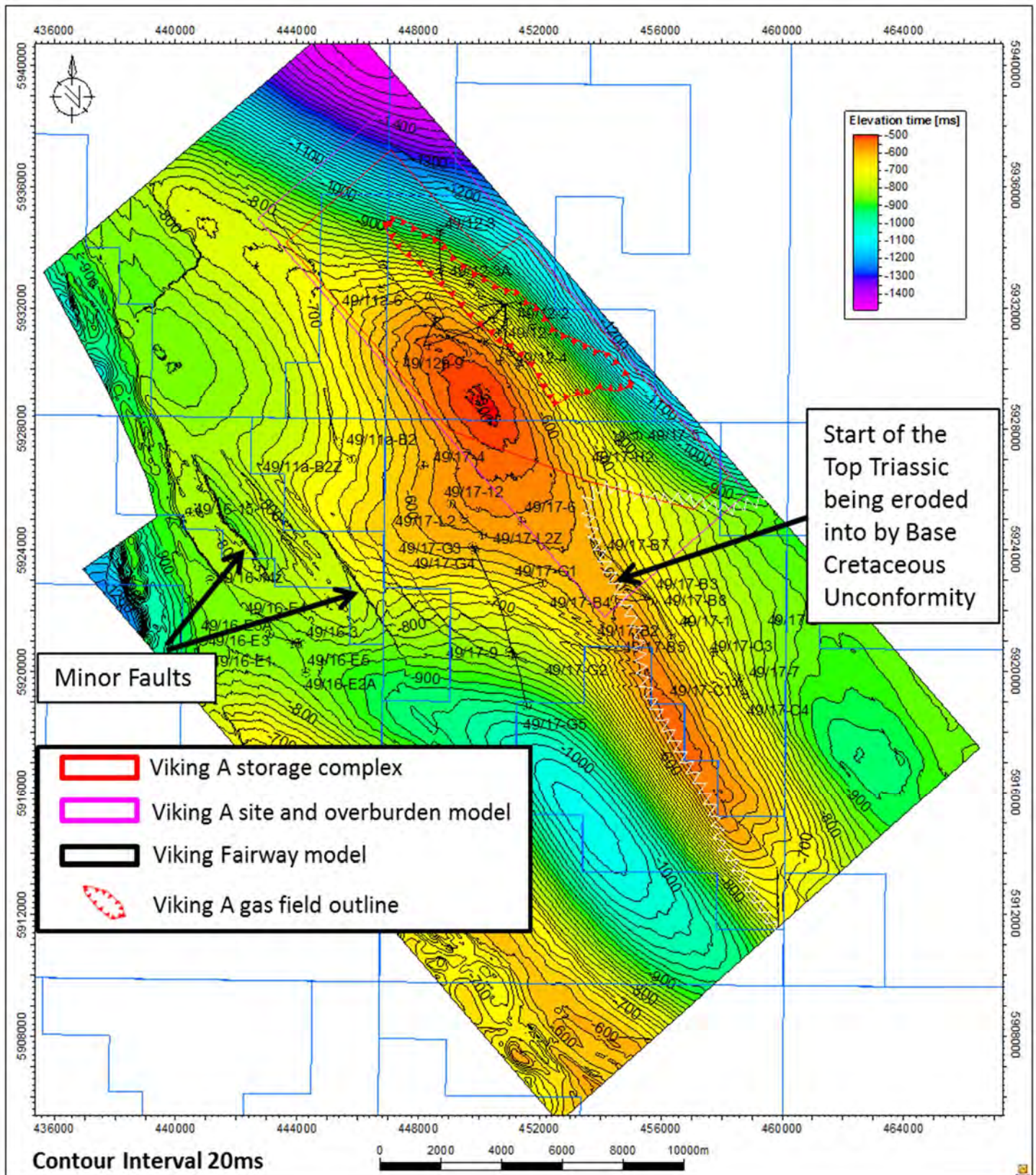


Figure 11-6 Base Chalk/ Base Cretaceous Unconformity Two-Way Time Map

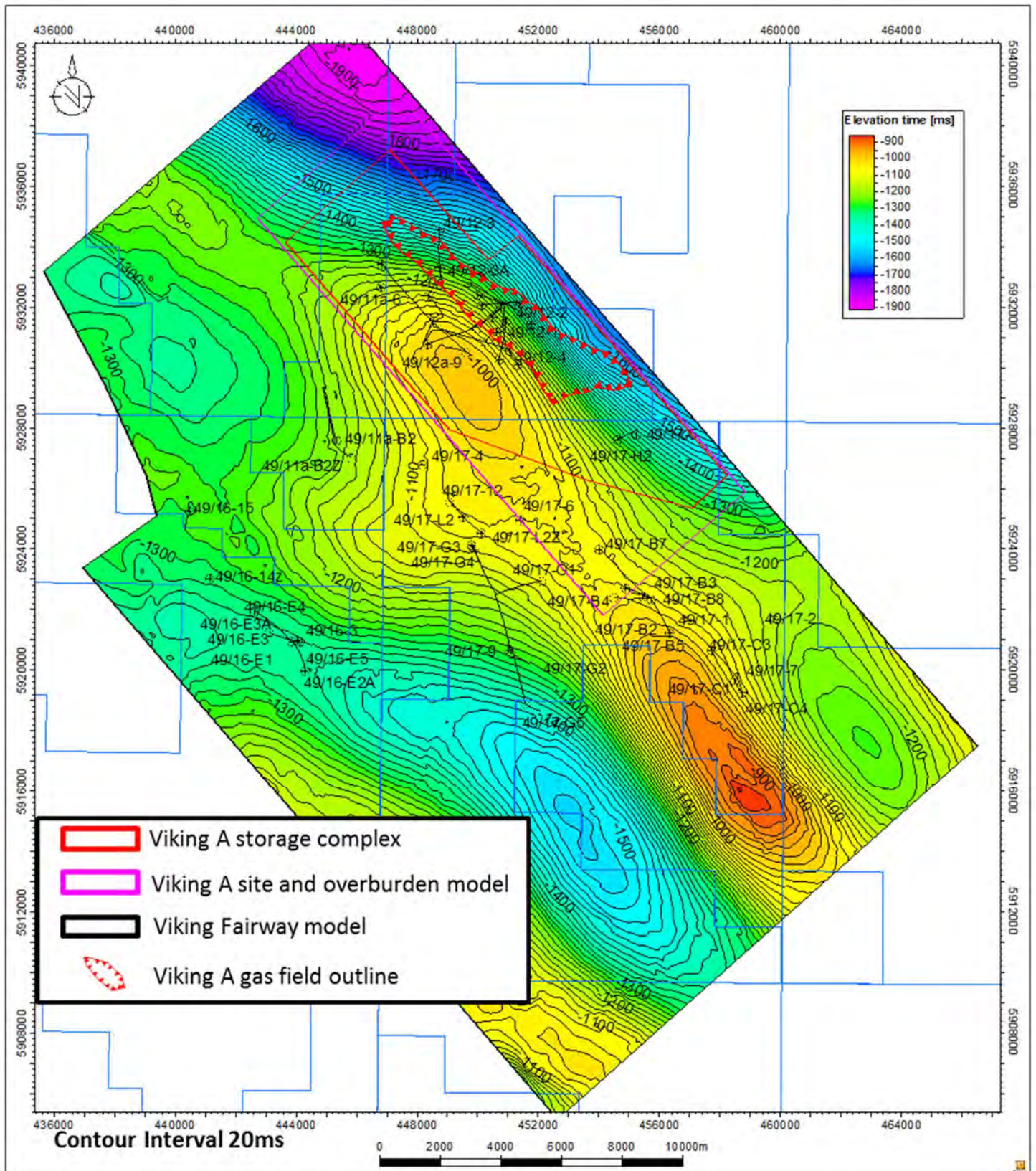


Figure 11-7 Top Triassic Two-Way Time Map

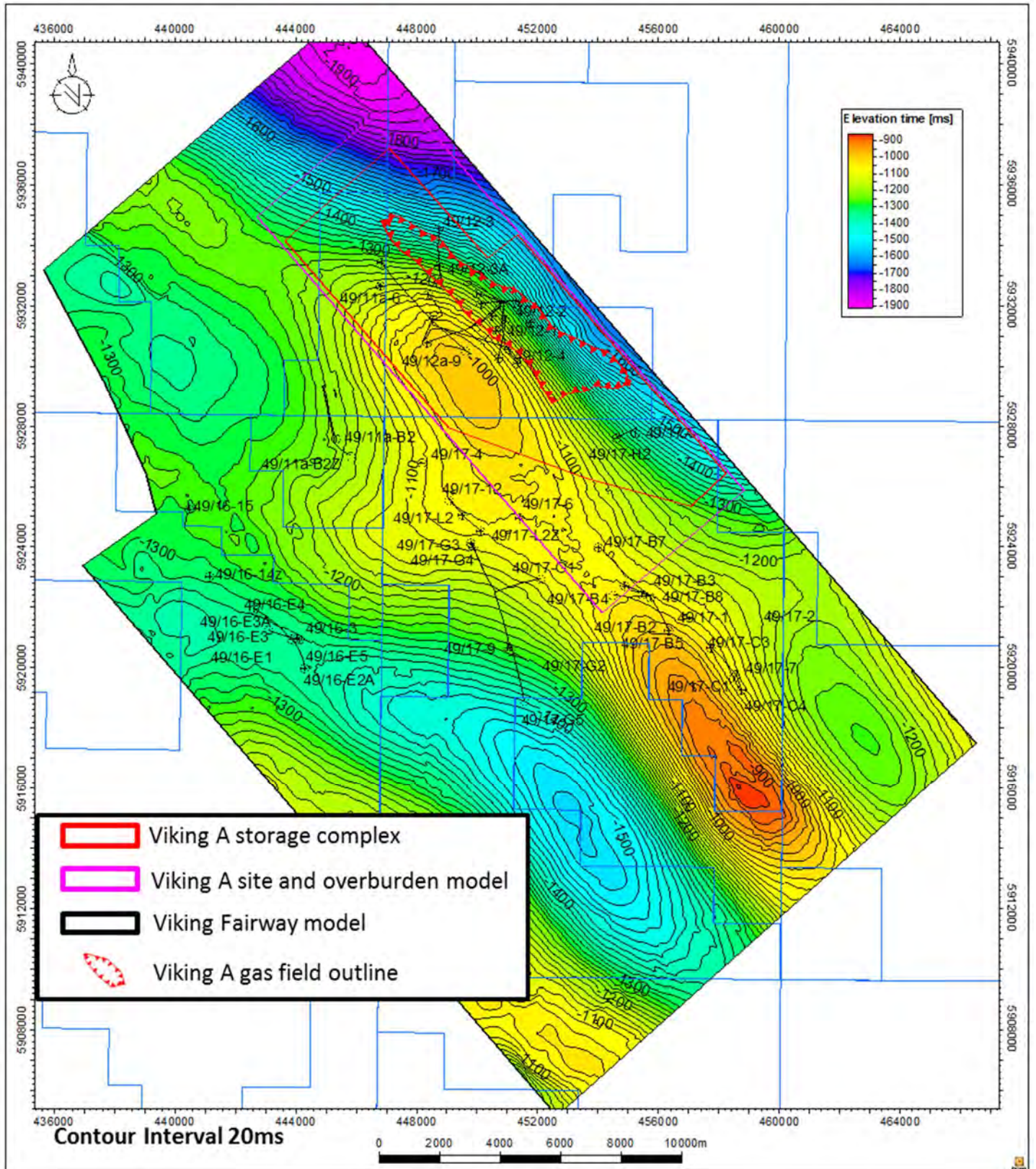


Figure 11-8 Top Bunter Sandstone Two-Way Time Map

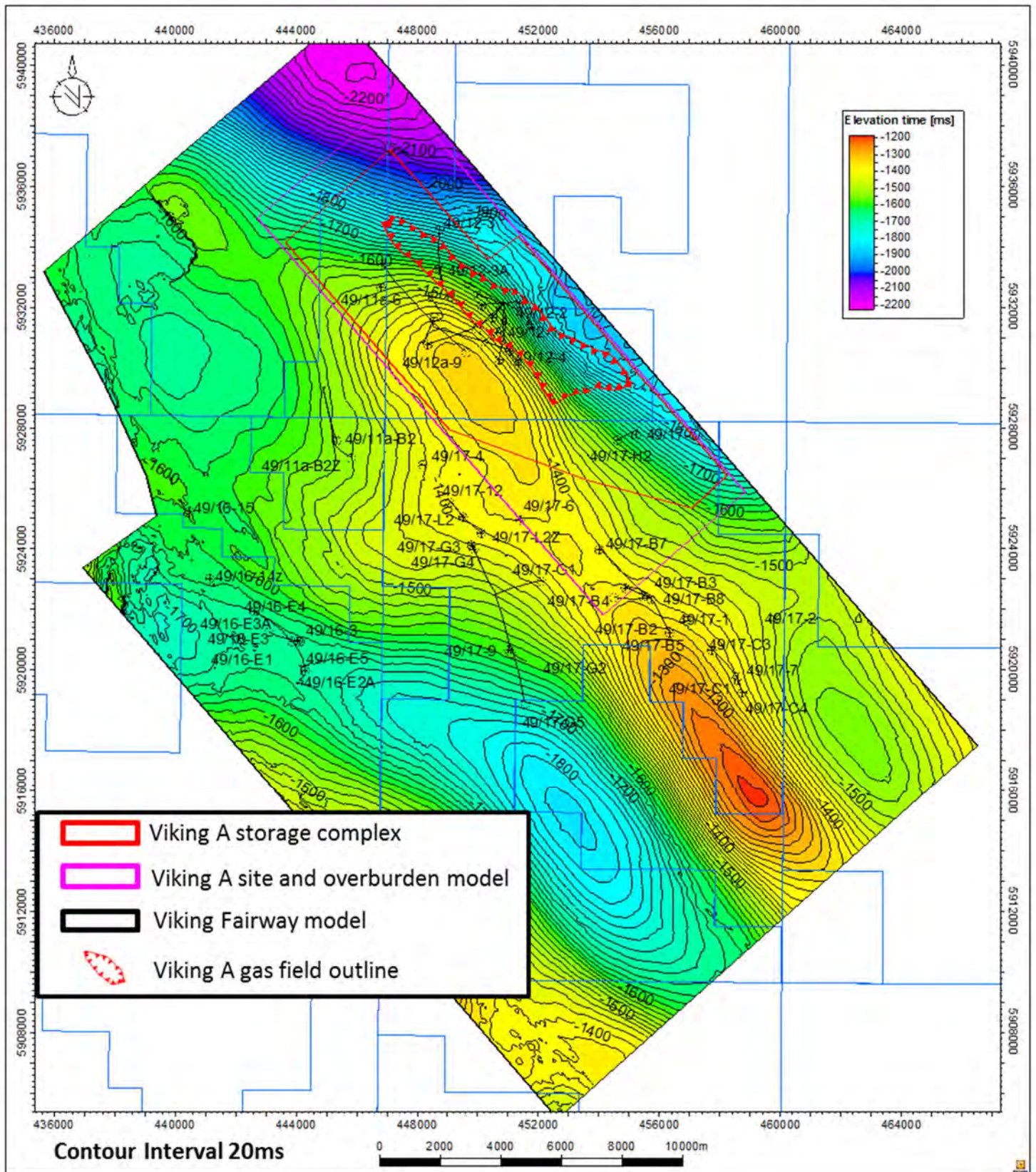


Figure 11-9 Top Zechstein Two-Way Time Map

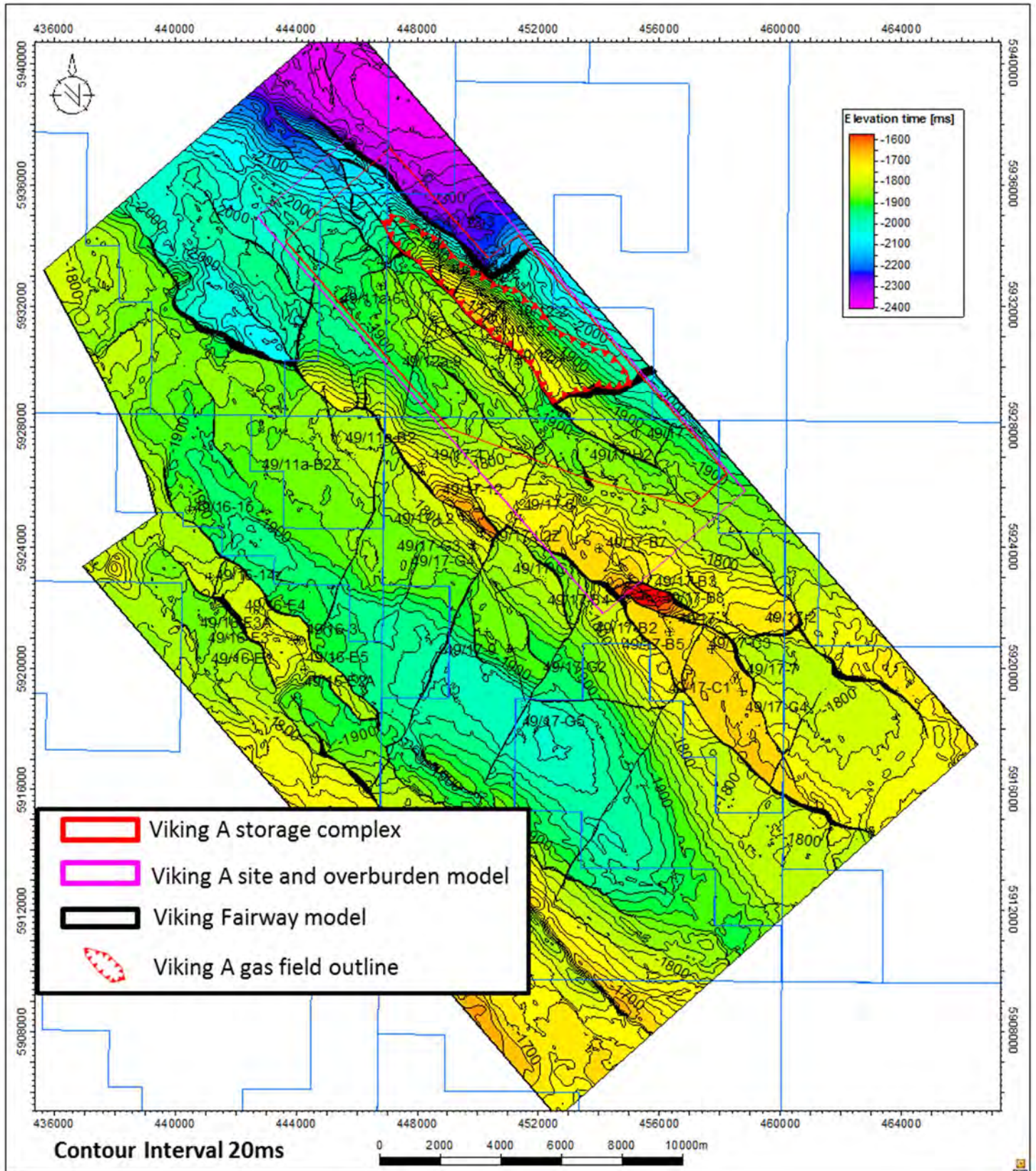


Figure 11-10 Top Lemn Sandstone Two-Way Time Map

11.4.2 Depth maps

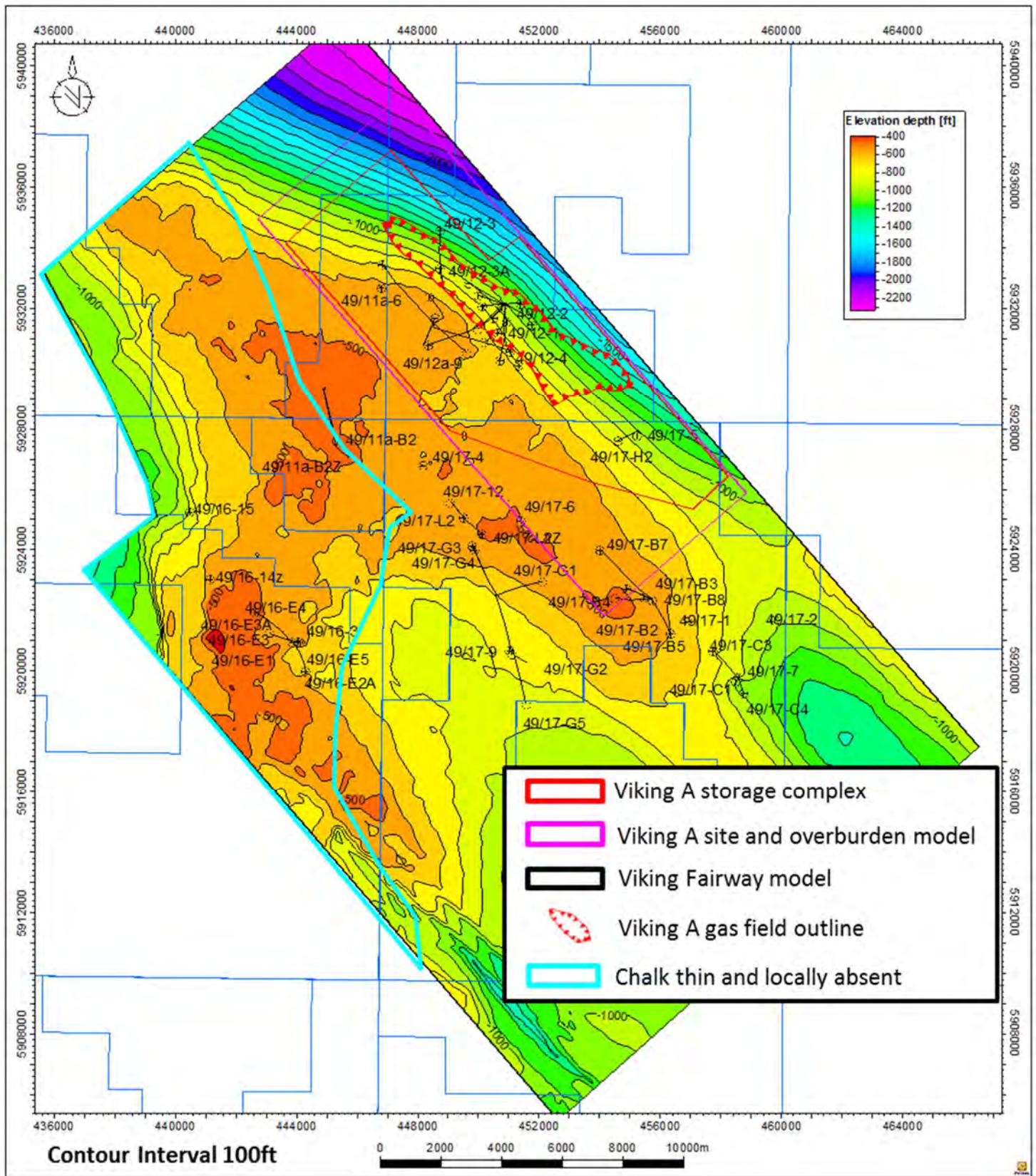


Figure 11-11 Top Chalk Depth Map

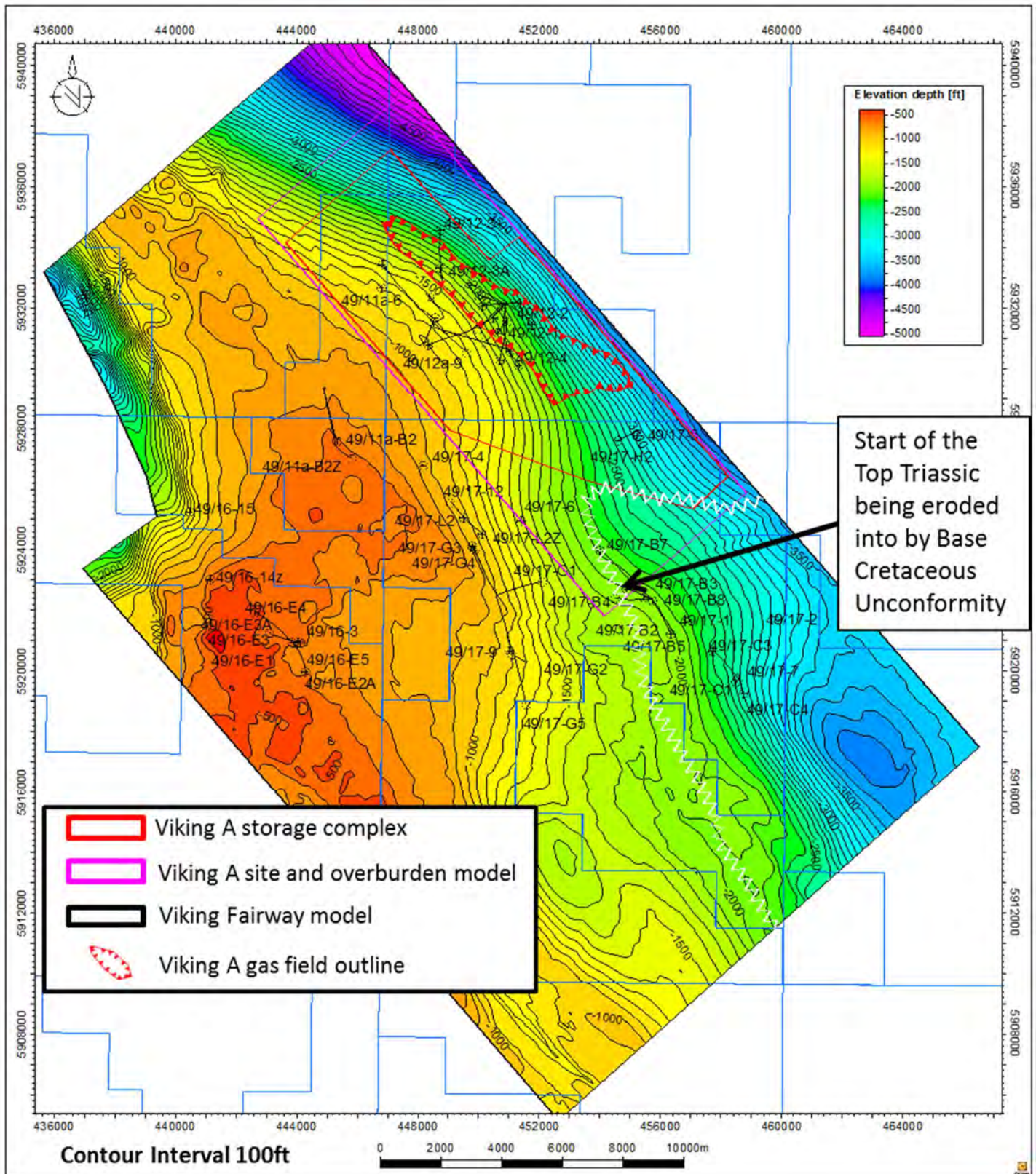


Figure 11-12 Base Chalk/Base Cretaceous Unconformity Depth Map

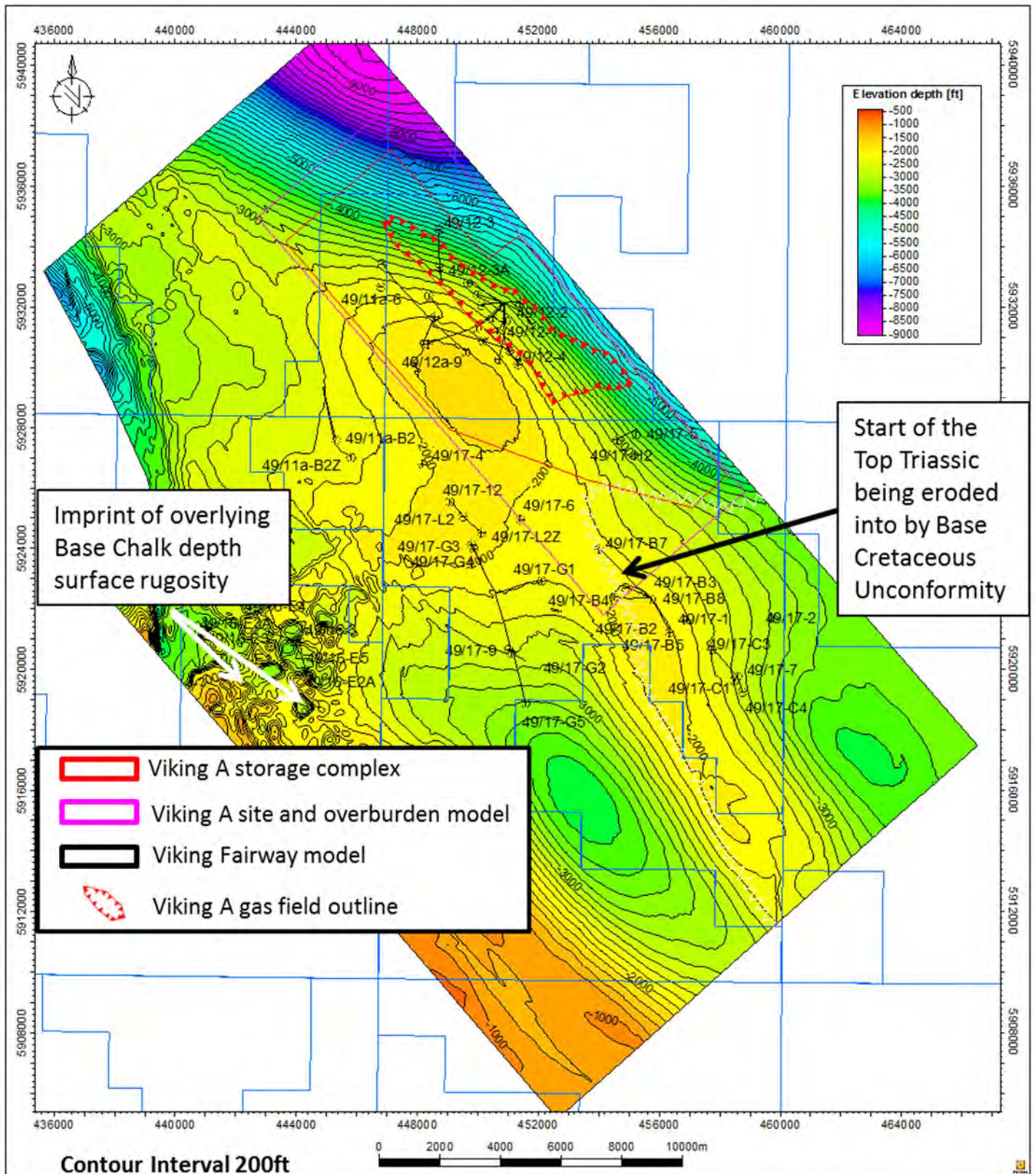


Figure 11-13 Top Triassic Depth Map

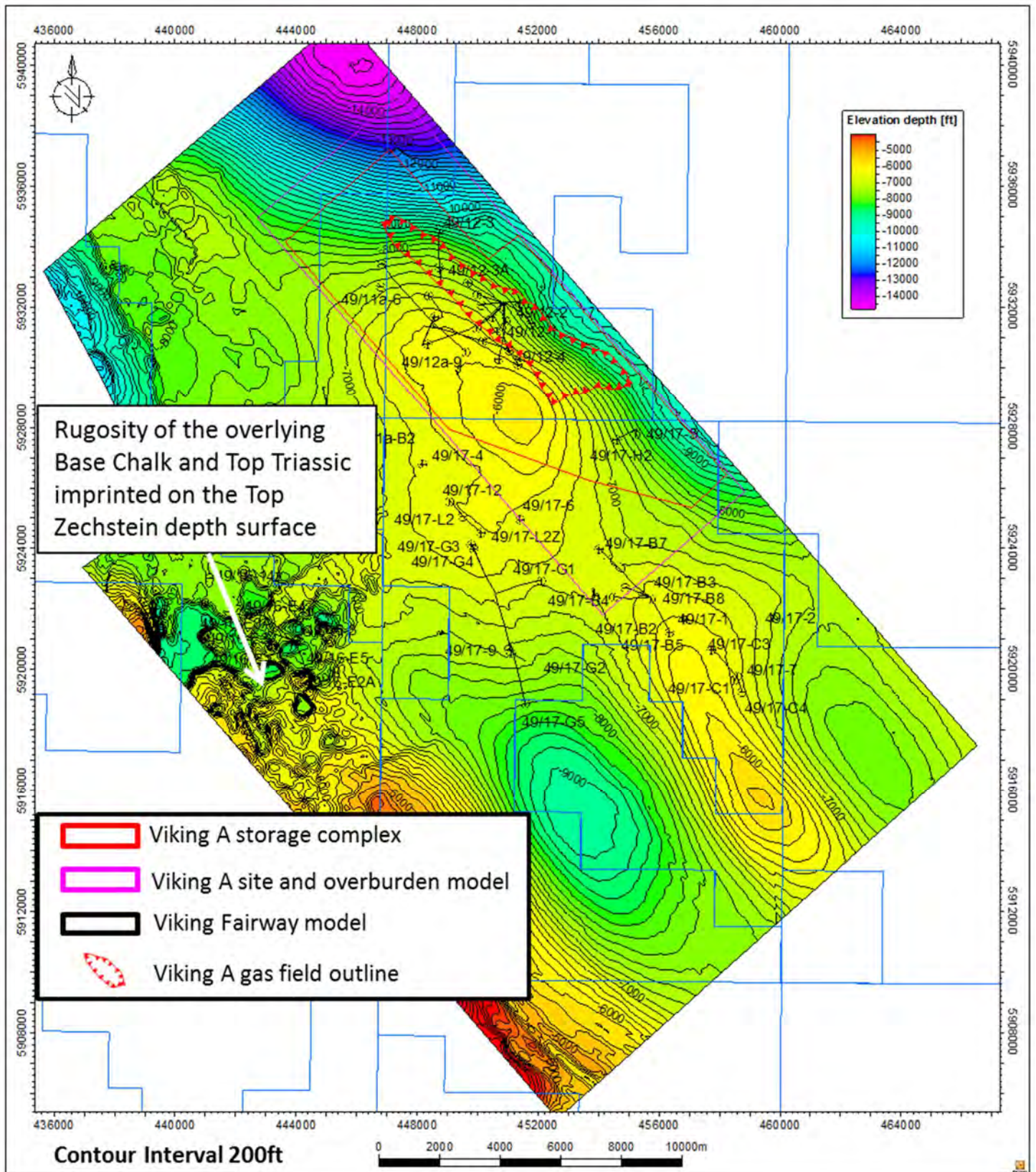
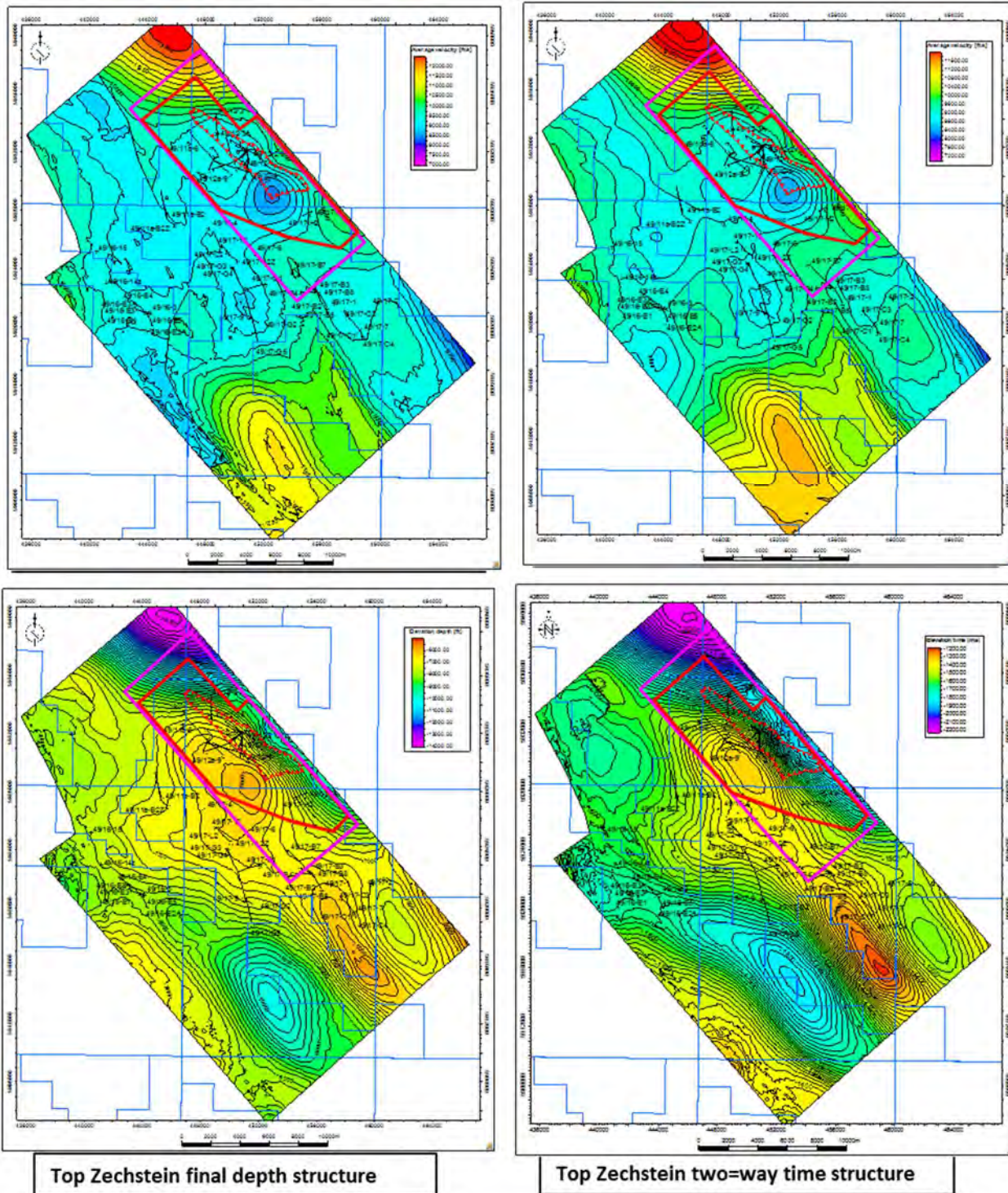


Figure 11-14 Top Zechstein raw Depth Map



- A. Average velocity grid from MSL to Top Zechstein is derived from the two-way time and raw depth grid
- B. Area of noise in the average velocity grid removed using a polygon and the surface is then regrided.
- C. Edited average velocity grid is then multiplied by the two-way time grid to give the final depth grid.
- D. Two-way time grid is shown along side for comparison.

Figure 11-15 Top Zechstein Depth Map Editing

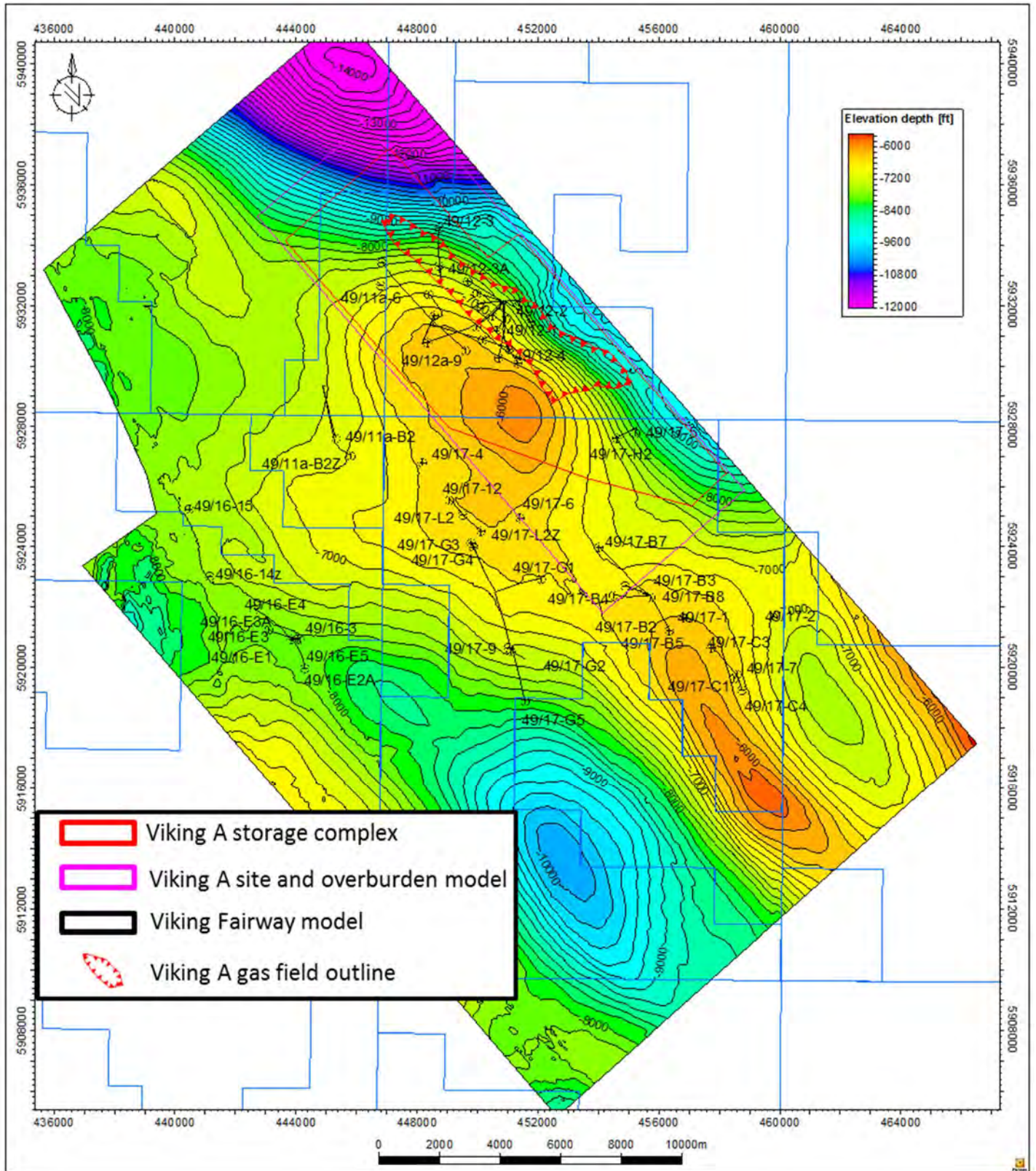


Figure 11-16 Top Zechstein Depth Map

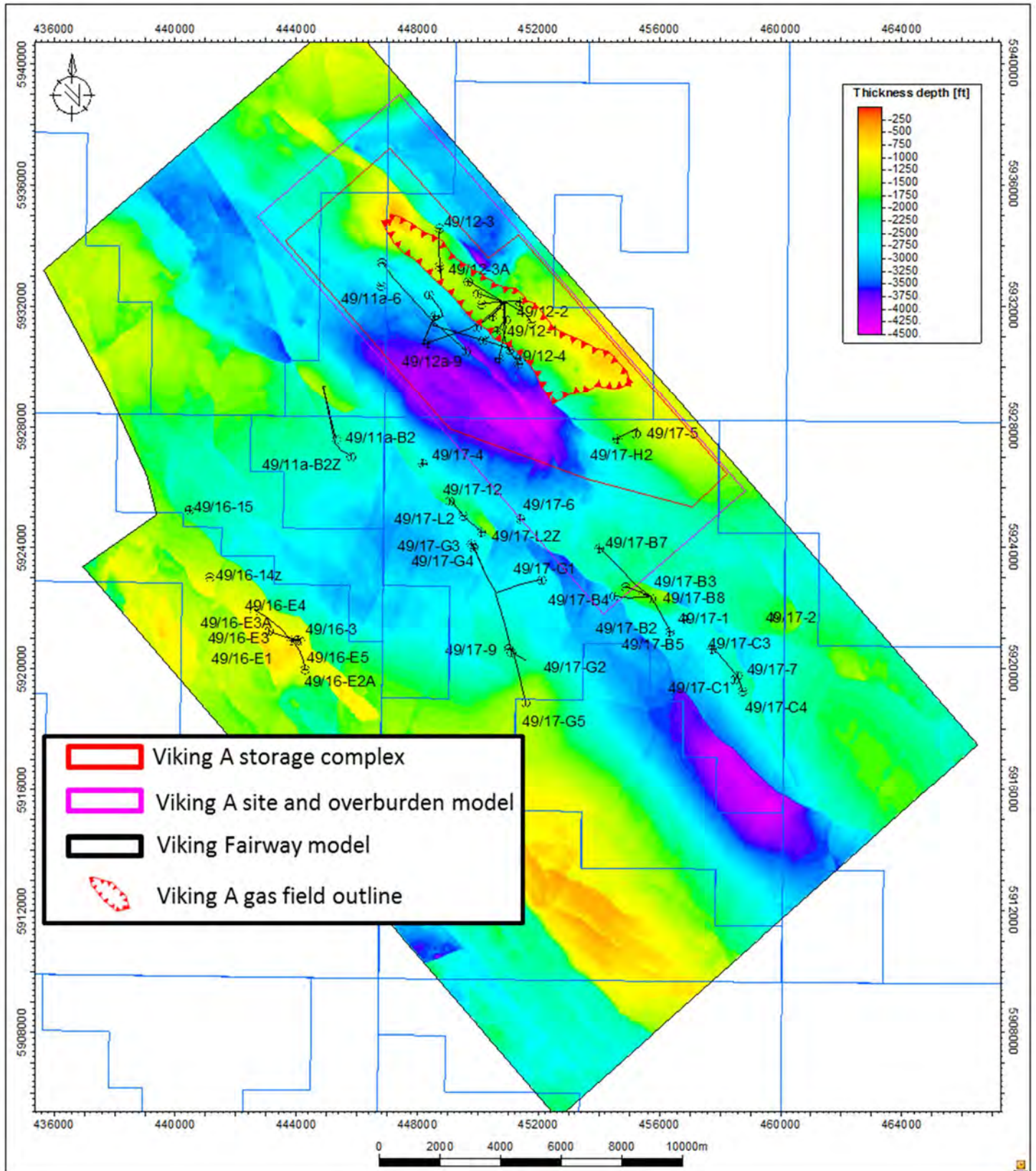


Figure 11-17 Zechstein Isochore

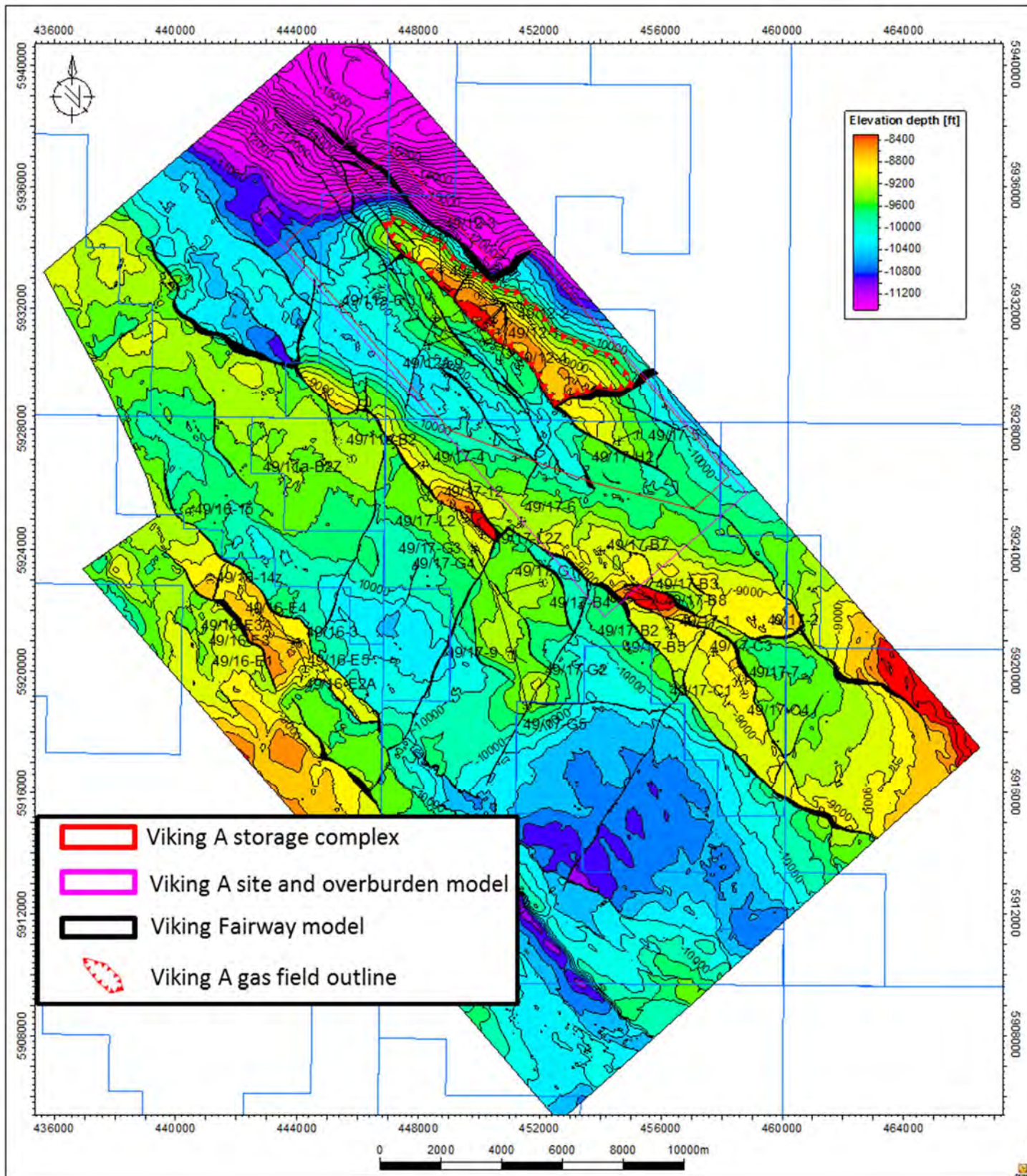


Figure 11-18 Top Leman Sandstone Depth Map

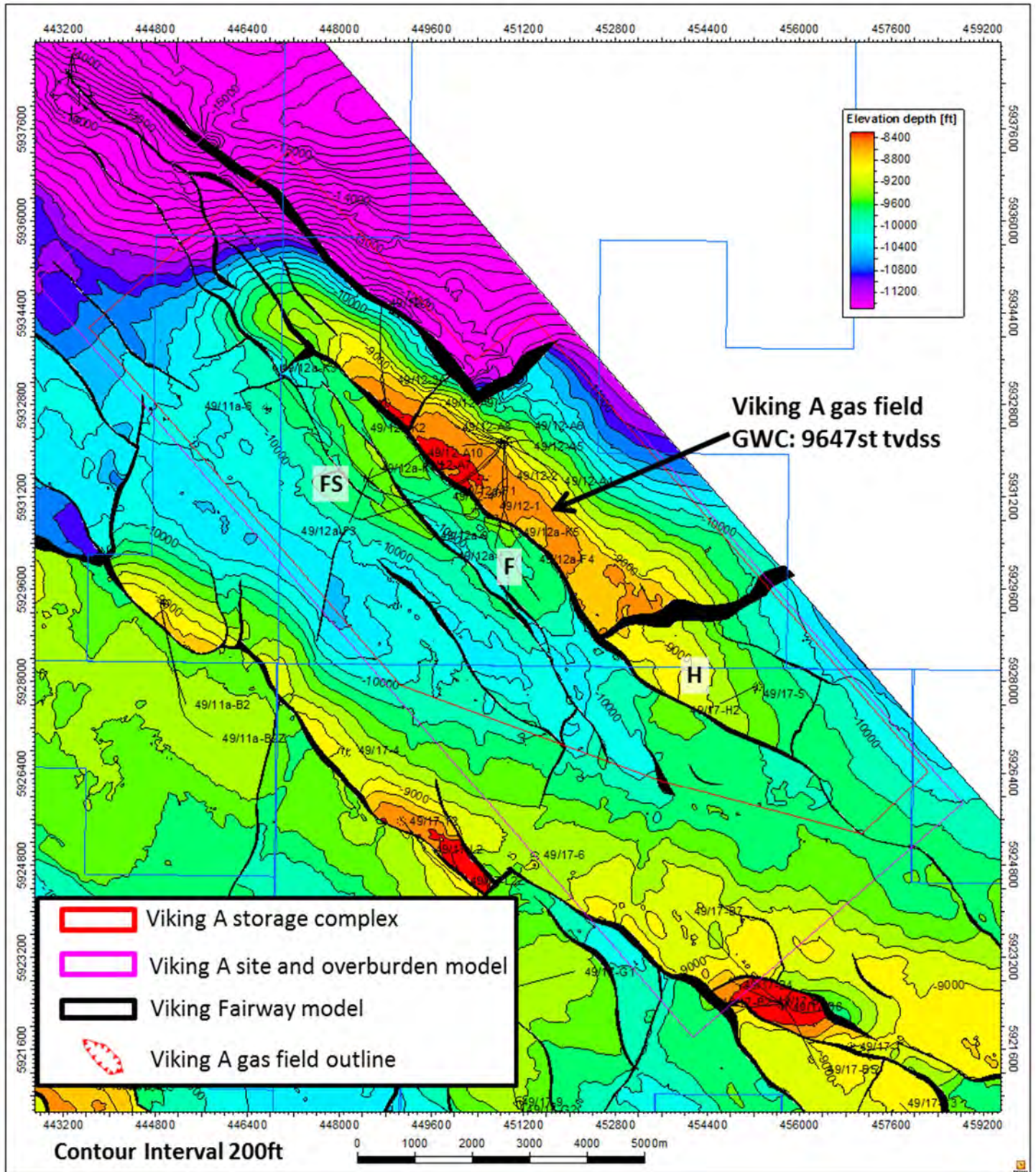


Figure 11-19 Viking A Top Lemman Sandstone Depth Map

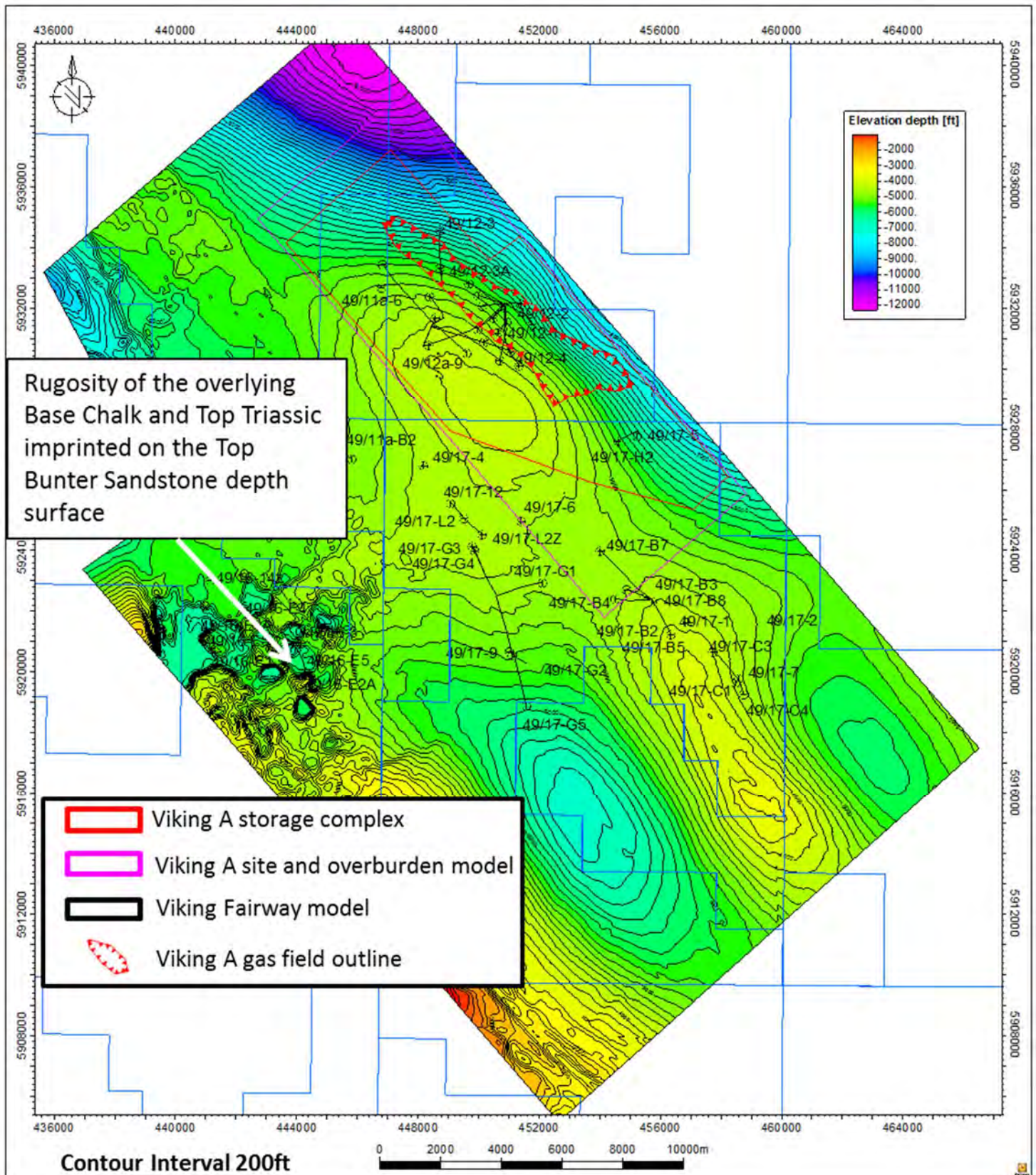
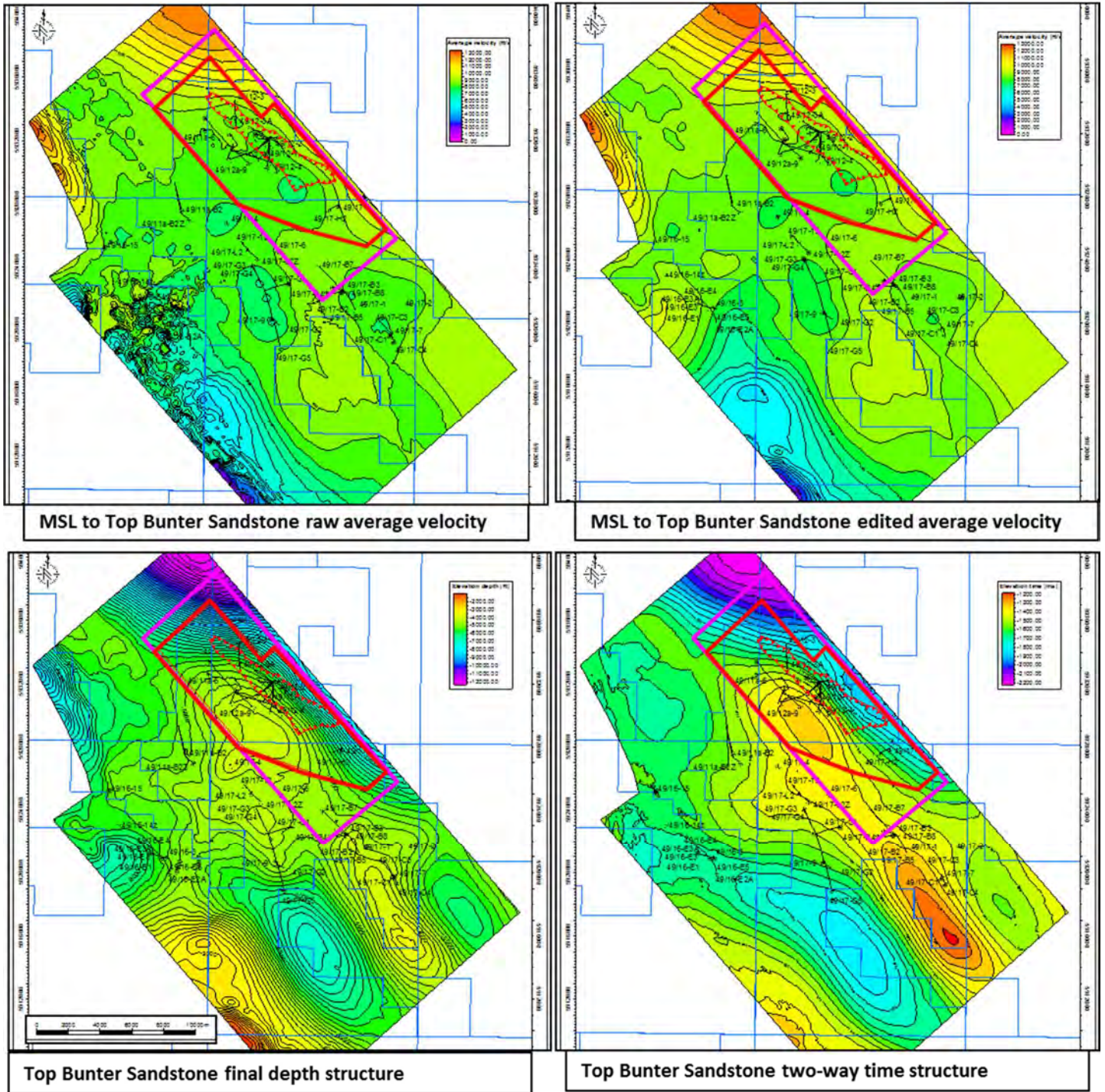


Figure 11-20 Top Bunter Sandstone Raw Depth Map



- A. Average velocity grid from MSL to Top Bunter Sandstone is derived from the two-way time and raw depth grid
- B. Area of noise in the average velocity grid removed using a polygon and the surface is then regridded.
- C. Edited average velocity grid is then multiplied by the two-way time grid to give the final depth grid.
- D. Two-way time grid is shown along side for comparison.

Figure 11-21 Top Bunter Sandstone Depth Map Editing

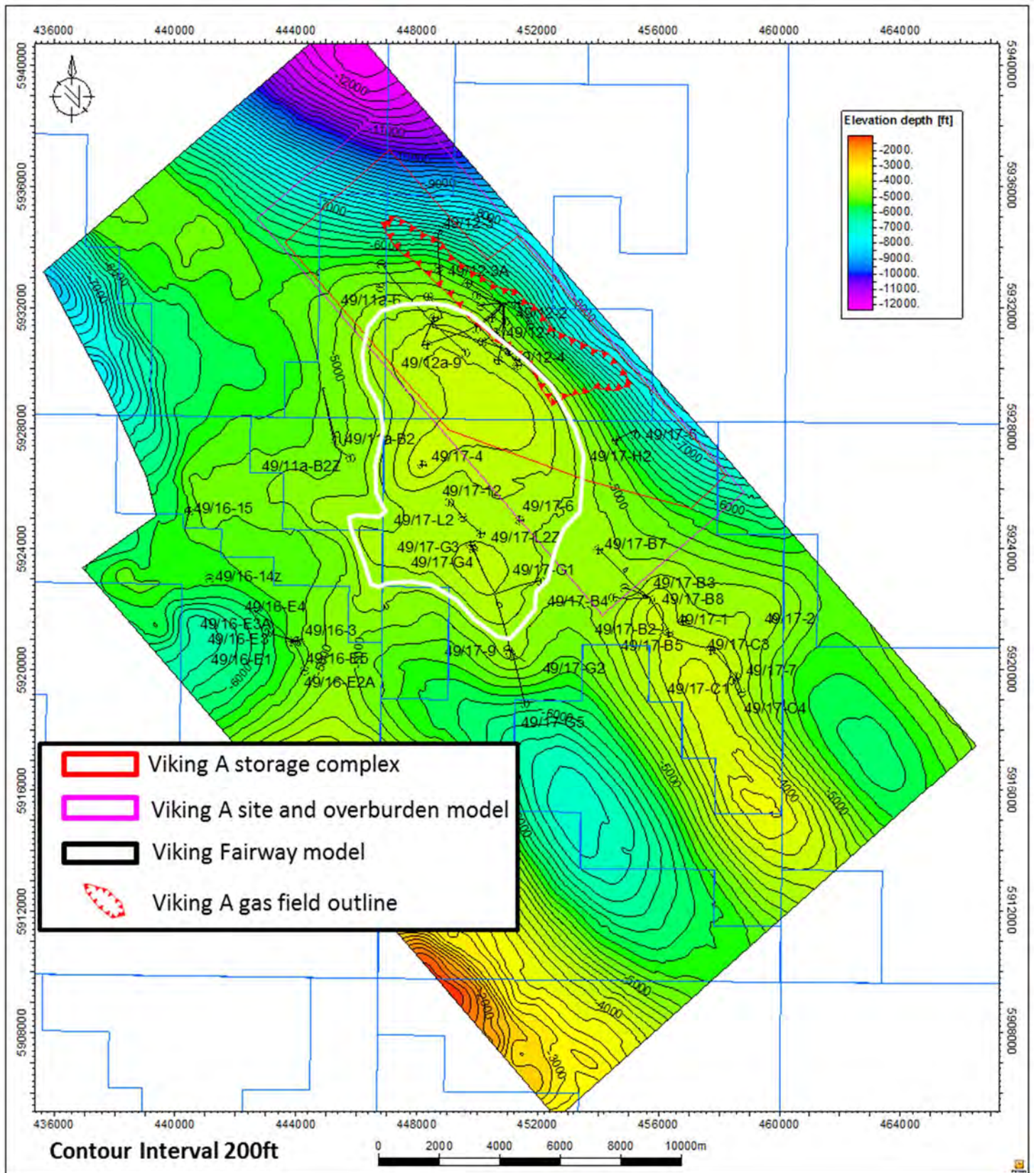


Figure 11-22 Top Bunter Sandstone Depth Map

11.4.3 CPI logs

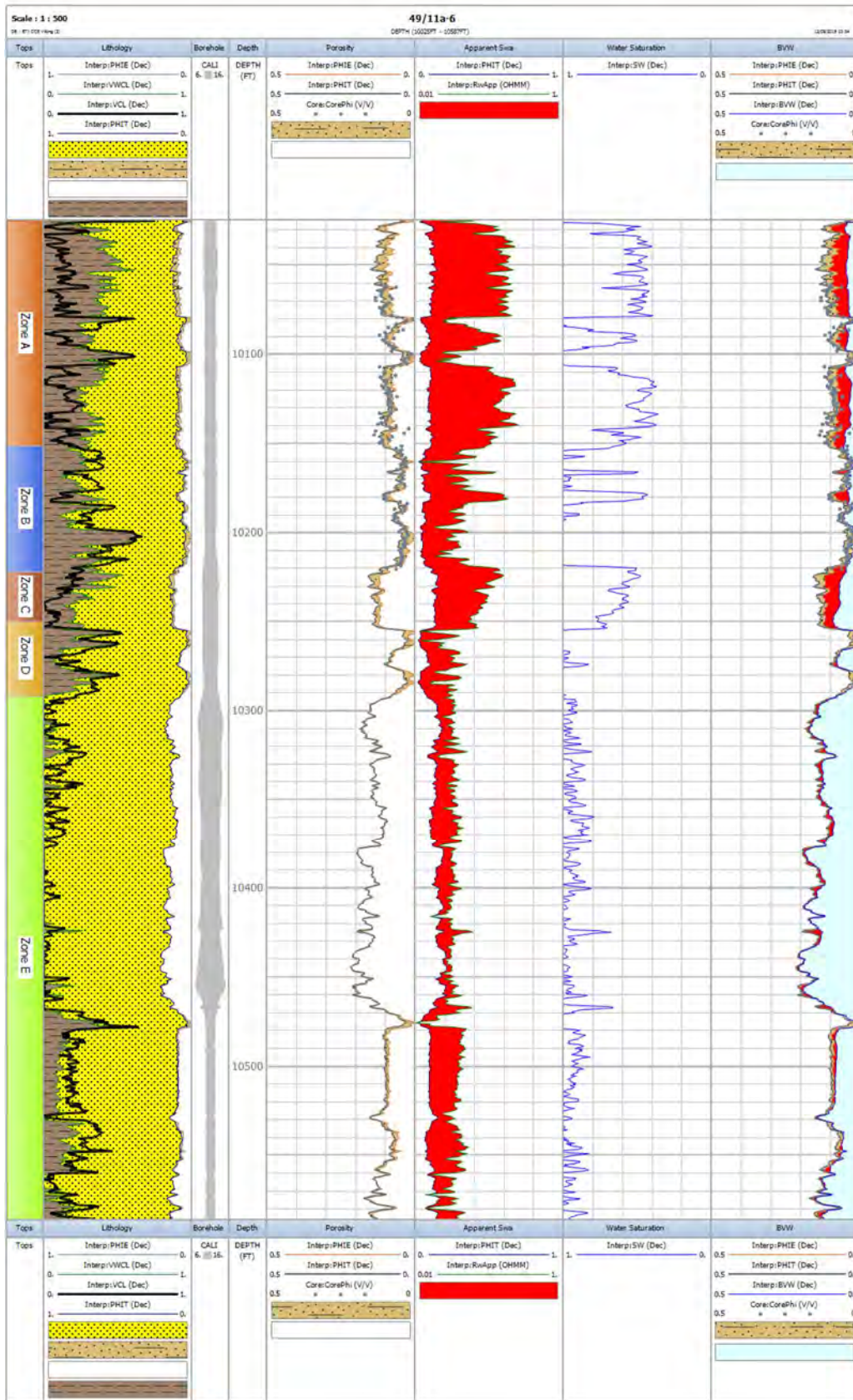


Figure 11-23 Well 49/11a-6 CPI

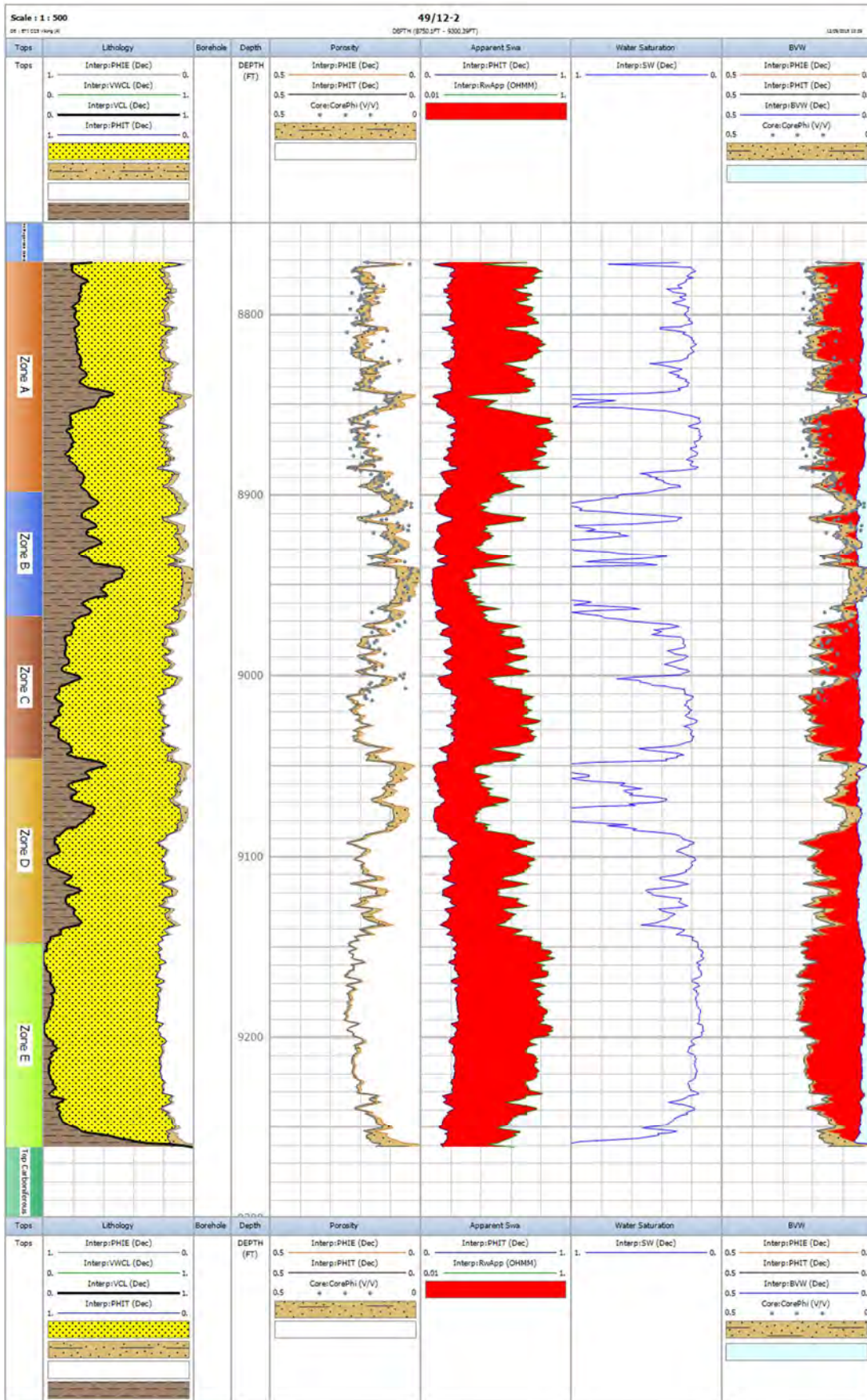


Figure 11-24 Well 49/12-2 CPI

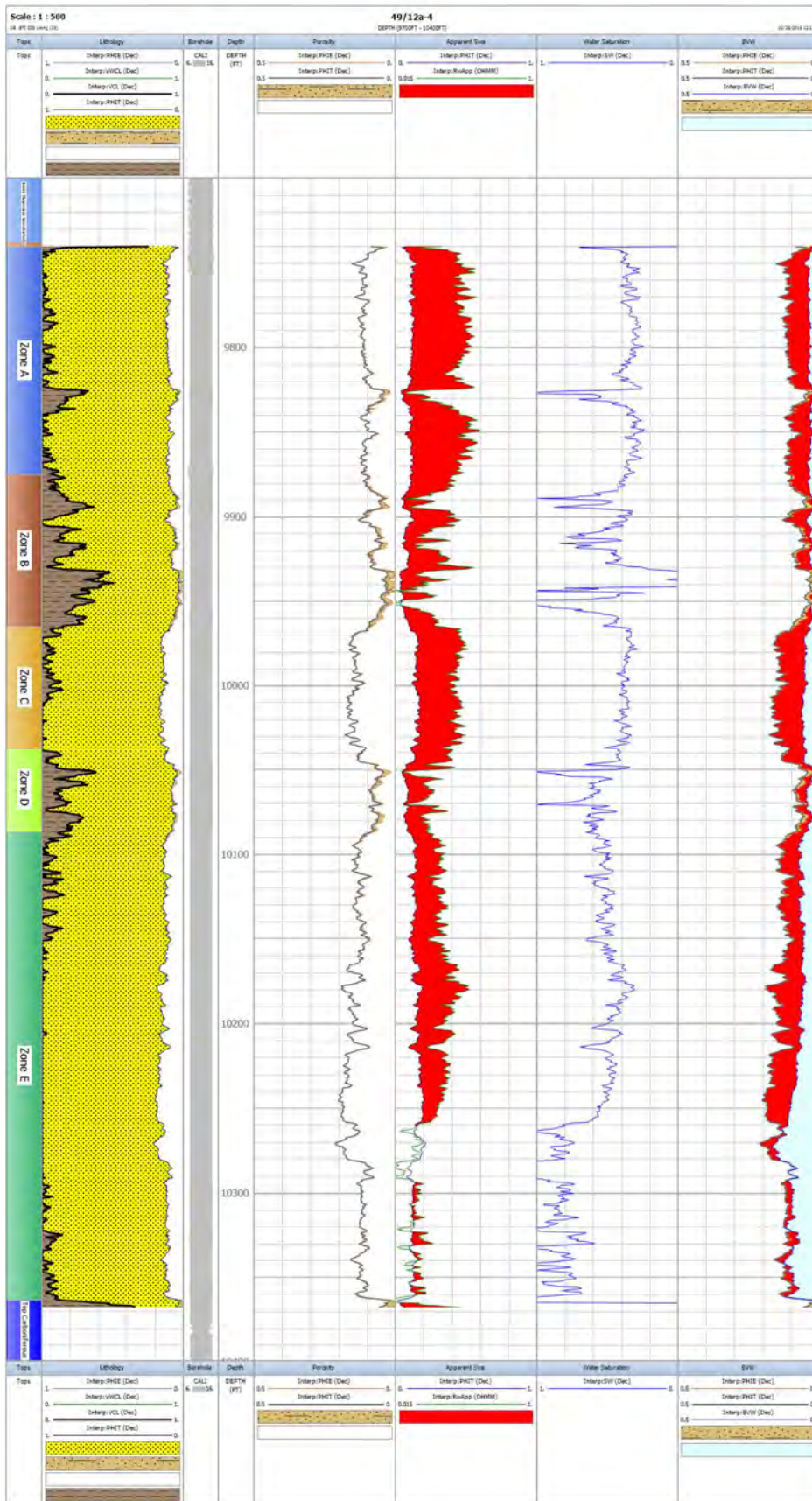


Figure 11-26 Well 49/12-4 CPI

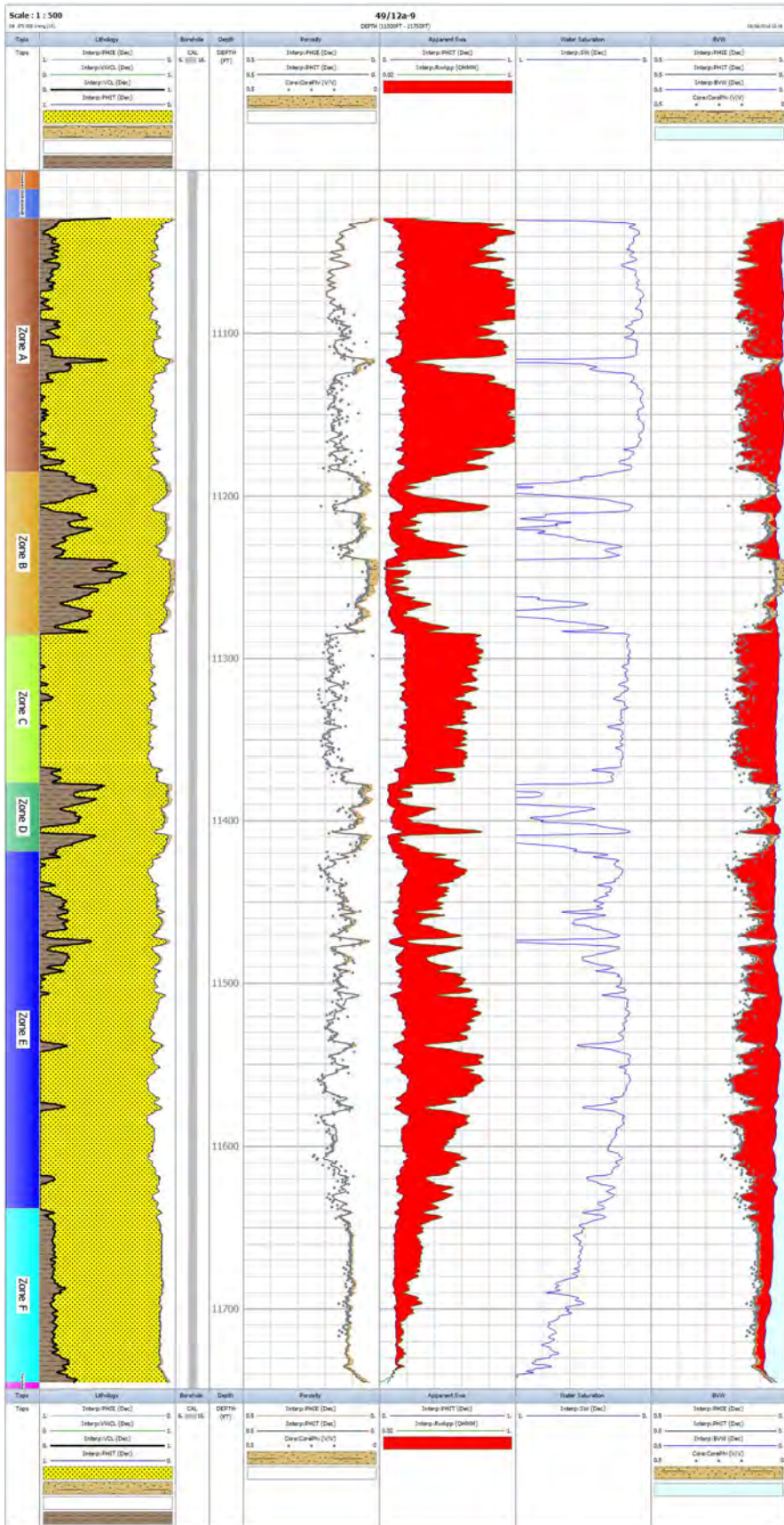


Figure 11-28 Well 49/12a-9 CPI

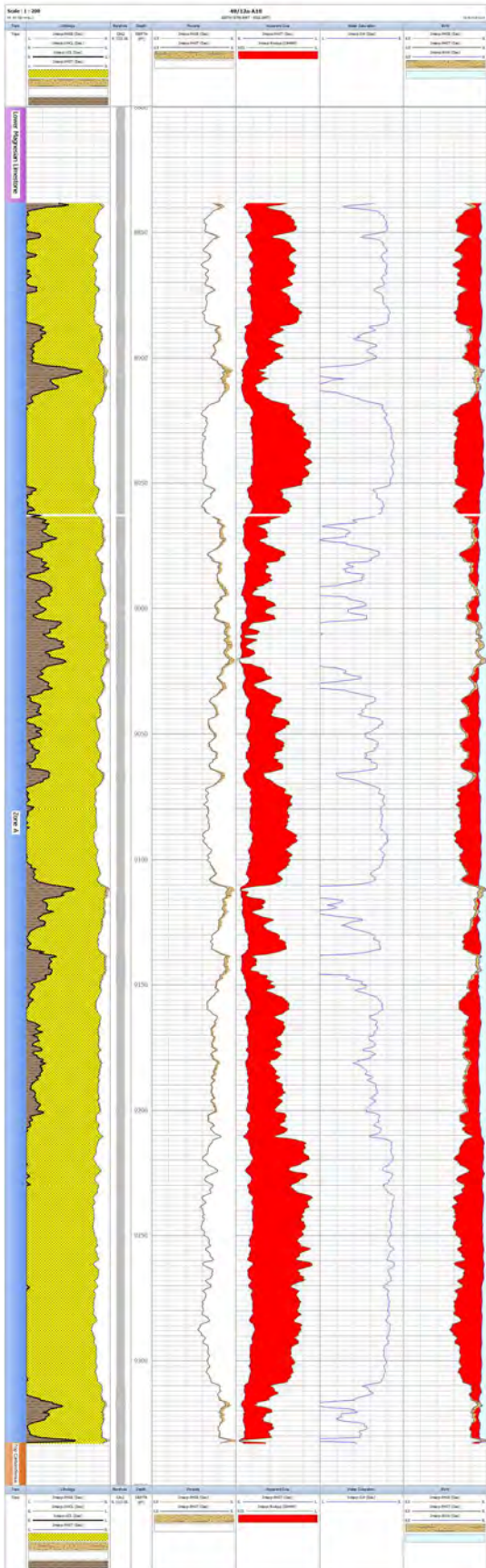


Figure 11-30 Well 14/12a-A10 CPI

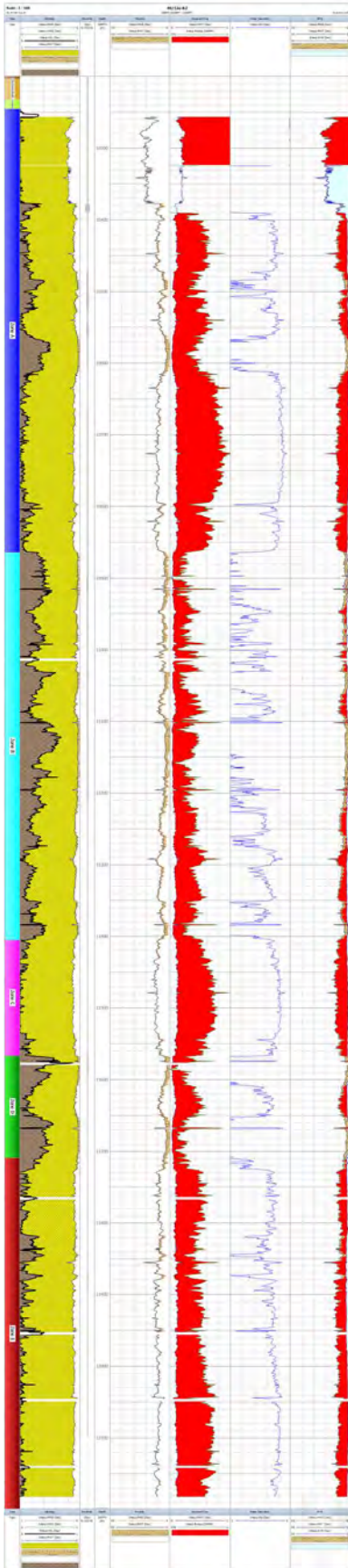


Figure 11-32 Well 49/12a-K2 CPI



Figure 11-33 Well 49/12a-K3 CPI

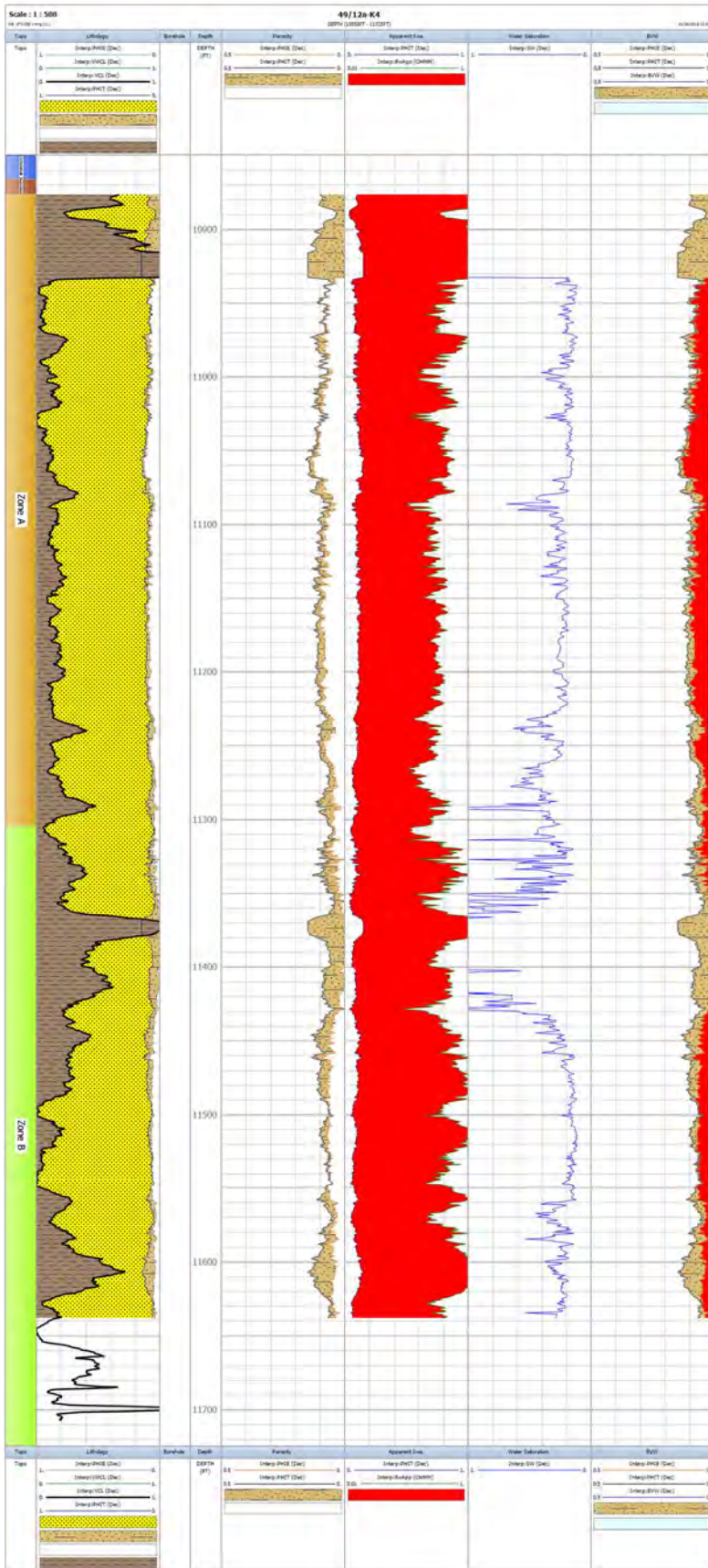


Figure 11-34 Well 49/12a-K4 CPI

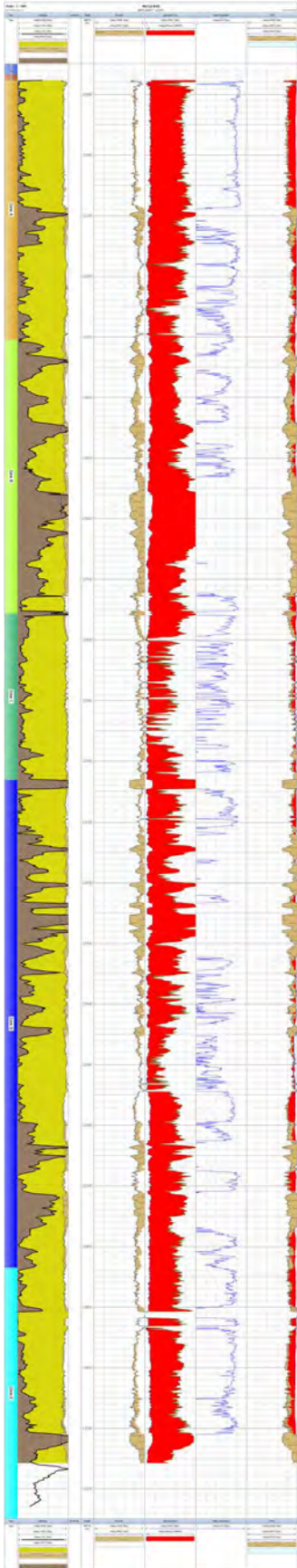


Figure 11-35 Well 49/12a-K4Z CPI

Well	Zone Name	Fault Block	Reservoir Summary				N/G	AvPhi	AvVcl
			Top [ft]	Bottom [ft]	Gross [ft]	Net [ft]			
49/11a-6	Zone A	Fs	10,025.0	10,151.0	126.0	53.8	0.427	0.089	0.113
49/12-2	Zone A	A	8,771.0	8,898.0	127.0	118.0	0.929	0.157	0.228
49/12-3	Zone A	A	9,098.5	9,236.5	138.0	125.5	0.909	0.154	0.038
49/12a-4	Zone A	Fs	9,740.5	9,875.0	134.5	118.3	0.879	0.110	0.027
49/12a-8	Zone A		11,082.0	11,518.0	436.0	166.8	0.382	0.129	0.096
49/12a-9	Zone A	Fs	11,029.0	11,185.0	156.0	144.4	0.925	0.155	0.057
49/12a-A10	Zone A	A	8,838.0	9,329.0	491.0	418.0	0.851	0.149	0.055
49/12a-A6	Zone A	A	9,750.0	9,902.0	152.0	127.3	0.837	0.150	0.137
49/12a-F1	Zone A	F	10,688.0	10,814.0	126.0	103.5	0.822	0.113	0.097
49/12a-K2	Zone A	F	10,245.0	10,864.0	619.0	436.5	0.705	0.128	0.050
49/12a-K3	Zone A	Fs	11,451.0	11,624.0	173.0	125.9	0.728	0.101	0.089
49/12a-K4	Zone A	Fs	10,876.5	11,304.0	427.5	189.0	0.442	0.094	0.132
49/12-K4Z	Zone A	F	10,876.0	11,304.0	428.0	172.5	0.403	0.095	0.077
49/11a-6	Zone B	Fs	10,151.0	10,222.0	71.0	7.0	0.099	0.086	0.185
49/12-2	Zone B	A	8,898.0	8,967.5	69.5	19.0	0.273	0.109	0.293
49/12-3	Zone B	A	9,236.5	9,298.5	62.0	26.5	0.427	0.101	0.141
49/12a-4	Zone B	Fs	9,875.0	9,965.0	90.0	25.0	0.278	0.094	0.097
49/12a-9	Zone B	Fs	11,185.0	11,285.0	100.0	28.5	0.285	0.117	0.132
49/12a-A6	Zone B	A	9,902.0	9,950.0	48.0	28.8	0.599	0.123	0.158
49/12a-F1	Zone B	F	10,814.0	10,879.0	65.0	8.1	0.124	0.099	0.120
49/12a-K2	Zone B	F	10,864.0	11,405.0	541.0	63.9	0.118	0.095	0.100
49/12a-K3	Zone B	Fs	11,624.0	11,804.0	180.0	39.0	0.217	0.103	0.122
49/12a-K4	Zone B	Fs	11,304.0	11,707.0	403.0	3.0	0.007	0.087	0.234
49/12-K4Z	Zone B	F	11,304.0	11,756.0	452.0	9.0	0.020	0.087	0.121
49/11a-6	Zone C	Fs	10,222.0	10,250.0	28.0	28.0	1.000	0.116	0.115
49/12-2	Zone C	A	8,967.5	9,046.0	78.5	75.7	0.964	0.165	0.140
49/12-3	Zone C	A	9,298.5	9,387.5	89.0	85.5	0.961	0.136	0.053
49/12a-4	Zone C	Fs	9,965.0	10,037.0	72.0	72.0	1.000	0.145	0.037
49/12a-9	Zone C	Fs	11,285.0	11,377.0	92.0	92.0	1.000	0.176	0.018
49/12a-A6	Zone C	A	9,950.0	9,988.0	38.0	8.5	0.224	0.112	0.131
49/12a-F1	Zone C	F	10,879.0	10,956.0	77.0	65.0	0.844	0.115	0.095
49/12a-K2	Zone C	F	11,405.0	11,567.0	162.0	150.4	0.928	0.111	0.042
49/12a-K3	Zone C	Fs	11,804.0	11,959.0	155.0	132.4	0.854	0.114	0.092
49/12-K4Z	Zone C	F	11,756.0	12,031.0	275.0	1.0	0.004	0.091	0.059
49/11a-6	Zone D	Fs	10,250.0	10,292.0	42.0	8.0	0.190	0.100	0.110
49/12-2	Zone D	A	9,046.0	9,148.0	102.0	78.2	0.767	0.154	0.149
49/12-3	Zone D	A	9,387.5	9,425.5	38.0	11.5	0.303	0.122	0.097
49/12a-4	Zone D	Fs	10,037.0	10,087.0	50.0	13.8	0.275	0.108	0.072
49/12a-9	Zone D	Fs	11,377.0	11,419.0	42.0	11.3	0.268	0.104	0.100
49/12a-A6	Zone D	A	9,988.0	10,057.0	69.0	48.3	0.699	0.137	0.188
49/12a-F1	Zone D	F	10,956.0	11,030.0	74.0	51.9	0.702	0.110	0.106
49/12a-K2	Zone D	F	11,567.0	11,709.0	142.0	13.5	0.095	0.091	0.099
49/12a-K3	Zone D	Fs	11,959.0	12,069.0	110.0	19.5	0.177	0.096	0.140
49/12-K4Z	Zone D	F	12,031.0	12,835.0	804.0	65.5	0.081	0.092	0.070
49/11a-6	Zone E	Fs	10,292.0	10,587.0	295.0	265.8	0.901	0.134	0.096
49/12-2	Zone E	A	9,148.0	9,261.0	113.0	107.7	0.953	0.201	0.069
49/12-3	Zone E	A	9,425.5	9,592.5	167.0	161.0	0.964	0.133	0.018
49/12a-4	Zone E	Fs	10,087.0	10,363.0	276.0	273.5	0.991	0.138	0.022
49/12a-9	Zone E	Fs	11,419.0	11,638.0	219.0	214.8	0.981	0.152	0.044
49/12a-A6	Zone E	A	10,057.0	10,294.5	237.5	185.5	0.781	0.150	0.142
49/12a-F1	Zone E	F	11,030.0	11,233.0	203.0	195.4	0.962	0.141	0.033
49/12a-K2	Zone E	F	11,709.0	12,182.0	473.0	362.6	0.767	0.104	0.044
49/12a-K3	Zone E	Fs	12,069.0	14,103.5	2,034.5	1,680.5	0.826	0.116	0.126
49/12-K4Z	Zone E	F	12,835.0	13,229.0	394.0	114.5	0.291	0.091	0.111

Figure 11-36 Petrophysical summary for all zones

11.5 Appendix 5 – MMV Technologies

Monitoring, measurement and verification (MMV) of any CO₂ storage site in the United Kingdom Continental Shelf (UKCS) is required under the EU CCS Directive (The European Parliament And The Council Of The European Union, 2009) and its transposition into UK Law through the Energy Act (Energy Act, Chapter 32, 2008). A comprehensive monitoring plan is an essential part of the CO₂ Storage Permit.

The four main purposes of monitoring a CO₂ storage site are to:

- Confirm that the actual behaviour of the injected CO₂ conforms with the modelled behaviour.
- Confirm that there is no detectable leakage from the storage reservoir and defined storage complex.
- Confirm that the storage site will permanently contain the injected CO₂.
- Acquire data to update reservoir models to refine future CO₂ behaviour predictions.

The storage site has been carefully selected to ensure secure containment of the CO₂ and so loss of containment is not expected. A site monitoring plan needs to prove that the integrity of the store has not been compromised and build confidence that the store is behaving as predicted.

The monitoring plan is based on a risk assessment of the storage site and is designed to prevent risks, or mitigate them, should they occur. The plan is also dynamic, meaning that it will be updated throughout the life of the project as new data are acquired, or perhaps as new technologies become commercial.

The two elements of the monitoring plan are discussed in the following sections:

- Base Case monitoring plan.
- Corrective measures plan.

11.5.1.1 Base Case Monitoring Plan

The base case plan is one that is scheduled and consists of baseline, operational and post-closure monitoring activity.

Baseline monitoring is carried out prior to injection and provides a baseline against which to compare all future results to. Since all future results will be compared to these pre-injection data, it is very important to ensure a thorough understanding of what the baseline is so that any possible deviations from it can be detected with greater confidence.

Operational monitoring is carried out during injection and to ensure that the CO₂ is contained and that the injection process and performance of the store is as expected. Data acquired from this monitoring phase will be used to update and history match existing reservoir models. The data will also be used to revise and update the risk assessment. Data such as flow, pressure and temperature at injection wellheads will be used for quantification of the injected CO₂ for accounting and reporting under the EU Emissions Trading Scheme (The European Parliament and the Council of the European Union, 2012).

As part of the storage permit application, the monitoring plan should include surface facilities and equipment process monitoring to demonstrate that the pipeline and facilities are operating as designed.

Post-closure monitoring takes place after cessation of injection with the primary purpose to confirm that the storage site is behaving as expected. Within the UK the anticipated requirement is for 20 years of post-closure monitoring, after which time the Department of Energy and Climate Change (DECC), or their

successor will take on the storage liabilities, assuming the site shows conformance. A post-closure baseline will be carried out prior to post-closure monitoring for all future results to be compared against.

Post-handover monitoring may be required in the UK by DECC following handover of the storage liabilities. This would likely be negotiated between the CO₂ Storage Operator and DECC during the post-closure monitoring phase.

As discussed above, the monitoring plan is dynamic and will be updated and revised with data collected and interpreted from the monitoring activities. The plan will also be updated if new CO₂ sources are to be injected into the storage site or if there are significant deviations from previous modelling as a result of history matching.

Annual reporting to DECC will include information about site performance and may include commentary around any site-specific monitoring challenges that have occurred.

11.5.1.2 Corrective Measures Plan

The corrective measures plan is deployed in case of detection of a 'significant irregularity' in the monitoring data, or leakage, and includes additional monitoring to further identify the irregularity and remediation options should they be required.

A 'significant irregularity' is defined in the CCS Directive as:

“any irregularity in the injection or storage operations or in the condition of the storage complex itself, which implies the risk of a leakage or risk to the environment or human health.”

Corrective measures are defined in the CCS Directive as:

“any measures taken to correct significant irregularities or to close leakages in order to prevent or stop the release of CO₂ from the storage complex.”

The four main parts to the corrective measures plan are:

- Additional monitoring to understand the irregularity and gather additional data;
- Risk assessment to understand the potential implications of the irregularity;
- Measures to control or prevent the irregularities and;
- Potential remediation options (if required)

If any corrective measures are taken, their effectiveness must be assessed.

11.5.2 Monitoring Domains

Within the storage site and complex there are several monitoring domains, which have different monitoring purposes Table 11-8.

Monitoring domain	Monitoring purpose
Storage reservoir	Confirm that the CO ₂ is behaving as predicted
Injection wells	Ensure safe injection process, collect data to update reservoir models for CO ₂ prediction and detect any early signs of loss of containment
Storage complex (including P&A wells)	Detection of CO ₂
Seabed/ atmosphere	Detection of CO ₂ Quantification of CO ₂ leakage

Table 11-8 Monitoring domains

11.5.3 Monitoring Technologies

Many technologies which can be used for offshore CO₂ storage monitoring are well established in the oil and gas industry.

Monitoring of offshore CO₂ storage reservoirs has been carried out for many years at Sleipner and Snohvit in Norway and at the K12-B pilot project in the Netherlands. Onshore, Ketzin in Germany has a significant focus on developing MMV research and best practice.

A comprehensive list of existing technologies has been pulled together from NETL (2012) and IEAGHG (2015).

NETL (2012) references a "field readiness stage" for each technology, based on its maturity:

- Commercial
- Early demonstration
- Development

IEAGHG (2015) included an estimate of the cost of some offshore technology.

To help map each monitoring technology's relevance and applicability to a generic storage site in the North Sea, a Boston square plot was used. This is a useful tool, which has been used on previous CO₂ storage projects such as in Salah (operational) and Longannet (FEED study).

Along the x-axis of the plot is the relative cost (low to high) and along the y-axis is the relative value of information (VOI) benefit (high to low) and so each monitoring technology is plotted according to these parameters. The Boston square can then be divided into four quadrants, which help to refine the choice of monitoring technologies:

"Just do it" - technologies with low cost and high VOI - these should be included as standard in the monitoring plan

"Park" - technologies with high cost and low VOI- these should be excluded from the plan

"Consider" - technologies with low cost but also a low VOI - these should not be ruled out due to their low cost

"Focussed application" - technologies with a high cost but a high VOI- these may be deployed less frequently, over a specific area or included in the corrective measures plan

Note that the Boston square is for this stage in the project and would likely be modified following additional work to refine costs and benefits of the technologies for this site.

The Boston Square for a generic North Sea storage site is shown in Figure 11-37 and Table 11-9 provides additional information about each technology and the rationale for technologies in each quadrant.

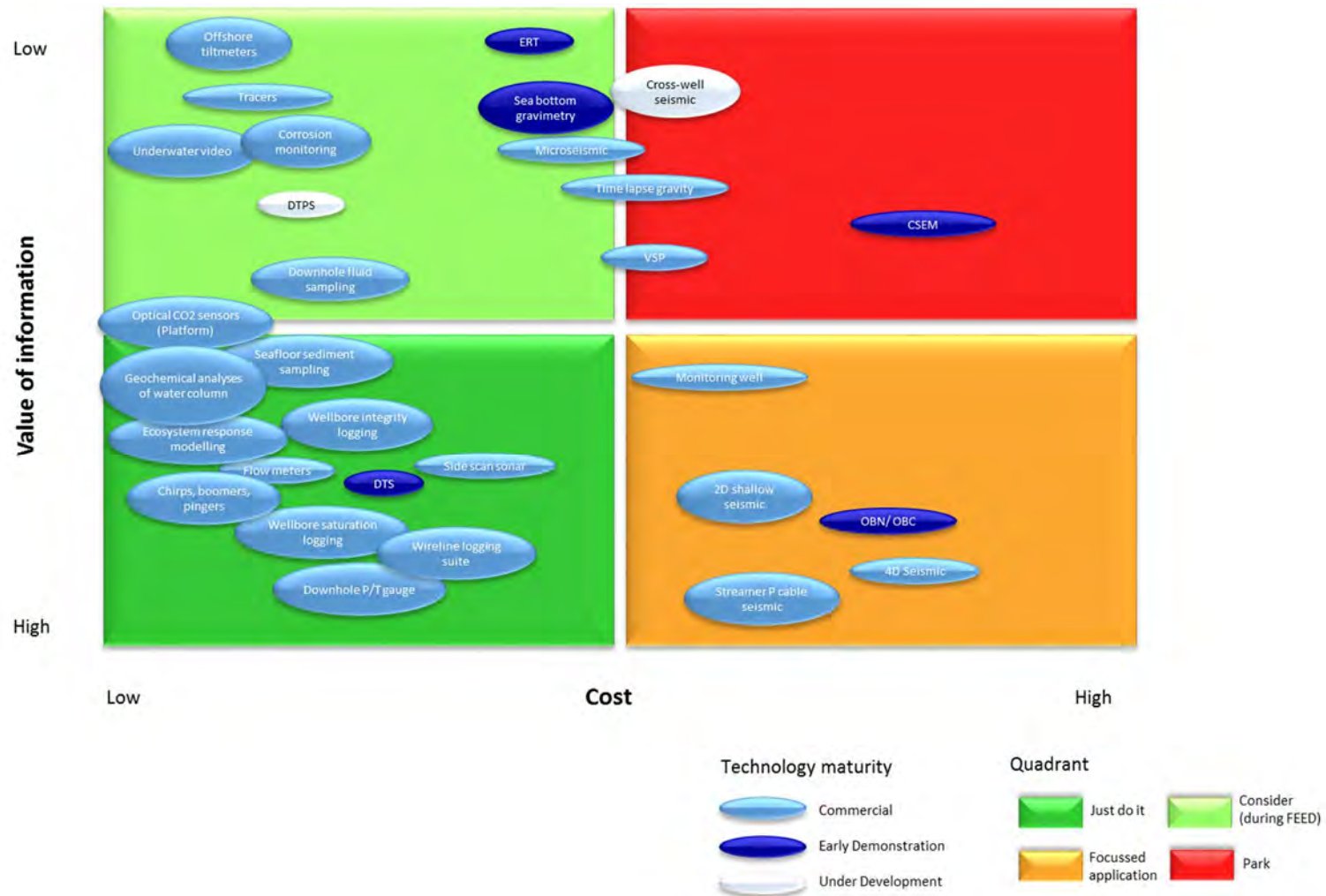


Figure 11-37 Boston square plot of monitoring technologies applicable offshore

11.5.4 Technologies for monitoring offshore

The table in the following pages contains technologies suitable for monitoring offshore.

Monitoring Domain	Type	Field Readiness	Technology	Applicability to Offshore	Description	Boston Square Box	Comments/ rationale
Subsurface	Wireline Logging Tool	Commercial	Density logging	Platform and subsea	Standard wireline tool that provides information about a formation's bulk density along borehole length. Bulk density relates to the rock matrix and pore fluid so can be used to infer pore fluid and characterise reservoir models. Uses gamma rays (radioactive source) and detector that detects their scatter, which is related to the formation's electron density.	Just do it	Used for formation characterisation in reservoir models
Subsurface	Wireline Logging Tool	Commercial	Sonic logging	Platform and subsea	Standard wireline tool in the oil and gas industry. Measures velocity of both compressional and shear waves in the subsurface and transit times of acoustic wave. Could detect changes in pore fluid from CO ₂ due to velocity contrasts between CO ₂ and brine.	Just do it	Used for formation characterisation in reservoir models
Subsurface	Wireline Logging Tool	Commercial	Dual-induction logging	Platform and subsea	Resistivity logging - detects resistivity contrast between CO ₂ (resistive) and water (conductive).	Just do it	Used for formation characterisation in reservoir models
Subsurface	Wireline Logging Tool	Commercial	Wellbore integrity logging	Platform and subsea	Well integrity logging focusses on determining the integrity of the wellbore (and its cement, casing etc.) and is important for safe injection operations and reduces leakage risk. i.e. Cement bond logging (CBL) and formation bond logging (VDL)	Just do it	Well integrity logging is considered essential for determining injection well integrity during operations.

Monitoring Domain	Type	Field Readiness	Technology	Applicability to Offshore	Description	Boston Square Box	Comments/ rationale
Subsurface	Wireline Logging Tool	Commercial	Pulsed neutron tool (PNT)	Platform and subsea	A standard wireline tool using pulsed neutron techniques to measure CO ₂ saturation. Sensitive to changes in reservoir fluids and can distinguish between brine, oil and CO ₂ . PNT will not detect CO ₂ dissolved in brine.	Just do it	Used for formation characterisation in reservoir models
Subsurface	Permanent Downhole Tool	Early Demonstration Stage	Distributed temperature sensor (DTS)	Platform and subsea	Permanent down-hole optical fibre tools which can detect temperature at ~1m intervals along the wellbore. Can measure in real time and may be able to detect CO ₂ migration from reservoir with associated temperature drop or any fluid temperature fluctuations which could indicate a poorly sealed wellbore.	Just do it	Considered essential to ensure integrity of injection operations. Also used to update reservoir models.
Subsurface	Permanent Downhole Tool	Development Stage	Distributed thermal perturbation sensor (DTPS)	Platform and subsea	DTPS measures the thermal conductivity of the formation and can estimate CO ₂ saturation within the zone of injection (decrease in bulk thermal conductivity indicates an increase in CO ₂ saturation). Equipment includes an electrical heater with DTS.	Consider	The technology is at development stage so monitor its maturation and consider inclusion in FEED.

Monitoring Domain	Type	Field Readiness	Technology	Applicability to Offshore	Description	Boston Square Box	Comments/ rationale
Subsurface	Permanent Downhole Tool	Commercial	Corrosion monitoring	Platform and subsea	CO ₂ with brine can be corrosive and so corrosion monitoring can be used to prevent potential failures within the injection system. Two techniques: (i) expose a removable piece of casing to the corrosive fluid for a set amount of time, remove it and analyse it (ii) install a corrosion loop with the injection system which can be removed and examined for signs of corrosion	Consider	Wellbores will be designed to minimise corrosion and injection CO ₂ will be dehydrated to minimise corrosion. Therefore uncertainty over benefit. To consider further in FEED.
Subsurface	Permanent Downhole Tool	Commercial	Downhole wellhead Pressure/ Temperature gauges &	Platform and subsea	Located in the storage reservoir and can give continuous reservoir pressure and temperature throughout field life. The injected CO ₂ will be at a lower temperature than reservoir temperature so can differentiate between CO ₂ and brine. Pressure and Temperature data can be used as input to reservoir models. Pressure can be used to confirm mechanical integrity of wellbore. Can be used at monitoring wells to aid in detection of CO ₂ arrival (CO ₂ may be at lower temperature and higher pressure than fluids in the formation). Deployment required under the EU Storage Directive	Just do it	Required under the EU Storage Directive and considered essential to ensure integrity of injection operations and to update reservoir models.
Subsurface	Permanent Downhole Tool	Commercial	Flow meters	Platform and subsea	Directly measure rate and volume of injected CO ₂ . Different types: differential pressure meters, velocity meters, mass meters. Used for reporting of injected volumes of CO ₂ .	Just do it	Essential for reporting on injected volumes of CO ₂ .

Monitoring Domain	Type	Field Readiness	Technology	Applicability to Offshore	Description	Boston Square Box	Comments/ rationale
Subsurface	Permanent Downhole Tool		Subsurface Fluid Sampling and Tracer Analysis	Platform and subsea	Collection of liquid or gas samples via wells (from either reservoir or overlying formation) for geochemical analysis of changes in reservoir due to CO ₂ or identify any tracers. Data can be used to constrain reservoir simulation modelling (e.g. fluid chemistry, CO ₂ saturation etc). Challenges with additional reservoir fluids of hydrocarbon and brine and preserving samples at reservoir temperature and pressure.	Consider	Moderate cost and can be conducted during wireline runs. To be more fully considered during FEED

Subsurface	Seismic Method	Early Demonstration	Microseismic/ passive seismic	Platform and subsea	Microseismic/ passive seismic monitoring includes installation of geophones down the wellbore when the wells are drilled and may provide real-time information on hydraulic and geomechanical processes taking place within the reservoir. This may give useful insight into reservoir and caprock integrity during the injection process. Challenges with reliability of sensors.	Consider	Moderately high cost and uncertainty over reliability of sensors and of information benefit (since caprocks in five storage sites are excellent). To be more fully considered during FEED.
-------------------	----------------	---------------------	-------------------------------	---------------------	--	----------	--

Monitoring Domain	Type	Field Readiness	Technology	Applicability to Offshore	Description	Boston Square Box	Comments/ rationale
Subsurface	Seismic Method	Commercial	4D/time-lapse 3D seismic	Platform and subsea	Reflection 3D seismic uses the acoustic properties of geological formations and pore fluid to image the subsurface in a 3D volume. 4D seismic involves repeating the 3D survey over time to detect any changes. Each CO ₂ storage site is unique and site-specific modelling is required to understand if reflection seismic will detect CO ₂ at that specific site	Focussed application	High cost, but it may provide extremely useful insight into plume extent for certain sites in the North Sea. Can also be used in corrective measures plan if loss of containment to overburden is suspected.
Subsurface	Seismic Method	Commercial	2D seismic		A seismic survey with closely spaced geophones along a 2D seismic line to give greater resolution at shallower depths.	Focussed application	This may be usefully deployed in a corrective measures plan seeking to detect CO ₂ in the shallow overburden.
Subsurface	Seismic Method		Streamer - P Cable seismic	Platform and subsea	High resolution 3D seismic system for shallow sections (<1000m) so could be used for imaging the overburden	Focussed application	This may be usefully deployed in a corrective measures plan seeking to detect CO ₂ in the shallow overburden.

Monitoring Domain	Type	Field Readiness	Technology	Applicability to Offshore	Description	Boston Square Box	Comments/ rationale
Subsurface	Seismic Method	Development	Ocean bottom nodes (OBN) and cables (OBC)	Platform and subsea	Multicomponent (p and s-wave recording) geophones placed on the seabed and can provide full azimuth coverage. Can provide data near platforms (unlike towed streamers which have an exclusion radius)	Focussed application	Multicomponent seismic may provide greater cost-benefit analysis over field life. Analysis to be carried out for specific sites during FEED.
Subsurface	Gravity	Early Demonstration	Time lapse seabottom gravimetry	Platform and subsea	Use of gravity to monitor changes in density of fluid resulting from CO ₂ due to the fact that CO ₂ is less dense than the formation water. Resolution of gravity surveys is much lower than seismic surveys. Time-lapse could track migration and distribution of CO ₂ in the subsurface. Deeper reservoirs are also less suitable for gravity monitoring. Technology example: remotely-operated vehicle-deployable-deep-ocean gravimeters (ROVDOG)	Consider	Relatively low cost, but often requires a larger CO ₂ plume before detection. Technology sensitivity modelling to be done during FEED to understand minimum plume detection limits.

Monitoring Domain	Type	Field Readiness	Technology	Applicability to Offshore	Description	Boston Square Box	Comments/ rationale
Subsurface	Electrical Techniques	Development	Controlled-source Electomagnetic (CSEM) survey	Platform and subsea	Seabottom CSEM (Controlled Source Electro Magnetic) surveying is a novel application of a longstanding technique, currently at a quite early stage of development. It involves a towed electromagnetic source and a series of seabed receivers that measure induced electrical and magnetic fields. These can be used to determine subsurface electrical profiles that may be influenced by the presence of highly resistive CO ₂ . Challenges of technique in shallow water (<300m) and offshore deployment is logistically complex.	Park	Costly and challenging to deploy, still in early stages of development. However, modelling during FEED will determine whether this is likely to provide any benefit.
Subsurface	Electrical Techniques	Early Demonstration	Electrical resistivity tomography (ERT)		Electrodes used to measure pattern of resistivity in the subsurface and can be mounted on outside of non-conductive well casing. Can have Cross-well ERT or surface-downhole ERT configurations, depending on scale of imaging	Consider	Modelling during FEED to understand the benefit of this technology
Subsurface			Monitoring well		An additional well drilled for the purpose of monitoring, with no intent to inject CO ₂ into it. CO ₂ breakthrough at the monitoring well can give insight into plume movement (rates, extent, etc) through the reservoir and pressure and temperature measurements can provide information on aquifer connectivity. The draw-back is that monitoring wells can be expensive and only give one point source measurement.	Focussed application	A redundancy well is currently considered, which will monitor when not injecting.

Monitoring Domain	Type	Field Readiness	Technology	Applicability to Offshore	Description	Boston Square Box	Comments/ rationale
Subsurface	Seismic Method	Commercial	Vertical Seismic Profiling (VSP)	Platform and subsea	VSPs have seismic source in water column (offshore) or at surface (onshore) and geophones at regular intervals down the wellbore to produce a high-resolution near-wellbore image (300 to 600m away). Time-lapse VSPs are repeated over time to understand any changes. May be challenges with repeatability as reliability of sensors is a key issue	Park	Moderately expensive offshore and value of information uncertain compared with other technologies of similar or less cost - modelling during FEED.
Subsurface	Seismic Method	Early Demonstration	Cross-well seismic	Platform and subsea	Borehole seismic using seismic source in one well and receiver array in nearby well to build up a velocity map between the wells. Requires wellbore access and good coordination with other monitoring activities.	Park	Challenging regarding wellbore access and uncertainty over value of information.
Seabed/ water column	Seismic method	Commercial	Chirps, boomers & pingers	Platform and subsea	Very high resolution surface seismic surveys which may detect bubble streams. AUV systems have chirp transducers.	Just do it	Relatively low cost and can be used to rule out bubble streams at seabed and around abandoned/injection wellheads which may indicate loss of containment.

Monitoring Domain	Type	Field Readiness	Technology	Applicability to Offshore	Description	Boston Square Box	Comments/ rationale
Seabed/ water column	Seabed Method	Commercial	Side sonar scan	Platform and subsea	Sidescan sonar, a towed echo sounding system, is one of the most accurate tools for imaging large areas of the seabed. Sidescan sonar transmits a specially shaped acoustic beam perpendicular to the path of the support craft (which could include AUV or ROV), and out to each side. It can detect streams any bubbles, for example around abandoned or injection wellheads which penetrate the storage complex.	Just do it	Can be used to rule out bubble streams at seabed and around abandoned/injection wellheads which may indicate loss of containment.
Seabed/ water column	Seabed Method	Commercial	Underwater Video	Platform and subsea	Recording and high definition images of bubbles and other features which could indicate CO ₂ at seabed/ water column. Qualitative - cannot resolve size or shape of bubbles.	Consider	Consider inclusion as additional monitoring in corrective measures plan.
Seabed/ water column	Surface displacement monitoring	Development	Offshore tiltmeters	Platform and subsea	Reservoir pressure changes from CO ₂ injection can cause surface deformation and so vertical displacement of seabed may indicate that this has occurred. GPS system may be able to measure this to 5mm accuracy. Measuring subsidence or uplift may provide evidence of containment and conformance.	Consider	Moderate cost but modelling required to understand detectability limit for store depth and injected CO ₂ volumes and therefore information benefit.

Monitoring Domain	Type	Field Readiness	Technology	Applicability to Offshore	Description	Boston Square Box	Comments/ rationale
Seabed/ water column	Geochemical Monitoring of water column	Commercial	Geochemical analyses of water column	Platform and subsea	CTD (conductivity, temperature and depth) probes from survey ships or platforms (for continuous measurement) can measure water column conductivity, used in addition to pH pCO ₂ , dissolved O ₂ and other chemical components, any anomalous chemistry can be detected. Requires good baseline measurements and may have challenges detecting small quantities of CO ₂ due to dispersion.	Just do it	Relatively cheap and can be used to rule out loss of containment of CO ₂ to seabed over a large area and also around wellheads. Carry out survey at same time as side-scan sonar
Seabed/ water column	Tracer		Tracers		CO ₂ soluble compounds injected along with the CO ₂ into the target formation. Act as a "fingerprint" for the CO ₂ in case of any leakage.	Consider	Tracers are in the "Consider" box as they are of moderate cost, but low benefit as containment loss at the storage sites is not expected. To explore further during FEED.
Seabed/ water column	Seabed Method		Seafloor sediment samples	Platform and subsea	Sediment samples are extracted from the seabed (for example using a Van Veen Grab, vibro corer, CPT+BAT probe, hydrostatically sealed corer) and analysed for CO ₂ content. The CO ₂ content may give insight into CO ₂ flux (if any) above abandoned wellbores which penetrate the storage complex. Requires a good baseline to detect CO ₂ above background levels.	Just do it	Relatively cheap and can be used to rule out loss of containment of CO ₂ to seabed over a large area and also around wellheads. Carry out survey at same time as side-scan sonar

Monitoring Domain	Type	Field Readiness	Technology	Applicability to Offshore	Description	Boston Square Box	Comments/ rationale
Seabed/ water column	Seabed Method		Ecosystem response monitoring	Platform and subsea	Time-lapse sediment sampling may detect changes in seabed flora and fauna from CO ₂ . Baseline survey key to determine normal behaviour and CO ₂ concentrations	Just do it	Relatively cheap and can be used to rule out loss of containment of CO ₂ to seabed over a large area and also around wellheads. Carry out survey at same time as side-scan sonar
Atmospheric	Optical CO ₂ Sensors	Commercial	e.g. CRDS, NDIR-based CO ₂ sensors, DIAL/ LIDAR	Platform only	<p>All sensors optical CO₂ sensors measure absorption of infrared radiation (IR) along the path of a laser beam</p> <p>Cavity ring-down spectroscopy (CRDS): Sensors to measure continuous or intermittent CO₂ in air. Works better over smaller areas and may be difficult to detect any CO₂ release from background CO₂ emissions. Relatively cheap and portable.</p> <p>Non-dispersive infrared (NDIR) spectroscopy. CO₂ detectors for health and safety monitoring.</p> <p>Light detection and ranging (LIDAR).</p>	Just do it	Atmospheric CO ₂ sensors will be essential if platform (including unmanned) injection facilities. For health and safety of personnel inspecting or maintaining platform. Modelling required during FEED to understand which atmospheric CO ₂ sensors should be installed.

Table 11-9 Offshore technologies for monitoring

11.5.5 Outline Base Case Monitoring Plan

For the monitoring schedule, please see Section 3.7.

A dedicated monitoring well has not been included in the plan, but instead a redundancy injection well, which will monitor when not in use.

The surface facilities include an unmanned platform with occasional personnel carrying out inspections and maintenance. There will be a requirement for some

atmospheric CO₂ monitoring, perhaps using optical CO₂ sensors, to ensure the safety of these personnel.

Monitoring of pipeline wall thickness and valve seal performance will be carried out as part of routine maintenance and the pipeline has been designed to receive pigs.

Monitoring technology/ workscope	Rationale	Timing
Seabed sampling, ecosystem response monitoring, geochemical analyses of water column	Baseline sampling to understand background CO ₂ concentrations in the sediment and water column to benchmark any future surveys against.	1-2 years prior to injection
Sidescan sonar survey Chirps, boomers & pingers	Baseline sidescan sonar survey to benchmark future surveys. Looking to detect any pre-existing bubble streams on seabed or around abandoned wellheads and map pock-marks.	1-2 years prior to injection
Seismic survey	Baseline survey required for 4D seismic.	1-2 years prior to injection
Wireline logging suite (incl well bore integrity)	Part of the drilling programme to gather data on the reservoir, overburden and wellbore for baseline update to reservoir models.	During drilling programme
Installation of Distributed Temperature Sensor (DTS), downhole and wellhead P/T gauge and flow meter	DTS for real-time monitoring of temperature along the length of the wellbore, which can indicate CO ₂ leakage through tubing. Downhole pressure and temperature monitoring is considered essential to ensure injection integrity & required under EU Storage Directive; flow meter for reporting.	Permanent installation once wells drilled

All surveys to be carried out over the storage complex

Table 11-10 Baseline monitoring plan

11.5.6 Operational Monitoring Plan

Monitoring technology/ workscope	Rationale	Timing
Wireline logging suite (incl well bore integrity)	Gather data on the reservoir, overburden and wellbore integrity to ensure injection integrity and update reservoir models.	Every 10 years
4D seismic survey	Used to detect plume extent and update geological and dynamic models. Also looking for any early-warning signs of loss of containment, such as unexpected lateral or vertical migration of CO ₂ within the storage complex.	Every 5 years
Sidescan sonar survey Chirps, boomers & pingers	Used to detect any bubble streams around abandoned wellheads, on the seabed or around pock-marks, which could indicate loss of containment to seabed.	Every 5 years
Seabed sampling, ecosystem response monitoring, geochemical analyses of water column	Used to detect any evidence of elevated CO ₂ concentrations in sediment or water column which may indicate loss of containment.	Every 5 years
DTS, downhole and wellhead P/T gauge and flow meter readings	DTS for real-time monitoring of temperature along the length of the wellbore, which can indicate CO ₂ leakage through tubing. Downhole pressure and temperature monitoring is required under EU Storage Directive, can be used to update models and is considered essential to ensure injection integrity. Flow meter for reporting.	Continuous
Data management	To collate, manage, interpret and report on monitoring data.	Continuous

All surveys to be carried out over the storage complex

Table 11-11 Operational monitoring plan

11.5.7 Post-Closure Monitoring Plan

Monitoring technology/ workscope	Rationale	Timing
4D seismic survey	Detect plume extent at end of injection operations and monitor to show site conformance prior to handover.	1 year post injection, then every 5 years
Seabed sampling, ecosystem response monitoring, geochemical analyses of water column	Used to detect any evidence of elevated CO ₂ concentrations in sediment or water column which may indicate loss of containment	1 year post injection, then every 5 years
Sidescan sonar survey Chirps, boomers & pingers	Looking to detect any bubble streams around abandoned wellheads, seabed or pock-marks and set a baseline for post-closure and post-handover monitoring.	1 year post injection, then every 5 years
Data interpretation, management and reporting	To collate, manage, interpret and report on monitoring data.	Continuous

All surveys to be carried out over the storage complex

Table 11-12 Post closure monitoring plan

11.5.8 Corrective Measures – Remediation Options

For each key risk event a remediation option (or options) is defined and an associated high level cost is associated. Options to improve the integrity status are identified.

11.5.8.1 Well Containment Risks

This section examines the containment risks from wells in the Viking field. The following well types are (or will be) present in the reservoir if it is developed for CO₂ storage:

- Previously abandoned wells.
- Pre-existing wells that are operational, shut-in or suspended (to be abandoned).
- CO₂ injection wells.
- Observation wells for data gathering (optional).
- Wells drilled for CO₂ storage that are abandoned during the storage project's lifetime.

The assumption is that pre-existing wells were not designed for CO₂ injection or any other role in a CO₂ storage project and will be unsuitable for conversion to that purpose and will, therefore, be abandoned.

All wells present a CO₂ containment risk: migration past the designed pressure containment barriers of the well to the biosphere (atmosphere or ocean). The possible well containment failures are:

- Flow through paths in poor casing cement sheaths or cement plugs.
- Flow through paths in casing cement sheaths created by pressure cycling.

- Flow through a cement sheaths or plugs degraded by contact with CO₂ or carbonic acid.
- Corrosion of tubulars, metallic well components or wellhead by carbonic acid.
- Degradation of elastomers by contact with CO₂ or carbonic acid.
- Blowout whilst drilling an injection/observation well.
- Blowout whilst conducting a well intervention on an injection/observation well.

Several studies in recent years have comprehensively assessed containment risk. The following analysis of the containment risks is a summary of these reports (Jewell & Senior, 2012) (DNV, 2011) (Decision Gate Approach to Storage Site Appraisal, Mott MacDonald Report C12MMD002B, 2012).

All active wells that are part of the CO₂ injection system (injectors, observation, pressure maintenance) should be designed and constructed not to leak in service and will satisfy the well integrity requirements set out in the governing legislation and guidance (Offshore Installation & Wells (Design and Construction etc.) Regulations 1996) (Oil and Gas UK, 2012). Wells will also be designed to facilitate the most secure abandonment when they are taken out of service.

Abandoned wells that penetrate the storage reservoir pose a leak risk because they provide a direct pathway to the surface. There are three abandoned well types to consider:

- Pre-existing wells that are operational, shut-in or suspended and were abandoned as part of the development of the storage field.
- Wells drilled for CO₂ storage that are abandoned during the storage project's lifetime.
- Previously abandoned wells.

Pre-existing, still operational, wells in the field will be abandoned before injection starts, using the latest standards and practices to make them safe in a CO₂ storage environment. The well construction itself may not be suitable for a CO₂ environment (e.g. material selection for corrosion resistance).

CO₂ injection wells (or related observation or water abstraction wells), which are decommissioned during the life of the storage facility, will be designed to be abandoned using the latest standards and practices. Both well types that provides confidence in the long-term containment.

Previously abandoned wells (exploration and appraisal wells from earlier hydrocarbon development) may have been abandoned in a way that is inadequate for a CO₂ storage environment because of their outdated construction design and abandonment practices (see section 6). In addition, record keeping for abandoned wells is not always complete and it may not be possible to determine how a particular well was abandoned. Crucially, these wells will have been cleared to approximately 15ft below the seabed; the wellhead and all casing strings close to the seabed will have been cut and recovered, access into an abandoned well is very complex and expensive. It is unlikely that this would be attempted to remediate a perceived risk, but only in the event of a major loss of containment.

11.5.8.2 Well Containment Envelope

All wells in the field (including abandoned wells) will have a defined pressure containment envelope: the barriers that prevent an unplanned escape of fluids from the well. There must be suitable barriers in place that isolate the hazard from the surface throughout the well life.

Barriers that form the well pressure containment envelope must be monitored and maintained for the life of the well (not normally applied to abandoned wells). If a barrier is found to be not fully functional then the well monitoring and management processes identify this and initiate appropriate remediation.

11.5.8.3 Containment Risks and Remediation Options

The following tables catalogue the well containment failure mode and the associated effect, remediation and estimated cost (it is assumed that the wells are offshore). The remediation options available will be specific to the well and depend on:

- The type of failure.
- The location of the failure.
- The overall design of the well.

ACTIVE WELL			
Risk Event	Effect	Remediation	Cost
Blowout during drilling	Possible escape of CO ₂ to the biosphere.	Standard procedures: shut-in the well and initiate well control procedures.	\$3-5 million (5 days & tangibles).
Blowout during well intervention	Possible escape of CO ₂ to the biosphere.	Standard procedures: shut-in the well and initiate well control procedures.	\$2-3 million (3 days & tangibles).
Tubing leak	Pressured CO ₂ in the A-annulus. Sustained CO ₂ annulus pressure will be an unsustainable well integrity state and require remediation.	Tubing replacement by workover.	\$15 -20 million (16 days & tangibles).
Packer leak	Pressured CO ₂ in the A-annulus. Sustained CO ₂ annulus pressure will be an unsustainable well integrity state and require remediation.	Packer replacement by workover.	\$15 -20 million (16 days & tangibles).
Cement sheath failure (Production Liner)	Requires: a failure of the liner packer or failure of the liner above the production packer before there is pressured CO ₂ in the A-annulus. Sustained CO ₂ annulus pressure will be an unsustainable well integrity state and require remediation.	Repair by cement squeeze (possible chance of failure). Requires the completion to be retrieved and rerun (if installed).	\$3-5 million (5 days & tangibles). \$18-25 million (if a workover required).

ACTIVE WELL				
Risk Event	Effect	Remediation	Cost	
Production failure	Liner	Requires: a failure of the liner above the production packer and a failure of the cement sheath before there is pressured CO ₂ in the A-annulus. Sustained CO ₂ annulus pressure will be an unsustainable well integrity state and require remediation.	Repair by patching (possible chance of failure) or running a smaller diameter contingency liner. Requires the completion to be retrieved and rerun (if installed). Will change the casing internal diameter and may have an impact on the completion design and placement. Repair by side-track.	\$3-5 million (3 days & tangibles). \$18-25 million (if a workover required). Side-track estimated to be equal to the cost of a new well - \$55 million (60 days & tangibles).
	sheath (Production Casing)	Requires: a failure of the Production Liner cement sheath or a pressurised A-annulus and failure of the production casing before there is pressured CO ₂ in the B-annulus. Sustained CO ₂ annulus pressure will be an unsustainable well integrity state and require remediation.	Repair by cement squeeze (possible chance of failure). Requires the completion to be retrieved and rerun (if installed).	\$3-5 million (5 days & tangibles). \$18-25 million (if a workover required).

ACTIVE WELL			
Risk Event	Effect	Remediation	Cost
Production Casing Failure	<p>Requires: a pressurised A-annulus and a failure of the Production Casing cement sheath before there is pressure CO₂ in the B-annulus. Sustained CO₂ annulus pressure will be an unsustainable well integrity state and require remediation.</p>	<p>Repair by patching (possible chance of failure). Requires the completion to be retrieved (if installed). Will change the casing internal diameter and may have an impact on the completion design and placement.</p>	<p>\$3-5 million (3 days & tangibles). \$18-25 million (if a workover required). Side-track estimated to be equal to the cost of a new well - \$55 million (60 days & tangibles).</p>
Safety critical valve failure – tubing safety valve	<p>Inability to remotely shut-in the well below surface. Unsustainable well integrity state.</p>	<p>Repair by: installation of insert back-up by intervention or replacement by workover</p>	<p>£1 million to run insert (1 day & tangibles). \$18-25 million (if a workover required).</p>
Safety critical valve failure – Xmas Tree valve	<p>Inability to remotely shut-in the well at the Xmas Tree. Unsustainable well integrity state.</p>	<p>Repair by valve replacement.</p>	<p>Dry Tree: < \$1 million (costs associated with 5 days loss of injection, tangibles and man days). Subsea: \$5-7 million (vessels, ROV, dive support & tangibles).</p>

ACTIVE WELL			
Risk Event	Effect	Remediation	Cost
Wellhead seal leak	<p>Requires:</p> <p>a pressurised annulus and multiple seal failures</p> <p>before there is a release to the biosphere.</p> <p>Seal failure will be an unsustainable well integrity state and require remediation.</p>	<p>Possible repair by treatment with a replacement sealant or repair components that are part of the wellhead design. Highly dependent on the design and ease of access (dry tree or subsea).</p> <p>May mean the well has insufficient integrity and would be abandoned.</p>	<p>Dry Tree: <\$3 million (costs associated with 7 days loss of injection, tangibles and man days).</p> <p>Abandonment \$15-25 (21 days & tangibles).</p>
Xmas Tree seal leak	<p>Requires multiple seal failures before there is a release to the biosphere.</p> <p>Seal failure will be an unsustainable well integrity state and require remediation.</p>	<p>Possible repair by specific back-up components that are part of the wellhead design. Highly dependent on the design and ease of access.</p> <p>May mean the Xmas Tree need to be removed/recovered to be repaired. This is a time consuming process for a subsea tree.</p>	<p>Dry Tree: <\$3 million (costs associated with 7 days loss of injection, tangibles and man days).</p> <p>Subsea: \$12-15 million (12 days & tangibles).</p>

Table 11-13 Active well containment failure modes and associated effects and remediation options

ABANDONED WELL			
Risk Event	Effect	Remediation	Cost
Well Leak	Escape of CO ₂ to the biosphere.	Re-entry into an abandoned well is complex, difficult and has a very low chance of success.	Relief well: \$55 million (60 days & tangibles).
	Only the final event – leak to the biosphere – will be detected.	A relief well is required.	

Table 11-14 Abandoned well containment failure modes and associated effects and remediation options

11.6 Appendix 6 – Well Basis of Design

11.6.1 Wellbore Stability

In order to drill a well in the subsurface it is essential to understand the safe operating window (the wellbore pressure required to prevent ingress of formation fluids and to prevent hole collapse, while avoiding the fracturing of the formation, which could lead to loss of well fluids (mud) and thus loss of well pressure control). In order to define this window, a 1D analytical wellbore stability analysis of key wells on the structure was performed in order to determine fracture gradient, breakout line and the mud window to drill hole with no breakouts or losses. The fracture gradient and stress analysis work is described in Appendix 9. The basic work flow in Drillworks 5000 was supplemented with safe mud weight windows and optimal wellbore trajectory analysis for the original reservoir pressure condition and for the potential depleted reservoir pressure condition. Note, the safe mud weight ranges are for zero losses and zero breakouts so they may be somewhat conservative.

11.6.1.1 Safe Mud Weight Windows -Original Reservoir Pressure Condition

Well 49/12-2

- No MW used data found for this well.
- A safe MW would vary in the layers between 10 to 14 ppg (for a vertical well) as specified in the right plot.
- The halite layers could be drilled with a MW within this range (e.g. 12 ppg) but it will require care as there may be thin intervals of highly overpressured dolomite that could produce large kicks

Well 49/11a-6

- The MW used varied from 8.6 to 11.5 ppg (black dots in right plot)

- Tight hole was reported in the Bunter Sandstone due to halite within this layer
- Losses were reported at different depths including the upper part of the Lemman Sandstone with a MW around 11 ppg. This appeared to be because of an open fault at this depth taking fluid at any overbalance above hydrostatic. The MW was dropped to 9.0 ppg but tight hole was then reported within Stassfurt halite, probably due to salt creep. This was managed by reaming.
- For the Lemman Sandstone a safe MW would be 9 to 14 ppg for a vertical well with no faulting. The MW should be kept close to 9.0 ppg if conductive faults are known or suspected.
- For the overburden layers a safe MW would vary between 9 to 13 ppg (for a vertical well).
- The halite layers could be drilled with the MW range suggested but it will require special care (drilled OK with ~10ppg)

Well 49/12a-K4

- The MW used were from 9.1 to 10.85 ppg (black dots in the plot)
- For the Lemman layer a safe MW would be between 9.5 to 14 ppg (for a vertical well)

Well 49/12a-K5

- The MW used in this well varies from 9.4 to 10.9 ppg (black dots in the plot)
- Losses reported at 14915 ft (Below Lemman Sandstone)
- Based on these uncalibrated strengths, for the Lemman layer a safe MW would be between 10 to 12 ppg (for a vertical well)

Well 49/12-A6

- The MW used in this well varies from 9.2 to 10.8 ppg (purple diamonds in the plot)
- For the Rotliegend a safe MW would be between 10 to 14 ppg (for a vertical well)
- For the immediate layer above Rotliegend (L.Magnesium), a safe MW would be between 9 to 12 ppg (for a vertical well)

Well 49/12-A10

- The MW used in this well varies from 8.9 to 10.8 ppg (purple diamonds in the plot)
- For the Rotliegend a safe MW would be between 10.5 to 14 ppg (for a vertical well)
- For the immediate layer above Rotliegend (L.Magnesian), a safe MW would be between 9 to 11 ppg (for a vertical well)

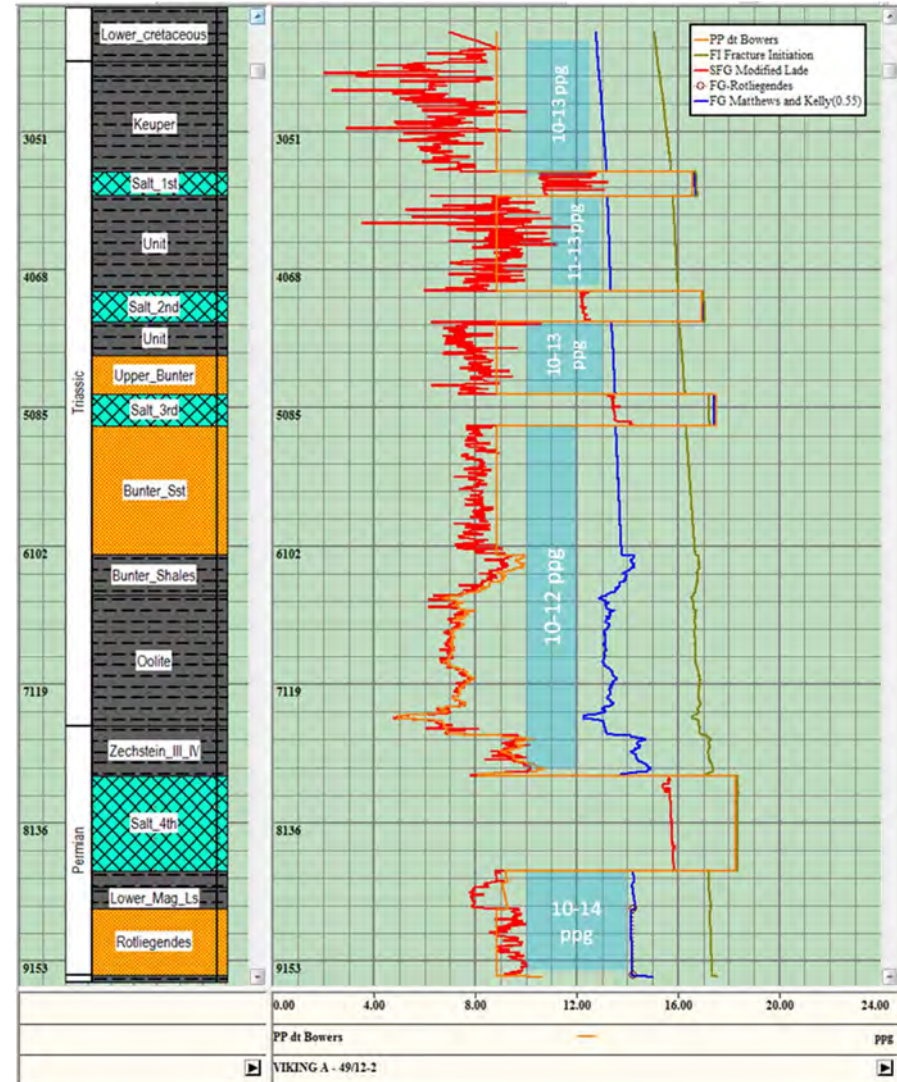


Figure 11-38 Viking A Well 49/12-2 (original condition) Safe mudweight analysis

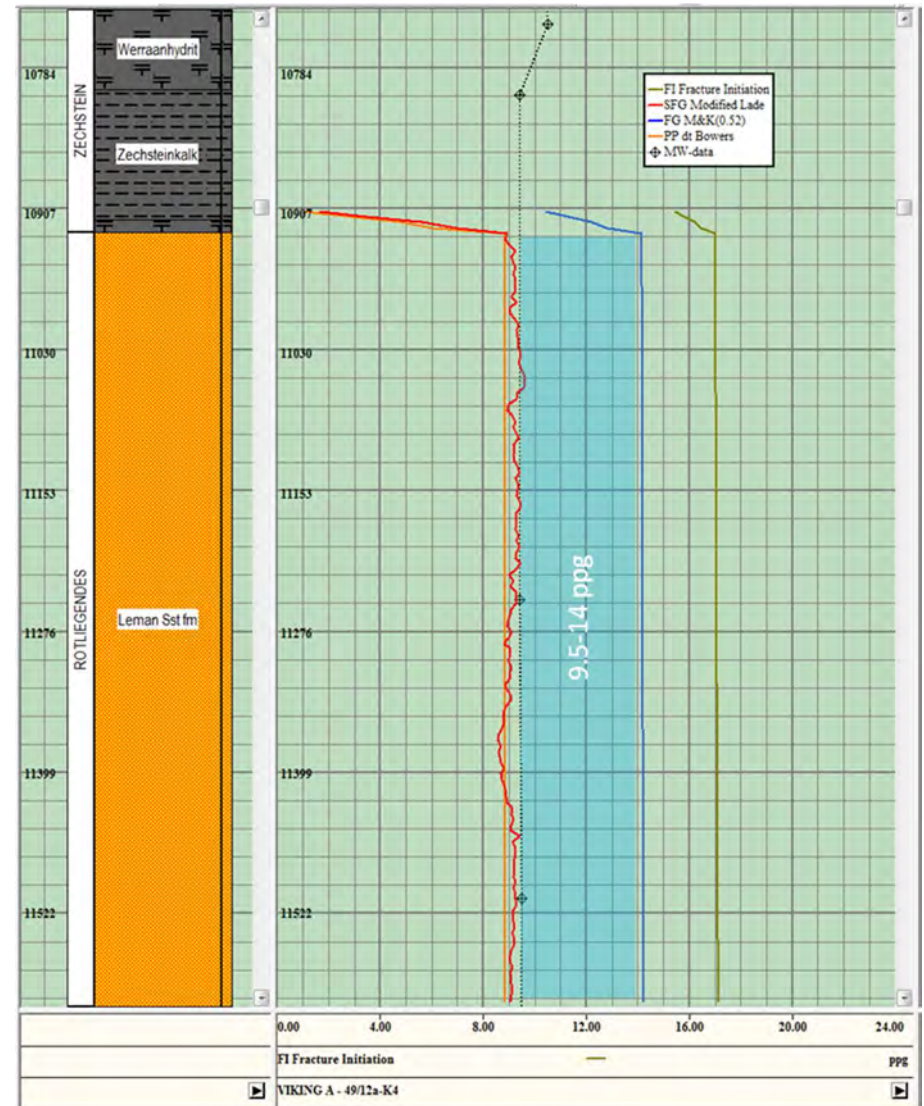
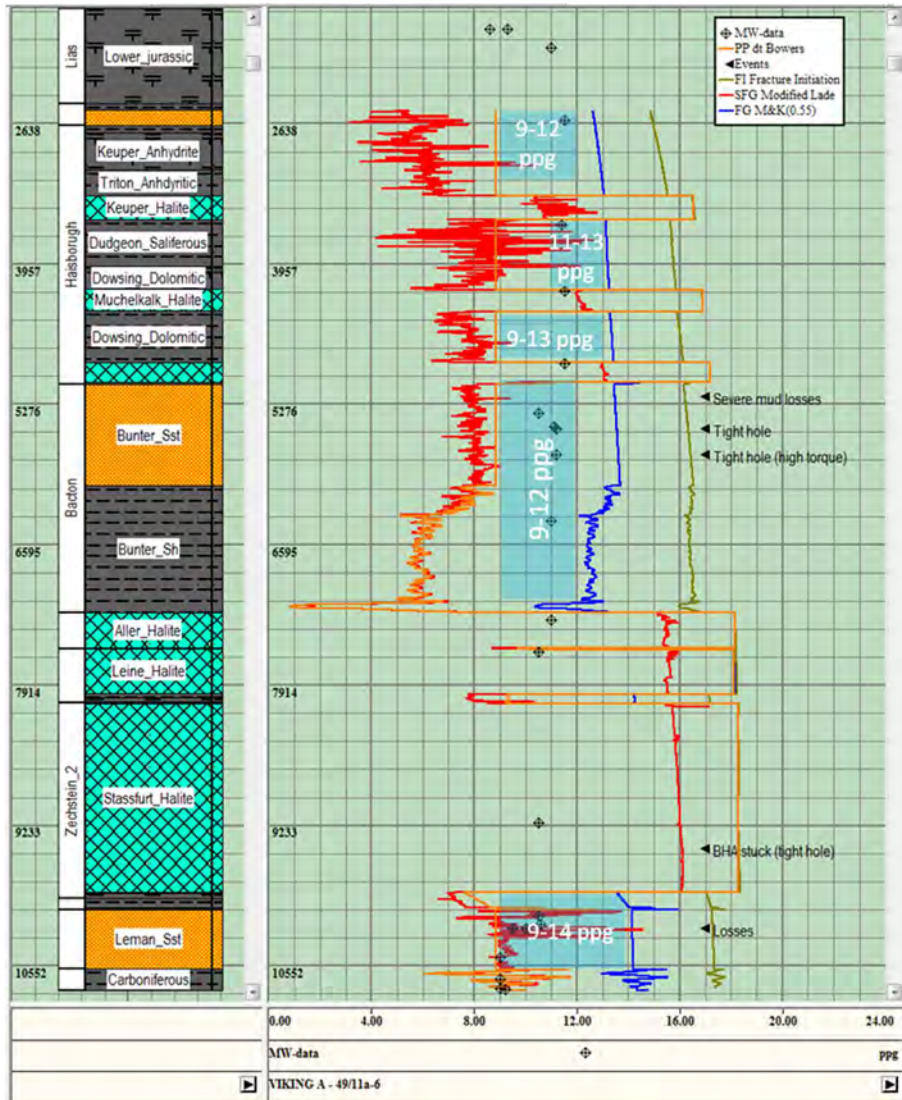


Figure 11-39 Viking A Well 49/11a-6 (original condition) Safe mud weight analysis

Figure 11-40 Viking A Well 49/12a-K4 (original condition) Safe mud weight analysis

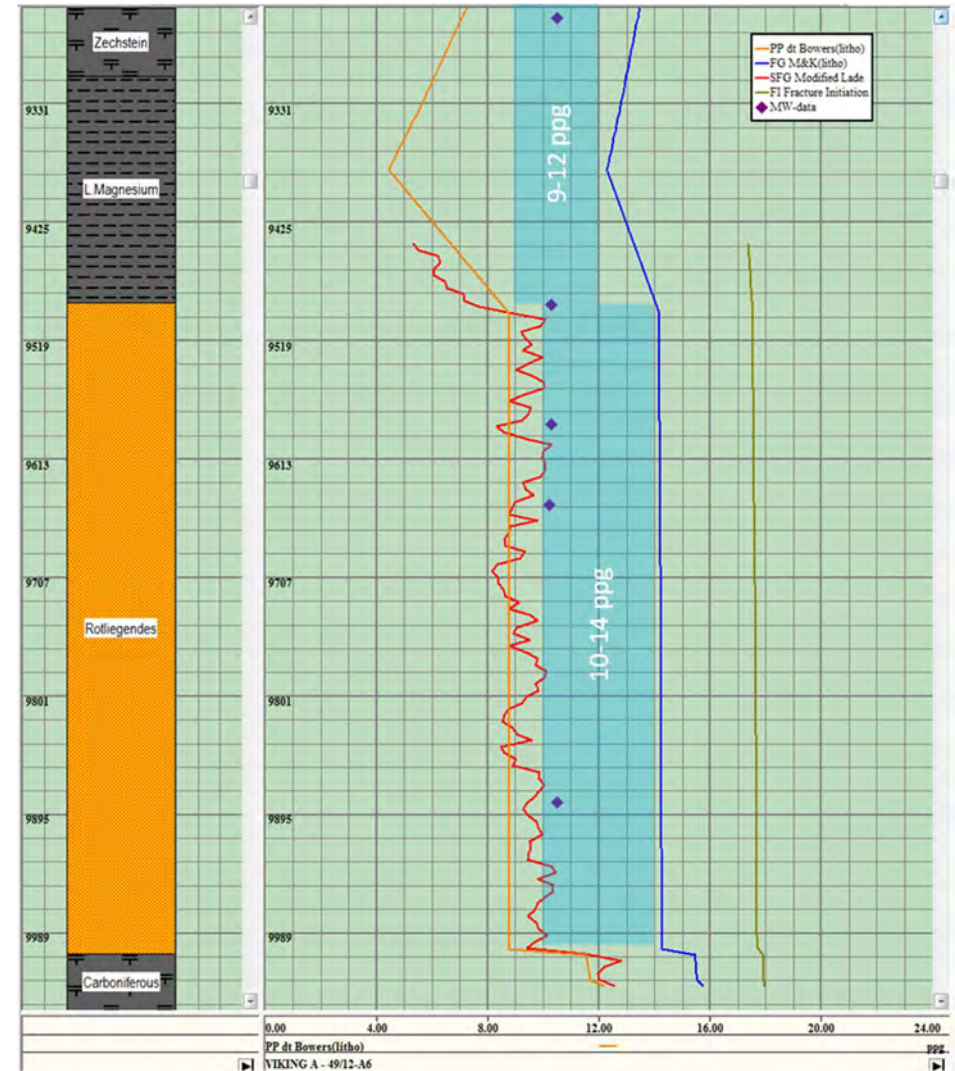
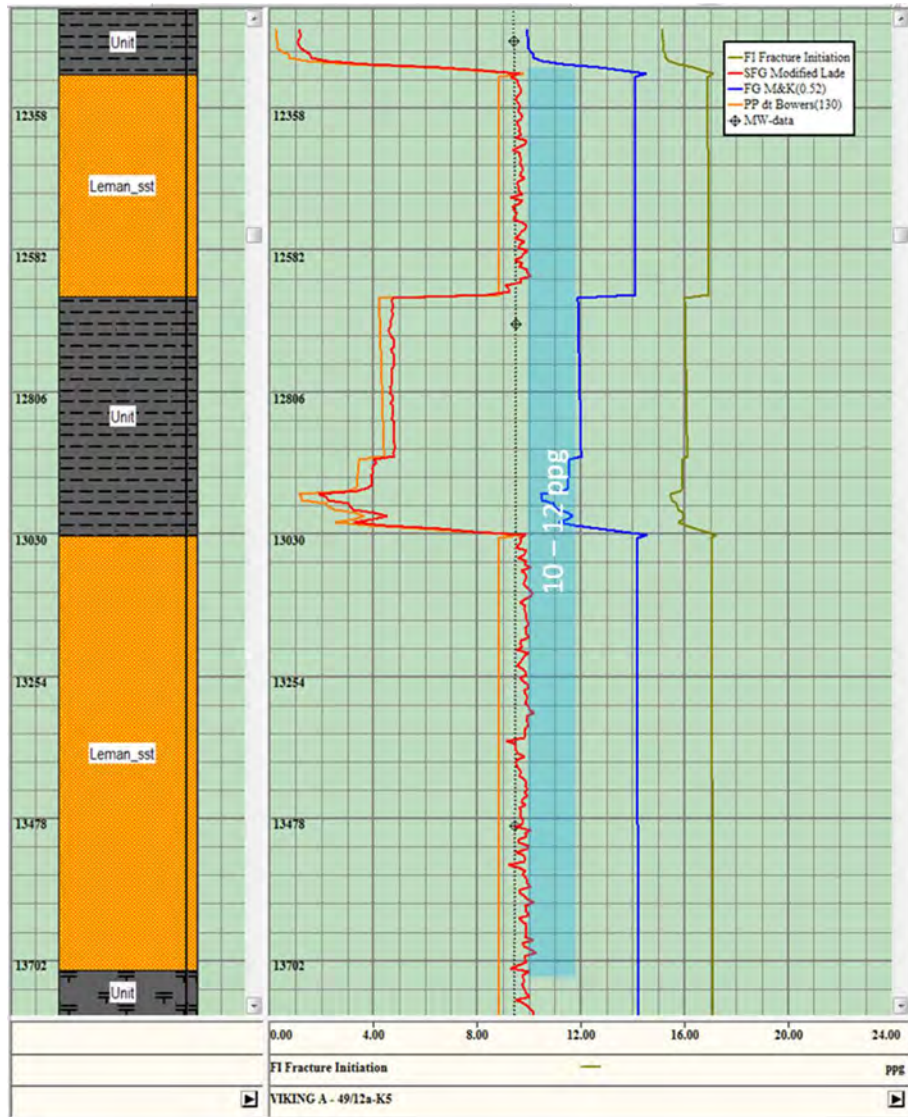


Figure 11-42 Viking A Well 49/12-A6 (original conditions) Safe mud weight analysis

Figure 11-41 Viking A Well 49/12a-K5 Safe mud weight analysis

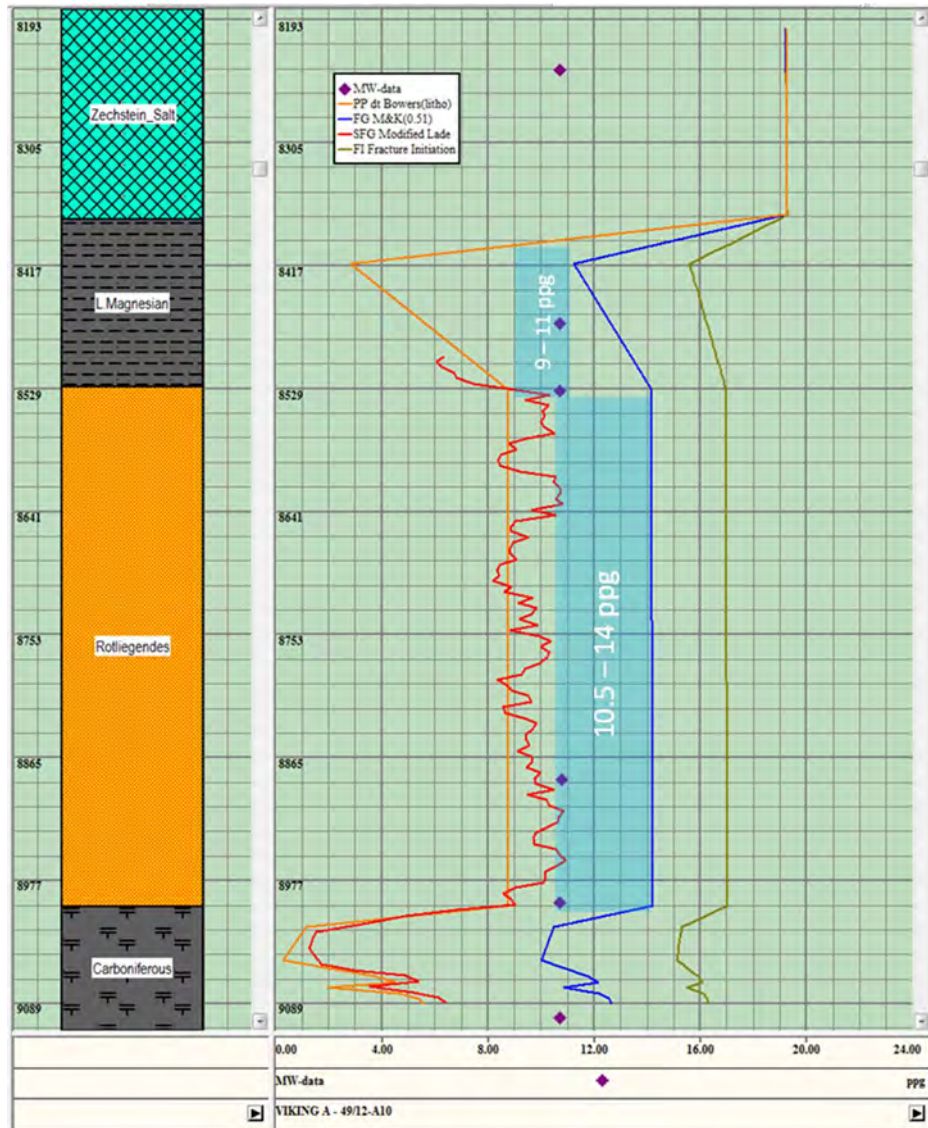


Figure 11-43 Viking A Well 49/12-A10 (original conditions) Safe mud weight analysis

11.6.1.2 Wellbore Trajectory Analysis

The figures below indicate the variation of the minimum mud weight to prevent any breakout with changes in wellbore inclination and orientation.

Figure 11-44 shows the Rotliegend at 9000 ft TVD in the well 49/12-2, where a horizontal well with NW-SE orientation would increase the MW by up to 1.6 ppg (11.6ppg).

Figure 11-45 shows the Rotliegend at 10094 ft TVD (Leman Sandstone) in the well 49/11a-6, where a horizontal well with NW-SE orientation would increase the MW by up to 1.0 ppg (10ppg).

Figure 11-46 shows the Rotliegend at 11070 ft TVD (Leman Sandstone) in the well 49/12a-K4, where a horizontal well with NW-SE orientation would increase the MW by up to 1.6 ppg (11.1ppg).

Figure 11-47 shows the Rotliegend at 13254 ft TVD in the well 49/12a-K5, where a horizontal well with NW-SE orientation would increase the MW by up to 1.8 ppg (11.8 ppg).

Figure 11-48 shows the Rotliegend at 9613 ft TVD in the well 49/12-A6, where a horizontal well with NW-SE orientation would increase the MW by up to 1.4 ppg (11.4 ppg).

Figure 11-49 shows the Rotliegend at 8609 ft TVD in the well 49/12-A10, where a horizontal well with NW-SE orientation would increase the MW by up to 2.2 ppg (12.7 ppg).

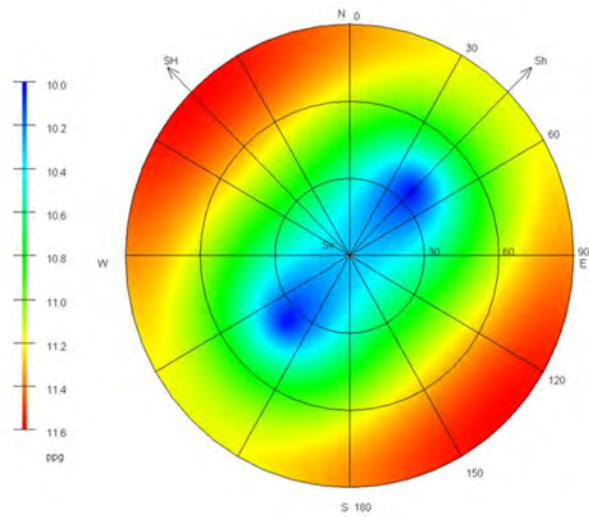


Figure 11-44 Viking A Well 49/12-2 (original condition) Well trajectory analysis

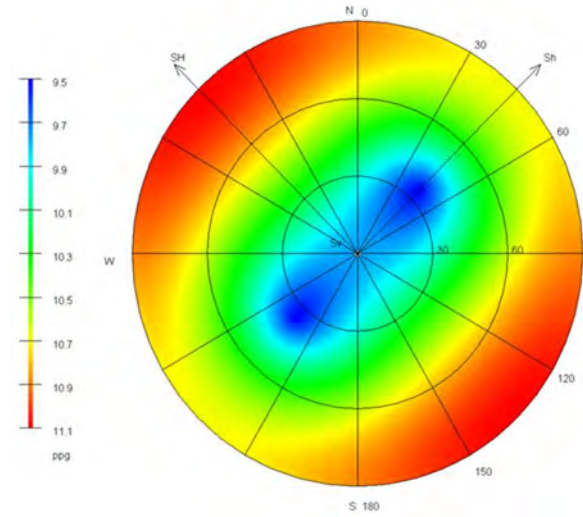


Figure 11-46 Viking A Well 49/12a-K4 (original condition) Well trajectory analysis

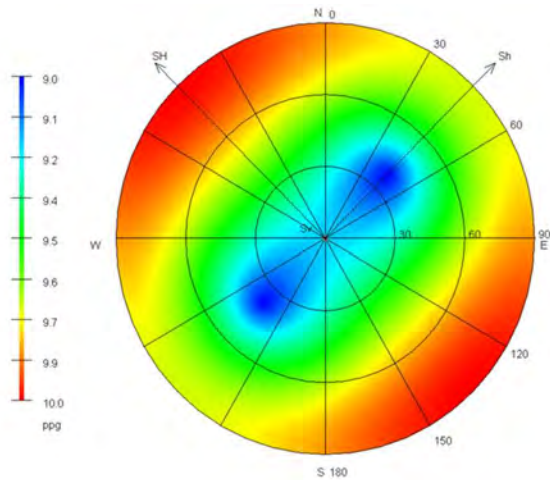


Figure 11-45 Viking A Well 49/11a-6 (original condition) Well trajectory analysis

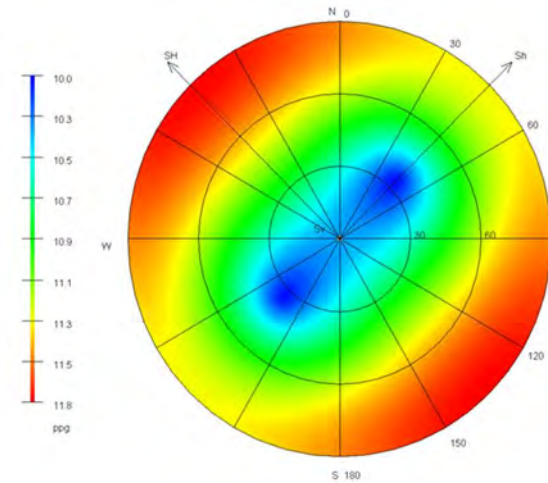


Figure 11-47 Viking A Well 49/12a-K5 (original condition)

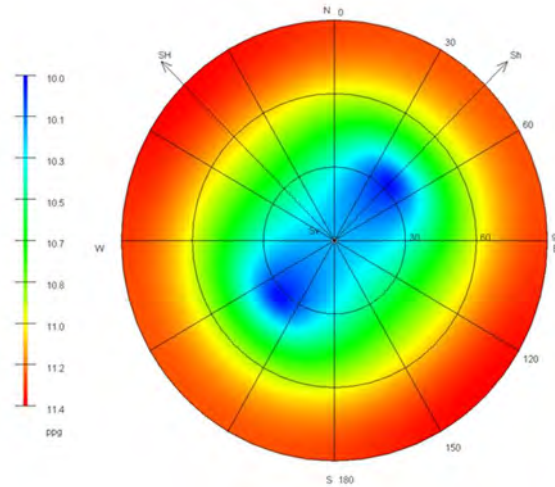


Figure 11-48 Viking A Well 49/12-A6 (original condition) Well trajectory analysis

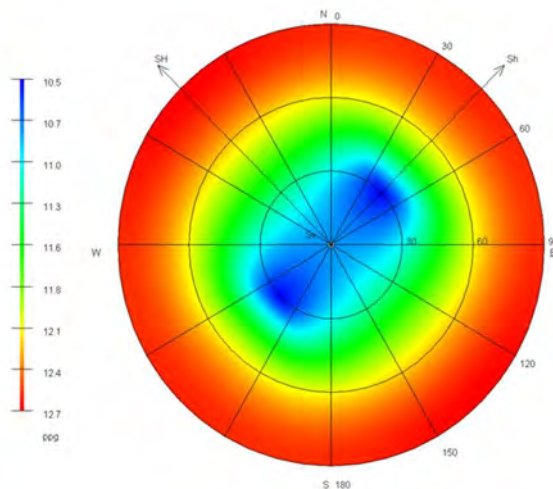


Figure 11-49 Viking A Well 49/12-A10 (original condition) Well trajectory analysis

11.6.1.3 Safe Mud Weight Windows – Depleted Reservoir Pressure Conditions

For the Rotliegend group, the changes in the safe MW due to depletion:

Well 49/12-2

- Original Condition: between 10 to 14 ppg (for a vertical well)
- Depleted Condition: between 5 to 10 ppg (for a vertical well)

Well 49/11a-6

- Original Condition: between 9 to 14 ppg (for a vertical well)
- Depleted Condition: between 3 to 10 ppg (for a vertical well)

Note that the likely presence of conductive faults means that as low a mud weight as possible is probably best.

Well 49/12a-K4

- Original Condition: between 9.5 to 14 ppg (for a vertical well)
- Depleted Condition: between 4 to 10 ppg (for a vertical well)

Well 49/12a-K5

- Original Condition: between 10 to 12 ppg (for a vertical well)
- Depleted Condition: between 5 to 10 ppg (for a vertical well)

Well 49/12-A6

- Original Condition: between 10 to 14 ppg (for a vertical well)
- Depleted Condition: between 5 to 10.5 ppg (for a vertical well)

Well 49/12-A10

- Original Condition: between 10.5 to 14 ppg (for a vertical well)
- Depleted Condition: between 6 to 10.5 ppg (for a vertical well)

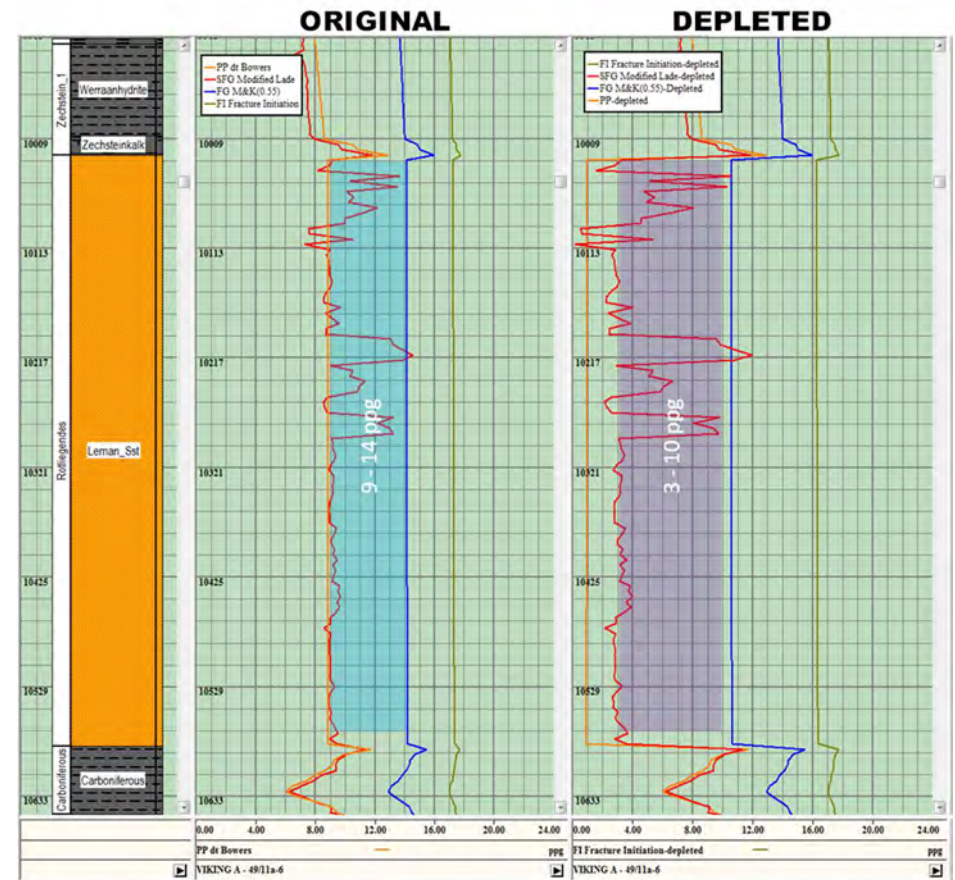
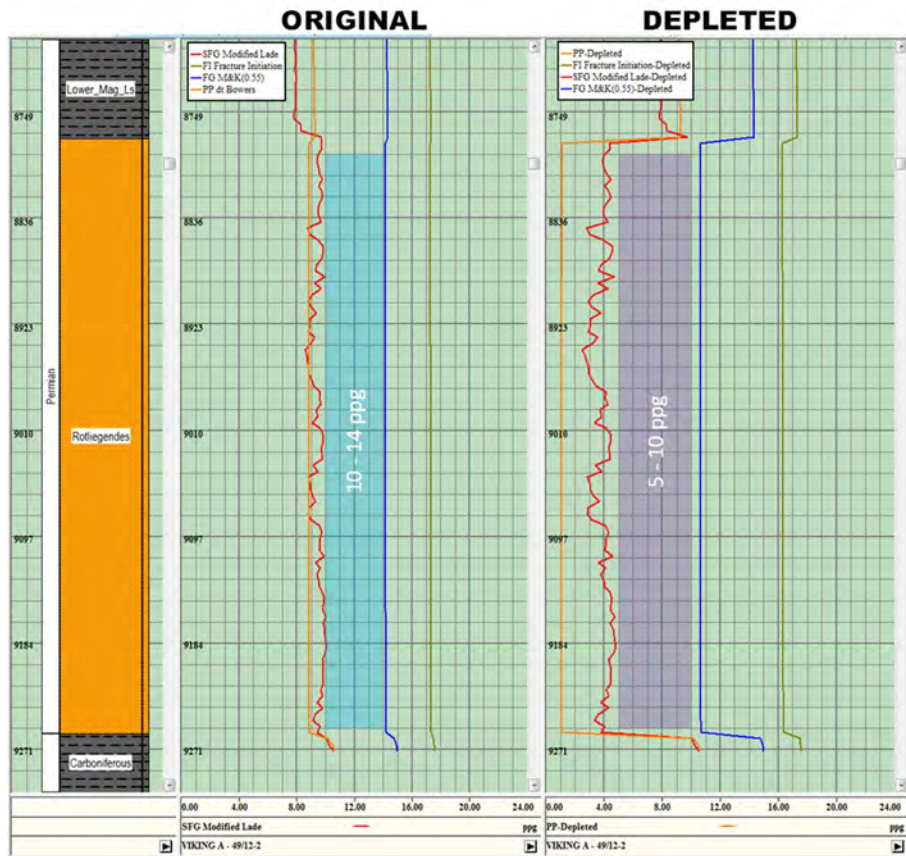


Figure 11-50 Viking A Well 49/12-2 (original/depleted) Safe mud weight analysis

Figure 11-51 Viking A Well 49/11a-6 (original/depleted) Safe mud weight analysis

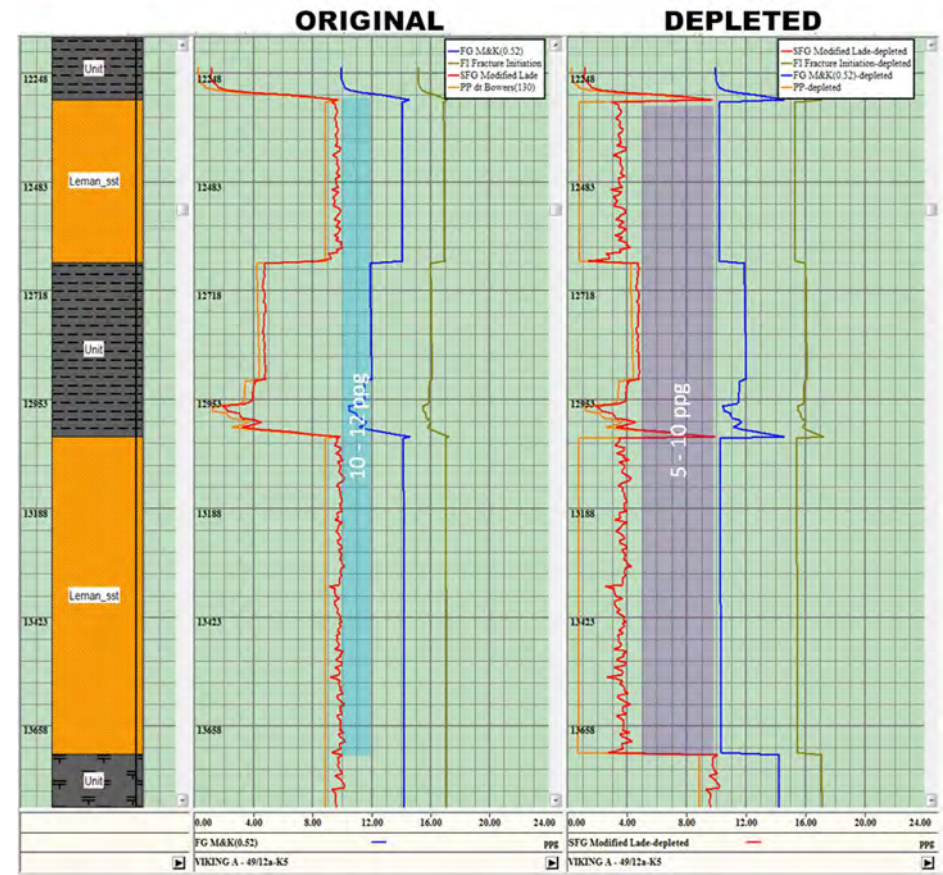
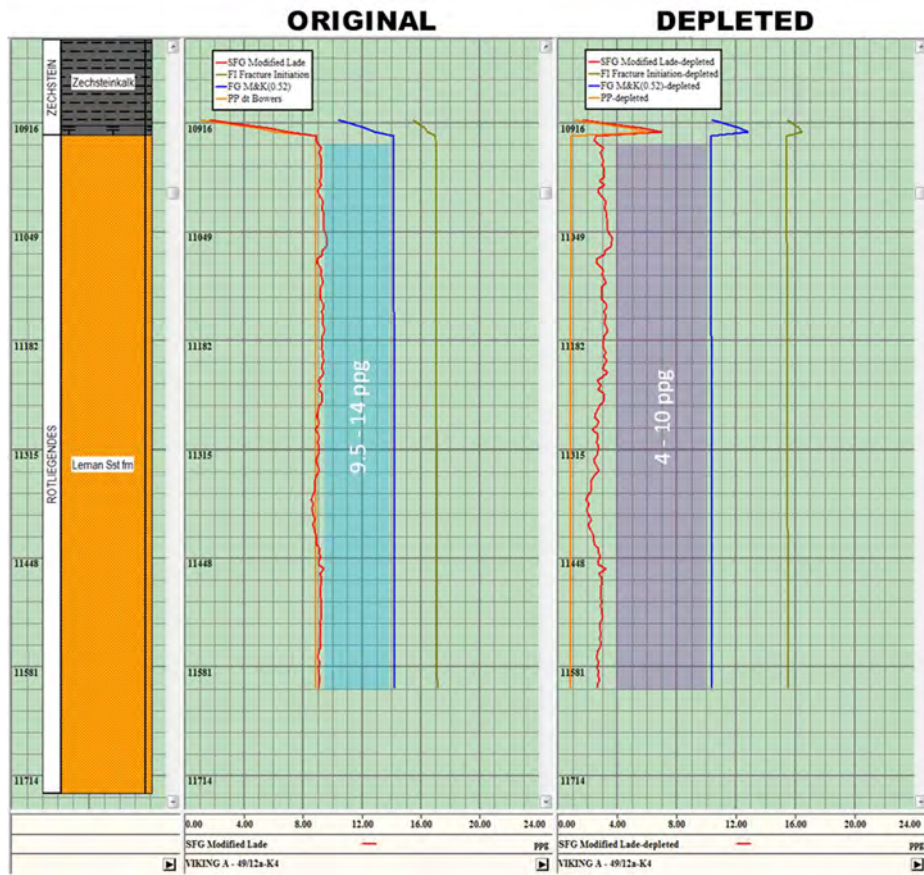


Figure 11-52 Viking A Well 49/12a-K4 (original/depleted) Safe mud weight analysis

Figure 11-53 Viking A Well 49/12a-K5 (original/depleted) Safe mud weight analysis

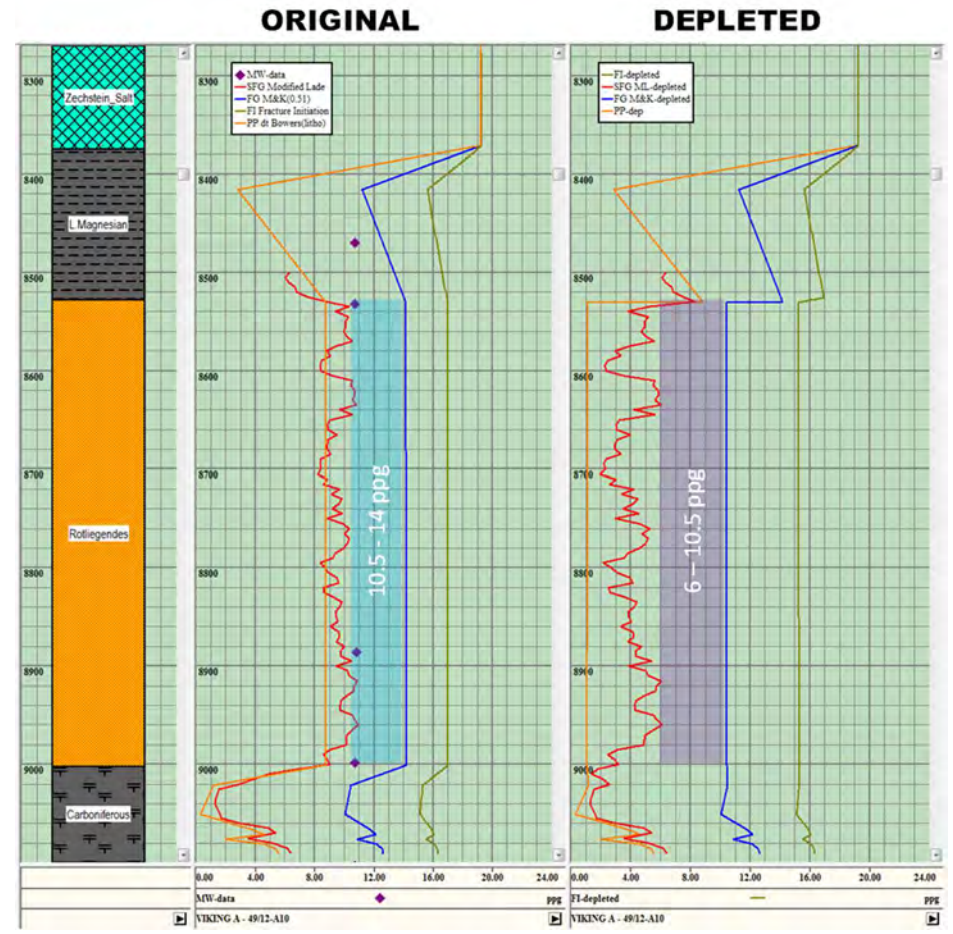
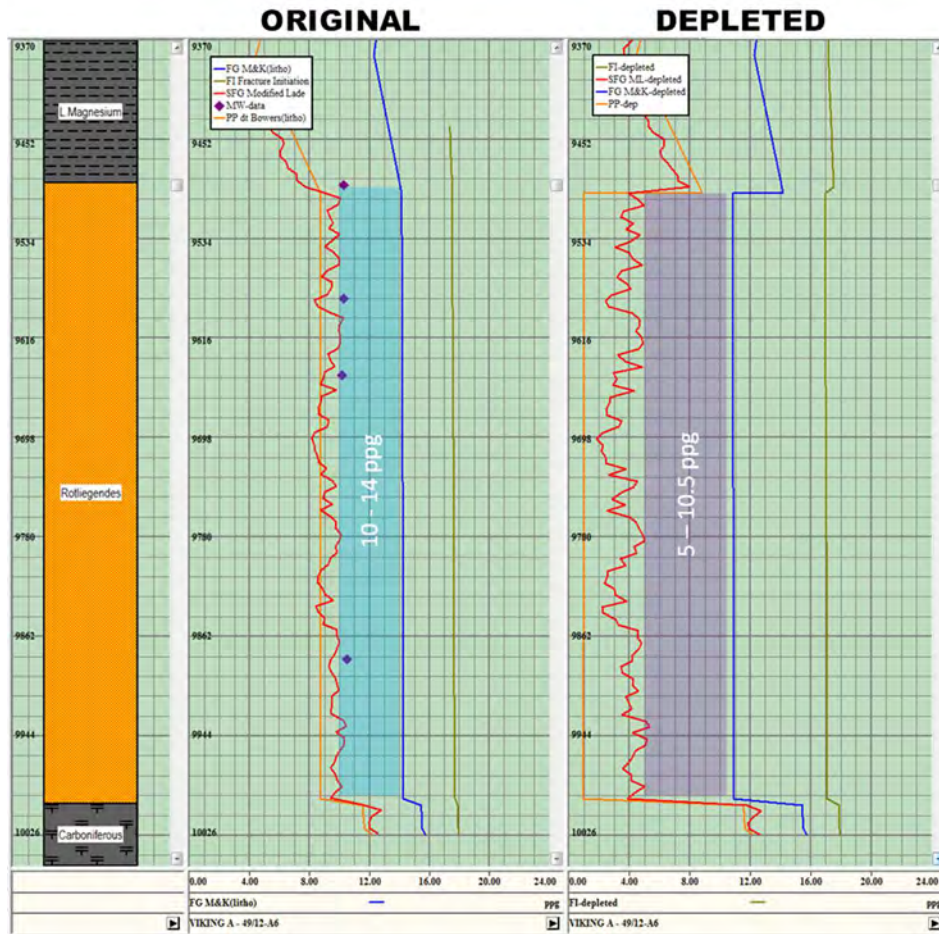


Figure 11-54 Viking A Well 49/12-A6 (original/depleted) Safe mud weight analysis

Figure 11-55 Viking A Well 49/12-A10 (original/depleted) Safe mud weight analysis

11.6.1.4 Wellbore Trajectory Analysis – Depleted Reservoir Condition

The figures below indicate the variation of the minimum mud weight to prevent any breakout with wellbore inclination and orientation taking into account a depleted reservoir pressure in the Rotliegend group.

Figure 11-56 shows the depleted Rotliegend at 9000 ft TVD in the well 49/12-2, where a horizontal well with NW-SE orientation would increase the MW by up to 2.9 ppg (7.9 ppg).

Figure 11-57 shows the depleted Rotliegend at 10094 ft TVD (Leman Sandstone) in the well 49/11a-6, where a horizontal well with NW-SE orientation would increase the MW by up to 1.9 ppg (4.9ppg).

Figure 11-58 shows the depleted Rotliegend at 11070 ft TVD (Leman Sandstone) in the well 49/12a-K4, where a horizontal well with NW-SE orientation would increase the MW by up to 2.8 ppg (6.8ppg).

Figure 11-59 shows the depleted Rotliegend at 13254 ft TVD (Leman Sandstone) in the well 49/12a-K5, where a horizontal well with NW-SE orientation would increase the MW by up to 3 ppg (8 ppg).

Figure 11-60 shows the depleted Rotliegend at 9613 ft TVD in the well 49/12-A6, where a horizontal well with NW-SE orientation would increase the MW by up to 2.4 ppg (7.4 ppg).

Figure 11-61 shows the depleted Rotliegend at 8609 ft TVD in the well 49/12-A10, where a horizontal well with NW-SE orientation would increase the MW by up to 3.8 ppg (9.8 ppg).

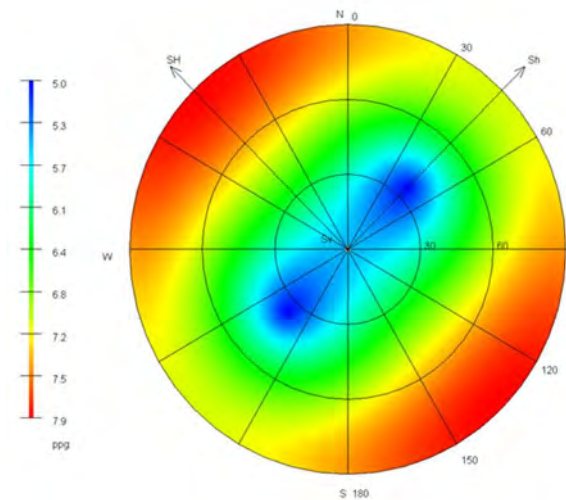


Figure 11-56 Viking A Well 49/12-2 (depleted condition) Well trajectory analysis

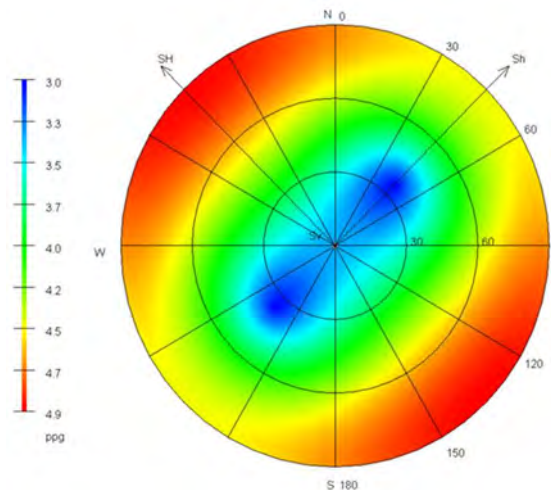


Figure 11-57 Viking A Well 49/11a-6 (depleted condition) Well trajectory analysis

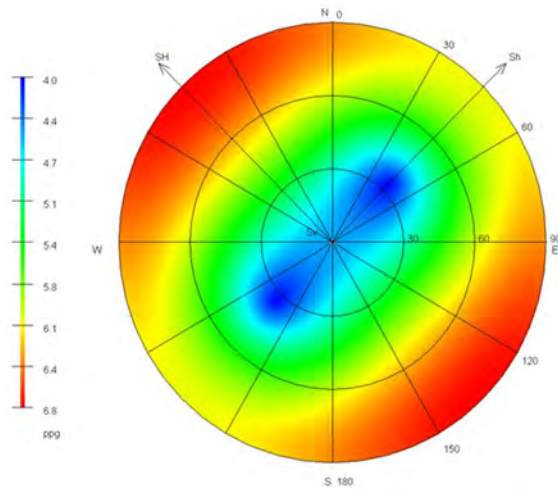


Figure 11-58 Viking A Well 49/12a-K4 (depleted condition) Well trajectory analysis

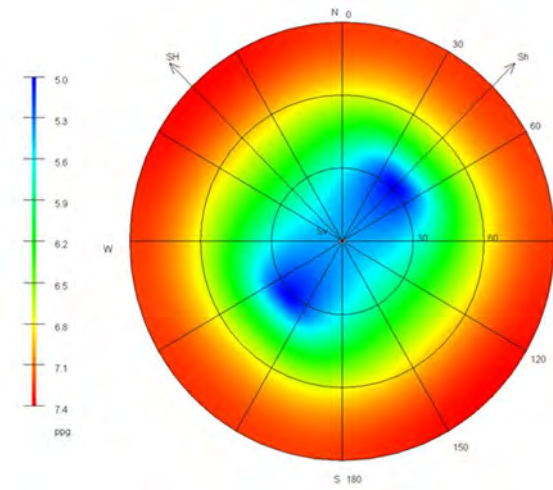


Figure 11-60 Viking A Well 49/12-A6 (depleted condition) Well trajectory analysis

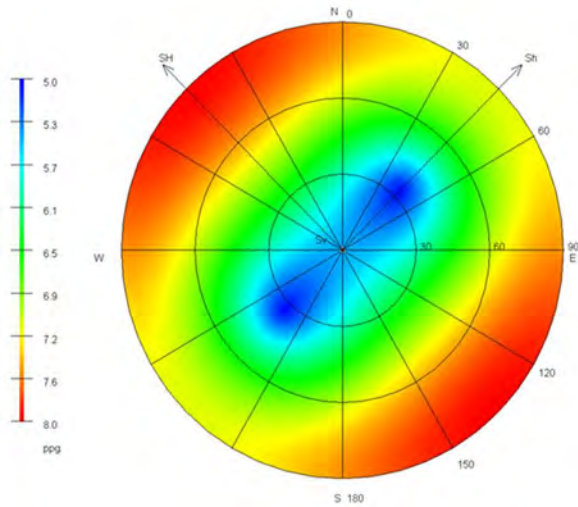


Figure 11-59 Viking A Well 49/12a-K5 (depleted condition) Well trajectory analysis

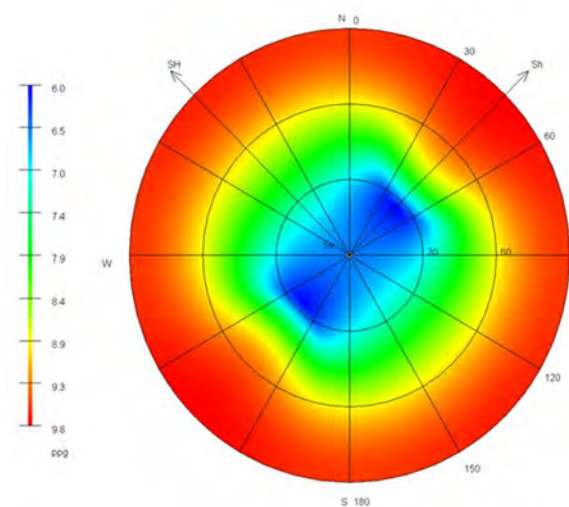


Figure 11-61 Viking A Well 49/12-A10 (depleted condition) Well trajectory analysis

11.6.1.5 Conclusions

- 1D geomechanical analysis of existing wells and pore pressure depletion estimation indicates that a potential depleted SHmin gradient could be around 0.54 psi/ft in the Leman Sandstone and that vertical wells can be drilled through the overburden and Leman Sandstone with 10 ppg as a maximum mud weights. The actual depleted condition in the Leman Sandstone has not been confirmed with field data.
- For vertical wells in this sequence, the recommended mud weight is around 5-10 ppg. Some basic analysis on required mud weights at different injector orientations has been performed within the Leman Sandstone. In general, mud weight increases of 1.9 to 3.0 ppg are sufficient to prevent breakouts for the worst orientation (horizontal wells parallel to SHmax).
- Assumptions are made that the regional NW-SE in-situ Shmax stress orientation is relevant to the Viking structure. Real Shmax azimuth may be different (e.g. oriented N-S parallel to local structure).
- Note the reported static mud weight windows are for drilling 'gun barrel' hole with no losses. If some breakout is tolerated and or losses can be managed with LCM then the real mud window could be larger.
- No core has been available to calibrate the strength (breakout) information. This would need optimising for any planned wells.
- The Leman Sandstone sometimes contains conductive faults that can take significant losses at pressures below the fracture gradient. As a result, active loss control procedures and/or as low a mudweight as possible are recommended whilst drilling the Leman to prevent excessive mud loss. If a low mudweight is required, casing off of the Zechstein salt is probably desired to prevent problems with salt creep – particularly with the depleted conditions expected.
- The wellbore trajectory analysis has been made on Leman Sandstone levels only. For any planned wells a predicted MW window would need to be generated based on expected lithologies vs planned trajectory. This could indicate different mud weights are required to maintain stability in some of the shallower units drilled at a higher angle than existing vertical wells.
- For drilling the thick salt sections, a number of factors need to be considered:
 - K/Mg salts can be very plastic and seal off the drill string very quickly. Often occur near the top of each evaporate sequence in the Zechstein. Manage by reaming or water pills.
 - Avoid creating washouts during drilling as this can lead to problems with differential stresses on the casing and possible collapse.
 - Isolated dolomite stringers or larger 'rafts' within the salt maybe at lithostatic or higher pressure. Can produce 16-19 ppg kicks. Use 3D seismic to navigate around larger ones.
 - Plattendolomite at base Zechstein may sometimes contain H₂S at 15-120 ppm derived from the Kupferschiefer.
 - To properly case off the salt above depleted Leman, casing would need to be set in the Zechstein Anhydrite 1 at base Zechstein or within any Rotliegend claystone that may be present above or in the upper part of the Leman Sandstone.

11.6.2 Well Design

In order to develop the depleted Viking gas fields for carbon capture and storage, both CO₂ injection and monitoring wells will be required. The CO₂ injectors will be J-shaped, high angle wells in order to optimise dense phase CO₂ injection performance. The monitoring well will also be J-shaped to allow it to be used as a spare injector, should the need arise.

The purpose of this section of the report is to:

- Identify well design risks and drilling hazards based on the available offset well data.
- Generate a preliminary well design for the identified injection and monitoring wells.
- Provide high level time and cost estimates for each well type.

This report proposes a conceptual well design that could form the basis of a detailed well design. It should be stressed that the well design suggested herein is not fully developed and may be subject to change following detailed engineering analysis.

11.6.2.1 Offset Review

Well data from available sources on the CDA database has been analysed in order to identify inputs for designing the Viking CO₂ injection and monitoring wells. The key findings are as follows:

Surface Hole and Conductor

In the area, the conductor has been set using two differing techniques, these being:

- Drill a 36" or 32" hole section to approximately 100m below seabed, and then run and cement a 30" or 26" conductor.

- Drive a 26" conductor to approximately 95m.

Both techniques have been applied successfully, with no hole or installation problems occurring.

Surface Hole Section and Casing

The surface hole sections have been drilled to 30m below the top of the Triton Anhydrite at approximately 750m TVDSS. This setting depth was selected to:

- Provide sufficient formation strength to drill the next hole section with a weighted mud system.
- Isolate the reactive Winterton Clay.

All surface hole sections were drilled using seawater, with bentonite sweeps being used to assist with hole cleaning.

Some surface hole sections were directionally drilled, with inclination being nudged up to 20°. The main reason for conducting directional drilling at shallow depths was to provide separation from offset platform wells. Therefore, should anti-collision issues dictate that directional drilling in the surface hole section is a requirement in a future development application, offset data suggests that this is possible.

No major problems occurred when drilling the surface hole sections, however, the following issues were recorded as being potentially problematic:

- The Triassic Winterton clays can be reactive when drilled with seawater, and are prone to swelling.
 - KCl water based mud was spotted at section TD instead of conventional spud mud, in order to reduce the rate of clay swelling prior to running the surface casing string.

- Chert was present in the Chalk formation overlying the Winterton Clay, which led to high vibration and slow rates of penetration (ROP).

First Intermediate Hole Section and Casing

The first intermediate hole section was drilled to 100m below the top of the Zechstein formation at approximately 2,100m TVDSS. This setting depth was selected to:

- Isolate the weaker Bunter shale prior to drilling the mobile Zechstein salt sequences.
- Provide sufficient formation strength to contain over-pressure from Platten Dolomite rafts, should one of these be encountered.
- Allow the use of a salt-saturated mud system in the Zechstein formations.
- Allow the use of water based pills to free stuck drillstrings in the mobile salt sequences (should these be required) without exposing the Bunter shale and Haisborough Group clays to uninhibited water based fluids.

The findings from the intermediate hole section offset analysis were as follows:

- The hole sections were drilled with both KCl salt-saturated water based and oil based mud systems, with the management of drilled cuttings being the deciding basis upon which the mud system was selected. Both systems were successfully used, however, the following issues were observed when drilling with the water based system:
 - Tight hole and stuck pipe occurred in the mobile salts encountered in the Keuper, Muschelkalk and Rot halites.

- Shale sloughing and hole enlargement occurred in the Muschelkalk clays with 10.5 ppg water based mud. However, upon raising the mud weight to 11.0 ppg, wellbore stability was regained.

- Low level mud losses (i.e. up to 15 barrels per hour (bph)) were observed at the top of the Bunter Sand with 11.0 ppg mud weight.
- The Bunter Sand is abrasive, and this led to slow ROPs and increased rates of bit and BHA wear. Additional trips were required to replace worn bits and eroded BHA components.
- No problems were recorded running and cementing casing.

11.6.2.2 Second Intermediate Hole and Production Casing

The second intermediate hole section was drilled through the Zechstein sequence, with production casing being set in the Werra Anhydrite directly above the Rotliegend reservoir sands. This setting depth was selected to:

- Isolate the Zechstein salt sequences prior to drilling the reservoir with a dedicated drill-in fluid.
- Isolate any over-pressured dolomite rafts.
- Minimise the risk of losses when cementing casing across the mobile Zechstein halites.
 - Fully circumferential cement coverage is a necessity if casing collapse due to mobile salt point loading is to be avoided.

The findings from the second intermediate hole section offset analysis were as follows:

- Both KCl salt-saturated water based mud and oil based mud were effective in maintaining gauge hole and minimising wash-outs in the halite sections.
- Casing collapse in the early Viking wells (i.e. before 1985) was a common occurrence. However, the wells drilled after this date used high collapse casing with enhanced cementing techniques to effectively minimise the risk of casing collapse.
- Over-pressured Platten and Haupt Dolomite rafts were encountered on many occasions in the early Viking wells, with kicks and well control problems occurring. However, enhanced seismic processing techniques have now made it possible to reduce the risk of encountering a floating dolomite raft, with the incidence of well control events reducing. Therefore, the risk of inadvertently drilling into an over-pressured dolomite raft has been significantly reduced.
- Mobile salt movement has led to stuck pipe on multiple occasions. However, the drillstring was freed on most occasions by spotting a freshwater pill across the stuck zone and dissolving salt around the drillstring.
- Running casing has on occasion been problematic, with the casing shoe hanging up on dolomite and anhydrite ledges in washed out sections of salt.
- Cementing the earlier Viking wells was problematic, with cement coverage in over-gauge sections leading to mobile salt point loading and casing collapse.

Production Hole Section and Liner

The production hole section was drilled through the Rotliegend reservoir sands, with many of the latter wells being drilled horizontally in order to maximise

production rates. The reservoir section was either cased and perforated, or completed with a slotted liner.

The Rotliegend Sands were drilled with both water-based drill-in fluids and oil based muds, with both systems being effective as a drilling fluid. On occasion, low level losses occurred, however, in the majority of cases, drilling the reservoir hole section and running the liner was problem free.

It should be noted that none of the offset wells reviewed were drilled into a depleted reservoir. As such, none of the reviewed wells encountered any of the problems associated with low pore pressure such as:

- Losses caused by a reduction in formation strength.
- Differential sticking.
- Wellbore instability.

11.6.2.3 Drilling Risks and Hazards

The following drilling risks and hazards been identified from the available offset data.

Shallow Gas

At present, it is assumed that shallow gas will not be present below the platform location. However, this will be confirmed when the results of the shallow gas survey are available. In the event that shallow gas is identified at the selected platform location, the location will be moved.

Shallow Swelling Clays

The Triassic Winterton Clays swell when exposed to seawater or water based drilling fluids. Therefore, the length of time in which they are left open should be minimised. This situation has been managed in the offset wells by:

- Setting surface casing directly below the base of the Winterton formation (in the Triton Anhydrite).
- Displacing the hole to KCl water based mud at section TD instead of conventional spud mud in order to reduce the rate of clay swelling prior to running the surface casing string.

Reactive Clay

Shale sloughing and hole enlargement has occurred in the offset wells when drilling the Muschelkalk Clay with water based systems, suggesting that the shales are chemically reactive. This problem was managed by increasing the mud weight from 10.5 ppg to 11.0 ppg, however, it is recommended that consideration be given to using oil based mud in order to eliminate water induced chemical reactivity.

Triassic Halites

The Triassic salts are known to be mobile, with instances of tight hole and stuck pipe having occurred in the Keuper, Muschelkalk and Rot halites. Two mud systems have been used when drilling these formations, these being salt-saturated water-based mud or oil-based mud. Either is considered acceptable for use; however given that benefits can also be realised by drilling the Muschelkalk clays with oil based mud, it is recommended that this system is selected for use.

In order to minimise salt movement, it is important to select the correct mud weight. Offset data suggests that a mud weight of 11.0 ppg will be successful in preventing salt movement in these halites, however this is inclination dependent. It is recommended that detailed modelling be conducted during the FEED stage to confirm the mud weights required to maintain wellbore stability in the Muschelkalk clay and halite formations at the inclinations planned.

Losses to the Bunter Sand

Low level mud losses have been recorded at the top of the Bunter Sand with 11.0 ppg mud weight. This mud weight is required to maintain wellbore stability in the Triassic Halites and Muschelkalk Clay, therefore, loss management must be considered. During the FEED stage, it is recommended that lost circulation materials are assessed for effectiveness and that a detailed loss management strategy is devised for the Bunter Sand.

Zechstein Salt Movement

The Zechstein salts are known to be mobile, with instances of tight hole and stuck pipe having occurred on many occasions. Two mud systems have been used when drilling these formations, these being salt-saturated water-based mud or oil-based mud, with either being considered acceptable for use.

When salt movement has led to a stuck drillstring, this has been rectified by spotting a freshwater pill across the stuck zone, and dissolving the salt.

In order to minimise salt movement, it is important to select the correct mud weight. Offset data suggests that a mud weight of 10.5 to 11.0 ppg will be successful in preventing salt movement, however this is inclination dependent. It is recommended that detailed modelling be conducted during the FEED stage to confirm the mud weights required to reduce the rate of salt creep at the inclinations planned.

Over Pressured Dolomite Rafts

Floating dolomite rafts containing over-pressured brine and gas have been encountered in the Viking area. Drilling into a raft can lead to a well control incident, with high surface pressures. The most effective method of mitigating this risk is to avoid drilling into a dolomite raft, and this can be achieved by

positioning the well to avoid seismically observable rafts. However, it should be recognised that some rafts may be small and below the range of seismic resolution. Therefore, the risk associated with encountering an over-pressured dolomite raft cannot be eliminated, and the casing design and well control programme should be designed on the assumption that a dolomite raft is encountered.

Cementing in the Zechstein and Casing Collapse

Zechstein salt induced casing collapse was a common occurrence in the early Viking wells (i.e. before 1985), with this occurring for the following reasons:

- The collapse rating of the casing was insufficient to withstand the forces imposed by mobile salt sections.
- Casing strings were inadequately cemented across the Zechstein, leading to salt point loading opposite casing without complete circumferential cement coverage.

The risk of failure can be mitigated by using high collapse strength casing, and by designing the drilling fluid and cement job to increase the probability of full cement coverage over the entire length of the Zechstein open hole section. The mitigation methods include:

- Drill the hole section with oil based mud to increase the likelihood of delivering a gauge hole and avoiding washed out sections.
- Centralise the casing string over the entire length of the open hole to optimise annular stand-off.
- Maximise cement displacement rates to ensure full mud and cement displacement.
- Use a spacer train system which will remove the oil based mud residue while minimising salt wash-outs.

Depleted Rotliegend Sand

The Rotliegend reservoir sand is known to be highly depleted, and this will generate the following problems:

Loss of formation strength: Depleted formations lose formation strength, with the reduction in fracture gradient being proportional to the reduction in pore pressure. Reservoir mud weights must be maintained at a level which keeps equivalent circulating density (ECD) below the depleted fracture gradient in order to avoid losses.

Differential sticking: Drilling with a fluid column will generate a significant overbalance against the formation, which could lead to differential sticking. This risk may be mitigated by:

- Drilling with as low a mud weight as possible to reduce the differential pressure.
- Using a drilling fluid which generates a tight filter cake.
- Using stabilised drillpipe to reduce the drillstring surface area in contact with the borehole wall.

Wellbore instability: The Rotliegend Sand is predicted to require a minimum mud weight of up to 8.0 ppg to avoid wellbore instability. Given that the depleted formation strength is predicted to be 10.5 ppge, in this instance, a mud weight can be selected which maintains wellbore stability even under depleted conditions.

11.6.2.4 Directional Profiles

Reservoir Targets

The following reservoir targets have been identified for the Rotliegend reservoir:

Target Name	TVDSS (m)	UTM North (m)	UTM East (m)
INJ-01 Top Rotliegend	2,598.9	5,931,001.0	451,161.7
INJ-01 TD	2,844.7	5,931,272.0	451,473.2
INJ-02 Top Rotliegend	2,556.3	5,931,975.0	449,877.5
INJ-02 TD	2,703.3	5,932,169.0	449,708.5
INJ-03 Top Rotliegend	2,593.3	5,930,401.0	451,911.2
INJ-03 TD	2884.0	5,930,019.0	452,243.5

Table 11-15 Viking A reservoir targets

The coordinate system in use is UTM, ED50 Common Offshore, Zone 31N (0° to 6° East)

Note: Well INJ-03 is currently defined as the monitoring well and/or spare injector.

Surface Location

A central surface location for the platform site has been selected, with the coordinates being:

- 5,930,500m North
- 451,000m East

The platform surface location and position for each well is shown in the spider plot below:

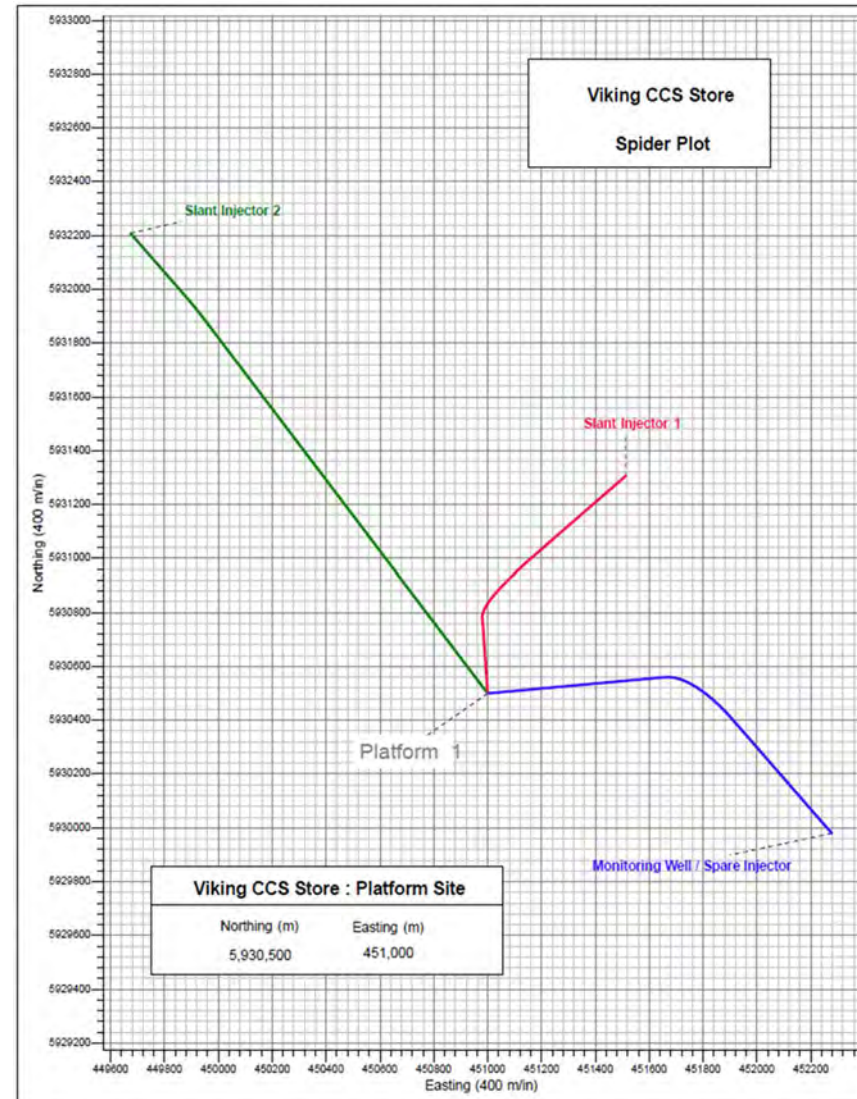


Figure 11-62 Platform directional spider plot

Directional Design

The platform and well reservoir locations have been selected for conceptual well design purposes; however, it should be noted that these locations have not been optimised for reservoir management or directional drilling purposes. Therefore, it is recommended that the wells are re-planned and anti-collision scans conducted during the FEED stage when the target locations have been finalised.

The conceptual directional plans for the CO₂ injectors have been designed on the following basis:

- All wells will be drilled as slant wells, including the monitoring well which will also act as a spare injector.
- All wells will be drilled vertically to 640m TVDSS (i.e. to below the surface casing shoe).
- All wells will be kicked off below 640m MD, with a planned dogleg severity of 3.0° per 30m. The wells will be built to the required tangent angle, while turning the wellpath onto the required azimuth.
- A build section will be drilled from the surface shoe to the depth at which inclination is sufficient to reach the identified reservoir target.
- A turn and build / drop section will be drilled in the 12 ¼” hole section to deliver an inclination of 60° at the top of the Rotliegend Sand while turning the well path onto the desired azimuth.
- The reservoir section will be drilled as a tangent section, holding inclination at 60° to TD below the base of the Rotliegend Sand.

Directional profiles have been prepared for each injection well based on the reservoir targets and directional drilling limitations, as follows:

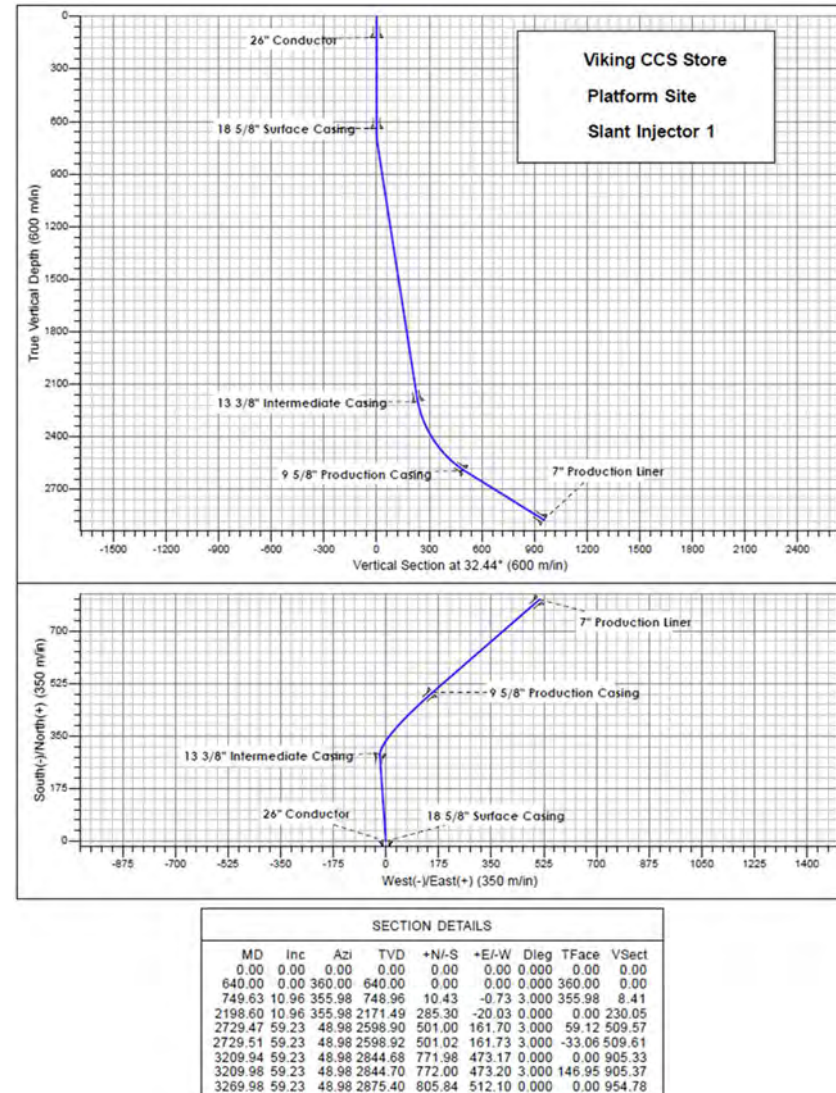


Figure 11-63 Slant injector 1 directional profile

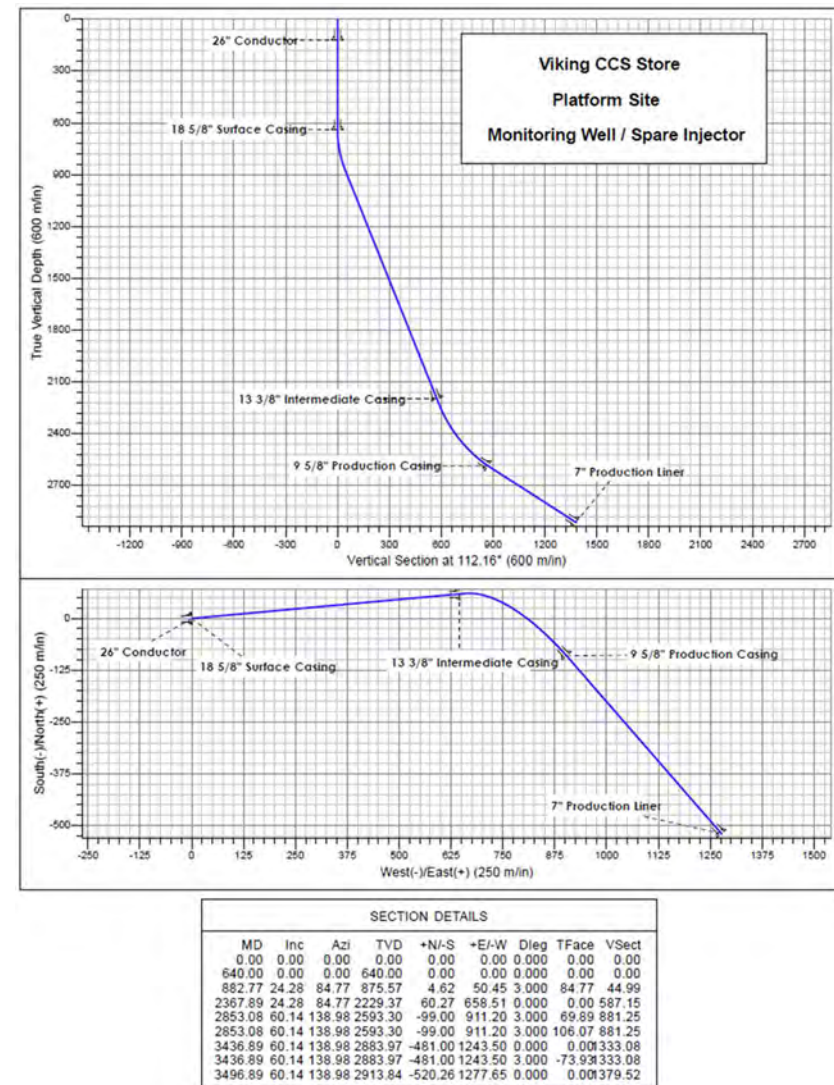
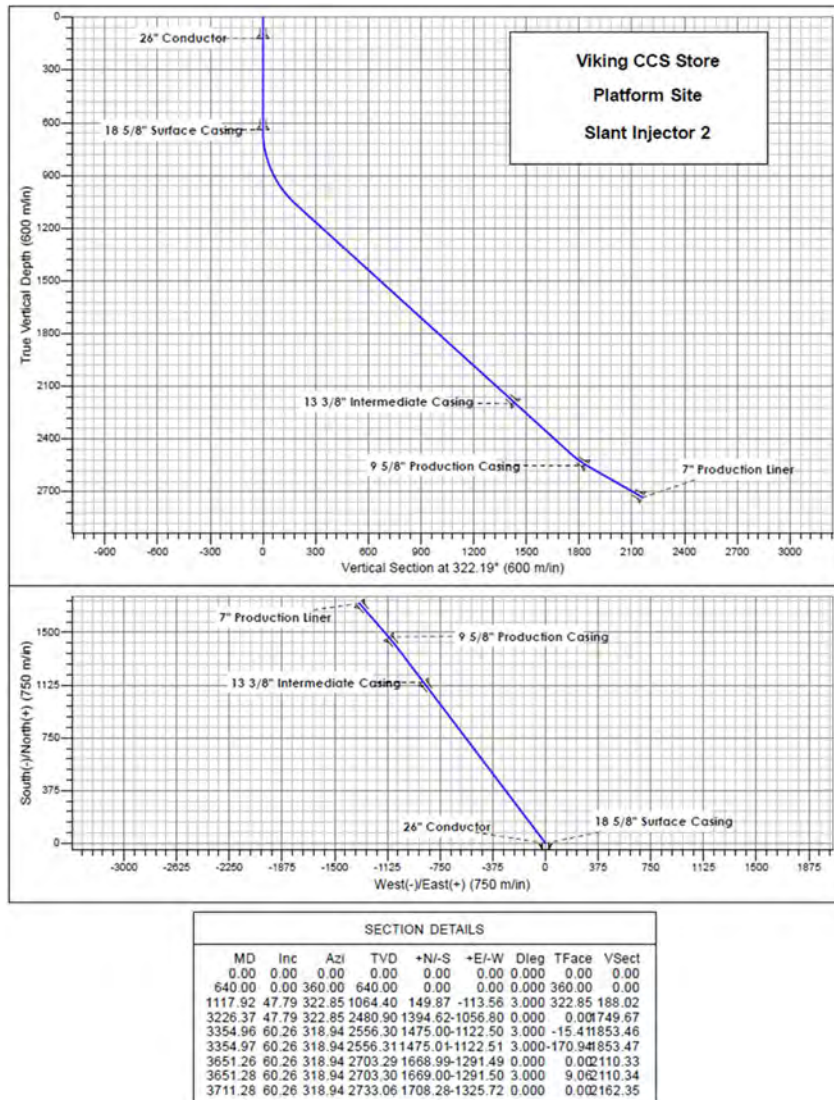


Figure 11-64 Slant injector 2 directional profile

Figure 11-65 Monitoring Well / Slant injector 3 directional profile

11.6.2.5 Detailed Well Design

CO₂ Injector

Conductor

To reduce the risk of shallow soil destabilisation, the conductor string is normally driven to depth on platform wells in the Southern North Sea, and this method has been selected for setting the conductors in the Viking area. The conductor setting depth has been specified as 95m below the mudline for the following reasons:

- Conductors have been successfully driven to this depth regionally.
- The formation strength at this depth should be sufficient to hold a mud weight of 10.0 ppg (recommended spud mud weight prior to running surface casing), and allow returns to be taken to the rig floor elevation.

The selected conductor size is 26" which is compatible with the selected well design, while minimising the tubular diameter for driving efficiency.

22" Surface Hole and 18 5/8" Casing Setting Depth

The 13 3/8" intermediate casing setting depth has been defined as the top of the Zechstein at approximately 2,200m TVDSS. This setting depth has been selected in order to:

- Isolate the weaker Bunter Shale prior to drilling the mobile Zechstein salt sequences.
- Provide sufficient formation strength to contain over-pressure from a Platten Dolomite raft, should these be encountered.

17 1/2" Intermediate Hole and 13 3/8" Casing Setting Depth

The 13 3/8" intermediate casing setting depth has been defined as the top of the Zechstein at approximately 2,200m TVDSS. This setting depth has been selected in order to:

- Isolate the weaker Bunter Shale prior to drilling the mobile Zechstein salt sequences.
- Provide sufficient formation strength to contain over-pressure from a Platten Dolomite raft, should these be encountered.

12 1/4" Intermediate Hole and 9 5/8" Production Casing Setting Depth

The 12 1/4" intermediate hole section will be drilled through the Zechstein formations, and will be cased off prior to drilling the reservoir section. The 9 5/8" production casing will be set in the Werra Anhydrite directly above the Rotliegend reservoir sands in order to:

- Isolate the Zechstein salt sequences prior to drilling the reservoir with a dedicated drill-in fluid.
- Isolate any over-pressured dolomite rafts.
- Maximise the probability of obtaining a good cement job across the mobile Zechstein halites. This provides the following advantages:
 - The risk of a poor cement job is reduced, thereby minimising the risk of casing collapse due to mobile salt point loading.
 - Note: Fully circumferential cement coverage is a necessity if casing collapse due to mobile salt point loading is to be avoided.
 - The cement design can be optimised to provide isolation from the reservoir, thereby minimising the risk of CO₂ leakage from the reservoir.

- The probability of delivering a good cement job for end of life abandonment purposes is increased.

8 ½" Production Hole and Sand Screen Setting Depth

The 8 ½" hole section will be drilled through the Rotliegend Sand, with the section length being optimised for CO₂ injection purposes.

A 7" liner will be run to TD and cemented across its entire length for reservoir management and zonal isolation purposes.

End of Life Well Abandonment

The casing sizes and setting depths have been selected to ensure that the well can be abandoned at the end of field life by placing cement plugs inside cemented 9 5/8" production casing and opposite the anhydrites and halites of the Zechstein sequence. These formations have sufficient strength to contain reservoir pressure; therefore, by placing the abandonment plugs opposite these formations, store integrity will be assured.

Casing Metallurgy

When selecting the casing materials for CO₂ injectors, the following issues should be taken into consideration:

- Corrosion caused by exposure to CO₂.
- Material selection for low temperature.

For casing strings with no direct exposure to the CO₂ injection stream, CO₂ corrosion resistant materials are not required. Therefore, the following casings strings may be specified using conventional carbon steel grades:

- 26" conductor
- 18 5/8" surface casing

- 13 3/8" intermediate casing
- 9 5/8" production casing above the production packer

However, below the production packer, the casing and liner components will be exposed to injected CO₂. The corrosion potential will be dependent upon the water content of the injected CO₂, and/or latent water in the wellbore; however, some form of corrosion resistant alloy (CRA) will be required. The most commonly used CRA for CO₂ corrosion resistance is 13Cr and this would probably be suitable for the casing strings exposed to the injection stream below the production packer. However, it is recommended that detailed modelling be conducted during the FEED stage to confirm that this material is suitable for the injection stream specification. The strings to be designed using CRA materials are:

- 9 5/8" production casing below the production packer
- 7" production liner

When selecting the casing materials, it should also be noted that all casing strings could be exposed to low temperatures. The worst case happens during transient conditions which occur when wellbore pressure is released. A reduction in wellbore pressure can occur due to planned operations (i.e. when pressure is bled off to test a downhole safety valve or during well servicing activities), or when an unplanned event occurs (i.e. there is a leak at the wellhead). When wellbore pressure is released either by design or unexpectedly, dense phase (liquid) CO₂ will revert to its gaseous phase. At the liquid / gas interface, temperatures can be as low as -78oC, and heat transfer will lead to the near wellbore casing materials being exposed to low temperatures. In order to determine the minimum temperature that each casing string could be exposed to, modelling will be required, and this should be conducted during the detailed design phase.

When metals cool they lose toughness, which could become an issue when subjected to mechanical load. Therefore, in order to demonstrate that the selected casing grades are suitable for the modelled temperatures, low temperature impact toughness testing should be conducted by the steel suppliers, to confirm that the selected tubular is suitable for a low temperature application.

The monitoring well will not be exposed to the same concentrations of CO₂ and/or water as an injector. However, it is recommended that the selected casing grades are the same for a monitoring well as for an injector. This should provide the following benefits:

- Reservoir management flexibility is provided (i.e. it would ease conversion of a monitoring well to an injector).
- It would minimise the number of differing casing joints and string components purchased.

Wellhead Design

As with the casing materials, the wellhead components must also be designed to provide suitable low temperature performance and corrosion resistance. Wellhead component temperature rating is specified in API 6A with a class being assigned to reflect the temperature range to which the components are rated. For CO₂ injection wells, API 6A class K materials may be suitable, as the low temperature rating of these materials is -60oC. This should be acceptable for CO₂ injection purposes; however, it is recommended that detailed modelling is conducted for each wellhead component to confirm the lowest temperature to which they may be exposed, and that suitable materials are being selected.

In addition, the wellhead components which are directly exposed to the CO₂ injection stream should be specified from CO₂ resistant alloys.

Negative Wellhead Growth

When CO₂ injection commences, well temperatures are expected to drop. This could lead to casing contraction and negative wellhead growth (i.e. the wellhead made up to the surface casing will move lower, and the tensile stresses in the 13 3/8" and 9 5/8" casing strings will decrease). This scenario should be modelled during the detailed design phase, to confirm that the selected casing strings remain within their tensile and compression design limits.

In addition, wellhead downward movement could lead to the wellhead, annulus valves and flowline clashing with the top of the conductor. Therefore, it is recommended that casing contraction is modelled during the detailed design phase to determine the movement magnitude, and to confirm that the gap between the top of the conductor and the surface casing starter wellhead is sufficient to prevent component clashes.

Drilling Fluids Selection

22" Surface Hole Section

This hole section should be drilled with seawater and viscous sweeps, taking returns to the rig. At section TD, the hole should be displaced to 10.0 ppg KCl water based mud, in order to reduce the rate of clay swelling and maintain wellbore stability prior to running the surface casing string.

The 22" hole section will initially be drilled through the Cretaceous Chalk, and this formation is known to produce sticky hole conditions, and high torques. However, chalk reacts well to being drilled with seawater, as the fines produced are constantly being diluted. In addition, faster ROPs can be obtained by drilling on-balance, and should losses occur, the cost implications will be minimal.

17 ½" Hole Section

This hole section should be drilled with 11.0 ppg oil based mud, taking returns to the rig. Oil based mud has been selected to:

- Avoid chemical reactivity and maintain borehole stability in the Muschelkalk Clay.
 - In some offset wells, shale sloughing and hole enlargement problems occurred in the Muschelkalk Clay when drilling with water based mud, suggesting that the shales are chemically reactive. This problem was managed by increasing the mud weight from 10.5 ppg to 11.0 ppge; however, using oil based mud will eliminate water induced chemical reactivity.
- Maintain borehole stability in the Triassic Halites (i.e. prevent mobile salt movement).
- Provide increased lubricity in the Bunter Sand and reduce the risk of bit or BHA component failure due to abrasion.
- Maintain gauge hole in order to reduce the risk of hole cleaning problems and increase the probability of obtaining a good cement bond.

It should be recognised that cuttings collection and management will be an important issue when using oil based mud. Therefore, this factor should be addressed early in the planning process, when selecting the rig.

12 ¼" Hole Section

The 12 ¼" intermediate hole section will be drilled through the Zechstein formations, and should be drilled with oil based mud, taking returns to the rig.

Oil based mud has been selected in order to avoid washouts in the salt formations and deliver a gauge hole for cementing purposes.

In order to minimise salt movement, it is important to select the correct mud weight. Offset data suggests that a mud weight of 10.5 to 11.0 ppg will be successful in preventing salt movement, however this is inclination dependent. It is recommended that detailed modelling be conducted during the FEED stage to confirm the mud weights required to reduce the rate of salt creep at the inclinations planned.

8 ½" Hole Section

The 8 ½" reservoir hole section should be drilled with oil-based mud weighted to 8.8 ppg (or lower if possible). This mud system has been selected in order to:

- Use a conventional mud system with as low a weight as possible.
 - Base oil has a lower density than water, thereby providing lower weights than water based muds.
- Deliver lower ECD's, thereby ensuring that ECD does not exceed the predicted formation strength under depleted conditions. ECD may be minimised by adopting the following practices:
 - Use ultra-fine barite to lower the rheological profile.
 - Use the lowest pump rate commensurate with efficient hole cleaning.
 - Reduce the yield a point and plastic viscosity of the mud system to the lowest values commensurate with efficient hole cleaning.
- Reduce the differential sticking risk by:

- Keeping the mud weight as low as possible, thereby reducing the differential pressure applied to the drillstring.
- Generating a tight filter cake, thereby reducing the contact area between the drillstring and the borehole wall.

In addition, oil based mud provides the following benefits:

- It minimises formation damage in the reservoir by building a tight filter cake and reducing the depth of filtrate invasion.
 - It should be noted that oil-based mud can also cause damage in the Rotliegend Sand, if incorrectly specified. Fluid loss to the reservoir can affect porosity; therefore it is important to maintain mud system fluid loss at very low levels. In addition, filter cake deposition must be tightly controlled, to ensure that any damage that does occur is local to the wellbore, allowing the perforation tunnels to extend beyond the damaged zones.
- It can deliver higher ROPs.
- It increases lubricity and reduces the rate of erosion to bit and BHA components caused by the abrasive sandstone cuttings.

It should be recognised that cuttings collection and management will be an important issue when using oil based mud. Therefore, this factor should be addressed early in the planning process, when selecting the rig.

Cement Programme

18 5/8" Surface Casing

The 18 5/8" surface casing should be cemented back to the mudline using conventional cement slurries.

13 3/8" Intermediate Casing

The purpose of the 13 3/8" cement job is primarily to provide a strong shoe prior to drilling the Zechstein sequence, and a tail slurry should be used to generate the compressive strength required to meet this objective.

The 13 3/8" casing should be cemented back to 100m inside the 18 5/8" shoe in order to save suspension or abandonment costs, while minimising the risk of cement contamination at the mudline hanger.

Conventional lead and tail slurries should be selected for this cement job.

9 5/8" Production Casing

The purpose of the 9 5/8" cement job is to:

- Isolate the Zechstein formation prior to drilling the Rotliegend Sand.
- Provide full cement coverage across the Zechstein halites to prevent salt point loading and casing collapse.
- Prevent CO₂ leakage from the reservoir.

A single slurry should be used to generate the compressive strength required to meet these objectives.

The 9 5/8" casing should be cemented back to 200m inside the 13 3/8" shoe in order to:

- Ensure full cement coverage across all mobile halite sequences.
- Cement off all open formations, and minimise leak paths from the Rotliegend Sand.
- Optimise the end of field life abandonment design.

7" Production Liner

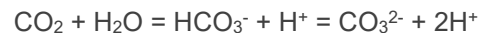
The purpose of the 7" cement job is to provide zonal isolation in the reservoir and prevent CO₂ leakage. The liner should be cemented over its entire length to the liner hanger using a single slurry at a low weight (to minimise the risk of cementing losses).

- The combined cement slurry and mud weight should be designed to ensure that the cementing ECD does not exceed 10.5 ppge.
- The cement displacement rate should be minimised to reduce the risk of losses.
- Consideration should be given to placing expandable casing packers at any zones critical to zonal isolation, in order to provide a secondary isolation mechanism should cementing losses occur.

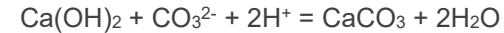
Production Casing and Liner Cement Design

At present, it is planned to cement the production casing and liner strings using conventional Portland Class G cement. The interaction between Portland cement and CO₂ is as follows:

- Carbonic acid will form when water and CO₂ are present:



- When cement and carbonic acid are in contact, cement dissolution and carbonate precipitation (also called cement carbonation) occurs. This process forms an insoluble precipitate and leads to lower porosity because calcium carbonate has a higher molar volume than Ca(OH)₂ (i.e. cement). This reduces the CO₂ diffusion rate into the cement and is therefore a self-healing mechanism (Shen and Pye, 1989). The precipitation mechanism is:



Due to the carbonation effect, cement degradation is a very slow process. Lab testing has been conducted by various parties in order to determine the rate of degradation, with a summary of the test results shown in Table 11-16.

For comparison purposes, the reservoir pressure is predicted to vary between 35 and 270 bar. As such, the rate of cement degradation predicted by Bartlett-Gouedard may be the most appropriate measurement to use. This suggests that cement would degrade at a rate of 2.5m per 10,000 years. Given that the length of cement behind the 9 5/8" production casing is designed to cover approximately 700m to 750m, it may be concluded that the rate of conventional class G cement degradation makes the selection of this cementing material suitable for use.

However, the loss of integrity due to degradation is not the only factor to be considered when selecting the cement type. The creation of micro-annuli due to thermal cycling should also be taken into consideration, as the wellbore could be exposed to low temperatures at certain stages of the CO₂ management process.

CO₂ resistant cements are available from the main cementing service providers, with the chemistry being well understood. These specialist cements have been

Reference	Cement Class	Test Pressure (bar)	Test Temperature (°C)	Cement degradation per 1,000 years (mm)	Cement degradation per 10,000 years (mm)
Bartlet-Gouedard	G	280	90	776	2,454
Bartlet-Gouedard	G	280	90	646	2,042
Duguid et al	H	1	23	29	92
Duguid et al	H	1	23	16	50
Duguid et al	H	1	23 / 50	99	314
Duguid et al	H	1	23 / 50	74	234
Lecolier et al	Conventional	150	120	1,648	5,211
Shen & Pye	G	69	204	3,907	12,354
Bruckdorfer	A	207	79	184	583
Bruckdorfer	C	207	79	152	480
Bruckdorfer	H	207	79	228	721
Bruckdorfer	H + flyash	207	79	250	789

Table 11-16 Cement degradation rates in CO₂ laboratory test results

used in CO₂ environments, however, they can be problematic to handle as they are incompatible with conventional cementing products. Therefore, when selecting the preferred cement type it is recommended that conventional cements are compared with CO₂ resistant systems, and that the selection is based on best practices and standards in place at the time of drilling.

Consideration should also be given to annular packers (casing deployed). These can have elastomer or metal seals, and reduce the risk of an annular leak path (micro-annulus) through the expansion and contraction of the casing during cementing operations.

11.6.3 Completion Design

11.6.3.1 Lower Completion

The lower completion consists of a 7" cemented and perforated liner. No sand control is incorporated in the base case following the recommendations of the sanding risk review.

Perforating options include:

- TCP shoot and pull
- TCP gun drop
- Coiled tubing conveyed perforating
- Wireline perforating

As the well is below hydrostatic, TCP shoot and pull could cause significant formation damage when the well is killed after perforating. TCP gun drop is discounted due to the requirement to maintain a large capacity sump for sand production. Coiled Tubing conveyed perforating could be considered, as larger gun lengths can be run. However, through tubing wireline perforating appears to be the most cost effective solution. Consideration could be given to dynamically underbalanced guns in order to help with perforation clean-up.

11.6.3.2 Upper Completion

The upper completion consists of a 7" tubing string, anchored at depth by a production packer in the 9-5/8" production casing, just above the 7" liner hanger. Components include:

- 7” 13Cr tubing (weight to be confirmed with tubing stress analysis work) with higher grade CRA from Barrier Valve to tailpipe
- Tubing Retrievable Sub Surface Safety Valve (TRSSSV)
- Deep Set Surface-controlled Tubing-Retrievable Isolation Barrier Valve (wireline retrievable, if available)
- Permanent Downhole Gauge (PDHG) for pressure and temperature above the production packer
- Optional DTS (Distributed Temperature Sensing) installation
- 9-5/8” V0 Production Packer

The DTS installation will give a detailed temperature profile along the injection tubulars and can enhance integrity monitoring (leak detection) and give some confidence in injected fluid phase behaviour. The value of this information should be further assessed, if confidence has been gained in other projects (tubing leaks can be monitored through annular pressure measurements at surface, leaks detected by wireline temperature logs and phase behaviour modelled with appropriate software). If possible, the DTS should be run across the full sandface (possibly behind casing) in order to provide an injection profile and monitor minimum temperatures in the wellbore.

11.6.3.3 Completion Metallurgy

Initial Assumptions

It is assumed that the injected fluid will be predominantly CO₂ with small concentrations of water, oxygen and nitrogen. Other minor impurities may exist however it will not be present in high enough concentrations to cause corrosion/cracking issues.

Metallurgy Selection

The selection of the metallurgy for flow wetted components of the CO₂ injection wells depends on the final composition of the supply stream. For pure CO₂, with negligible water content (<300ppmv), carbon steel is suitable. As contaminants increase, metallurgy specifications change and a higher spec is normally required. The table below indicates the impact of various contaminants.

Contaminants	Selectable materials
CO ₂ only	Carbon steel
CO ₂ + H ₂ O / O ₂	13Cr
CO ₂ + H ₂ S	25Cr
CO ₂ + H ₂ S + O ₂	Nickel Alloy
CO ₂ + NO ₂ /SO ₂	GRE

Table 11-17 Material selection vs contaminants

While nitrogen, methane and some other gases may also be present in the injected fluid, they do not react with the injection tubulars and therefore have no significance with regards to material selection.

NO₂ and SO₂ can increase corrosion rates in 13%Cr, but only when present in significant quantities or at high temperatures (>140°C for NO₂ and >70°C for SO₂). Viking reservoir temperature is moderate (~84°C) and therefore only the quantity and impact of SO₂ needs further assessment.

Given that liquid water may be present in the system (out of spec conditions or following water wash operations), a minimum spec of 13%Cr is recommended for all flow wetted components, including production tubulars and tubing

hangers. Note that it is expected that out of spec conditions will be transient, with flow wetted components only exposed to these conditions for a short period of time. If longer periods of exposure are expected, then metallurgy requirements may be increased to suit.

It is expected that the supply stream will have negligible H₂S content, and the Viking reservoir gas is expected to be free of this contaminant, although there is the possibility that some reservoir souring may have occurred since last gas production (SRB contamination). A gas sample should be acquired before abandonment of the current production wells in order to test for any H₂S presence.

It should also be noted that later in field life, as pressure in the reservoir increases to a point where partial pressures become more of a concern for corrosion, no water washes are expected and the near wellbore is likely to be fully dehydrated. This means that there is no (or very limited) water phase present. Corrosion to the reservoir liner is not considered a threat to well integrity, so 13CR is acceptable. However, in order to maintain long term integrity in injector wells, it is recommended that the bottom joints of production casing (up to and across the production packer and setting depth of any abandonment plug) is upgraded to a nickel alloy. Duplex material (25CR) may be suitable, pending further investigation, but given the moderate cost uplift for a few hundred feet of casing, the higher grade is recommended. Similarly, upper completion equipment, from tailpipe up to and including the production packer and deep set downhole shut-in valve, should be upgraded to Nickel alloy (or Austenitic stainless steels).

Material grade is limited to 80ksi (L-80) due to the potential for low temperatures. Further work is recommended to determine the minimum temperatures likely to

be seen during transient events such as blow down, and to ensure any material recommended is suitable for these extreme conditions.

11.6.3.4 Elastomers

NBR nitrile elastomer can be used within the temperature range of -30 to 120°C [S13] and is therefore suitable for CO₂ injection wells. This elastomer gives the lowest operating temperature among the typical downhole elastomers.

The major issue associated with elastomers and CO₂ is the loss of integrity due to explosive decompression. This occurs due to the diffusion of CO₂ into the elastomer and the rapid expansion of absorbed CO₂ during rapid decompression (or blow down). While blow down is not planned to occur in the Viking wells under normal operation conditions, unexpected / unplanned events may occur. An elastomer that is more tolerant of rapid gas decompression with the same low temperature capability is recommended, such as specially formulated HNBR elastomers.

11.6.3.5 Flow Assurance

Hydrates

Hydrates may be an issue at very low temperatures, providing water is present and CO₂ gas phase. The injection of MEG (glycol) where low temperature events occur may help mitigate this issue (see discussion of ice below). In the unheated phase injection system for Viking, the primary risk of hydrate formation is during re-start operations following wash water injection. Further work on this area is recommended in FEED.

Ice

Ice will be expected to form if fresh water (e.g. condensed water or halite wash water) is present and temperatures drop to below 0°C. High saline brines

(150,000 to 220,000ppm), such as is present in the reservoir, may freeze if temperatures drop below -13°C.

CO₂ injection is unlikely to reduce temperature to this low temperature in the well (see near wellbore modelling). However, unplanned blowdowns or local pressure drops may drop temperatures to these levels through Joules-Thomson effects. Intervention operations, where CO₂ may be vented in the presence of water, should carry the contingency of inhibitors such as MEG. Detailed operation planning is required in order to confirm requirements and concentrations.

A flow control choke is required in order to control the distribution of flow to individual wells and in some circumstances, such as start-up, to provide some back pressure for the delivery system. Pressure drops across the choke may result in significant temperature drops. This is only problematic in a flow assurance context if free water is continuously present in the delivery system upstream of the choke. Choke modelling will be required in order to determine the extent of this issue, and the knock on effect in downhole temperature. Mitigations include the addition of heating upstream of the choke and / or the continuous injection of ice inhibitors (e.g. MEG). Heating is the more appealing solution, as the effect of continuous MEG injection on the reservoir is unknown. System design, where the well is operating with the choke mostly open is the preferred solution.

11.6.4 Intervention Programme

Intervention requirements for the CO₂ injection wells are not well defined at present due to lack of analogue experience. It is expected that some well performance logging will be required (production logging or PLT) in order to monitor injection profile should DTS installation prove problematic. Remedial

stimulation may be required if formation damage occurs through plugging. Some sand clean-out may be required if the base case perforated cemented liner completion option is pursued rather than an installed sand control.

11.6.5 Time and Cost Estimates

High level time and cost estimates have been generated for project evaluation purposes, and are based on the following assumed activity throughout field life:

VIKING - PROJECT SEQUENCE						
Well Type	0	5	10	15	20	26
Platform 1						
Drill and Complete New Injection Well	2					
Drill and Complete New Monitoring Well / Spare Injector	1					
Workover			1			
Local Sidetrack from Existing Platform Slot			2			
Abandonment						3

Table 11-18 Field life well activity

The schedule above is based on the following assumptions, and can be considered highly conservative:

- We have a four slot platform and that 3 wells (2 plus one spare / monitoring well) are drilled.
- Injector well life is extended to 26 years (compared to a standard 20 year well life assumption), through experience on other CO₂ injectors and by increasing metallurgy, material and fatigue resistance specs.

- Two dense phase injection wells are required to fulfil the storage contract, with one contingent well (designated as the monitoring well) at all times in case of a well outage
- The two dense phase wells (7” tubing) will require 1 local sidetrack (where new formation is drilled from the existing wellbore) contingency due to unforeseen formation damage issues after 10 years. With only 16 years injection until the end of field life, no additional mechanical failures (workovers) are expected, other than that during the sidetrack (the sidetrack requires the tubing to be pulled)
- Sidetracks with twin initial injector wells
- A monitoring well / spare well will be drilled at the same time. This well will not require sidetrack due to intermittent use, but may require workover after 10 yrs or thereabouts to replace tubing (possibly to a smaller size or for mechanical failure issues)
- Workovers and sidetracks will be planned as campaigns in order to reduce rig mobilisation costs
- All 3 wells will be abandoned at the end of field life – 26 yrs
- No appraisal well is required for the Viking field; as sufficient reservoir data is available from the current production wells.

- The rate for a standard North Sea jack-up rig is assumed to be \$150,000 per day.
 - The exchange rate is assumed to be £1.00 = \$1.50.
- The inclination for all wells is within wire lining capability. Therefore, it has been assumed that the wells will be perforated through the completion using electric line as the deployment method.

The time and cost estimate summary for all wells is as follows:

VIKING COST MODEL		
Well Cost Summary Table		
Well Name	Days	Well Cost (£,000)
Year 0		
Platform Injector 1	68.3	26,142.5
Platform Injector 2	61.8	23,932.5
Monitoring Well 1 / Spare Injector 3	66.8	25,432.5
Year 10		
Workover 1	25.2	10,067.5
Local Sidetrack 1	57.9	20,292.5
Local Sidetrack 2	62.9	21,597.5
Year 26		
Abandonment Platform Injector 1	31.2	8,970.0
Abandonment Platform Injector 2	24.7	6,760.0
Abandonment Monitoring Well 1 / Spare Injector 3	31.2	8,385.0
TOTAL	429.7	151,580.0

Table 11-19 Time and cost estimate summary

Typical time and cost estimates for each identified well activity are as follows:

The time and cost estimates listed below are based on the following assumptions:

- The time estimates are based on performance data obtained from the offset wells analysed for this study.
- The wells will be drilled through a normally unmanned installation (NUI) using a standard North Sea jack-up rig.

VIKING COST MODEL							
Well : Platform Injector 1							
Location : Viking Platform							
Location Sequence Position : 1							
Activity	Days	Rig Cost per Day (£,000)	Phase Rig Cost (£,000)	Spread Cost per Day (£,000)	Phase Spread Cost (£,000)	Tangible Costs (£,000)	Total Phase Cost (£,000)
Fixed Price Costs							
Well management fees						250	250
Insurance						200	200
Site survey						300	300
Pre-drill studies						150	150
DTS Installation						600	600
Time Related Costs							
Move rig to location and jack-up over platform	5.0	100	500	150	750		1,250
Drive conductor	1.0	100	100	150	150	200	450
Drill 22" surface hole	2.5	100	250	150	375		625
Run and cement 18 5/8" surface casing. Nipple up BOPE	4.0	100	400	150	600	800	1,800
Drill 17 1/2" intermediate hole	6.0	100	600	150	900		1,500
Run and cement 13 3/8" intermediate casing	3.0	100	300	150	450	700	1,450
Drill 12 1/4" intermediate hole	5.0	100	500	150	750		1,250
Run and cement 9 5/8" production casing	3.0	100	300	150	450	800	1,550
Drill 8 1/2" reservoir hole	6.0	100	600	150	900		1,500
Log reservoir	2.0	100	200	150	300	200	700
Run and cement 7" liner	3.0	100	300	150	450	400	1,150
Displace to kill weight completion fluid	2.0	100	200	150	300		500
Run completion	4.0	100	400	200	800	900	2,100
Nipple down BOPE. Install Xmas tree	2.0	100	200	200	400	500	1,100
Perforate well on wireline	2.0	100	200	200	400	600	1,200
Suspend well pending CO ₂ injection	2.0	100	200	200	400		600
Move rig off location	0.0	100	0	200	0		0
Contingency at 30%	15.8	100	1,575	150	2,363	1,980	5,918
TOTAL	68.3		6,825		10,738	8,680	26,143

Table 11-20 Platform injector time and cost estimate

VIKING COST MODEL							
Well : Monitoring Well / Spare Injector 3							
Location : Viking Platform							
Location Sequence Position : 3							
Activity	Days	Rig Cost per Day (£,000)	Phase Rig Cost (£,000)	Spread Cost per Day (£,000)	Phase Spread Cost (£,000)	Tangible Costs (£,000)	Total Phase Cost (£,000)
Fixed Price Costs							
Well management fees						250	250
Insurance						200	200
Site survey							0
Pre-drill studies							0
DTS Installation						600	600
Time Related Costs							
Move rig to location and jack-up over platform	0.0	100	0	150	0		0
Drive conductor	1.0	100	100	150	150	200	450
Drill 22" surface hole	2.5	100	250	150	375		625
Run and cement 18 5/8" surface casing. Nipple up BOPE	4.0	100	400	150	600	800	1,800
Drill 17 1/2" intermediate hole	6.0	100	600	150	900		1,500
Run and cement 13 3/8" intermediate casing	3.0	100	300	150	450	700	1,450
Drill 12 1/4" intermediate hole	5.0	100	500	150	750		1,250
Run and cement 9 5/8" production casing	3.0	100	300	150	450	800	1,550
Drill 8 1/2" reservoir hole	6.0	100	600	150	900		1,500
Log reservoir	2.0	100	200	150	300	200	700
Run and cement 7" liner	3.0	100	300	150	450	400	1,150
Displace to kill weight completion fluid	2.0	100	200	150	300		500
Run completion	4.0	100	400	200	800	900	2,100
Nipple down BOPE. Install Xmas tree	2.0	100	200	200	400	500	1,100
Perforate well on wireline	2.0	100	200	200	400	600	1,200
Suspend well pending CO ₂ injection	2.0	100	200	200	400		600
Move rig off location	5.0	100	500	200	1,000		1,500
Contingency at 30%	14.3	100	1,425	150	2,138	1,845	5,408
TOTAL	66.8		6,675		10,763	7,995	25,433

Table 11-21 Monitoring well time and cost estimate

VIKING COST MODEL							
Well : Workover 1							
Location : Viking Platform							
Location Sequence Position : 1							
Activity	Days	Rig Cost per Day (£,000)	Phase Rig Cost (£,000)	Spread Cost per Day (£,000)	Phase Spread Cost (£,000)	Tangible Costs (£,000)	Total Phase Cost (£,000)
Fixed Price Costs							
Well management fees						250	250
Insurance						200	200
Site survey						300	300
Pre-drill studies							0
DTS Installation						600	600
Time Related Costs							
Move rig to location and jack-up over platform	5.0	100	500	150	750		1,250
Kill well and set suspension plugs	2.0	100	200	150	300		500
Nipple down Xmas tree. NU BOPE	2.0	100	200	150	300		500
Pull suspension plugs and completion	3.0	100	300	150	450		750
Perform scraper run and displace to completion fluid	2.0	100	200	150	300		500
Run completion	4.0	100	400	200	800	900	2,100
Nipple down BOPE. Install Xmas tree	2.0	100	200	200	400	500	1,100
Pull plug from tailpipe	0.5	100	50	200	100		150
Displace well to CO ₂	1.0	100	100	200	200		300
Suspend well pending CO ₂ injection	2.0	100	200	200	400		600
Move rig off location	0.0	100	0	200	0		0
Contingency at 30%	1.7	100	165	150	248	555	968
TOTAL	25.2		2,515		4,248	3,305	10,068

Table 11-22 Workover time and cost estimates

VIKING COST MODEL							
Well : Local Platform Sidetrack 1 (out of 9 5/8" casing)							
Location : Viking Platform							
Location Sequence Position : 2							
Activity	Days	Rig Cost per Day (£,000)	Phase Rig Cost (£,000)	Spread Cost per Day (£,000)	Phase Spread Cost (£,000)	Tangible Costs (£,000)	Total Phase Cost (£,000)
Fixed Price Costs							
Well management fees						250	250
Insurance						200	200
Site survey							0
Pre-drill studies						150	150
DTS Installation						600	600
Time Related Costs							
Move rig to location and jack-up over platform	0.0	100	0	150	0		0
Kill well and set suspension plugs	2.0	100	200	150	300		500
Nipple down Xmas tree. NU BOPE	2.0	100	200	150	300		500
Pull suspension plugs and completion	3.0	100	300	150	450		750
Set abandonment cement plugs	2.0	100	200	150	300		500
Perform scraper run and displace to mud	2.0	100	200	150	300		500
Set whipstock and mill window	1.5	100	150	150	225	100	475
Drill 8 1/2" section	5.0	100	500	150	750		1,250
Run and cement 7" liner	3.0	100	300	150	450	500	1,250
Drill 6" reservoir section	7.0	100	700	150	1,050		1,750
Log reservoir	2.0	100	200	150	300		500
Run and cement 4 1/2" liner	3.0	100	300	150	450	300	1,050
Displace to kill weight completion fluid	2.0	100	200	150	300		500
Run completion	4.0	100	400	200	800	900	2,100
Nipple down BOPE. Install Xmas tree	2.0	100	200	200	400	500	1,100
Perforate well on wireline	2.0	100	200	200	400	600	1,200
Suspend well pending CO ₂ injection	2.0	100	200	200	400		600
Move rig off location	0.0	100	0	200	0		0
Contingency at 30%	13.4	100	1,335	150	2,003	1,230	4,568
TOTAL	57.9		5,785		9,178	5,330	20,293

Table 11-23 Local sidetrack time and cost estimate

VIKING COST MODEL							
Well : Platform Injector 1 - Permanent abandonment							
Location : Viking Platform							
Location Sequence Position : 1							
Activity	Days	Rig Cost per Day (£,000)	Phase Rig Cost (£,000)	Spread Cost per Day (£,000)	Phase Spread Cost (£,000)	Tangible Costs (£,000)	Total Phase Cost (£,000)
Fixed Price Costs							
Well management fees						250	250
Insurance						200	200
Site survey						300	300
Pre-drill studies						150	150
Time Related Costs							
Move rig to location and jack-up over platform	5.0	100	500	150	750		1,250
Kill well and set suspension plugs	2.0	100	200	150	300		500
Nipple down Xmas tree. NU BOPE	2.0	100	200	150	300		500
Pull suspension plugs and completion	3.0	100	300	150	450		750
Set abandonment cement plugs on top of packer	2.0	100	200	150	300		500
Set 9 5/8" bridge plug	1.0	100	100	150	150		250
Cut and pull 9 5/8" casing from 100ft below 18 5/8" shoe	3.0	100	300	150	450		750
Cut and pull 13 3/8" casing from 100ft below 18 5/8" shoe	3.0	100	300	150	450		750
Set shallow abandonment cement plug	1.0	100	100	150	150		250
Nipple down BOPE	1.0	100	100	150	150		250
Cut and pull 18 5/8" casing and 26" conductor	1.0	100	100	150	150		250
Move rig off location	0.0	100	0	150	0		0
Contingency at 30%	7.2	100	720	150	1,080	270	2,070
TOTAL	31.2		3,120		4,680	1,170	8,970

Table 11-24 Well abandonment time and cost estimate

11.7 Appendix 7 – Cost Estimate

Provided separately in Excel and PDF formats.

11.8 Appendix 8 – Methodologies

11.8.1 Offshore Infrastructure Sizing

Methodology:

The preliminary calculations are based on fluid flow equations as given in Crane Corporation (Crane Corporation, 1988) and were performed to provide a high level estimate of pressure drop along the pipeline routes.

Erosional Velocity: $V_e = c/\sqrt{\rho}$

Where;

V_e = Erosional Velocity (m/s)

c = factor (see below)

ρ = Density (kg/m³)

Industry experience to date shows that for solids-free fluids, values of $c = 100$ for continuous service and $c = 125$ for intermittent service are conservative. For solids-free fluids where corrosion is not anticipated or when corrosion is controlled by inhibition or by employing corrosion resistant alloys, values of $c = 150$ to 200 may be used for continuous service; while values of up to 250 may be used for intermittent service (American Petroleum Institute, 1991).

Velocity: $V = 4Q/\pi d^2$

Where,

V = Velocity (m/s)

Q = Mass flow rate (MTPa)

Reynolds Number: $Re = \frac{\rho V d}{\mu}$

Darcy Friction Factor: The friction factor is obtained from the Serghides' solution of the Colebrook-White equation.

$$A = -2 \log_{10} \left(\frac{\varepsilon/D}{3.7} + \frac{12}{Re} \right), \quad B = -2 \log_{10} \left(\frac{\varepsilon/D}{3.7} + \frac{2.51A}{Re} \right), \quad C = -2 \log_{10} \left(\frac{\varepsilon/D}{3.7} + \frac{2.51B}{Re} \right), \quad f = \left(\frac{A - (B - A)^2}{C - 2B + A} \right)^{-2}$$

Pressure drop for single phase fluid flow: $\Delta P = \frac{f L \rho V^2}{\mu}$

Pipeline	Pipeline OD	Mass Flow Rate	Route Length	Pipe Roughness	Fluid Phase	Pressure Drop per km	Pressure Drop
Barmston Viking NUI	to 20" (508mm)	2.5MTPa	185km	0.045	Liquid/Dense ^[1]	0.031 bar	6.0 bar
		5MTPa				0.119 bar	23.2 bar
		7.5MTPa				0.231 bar	45.0 bar
		10MTPa				0.469 bar	91.1 bar

Table 11-25 Barmston to Viking A NUI pipeline pressure drop

Notes:

- Density of 980.3kg/m³ and viscosity of 0.1016 kg/sm

Preliminary wall thickness calculations to PD8010 Part 2 (British Standards Institution, 2015) have also been performed. As the product is dry CO₂ composition, carbon steel is sufficient for the pipeline however the material specification will require particular fracture toughness properties to avoid ductile fracture propagation. The resulting pipeline configurations are summarized in Table 11-26.

Parameter	Barmston to Viking NUI
Outer Diameter	508mm
Wall Thickness	17.5mm
Corrosion Allowance	1mm
Material	Carbon Steel
Corrosion Coating	3 Layer PP
Weight Coating	Concrete Weight Coating
Pipeline Route Length	185km
Installation	S-Lay
Crossings	8

Table 11-26 Viking A development pipeline specifications

As discussed within Section 5 of the report, there are several high ranking potential storage sites along the Viking A pipeline route and in the vicinity of the NUI. The 20” pipeline above has been sized for a mass flow rate of up to 7.5 MTPA. Should subsequent studies determine that there is merit in pre-investing in a significantly larger pipeline to allow for further expansion of CO₂ storage), the table below summarises at a high level the additional CAPEX associated with procurement, fabrication and installation of pipelines up to 30” diameter, to deliver up to 10 or 15 MTPA of CO₂ to the Viking A NUI.

Note that no consideration has been given to any additional CAPEX associated with procuring such large diameter pipelines in non-standard wall thicknesses, or any modifications to the Barmston pump station that may be required to provide the required compression.

The current base case Transportation CAPEX for the 20” pipeline capable of delivering up to 7.5 MTPA is £224.6 MM (see Section 6).

Note that, if there were no requirement for additional ullage the pipeline diameter could be reduced to 18” (delivering 5 MTPA) and would result in a saving of approximately £10 MM versus a 20” pipeline.

OD	MASS FLOW RATE = 10 MTPA				MASS FLOW RATE = 15 MTPA			
	DP (bar)	MAOP (bar) ^[1]	WT (mm)	CAPEX (£ MM)	DP (bar)	MAOP (bar) ^[1]	WT (mm)	CAPEX (£ MM)
24”	35.6	195.6	22.2	272.8	79.5	239.5	26.97	301.6
26”	23.6	183.6	22.2	284.6	52.7	212.7	25.4	305.8
28”	16.1	176.2	23.8	308.4	36.0	196.0	25.4	319.7
30”	11.4	171.4	23.8	321.3	25.2	185.2	25.4	333.7

Table 11-27 CAPEX associated with a larger diameter pipeline from Barmston to Viking A NUI

11.8.2 Cost Estimation

The CAPEX, OPEX and ABEX have been calculated for the engineering, procurement, construction, installation, commissioning, operation and decommissioning of the Viking facilities. The OPEX has been calculated based on a 26 year design life.

An overview of the Viking development (transportation, facilities, wells) is given in Section 5. The cost estimate is made up of the following components:

- Transportation: Pipeline, landfall and structures along the pipeline
- Facilities: NUI – Jacket / Topsides, Template, Power cable
- Wells: Drilling and the well materials and subsurface materials
- Other: Anything not covered under transportation, facilities or wells.

The cost estimate WBS adopted throughout is shown in Table 11-28. A 30% contingency has been included throughout.

CAPEX (Transport, Facilities, Wells, Other)	
Pre-FID	Pre-FEED
	FEED
Post FID	Detailed Design
	Procurement
	Fabrication
	Construction and Commissioning
OPEX (Transportation, Facilities, Wells, Other)	
Operating Expenditure 26 year design life	
ABEX (Transportation, Facilities, Wells, Other)	

Decommissioning, Post Closure Monitoring, Handover

Table 11-28 Cost estimate WBS

11.8.3 Power Cable

The critical and greatest cost sensitive elements of securing a power connection to the Viking Site are:

- the land and subsea cable route (and length);
- seabed conditions for installing the submarine cable;
- working windows during offshore installation (weather and conditions);

- maintaining a high quality installation (to minimise on cable faults) during installation

11.8.3.1 Technologies

This section provides an overview of the technologies available for the provision of a high voltage offshore electrical supply to the Viking Site. It provides a high level description of the relevant features of an offshore connection based on economically feasible technologies. Budgetary costs for each technology are presented in the next section.

The majority of electricity systems throughout the world are Alternating Current (AC) systems. The voltage level is relatively easy to change when using AC electricity, which means a more economical electricity network can be developed to meet power requirements. However, AC systems incur a reactive power loss due to inductance and capacitance which are proportionately larger than comparable DC systems.

Direct Current (DC) electricity did not develop as the means of transmitting large amounts of power as it is difficult to transform to different voltages. However, HVDC has recently become attractive for relatively long transmission connections (such as the extension of an existing AC system or when providing inter-connections between different transmission systems) as HVDC technologies: cable and power electronics, have become more efficient and economic. HVDC incurs lower operating losses than AC systems; however, this is offset by an increase in capital cost of AC-DC converter stations that are required at each end of the HVDC link to connect AC systems together.

The electricity transmission network in England is owned and maintained by National Grid and operates at 275kV and 400kV. The distribution networks are owned and operated by Distribution Network Operators (DNO) who operate in

specific geographic areas at voltages which range from LV up to 132kV. The UK electricity transmission, distribution and market is regulated by OFGEM. In general terms higher voltage systems incur lower lifetime losses and have higher power capacities, though they incur significant levels of capital investment and cost more to repair in the event of failure.

There are two main technologies that can be used to provide high voltage connections offshore. These technologies have different features which affect how, when and where they can be used. The main technology options for offshore high voltage connections are: -

1. AC underground land and subsea cables and
2. High Voltage Direct Current (HVDC) land and subsea cables combined with at least two AC-DC converter stations

In the case of the Viking offshore connection any cables will be required to connect to substations at either end. With a demand of circa 10MW the land connection will likely be to a distribution network, which is owned and operated by an incumbent DNO. The offshore connection will be to an offshore substation that, depending upon the technology employed, will comprise conversion equipment to provide a suitable operating voltage for the heater system (typically 690V AC) and a suitable electrical system topology to meet with defined security, resilience and availability requirements of the overall CO₂ storage process.

The following is a brief overview of the technologies required to create an electrical high voltage connection between a public on-shore DNO network and an offshore privately owned distribution network incorporating the CO₂ storage process heating system.

11.8.3.2 Underground Cables

Underground cable systems are made up of two main components - the cable and connectors. Connectors can be cable joints, which connect a cable to another cable, or terminations which connect the cable to other equipment (such as switchgear or transformers or overhead lines), generally within a substation.

Cables consist of an electrical conductor in the centre, which is usually copper or aluminium, surrounded by insulating material and sheaths of protective metal and plastic. In subsea cables a layer of armouring is also incorporated to improve cable mechanical protection. The insulating material ensures that although the conductor is operating at a high voltage, the outside of the cable is at zero volts (and therefore safe).



Figure 11-66 Examples of underground cables

Underground cables connect to above-ground electrical equipment at substations which are enclosed within a fenced compound.

An electrical characteristic of a cable system is capacitance between the conductor and earth. Capacitance causes a continuous 'charging current' to flow: the magnitude of which is dependent on the length of the cable overhead line (the longer the cable, the greater the charging current) and the operating

voltage (the higher the voltage the greater the current). Charging currents have the effect of reducing the power transfer through the cable. High cable capacitance also has the effect of increasing the voltage along the length of the overhead line, reaching a peak at the remote end of the cable.

It is possible to reduce cable capacitance by connecting reactive compensation equipment to the cable, either at the ends of the cable, or, in the case of longer cables, at regular intervals along the route. Specific operational arrangements and switching facilities at points along the cable may also be needed to manage charging currents.

High voltage underground cables should be regularly maintained and inspected. Cable integrity tests are relatively straightforward and combined with continuous monitoring systems cables are relatively reliable and available assets. However, cable faults can result in lengthy down-times unless there are alternative sources of supply otherwise the cable will not be available for use until the repair is completed. Land based cable systems at 33kV may take a few hours to repair, whereas cables operating at 132kV and above repairs may take days (or weeks if spare cable and joints are not readily available). Subsea cable repairs require specialist vessels and diving operations. For this reason, asset owners often place operation, maintenance and repair contracts with specialist contractors.

Identifying faults in land based underground cables often requires multiple excavations to locate the fault and some repairs require removal and installation of new sections of cable, which can take a number of weeks to complete.

Identifying faults in subsea cables is more difficult than land cables as diving and/or Remote Operated Vehicle (ROV) operations are required and repairs require specialist cable laying and jointing vessels.

The installation of land based underground cables requires significant civil engineering works.

The construction swathe required for a single, 3-phase, 33kV AC underground cable would be around 7-15m, with a trench approximately 1m deep by 1m wide. At higher voltages the construction swathes increase and cable trench width increases. In some cases two or more cables may be required to meet the require power capacity, in this case the swathe and trench widths increase proportionally.



Figure 11-67 Example of a construction swathe for a land cable

Each of the two main components that make up land based underground cable system has a typical design life of 40 years. Subsea cables have lower design lives, due to their harsher environment, and are typically 20-25 years.

Subsea cables up to 132kV can incorporate a fibre optic cable bundle within the power cable. This saves having to install a separate fibre cable at the same time as installing the power cable. The fibres can be used for operational telecommunications, protection and SCADA systems as well as having the potential for continuous cable monitoring (such as DTS).

Asset replacement is generally expected at the end of design life. However, asset replacement decisions (that are made at the end of design life) should account for the actual asset condition and may lead to actual life being longer than the design life.

Installation costs associated with cable systems are very sensitive to the type of ground conditions encountered and routes should be planned with great care. Subsea cables are often shallow buried to provide increased protection against the marine environment and any vessel operations. The seabed environment and cable route corridor is therefore as critical as it is on land.

A transition is required between the offshore cable and the land based cable systems. Subsea cables are typically winched onto shore and brought to a suitably located 'transition joint bay'. This connects the offshore cable to the land cable system. Joint bays can take up a relatively large area, approximately 10-20m long (for 33kV – 132kV) and 5-10m wide. A separate joint bay is required for each 3-phase cable.

11.8.3.3 High Voltage Direct Current (HVDC)

HVDC technology can now provide efficient solutions for the bulk transportation of electrical energy between AC electricity systems (or between points on an electricity system).

There are circumstances where HVDC has advantages over AC generally over very long distances >60km or between different, electrically separate systems, such as between different countries.

Proposed large scale offshore wind farms to be located over 60km from the coast of the UK are likely to be connected using HVDC technology as an alternative to an AC subsea cable. This is because AC subsea cables over 60km long incur a number of technical limitations, such as high charging currents and the need for reactive compensation equipment.

The connection point between AC and DC electrical systems has equipment that can convert AC to DC (and vice versa), known as a converter. The DC electricity is transmitted at high voltage between converter stations.

HVDC can offer advantages over AC underground cable, such as:

1. Two cables per circuit* (+ and -) is required for HVDC whereas a minimum of three-phase system (i.e. three cables or a three-core cable) is required for AC;
2. reactive compensation mid-route is not required for HVDC;
3. Cables with smaller cross sectional areas can be used (compared to equivalent AC system rating).

* It is possible to deploy a single cable system and use the ground as a return. However, this increases risks of ground potential rise along the route and may have a greater impact to the environment than a symmetrical bipolar cable. In this report a two cable system has been considered, further studies may confirm that an earth return system is acceptable.

HVDC systems have a design life of about 20 years. This design life period is on the basis that large parts of the converter stations (valves and control systems) would be replaced after 20 years.

Asset replacement is generally expected at the end of design life. However, asset replacement decisions (that are made at the end of design life) should account for the actual asset condition and may lead to actual life being longer than the design life.

11.8.3.4 DNO Connection and Metering

A physical and electrical connection must be made to an existing electricity network if power is to be exported (or imported) by the DNO.

The DNO will charge a fixed amount for infrastructure required to supply the requested power (or a proportion thereof if the power is shared by a number of customers). In addition, if the request exceeds the power capacity at that point of the DNO network they may also charge a proportion of costs for increasing the supply capacity on their network (known as upstream reinforcement). The connection charges are therefore sensitive to a) the requested power and b) the state of the existing network in proximity to the point of connection.

The final connection to the DNO network must be made by the DNO. The DNO is obliged to quote for all necessary equipment to the point at which the customer takes their supply, however, in cases where other equipment is necessary the customer may obtain quotes from other authorised installers (so long as the equipment meets the DNO requirements).

In general, the fixed charge covers Opex costs, however if the equipment the DNO installs is only required for a single customer it may be appropriate to split

Capex and Opex costs. In general, DNO assets are inspected and maintained periodically on 4, 8 and 12 year cycles.

A meter operator is selected by the customer and is normally metered at the point of connection with the DNO. Metering and meter tariffs will be set by the operator and DNO and will be charged based upon units of electricity used.

11.8.3.5 Substations

Substations contain switchgear (to enable safe connection and disconnection of sections of network) and in certain instances, transformers which step-up or step-down voltage levels to suit overall system requirements.

11.8.3.6 Viking Network Concept Topologies

The following illustrate typical connections for a 10MW electrical load:

	33kV - 690V	132kV (11kV) 690V	HVDC
Connection Voltage (kV)	33	132	60
# of heaters	4	4	4
Rating of Heater (MW)	2.5	2.5	2.5
Aggregate Power (MW)	10	10	10
Power Factor (AC)	0.95	0.95	-
Total Apparent Power (MVA)	11	11	-
Current (A)	203	51	83

Table 11-29 Typical electrical connections for a 10 MW electrical load

Three conceptual network topologies are included in the economic evaluation. The single circuit (non-firm) connection is the simplest arrangement. The firm supply arrangement includes duplicated circuits and the final arrangement shows a HVDC with AC-DC convertor stations. The following diagrams illustrate these topologies.

HVAC NON-FIRM SUPPLY (Single Circuit)



HVAC FIRM SUPPLY (Duplicate Circuits for improved resilience and security)



HVDC SUPPLY



Figure 11-68 Possible electrical topologies for the Viking A development

The following table provides a generic appraisal of the merits of each connection type:

	Single Circuit	Duplicate Circuits	HVDC
Capex	Low	Medium	High
Opex	Low	Medium	High
Complexity	Simple	Medium	Complex
Typical Asset Life (yr)	40 (subsea 20)	40 (subsea 20)	25
Security/Resilience	Low	High	Medium

Table 11-30 Appraisal of electrical connection types

11.8.3.7 Economic Appraisal

For the economic appraisal of connections, it is necessary to make a comparative assessment of the lifetime costs associated with each technology that is considered to be feasible. This section provides an overview of the cost information that is publically available and that which is based on experience of working within DNO's.

There is some publically available information for Capex and Opex costs for subsea cable and HVDC technologies; however they tend to be focussed on offshore windfarm development. The power requirements for offshore wind have increased significantly in the past 10 years and most modern technology is designed for 300MW -1,000MW. A 10MW supply, as anticipated at Viking, is small in comparison. The cost of a smaller capacity (when considering HVDC) does not necessarily mean a lower Capex and Opex cost per unit of power as HVDC technologies have been designed specifically for higher power rating.

The Troll A offshore HVDC Platform is the closest comparable system to Viking, with a 40MW total power requirement over a 68km link comprising +/-60kV HVDC technology and was commissioned in 2005.

It is anticipated that a 33kV connection over 90km and circa 10MVA is towards the limit of voltage drop and capacitive charging/reactive power limits of standard cable systems. This report is not intended to engineer a solution, but further investigation will be required (reactive compensation or non-standard cable sizes may need to be added to this appraisal) in order that a 33kV connection is proved feasible.

11.8.3.8 Capital Cost Estimates

Initial Capex estimates are based on the high level scope of works defined for each option in respect of each technology option that is considered to be feasible. The high level scope effectively being outlined in the previous section.

Capex Option Costs (£GBP)								
Arrangement (typical 40 year asset life)	Planning Design &	Preliminaries & Project Management	DNO Connection	Offshore Substation	Onshore Substation	Land Cable	Subsea Cable	Total (£)
33kV Firm	1,009,000	1,720,000	200,000	3,500,000	-	4,940,000	68,400,000	79,769,000
33kV Non-Firm	1,009,000	1,720,000	100,000	2,000,000	-	2,600,000	36,000,000	43,429,000
132kV Firm	1,009,000	1,720,000	2,000,000	6,000,000	-	19,000,000	207,000,000	236,729,000
132kV Non-Firm	1,009,000	1,720,000	1,000,000	3,000,000	-	10,000,000	108,000,000	124,729,000
HVDC Non-Firm	1,151,914	1,720,000	1,000,000	3,300,000	3,300,000	5,000,000	45,000,000	60,471,914

Table 11-31 Capital cost estimates for a range of subsea electrical cable options

Notes:

1. Capital costs for all technologies are based upon rural/arable land installation with no major obstacles (examples of major obstacles would be roads, rivers, railways etc.) and subsea installations in beds that are conducive to 250m lay in an hour.
2. All underground AC cable technology costs are for direct buried installations only and 1 core per phase (i.e. a 3 core cable or 3 x single core cables)
3. AC cable installation costs exclude the cost of reactors and reactive compensation
4. Asset life is typically 40 years; manufacturing bespoke design life assets of 20 years is not considered to be cost effective.

11.8.3.9 Maintenance and Repair Costs (based on 2015 prices)

The maintenance and repair costs associated with each option vary significantly. Most high voltage electrical equipment is inspected and maintained regularly to ensure system performance is maintained. More complex equipment, like HVDC converters, have higher maintenance costs due to their specialist parts. Critical HV cables often incorporate cable temperature monitoring (and in some cases a means to detect partial discharge) so the asset condition can be continually assessed.

Table 11-32 provides an estimate of inspection, maintenance and repair costs of the major electrical components based on 2015 prices.

This report does not take account of replacement costs, except in the case of HVDC where the design life is typically less than the nominal 25 year design life anticipated. In general high voltage electrical assets have design lives of 40 years, with the exception of sub-sea cables where 25 years is more commonplace.

The following provides a high level summary of common replacement requirements applicable to specific technology options.

1. AC underground cable - At the end of their initial design life, circa 40 years, replacement costs for underground cables are estimated to be equal or potentially slightly greater than the initial capital cost. This is because of works being required to excavate and remove old cables prior to installing new cables in their place in some instances.
2. HVDC - It should be noted at the end of the initial design life, circa 20 years, replacement costs for HVDC are similar to install costs.

Asset	Description	Maintenance Regime	Unit Cost (£)	Frequency (1/yr)	Annual Maintenance Costs (£/year)	Repair	Repair Time (Est)	Repair Cost (£)	Repair Notes	
Land Cable	Single core, 3-Phase XLPE cable installed in the verge of highway	Inspection yearly	4	7,400	0.25	1,850	33kV Cable, 20m with joints and install	0.3w	15,000	Costs inclusive of labour and materials and assumes spare materials held
Subsea Cable	Three-core, 3-Phase XLPE cable	Inspection yearly	2	15,000	0.5	7,500	Vessel, jointing, ROV, Cable	1w	300,000	Costs inclusive of labour and materials and assumes spare materials held
Fluid Filled Transformer	33/11kV transformer 20/40MVA	Inspection & Maintenance 4 yearly. Assumes no oil change required	4	12,000	0.25	3,000	Replace Tx	8w	600,000	Costs inclusive of labour and materials (33kV transformer) and assumes spare materials held (note 33kV transformer lead time typically 32w)
AC GIS Switchgear	33kV GIS Switchgear	Inspection yearly	8	7,400	0.125	925	Replace CB	4w	45,000	Costs inclusive of labour and materials (33kV GIS CB) and assumes spare materials held (note 33kV CB lead time typically 24w)
HVDC VSC Converter	HVDC Converter with associated DC switchgear and transformer	Inspection & Maintenance yearly	2	13,000	0.25	3,250	Replace Components	4w	-	Spares should be procured or contract placed with OEM for spares provision, Cost of this is unknown at this time.

Table 11-32 Maintenance and repair cost estimates for subsea cabling options

11.8.3.10 Annual Electrical Losses and Cost

Losses occur in all electrical equipment and are related to the operation and design of the equipment. The main losses within a power system come from heating losses associated with the resistance of the electrical components, often referred to as I²R losses. As the load (the amount of power each circuit is carrying) increases, the current increases and thus losses increase. There are also smaller losses in AC systems associated with magnetisation of inductive assets and dielectric losses associated with capacitive assets. These are independent of size of the load. For the purpose of this report these have been ignored as they are small in comparison to the load losses.

In all AC technologies the power losses are calculated directly from the electrical resistance properties of each technology and associated equipment. A summary of asset resistance data for each technology option is included in Table 11-33.

The process of converting AC power to DC is not 100% efficient. Power losses occur in all elements of the converter station: the valves, transformers, reactive compensation/filtering and auxiliary plant. Manufacturers typically represent these losses in the form of an overall percentage.

Asset	Resistance (Ohms/unit)	I ² R Loss at Max Current (kW/unit)	% of capacity (11MVA/unit)
33kV Cable Single Circuit (Non-Firm) 1 x 240mm ² Cu, 3 core, XLPE	0.041	4.56	0.041%
132kV Single Circuit (Non-Firm) 1 x 185mm ² Cu, 3 core, XLPE	0.130	0.90	0.008%
33kV Transformer	0.5	56.6	0.51%
132kV Transformer	2.5	17.4	0.16%

Table 11-33 Typical AC load losses

11.8.3.11 Distribution Use of System Charges and Tariffs

All DNO's are required to publish statements on their use of system charges for customers. Tariff and charges for 22kV connections and above are bespoke and calculated on the required capacity and network security, availability, reliability and capacity requirements.

It is likely the DNO would categorise Viking A as a Designated EHV connection and thus a bespoke fixed charge and variable charge may be levied, dependent upon capital contributions for the initial connection.

In OFGEM's project discovery document they estimate the cost of electrical energy to be £50/MWh. Using this as a datum the annual cost of energy would be:

$$50 \times 24 \times 365 \times 10 = \text{£}4,380,000$$

11.8.3.12 Overall Costs Estimate

The following table provides an overview of each option and a summary of Capital and Operational expenditure. The OPEX costs are based on 2015 estimates and thus need to be discounted using appropriate rates to account for overall lifetime costs.

Note the energy costs have been calculated based on £50/MW. A sensitivity on the energy cost has been performed and is included in Section 6.2.1.

Arrangement	CAPEX	OPEX - Annual Costs		
		Operational Cost	Cost of Energy	Cost of Losses
33kV Firm	£79,769,000	£25,625	£4,380,000	£111,933
33kV Non-Firm	£43,429,000	£13,275	£4,380,000	£223,867
132kV Firm	£236,729,000	£25,625	£4,380,000	£23,573
132kV Non-Firm	£124,729,000	£13,275	£4,380,000	£47,146
HVDC Non-Firm	£60,471,914	£15,600	£4,380,000	£507,654

Table 11-34 Opex cost estimates for subsea cabling options

11.8.4 Petrophysics

For the purposes of quantitative evaluation of reservoir rock properties from wireline logs, a standard oilfield approach to formation evaluation has been adopted. This is outlined below and illustrated in Figure 11-69.

11.8.4.1 Parameter Definition

Formation Temperature Gradient

Formation temperatures were taken from the maximum reported bottom hole temperature on the field wireline prints or composite logs from TD and intermediate logging runs. These data were plotted and a regression line fitted to estimate temperature over the intervals of interest (Figure 11-70).

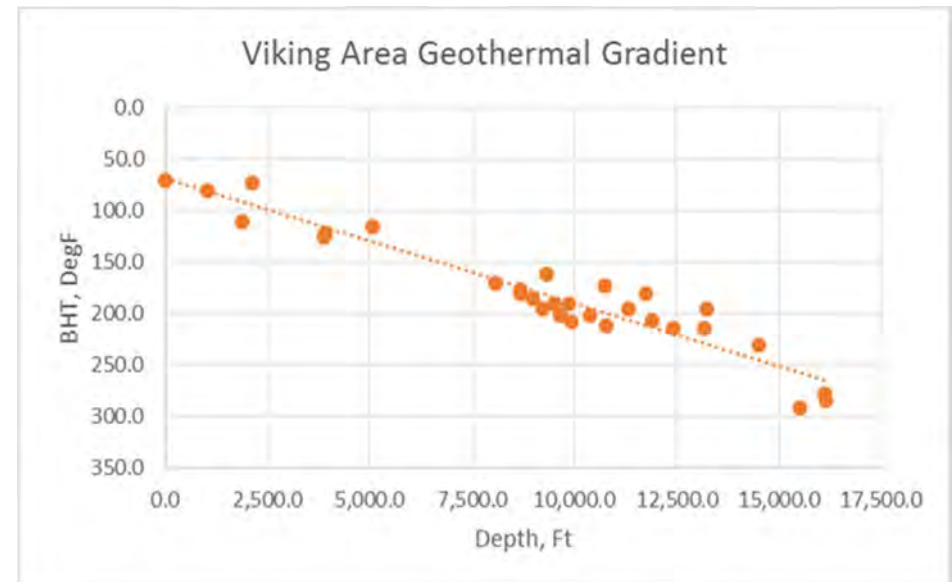
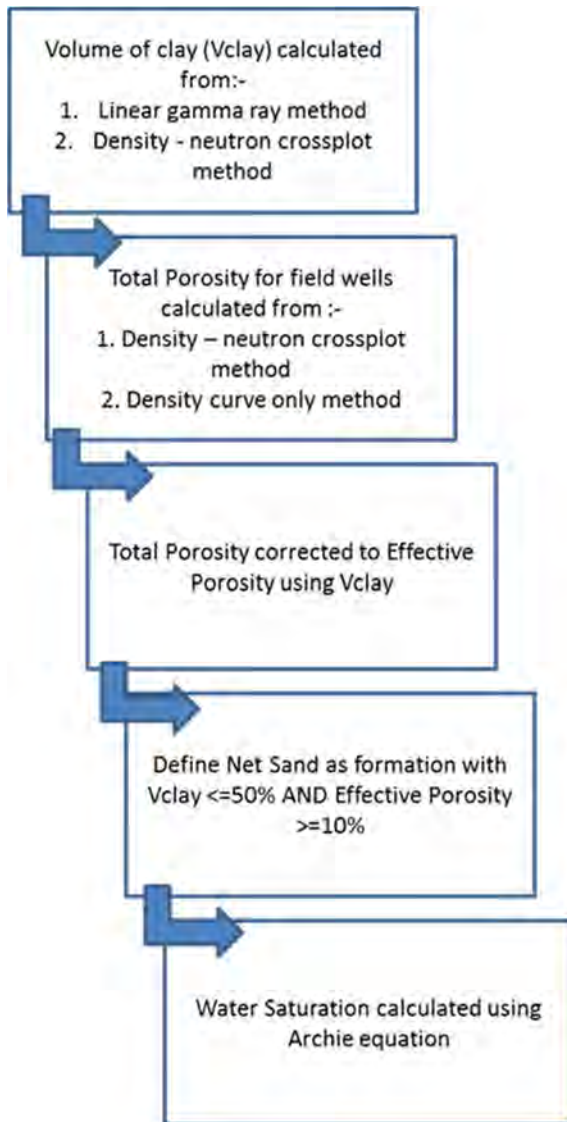


Figure 11-70 Recorded bottom hole pressure from wireline data

For this study a single geothermal gradient is assumed; assuming a linear free regression model through these data, the temperature gradient, in degrees Fahrenheit, is estimated using the following equation:

$$BHT = 0.013 * TVD + 65$$

BHT = Bottom Hole Temperature [DegF]

TVD = True vertical depth [ft]

This results in a formation temperature between 150 °F and 170 °F over the zone of interest.

Figure 11-69 Summary of petrophysical workflow

Formation Water Resistivity

R_{wa} is calibrated in all the water zones and gives a fairly consistent estimate of formation water resistivity. Formation water resistivity (R_w) is assumed to be 0.0545 at 60 °F for the core area of this study.

Electrical Resistivity Properties

The only SCAL data available for this study is from well 49/12a-9; these measurements include electrical properties for the reservoir sands. Figure 11-71 and Figure 11-72 are the formation resistivity factor and resistivity index, these data display considerable scatter.

There is considerable variance in the documented parameters used on a well by well basis, for example the operators’ final well report for the 14/12a-9 well recommends slightly different values to these plots and the operator petrophysical model, has slightly different values.

Source	a	m	n
SCAL Crossplot	1.0	1.71	1.75
49/12a-9 Final Well Report	1.0	1.98	1.76
Operator Petrophysical Model	1.0	1.90	1.59

Table 11-35 Uncertainty in Archie parameters

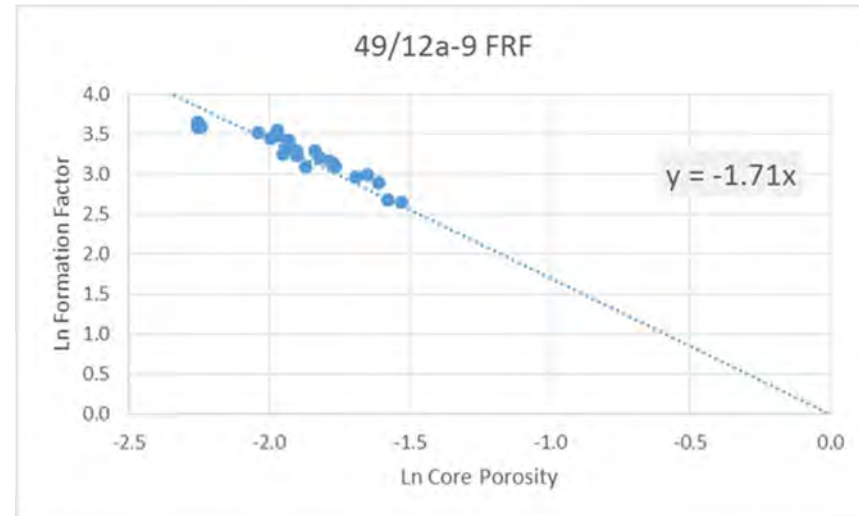


Figure 11-71 Measured formation resistivity factor 'm'

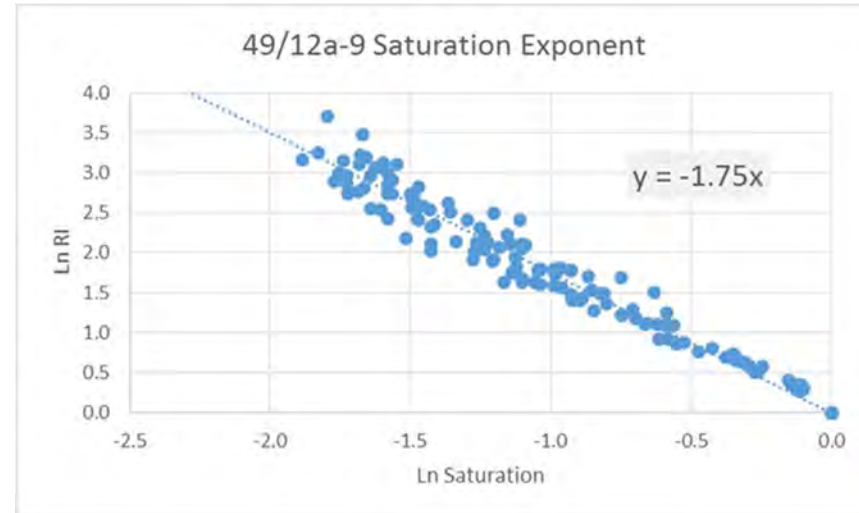


Figure 11-72 Measured formation saturation component 'n'

For this study it has been assumed that there is a more comprehensive database for the operator to define its petrophysical model, on this basis the Operators model parameters have been selected for these interpretations.

Using the average estimated porosity of 12.6% and assuming 20 ohm m resistivity in hydrocarbon bearing zone, the effect of varying the Archie parameters between the operator model and the plotted SCAL data is less than 1 saturation unit.

	a	m	n	F	Sw v/v
Model	1.0	1.90	1.59	51.203	0.157
SCAL	1.0	1.71	1.75	34.544	0.149

Table 11-36 Impact of uncertainty on Sw

A total of 15 capillary pressure measurements, Figure 11-73, were made on core from 49/12a-9. Ten saturation injection tests are using brine and five are using mercury injection fluid.

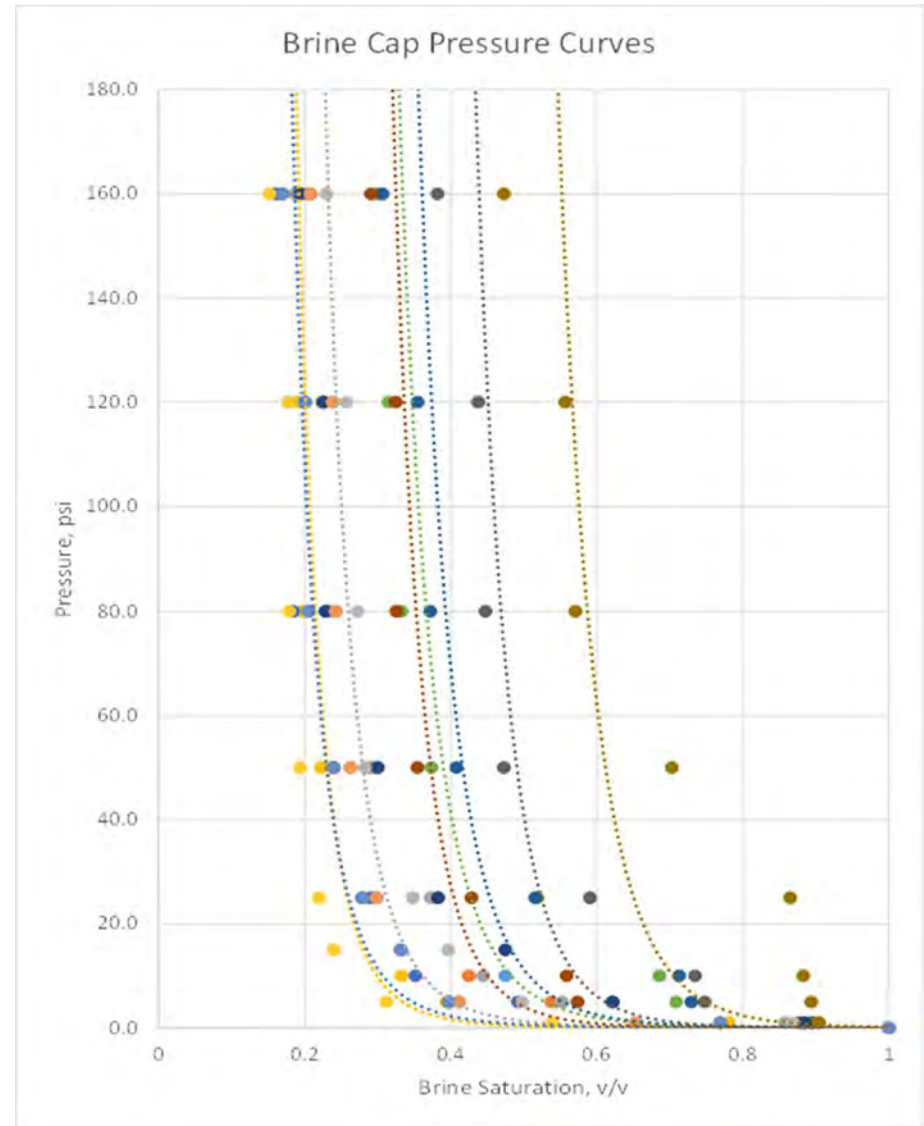


Figure 11-73 Capillary pressure samples

Formation Resistivity

The deepest penetrating resistivity curve is always used as the measurement for true formation resistivity. No additional environmental corrections are applied to these curves as the data archived by CDA does not give a detailed history of any resistivity post-processing

11.8.4.2 Clay and Shale Volume Estimates

The volume of clay in the reservoir is estimated by two independent deterministic methods.

Gamma Ray

The simplest model, for quartz sandstone, is to assume a linear relationship between clean and clay end-points. Figure 11-74 is a multi-well histogram for the Lemman Sandstone in Viking; these data show a good multi-modal response with a confident definition of both the clean sand and shale response from all wells. The average clean sand and shale points are 30 and 103 API respectively, for each well these may be slightly shifted on a zone by zone basis.

The linear model gamma ray Vclay equation is shown below:

$$V_{Clay} = (GR_{log} - GR_{min}) / (GR_{max} - GR_{min})$$

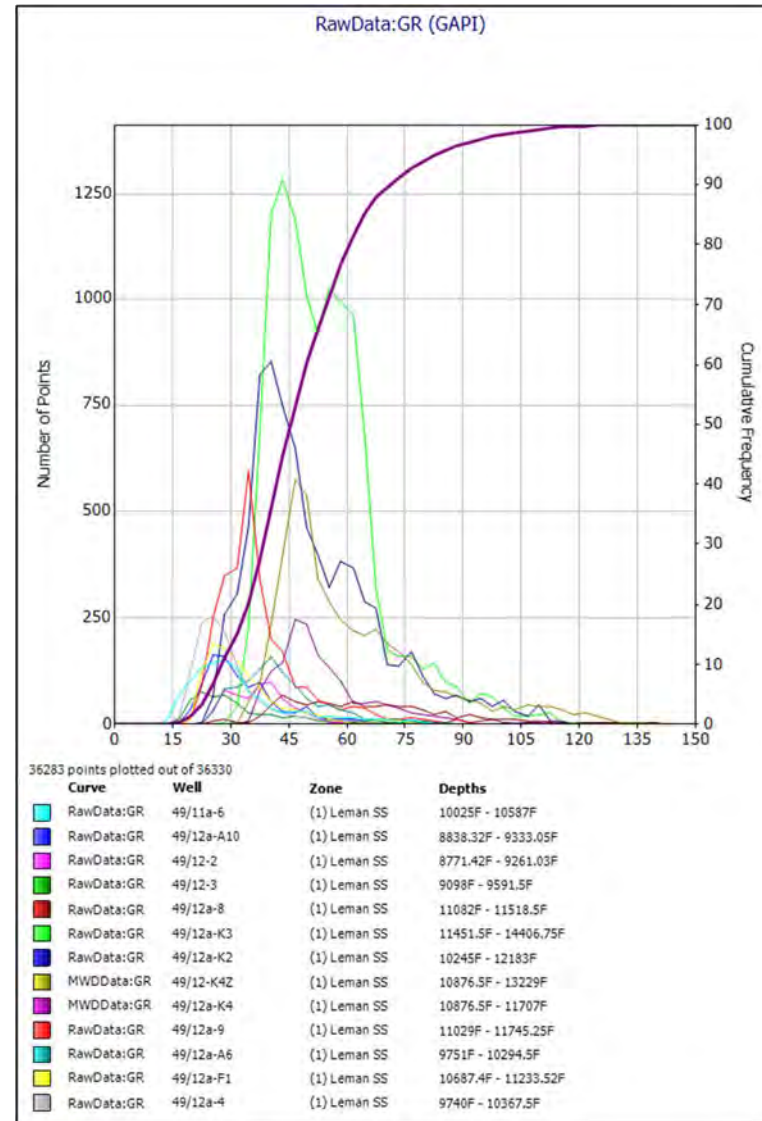


Figure 11-74 Multi-well gamma ray distribution

Neutron – Density Crossplot.

“Double” clay indicator models use a cross-plot method that defines clean sand line and a clay point. The volume of clay is then estimated as the distance the data falls between the clay point and the clean sand line.

Figure 11-75 is a multi-well crossplot of the Neutron-Density over the Leman Sandstone zone of interest. These data fall on a consistent ‘clean’ sand line with an expected global ‘clay-point’ falling at approximately 0.21 p.u. and 2.66 g/cc respectively for the Neutron and Density.

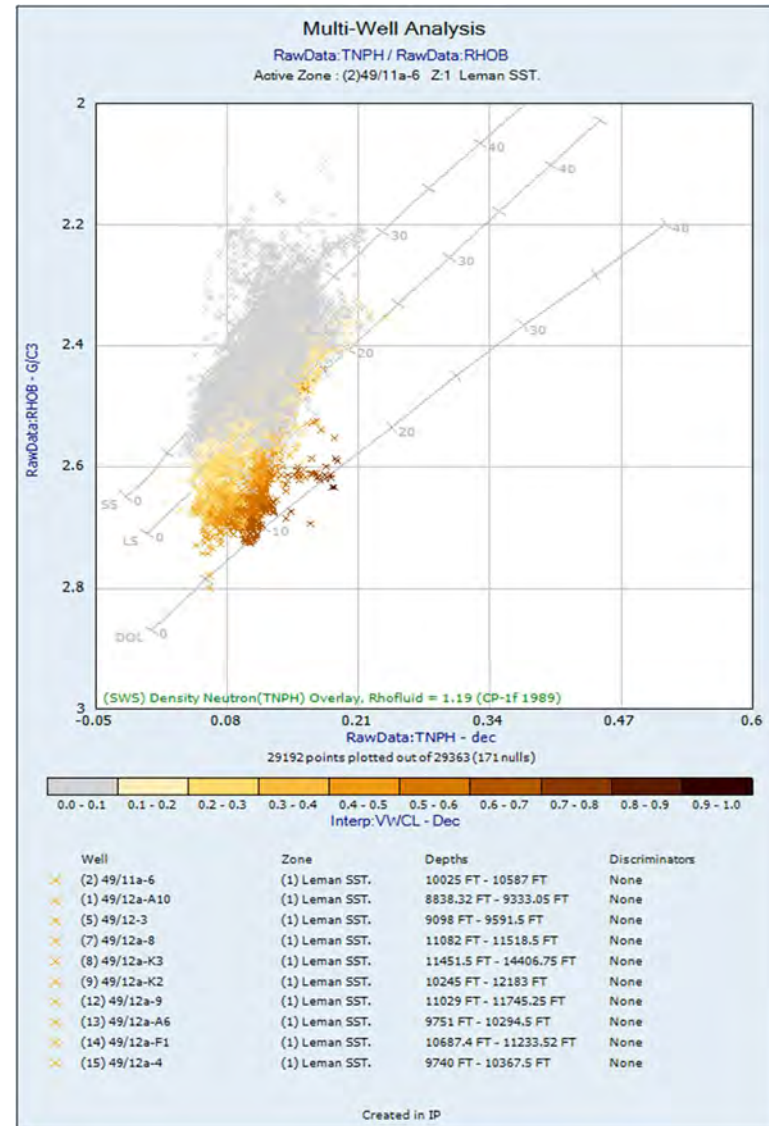


Figure 11-75 Multi-well neutron density crossplot

11.8.4.3 Porosity and Water Saturation

The estimation of porosity and water saturation are coupled as an iterative process such that any parameter update during the calculation of porosity or water saturation will result in porosity and water saturation being recalculated; furthermore, if it becomes necessary to fine-tune the clay model this will cycle back to update the volume clay models for the same interval.

Porosity Model

Porosity is calculated using either the single curve Density model or Density – Neutron crossplot method with option to calculate sonic porosity if the condition of the borehole is too poor to acquire accurate density data.

Borehole conditions are estimated from limits set for the calliper and the density DRHO curves, if these limits are exceeded sonic is substituted as the most appropriate porosity method. A clay volume fraction correction is made to estimate ‘effective’ porosity from the ‘total’ porosity calculation.

A total of 846 core grain measurements were available, Figure 11-76, the data plots with a mean grain density of 2.69g/cc, slightly greater than the expected value for a wholly quartz dominated matrix sandstone.

	Core Grain Density				
	Valid N	Mean	Minimum	Maximum	Std. Dev.
Grain Density	846	2.693	2.640	2.910	0.025

Table 11-37 Core grain density summary

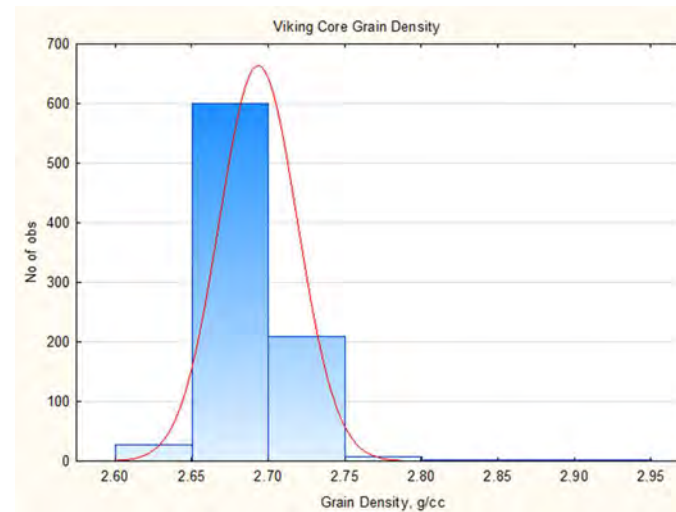


Figure 11-76 Measured core grain density

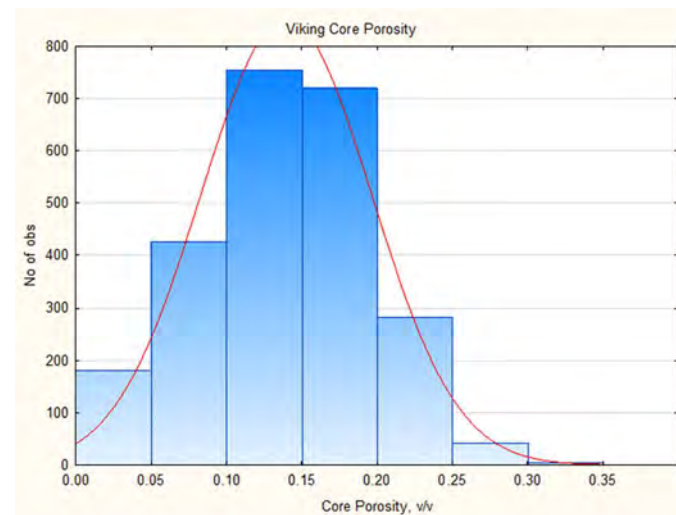


Figure 11-77 Measured core porosity

Variable	Core Porosity Distribution			
	Valid N	Mean	Maximum	Std. Dev.
Core Phi	2409	0.139	0.330	0.056

Table 11-38 Core porosity summary

Where core porosity data is available, the best fit porosity model to the core data is noted and then preferentially selected for un-cored intervals and wells. Figure 11-77 is the distribution of the core porosity data, the plot has 2,409 valid data points, the plot suggests there is a well-defined ‘normal’ distribution within this data set with a mean porosity of 13.9%.

Water Saturation

Water Saturation is calculated in the deep zone of the reservoir (Sw) and the invaded zone (Sxo) using deep and shallow resistivity respectively; where oil based mud is used as the drilling fluid an approximation of the invaded zone saturation is made with defined limits using an Sxo ratio factor.

Archie saturation exponents, a = 1.00, m = 1.90, n = 1.59, are taken from the Operators Petrophysical Model and validated in the water zones with Pickett plots; the ‘a’ and ‘m’ parameters are consistent with the expected values for a clastic reservoir; the saturation exponent ‘n’ is slightly lower than expected.

11.8.4.4 Petrophysical Parameter Selection

Table 11-39 details parameter used to estimate shale and clay volume:

Well	Petrophysical Parameters for Clay and Shale Models			
	GR _{Clean}	GR _{Shale}	NPHI _{Shale}	RHO _{Shale}
49/11a-6	25	100	0.209	2.662
49/12-2	25	92		
49/12-3	25	90	0.209	2.658
49/12a-4	25	94	0.209	2.660
49/12a-8	38	131	0.209	2.660
49/12a-9	25	121	0.209	2.660
49/12-A6	25	94	0.209	2.660
49/12-A10	25	94	0.209	2.660
49/12a-F1	25	90	0.209	2.715
49/12a-K2	30	101	0.209	2.660
49/12a-K3	38	104	0.215	2.600
49/12a-K4	37	111		
49/12a-K4Z	40	119		
49/17-5	No Log Data			
Averages	29.5	103.2	0.210	2.660

Table 11-39 Clay parameter selection

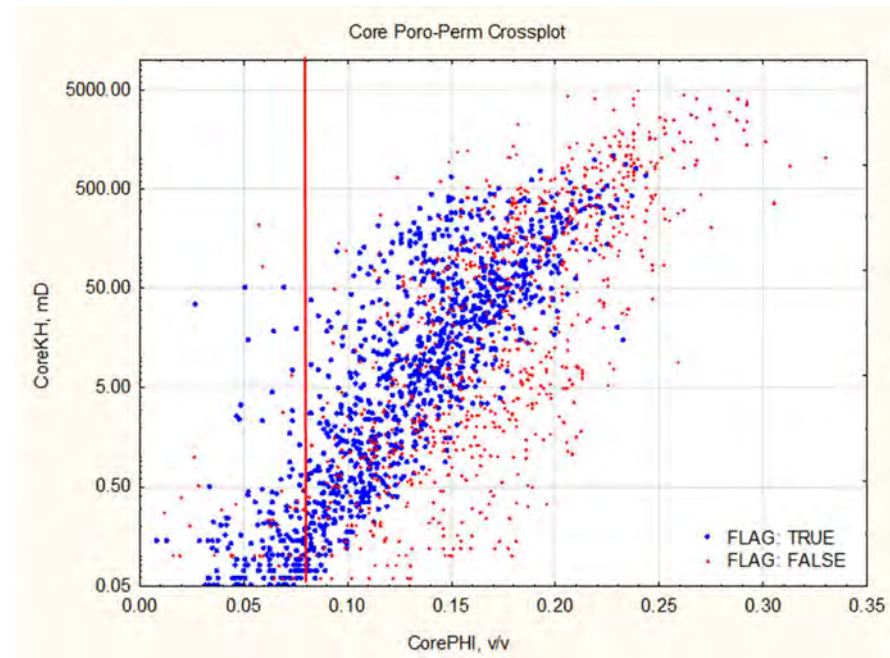
Table 11-40 details parameter used to estimate porosity and water saturation:

Petrophysical Parameter Selection for Porosity and Saturation Model			
Well	Phi Model	Rw at 60 DEGF	Sw Model
49/11a-6	NDXplot	0.0206	Archie
49/12-2	NDXplot	0.0206	Archie
49/12-3	NDXplot	0.0206	Archie
49/12a-4	NDXplot	0.0206	Archie
49/12a-8	NDXplot	0.0206	Archie
49/12a-9	NDXplot	0.0206	Archie
49/12-A6	Questionable RT Data		
49/12-A10	NDXplot	0.0206	Archie
49/12a-F1	NDXplot	0.0206	Archie
49/12a-K2	NDXplot	0.0206	Archie
49/12a-K3	NDXplot	0.0206	Archie
49/12a-K4	Sonic		Archie
49/12a-K4Z	Sonic		Archie

Table 11-40 Porosity and water saturation parameter selection

11.8.4.5 Cut off and Summation Definitions

A cut-off of less than 50% clay content has been selected to define “sandstone”, 8% porosity is the minimum for the sands to be considered of net reservoir. Figure 11-78 is a crossplot of the Viking porosity and permeability core data categorised by a flag (blue) to discriminate the data from the four cored wells in the study area; the permeability in the study area is slightly lower compared to the full permeability population. The 8% porosity cut-off is recommended in the Operators Petrophysical model and discriminates permeability of less than 0.1mD.



Core from site area (blue); Other Viking core (red)

Figure 11-78 Core porosity-permeability cross plot

11.8.4.6 Capillary Pressure

A total of 15 capillary pressure measurements, Figure 11-73, were made on core from 49/12a-9. Ten saturation injection tests are using brine and five are using mercury injection fluid.

A normalised J-Function is used to fit the capillary pressure data to predict gas saturation at reservoir conditions. The function assumes gas and water density of 0.20 g/cc and 1.10 g/cc respectively and Reservoir Quality Indicator (“RQI”) is used to group these data into a common pore geometry, Figure 11-79.

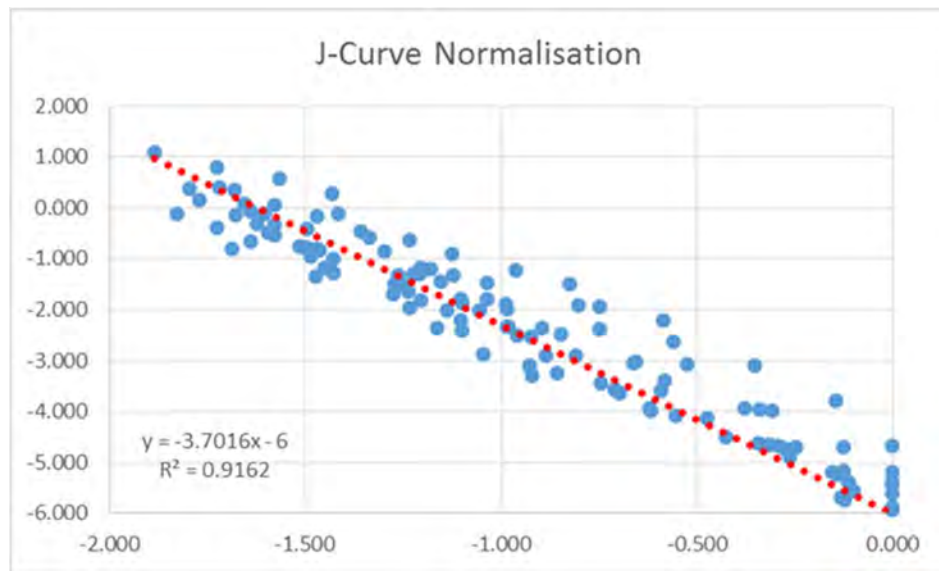


Figure 11-79 J-Curve trend normalisation

The saturation function assumes that permeability is estimated and has the following form:

$$Sw_j = (6.1204 * Height * 0.0314 * \sqrt{k/\phi})$$

Height in Ft

k = Permeability, mD

Ø = Porosity, v/v

Figure 11-80 is the resulting saturation estimation for increasing permeability assuming a constant porosity of 12.5%

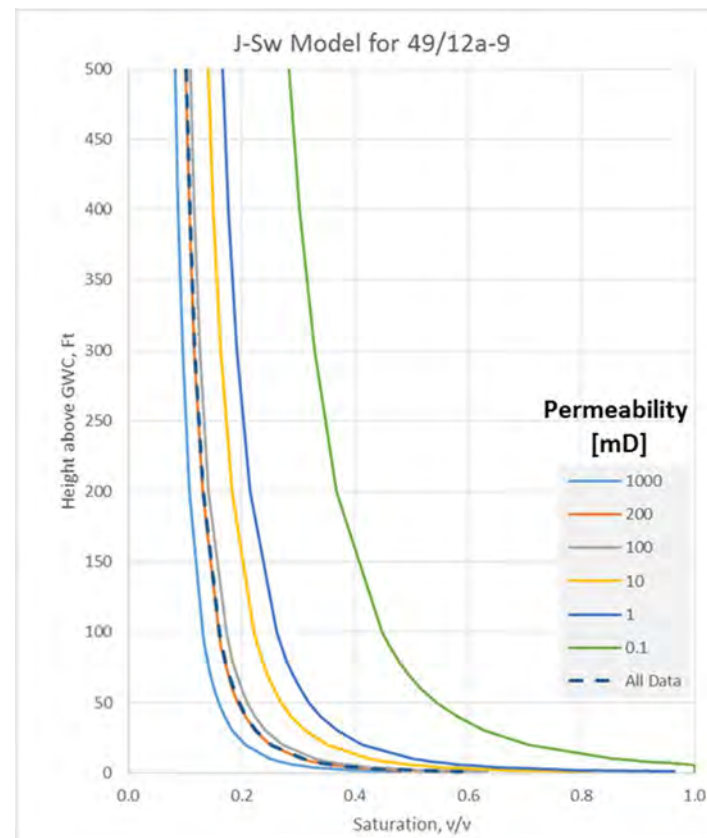


Figure 11-80 Capillary Based Sw height curves

11.8.5 Geochemistry

11.8.5.1 Objective

Geochemical modelling of the primary caprock for the Viking gas field, UKCS was carried out to evaluate the likely impact of CO₂ injection on the rock fabric and mineralogy following the injection period and the long term post-closure period. The main objective was to gain a better understanding of the key geochemical risks to injection site operation and security of storage. Specifically, the main objective in this study was to assess if, increasing the volume (partial pressure) of CO₂ in the Lemn Sandstone reservoir sands leads to mineral reactions which result in either an increase or decrease of the porosity and permeability of the overlying Kupferschiefer and Zechstein Formation caprocks.

11.8.5.2 Methodology

A study methodology was developed to answer a key question:

- Will increasing the amount (partial pressure) of CO₂ in the Lower Permian Lemn Sandstone lead to mineral reactions which result in either increase or decrease of porosity and permeability of the Kupferschiefer and Zechstein Formation sealing lithologies which overlie the field reservoir sandstones?

The work flow followed is shown in Figure 11-81. Water and any gas geochemical data, and mineral proportion data from the reservoir and the caprock (representing the pre-CO₂ injection conditions) were collected from field and analogue data available in the public domain.

As a general approach, following data QC, the initial gas-water-rock compositions were modelled, using a range of CO₂ partial pressures and temperatures, using two approaches:

- The first, and simplest, modelling approach is to assume that there is instant equilibrium between minerals, aqueous solution and changing gas composition. The extent of this type of reaction is thus simply a function of the amount of CO₂ that has arrived at the reaction site (as reflected in the fugacity [as stated approximately the partial pressure] of CO₂).
- A more subtle approach involves a kinetic approach that requires a range of further inputs including rate of reaction (e.g., dissolution), and textural controls on dissolution such as grain size (which is reflected in the specific surface area per unit mass or unit volume. In this study, only kinetic modelling was undertaken on the caprocks.

All modelling was undertaken using Geochemists Workbench.

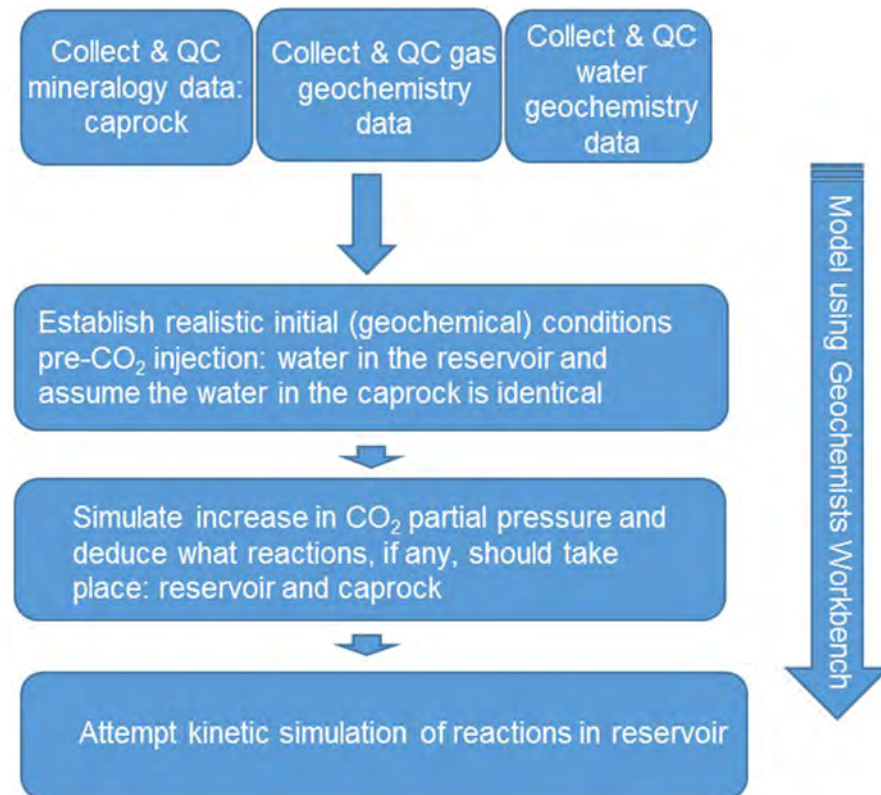


Figure 11-81 Geochemical modelling workflow

11.8.5.3 Data Availability

1. Quantitative caprock mineralogy data from the Kupferschiefer and Zechstein in the Viking field vicinity were not available to this study. Analogous data from the Kupferschiefer were taken from other parts of the Permian Basin.
2. Viking field gas compositional data are available and have been used in this study.

3. Some water compositional data were available from Viking-Phoenix and adjacent fields but they are not credible due to unusual reported concentrations of various species (K, Ca, Mg, Fe etc.) and unexplained differences between the reported data and the overall published field salinity.

11.8.5.4 Water Geochemistry

The water compositional data available to this study are shown in Table 11-41

As mentioned above, although water compositional data were available in the CDA, the data are considered unreliable and have not been used:

- Numerous water compositions reported for Viking-Phoenix and Jupiter but none of them are credible. The published water salinity is 220,000 ppm (Riches, 2003) so all values significantly lower must be contaminated or represent poor lab practice (see 'Salinity' data in upper part of Table 11-41). Sodium was not directly analysed for Viking and Jupiter waters; this is not ideal practice since it assumes that all other analyses are perfect (there is no way of checking data quality). Some reported values have unusually, ultra-high potassium, magnesium or iron relative to sodium while others have oddly high sulphate or bicarbonate concentrations.
- Instead, credible data from other SNS Leman Sandstone reservoirs (see lower part of Table 11-41) have been used for geochemical modelling (Warren & Smalley, 1994). Notice that all these four analyses are similar with high calcium and strontium (compared to NNS Jurassic fields for example) and have appropriate reported salinity values.

mg/L	K+	Na+ (calc, not measured for Viking)	Mg++	Ca++	Sr++	Ba++	Fe++	Cl-	SO4--	HCO3-	pH	salinity (TDS)	% charge difference
Phoenix 49/12a-K5	5016	36300	883	1556	13.6	0.5	970	65510	3251	2418	7.6	115918.1	-1.63
Jupiter 49/22-N6	17700	83000	798	2683	92.5	0	53	148770	3131	603	7.2	256830.5	-0.06
Jupiter 49/23-A8	18100	27500	1408	8168	59	0.8	1430	67550	10970	6320	7.9	141505.8	-0.05
Phoenix 49/12a-K5	16650	75950	862	2743	95.7	0	73	137380	2923	544	7.4	237220.7	-0.04
Jupiter 49/22-N6	2711	19000	13250	10850	35.2	6	25350	121060	996	0	2.4	193258.2	0.00
Jupiter 49/23-A8	18950	29850	1487	8670	64.2	0.7	1498	72430	12047	6210	7.9	151206.9	-0.05
Phoenix 49/12a-K5	2862	15950	13150	10650	35.4	6	24300	114390	1122	0	2.7	182465.4	0.02
Phoenix 49/12a-K3	926	35750	495	1951	44.8	1.3	59	60250	940	126	5.3	100543.1	-0.04
Phoenix 49/12a-K3	862	28100	495	1987	46.7	1.1	73	48640	779	107	5.1	81090.8	-0.08
Phoenix 49/12a-K3	1409	22900	1069	4327	114	1.9	239	47570	292	0	4.1	77921.9	-0.03
Phoenix 49/12a-K3	887	13350	664	2572	68.3	1.6	348	28270	213	0	4.1	46373.9	-0.09
Amethyst	1230	61800	2520	22000	1030	0	312	149000	830	155	6.03	238877	-1.97
Clipper	2350	70450	3500	23900	1045	4	215	165240	565	0	4.78	267269	-0.39
Ravenspurn	4820	66100	2850	26930	1160	14	295	163100	470	0	3.74	265739	0.04
Welland	1530	72650	4760	14030	460	4	145	152300	425	67	5.14	246371	0.01

Table 11-41 Water geochemical composition data used in modelling

11.8.5.5 Gas Geochemistry

Gas geochemical data for the Viking field were taken from a single well (49/12-A9). The pre-CO₂ injection CO₂ content is about 0.5 mol. %, typical of many SNS Permian reservoirs.

Component	Wt. %	Mol. %
Nitrogen	3.77	2.44
Hydrogen Sulphide	0.00	0.00
Carbon Dioxide	1.28	0.53
Methane	80.06	90.62
Ethane	6.83	4.13
Propane	2.69	1.11
Isobutane	0.75	0.23
N-Butane	0.85	0.27
Isopentane	0.38	0.10
N-Pentane	0.34	0.09
Hexanes	0.45	0.10
Heptanes	0.70	0.13
Octanes	0.55	0.09
Nonanes	0.34	0.05
Decanes	0.22	0.03
Undecanes	0.16	0.02
Dodecanes	0.11	0.01
Tridecanes	0.12	0.01
Tetradecanes	0.08	0.01
Pentadecanes +	0.32	0.03
Total	100.00	100.00

Table 11-42 Gas geochemical composition data used in modelling

11.8.5.6 Caprock Mineralogy

An extensive literature search led to no quantitative (XRD) mineralogy data for the caprocks sitting on top of the Viking sandstone reservoir. At the site, the Permian Leman sandstone is directly overlain by a thin layer of Kupferschiefer (a black, pyritic and dolomitic shale), above which are the dolomite, dolomitic

limestones and anhydrite of the Zechstein sequence. The analogue compositions for each caprock type used in the geochemical modelling work were as follows:

- Kupferschiefer: composed of a pyritic dolomitic shale modelled to contain: 21% quartz, 5% kaolinite, 54% illite, 5% pyrite, 5% chlorite and 10% dolomite (Bechtel et al., 2000).
- Zechstein: composed of 3 caprock types: (a) 98% dolomite, 2% anhydrite (b) 55% anhydrite and 45% dolomite and (c) 98% anhydrite and 2% dolomite.

11.8.5.7 Results

Mineral Reactions in the Caprock Lithologies

The key mineral reactants and products likely in the Kupferschiefer and Zechstein Formations (in the presence of injected CO₂) are listed below:

- The Kupferschiefer contains a range of minerals that are reactive to CO₂, and to the saline and Ca- and Sr-rich formation fluids. Chlorite reacts relatively quickly (Armitage, et al., 2013) leading to growth of dolomite (with the incoming CO₂). Kaolinite also reacts with the Na-rich formation water and incoming CO₂ to create dawsonite (Na-Al-carbonate). Muscovite also partly reacts with Na-rich formation water and incoming CO₂ to create dawsonite (Na-Al-carbonate). The clay-breakdown reactions liberate silica resulting in a net volume increase in quartz.
- The Zechstein anhydrite is stable in the presence of CO₂ but dolomite tends to partially dissolve in the increasingly acid pore waters due to carbonic acid formation.

Kinetic Modelling: Caprock

Kupferschiefer Formation

In order to evaluate the kinetic effects on the caprock, models reacting 5 mol CO₂ (g) over 10,000 years at 80°C (representative of 9000 ft TVDSS) for the selected Kupferschiefer composition were run. Kinetic dissolution constraints for illite, kaolinite and chlorite were taken from (Xu, Sonnenthal, Spycher, & Pruess, 2006)

The key results derived from the kinetic modelling are shown in Table 11-43 and in Figure 11-82. Table 11-43 shows the modelled relative mineral volume change in the Kupferschiefer caprock after CO₂ has been injected into the underlying reservoir (and simulates the impact if CO₂ migrates into the overlying caprock).

The main changes modelled in the Kupferschiefer caprock are the major dissolution of kaolinite due to CO₂ influx, the relatively minor loss of muscovite (illite) over 10,000 years of addition of CO₂ and the replacement of Mg, Si and Al-bearing chlorite. The products of this clay mineral breakdown are shown by the increase in volume of the quartz, dolomite and dawsonite in Figure 11-82 and Table 11-43.

Overall, there is a solid volume increase (Table 11-43) due to CO₂ flooding of the Kupferschiefer Formation meaning that there is no increase in porosity and thus no increase in permeability. The solid volume increase is considerable probably leading to significant loss of porosity and permeability of the top seal. Migration of CO₂ into the Kupferschiefer caprock should not initiate leakage from the top seal.

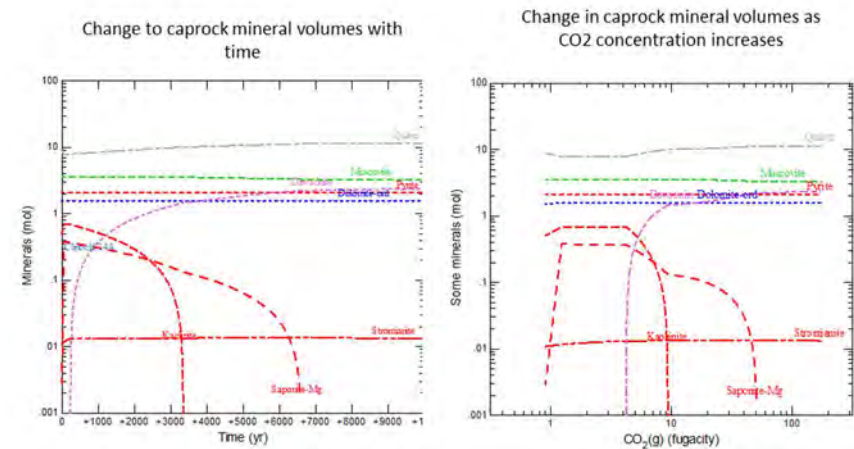


Figure 11-82 Mineral dissolution and growth with time and CO₂ concentration

top seal mineral	Time = 0 after equilibration	5,000 years	10,000 years
Quartz	200.00	242.80	258.80
Albite	0.00	0.00	0.00
K-feldspar	0.00	0.00	0.00
Kaolinite	50.00	0.00	0.00
Illite	500.00	481.60	459.45
Chlorite	50.00	0.00	0.00
Pyrite	50.00	50.00	50.00
Dawsonite	0.00	110.20	139.50
Anhydrite	0.00	0.00	0.00
Strontinite	0.00	0.53	0.51
Dolomite	92.76	100.70	100.70
Alunite	0.00	0.00	0.00
	942.76	985.83	1008.96
Fractional volume change		1.05	1.07

Table 11-43 Kinetic modelling mineral volume results for the Kupferschiefer Formation

Zechstein Formation

Geochemical kinetic simulations for each of the three Zechstein lithologies were run to assess the impact of migrating CO₂ from the underlying Leman

Sandstone. As with the Kupferschiefer, models reacting 5 mol CO₂ (g) over 10,000 years at 80°C (representative of 9000 ft TVDSS) for the selected Zechstein caprock compositions were run. Kinetic dissolution constraints for all minerals were again taken from Xu et al. (2006). The results of the kinetic modelling are shown in Figure 11-83 to Figure 11-85. Table 11-44 summarises the mineral volumetric impact of CO₂ migration into the Zechstein caprock.

For the Zechstein Dolomitic caprock (98% dolomite, 2% anhydrite), the models (Figure 11-83) indicate that only very minor dissolution of dolomite will occur on contact with CO₂. The minor (2%) anhydrite content will undergo no change, although any Sr-sulphates (e.g. strontianite) may undergo minor dissolution.

A similar result (Figure 11-84) was shown for the Zechstein Anhydritic Dolomite caprock lithology (55% anhydrite, 45% dolomite). Once again, very minor dissolution of dolomite due to CO₂ influx was observed with minor change in Sr-sulphate mineral volume. No change in anhydrite volume was seen.

The increase in anhydrite content of the Zechstein Anhydritic (98% anhydrite) caprock makes no difference to the simulation results; as Figure 11-85 shows, a similarly minor loss of dolomite and Sr-sulphate are the only observable changes.

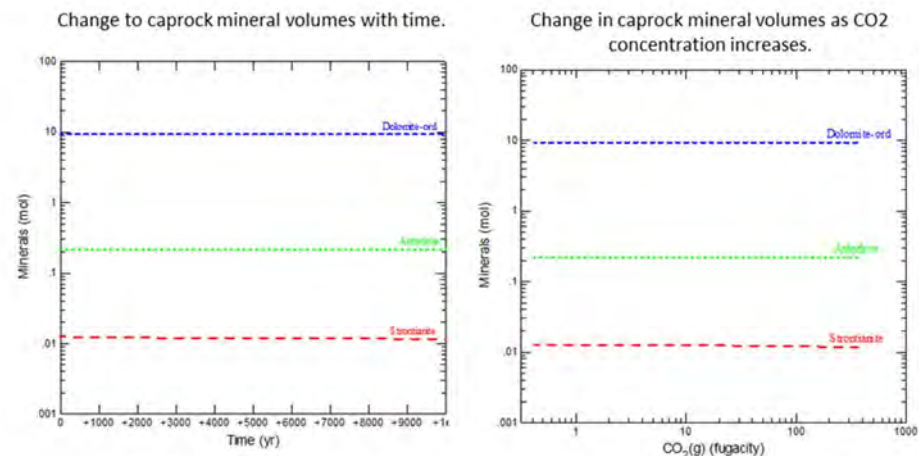


Figure 11-83 Mineral dissolution and growth with time and CO₂ concentration (Zechstein Dolomitic caprock)

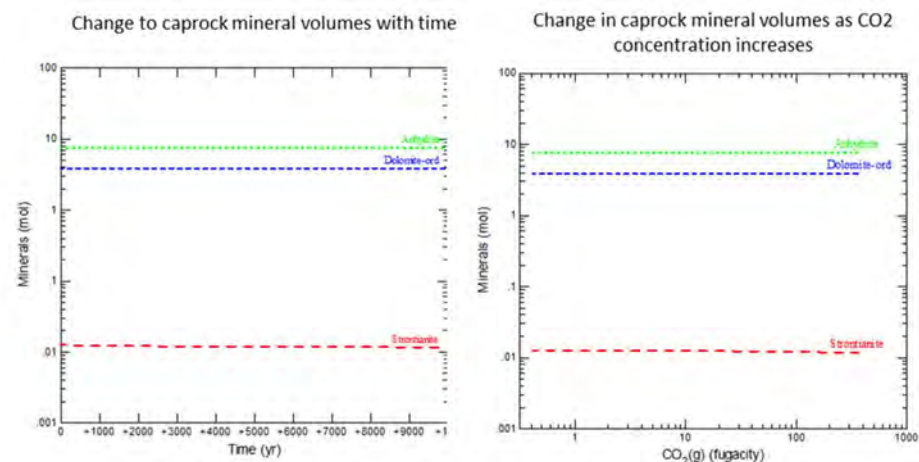


Figure 11-84 Mineral dissolution and growth with time and CO₂ concentration (Zechstein Anhydritic Dolomitic caprock)

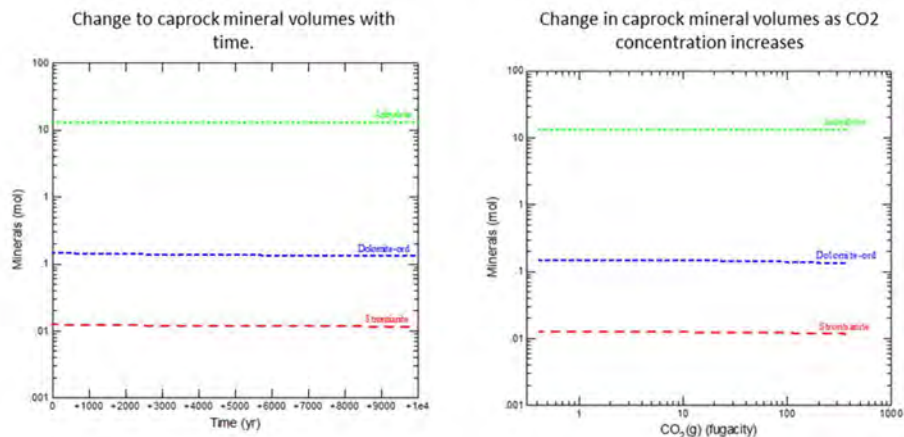


Figure 11-85 Mineral dissolution and growth with time and CO₂ concentration (Zechstein Anhydritic caprock)

Table 11-44 shows the overall mineral volume impact of migration of CO₂ into the Viking field Zechstein caprocks. The main changes are:

1. Dolomite undergoes a small amount of dissolution as CO₂ injection proceeds and pH drops.
2. Sr-sulphate initially forms due to the elevated Sr in the formation water – it then partially dissolves

Overall, there is a very small solid volume decrease due to CO₂ flooding of the Zechstein Formation where dolomite is present, meaning that there is a very small increase in porosity. Where dolomite is absent there is no reaction and no volume change.

Caprock mineral	Time = 0 after equilibration	5,000 years	10,000 years
Anhydrite	10.06	10.08	10.09
Strontianite	0.49	0.47	0.46
Dolomite	599.60	598.80	598.50
	610.15	609.35	609.05
Fractional volume change		0.999	0.998

Caprock mineral	Time = 0 after equilibration	5,000 years	10,000 years
Anhydrite	350.00	350.10	350.10
Strontianite	0.49	0.47	0.46
Dolomite	250.00	248.80	248.50
	600.49	599.37	599.06
Fractional volume change		0.998	0.998

Caprock mineral	Time = 0 after equilibration	5,000 years	10,000 years
Anhydrite	600.00	600.10	600.10
Strontianite	0.49	0.48	0.45
Dolomite	10.00	8.79	8.47
	610.49	609.37	609.02
Fractional volume change		0.998	0.998

Table 11-44 Results for the simulated Zechstein Formation caprock lithologies (dolomitic, anhydritic dolomite and anhydritic)

11.8.5.8 Conclusions

In summary, by flooding the Viking field Leman sandstone reservoirs with CO₂, the overlying caprock lithologies are unlikely to be geochemically-affected in a manner which significantly alters the existing permeability character.

In the clay-rich Kupferschiefer:

1. The kaolinite and, to a lesser extent illite, react with sodium in the formation water and the incoming CO₂ to create dawsonite and quartz
2. Chlorite reacts to form dolomite (and dawsonite and quartz)

These reactions lead to a solid volume increase thus diminishing porosity and permeability

The Zechstein may undergo minor dissolution due to the presence of CO₂ where dolomite is present but anhydrite is fully stable.

11.9 Appendix 9 – Fracture Pressure Gradient Calculation

Fracture pressure is related rock strength, applied stress and pore pressure in the reservoir. As a produced field, the Viking A reservoir has depleted in pressure from its original state to the current state, and thus the fracture pressure has also changed over time. In order to derive the current fracture pressure (and the likely future fracture pressure as the reservoir is re-pressured through CO₂ injection), the original fracture and pore pressure needs to be fully understood.

In order to determine fracture (and pore) pressure in the Viking, an analysis of available log data was carried out using DrillWorks 5000. The following tasks were performed for selected wells in each field (basic workflow):

- Overburden or Vertical stress (SV): based on bulk density log
- Pore pressure calculation: from RFT data
- Fracture Gradient or minimum horizontal stress (Shmin): Matthews and Kelly method calibrated with reference fracture gradient (0.74 psi/ft)
- Poisson's ratio: based on sonic log
- UCS: Lal's law correlation applied to the sonic log
- Stress regime: normal assumed (SV>SH>Shmin)
- Maximum horizontal stress (SH) calculated from SV and Shmin
- Stress orientation from the World Stress map

The combination of Kupferschiefer-loss of porosity and the stability of the anhydrite-dominated Zechstein probably means there is negligible risk of top seal dissolution due to elevated CO₂ concentration in the reservoir.

This process utilises log derived geomechanical properties combined with elastic stress calculations. The modified Lade shear failure criterion was applied. This utilises all three principal stresses and is generally less conservative than the Mohr-Coulomb failure criterion.

Public domain data suggests a fracture gradient of 0.74 psi/ft (source material in the Reference section), therefore the calculated fracture gradient is calibrated to this reference fracture gradient and compared with any specific FIT or LOT data that is available. The calculated breakout criterion and fracture gradient lines are combined with information on drilled mud weights and any drilling issues (tight hole, losses) to provide a qualitative calibration on the rock property / stress system.

11.9.1 Stress Orientation

The World Stress Map is a global reference for tectonic stress data when there is no any other data available (e.g. reliable dual arm calliper or image log data). The web link is in the References section.

The regional maximum horizontal stress (SH) is aligned NW-SE, and therefore the Shmin is aligned NE-SW. The presence of halite layers may allow local structure related stress orientation variations in the overburden compared to the underlying Leman Sandstone.

The Viking A Rotliegend structural alignment is also NW-SE, Shmax is often parallel to the main structural grain in the North Sea

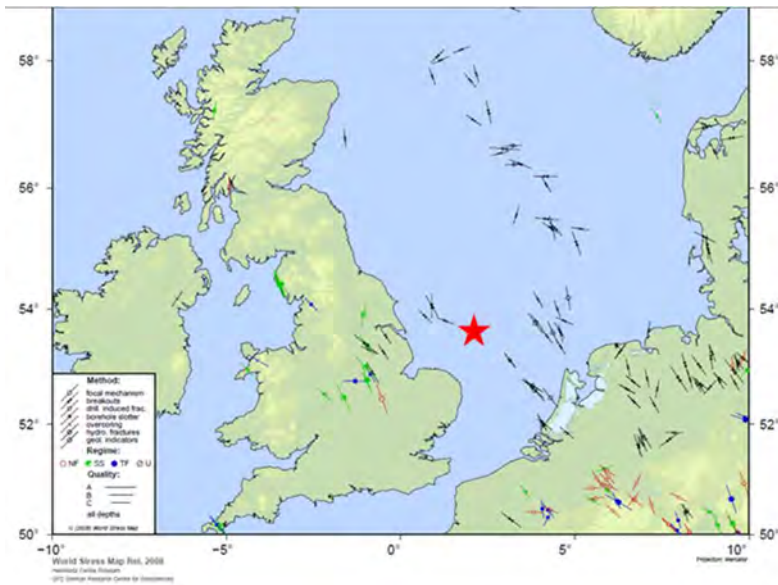


Figure 11-86 Viking stress orientation

11.9.2 Wells Evaluated

Available Logs were obtained from the CDA website. The analysis was focused on six wells to cover the Viking A field: 49/12-2, 49/11a-6, 49/12a-K4, 49/12a-K5, 49/12-A6 and 49/12-A10



Figure 11-87 Viking A field

11.9.3 Stress Path and Rock Mechanical Properties

The figures in this section describe the calculated stress curves and log derived rock mechanical properties in each well. Note that these wells were drilled and logged when the reservoir was at (or close to) original pore pressure (i.e. before significant depletion). Note also that the Lemman Sandstone (reservoir rock) is a sub-unit of the Rotliegend Group, but can in this specific case be considered interchangeable (different logs have different nomenclature).

The calculated stress curves figures show pore pressure (orange line), minimum horizontal stress (red line), maximum horizontal stress (black line) and overburden (magenta line). The following considerations were used to calculate the stress path:

- Pore pressure based on RFTs in the Rotliegend group.
- Minimum horizontal stress (Shmin) calculated by Matthews and Kelly and calibrated with reference fracture gradient (0.74 psi/ft) in Lemman sandstone
- Normal stress regime assumed. Maximum horizontal stress calculated from average of Shmin and overburden (Sv)
- Halite Shmin gradient treated as lithostatic.

For wells 49/12a-K4, 49/12a-K5, 49/12-A6 and 49/12-A10, the log data was only available around the Rotliegend formation. Therefore the analysis was carried out only where log data is available. It is important to mention that there are several halite layers above Rotliegend (five layers in 49/12a-K4, four layers in 49/12a-K5, one layer in 49/12-A6 and two layers in 49/12-A10) and this was not taken into account in this analysis due to the lack of log data. However the wells 48/12-2 and 49/11a-6 could be used as a guide for upper layers (their logs start from approximately 2500' TVD).

The minimum horizontal stress curves were compared with LOT/FITs available as follows:

Wells 49/12-2, 49/12-A6 and 49/12-A10:

- No FIT/LOT data found for these three wells

Well 49/11a-6

- LOT from 20" shoe is high, probably close to the fracture initiation pressure rather than minimum horizontal stress
- FIT from 9 $\frac{5}{8}$ " was performed in a halite layer (lithostatic gradient assumed).

Well 49/12a-K4

- FIT data is available in this well (however no logs are available at these depths)

Well 49/12a-K5

- FIT at 7" is close to the start of the Shmin predicted

The rock mechanical properties figures depict the following rock mechanical properties derived from logs:

- Poisson's ratio (black line)
- Friction angle (blue line)
- Rock strength (UCS) (purple line)

For the well 49/11a-6, the sonic log suffers from cycle skipping within the Lemman Sandstone. This means the spikes of low FA and UCS values are probably erroneous and have been ignored in the analysis.

Wells 49/12-A6 and 49/12-A10 do not have sonic log available. The sonic logs used were calculated based on the density log (inverted Gardner function).

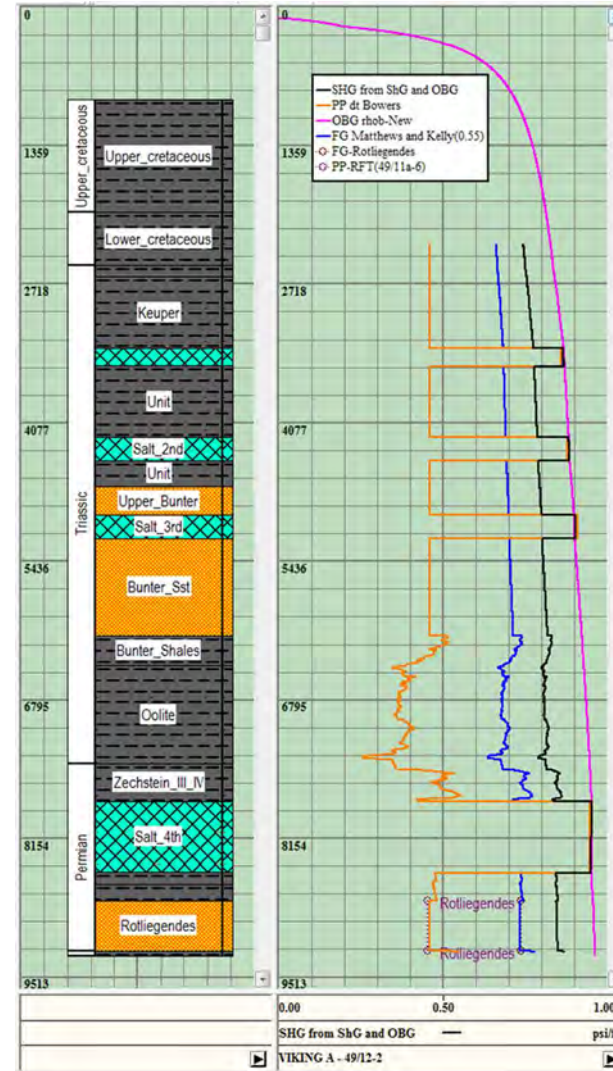


Figure 11-88 Viking A Well 49/12-2 Calculated stress curves

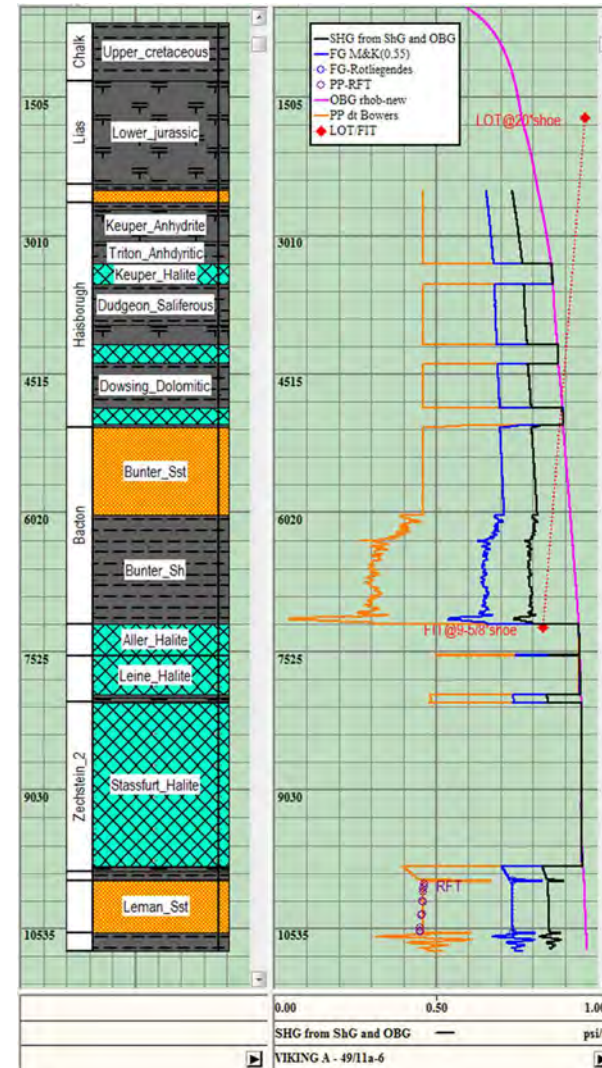
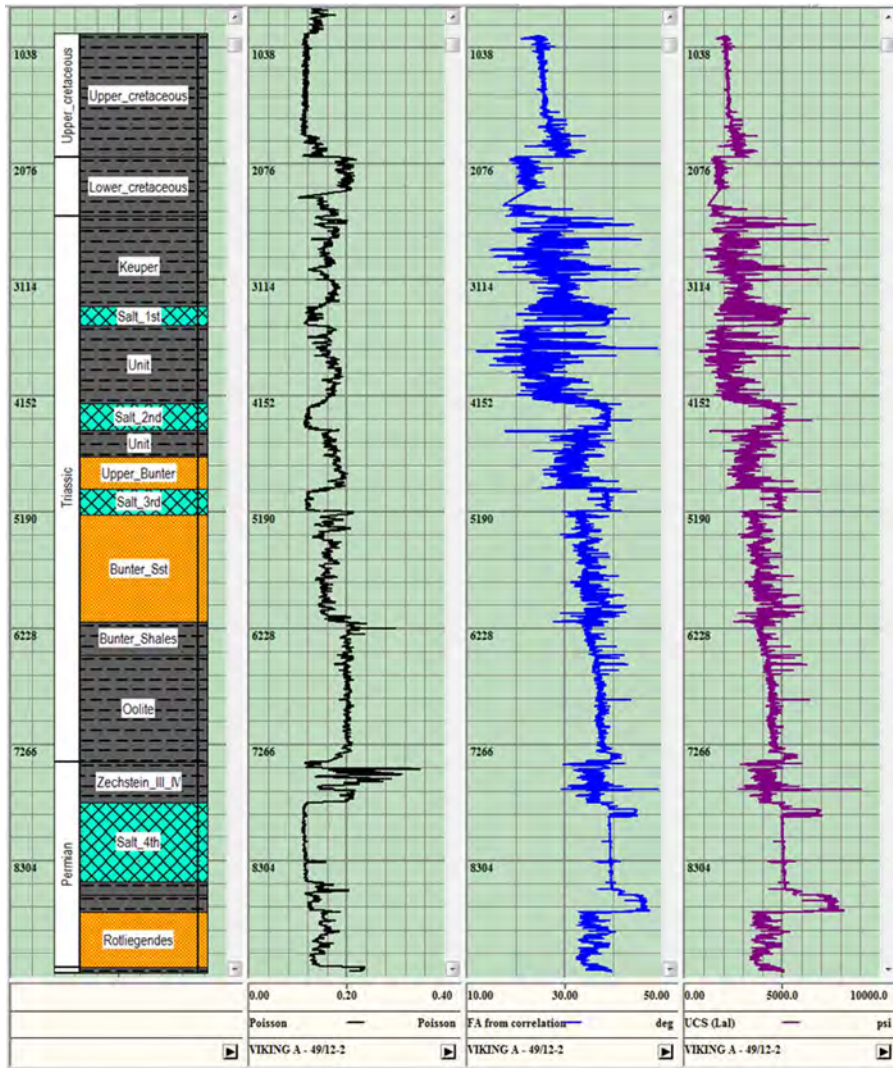


Figure 11-89 Viking A Well 49/12-2 Rock mechanical properties

Figure 11-90 Viking A Well 49/11a-6

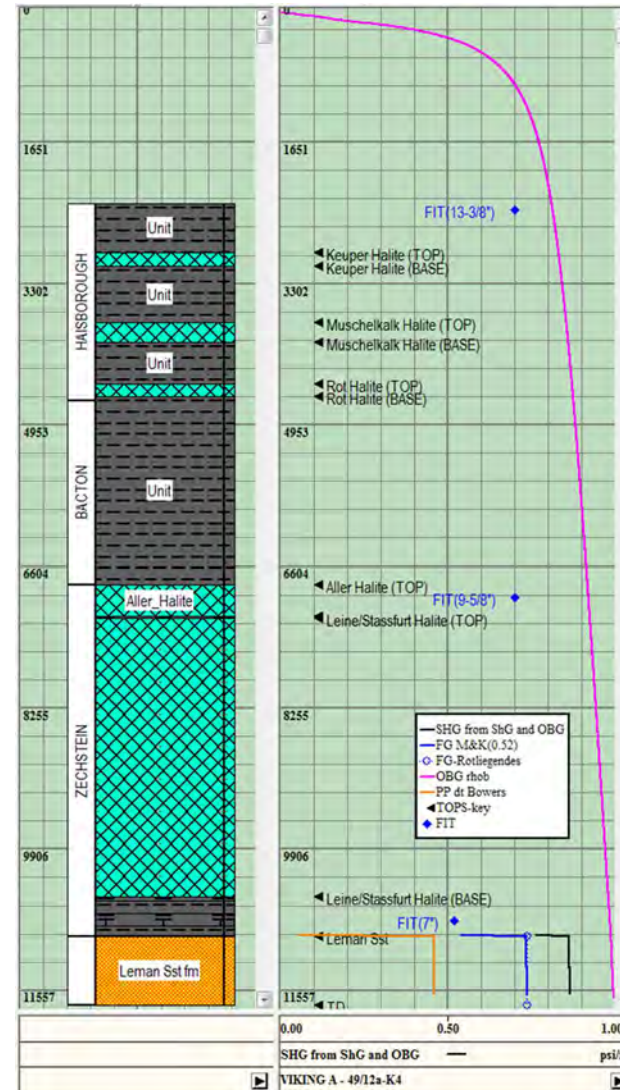
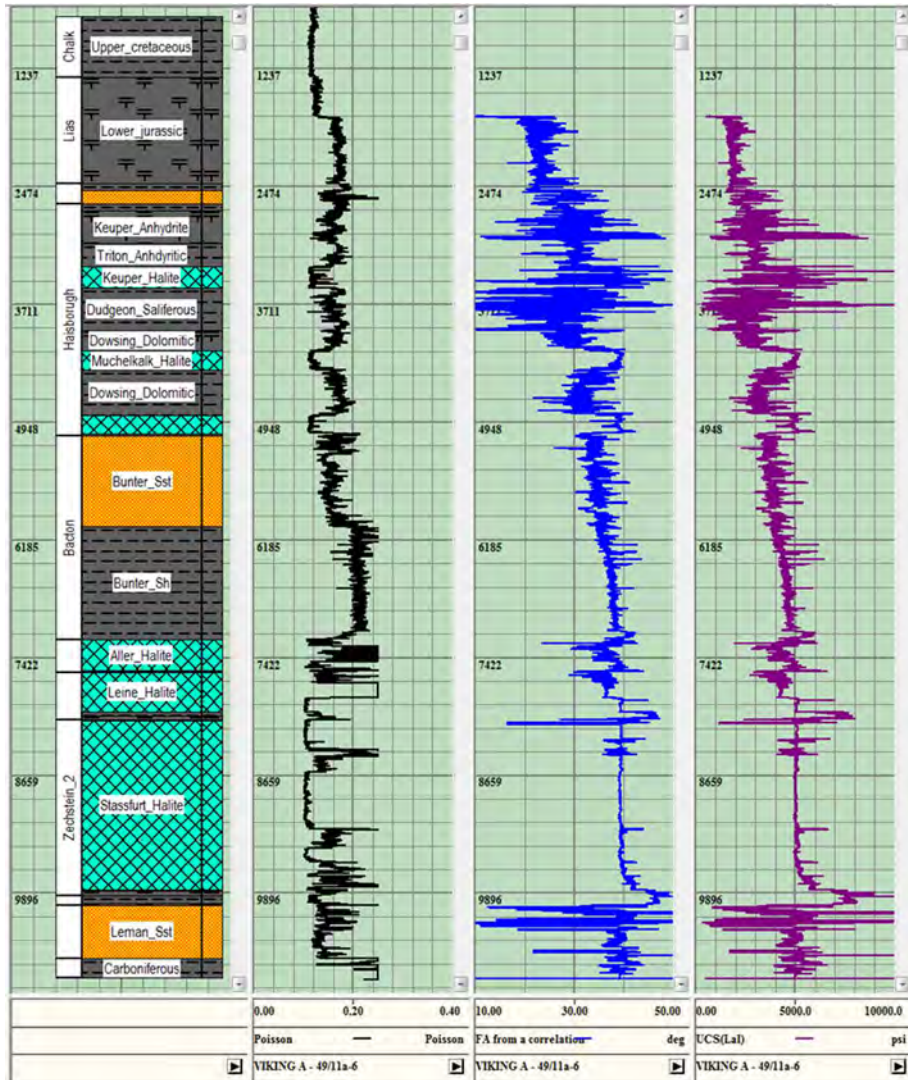


Figure 11-91 Viking A Well 49/11a-6

Figure 11-92 Viking A Well 49/12a-K4

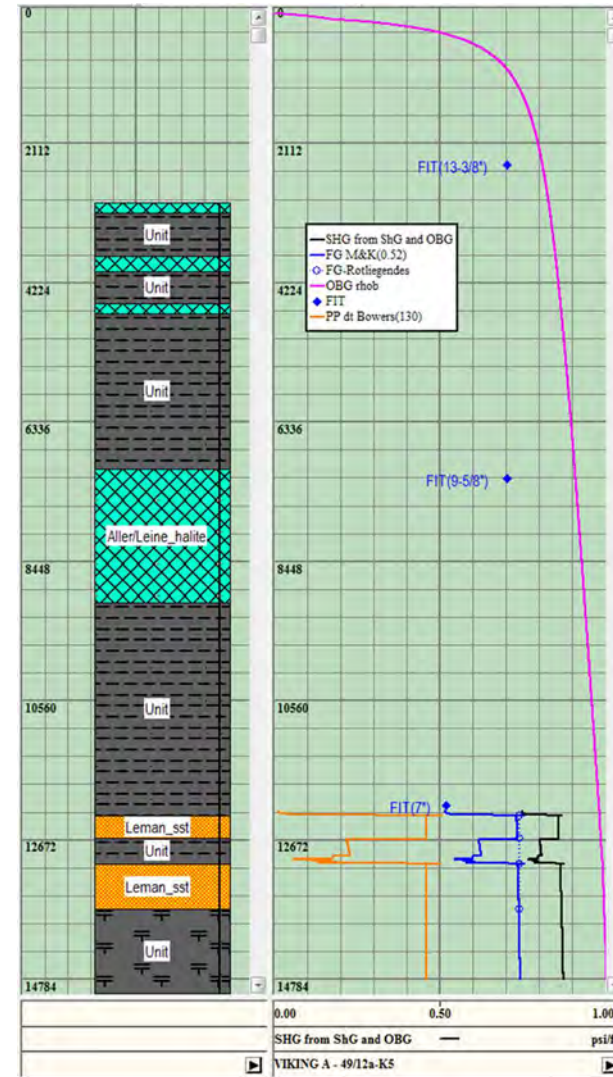
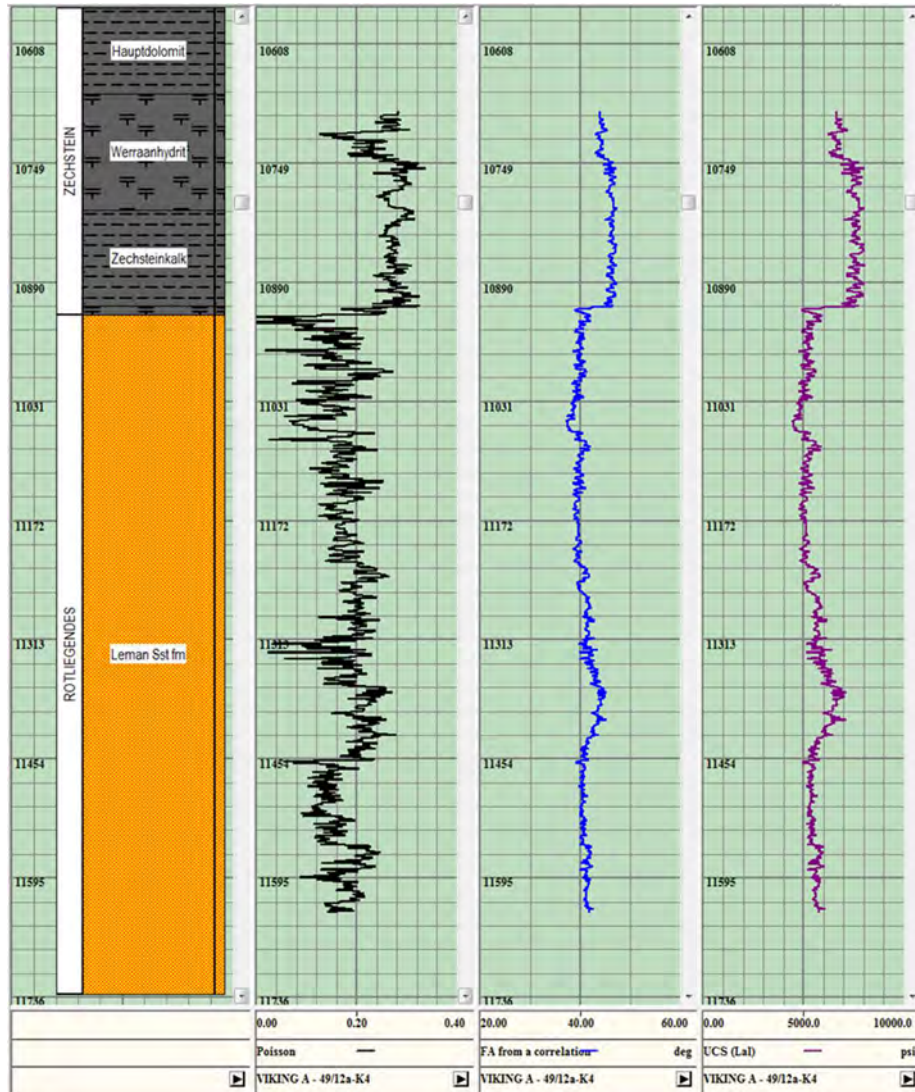


Figure 11-93 Viking A Well 49/12a-K4 Rock mechanical properties

Figure 11-94 Viking A Well 49/12a-K5 Calculated stress curves

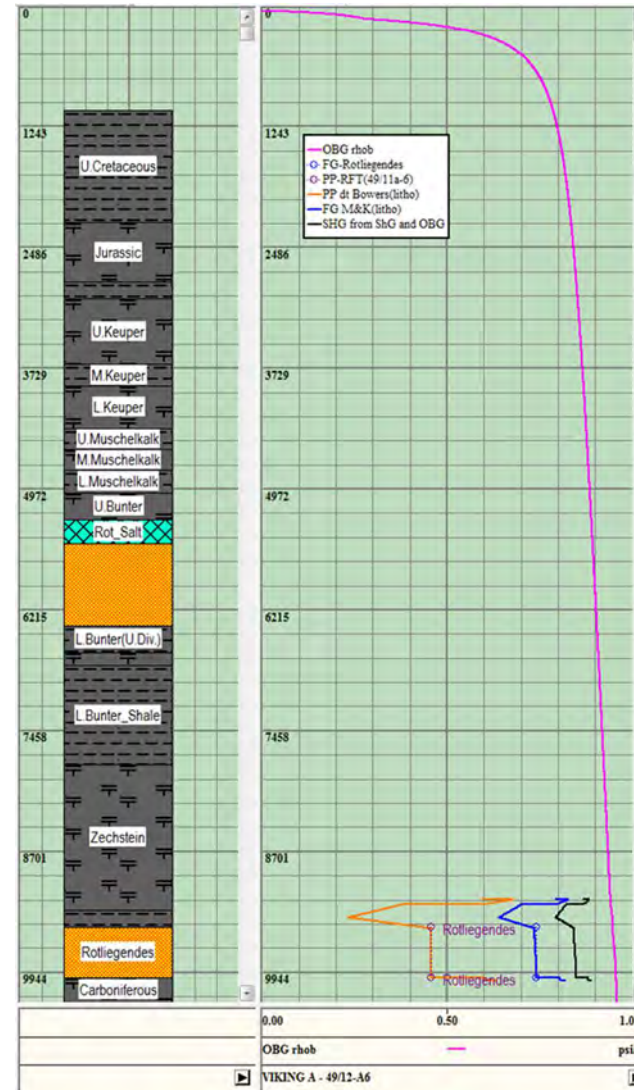
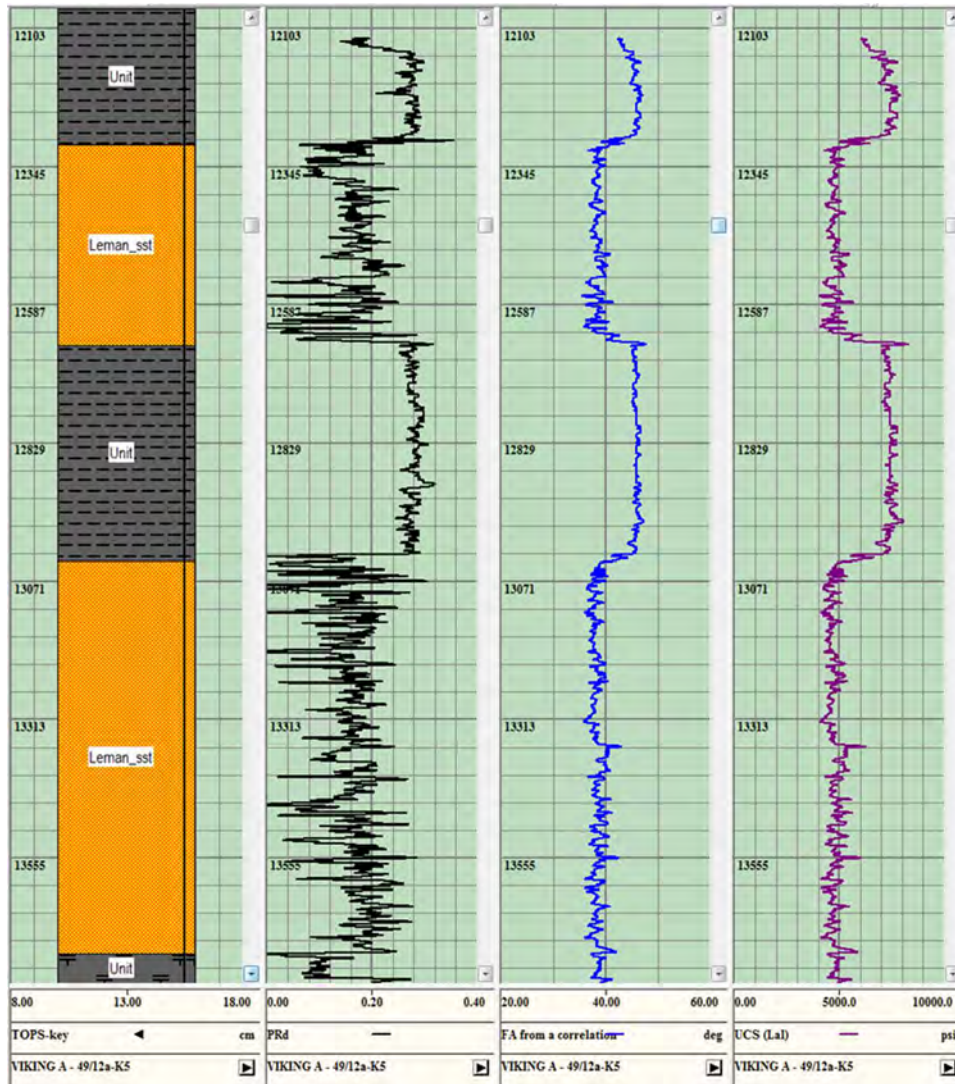


Figure 11-95 Viking A Well 49/12a-K5 Rock mechanical properties

Figure 11-96 Viking A Well 49/12-A6 Calculated stress curves

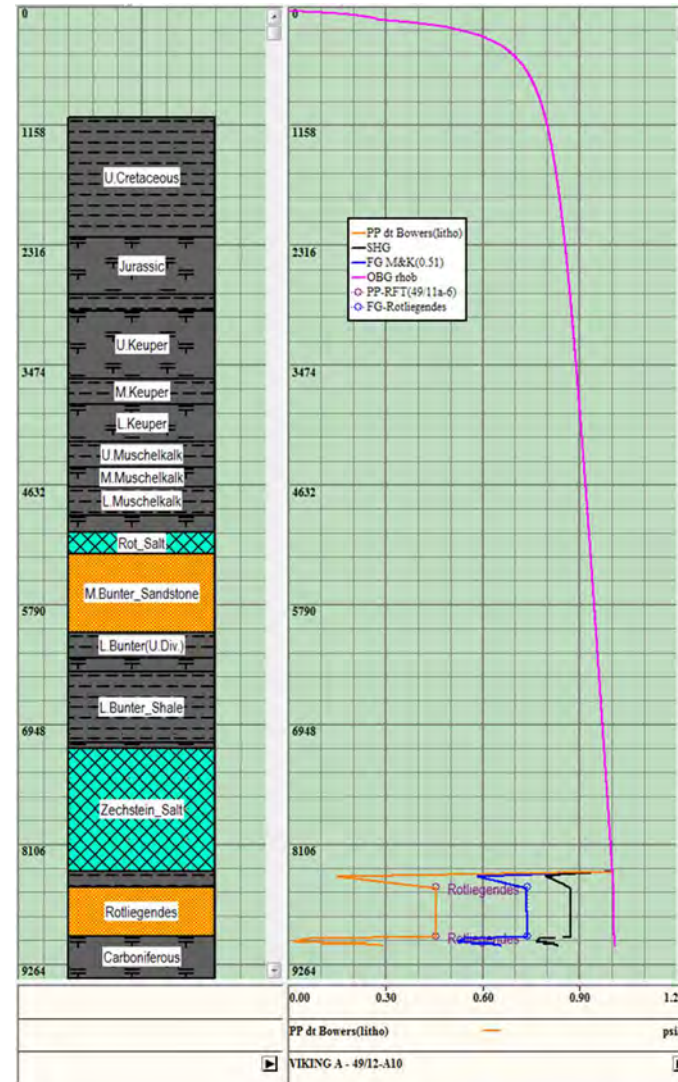
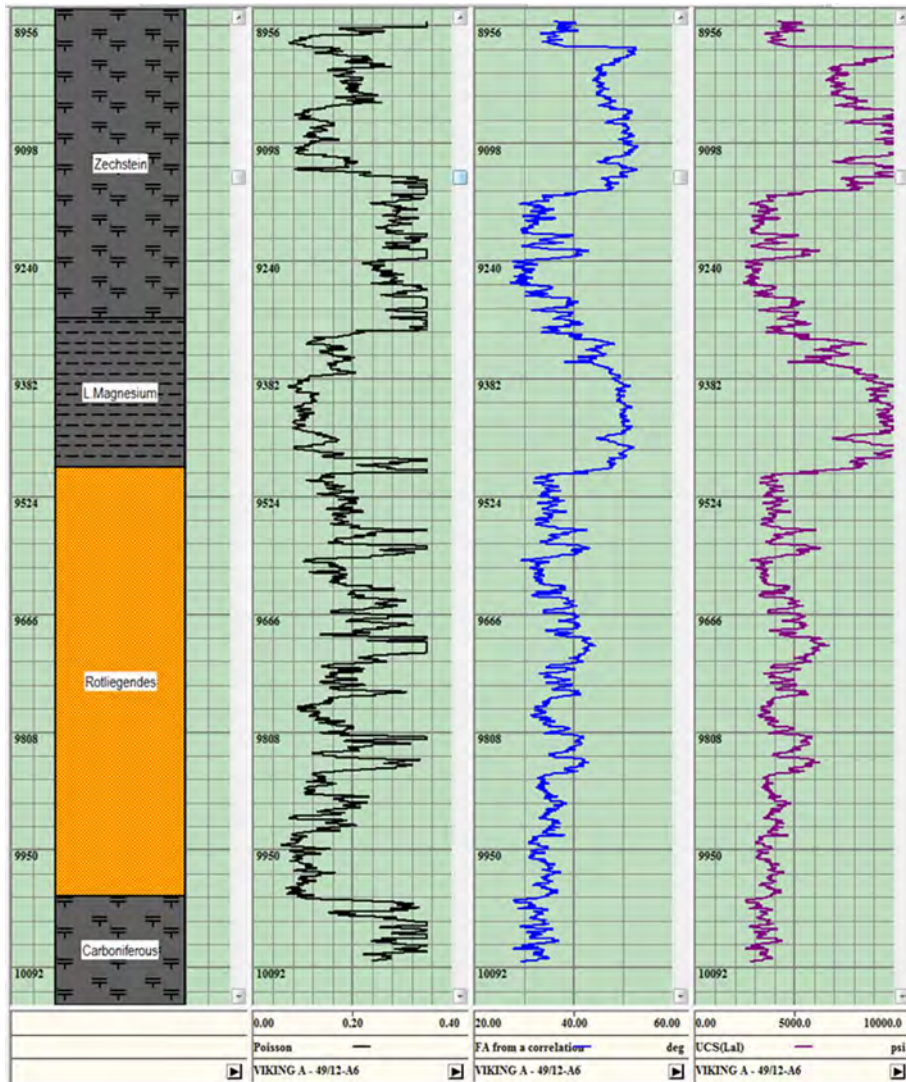


Figure 11-97 Viking A Well 49/12-A6 Rock mechanical properties

Figure 11-98 Viking A Well 49/12-A10 Calculated stress curves

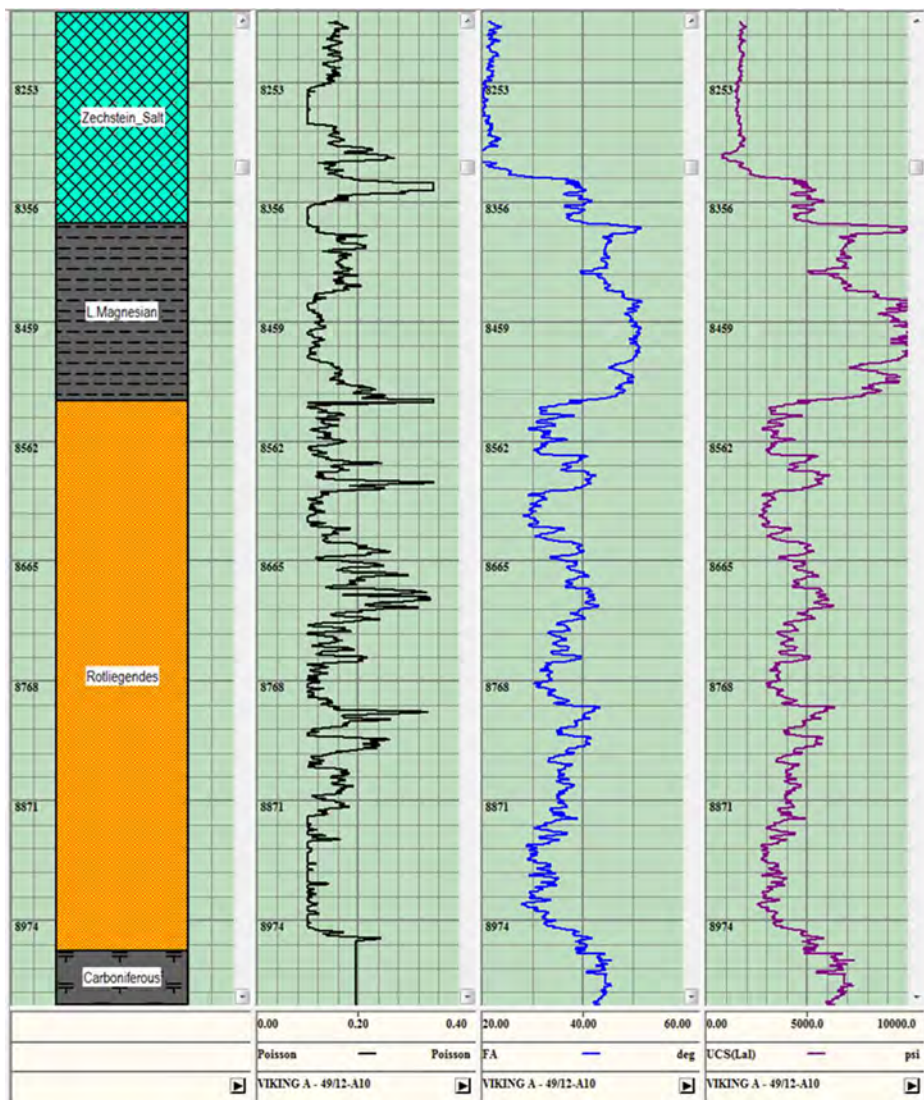


Figure 11-99 Viking A Well 49/12-A10

It can be concluded from this analysis that the fracture gradient from literature of 0.74psi/ft can be supported and that the original pore pressure is 0.46 psi/ft. These values are used in the following depletion analysis.

11.9.4 Depletion Analysis – Poroelasticity

Depletion in a reservoir can lower the fracture gradient due to a combination of Biot’s factor (pore pressure effectiveness) and Poisson’s ratio (lateral strain/vertical strain). During depletion the total stress stays the same (weight of rock doesn’t change) but the effective vertical stress (σ_v) increases as;

$$\Sigma_v = S_v - \alpha P_p$$

Where:

α = Biot’s factor.

The effective horizontal stresses also increase with depletion but the increasing vertical strain causes an increase in lateral strain that counteracts the horizontal stress increase. This means the net result is a total horizontal stress decrease during depletion. The equation for the change in total horizontal stress with pore pressure change (stress path or λ) is shown below:

$$\lambda = \alpha((1-2\nu)/(1-\nu)) = \Delta S_h / \Delta P_p \quad \text{e.g. Zoback (2007)}$$

Where:

α = Biot’s factor

ν = Poisson’s ratio.

This formula is valid where the reservoir width is equal or higher than ten times (10x) the reservoir height (to prevent stress arching).

Even if this relationship is broadly correct, there is the potential for hysteresis if the reservoir pressure is increased from the depleted state. The worst case scenario for fracturing the reservoir is that during injection, the fracture gradient stays similar to the depleted fracture gradient.

The impact of the changes in reservoir pressure on the overburden units will be much less, meaning the seals should still have fracture gradients close to original conditions. If there are any stress arching effects, then the horizontal stresses may increase slightly.

Depleted fracture gradient, using this formula, was determined by DrillWorks 5000. The following considerations were taken to calculate the fracture gradient at depleted condition in DrillWorks 5000:

- The depletion condition was applied only to the Rotliegendes Group.
- The depleted pore pressure was assumed to be 500 psi (see section 3.6)
- The Breckels & Van Eekelen correlation and the Matthews & Kelly correlations have almost the same output at depleted conditions. Therefore, the Matthews & Kelly correlation will be used to identify the depleted fracture gradient condition for all the wells in Viking A

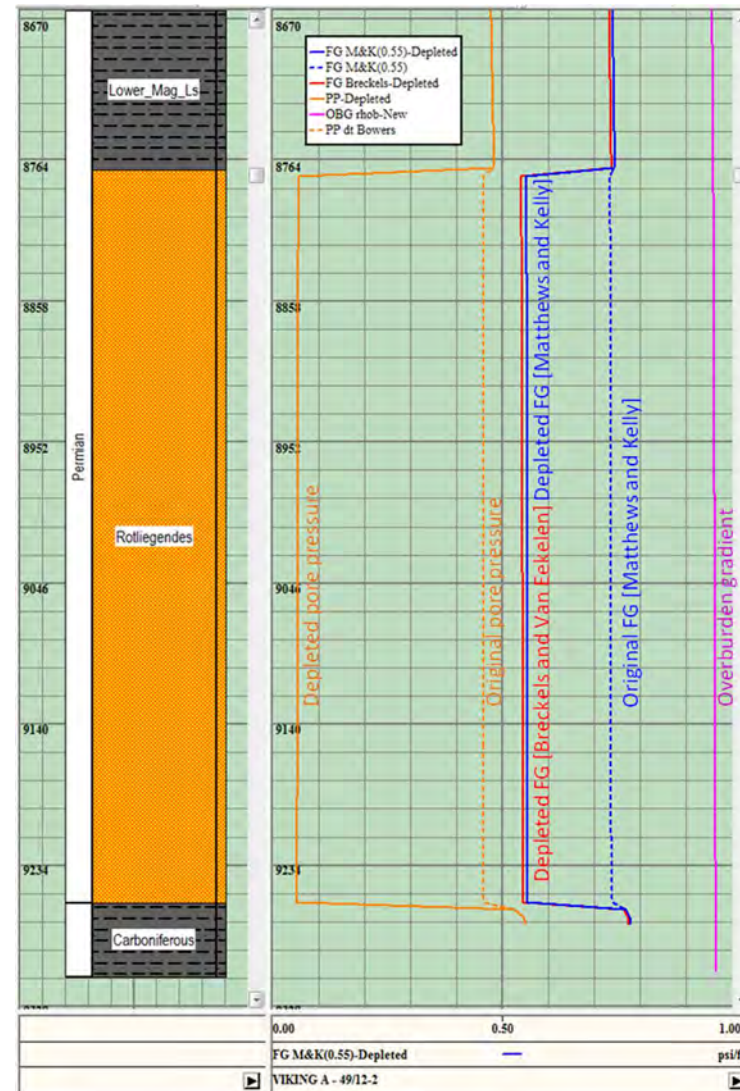


Figure 11-100 Viking A Well 49/12-2 Depleted fracture gradient analysis

For the Viking A, this work resulted in a depleted fracture gradient of 0.54 psi/ft. However, this simple relationship can only be used as a rough guide to the potential change in fracture gradient as it assumes a vertical stress with elastic response control on the horizontal stress system with depletion. The actual stress path may be affected by local variations in far field tectonic stresses, depletion variability, lithological changes or the local structure (folds and faults).

These variables can be more accurately modelled in a full field 3D geomechanical model, such as that available in Schlumberger's Petrel platform. A 3D model was constructed for the Viking field to explore fault re-activation during the depletion / re-pressurisation cycle (Appendix 11) which gave a more conservative depleted fracture gradient of 0.43 psi/ft using the Mohr Coulomb relationship (see resultant fracture gradient ramp in Figure 3 15). It is also worth noting that the higher depleted fracture pressure gradient of 0.54 psi/ft is supported by the Modified Drucker-Prager relationship.

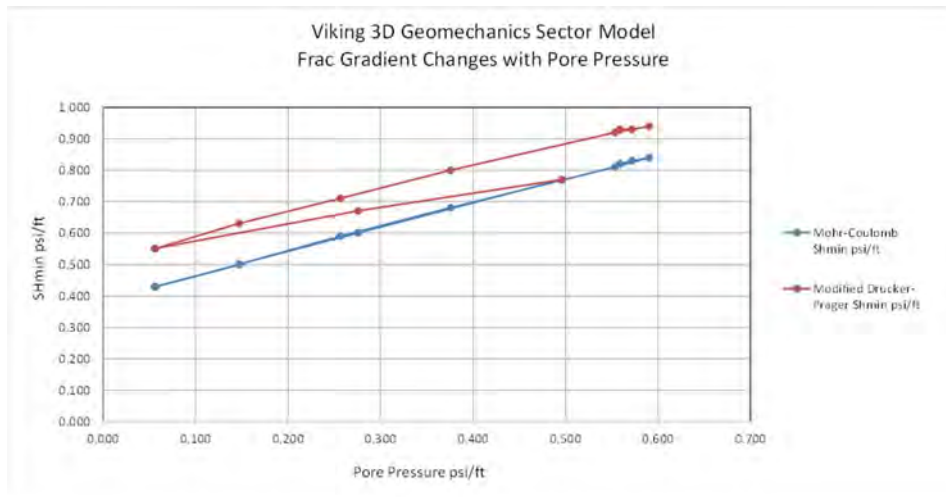


Figure 11-101 Stress paths for Viking at the 49/12-2 well location

11.9.5 Conclusions

- Assumptions are made that the regional NW-SE in-situ maximum horizontal stress orientation is relevant to the Viking structure. Real maximum horizontal stress azimuth may be different.
- The actual depleted condition in the Leman Sandstone is not confirmed with field data, at the moment the estimation is based on the correlation used (Matthews and Kelly).
- The average pore pressure gradient in the wells analysed were 0.46 psi/ft. The assumed average depleted pore pressure gradient was 0.047 psi/ft (based on an assumed depleted pore pressure of 500 psi).
- No core has been available to calibrate the strength (breakout) information.
- Based on the analyses presented here, a valid working assumption for a depleted fracture gradient in Viking is 0.54 psi/ft. The original (un-depleted) fracture gradient has been confirmed as 0.74 psi/ft. Note this is likely to increase as the reservoir is pressurised although that is not guaranteed. For the purposes of this study, well design will adopt this value as base case, with operational contingencies discussed should fracture gradient be lower.
- It should also be noted that 3D geomechanical modelling (Appendix 11) has established a larger range of fracture pressures, with a low end being 0.43 psi/ft. At the time of writing, the 0.43 psi/ft value was adopted, and the safe operating range was therefore taken as 90% of this (i.e. 0.387 psi/ft). For the purposes of this study initial reservoir injection limits will honour this value.

- The development of the fracture gradient as the reservoir re-pressures is also discussed in the 3D Geomechanics section. There is considerable uncertainty over the stress path during reservoir re-pressurisation (fracture pressure hysteresis), and this is considered a high project risk. However, this can be considerably de-risked by determining the true depleted fracture pressure as a starting point. It is recommended that the current operators of the Viking field are approached, prior to field abandonment, in order to acquire fracture pressures from the current well stock (extended leak off tests for example).

11.10 Appendix 10 – Subsurface Uncertainty Analysis

A number of subsurface and development uncertainties were identified through the course of the project and assessed for their impact on CO₂ injectivity and site performance.

The reference case is described with respect to the sensitivity parameters in Table 11-46 but for clarity the main input parameters presented throughout the body of this report are consolidated in Table 11-45, provided as a summary.

The uncertainty parameters and the associated range of values is summarised in the sensitivity matrix in Table 11-46 below.

The results are tabulated in Table 11-47 and also displayed in Figure 11-102, a bar chart showing the capacity and in Figure 11-103, a bar chart showing the duration of the injection period for each case.

Injection into the Viking A site ceases when any cell in the model violates the imposed pressure constraint which is 90% of the fracture pressure. The injected mass at this time represents the storage capacity of the Viking site. Based on the sensitivity analysis the range of capacity for Viking is 82.7Mt to 158.8MT, with a reference case capacity of 134.5MT. The parameters that have the biggest impact on capacity are the fracture pressure limit and the connected GIIP volume.

The impact of the key uncertainty parameters on site performance is discussed in more detail in the following sections.

Input Parameter	Value / Description
Datum depth (mTVDSS)	2544
Initial Pressure (pre-injection) at datum (bar)	34.1
Temperature at datum (°C)	83.8
Rock compressibility (1/bar)	1.423x 10 ⁻⁵
CO ₂ density at datum (kg/m ³)	56 - 799
CO ₂ viscosity at datum (cp)	0.017 – 0.069
Brine Salinity (NaCl eq.) (ppm)	220000
Porosity (mean) (fraction)	0.13
Permeability (model mean / range) mD	49.2 (0 – 962)
Aquifer Volume (MMm ³)	806.5
Well Number	2
Injection Rate per well (Mt/y)	5
Tubing Size (“)	7”

Table 11-45 Key input parameters to the reference case dynamic model

Note that the density and viscosity ranges refer to conditions at the start and end of injection.

Uncertainty Parameter	Unit	Input Values		
		Low	Reference	High
Pre-injection reservoir pressure	bara	20.4	34.1	47.1
Fault seal	m ³	sealed	open	-
Fracture pressure limit (bar/m)	bar/m	0.09	0.15	-
Connected Volume in Block A	MMm ³ (Bscf)	36 (1269)	44 (1553)	52 (1837)
Permeability (kx)	mD	26	78	230
kv/kh		0.20	0.58	-
Connection through zones B and D		-	None	Low transmissibility
Number of wells		-	2	5
Injection rate	MT/y	2	5	10

Table 11-46 Subsurface uncertainty parameters and associated range of values

Uncertainty Parameter	Capacity	Length of injection profile (years)	
		Total	Heated Phase
	(MT)		
Reference	134.5	26.9	19.7
Low pre-injection pressure	140.4	28.1	22.3
High pre-injection pressure	127.9	25.6	19.4
Fault seal	82.7	16.5	16.0
Low fracture pressure	90.0	18.0	18.0
Low connected volume	109.2	21.8	16.8
High connected volume	158.8	31.8	24.1
Low Perm _x	129.1	25.8	19.0
High Perm _x	137.5	27.5	21.3
Low Kv/kh	127.5	25.5	19.3
Connection through zones B and D	137.7	27.5	19.7
Number of wells: 5	133.4	26.7	21.6
Injection rate 2MT/y	136.3	68.2	55.4
Injection rate 10MT/y	130.4	13.0	8.5

Table 11-47 Comparison of injection profile for the uncertainty cases

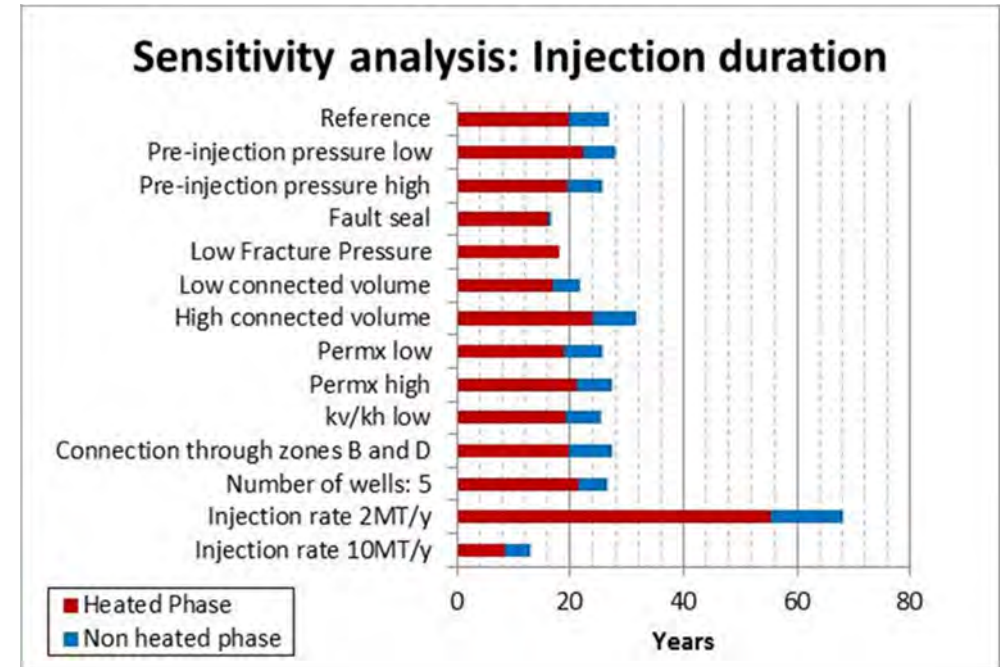
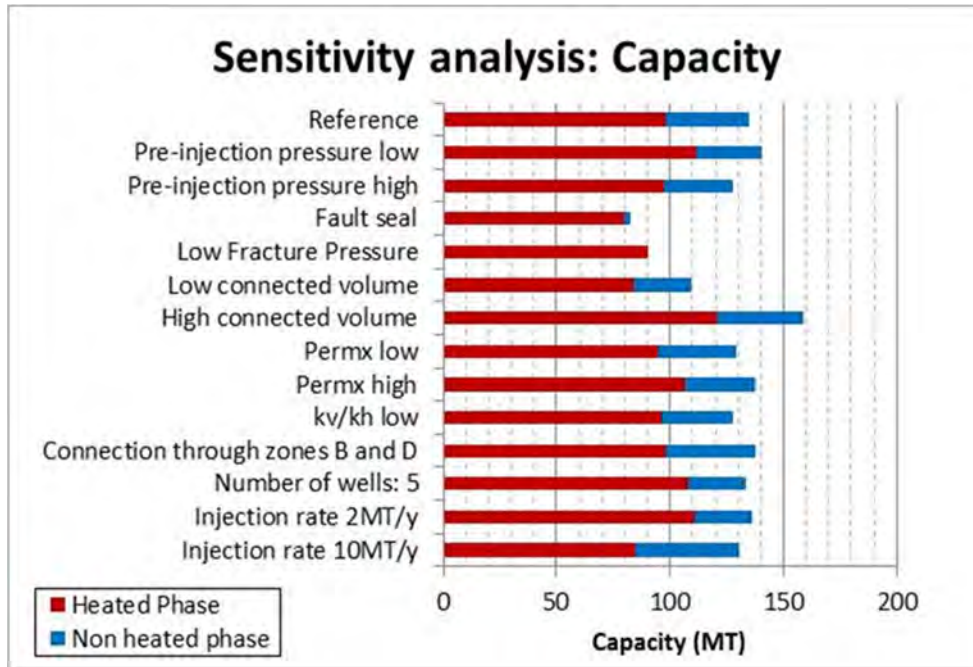


Figure 11-102 Comparison of capacity per case

Figure 11-103 Comparison of injection duration per case

11.10.1 Depleted Reservoir Pressure

Viking Block A was produced from October 1972 until April 1991, using ten gas producers. The production from Block A was reported in the literature to be 1124 Bscf, (Riches, 2003).

Some pressure data was supplied by the Operator for Viking A in the form of a single reservoir pressure and this has been used in combination with pressure data sourced from CDA abandonment reports to estimate the reservoir pressure at the start of CO₂ injection to be 34.1bara at a depth of 2544m tvdss. The model has been initialised with this pressure in all regions. As there is considerable uncertainty in the pressure depletion, sensitivities were run using initial pressures of 20.8 bara and 48.4 bara to evaluate the impact of the pressure uncertainty in the site storage performance. The capacity for the low and high pressure cases are 140.4MT (4% greater than reference case) and 127.9MT (5% reduction from reference case) respectively. The injection forecasts are shown in Figure 11-104.

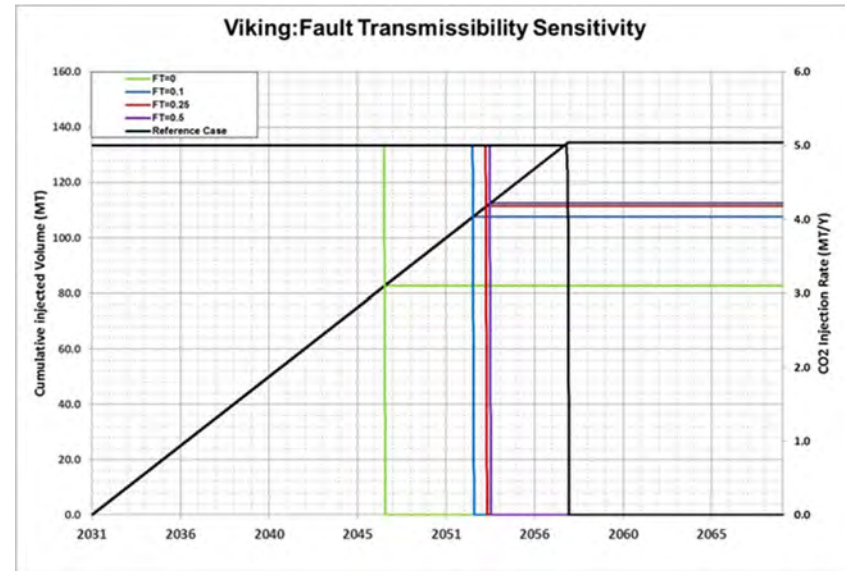


Figure 11-104 Injection forecasts for reservoir pressure sensitivities

11.10.2 Fault Seal

Fault seal influences the connected pore space available for CO₂ storage. The fault to the north west of the injection wells could potentially act as a barrier as there were no gas production wells drilled into the north west region to determine whether or not there is communication across the fault. If the fault is sealing the capacity is reduced from 134.5MT to 82.7MT. In this case the connected GIIP is 1225Bscf, compared to the non-sealing case GIIP volume of 1553Bscf. The location of the fault is shown in Figure 11-105

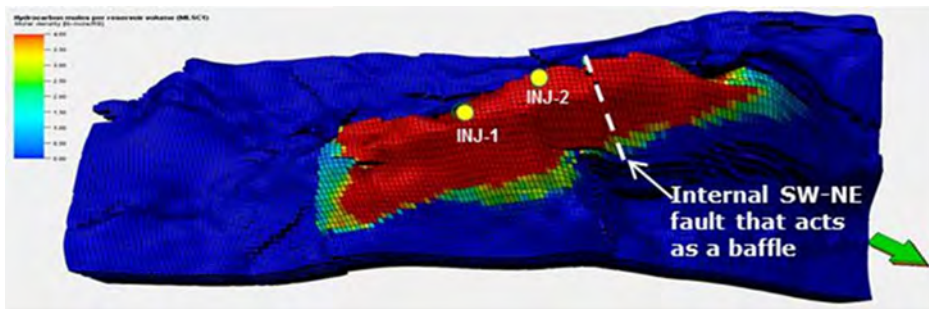


Figure 11-105 North West fault location shown on CO₂ distribution map at the end of injection

The impact of partially sealing the fault was also tested and the injection forecasts for the fault seal sensitivities are shown in Figure 11-106.

With the fault sealed the pressure build up in zone A is more rapid than in the reference case as pressure cannot dissipate to the lower zones as the only communication pathway is through the fault. The pressure constraint is first violated in zone A but the lower zones have not yet reached the fracture pressure constraint and still have some storage potential.

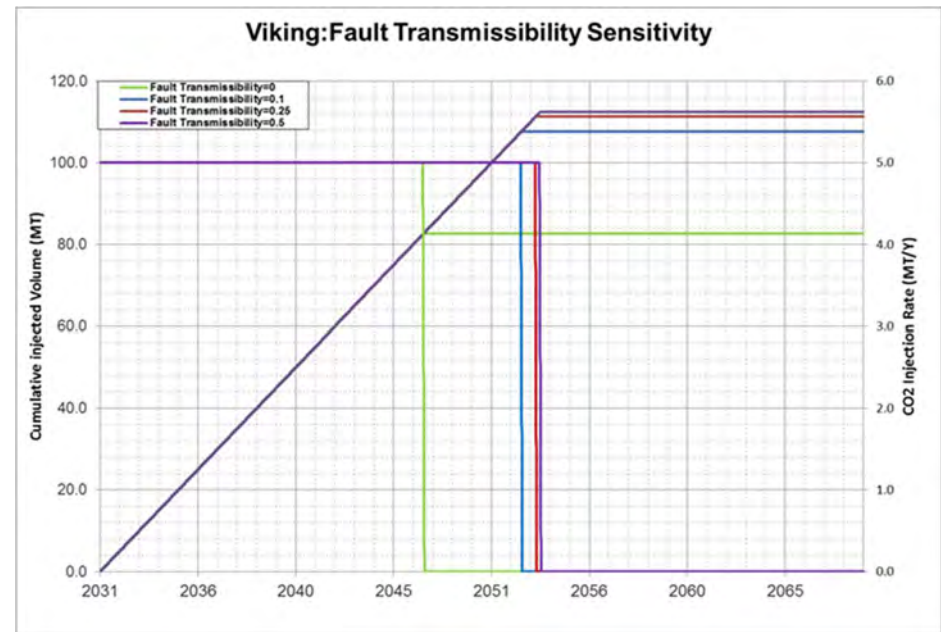


Figure 11-106 Injection forecasts for fault sealing sensitivities

11.10.3 Fracture Pressure Gradient

There is some uncertainty associated with the fracture pressure limit prediction, particularly for a depleted gas field, due to the uncertainty in the depleted reservoir pressure and also the uncertainty associated with the change in fracture pressure during re-pressurisation. A conservative approach has been adopted for the dynamic modelling. To avoid any chance of fracturing the reservoir the maximum pressure is limited to 90% of the fracture pressure. The model is set up so that if the pressure in any cell in the model reaches the pressure limit, injection will be stopped. At the start of CO₂ injection, into the depleted reservoir, the fracture pressure is estimated to be 0.097bar/m (0.43psi/ft). The most likely case is that the fracture pressure gradient will return to the initial fracture pressure gradient (pre-production) of 0.167bar/m (0.74psi/ft).

In the reference case the pressure constraint is set as 90% of 0.167bar/m, 0.1503bar/m. The worst case scenario is that the fracture pressure remains at the low depleted fracture pressure during injection but this is considered to be very unlikely. In this case the capacity is reduced from 134.5MT to 90MT.

A relationship between pressure gradient and injection capacity was developed for Viking A which can be used to ascertain injection capacity for different fracture pressure gradient values as shown in Figure 11-107 below.

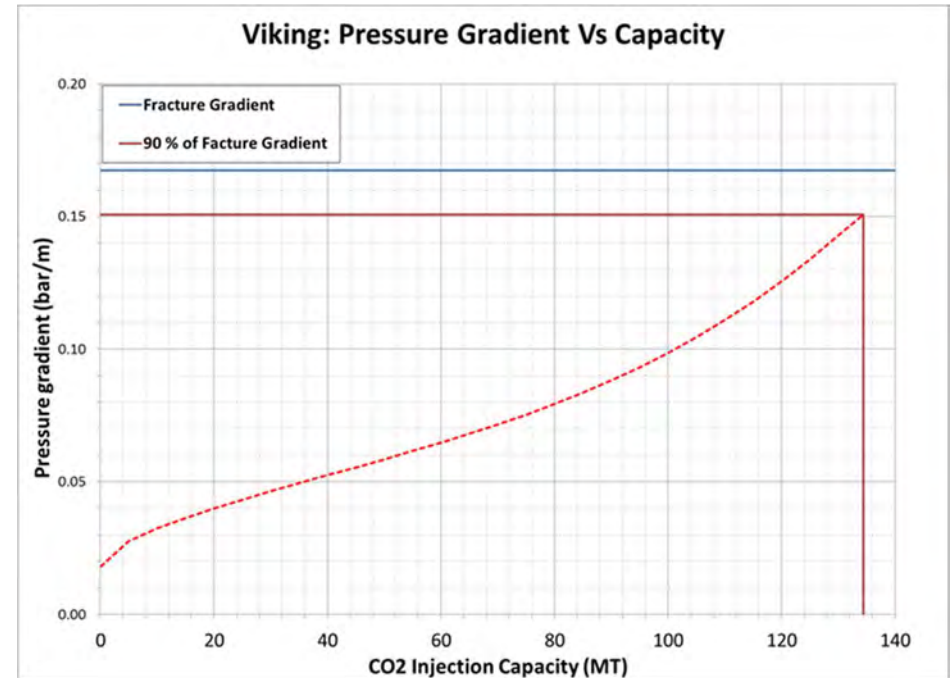


Figure 11-107 Fracture pressure gradient vs injection capacity

11.10.4 Connected Pore Volume

The uncertainty in the connected pore space has been discussed previously with regards to the uncertainty in the connected GIIP in Block A. To evaluate the impact of this uncertainty on the site performance a pore volume multiplier was applied in the model to represent a low case (-18% GIIP) which matches the results of the material balance analysis and a high case (+18% GIIP) which captures the structural uncertainty related to the depth conversion and improved reservoir connectivity. The capacity for the low and high cases is 109MT and 159MT respectively. The injection profiles for the connected volume sensitivities are shown in Figure 11-108.

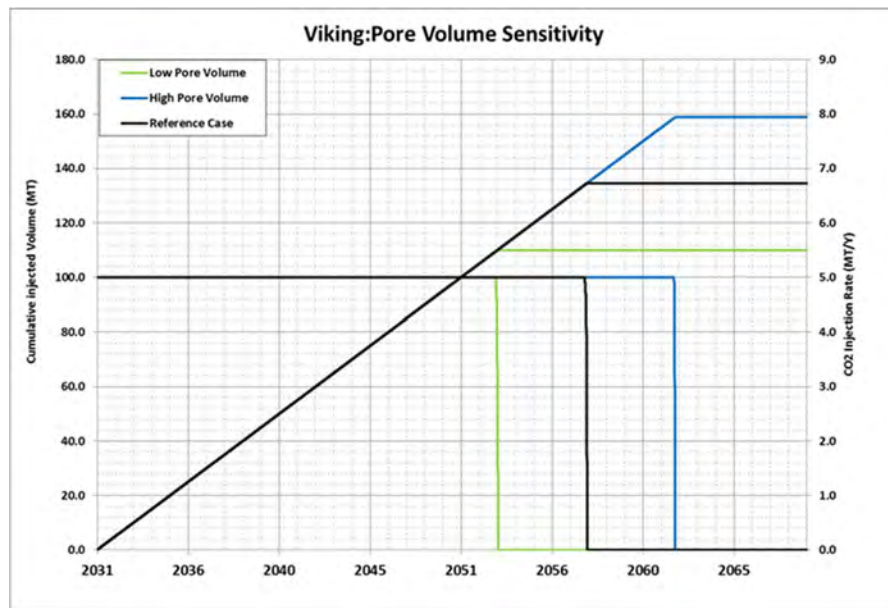


Figure 11-108 Injection forecasts for pore volume sensitivities

11.10.5 Permeability

There is good well control in Block A resulting in reasonable confidence in the permeability prediction. However, there are areas in the Viking field that are reported to have productivity issues. The average permeability in the Viking A is 78mD, with a maximum permeability of approximately 1D. Sensitivities were run to evaluate the impact of permeability on the injection performance. Low and high cases were run with an average permeability of 26mD and 230mD respectively. There was a small impact on capacity, a reduction of 4% in the low case and an increase of 2% in the high case. It should also be noted that the wells could not sustain a rate of 2.5MT/y for the final year of the injection life in the low case. The injection profiles for the permeability sensitivities are shown in Figure 11-109.

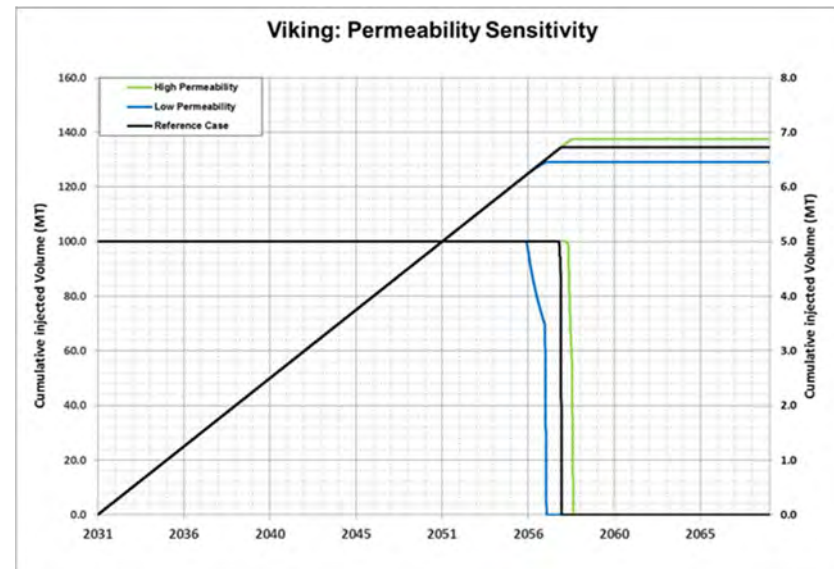


Figure 11-109 Injection forecasts for the horizontal permeability sensitivities

11.10.6 Vertical Connectivity

The vertical connectivity is impacted by two modelling parameters, the ratio of vertical permeability to horizontal permeability (k_v/k_h) within the reservoir layers and also the transmissibility between the layers. In Viking A zone B and zone D are modelled as non net layers as they represent the Sabkha silts and there is no transmissibility across these layers. Sensitivities were run to test the impact of a lower k_v/k_h assumption (0.2mD) and also the introduction of some transmissibility through zones B and D. In the low k_v/k_h case the capacity was reduced by 5%. In the case where transmissibility was included in zones B and D the capacity was increased by 2%.

11.10.7 Relative Permeability

Relative permeability does not impact site performance as the water in Viking A is not mobile and the relative movement between CO₂ and methane is dominated by density and viscosity differences. However, a sensitivity to relative permeability inputs was carried out to confirm that this is the case. The reference case and alternative gas curve are shown in Figure 11-110 below. The impact on the injection profile is negligible.

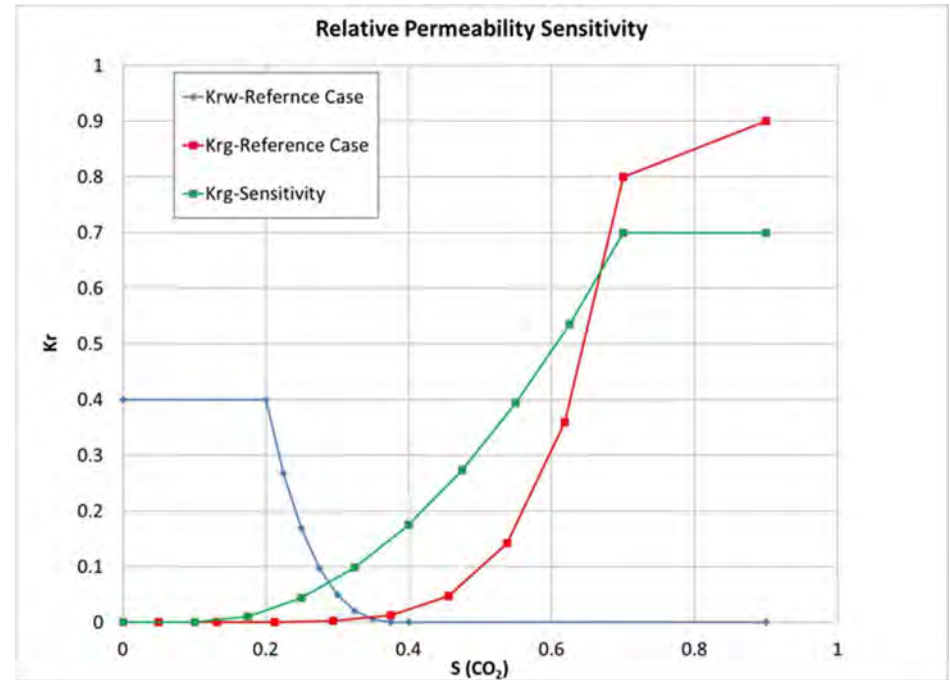


Figure 11-110 Viking A relative permeability functions

11.10.8 Rate Sensitivity

As part of the injection site development evaluation the optimum injection rate for the site is determined. Three rate cases were evaluated for Viking A, 2Mt/y, 5Mt/y and 10Mt/y. As with most sites, a lower injection rate does improve the site capacity but in this case the capacity was increased by only 1.3% and it required over 68 years to fill the site. The high injection rate of 10Mt/y resulted in a reduced capacity of 3% and a short injection life of 13 years. The rate of 5Mt/y is considered, at this stage, to be the optimal rate for Viking A. The injection profiles for the rate sensitivity cases are shown in Figure 11-111 below.

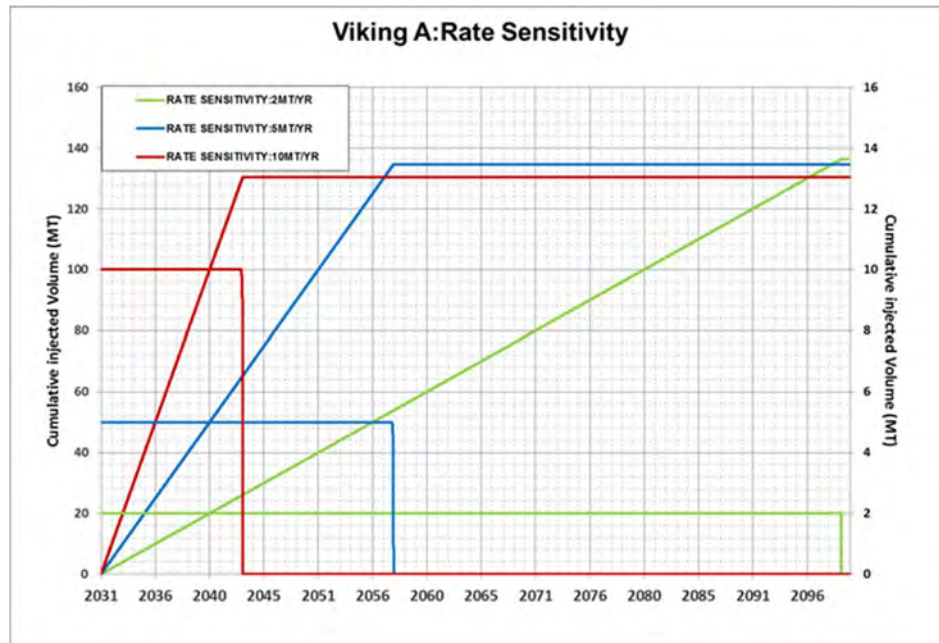


Figure 11-111 Injection forecasts for the horizontal permeability sensitivities

11.11 Appendix 11 – 3D Geomechanical Modelling

11.11.1 Introduction

A 3D geomechanical model was constructed to investigate the possibility of seal breach and/or fault reactivation in a sub-area of the crest of the Viking A and F structures and the effects on the fracture gradient of depletion during gas production followed by injection. The process involves creating a small-strain finite element model (i.e. the grid is not deformed) that allows elastic stress/strain relations and plastic failure effects to be investigated as a response to the actual production and proposed injection scheme(s). These reported parameters include the following:

1. Displacement vectors to assess degree of overburden uplift
2. Failure criteria thresholds (shear or tensile) in the Bunter Sandstone or overburden
3. Matrix strains
4. Fault reactivation strains
5. Total and effective stress evolution
6. Stress path analysis (elastic response to pore pressure changes)

The Viking A Petrel primary static model was used as a basis for building a simplified 3D geomechanical model. This model has the same top and base as the primary static model within the Lemman Sandstone. Two main runs were made (both non-linear) Mohr-Coulomb and Modified Drucker-Prager.

11.11.2 3D Geomechanical Modelling Process

The various steps required to construct, initialise, run and analyse a 3D geomechanical model are listed below.

1. Area is selected and layering scheme identified. Layering scheme covers all units from Top Lemman Sandstone upwards to Seabed. Area Viking A and F as per the primary static model (see Figure 11-112).
2. Explicit surfaces used to generate a grid and zones over the area of interest. Lemman Sandstone given 10 layers, other zones given 1-10 cells to allow relatively gradual changes in cell thickness (Figure 11-113).
3. Generate a geomechanical grid. This is a semi-automated process that adds geometrically expanding cells to the model sides (sideburden) and base (underburden). The sideburdens provide a buffer between the model and the boundary conditions. Note the edges of the lateral boundaries are defined by relatively stiff homogeneous plates approximately 50m thick. The underburden thickens the model and prevents buckling.
4. Geomechanical properties were upscaled and distributed from logs in 49/12-2, 49/11a-6, 49/12A-K4Z and 49/12A-K5. Young's Modulus, Poisson's Ratio and Uniaxial Compressive Strength (UCS) values generated from logs in Drillworks were used here and distributed using kriging to create smoothly varying properties within the layers from Carboniferous to Seabed (Figure 11-114).
5. Geomechanical Materials (e.g. sandstone, shale, salt, faultrock) can be selected from a library and made available to the project. These materials can be assigned to cells based on regions (reservoir, sideburden etc.) or specific cell indices. The library materials are used in undefined areas in the log derived properties. The default is to create elastic properties (bulk density, Young's modulus, Poisson's ratio, Biots factor, thermal expansion coefficient and porosity). For this project, Mohr-Coulomb failure function properties for plastic failure

analysis were also created (UCS, friction angle, dilation angle and tensile failure threshold). These parameters were defined over the Lemna Sandstone within the reservoir area plus two sideburden cells only. These elastic and plastic materials can be overridden by the properties upscaled and distributed in Petrel (see point 4).

6. Salt (halite) properties were treated differently to the other units. One variant was created –WkHal created by assigning the material library salt properties that have a low Young's modulus and high Poisson's ratio and thermal expansion coefficient (see Figure 11-114). This was done to allow the spectrum of possible salt behaviours to be modelled. In reality salt acts as a viscous fluid over geological time and equilibrates to the lithostatic stress state. This can also occur over week to year timeframes depending on the depth and geothermal gradient. However, the instantaneous response obtained from logs or from slightly longer term laboratory tests at surface conditions indicate halite often has moderately high Young's modulus and low to moderate Poisson's ratio values. Petrel geomechanics does not yet contain a salt creep model so the highly compliant elastic properties variant has been used as a proxy for the stress state obtained via viscous flow. This is generally regarded as adequate for small strains.
7. Fault properties are defined as shear and normal stiffness, cohesion and tensile strength in the material library. These properties are assigned to cells cut by surfaces representing the faults (see Figure 11-115).
8. Pressure / saturation properties are created using pressure vs depth equations and/or upscaled from Eclipse. Single steps are used for initialisation models to allow the stresses to be matched in certain layers (e.g. clastics and carbonates in one step and salt layers in

another to get lithostatic stresses). Multiple pressure steps are used to model the geomechanical responses to the injection pressure steps. Here, variable sized steps of between 3 and 41 years have been used.

9. Boundary condition properties are created to setup the boundary condition SHmin stress magnitude, the SHmax/SHmin ratio and the SHmin orientation. These are modified to get a match to expected stress trends in the initialisation models. For the multi pressure runs, the starting stresses (6 component tensor) were defined explicitly by splicing the initialisation total stress properties from the sandstone and lithostatic salt stress cases.
10. The cases were setup by selecting the relevant properties folders from items 5 to 8 and defining the run as either linear (elastic) or non-linear (plastic). Non-linear runs utilise the Mohr-Coulomb materials defined in steps 4 and 5.

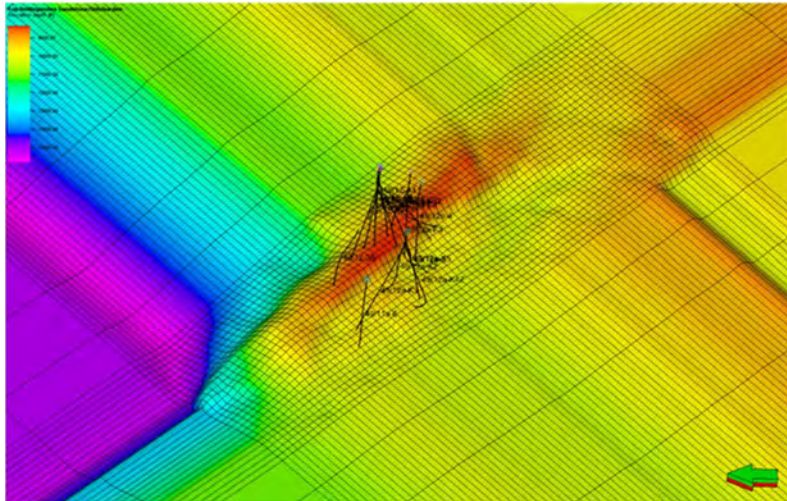


Figure 11-112 View to SE of Viking A and Viking F top Lemman sandstone surface in the geomechanical model

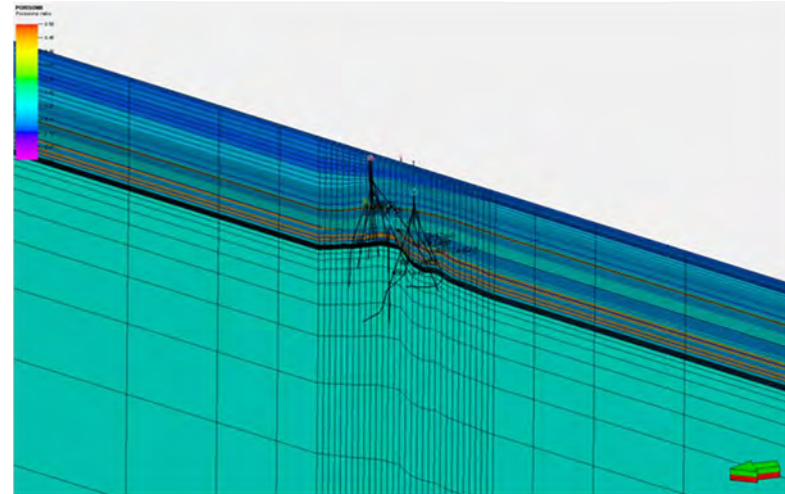


Figure 11-114 Poisson's ratio in the geomechanical model, high values are for the salt layers

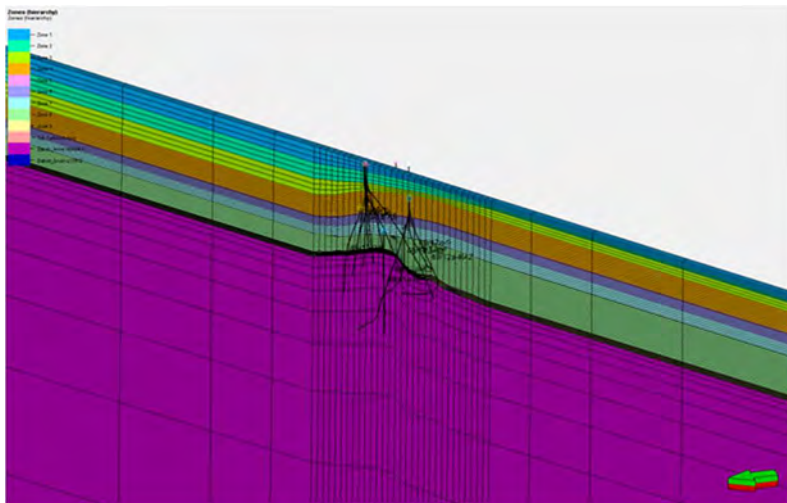


Figure 11-113 Geomechanical model zonation in SW-NE section through crest



Figure 11-115 Fault cells (plastic shear strain property) at K layer 58 in the Lemman sandstone

11.11.3 Geomechanics Results

One case was run with non-linear Mohr-Coulomb material properties and one with Drucker-Prager material properties within the Lemna Sandstone. Both were run in non-linear mode with faults. This was primarily to assess the impact of depletion followed by injection on the fracture gradient and the potential for fault reactivation. As described in the 1D analysis report, poroelastic theory predicts that the fracture gradient decreases during depletion and increases during repressurisation (injection). However, the exact trends these stress paths take may vary between each phase. There is also the potential for significant hysteresis such that the depleted fracture gradient only increases a little or not at all during subsequent injection (Santarelli, Havmoller, & Naumann, 2008). There are a number of factors that can lead to this effect including reservoir geometry, reservoir geomechanics property values compared to the surrounding rock, geometry and properties of faults and the temperature of the injected fluid. A full investigation of all these effects is beyond the scope of this project.

11.11.3.1 Mohr-Coulomb

The purpose of this study was to run some scenarios to assess the potential for depletion / injection pressure related failure in the Rotliegend Sandstone, the caprock lithologies or the reservoir faults. Therefore, the model was run with Mohr-Coulomb and Modified Drucker-Prager failure mode parameters, the inclusion of faults and run in non-linear mode. In addition, some geomechanics plug-ins were tested that can provide detailed information on potential areas of fault slip and modelled microseismic event locations and magnitudes at a given timestep.

The pore pressure properties varied both with time and space as the post-depletion injection scheme started in Viking F and moved to Viking A (see Figure

11-116). The virgin pressure (at the datum depth of 8800 ft TVDs around 49/12-2) was around 4360 psi and the depleted pressure went down to around 500 psi. The final injection pressure in 2058 is modelled as around 5250 psi.

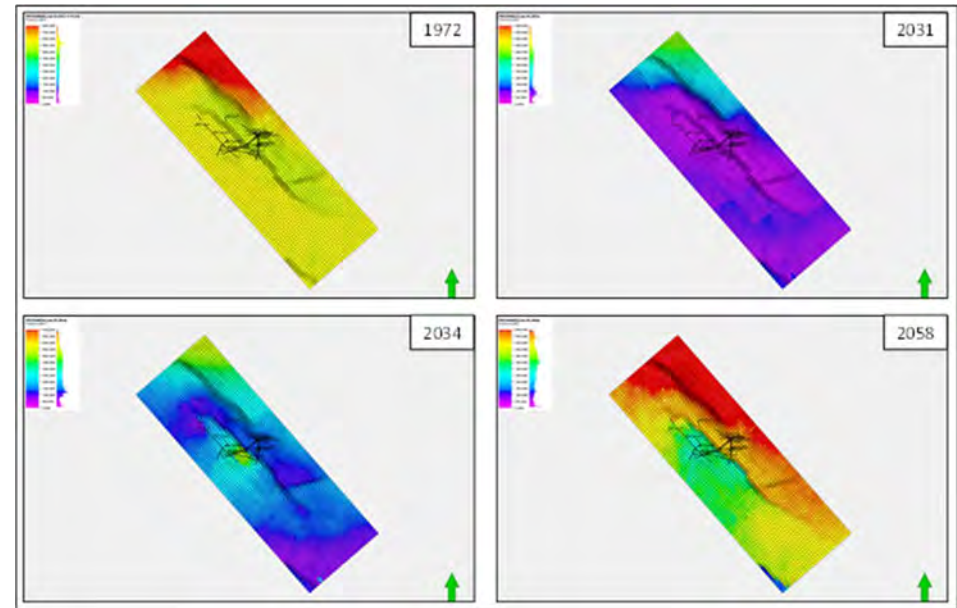


Figure 11-116 Viking pressure evolution from virgin conditions (1972), depleted state (2031), early injection in Viking F (2034) and late injection in Viking A (2058) Map from K layer 58 within the Lemna Sandstone

The main results from the analysis are shown in Figure 11-117. The vertical displacement at end production is around -0.5 ft at seabed and similar throughout the overburden. The displacement is partially reversed in 2034 during Viking F injection. At end Viking A injection in 2058, the overburden is lifted on the NE side (Viking A) to 0.08 ft consistent with the overpressure from virgin conditions. Similarly, the elastic strain in the Lemna Sandstone is positive during depletion and reversed to dilational strain over Viking A at end injection.

Plastic strain in the matrix is minimal with some very minor shear failure in 196 cells associated with the faults at end depletion in 2031.

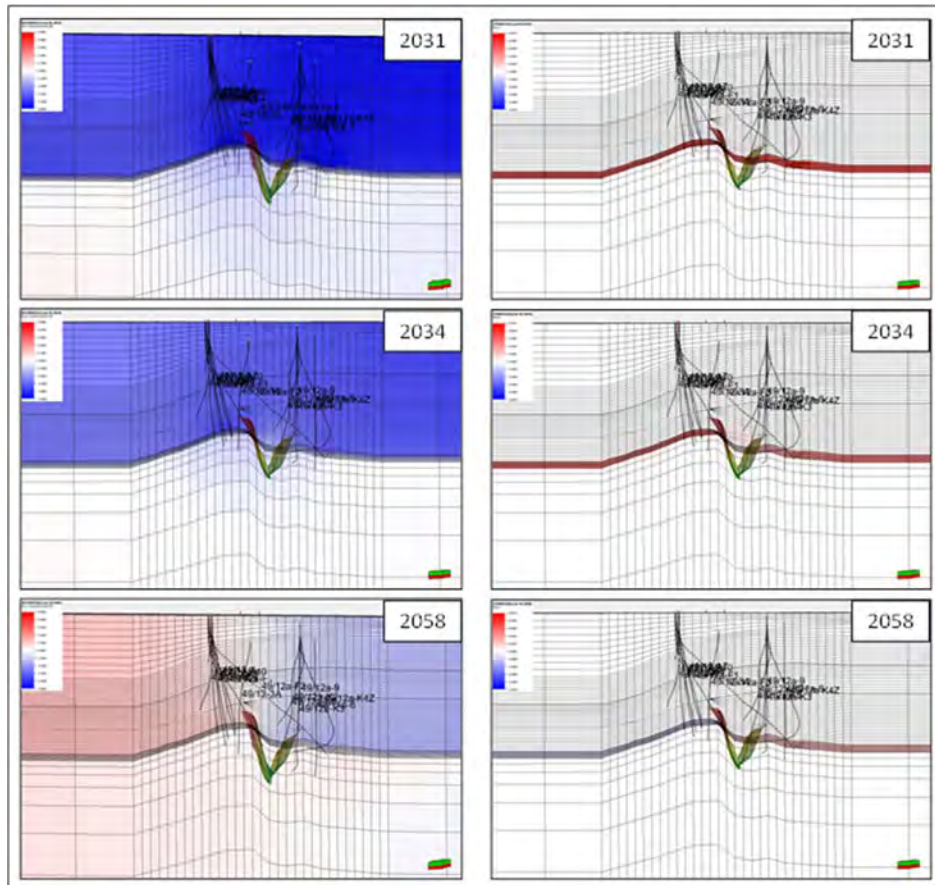


Figure 11-117 Mohr-Coulomb run LH column ROCKDISZ on Viking crest at key timesteps described in text RH column STRAINZZ property

The modelled faults indicate some elastic and plastic strain on the faults as a result of depletion. Figure 11-115 shows a K slice of the plastic shear strain

property. Figure 11-118 shows the fault related plastic shear strain at end depletion filtered at values less than -0.000001 (i.e. more negative equals higher shear strains). All of these higher strains occur within the Lemna and not in the caprocks. These small fault related plastic shear strain values have been converted into microseismic moment magnitude events which are shown in Figure 11-119. The event magnitudes range from -4.65 to -2.74 . Based on the table published by Bohnhoff et.al. (2010) (see Table 11-48) these are in the Femto to Pico categories. These events are associated with slip planes of 0.01-1m length scales and 0.0004-0.04 mm displacements and they are highly unlikely to cause any detectable leak pathways.

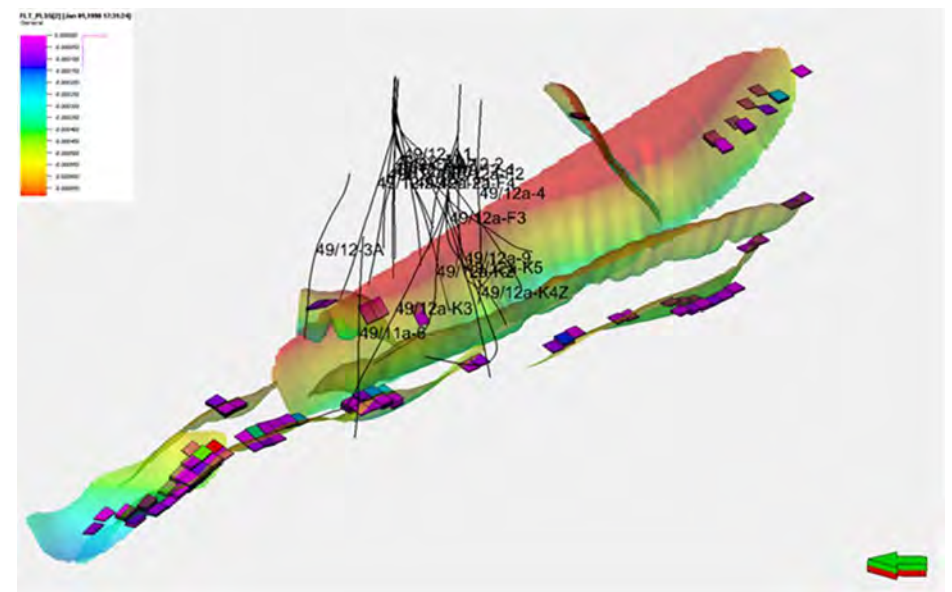


Figure 11-118 Mohr-Columb run, fault related plastic shear strain at end depletion

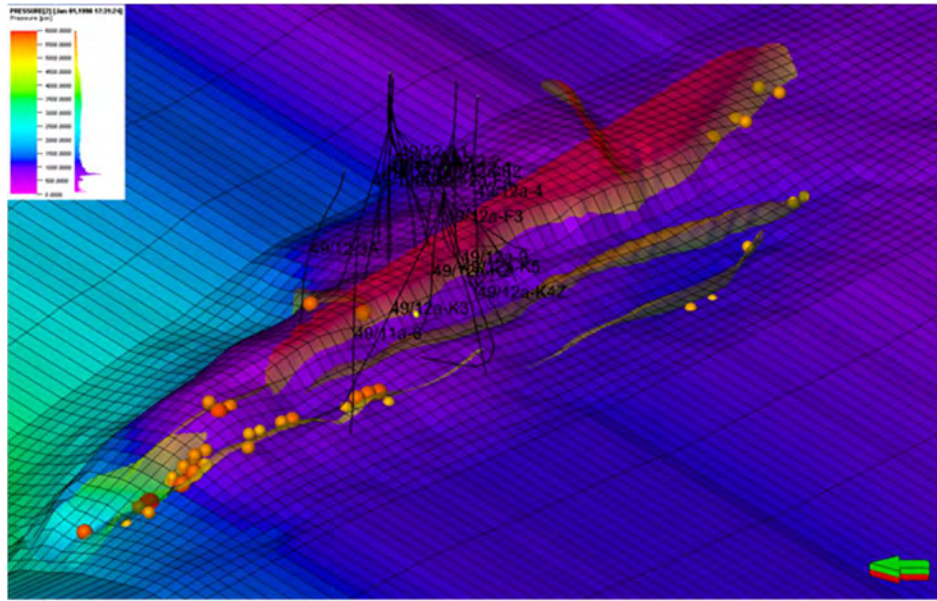


Figure 11-119 Mohr-Coloumb run, microseismic events associated with fault related plastic strains. Events scale in size and colour from magnitude -4.56 to -2.74 and yellow to red respectively

Magnitude Range	Class	Length Scale	Displacement Scale
8-10	Great	100-1,000 km	4-10 m
6-8	Large	10-100 km	0.4-4 m
4-6	Moderate	1-10 km	4-40 cm
2-4	Small	0.1-1 km	4-40 mm
0-2	Micro	10-100 m	0.4-4 mm
-2-0	Nano	1-10 m	40-400 μ m
-4 to -2	Pico	0.1-1 m	4-40 μ m
-6 to -4	Femto	1-10 cm	0.4-4 μ m
-8 to -6	Atto	1-10 mm	0.04-0.4 μ m

Table 11-48 Seismic event magnitudes vs length scales

11.11.3.2 Modified Drucker-Prager

Drucker-Prager can be simplistically defined as a smoothed version of the Mohr-Coulomb failure function. The Drucker-Prager yield surface shape varies depending on which Mohr-Coulomb principal stress vertices it is fitted to. The modified version accounts for changes in the material responses in the tensile region (tensile cut-off) and at high confining stresses (end cap). Only the material properties in the non-linear material are updated, all other parameters (stress field, fault properties, pore pressures) are the same as the Mohr-Coulomb run.

The results are broadly similar to the Mohr-Coulomb runs although there are some important differences.

Figure 11-120 shows the vertical displacement and strain properties at key steps in the pressure history. The amount of vertical displacement (max 0.65ft) and internal Lemman matrix elastic strain at end depletion is greater compared to the Mohr-Coulomb run. The Lemman matrix plastic vertical strain is also more developed at end depletion in 1990 compared to the Mohr-Coulomb run with all Lemman cells displaying some minor plastic strain.

There is also increased predictions of microseismic activity with all faults displaying pico scale events by end depletion in 1990 (see Figure 11-121) and a few fault locations also showing small events during injection between 2034 and 2058. None of these events are in the caprock and they appear to be restricted to the plastic strain occurring within the Lemman.

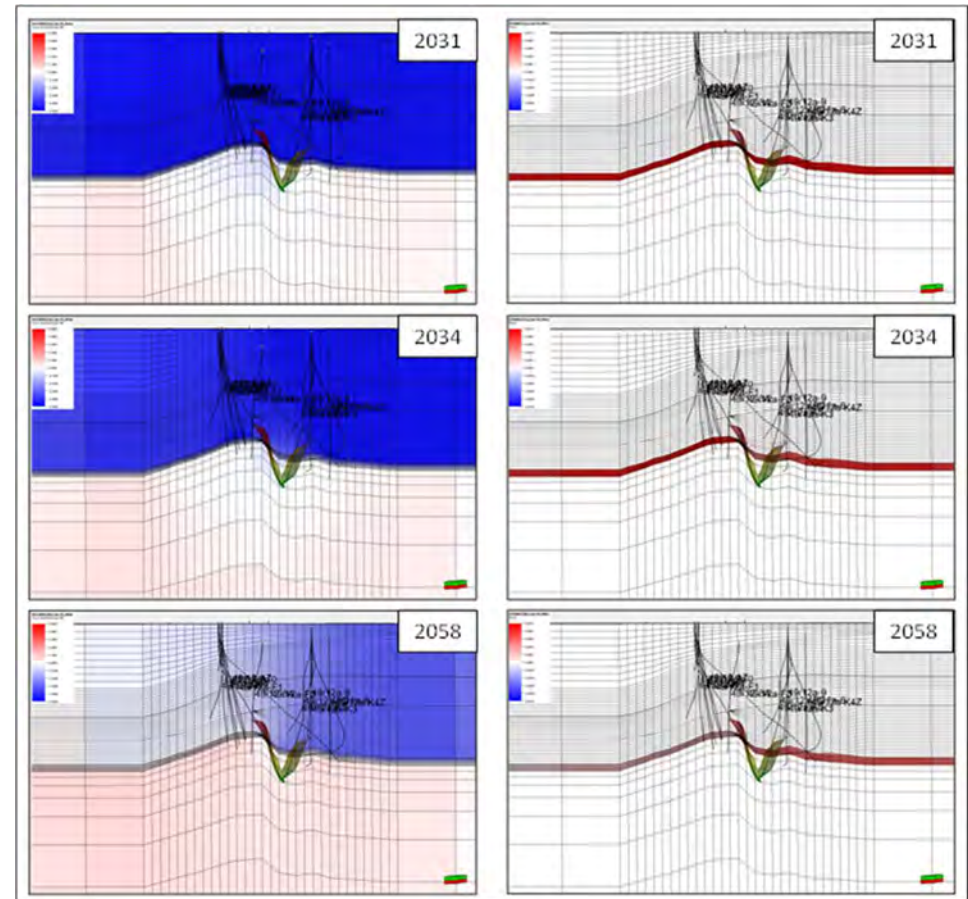


Figure 11-120 Modified Drucker-Prager run, LH column ROCKDISZ on Viking crest at key timesteps RH column, STRAINZZ property

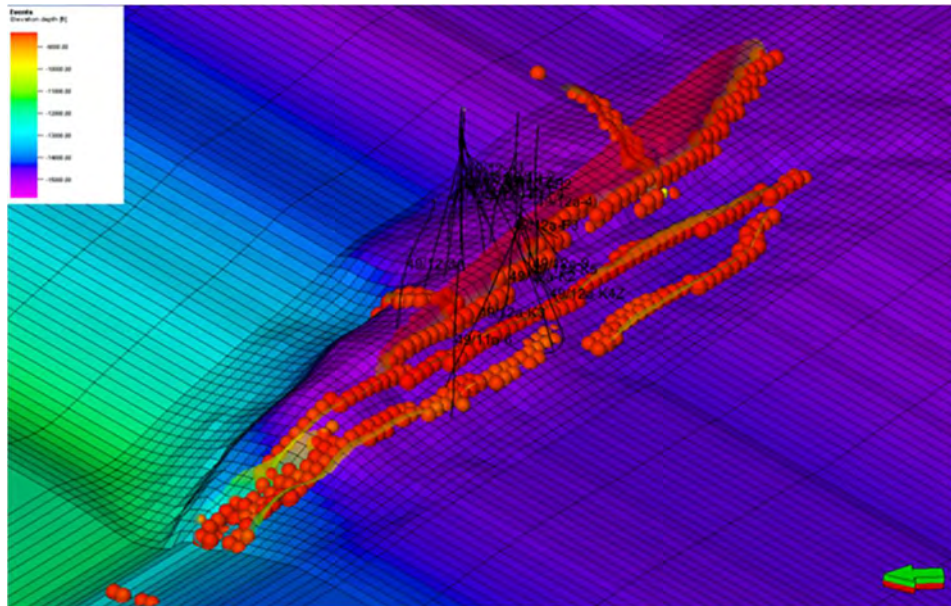


Figure 11-121 Modified Drucker-Prager run, microseismic events associated with plastic shear strain at end production in 1990. Events scale in size and colour from magnitude -3.88 to -2.16 and yellow to red respectively

11.11.4 Discussion and Conclusion

The results above indicate that varying levels of elastic and plastic strain can be modelled on Viking but virtually all of it is restricted to within the Lemna Reservoir interval. Some minor ‘pico’ scale seismic events have been modelled that can be widespread on faults or more localised. Most of these would have occurred during production but a few may occur during injection. Note that the absolute amounts of displacement associated with these events is unlikely to cause significant failure and/or fault reactivation.

The stress path is the change in total minimum principal stress (SHmin or fracture gradient) with depletion. This is due to the poroelastic effect for

reservoirs that have an approximate width vs height ratio of $\geq 10:1$ (Zoback 2007). The Modified Drucker-Prager depleted fracture gradient is at 0.55 psi/ft (using the 49/12-2 location) as opposed to 0.43 psi/ft for Mohr Coulomb (see Figure 11-122). The end injection fracture gradient for Modified Drucker-Prager is also higher at around 0.94 psi/ft compared with 0.83 psi/ft for Mohr-Coulomb. This is getting close to the overburden gradient which would need managing.

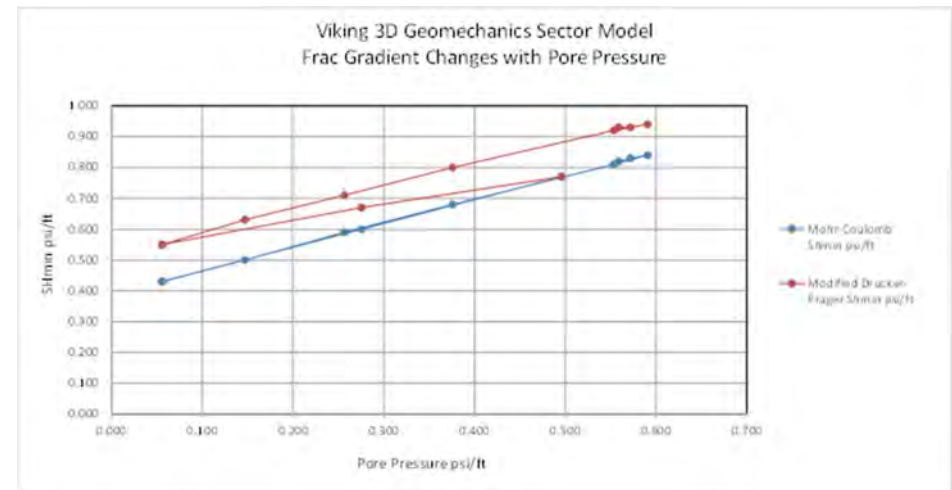


Figure 11-122 Stress paths for Viking at the 49/12-2 well location

The 3D geomechanical modelling indicates that with variable material properties and stress paths and the inclusion of faults on the structure, the plastic strains and associated slip events are of a very small size. Note that all the properties in this model are log derived and uncalibrated to core or other data so other values are possible for key parameters such as rock strength and the elastic moduli. However, the Lemna Sandstone is usually a well cemented hard rock so extensive strain of the matrix is unlikely. It is also possible that hysteresis of the fracture gradient could occur after depletion (Santarelli, Havmoller, &

Naumann, 2008) which is a remaining risk. Weaker faults could occur which may lead to larger plastic strains over larger areas. However, the change in fault properties would have to be significant to produce appreciable plastic strains. This is regarded as unlikely.

RISK REGISTER

Viking - depleted gas field site

Document: D34 1011875 WPSE Report - Appendix G1 Risk Register

Risk ID	Risk description/ event	Consequence of risk/ impact on project	Likelihood	Impact	Likelihood x impact	Comments (if applicable)	Controls (mitigation actions)	Potential remediation options	High level cost
1	Storage and injectivity of Leman Sandstone different (poorer) than forecast	Significant uncertainty over final cost of project, potential to reduce timescale of injection operations, reputational impact and fines	2	4	8		Appraisal well and well test to understand injectivity	Work-over/ stimulate wells. Drill additional wells	
2	Drilling activities near the storage site (either for O&G or CO2 storage)	Potential to compromise caprocks of storage site and provide an additional migration pathway to the near-surface/surface	1	4	4		Work closely with DECC to understand future drilling activities in the area and then work closely with Operators to ensure their drilling operations do not compromise storage integrity		
3	Future O&G extraction operations hindered by presence of CO2 in storage site	Presence of injected CO2 may hinder extractive operations near the storage site by obscuring seismic traces (eg in prospective formations below the storage site) or making drilling process more difficult. Drilling through formation with supercritical CO2 might cause blow out or loss of containment. May be requirement to pay compensation	1	4	4		Work closely with DECC to understand future drilling activities in the area and then work closely with Operators to ensure their drilling operations do not compromise storage integrity		
4	Accidental or intentional damage to injection process or storage site that disrupts storage site	Depending on scale of damage, could result in release of CO2 to seabed via well bore, injection being stopped, reputational and financial implications	1	4	4	Very low probability event but could have significant impact on storage system by disrupting expected evolution of the system	Monitoring of site to ensure operations are as expected	Shut in wells, further work to understand the scale of the damage, potentially require new injection site.	
5	Seismic event compromises store integrity		1	1	1	The North Sea is a fairly quiescent area and far from plate boundaries so likelihood of large-scale seismicity is very low	Monitoring of site to ensure operations are as expected	Shut in wells, further work to understand the scale of the damage, potentially require new injection site.	
6	Loss of containment of CO2 from primary store to overburden through caprock	Unexpected movement of CO2 outwith the storage site, but within the storage complex in the overburden, considerable reputational impact, large fine likely	1	3	3		Secondary store site in Bunter Sandstone as additional barrier to surface	Re-entry into an abandoned well is complex, difficult and has a very low chance of success.	Relief well: \$55 million (60 days & tangibles).
7	Loss of containment from primary store to overburden through caprock & P&A wells	Unexpected movement of CO2 outwith the storage site, but within the storage complex in the overburden, considerable reputational impact, large fine likely	1	3	3	Within Site A: 31 wells - 10 P&A - 4 legacy wells sampled (4/10); 2 wells abandoned per spec - 2 weren't (1960, 1970); don't meet: 49/12-2 = limited well info - did not meet spec; TOC unknown, cement plug too small & not lapped with cement; 20" casing cut; 49/12-3 - did not meet spec, limited well info, TOC unknown, 20" casing cut, cement plug too small & not lapped with cement; h/c gas buffer at top reservoir so if any leakage via legacy wells would be h/c rather than CO2. Only a leak to the biosphere will be detected.	Secondary store site in Bunter Sandstone as additional barrier to surface	Re-entry into an abandoned well is complex, difficult and has a very low chance of success.	Relief well: \$55 million (60 days & tangibles).
8	Loss of containment from primary store to overburden through caprock & inj wells	Unexpected movement of CO2 outwith the defined storage complex in the overburden, considerable reputational impact, large fine likely	1	3	3	Injection wells designed for CO2 use so low likelihood of loss of containment.	Injection wells designed to have low risk of loss of containment; downhole P/T gauges and DTS along the wellbore as part of monitoring plan to detect first signs of loss of integrity.		
9	Loss of containment from primary store to overburden through caprock & suspended wells	Unexpected movement of CO2 outwith the defined storage complex in the overburden, considerable reputational impact, large fine likely	1	3	3	Suspended wells will be abandoned to current spec.	Suspended wells will be abandoned to current spec. Secondary store site in Bunter Sandstone as additional barrier to surface		
10	Loss of containment from primary store to overburden via P&A wells	Unexpected movement of CO2 outwith the defined storage complex in the overburden, considerable reputational impact, large fine likely	2	3	6	Within Site A: 31 wells - 10 P&A - 4 legacy wells sampled (4/10); 2 wells abandoned per spec - 2 weren't (1960, 1970); don't meet: 49/12-2 = limited well info - did not meet spec; TOC unknown, cement plug too small & not lapped with cement; 20" casing cut; 49/12-3 - did not meet spec, limited well info, TOC unknown, 20" casing cut, cement plug too small & not lapped with cement; h/c gas buffer at top reservoir so if any leakage via legacy wells would be h/c rather than CO2. Only a leak to the biosphere will be detected.	Secondary store site in Bunter Sandstone as additional barrier to surface	Re-entry into an abandoned well is complex, difficult and has a very low chance of success.	Relief well: \$55 million (60 days & tangibles).
11	Loss of containment from primary store to overburden via injection wells	Unexpected movement of CO2 outwith the defined storage complex in the overburden, considerable reputational impact, large fine likely	2	3	6	Injection wells designed for CO2 use so low likelihood of loss of containment. Secondary store site in Bunter Sandstone as additional barrier to surface. Only a leak to the biosphere will be detected.	Injection wells designed to have low risk of loss of containment; downhole P/T gauges and DTS along the wellbore as part of monitoring plan to detect first signs of loss of integrity.		
12	Loss of containment from primary store to overburden via suspended wells	Unexpected movement of CO2 outwith the defined storage complex in the overburden, considerable reputational impact, large fine likely	2	3	6	Suspended wells will be abandoned to current spec. Secondary store site in Bunter Sandstone as additional barrier to surface. Only a leak to the biosphere will be detected.			
13	Loss of containment from primary store to upper well/ seabed via P&A wells	CO2 to seabed. Environmental, national reputation and cost implications	2	4	8		Seabed monitoring around abandoned wellheads to detect any signs of loss of containment	Re-entry into an abandoned well is complex, difficult and has a very low chance of success.	Relief well: \$55 million (60 days & tangibles).
14	Loss of containment from primary store to upper well/ seabed via injection wells	CO2 to seabed. Environmental, national reputation and cost implications	2	4	8		Injection wells designed to have low risk of loss of containment; downhole P/T gauges and DTS along the wellbore as part of monitoring plan to detect first signs of loss of integrity.		
15	Loss of containment of CO2 from primary store to seabed via combination of both caprock and wells		1	4	4				
16	Loss of containment from primary store to underburden via existing wells		1	2	2	Existing wells drilled through the storage site aiming for deeper targets do not go below the complex & are all in shale		Stop injection; risk assessment; corrective measures plan	
17	Primary store to underburden via store floor (out with storage complex)		1	3	3	CO2 movement within Carboniferous			
18	Fault reactivation through primary caprock		1	2	2	Zechstein Salt caprock so v low chance of permeable pathway; faults do not go that far into the Zechstein; salt "self healing"	Maximum reservoir pressure during injection set to 90% of reservoir fracture pressure	Stop injection, corrective measures plan, inject at reduced pressure, limit injection volumes	
19	CO2 flow through unreactivated, permeable fault in primary caprock		1	2	2	Zechstein Salt so v low chance of permeable pathway & faults don't go that far into the Zechstein; gas column held for millions of years	n/a		
20	Thermal fracturing of primary caprock from injection of cold CO2 into a warm reservoir		1	2	2	Zechstein Salt so v low chance of permeable pathway & faults don't go that far into the Zechstein; thermal conductivity of the salt		Stop injection, corrective measures plan, limit injection volumes/rate	
21	Mechanical fracturing of primary caprock from injection pressure of CO2 exceeding the fracture pressure of the caprock		1	2	2	Zechstein Salt caprock has v high fracture pressures and therefore is v v hard to fracture - v very low likelihood. Also is "self healing" so v low chance of permeable pathway			
22	CO2 and brine react with minerals in caprock and create permeability pathway		1	2	2	On flooding the Viking field with CO2, the clay-rich Kupferschiefer is unlikely to be affected in a way that increases permeability. This is because The kaolinite and, to a lesser extent illite, react with sodium in the formation water and the incoming CO2 to create dawsonite and quartz Chlorite reacts to form dolomite (and dawsonite and quartz) These reactions lead to a solid volume increase thus diminishing porosity and permeability The Zechstein may undergo minor dissolution due to CO2 injection where dolomite is present but anhydrite is fully stable. The combination of Kupferschiefer loss of porosity and unreactiveness of anhydrite-dominated Zechstein probably means there is negligible risk of top seal dissolution due to elevated CO2 concentration in the reservoir.	None required		
23	Buoyant CO2 exerts caprock to pressures beyond the capillary entry pressure enabling it to flow through primary caprock		1	2	2	Zechstein Salt has v v permeability so v low chance of permeable pathway		Stop injection, corrective measures plan, inject at reduced pressure, limit injection volumes to reduce column height of CO2,	
24	Geology of caprock lithology is variable and lacks continuity such that its presence cannot be assured across the whole site		1	2	2	No evidence. Gas shows in dolomites which have salt above & below		Stop injection, corrective measures plan	
25	Relative permeability curves in the model move the CO2 too slowly within the primary store relative to reality	In the unlikely event that CO2 did migrate faster than expected and laterally exit the primary store, this would be unexpected migration but at reservoir level. Considerable impact on reputation and large fine likely.	1	3	3	Not an issue at this site h/c depleted field	Site specific relative permeability study from core in appraisal well to constrain curves	Stop injection, corrective measures plan, re-model expected CO2 plume movement with new data and re-assess injection volumes to ensure containment integrity.	
26	Permeability anisotropy causes the CO2 to move more quickly than expected		2	3	6	Site A has higher permeability than other parts of Viking.			
27	Depth conversion uncertainty	In the unlikely event that the depth conversion uncertainty caused CO2 to laterally exit the primary store, this would be unexpected migration but at reservoir level. Considerable impact on reputation and large fine likely.	1	3	3	Gas field - position of the spill pt could move laterally, but injecting a long way from spill point so not an issue			
28	Depletion or pressure gradient from nearby fields	In the unlikely event that depletion or pressure gradient from nearby fields caused CO2 to laterally exit the primary store, this would be unexpected migration but at reservoir level. Considerable impact on reputation and large fine likely.	1	3	3	Not connected to other blocks within Viking based on knowledge of fields	Model impacts; good engagement with other operators in the area to understand impact	Stop injection until situation understood; further detailed work	
29	Impact of injection and CO2 storage on nearby fields is greater than expected	Pressure build up quicker than expected so reduces storage capacity, potential loss of credibility of CCS projects	1	2	2	Not connected to other blocks within Viking based on knowledge of fields	Draft process for dispute resolution with nearby subsurface users	Stop injection until situation understood; further detailed work	
30	Well placement error	In the unlikely event that the well was drilled at the edge of the storage complex and caused CO2 to laterally exit the primary store, this would be unexpected migration but at reservoir level. Considerable impact on reputation and large fine likely.	1	1	1	Not an issue at this site because it is an existing gas field with good well control			
31	Inject in wrong zone of reservoir or damage reservoir	In the unlikely event that CO2 was injected into the wrong zone or the reservoir was damaged and caused CO2 to laterally exit the primary store, this would be unexpected migration but at reservoir level. Considerable impact on reputation and large fine likely.	1	1	1	Only one zone to inject into	Downhole P/T gauges and DTS along the wellbore as part of monitoring plan to detect first signs of loss of integrity.		
32	CO2 becomes dissolved in water and laterally exits the primary store	Even if it exits the primary store laterally, the impact would be limited as will be geographically stable.	2	1	2	Potential to do so but uncertainty around this. Unconformity present			
33	CO2 bubble expands beyond spill point and laterally exits the primary store		1	1	1	No spill point - negligible			
34	CO2 flow across bounding faults and laterally exits the primary store	CO2 in water is acidic - Zechstein at base has carbonate - could be carbonates in fact; CO2 in water deeper; faults have kept h/c sealed for millions of years; even if in to Zechstein - cant move anywhere	2	1	2				




35	CO2 migration out with secondary store (Bunter)	CO2 migration out with the storage complex	1	3	3	Due to significant Haisburgh Group and faults between secondary store (Bunter Sandstone) and surface, low likelihood of occurrence			
36	Blowout during drilling	Possible escape of CO2 to the biosphere.					Mapping of shallow gas, understanding subsurface pressure regime for appropriate mud weight, drilling procedures	Standard procedures: shut-in the well and initiate well control procedures.	\$3-5 million (5 days & tangibles)
37	Blowout during well intervention	Possible escape of CO2 to the biosphere.					Mapping of shallow gas, understanding subsurface pressure regime for appropriate mud weight, drilling procedures	Standard procedures: shut-in the well and initiate well control procedures.	\$2-3 million (3 days & tangibles)
38	Tubing leak	Pressured CO2 in the A-annulus. Sustained CO2 annulus pressure will be an unsustainable well integrity state and require remediation.					Downhole P/T gauges and DTS along the wellbore as part of monitoring plan to detect first signs of loss of integrity.	Tubing replacement by workover.	\$15-20 million (16 days & tangibles)
39	Packer leak	Pressured CO2 in the A-annulus. Sustained CO2 annulus pressure will be an unsustainable well integrity state and require remediation.						Packer replacement by workover.	\$15-20 million (16 days & tangibles)
40	Cement sheath failure (Production Liner)	Sustained CO2 annulus pressure will be an unsustainable well integrity state and require remediation.				Requires: - a failure of the liner packer or - failure of the liner above the production packer before there is pressured CO2 in the A-annulus.		Repair by cement squeeze (possible chance of failure). Requires the completion to be retrieved and rerun (if installed).	\$3-5 million (5 days & tangibles). \$18-25 million (if a workover required)
41	Production Liner failure	Sustained CO2 annulus pressure will be an unsustainable well integrity state and require remediation.				Requires: - a failure of the liner above the production packer and - a failure of the cement sheath before there is pressured CO2 in the A-annulus.		Repair by patching (possible chance of failure) or setting a smaller diameter contingency liner. Requires the completion to be retrieved and rerun (if installed). Will change the casing internal diameter and may have an impact on the completion design and placement. Repair by side-track.	\$3-5 million (3 days & tangibles). \$18-25 million (if a workover required). Side-track estimated to be equal to the cost of a new well - \$55 million (60 days & tangibles).
42	Cement sheath failure (Production Casing)	Sustained CO2 annulus pressure will be an unsustainable well integrity state and require remediation.				Requires: - a failure of the Production Liner cement sheath or - a pressurised A-annulus and - failure of the production casing before there is pressured CO2 in the B-annulus.		Repair by cement squeeze (possible chance of failure). Requires the completion to be retrieved and rerun (if installed).	\$3-5 million (5 days & tangibles). \$18-25 million (if a workover required)
43	Production Casing Failure	Sustained CO2 annulus pressure will be an unsustainable well integrity state and require remediation.				Requires: - a pressurised A-annulus and - a failure of the Production Casing cement sheath before there is pressure CO2 in the B-annulus.		Repair by patching (possible chance of failure). Requires the completion to be retrieved (if installed). Will change the casing internal diameter and may have an impact on the completion design and placement.	\$3-5 million (3 days & tangibles). \$18-25 million (if a workover required). Side-track estimated to be equal to the cost of a new well - \$55 million (60 days & tangibles).
44	Safety critical valve failure – tubing safety valve	Inability to remotely shut-in the well below surface. Unsustainable well integrity state.						Repair by: - installation of insert back-up by intervention or - replacement by workover	\$1 million to run insert (1 day & tangibles). \$18-25 million (if a workover required)
45	Safety critical valve failure – Xmas Tree valve	Inability to remotely shut-in the well at the Xmas Tree. Unsustainable well integrity state.						Repair by valve replacement.	Dry Tree: < \$5 million (costs associated with 5 days loss of injection, tangibles and man days). Subsea: \$5-7 million (vessels, ROV, dive support & tangibles).
46	Wellhead seal leak	Seal failure will be an unsustainable well integrity state and require remediation.				Requires: - a pressurised annulus and - multiple seal failures before there is a release to the biosphere.		Possible repair by treatment with a replacement sealant or repair components that are part of the wellhead design. Highly dependent on the design and ease of access (dry tree or subsea). May mean the well has insufficient integrity and would be abandoned.	Dry Tree: < \$3 million (costs associated with 7 days loss of injection, tangibles and man days). Abandonment \$15-25 (21 days & tangibles).
47	Xmas Tree seal leak	Seal failure will be an unsustainable well integrity state and require remediation.				Requires multiple seal failures before there is a release to the biosphere.		Possible repair by specific back-up components that are part of the wellhead design. Highly dependent on the design and ease of access. May mean the Xmas Tree need to be removed/recovered to be repaired. This is a time consuming process for a subsea tree.	Dry Tree: < \$5 million (costs associated with 7 days loss of injection, tangibles and man days). Subsea: \$12-15 million (12 days & tangibles).

Impact categories (CO2QUALSTORE)

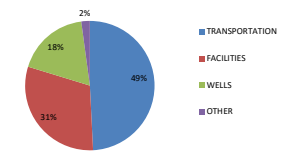
No.	1	2	3	4	5
Name	Very Low	Low	Medium	High	Very High
Impact on storage integrity	None	Unexpected migration of CO2 inside the defined storage complex	Unexpected migration of CO2 outside the defined storage complex	Leakage to seabed or water column over small area (<100m2)	Leakage seabed water column over large area (>100m2)
Impact on local environment	Minor environmental damage	Local environmental damage of short duration	Time for restitution of ecological resource <2 years	Time for restitution of ecological resource 2-5 years	Time for restitution of ecological resource such as marine Biosystems, ground waters >5 years
Impact on reputation	Slight or no impact	Limited impact	Considerable impact	National impact	International impact
Consequence for Permit to operate	None	Small fine	Large fine	Temporary withdrawal of permit	Permanent loss of permit

Likelihood categories (CO2QUALSTORE)

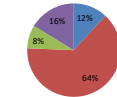
No.	1	2	3	4	5
Name	Very Low	Low	Medium	High	Very High
Description	Improbable, negligible	Remotely probably, hardly likely	Occasional, likely	Probable, very likely	Frequent, to be expected
Event (E)	Very unlikely to occur during the next 5000 years	Very unlikely to occur during injection operations	Likely to occur during injection operations	May occur several times during injection operations	Will occur several times during injection operations
Frequency	About 1 per 5000 years	About 1 per 500 years	About 1 per 50 years	About 1 per 5 years	About 1 per year or more
Feature (F)/ Process (P)	Disregarded	Not expected	50/50 chance	Expected	Sure

PROJECT	Strategic UK Storage Appraisal Project		LEVEL 2 COST ESTIMATE		  	
TITLE	SITE 5: VIKING					
CLIENT	ETI					
REVISION	A1					
DATE	08/03/2016					
Category	Comment	Primary Cost (£ MM)	Overheads (£ MM)	Total Cost excl. Contingency (£ MM)	Contingency (%)	Total Cost inc. Contingency (£ MM)
A. Pre-Final Investment Decision (Pre-FID)	Including Pre-FEED / FEED Design and Engineering	15.6	5.8	21.4		27.8
A1.1	Transportation	0.6	0.2	0.8		1.0
A1.2	Facilities	8.8	4.0	12.8		16.7
A1.3	Wells	2.0	0.2	2.2		2.9
A1.4	Other	4.3	1.3	5.6		7.2
A1.4.1	Seismic and Baseline Survey	1.3	0.1	1.4	30%	1.8
A1.4.2	Appraisal Well	0.0	0.0	0.0		0.0
A1.4.3	Engineering and Analysis	2.0	0.2	2.2		2.9
A1.4.4	Licensing and Permits	1.0	1.0	2.0		2.6
B. Post-Final Investment Decision (Post-FID)		311.8	18.9	330.7		428.6
B1.1	Transportation	165.9	6.1	171.9		223.5
B1.1.1	Detailed Design	0.4	0.1	0.5		0.7
B1.1.2	Procurement	71.8	4.8	76.6	30%	99.6
B1.1.3	Fabrication	22.0	1.2	23.2		30.1
B1.1.4	Construction and Commissioning	71.6	0.0	71.6		93.1
B1.2	Facilities	87.8	6.5	94.2		122.5
B1.2.1	Detailed Design	10.0	3.0	13.0		16.9
B1.2.2	Procurement	27.7	3.1	30.9	30%	40.1
B1.2.3	Fabrication	5.9	0.4	6.3		8.1
B1.2.4	Construction and Commissioning	44.1	0.0	44.1		57.4
B1.3	Wells	57.2	5.3	62.5		79.9
B1.3.1	Detailed Design	2.0	0.2	2.2		2.9
B1.3.2	Procurement	15.3	1.5	16.8	30%	22.5
B1.3.3	Fabrication	0.0	0.0	0.0		0.0
B1.3.4	Construction and Commissioning	39.9	3.6	43.5		54.5
B1.4	Other	1.0	1.0	2.0		2.6
B1.4.1	Licensing and Permits	1.0	1.0	2.0	30%	2.6
C. Total Operating Expenditure (OPEX)		461.7	31.9	493.6		639.1
C1.1	OPEX - Transportation	55.5	2.9	58.4		75.9
C1.2	OPEX - Facilities	235.4	18.1	313.5	30%	407.6
C1.3	OPEX - Wells	38.3	3.6	41.9		52.0
C1.3.1	Well Sidetracks and Workovers	38.3	3.6	41.9		52.0
C1.4	Other	72.5	7.3	79.8		103.7
C1.4.1	Measurement, Monitoring and Verification	6.8	0.7	7.5		9.7
C1.4.2	Financial Securities	65.7	6.6	72.27	30%	94.0
C1.4.3	Ongoing Tariffs and Agreements	0.0	0.0	0.0		0.0
D. Abandonment (ABEX)		76.0	7.4	83.5		108.5
D1.1	Decommissioning - Transportation	22.5	2.2	24.7		32.1
D1.2	Decommissioning - Facilities	26.7	2.7	29.4	30%	38.2
D1.3	Decommissioning - Wells	16.7	1.9	18.6		24.1
D1.4	Other	10.1	0.7	10.8		14.1
D1.4.1	Post Closure Monitoring	6.8	0.7	7.4	30%	9.7
D1.4.2	Handover	3.4	0.0	3.4		4.4

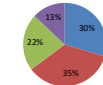
CAPEX BREAKDOWN [A+B]



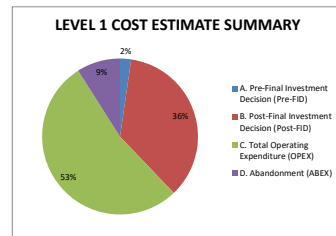
OPEX BREAKDOWN [C]



ABEX BREAKDOWN [D]



FIELD LIFE (YEARS)	26
CO2 STORED (MT)	130
DEFINITIONS	
TRANSPORTATION	CO2 PIPELINE SYSTEM (LANDFALL & OFFSHORE PIPELINE)
FACILITIES	NUIS, SUBSEA STRUCTURES, UMBILICALS, POWER CABLES
WELLS	ALL COSTS ASSOCIATED WITH CO2 INJECTION WELLS
OTHER	ANY AND ALL COSTS NOT COVERED WITHIN ABOVE
PRIMARY COST	PRIMARY CONTRACT COSTS
OVERHEAD	ADDITIONAL OWNER'S COSTS COVERING OWNER'S PROJECT MANAGEMENT, VERIFICATION, ETC



CAPEX / OPEX / ABEX BREAKDOWN SUMMARY - VIKING			
COST	TOTAL COST (£ MM)	CATEGORY	COST (£ MM)
CAPEX [A + B]	456.4	TRANSPORTATION	224.6
		FACILITIES	139.2
		WELLS	82.8
OPEX [C]	639.1	OTHER	9.8
		TRANSPORTATION	75.9
		FACILITIES	407.6
ABEX [D]	108.5	WELLS	52.0
		OTHER	103.7
		TRANSPORTATION	32.1
		FACILITIES	38.2
TOTAL	1204.0		1204.0

LEVEL 1 COST ESTIMATE SUMMARY				
Category	Primary Cost (£ MM)	Overheads (£ MM)	Total Cost excluding Contingency (£ MM)	Total Cost inc. Contingency (£ MM)
A. Pre-Final Investment Decision (Pre-FID)	15.6	5.8	21.4	27.8
B. Post-Final Investment Decision (Post-FID)	311.8	18.9	330.7	428.6
C. Total Operating Expenditure (OPEX)	461.7	31.9	493.6	639.1
D. Abandonment (ABEX)	76.0	7.4	83.5	108.5
TOTAL COST (CAPEX, OPEX, ABEX)			929.2	1204.0
COST CO2 INJECTED (£ PER TONNE)			£7.15	£9.26

PROJECT	Strategic UK Storage Appraisal Project
TITLE	SITE 5: VIKING
CLIENT	ETI
REVISION	A1
DATE	08/03/2016

TRANSPORTATION:
PROCUREMENT & FABRICATION

Pale Blue Dot.



Pipeline	Trunk Pipeline(s)	Infield Pipeline(s)
Number	1	
Route Length (km)	185	
Route Length Factor	1.05	
Pipeline Crossings	8	
Tee Structures	2	
Outer Diameter (mm)	508	
Wall Thickness (mm)	17.5	
Anode Spacing (m)	300	

No.	Item	Description	Unit Cost (£)	Unit	Qty	Total (£MM)	Overhead (£)	Description (Overheads)	Total Cost (£)
A. Pre-FID									
A1.1 Transportation - Pre FID									
A1.1.1	Pre-FEED	Lump Sum	£200,000	LS	1.00	£200,000	£90,000	Company Time Writing, Contractor Surveillance	£290,000
A1.1.2	FEED	Lump Sum	£350,000	LS	1.00	£250,000	£157,500	Company Time Writing, Contractor Surveillance	£407,500
B. Post FID									
B1.1 Transportation - Post FID									
B1.1.1	Detailed Design	Lump Sum	£400,000	LS	1.00	£400,000	£100,000	Company Time Writing, IVB, SIT, Insurance etc	£500,000
B1.1.2	Procurement	Pipeline from Barnston	-	-	-	-	-	Insurance and Certification	£75,625,026
B1.1.2.2	Insurance and Certification	Pipeline route	-	-	-	-	£500,000	Insurance and Certification	£500,000
B1.1.2.3	Geotechnical Testing	Pipeline route	£2,000	km	194	£388,500	£28,000	Documentation etc	£416,500
B1.1.2.4	Procurement - Linepipe (Trunk)	API 5L X65, OD 508mm, WT 17.5mm	£1,500	Te	41,121	£61,681,500	£3,700,890		£65,382,390
B1.1.2.5	Procurement - Coating (Trunk)	Corrosion Coating	£20	m	194,250	£3,885,000	£233,100	Logistics/Freight @ 6%	£4,118,100
B1.1.2.6	Procurement - Coating (Trunk)	Concrete Coating	£30	m	194,250	£5,827,500	£349,650		£6,177,150
B1.1.2.7	Procurement - Anodes (Trunk)	CP Protection	£45	Each	648	£29,138	£1,748		£30,886
B1.1.3	Fabrication		-	-	-	-	-		£23,182,500
B1.1.3.1	SSIV	Subsea Isolation Valve Structure	£1,500,000	LS	1	£1,500,000	£100,000	Contractor Surveillance	£1,600,000
B1.1.3.2	Spoolbase Fabrication	Coating Only (S Lay)	£50	m	194,250	£9,712,500	£50,000	Contractor Surveillance	£9,762,500
B1.1.3.3	Crossing Supports	Concrete Crossing Plinth/Supports	£100,000	Per Crossing	8	£800,000	£20,000	Contractor Surveillance	£820,000
B1.1.3.4	Tee-Piece Structure	To Facilitate Future Expansion	£5,000,000	Each	2	£10,000,000	£1,000,000		£11,000,000
Total (Excluding Contingency)									£101,005,026
Pre-FID Contingency (%)									30%
									£209,250
Post-FID Contingency (%)									30%
									£30,092,258
Total (Including Contingency)									£131,306,533

PROJECT	Strategic UK Storage Appraisal Project
TITLE	SITE 5: VIKING
CLIENT	ETI
REVISION	A1
DATE	08/03/2016

TRANSPORTATION:
CONSTRUCTION AND COMMISSIONING

Pale Blue Dot.



Pipeline	Trunk Pipeline(s)	Infield Pipeline(s)
Number	1	
Route Length (km)	185	
Route Length Factor	1.05	
Pipeline Crossings	8	
Outer Diameter (mm)	508	
Wall Thickness (mm)	17.5	
Anode Spacing (m)	300	
Landfall Required?	YES	

Landfall Cost	£25,000,000
---------------	-------------

Activity	Vessel	Dayrate (£)	Working Rate (m/hr)
Pipeline Route Survey	Survey Vessel	£100,000	750
Pipelay (Reel)	Reel Lay Vessel	£150,000	500
Pipelay (S-Lay)	S-Lay Vessel (14000Te)	£350,000	100
Trenching and Backfill	Ploughing Vessel	£100,000	400
Crossing Installation	Survey Vessel	£100,000	-
Spoolpiece Tie-ins	DSV	£150,000	-
Commissioning	Survey Vessel	£100,000	-
Pipelay (Carrier)	Pipe Carrier (1600Te)	£50,000	-
Structure Installation	DSV	£150,000	-
Seabed Rectification	Jet Trencher	£100,000	-

No.	Activity	Breakdown	Vessel	Day Rate (£)	Days	Sub-Total (£)	Total Cost (£)
-----	----------	-----------	--------	--------------	------	---------------	----------------

B. Post FID							
B1.1 Transportation - Post FID							
B1.1.4 Construction and Commissioning							
B1.1.4.1	Pipeline Route Survey	Mobilisation	Survey Vessel	£100,000	2	£200,000	£1,500,000
		Infield Operations			11	£1,100,000	
		Demobilisation			2	£200,000	
B1.1.4.2	Pipelay (S-Lay)	Mobilisation	S-Lay Vessel (14000Te)	£350,000	2	£700,000	£29,750,000
		Infield Operations			81	£28,350,000	
		Demobilisation			2	£700,000	
B1.1.4.3	Crossing Installation	Mobilisation	Survey Vessel	£100,000	2	£200,000	£2,800,000
		Infield Operations - 3 day per Crossing			24	£2,400,000	
		Demobilisation			2	£200,000	
B1.1.4.4	Spoolpiece Tie-ins	Mobilisation	DSV	£150,000	2	£200,000	£1,400,000
		Infield Operations			10	£1,000,000	
		Demobilisation			2	£200,000	
B1.1.4.5	Commissioning	Mobilisation	Survey Vessel	£100,000	2	£200,000	£600,000
		Infield Operations			2	£200,000	
		Demobilisation			2	£200,000	
B1.1.4.6	Structure Installation	Mobilisation	DSV	£150,000	4	£600,000	£1,350,000
		Infield Operations -SSIV & Tees			3	£450,000	
		Demobilisation			2	£300,000	
B1.1.4.7	Pipelay (Carrier)	Mobilisation	Pipe Carrier (1600Te)	£50,000	2	£100,000	£3,600,000
		Infield Operations - days per trip			68	£3,400,000	
		Demobilisation			2	£100,000	
B1.1.4.8	Seabed Rectification	Mobilisation	Jet Trencher	£100,000	2	£200,000	£1,400,000
		Infield Operations - days per trip			10	£1,000,000	
		Demobilisation			2	£200,000	
B1.1.4.8	Construction Project Management and Engineering		-	Lump Sum (10%)	-	£4,240,000	£4,240,000
B1.1.4.9	Landfall		-	Lump Sum	-	£25,000,000	£25,000,000
						Total (Excluding Contingency)	£71,640,000
						Contingency 30%	£21,492,000
						Total (Including Contingency)	£93,132,000

PROJECT	Strategic UK Storage Appraisal Project
TITLE	SITE 5: VIKING
CLIENT	ETI
REVISION	A1
DATE	08/03/2016

Facilities:
PROCUREMENT & FABRICATION

Pale Blue Dot.

COSTAIN

AXIS
WELL TECHNOLOGY
FROM CONCEPT TO COMPLETION

COSTS EXTRACTED FROM QUESTOR Exchange Rate (E.\$) 1.50

No.	Item	Description	Unit Cost (£)	Unit	Qty	Total (EMM)	Overhead (£)	Description (Overheads)	Total Cost (£)
A. Pre-FID									
A1.2 Facilities - Pre FID									
A1.2.1	Pre-FEED	4 Legged Jacket, Topsides	£3,237,160	LS	1	£3,237,160	£1,456,722	Company Time Writing, Contractor Surveillance	£4,693,882
A1.2.2	FEED	4 Legged Jacket, Topsides	£5,605,740	LS	1	£5,605,740	£2,522,583	Company Time Writing, Contractor Surveillance	£8,128,323
B. Post FID									
B1.2 Facilities - Post FID									
B1.2.1	Detailed Design	4 Legged Jacket, Topsides	£10,000,000	LS	1	£10,000,000	£3,000,000	Company Time Writing, IVB, SIT etc	£13,000,000
B1.2.2	Procurement	Jacket	-	-	-	-	-	-	£30,651,699
B1.2.2.1	Insurance and Certification	4 Legged Jacket	-	-	-	-	£584,667	Insurance and Certification	£584,667
B1.2.2.1.1	Jacket Steel		£1,333	Te	726	£968,000	£58,080		£1,026,080
B1.2.2.1.2	Piles		£1,301	Te	507	£659,438	£39,566	Logistics/Freight @ 6%	£699,004
B1.2.2.1.4	Anodes		£3,685	Te	47	£173,211	£10,393		£183,603
B1.2.2.1.5	Installation Aids		£1,127	Te	36	£40,584	£2,435		£43,019
B1.2.2.2	Insurance and Certification	Primary Steel	£1,087	Te	169	£183,647	£11,019	Insurance and Certification	£99,901,321
B1.2.2.2.1	Secondary Steel		£900	Te	101	£90,900	£5,454		£96,354.00
B1.2.2.2.4	Piping		£10,733	Te	30	£322,000	£19,320		£341,320.00
B1.2.2.2.5	Electrical		£19,200	Te	15	£298,000	£17,280		£315,280.00
B1.2.2.2.6	Instrumentation		£36,333	Te	15	£545,000	£32,700		£577,700.00
B1.2.2.2.7	Miscellaneous		£8,800	Te	18	£158,400	£9,504		£167,904.00
B1.2.2.2.8	Manifolding		£14,733	Te	19	£279,933	£16,796		£296,729.33
B1.2.2.2.9	Control and Communications	Sat Comms	£469,733	Te	2	£1,382,200	£82,522		£1,465,122.00
B1.2.2.2.10	General Utilities	Drainage, Diesel Storage etc	£50,000	Te	2	£100,000	£6,000	Logistics/Freight @ 6%	£106,000.00
B1.2.2.2.11	Vent Stack	Low Volume (venting done at beach)	£6,933	Te	35	£242,867	£14,560		£257,427.00
B1.2.2.2.12	Diesel Generators	Power Generation	£52,067	Te	5	£0	£0		£0.00
B1.2.2.2.13	Power Distribution		£36,967	Te	5	£169,333	£10,820		£180,153.33
B1.2.2.2.14	Emergency Power		£34,733	Te	2	£69,467	£4,168		£73,634.67
B1.2.2.2.15	Quarters and Helideck	50 Tt Helideck plus TR	£23,333	Te	70	£1,633,333	£98,000		£1,731,333.33
B1.2.2.2.16	Crane	Mechanical Handling	£19,267	Te	30	£578,000	£34,680		£612,680.00
B1.2.2.2.17	Lifboats	Freefall Lifboats	£24,400	Te	7	£172,800	£10,248		£183,048.00
B1.2.2.2.18	Chemicals, Infection	Chemicals, Pumps, Storage	£46,800	Te	10	£466,000	£27,960		£493,960.00
B1.2.2.2.19	PLR	Pig Receiver	£10,000	Te	2	£20,000	£1,200		£21,200.00
B1.2.2.2.20	Heaters	CO2 Heating	£300,000	Each	6	£1,800,000	£109,000		£1,909,000.00
B1.2.3	Power Supply - Cable+Onshore Tie-in	Connection into Local Distribution	£17,371,600	Each	1	£17,371,600	£1,042,296		£18,413,896
B1.2.3.1	Jacket Steel		£3,245	m	726	£2,355,628	£141,338		£2,496,966
B1.2.3.2	Piles		£1,022	m	507	£519,154	£31,089	Logistics/Freight @ 6%	£549,243
B1.2.3.3	Anodes		£755	Each	47	£35,501	£2,190		£37,691
B1.2.3.4	Installation Aids		£3,955	Each	36	£142,392	£8,544		£150,936
B1.2.3.2.1	Primary Steel		£5,467	Te	169	£923,867	£55,432		£979,299
B1.2.3.2.2	Secondary Steel		£7,200	Te	101	£727,200	£43,632		£770,832
B1.2.3.2.3	Equipment		£1,513	Te	75	£113,500	£6,810	Logistics/Freight @ 6%	£120,310
B1.2.3.2.4	Piping		£14,867	Te	30	£446,000	£26,760		£472,760
B1.2.3.2.5	Electrical		£26,467	Te	15	£397,000	£23,820		£420,820
B1.2.3.2.6	PLR	Pig Receiver	£25,000	Te	2	£50,000	£3,000		£53,000
B1.2.3.2.7	Miscellaneous		£10,867	Te	18	£195,600	£11,736		£207,336
B1.2.4	Construction and Commissioning		-	-	-	-	-		£44,137,057
B1.2.4.1	Power Cable Installation	Jumps sum	£21,714,500	Each	1	£21,714,500	£0		£21,714,500
B1.2.4.2	Installation Spread	Jacket Installation	£596,206	Days	28	£16,693,768	£0		£16,693,768
B1.2.4.3	Installation Spread	Topsides Installation	£135,533	Days	7	£948,733	£0		£948,733
B1.2.4.4	Tug Transport - Jacket	Mobilisation	£57,236	Days	4	£228,944	£0		£228,944
B1.2.4.4	Tug Transport - Jacket	Infield Operations	£57,236	Days	16	£915,776	£0		£915,776
B1.2.4.4	Tug Transport - Jacket	Demobilisation	£57,236	Days	4	£228,944	£0		£228,944
B1.2.4.5	Barge Transport - Jacket	Mobilisation	£8,672	Days	4	£34,688	£0		£34,688
B1.2.4.5	Barge Transport - Jacket	Infield Operations	£8,672	Days	56	£485,632	£0		£485,632
B1.2.4.5	Barge Transport - Jacket	Demobilisation	£8,672	Days	4	£34,688	£0		£34,688
B1.2.4.6	Tug Transport - Topsides	Mobilisation	£57,236	Days	4	£228,944	£0		£228,944
B1.2.4.6	Tug Transport - Topsides	Infield Operations	£57,236	Days	30	£1,717,080	£0		£1,717,080
B1.2.4.6	Tug Transport - Topsides	Demobilisation	£57,236	Days	4	£228,944	£0		£228,944
B1.2.4.7	Barge Transport - Topsides	Mobilisation	£8,672	Days	4	£34,688	£0		£34,688
B1.2.4.7	Barge Transport - Topsides	Infield Operations	£8,672	Days	70	£607,040	£0		£607,040
B1.2.4.7	Barge Transport - Topsides	Demobilisation	£8,672	Days	4	£34,688	£0		£34,688
Total (Excluding Contingency)									£107,069,984
Pre-FID Contingency (%)									30%
Post-FID Contingency (%)									30%
Total (including Contingency)									£139,190,980

PROJECT	Strategic UK Storage Appraisal Project
TITLE	SITE 5: VIKING
CLIENT	ETI
REVISION	A1
DATE	08/03/2016

WELLS:
COST SUMMARY

Pale Blue Dot.



Well Cost Summary (including 30% Contingency)		
Well Name	Days	Well Cost (£,000)
Year 0		
Platform Injector 1	68.3	26142.5
Platform Injector 2	61.8	23932.5
Monitoring Well 1 / Spare Injector	66.8	25432.5
Year 10		
Workover 1	25.2	10067.5
Local Sidetrack 1	57.9	20292.5
Local Sidetrack 2	62.9	21597.5
Year 40		
Abandonment Platform Injector 1	31.2	8970
Abandonment Platform Injector 2	24.7	6760
Abandonment Monitoring Well 1	31.2	8385
TOTAL	429.7	151580.0

Note: This figure does not include the PM & Eng costs.

Drilling Overhead Cost Summary	
Drilling Campaign	Overhead (EMM)
Platform Injector 1-2 + MW	3.60
Abandonment	1.85

OPEX Overhead Cost Summary	
OPEX Campaign	Overhead (EMM)
Workover + Local Sidetracks	3.60

Level 1 Cost Estimate Summary - Wells	
Total CAPEX (EMM)	82.8
Total OPEX (EMM)	52.0
Total ABEX (EMM)	24.1
TOTAL (EMM)	158.8

Activity	Wells Cost Estimate - Primary Cost Summary					Total Cost (£,000)
	Drilling Costs		Procurement Costs (£,000)			
	Phase Rig Cost (£,000)	Phase Spread Cost (£,000)	Contingency (£,000)	Procurement (£,000)	Contingency (£,000)	
Development Wells - CAPEX Breakdown						
Platform Injector 1	5,250	8,375	3,938	6,600	1,980	26,143
Platform Injector 2	4,750	7,625	3,563	6,150	1,845	23,933
Monitoring Well 1 / Spare Injector	5,250	8,625	3,563	6,150	1,845	25,433
Wells - OPEX Breakdown						
Workover	2,350	4,000	413	2,750	555	10,068
Local Platform Sidetrack 1	4,450	7,175	3,338	4,100	1,230	20,293
Local Platform Sidetrack 2	4,950	8,175	3,338	3,950	1,185	21,598
Wells - ABEX Breakdown						
Abandonment Platform Injector 1	2,400	3,600	1,800	900	270	8,970
Abandonment Platform Injector 2	1,900	2,850	1,425	450	135	6,760
Abandonment Monitoring Well 1	2,400	3,600	1,800	450	135	8,385

CAPEX Summary	Excluding Contingency (EMM)	Overhead (EMM)	Overhead Description	Sub-Total (EMM)	Contingency		Total Cost (EMM)
					%	EMM	
Pre-FEED / FEED PM & E	2.0	0.2	Company Time Writing, IVB, SIT, Insurance etc.	2.2	30%	0.7	2.9
Detailed Design PM & E	2.0	0.2		2.2	30%	0.7	2.9
Procurement	15.3	1.5		16.8	30%	5.7	22.5
Construction and Commissioning (Drilling)	39.9	3.60	Well Management Fees, Insurance, Site Survey, Studies etc.	43.5	30%	11.1	54.5
Total	59.2	5.5		64.7		18.1	82.8

OPEX Summary	Excluding Contingency (EMM)	Overhead (EMM)	Overhead Description	Sub-Total (EMM)	Contingency		Total Cost (EMM)
					%	EMM	
OPEX	38.3	3.60	Well Management Fees, Insurance, Site Survey, Studies etc.	41.9	30%	10.1	52.0

ABEX Summary	Excluding Contingency (EMM)	Overhead (EMM)	Overhead Description	Sub-Total (EMM)	Contingency		Total Cost (EMM)
					%	EMM	
ABEX	16.7	1.85	Well Management Fees, Insurance, Site Survey, Studies etc.	18.6	30%	5.6	24.1